



UNIVERSIDAD NACIONAL AUTÓNOMA DE MÉXICO

Maestría y Doctorado en Ciencias Bioquímicas

EFFECTO DE LA ALOPREGNANOLONA EN LA MIGRACIÓN E INVASIÓN DE
CÉLULAS DERIVADAS DE GLIOBLASTOMA HUMANO A TRAVÉS DE LA
ACTIVACIÓN DE LA PROTEÍNA CINASA cSrc.

TESIS

QUE PARA OPTAR POR EL GRADO DE:

Doctor en Ciencias

PRESENTA:

M. en C. Carmen Janín Zamora Sánchez

TUTOR PRINCIPAL

Dr. Ignacio Camacho Arroyo
[Facultad de Química, U.N.A.M.](#)

MIEMBROS DEL COMITÉ TUTOR

Dr. Mauricio Rodríguez Dorantes
[Instituto Nacional de Medicina Genómica](#)

Dr. Marco Antonio Velasco Velázquez
[Facultad de Medicina, U.N.A.M.](#)

Ciudad Universitaria, Ciudad de México. Mayo, 2023



Universidad Nacional
Autónoma de México

Dirección General de Bibliotecas de la UNAM

Biblioteca Central



UNAM – Dirección General de Bibliotecas
Tesis Digitales
Restricciones de uso

DERECHOS RESERVADOS ©
PROHIBIDA SU REPRODUCCIÓN TOTAL O PARCIAL

Todo el material contenido en esta tesis esta protegido por la Ley Federal del Derecho de Autor (LFDA) de los Estados Unidos Mexicanos (México).

El uso de imágenes, fragmentos de videos, y demás material que sea objeto de protección de los derechos de autor, será exclusivamente para fines educativos e informativos y deberá citar la fuente donde la obtuvo mencionando el autor o autores. Cualquier uso distinto como el lucro, reproducción, edición o modificación, será perseguido y sancionado por el respectivo titular de los Derechos de Autor.

ZAMORA SÁNCHEZ CARMEN JANÍN
Estudiante de Doctorado en Ciencias Bioquímicas
Presente

Los miembros del Subcomité Académico en reunión ordinaria del **12 de septiembre de 2022**, conocieron su solicitud de asignación de **JURADO DE EXAMEN** para optar por el grado de **Doctora en Ciencias**, con la réplica de la tesis "**Efecto de la alopregnanolona en la migración e invasión de células derivadas de glioblastoma humano a través de la activación de la proteína cinasa cSrc**", dirigida por el/la Dr(a). **CAMACHO ARROYO IGNACIO**.

De su análisis se acordó nombrar el siguiente jurado integrado por los doctores:

LIZANO SOBERÓN MARCELA	PMDCBQ	PRESIDENTE
ROCHA ZAVALETA LETICIA	PMDCBQ	SECRETARIO
IBARRA RUBIO MARÍA ELENA	PMDCBQ	VOCAL
VÁZQUEZ MARTÍNEZ EDGAR RICARDO	PMDCBQ	VOCAL
DRA. PATRICIA GARCÍA LÓPEZ	NO ACREDITADO	VOCAL

Sin otro particular por el momento, aprovecho la ocasión para enviarle un cordial saludo.

Atentamente
“POR MI RAZA HABLARÁ EL ESPÍRITU”
Cd. Universitaria, Cd. Mx., a 19 de septiembre de 2022



Coordinadora
Dra. Claudia Lydiá Treviño Santa Cruz

AGRADECIMIENTOS

A la Dirección General de Asuntos del Personal Académico (DGAPA) por la beca para obtención de grado del Programa de Apoyo a Proyectos de Investigación e Innovación Tecnológica (PAPIIT) de la UNAM, con clave de proyecto: IN217120.

Al comité tutor conformado por el Dr. Mauricio Rodríguez Dorantes y el Dr. Marco Antonio Velasco Velázquez, por su asesoramiento durante el desarrollo de este proyecto. Y a los miembros del jurado de tesis, por sus comentarios al presente trabajo.

Al Dr. Ignacio Camacho Arroyo por la tutoría principal de este proyecto de tesis y a la Unidad de Investigación en Reproducción Humana del Instituto Nacional de Perinatología – Facultad de Química de la Universidad Nacional Autónoma de México, en dónde se realizó el proyecto.

Asimismo, este trabajo contó con el apoyo del Programa de Apoyo a los estudios de Posgrado (PAEP), para la presentación del proyecto de tesis en el congreso: III Neurobiology Meeting of the Mexican Society for Biochemistry.

Esta tesis fue realizada gracias a la beca otorgada por el Consejo Nacional de Ciencia y Tecnología (CONACyT), con el registro de CVU: 589888.

AGRADECIMIENTOS Y DEDICATORIAS PERSONALES

Esta tesis, como todas, está enteramente dedicada a mis papás: **Alejandra y David**. Gracias por todo, absolutamente todo. Los amo.

Mi más profundo agradecimiento y estima al **Dr. Camacho**, es un gusto trabajar contigo, mil gracias siempre por tus enseñanzas, apoyo, confianza e impulso.

Muchas gracias a todas y cada una de las personas con las que me he cruzado en el **laboratorio de comunicación neuroendócrina** de la Facultad de Química, de todos he aprendido algo. Especialmente, quiero agradecerles a todas las mujeres que impiden que el lab se prenda en llamas: **Irene, Ale, Reyna y Karina**. Gracias también a las mejores amistades que hice en este lab: **Claudia, Karla y Saúl**, es un placer trabajar y compartir la vida con personas con tanta calidad humana como ustedes.

Gracias especiales e infinitas a **Omar**, un excelente ser humano y compañero de vida, gracias por ser una gran fuente de motivación, tu apoyo ha sido invaluable para culminar este proyecto.

A todos los que están o estuvieron en algún punto entre el inicio y el fin de mi proyecto de doctorado, gracias por la inspiración, estima, asistencia, motivación, enseñanzas y compañía: **Aliesha, Valeria, Gaby, Karina, Daniel, Alma**.

A mis mejores amigos: **Tomy y Osa**.

*“Soy de las que piensan que la ciencia tiene
una gran belleza. Un científico en su
laboratorio no es sólo un técnico: también es
un niño colocado ante fenómenos naturales
que lo impresionan como un cuento de
hadas.”*

Marie Curie

ÍNDICE

1	ÍNDICE DE ABREVIATURAS	9
2	RESUMEN.....	10
3	ABSTRACT	12
4	INTRODUCCIÓN.....	13
5	ANTECEDENTES.....	15
5.1	Características de los tumores del sistema nervioso central (SNC)	15
5.2	Características de los glioblastomas (GB)	19
5.3	Migración e invasión de las células de GB humanos	25
5.4	Cinasa cSrc en la migración e invasión celular de los GB.....	30
5.5	Generalidades sobre la alopregnanolona (3 α -THP)	33
5.6	Síntesis de alopregnanolona (3 α -THP).....	34
5.7	Mecanismos de acción de la 3 α -THP	39
5.8	Efectos de la 3 α -THP en cáncer	47
6	PLANTEAMIENTO DEL PROBLEMA	50
7	HIPÓTESIS.....	50
8	OBJETIVOS	51
8.1	OBJETIVO GENERAL.....	51
8.2	OBJETIVOS PARTICULARES	51
9	METODOLOGÍA	52
9.1	Cultivo celular	52
9.2	Ensayos de migración	52
9.3	Ensayos de invasión	54
9.4	Transfección y silenciamiento de las 3 α -HSD	55
9.5	Extracción de RNA total y RT-qPCR	57
9.6	Extracción de proteína y Western Blot	58
10	RESULTADOS.....	61
10.1	Efecto de la 3 α -THP sobre la migración de las células de GB.....	61

10.2	Efecto de la 3 α -THP sobre la capacidad de invasi3n de las c3lulas de GB	65
10.3	Caracterizaci3n de las 3 α -HSD (AKR1C1-4) en las l3neas celulares de GB.....	66
10.4	Efecto del silenciamiento de las 3 α -HSD sobre la migraci3n de c3lulas de GB tratadas con 3 α -THP	67
10.5	Efecto del silenciamiento de las 3 α -HSD sobre la invasi3n de c3lulas de GB tratadas con 3 α -THP	69
10.6	Efecto de la 3 α -THP sobre la activaci3n de la cinasa cSrc	69
10.7	Efecto de la 3 α -THP y el PP2 sobre la migraci3n de las l3neas celulares de GB..	73
10.8	Efecto de la 3 α -THP y el PP2 sobre la invasi3n de las l3neas celulares de GB.....	76
11	DISCUSI3N	78
12	CONCLUSIONES	85
13	PERSPECTIVAS	86
14	REFERENCIAS.....	87
15	ANEXOS.....	i
15.1	Caracter3sticas de las l3neas celulares utilizadas.....	i
15.2	Art3culos derivados del proyecto de doctorado.....	ii
15.2.1	Zamora-S3nchez, C.J.; Hern3ndez-Vega, A.M.; Gaona-Dom3nguez, S.; Rodr3guez-Dorantes, M.; Camacho-Arroyo, I. 5alpha-dihydroprogesterone promotes proliferation and migration of human glioblastoma cells. <i>Steroids</i> 2020 , 163, 108708, doi:10.1016/j.steroids.2020.108708. Factor de impacto:2.76.	
15.2.2	Zamora-S3nchez, C.J.; Bello-Alvarez, C.; Rodr3guez-Dorantes, M.; Camacho-Arroyo, I. Allopregnanolone Promotes Migration and Invasion of Human Glioblastoma Cells through the Protein Tyrosine Kinase c-Src Activation. <i>Int. J. Mol. Sci.</i> 2022 , 23, 4996, doi:10.3390/ijms23094996. Factor de Impacto: 6.208.	
15.2.3	Zamora-S3nchez, C.J.; Camacho-Arroyo, I. Allopregnanolone: Metabolism, Mechanisms of Action, and Its Role in Cancer. <i>Int. J. Mol. Sci.</i> 2023 , 24, doi:10.3390/ijms24010560. Factor de Impacto: 6.208.	
15.2.4	Bello-Alvarez, C.; Zamora-S3nchez, C.; Pe3a-Guti3rrez, K.; Camacho-Arroyo, I. Progesterone and its metabolite allopregnanolone promote invasion of human glioblastoma cells through metalloproteinase-9 and cSrc kinase. <i>Oncol. Lett.</i> 2023 , 25, 223, doi:10.3892/ol.2023.13809. Factor de Impacto: 3.111.	

-
- 15.3 Otras publicacioneslviii
- 15.3.1 González-Arenas, A., De la Fuente-Granada, M., Camacho-Arroyo, I., **Zamora-Sánchez, C. J.**, Piña-Medina, A. G., Segura-Uribe, J., & Guerra-Araiza, C. (2019). Tibolone Effects on Human Glioblastoma Cell Lines. *Archives of Medical Research*, 50(4), 187–196. <https://doi.org/10.1016/j.arcmed.2019.08.001>. **Factor de Impacto: 8.323.**
- 15.3.2 **[Capítulo de libro]** Camacho-Arroyo, I., Piña-Medina, A. G., Bello-Alvarez, C., & **Zamora-Sánchez, C. J.** (2020). Sex hormones and proteins involved in brain plasticity. In *Vitamins and Hormones* (pp. 145–165). Academic Press Inc. <https://doi.org/10.1016/bs.vh.2020.04.002>.
- 15.3.3 Hernández-Vega, A. M., Del Moral-Morales, A., **Zamora-Sánchez, C. J.**, Piña-Medina, A. G., González-Arenas, A., & Camacho-Arroyo, I. (2020). Estradiol Induces Epithelial to Mesenchymal Transition of Human Glioblastoma Cells. *Cells*, 9(9), 1–23. <https://doi.org/10.3390/cells9091930>. **Factor de Impacto: 7.666.**
- 15.3.4 Valdés-Rives, S. A., Arcos-Montoya, D., Fuente-Granada, M. de la, **Zamora-Sánchez, C. J.**, Arias-Romero, L. E., Villamar-Cruz, O., Camacho-Arroyo, I., Pérez-Tapia, S. M., & González-Arenas, A. (2021). LPA1 Receptor Promotes Progesterone Receptor Phosphorylation through PKC α in Human Glioblastoma Cells. *Cells*, 10(4), 807. <https://doi.org/10.3390/CELLS10040807>. **Factor de Impacto: 7.666.**
- 15.3.5 Bello-Alvarez, C., **Zamora-Sánchez, C. J.**, & Camacho-Arroyo, I. (2022). Rapid Actions of the Nuclear Progesterone Receptor through cSrc in Cancer. *Cells*, 11(12), 1964. <https://doi.org/10.3390/cells11121964>. **Factor de Impacto: 7.666.**

1 ÍNDICE DE ABREVIATURAS

3α-HSD	3 α -hidroxiesteroide deshidrogenasa(s)
3α-THP	Alopregnanolona
5α-DHP	5 α -Dihidroprogesterona
5α-R	5 α -reductasa
AKR1C1-4	Aldo ceto reductasa 1C1, 1C2, 1C3 y 1C4
cSrc	Proto-oncogen SRC, tirosina cinasa no receptor
DMEM	Medio de cultivo Eagle Modificado Dulbecco
GABA	Ácido γ -aminobutírico
GABA_AR	Receptor tipo A del ácido γ -aminobutírico
GB	Glioblastoma(s)
IDH	Isocitrato deshidrogenasa
MEC	Matriz extracelular
mPR	Receptor(es) membranal(es) de progesterona
P4	Progesterona
PP2	1-tert-Butil-3-(4-clorofenil)-1H-pirazolo[3,4-d]pirimidin-4-amina
PXR	Receptor X de pregnano
RP	Receptor de progesterona
sAKR1C1-3	siRNA comercial para AKR1C1-3
SFB	Suero fetal bovino

2 RESUMEN

La alopregnanolona (3α -THP), es uno de los metabolitos más estudiados de la progesterona (P4), una hormona esteroide. La 3α -THP tiene diversos efectos en el sistema nervioso central (SNC). Algunos de ellos son: promover la proliferación de células neurales y progenitoras gliales, inducir cambios en el citoesqueleto y aumentar la migración en las células gliales. Estos procesos celulares también se ven alterados en el cáncer, sin embargo, el efecto de la 3α -THP sobre estas enfermedades se ha estudiado muy poco. Los glioblastomas (GB) son los tumores primarios malignos más frecuentes y agresivos del SNC. Éstos se caracterizan por una alta capacidad de proliferación, migración e invasión. Se ha reportado que la 3α -THP promueve la proliferación de las células de GB e induce la migración de células de cáncer ovárico. En el presente trabajo se investigaron los efectos de la 3α -THP sobre la migración y la capacidad invasiva de células derivadas de GB humanos. También se evaluó la participación del metabolismo de la 3α -THP a través de las enzimas 3α -hidroxiesteroide deshidrogenasas (3α -HSD), que catalizan la oxidación de la 3α -THP a 5α -dihidroprogesterona (5α -DHP). Asimismo, se determinó el efecto de la inhibición de la cinasa cSrc, que está involucrada en la migración e invasión, en los efectos de la 3α -THP. La 3α -THP (100 nM) aumentó la migración e invasión de las líneas celulares U251, U87 y LN229, tres de las líneas celulares más utilizadas para ensayos in vitro con células de GB. Las células U251 y LN229 presentaron altos niveles de las 3α -HSD en comparación con astrocitos humanos. El silenciamiento de dichas enzimas no modificó los efectos de la 3α -THP sobre la migración e invasión. Por otro lado, la 3α -THP aumentó los niveles de la proteína cSrc fosforilada en el residuo Y416 a los 10 min de tratamiento en las células U251 y a los 15 min en las células U87 y LN229. Dicha marca de fosforilación está asociada a una mayor actividad de la proteína cSrc. Además, la inhibición farmacológica de cSrc con el fármaco PP2 disminuyó el efecto de la 3α -THP sobre la migración y la capacidad

invasiva de las células de GB. Estos resultados sugieren que la 3α -THP promueve la malignidad de los GB al incrementar la migración e invasión celulares mediante la activación de la cinasa cSrc y que dicho efecto es independiente de su metabolismo a través de las 3α -HSD.

3 ABSTRACT

Allopregnanolone (3α -THP) is one of the most studied metabolites of the steroid hormone progesterone (P4). 3α -THP has many effects on the Central Nervous System (CNS). It promotes the proliferation of neural and glial progenitor cells. Moreover, in glial cells, it induces cytoskeleton rearrangement and augments migration. Such cellular processes are often found to be altered in cancer. However, the effects of 3α -THP in such pathologies have been poorly studied. Glioblastoma (GB) is the most frequent and aggressive primary malignant tumor of the CNS. GB cells are characterized by a highly migrative potential and invasion of the brain parenchyma. It has been described the positive effects of 3α -THP on GB cell proliferation. It also promotes cell migration of ovarian cancer cells. Here, the effects of 3α -THP in the cell migration and invasion of cell lines derived from human GB cells were evaluated. Also, the relevance of 3α -THP metabolism by the 3α -hydroxysteroid dehydrogenases (3α -HSD), which catalyzes the interconversion of 3α -THP to 5α -Dihydroprogesterone (5α -DHP) was studied. Besides, we determined the role of cSrc kinase, a key regulator of cell migration and invasion processes, on the effects of 3α -THP. 3α -THP (100 nM) augmented migration and invasion of the human GB cell lines U87, U251, and LN229. Besides, the cell lines U251 and LN229 express higher levels of the 3α -HSD enzymes when compared to normal human astrocytes. In addition, 3α -HSD silencing did not modify the effect of 3α -THP on cell migration and invasion. 3α -THP also promoted the cSrc phosphorylation at the Y416 residue, associated with a hyper-activation of cSrc kinase at 10 (in the U251 cell line) and 15 min (U87 and LN229 cells) of treatment. The pharmacologic inhibition of cSrc decreased the effects of 3α -THP on cell migration and invasion. Together, these data suggest that 3α -THP promotes GB malignancy by increasing GB migration and invasion through the c-Src activation and independently of its 3α -HSD metabolism.

4 INTRODUCCIÓN

Los glioblastomas (GB) son uno de los tumores más frecuentes y agresivos del sistema nervioso central (SNC). Éstos representan más del 49% de todos los tumores malignos del SNC y se caracterizan por su alta actividad mitótica, capacidad invasiva y vascularización [1,2]. A pesar del tratamiento, la media de supervivencia de los pacientes con GB no es mayor a los 8 meses [3]. Además, los GB son más prevalentes en hombres que en mujeres, en una razón de 3: 2 [2]. Este comportamiento dimórfico, ha llevado al estudio de factores como las hormonas sexuales sobre la progresión de los GB. Las hormonas sexuales, y particularmente la progesterona (P4), promueven la malignidad tumoral al aumentar procesos como la proliferación, migración e invasión en líneas celulares de GBs humanos y en modelos *in vivo* [4–6].

La P4 se metaboliza en diversos tejidos, tales como las gónadas, placenta, glándulas adrenales y el SNC. Además de la P4, sus metabolitos también tienen efectos y diversos mecanismos de acción diferentes a los de la P4 en el SNC [7]. Sin embargo, la relevancia de dichos metabolitos se ha estudiado poco en cáncer siendo el cáncer de mama en el que más se ha explorado el papel de dichos esteroides. En este tipo de cáncer, los metabolitos de la P4 desempeñan un papel importante en el desarrollo tumoral, especialmente los α -reducidos como la 5α -dihidroprogesterona (5α -DHP) y la alopregnanolona (3α -THP). Cabe destacar que su síntesis se encuentra aumentada en el tejido tumoral con respecto al tejido no tumoral [8].

La 3α -THP es considerada un neuroesteroide, ya que se sintetiza activamente en las células del SN donde ejerce sus efectos de manera autocrina y paracrina: La 3α -THP es un esteroide inmunomodulador, promotor de la proliferación celular, agente mielinizante, ansiolítico y regulador de la función de diversos neurotransmisores [9–11]. Por el contrario, los niveles bajos de 3α -THP correlacionan con la presentación de patologías como Parkinson, Alzheimer, depresión y la depresión posparto [7]. Si bien,

estos efectos han llevado al desarrollo de terapias farmacológicas con 3α -THP o sus análogos sintéticos para el tratamiento de enfermedades neurológicas, también es cierto que algunos de dichos efectos pueden ser claves para favorecer la progresión tumoral.

En GB, hemos reportado que la 3α -THP aumenta el número y la proliferación de células U87 derivadas de un GB humano. Además, en dicho estudio, el tratamiento con finasterida, un inhibidor de la producción de 3α -THP, disminuyó parcialmente la proliferación de las células U87 [12]. La 3α -THP también regula la expresión de genes que promueven la proliferación y la migración celular [13]. En células Schwann de rata, se ha observado que la 3α -THP promueve la migración celular a través de la activación de la cinasa cSrc, una tirosina cinasa que regula la migración e invasión celulares [14].

Además de la 3α -THP, otros catabolitos de la P4 también son moléculas bioactivas. La 5α -DHP, el precursor directo de la 3α -THP, promueve la proliferación y la migración de las células de GB. Dicho efecto está mediado parcialmente por el receptor intracelular de P4 (RP) [15]. El catabolismo reversible de 5α -DHP a 3α -THP e incluso, de 3α -THP al metabolito menos activo y de desecho, 5α -pregnan- $3\alpha,20\alpha$ -diol, está regulado por enzimas con actividad de 3α -hidroxiesteroide deshidrogenasas (3α -HSD). Existen 4 isoformas en el genoma humano con dicha actividad: las *AKR1C1*, *AKR1C2*, *AKR1C3* y *AKR1C4* (abreviadas así por el nombre de la superfamilia de las aldo-ceto reductasas). Dichas enzimas se expresan en el SNC y pueden alterar la disponibilidad de la 3α -THP o enmascarar sus efectos al contribuir a la oxidación de la 3α -THP a 5α -DHP, cuyo efecto sobre la migración ya se reportó [13]. Por todo lo anterior, en el presente trabajo se determinó el efecto de la 3α -THP sobre la migración e invasión de células U251, U87 y LN229 de GB humano, tres de las líneas celulares más utilizadas en la literatura. Además, se determinó si dicho efecto es mediado por la activación de la cinasa cSrc. También se evaluó si el efecto de la 3α -THP se debe o no a su metabolismo a través de las 3α -HSD.

5 ANTECEDENTES

5.1 *Características de los tumores del sistema nervioso central (SNC)*

El término “tumores del sistema nervioso central (SNC)” se utiliza para englobar a más de 120 entidades patológicas localizadas en el parénquima cerebral, médula espinal, el revestimiento ependimal de la zona ventricular y las meninges. Cada uno tiene un espectro propio de presentación clínica, tratamiento y pronóstico. En primera instancia, estas neoplasias se clasifican en primarias si se originan *de novo* en el SNC, o en secundarias si son producto de la metástasis de un tumor surgido en un sitio diferente al SNC [2]. La nomenclatura de los tumores primarios del SNC está originalmente basada en las similitudes histológicas del tumor con las células normales del tejido de origen [16]. Actualmente, con el constante avance científico y tecnológico, además de la caracterización histopatológica de los tumores también se consideran aspectos moleculares y anatómicos para un mejor diagnóstico y tratamiento. En la presente sección se enfatiza en la información actual sobre el diagnóstico y tratamiento de los gliomas difusos de tipo adulto.

Los tumores del SNC se diagnostican a nivel mundial siguiendo el Sistema de Clasificación de los Tumores del Sistema Nervioso Central de la Organización Mundial de la Salud (OMS). La más reciente actualización de dicho sistema fue en 2021. De acuerdo con esta clasificación los tumores se organizan en “tipos” por su parecido con las células normales, así como por la edad de presentación de la enfermedad. Por ejemplo, la OMS hace distinción entre: *glioma difuso de tipo adulto*, o *glioma difuso de tipo pediátrico (de bajo o de alto grado)* tomando en cuenta si el tumor tiene características histopatológicas similares a las de las células gliales, y si se presenta en población adulta o infantil. Además, se propone que el diagnóstico incluya el nombre histopatológico de la enfermedad seguido de una coma y la o las características genotípicas de relevancia

clínica detectadas [17,18]. Por ejemplo: *Glioblastoma*, *IDH-silvestre* u *Oligodendroglioma*, *IDH-mutante* y *1p/19q-codeletados*.

Una vez determinado el sitio anatómico del tumor, éste se clasifica histopatológica y molecularmente, y se establece el tipo de glioma y su grado del tumor. Los gliomas difusos de tipo adulto son los astrocitomas, oligodendrogliomas y los glioblastomas (GB). Los astrocitomas en adultos pueden presentarse como tumores de grado 2, 3, o 4. Los oligodendrogliomas sólo son clasificados como tumores de grado 2 o 3, mientras que los GB constituyen tumores de grado 4 de malignidad [18].

El grado del tumor se determina a nivel histopatológico por la celularidad, la cantidad de eventos mitóticos, el índice de proliferación, la proliferación de la microvasculatura y la presencia de necrosis [19]. La presencia de varias de estas características está asociada con un crecimiento y diseminación mayor y, por lo tanto, con un mayor grado. Además de las características histológicas, se consideran marcadores moleculares que se resumen en la **Figura 1** [18,20].

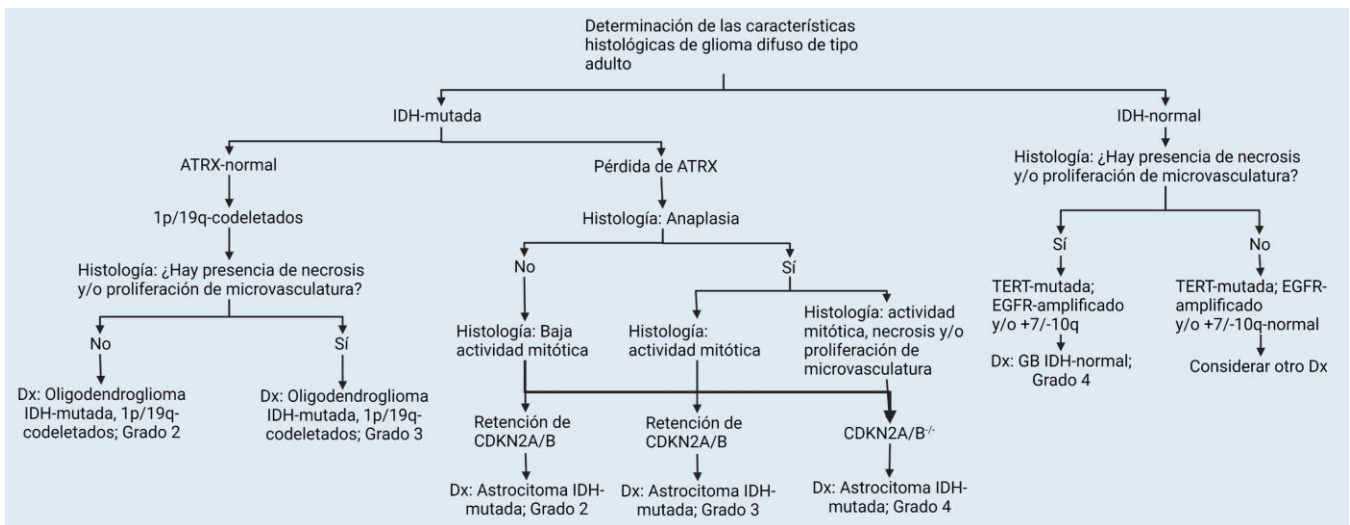


Figura 1. Características fenotípicas y genotípicas de los gliomas difusos de tipo adulto importantes a considerar para su diagnóstico. IDH: isocitrato deshidrogenasa; ATRX: ATRX remodelador de la cromatina; TERT: telomerasa transcriptasa reversa; EGFR: receptor del factor de crecimiento epidérmico; CDKN2A/B: Inhibidor de la cinasa dependiente de ciclina 2A/B. Imagen modificada de Antonelli et al., 2022 [20].

Las características histológicas de los gliomas difusos de tipo adulto por lo general son fáciles de identificar: Los astrocitomas son tejidos ricos en células astrocíticas con escaso citoplasma, elongadas o con forma irregular y con núcleos hipercromáticos. Los oligodendrogliomas presentan células densamente compactadas con núcleo redondeado y con “forma de huevo estrellado.” Además, presentan densas ramificaciones de vasos sanguíneos y microcalcificaciones. Los GB presentan un alto número de células astrocíticas, tejido muy desdiferenciado con células gigantes y granulares o con alto contenido lipídico [20,21]. En la **Figura 2** se presentan algunas de las imágenes típicas para el diagnóstico de los gliomas difusos de tipo adulto.

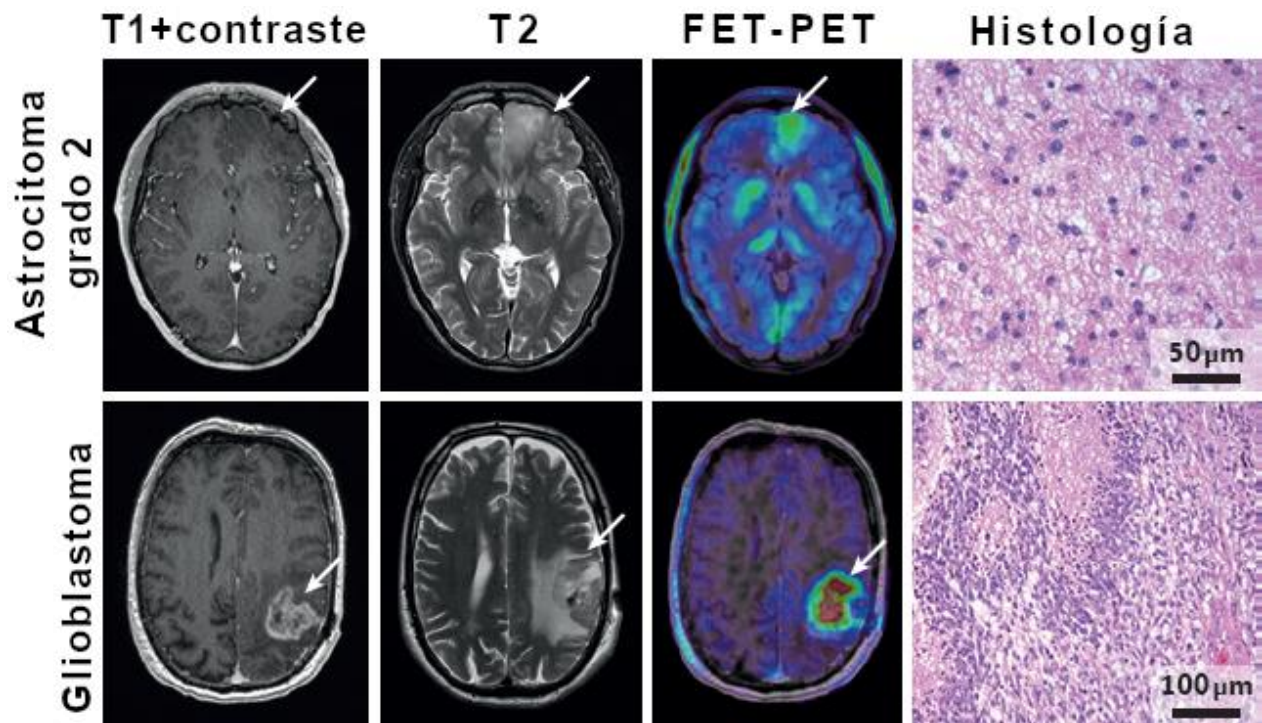


Figura 2. Imagenología y características histológicas de un astrocitoma de bajo grado de malignidad, y un glioblastoma. En las imágenes se indica la localización del tumor (flechas blancas). T1+contraste: Resonancia Magnética nuclear con agente de contraste (gadolinio); T2: Resonancia magnética potenciada en T2; FET-PET: Tomografía por emisión de positrones con ^{18}F -fluoro-etil tirosina como agente de contraste; Histología: Cortes histológicos teñidos con hematoxilina & eosina. Imagen modificada de Weller et al., 2015 [21].

De todos los tumores de SNC, los gliomas difusos de tipo adulto son los más comunes en la población mayor de 30 años. Dichos tumores tienen como característica común la infiltración difusa en el SNC. Los tumores que son diagnosticados originalmente con un grado de malignidad bajo tienden a progresar a grados más avanzados cuando recurren después del tratamiento [20]. Las características generales y clínicas de los gliomas difusos por grado de malignidad se presentan en la **Tabla 1**. Como se puede observar, los grados más avanzados tienden a ser mucho más infiltrantes hacia el tejido cerebral.

Tabla 1. Características generales de los gliomas difusos de tipo adulto de acuerdo con su grado de malignidad.

Grado de malignidad	Población afectada y tiempo de sobrevida	Características	Tratamiento
Grado 2	Adultos entre 30-40 años. Sobrevida de 5-10 años. Progresan a grados de mayor malignidad.	Invasivos, pero con baja proliferación. Con atipia celular (variación en el tamaño y la forma del núcleo) e hiper cromasia.	Resección quirúrgica máxima y quimio y/o radioterapia.
Grado 3	Adultos entre 40-60 años. Originados de novo (primarios) o de un tumor preexistente. Tienden a progresar. Sobrevida: 2-3 años.	Infiltrantes, alta actividad mitótica, atipia celular.	
Grado 4	Adultos entre 45-75 años. Originados de novo (primarios) o de un tumor preexistente. Sobrevida < 14 meses.	Alta proliferación, infiltración, vascularización. Resistencia a la apoptosis. Inestabilidad genómica, necrosis, pleomorfismo.	

Tomado de [2,20].

En México existen pocos estudios epidemiológicos con respecto a la incidencia de los tumores cerebrales. En datos recabados sobre México hasta el año 2020 la incidencia de los tumores cerebrales era de 1.6 % (el décimo octavo más común en la población mexicana). Lo anterior, sin hacer distinción entre el tipo de neoplasia cerebral. Al mismo tiempo, la mortalidad era del 2.8 % de todos los tipos de cáncer, ocupando el décimo tercer lugar en mortalidad debida a cáncer, de acuerdo con datos recabados por la base de datos GLOBOCAN (Global Cancer Observatory, por sus siglas en inglés) [22].

Asimismo, en la población mexicana entre 2000 y 2017, se ha reportado uno de los picos de mayor mortalidad por dichos tumores en el grupo etario entre los 65 y 69 años de edad y con una incidencia 1.2 veces mayor en hombres con respecto a mujeres [23].

Por otro lado, en Estados Unidos y Puerto Rico, la incidencia de las neoplasias cerebrales malignas es de 7.06 por cada 100,000 habitantes (en la población con más de 20 años de edad). De estos tumores malignos, los más frecuentes son los glioblastomas (GB, 14.3 % de todos los tipos de cáncer, 49.1 % de todos los tumores malignos del SNC y con una incidencia de 3.23 por cada 100,000 habitantes), de acuerdo con el Registro Central de Tumores Cerebrales de Estados Unidos (CBTRUS, por sus siglas en inglés: <http://www.cbtrus.org/index.html>) [2,24].

5.2 *Características de los glioblastomas (GB)*

Los GB son tumores de grado 4 y constituyen el tumor maligno de SNC más común en adultos. Los pacientes con GB tienen una media de supervivencia de 8 meses después del diagnóstico [2]. El pico de incidencia a nivel mundial de los GB está entre los 74 y 85 años, además, los hombres presentan una incidencia 1.6 veces mayor con respecto a las mujeres de cualquier edad. Lo que sugiere que hay factores inherentes al sexo involucrados en la incidencia de los GB [2]. Se ha visto que la expresión dimórfica de genes autosómicos, así como sexuales, aumenta el riesgo del sexo masculino a desarrollar GB (así como de otros tipos de cáncer) [25]. En el caso particular de los GB, se ha visto que genes supresores de tumores como ATRX (remodelador de la cromatina), KDM6A (desmetilasa), KDM5C (desmetilasa), y DDX3X (helicasa), codificados en el cromosoma X escapan a la inactivación de dicho cromosoma en individuos XX y confiere protección en individuos con este cariotipo ante la posible mutación heterocigota de dichos genes, con respecto a individuos XY [26].

Con respecto a las diferencias hormonales entre hombres y mujeres, se ha visto que los andrógenos promueven la progresión de los GB, mientras que el efecto de los estrógenos y progestágenos sobre estos tumores depende de los niveles de dichas hormonas y de la expresión de sus receptores. De manera general, se puede decir que a concentraciones fisiológicas tanto estrógenos como progestágenos inducen la progresión de la enfermedad [27].

Hasta el momento se sabe poco sobre los factores de riesgo ambientales y genéticos para la presentación de los GB. El único factor de riesgo de origen ambiental asociado al aumento en la incidencia de los GB es la radiación. Ésta puede ser ionizante, como la generada por bombas nucleares, o terapéutica y administrada durante la niñez o juventud para el tratamiento de tinea capitis y algunos tipos de cáncer como la leucemia [28,29]. Como factores de riesgo genéticos, se sabe que algunos síndromes familiares aumentan al doble el riesgo de desarrollar GB (y de gliomas difusos en general), tales como el síndrome de Li Fraumeni, Neurofibromatosis 1 y el síndrome de Lynch [30]. Dichos síndromes también están relacionados con una mayor predisposición hacia otros tipos de cáncer (**Tabla 2**).

Tabla 2. Síndromes Familiares asociados a mayor riesgo de presentar un GB.

Síndrome familiar	Genes afectados	Tipo de herencia	Predisposición a patologías
Li Fraumeni	<i>TP53</i>	Dominante	GB y otros cánceres cerebrales, cáncer de mama y sarcomas.
Lynch	<i>MSH2, MLH1, MSH6, PMS2</i>	Dominante	GB, cáncer endometrial y gastrointestinal.
Neurofibromatosis 1	<i>NF1</i>	Dominante	Tumores del sistema nervioso: Neurofibromas, Schwannomas, Astrocitomas y GB.
FAMMM: Familiar Atypical Multiple Mole Melanoma	<i>CDKN2A</i>	Dominante	Melanoma y gliomas difusos.

Tabla modificada de: Tonn et al., 2010 [30].

Por el contrario, patologías de carácter inmunológico, como el asma, el eczema y la rinitis alérgica son factores asociados a un menor riesgo para el desarrollo de GB. Esto ha llevado al planteamiento de la hipótesis de que la respuesta exacerbada del sistema inmune en estas patologías, aumenta la respuesta para la detección y destrucción temprana de células transformadas que pudieran resultar en la formación de los GB [28].

Diversos estudios indican que los GB surgen de la transformación maligna de células troncales neurales o células progenitoras de células gliales a células troncales cancerosas [31]. Por experimentos con cultivos primarios se ha visto que esta pequeña población de células troncales tumorales tiene el potencial de autorrenovarse y dividirse asimétricamente. Lo anterior promueve la proliferación de diversos linajes celulares que recapitulan las características de proliferación, migración, resistencia al tratamiento y heterogeneidad intratumoral [32]. En modelos murinos, además, la introducción de mutaciones en genes supresores de tumores *Nrf1*, *Trp53*, y *Pten*, induce la transformación celular sólo en células progenitoras neurales y preprogenitoras, y no en células maduras y con un linaje mucho más restringido como las neuronas [33–35].

La localización más frecuente de los GB es la región frontotemporal del cerebro, los lóbulos parietal y occipital, así como los ganglios basales [36–38]. Los GB se observan como grandes masas de tejido con un núcleo necrótico y hemorragias intratumorales internas evidentes, rodeados de una zona periférica altamente infiltrante y con el área peritumoral edematosa [30]. La sintomatología de los pacientes con GB es inespecífica, incluye déficit neurológico progresivo, debilidad, cefalea con o sin aumento de la presión intracraneal que empeora por las mañanas, al toser, realizar esfuerzo o inclinarse hacia adelante. También puede incluir dolor de cabeza similar al tensional, náuseas y vómito. La presentación de síntomas adicionales depende de la localización del tumor y puede incluir: Cambios en el comportamiento y la personalidad,

hemiparesia y disfasia (localización o daño en lóbulo frontal); convulsiones, alucinaciones auditivas, olfativas o *deja vus* (localización o daño en el lóbulo temporal); afectaciones en el lenguaje (localización o daño en el lóbulo parietal); o afectaciones en la visión (localización o daño en el lóbulo occipital) [30].

A nivel histológico, los GB se caracterizan por una alta cantidad de células astrocíticas, alta celularidad, pleomorfismo, atipia nuclear, alta actividad mitótica, proliferación de la microvasculatura y necrosis (**Figura 3**) [21,30]. Dadas las características histopatológicas su diagnóstico es muy sencillo, sin embargo, la determinación de marcadores moleculares que permitan su subclasificación es cada vez más importante para determinar el origen, el pronóstico, e incluso, un mejor tratamiento de la enfermedad [39,40].

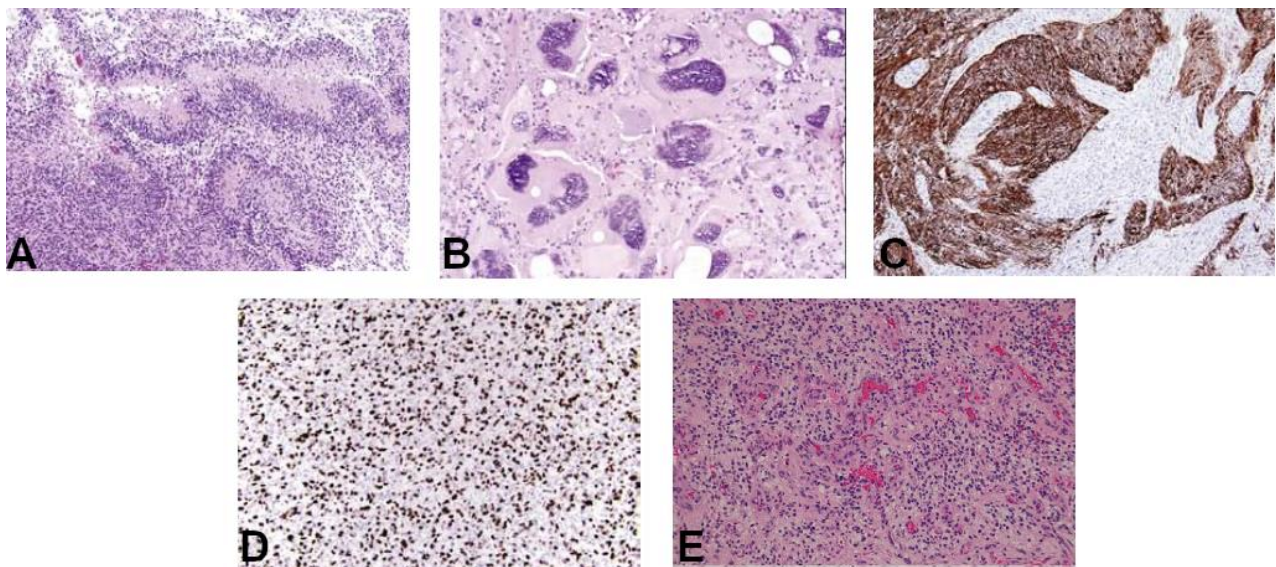


Figura 3. Imágenes representativas de las características típicas de los GB. **A:** Estructuras en pseudoempalizadas formadas por células tumorales alrededor de áreas necróticas. **B:** Células gigantes pleomórficas y multinucleadas. **C:** Inmunohistoquímica donde se muestra en color marrón la marca positiva del marcador de células gliales GFAP. **D:** Inmunohistoquímica donde se muestra en color marrón la marca positiva del marcador de proliferación celular Ki67. **E:** Proliferación de la microvasculatura. Imagen modificada de: Perry et al., 2016 y Tan et al., 2020 [39,40].

Actualmente la OMS considera la determinación del estado del gen de la enzima isocitrato deshidrogenasa (IDH) como uno de los marcadores más importantes para el diagnóstico de los GB [18]. Como se mencionó anteriormente, dentro de los gliomas difusos de tipo adulto, solo hay dos tipos de tumores de grado 4: Los GB y los astrocitomas de grado 4. La ausencia de mutaciones en cualquiera de los genes de la IDH (*IDH1* o *IDH2*) junto con la identificación histológica de las características típicas de un tumor de grado avanzado de malignidad (**Figura 1 y Tabla 1**), son suficientes para el diagnóstico de los GB. Además, los GB no poseen mutaciones adicionales clásicas de astrocitomas u oligodendrogliomas de bajo grado de malignidad tales como mutaciones en el gen *ATRX* y la codeleción de 1p/19q, típicas de los astrocitomas u oligodendrogliomas respectivamente (**Figura 1**). En la **Tabla 3** se presentan las diferencias entre los GB y los astrocitomas de grado 4.

Tabla 3. Características generales de los GB primarios y los astrocitomas de grado 4.

	GB; IDH-silvestre	Astrocitoma grado 4; IDH-mutante
Origen	Primario	Primario o secundario
Lesión precursora	No identificable; desarrollo de novo	Astrocitoma grado 2 o 3
Proporción	90 % de los casos totales	10 % de los casos totales
Razón Hombre: Mujer	1.6	1.05
Tiempo medio de historia clínica	4 meses	15 meses
Sobrevida media con TX:		
• Cirugía + radioterapia	9.9 meses	24 meses
• Cirugía + radioterapia + quimioterapia	15 meses	31 meses
Necrosis	Extensa	Limitada

TX = tratamiento. Modificada de [17].

Además, los GB se subclasifican en subtipos moleculares. La subclasificación está basada en las diferencias a nivel genómico identificadas gracias a los datos genómicos de cientos de muestras de GB depositadas en la base de datos del TCGA (The Cancer Genome Atlas, por sus siglas en inglés) [41]. Aunque los primeros estudios de clustering

para determinar las firmas genómicas de los GB definen 4 subtipos moleculares: clásico, neural, proneural y mesenquimal [41,42], otro estudio evaluó la expresión génica de células únicas para diferenciar las células del microambiente tumoral. Bajo estas condiciones, se considera al subtipo molecular neural como resultado de la contaminación de las muestras con tejido normal neuronal, de allí que consideren únicamente 3 subtipos moleculares: clásico, proneural y mesenquimal [43]. En dicho estudio Wang y colaboradores resaltan que más de un subtipo molecular puede ser identificado dentro de un solo tumor. Asimismo, se observó que hay una correlación inversa entre la cantidad de firmas génicas de los subtipos moleculares de GB y el pronóstico de los pacientes [43].

Esta última clasificación ha sido validada en otros estudios. Se ha visto que los subtipos clásico y neural presentan una mejor supervivencia y respuesta al tratamiento, con respecto al subtipo mesenquimal [44,45]. En relación con el dimorfismo sexual y los subtipos de GB también se ha visto una incidencia 2:1 en hombres respecto a mujeres, en los subtipos mesenquimal y neural, mientras que el subtipo clásico presenta una incidencia 1:1 [46].

El tratamiento estándar de los GB es el protocolo implementado por Stupp y colaboradores desde el año 2005. Como se mencionó en la **Tabla 1**, el tratamiento incluye la resección quirúrgica máxima posible del tumor, junto con la administración concomitante de radioterapia con quimioterapia [47,48]. El agente quimioterapéutico utilizado es la temozolomida, un profármaco de administración oral que se ioniza espontáneamente a pH fisiológico originando especies altamente reactivas que forman aductos con el DNA [49].

A pesar de lo anterior, existen diversos mecanismos de resistencia para revertir el daño inducido por la temozolomida. Uno de los principales es la sobreexpresión de enzimas reparadoras del daño al DNA. La O-6-metilguanina-DNA metiltransferasa

(MGMT) es la principal enzima involucrada en reparar el daño al DNA causado por la temozolomida [49,50]. La expresión de la MGMT está correlacionada con un peor pronóstico para los pacientes con GB debido a la poca respuesta al tratamiento estándar [51]. Si bien, los GB rara vez causan metástasis, tienden a recurrir después del tratamiento debido a su alta capacidad de proliferación e invasión [43].

5.3 Migración e invasión de las células de GB humanos

Dos de las características más significativas de los GBs, como ya se mencionó, son el potencial proliferativo y la capacidad de migración e invasión del parénquima cerebral. La migración e invasión son dos procesos altamente relacionados entre sí. La migración celular se define como la capacidad celular de cambiar de posición dentro de un tejido, mientras que la invasión es la capacidad de penetrar por barreras tisulares tales como la membrana basal o el intersticio estromal, por ejemplo [52]. Para que ocurra la migración, el cuerpo celular debe modificarse a fin de adaptarse y adherirse a la superficie de tránsito, mientras que la invasión requiere de la secreción de enzimas que favorezcan la proteólisis de los componentes de la matriz extracelular (MEC) [52,53]. Además, el proceso de migración puede llevarse a cabo por células individuales o de manera colectiva.

Los GB rara vez producen metástasis en otros órganos. Se han propuesto por lo menos tres hipótesis que explican por qué los GB tienen una baja tasa de metástasis: Si bien, las células tumorales se adhieren a los vasos sanguíneos, no son capaces de romper la membrana basal y entrar a la vasculatura. Otra hipótesis indica que los tejidos extracerebrales no tienen los factores de crecimiento necesarios para promover el crecimiento de los GB. Finalmente, los individuos con GB suelen no sobrevivir el tiempo suficiente para que la metástasis extracraneal sea evidente [54], muchos de los casos

reportados en la literatura sobre metástasis extracraneales de dichos tumores reportan una sobrevivencia de los pacientes por arriba de la promedio [55,56].

Histológicamente, se ha podido observar que las células tumorales presentan diversos fenotipos dependientes del contexto en el que se localicen [57,58]. Lo anterior se debe a que el cerebro es un órgano con características estructurales y biológicas variadas inherentes a la topología y función especializada neuronal, y las células tumorales adquieren propiedades plásticas que les permiten invadir y adaptarse. La alta capacidad invasiva de las células de GB es aún más evidente tras la recurrencia local o distante del tumor después de la resección quirúrgica. Las células que recurren guardan una relación filogenética con las clonas tumorales primarias. Esto indica que tras la resección, las células remanentes pueden proliferar, migrar e incluso invadir el hemisferio contralateral al sitio del tumor primario [59].

Las células de GB tienen tres vías de invasión principales: a través de los vasos sanguíneos, los tractos cerebrales y los espacios subaracnoideos [54]. Diversos modelos *in vivo*, así como análisis de reportes clínicos señalan que el método de migración más común es a través de los tractos cerebrales. En un alto porcentaje de los GB estudiados, dicho movimiento tiende a evitar la invasión de áreas anatómicas cerebrales específicas como la zona amigdalohipocámpica [58]. Para que este proceso ocurra se requiere que las células tumorales tengan activados mecanismos de migración e invasión celulares.

Histológicamente, la capacidad invasiva de las células de GB se hace patente en las diversas estructuras organizacionales de las células tumorales alrededor de tejido cerebral (**Figura 4**) [60]. Dichas estructuras fueron descritas por Scherer en los 80's [61]. Scherer clasifica dichas estructuras en *secundarias* al tumor primario cuando las células tumorales se encuentran agrupadas alrededor de células del tejido cerebral preexistente. Algunos ejemplos de lo anterior es el arreglo perineuronal y la *satelitos*. Esta última se refiere a la neurofagia reactiva que ejercen las células tumorales localizadas

alrededor de las neuronas, principalmente observado alrededor del soma y las dendritas de neuronas en la corteza cerebral. Algunas otras estructuras secundarias son el crecimiento superficial de las células tumorales sobre la corteza cerebral en la región subependimal de manera perivascular, intracortical o delimitado por los tractos de mielina, entre otras. Las *estructuras terciarias* son las que se pueden observar por la interacción de las células tumorales con las células mesenquimales.

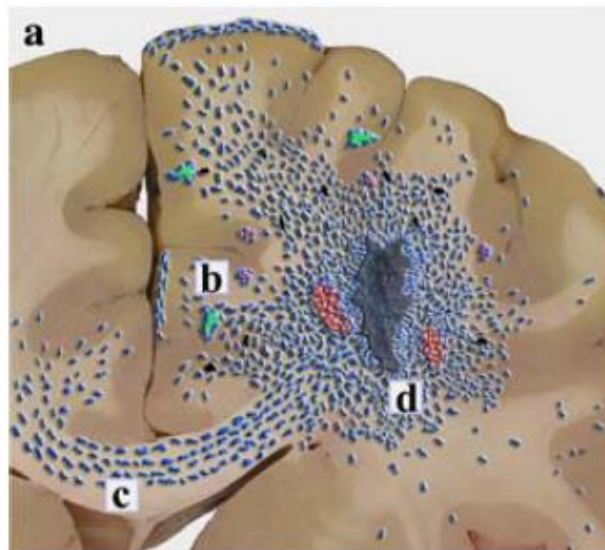


Figura 4. Representación esquemática del crecimiento de un GB. **a)** Las células tumorales se representan en azul, los vasos sanguíneos en rojo, neuronas en verde y células tumorales mitóticas en negro. Se pueden observar diversas estructuras reportadas por Scherer, como la acumulación perivascular de las células tumorales y la satelitosis neuronal, además del crecimiento subpial (**b**), el crecimiento intrafascicular a través del cuerpo caloso (**c**) y el arreglo en pseudo-palizada de las células tumorales alrededor del área necrótica (área gris oscura), de manera adyacente a esta zona, se observa proliferación tipo glomerulada de la microvasculatura (**d**). Modificada de Claes et al., 2007 [60].

Por otro lado, también se describen *estructuras propias* como aquellas que no dependen de la arquitectura del SNC, sino que son producto del potencial de crecimiento de las células tumorales. Tales como la formación de fibrosarcomas o la organización en pseudo-palizadas de las células tumorales alrededor de un área de necrosis [61]. Dichas estructuras, también pueden indicar características fenotípicas de las células tumorales que se encuentran ubicadas en un contexto particular. Por ejemplo,

las células en pseudo-palizadas localizadas alrededor de áreas necróticas son células tumorales que migran de forma colectiva hacia zonas menos hipóxicas y que expresan factores pro-angiogénicos como VEGF, IL-8 o HIF-1 α [58, 63].

Como ya se mencionó, la migración celular puede ocurrir de manera individual o colectiva. De forma individual se distinguen dos grandes fenotipos de células migratorias: ameboide y mesenquimal. Dichos fenotipos son fácilmente distinguibles dada la morfología celular. Las células con fenotipo ameboide tienen una morfología circular más o menos definida, las células mesenquimales presentan una forma alargada tipo fibroblasto. Sin embargo, pueden observarse también transiciones entre el espectro ameboide-mesenquimal debido a la respuesta adaptiva de las células hacia su microambiente [52,63,64]. El movimiento individual es un proceso rápido, mientras que el movimiento colectivo ocurre más lento ya que implica la coordinación entre un grupo de células que se mantienen adheridas entre sí y que rearreglan su citoesqueleto coordinadamente para crear la fuerza de tracción necesaria para moverse hacia la misma dirección [63]. Ambos tipos de migración celular se han identificado en los GB.

Uno de los factores más importantes para que las células de GB puedan migrar depende de la adhesión de las células a la MEC y a los componentes celulares de su entorno. El movimiento celular se mantiene por la interacción asimétrica entre la célula migratoria a través de la formación de protrusiones membranales –seudópodos, lamelipodia, filipodia o invadopodia— en el borde frontal de avance, y la MEC [65]. La forma, el tipo de protrusiones y la dinámica del citoesqueleto está regulado por proteínas de la familia de pequeñas GTPasas: RhoA, Rac y Cdc42. Dichas estructuras membranales se adhieren a la MEC y determinan la dirección de la migración celular a través de la formación de los complejos de adhesión focal [66]. Los complejos proveen de fuerza de tracción necesaria para el movimiento y son puntos de transducción de señales hacia el interior y exterior de la célula.

La formación de los complejos de adhesión focal depende de la interacción de un gran número de proteínas. Rac induce el ensamblaje de los polímeros de actina y la unión de integrinas y proteínas adaptadoras entre los filamentos de actina y la MEC. Las cinasas cSrc y FAK promueven la maduración del complejo y la transducción de señales necesarias para generar tensión entre la actina cortical y la fuerza de tracción hacia el frente celular unido a la MEC [65]. La fuerza de tracción es generada por RhoA, que induce la contractilidad de actomiosina y el desensamblaje de las integrinas y las proteínas adaptadoras. Mientras que Cdc42 regula la dirección de la migración y también participa en el ensamblaje de los polímeros de actina [67].

Las integrinas son receptores heterodiméricos formados por subunidades α y β que se localizan en la superficie celular y se unen a componentes de la MEC como la fibronectina, laminina y colágena [52]. En el caso de los GB, se observó una sobreexpresión de las subunidades $\alpha 5$ y $\beta 1$ que correlaciona con un aumento en la invasión celular a lo largo de los vasos sanguíneos [68,69]. En la cara interna de la membrana celular, las integrinas se unen a las proteínas adaptadoras. Algunas de las proteínas adaptadoras son paxilina (PAX), talina, vinculina, tenascina, α -actinina y p130Cas. Otras proteínas que no forman parte de las integrinas pero que también interactúan con componentes de la MEC son marcadores de superficie, los más comunes en las células troncales de GB son CD133, CD15 y CD44 [45].

Además, las células de GB modifican la MEC cerebral para favorecer la invasión del tejido cerebral sano. Las células de GB secretan al medio extracelular diversas metaloproteasas de matriz (MMPs), enzimas proteolíticas que degradan a las proteínas de la MEC tales como colágena, glicoproteínas y proteoglicanos como la fibronectina y la laminina [54,70]. Se ha visto que las MMPs mayormente expresadas en GB son MMP-2 y MMP-9, entre otras [70]. Otras metaloproteasas secretadas por las células de GB son las ADAMS (A Disintegrin and metalloproteinase, por sus siglas en inglés) y catepsinas [71,72].

5.4 *Cinasa cSrc en la migración e invasión celular de los GB*

La cSrc es la tirosina cinasa prototipo de la familia de tirosina cinasas no asociadas a receptores membranales (SFK, Src family kinases por sus siglas en inglés). Otras cinasas de la misma familia son Fyn, Lyn, Yes, entre otras [73]. cSrc es una de las cinasas más estudiadas y cuyo mecanismo de acción ha sido mejor descrito en la fisiopatología del cáncer. La cinasa cSrc promueve la progresión del cáncer ya que su activación desencadena la activación de diversas vías de señalización involucradas en promover la proliferación, el crecimiento celular y la migración e invasión celulares. En GB se ha visto que los genes de varios miembros de la familia SFK, así como cSrc, no presentan mutaciones ni sobreexpresión del mRNA, sino que han demostrado ser mucho más activos en las células de GB con respecto al tejido cerebral normal tanto por un aumento en su fosforilación (residuo Y416), como por ensayos de actividad, lo cual indica que la hiperactivación de dichas cinasas se debe a una señalización aberrante mediada por las proteínas activadoras de cSrc, tales como receptores de tipo tirosina cinasa o integrinas [74–76].

Los miembros de la SFK comparten similitud estructural. La zona con mayor variación entre los miembros de las SFK es su dominio N-terminal (NTD), que contiene al dominio SH4. Las modificaciones postraduccionales como la miristoilación o la palmitoilación de dicho residuo son determinantes para el anclaje de la proteína a la cara interna de la membrana celular. Seguido del dominio SH4 se localizan los dominios SH3 y SH2, que regulan interacciones proteína–proteína y la actividad catalítica de la cinasa, respectivamente. Las interacciones entre el dominio SH3 con otras proteínas son fundamentales para regular la función de las SFK [77,78]. Además, el dominio SH2 está unido al dominio SH1 por una región linker. El dominio SH1 es el centro catalítico de las SFK. El SH1 está unido al dominio C-terminal (CTD), misma que contiene una región de fosforilación autoinhibitoria (residuo Y530, en el caso de cSrc). De tal manera que

cuando la región C-terminal está fosforilada, se encuentra fuertemente unida a SH2, manteniendo un estado de inhibición enzimática [77].

Las SFKs, adquieren una conformación activa si ocurre la desfosforilación del residuo inhibitorio Y530 del CTD, o si ocurren cambios conformacionales debidos a la interacción de los dominios SH2 o SH3 con los motivos de poli-prolina de otra proteína [77]. Dichos cambios conformacionales inducen la exposición del residuo Y416 de cSrc susceptible a autofosforilación. Esta fosforilación promueve una estabilización permisiva para la unión de sustratos. En el caso de la cinasa cSrc, la desfosforilación del residuo Y530 puede ser catalizado por tirosina fosfatasas como la proteína-tirosina fosfatasa 1B [79], o la proteína tirosina fosfatasa α [80]. Mientras que las proteínas activadoras de cSrc son receptores a factores de crecimiento, integrinas, otras cinasas como FAK y receptores nucleares como el receptor a progesterona (RP) o a estrógenos (RE) o receptores a neurotransmisores [81–83]. Cabe destacar que más de uno de estos mecanismos es activado para regular la activación de cSrc en respuesta a un único estímulo. A través de estas interacciones cSrc regula diversos procesos celulares incluyendo la organización del citoesqueleto, la adhesión celular y la motilidad.

En la formación de los complejos de adhesión focal, las proteínas adaptadoras como PAX se unen a las integrinas y sirven como andamiaje para otras cinasas y pequeñas GTPasas. La fosforilación de PAX (residuos Y118 y Y31) promueve el reclutamiento de otras proteínas adaptadoras y la regulación de la señalización a otras proteínas, tales como FAK. La cinasa FAK fue inicialmente identificada como una proteína tirosina asociada a cSrc y que colocaliza con las integrinas de los complejos de adhesión focal. FAK se activa por autofosforilación (residuo Y397) y la interacción de dicha fosforilación y sus dos motivos de poli-prolina con el dominio SH3 de cSrc promueven la activación de ésta última. Además, cSrc fosforila a FAK en su CTD (residuos Y576 y Y577), induciendo un aumento en su actividad de cinasa [76]. Ambas

cinastas ya activas sirven como un punto de activación de otras proteínas que participan en diversas vías de señalización como Ras/Raf/MAPK y PI3K/Akt y Jak1/Jak2/STAT3 [83].

La activación transitoria de FAK y cSrc regula la migración e invasión en las células de GB al reclutar a otras proteínas a los complejos de adhesión focal [84]. Algunas de estas incluyen a las proteínas adaptadoras p130CAS, vinculina, talina y tensina [79]. Además, inducen la formación de los invadopodia en los GB [85]. El ensamblaje y desensamblaje dinámico de los complejos de adhesión focal y de estructuras como los lamelipodia, depende de la activación de proteínas efectoras de cSrc y de otras SFK. En la **Figura 5** se presenta un esquema de la estructura de los complejos de adhesión focal.

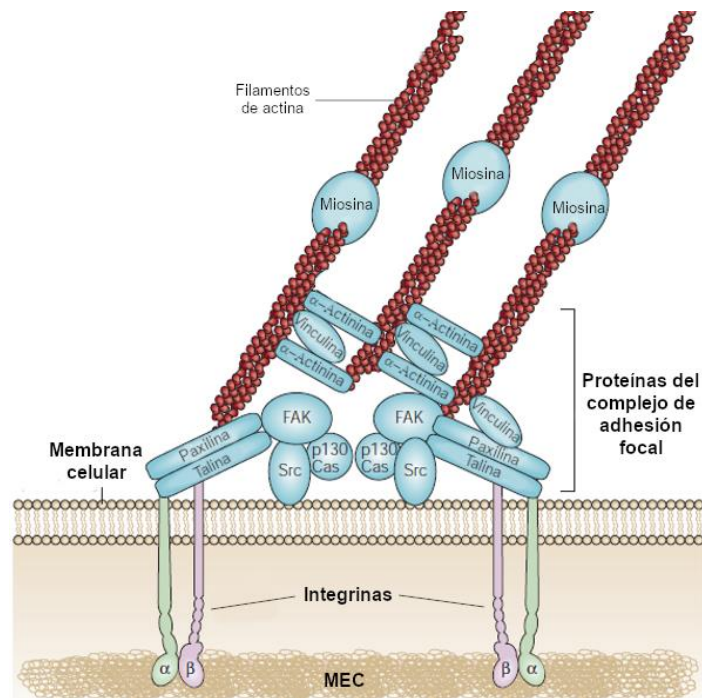


Figura 5. Estructura de un complejo de adhesión focal. Un contacto focal constituye un sitio de contacto entre la Matriz extracelular (MEC) y la célula. Las integrinas (heterodímeros de subunidades α y β) mantienen el contacto estrecho entre la MEC y el interior celular y sirven como punto de transducción de señales. En la cara interna de la membrana celular las integrinas se unen a proteínas adaptadoras: Paxilina, Talina, Vinculina y p130Cas. Estas sirven como andamio para la unión y activación de las cinasas cSrc y FAK, mismas que promueven la unión y estabilización de las fibras de actina y entrecruzadas con otras proteínas de citoesqueleto como α -Actinina y la Miosina. Imagen modificada de Mitra *et al.*, 2005 [84].

5.5 Generalidades sobre la alopregnanolona (3α -THP)

La alopregnanolona (3α -Tetrahidroprogesterona, 3α -THP) es un metabolito 5α -reducido de la progesterona (P4). La P4 se sintetiza en las gónadas, corteza adrenal, placenta y el SN. La P4 fue la primera hormona identificada secretada por el cuerpo lúteo involucrada con el mantenimiento del embarazo [86]. La 3α -THP y otros de sus isómeros como la pregnanolona fueron aislados de la orina de mujeres embarazadas en 1937 [87]. Dado que la P4 y sus metabolitos participan en el mantenimiento del embarazo, a estas moléculas se les denomina progestágenos [86].

En el SNC, la P4 puede ser sintetizada a partir del colesterol o de la pregnenolona. La pregnenolona fue uno de los primeros neuroesteroides identificados –esteroides con gran actividad biológica en el SNC—. En la década de los 80s se observó que los niveles de pregnenolona en SNC eran mayores que sus niveles plasmáticos, incluso en animales cuyos órganos esteroideogénicos habían sido resecados [88]. De allí que aumentara el auge en la investigación sobre el efecto de dichos esteroides en el cerebro más allá de la función reproductiva obvia que tienen.

La 3α -THP es por mucho, uno de los metabolitos de la P4 más estudiado. Dicho metabolito participa en el mantenimiento de la gestación y el proceso de lactancia [89,90], también participa en la regulación del eje hipotálamo-pituitaria-adrenales [90]. Además, tiene efecto antiinflamatorio [91,92]. En el SN, la 3α -THP induce el neurodesarrollo en mamíferos como los roedores y las ovejas [93], e induce la proliferación y la migración de neuronas y células gliales [14,94]. En enfermedades como el Parkinson, Alzheimer, trastorno de ansiedad generalizada, depresión y la depresión postparto, por mencionar algunas, se ha descrito una disminución en la expresión de las enzimas involucradas en la síntesis de 3α -THP o bien en sus niveles [11,95]. Dados los

efectos neuroprotectores y pro-proliferativos de la 3α -THP, puede especularse que también puede tener algún efecto promotor de la malignidad tumoral.

5.6 Síntesis de alopregnanolona (3α -THP)

La síntesis de la 3α -THP depende de la disponibilidad de P4 en la célula esteroidogénica. La P4 es producida por las células del SN a partir del colesterol o la pregnenolona [96]. Además, su catabolismo requiere enzimas de fase 1 del metabolismo de xenobióticos: monooxigenasas de la familia P450, oxidorreductasas de cadena corta (SDR), miembros de la familia de las aldo-ceto reductasas (AKR), así como otras enzimas del metabolismo de fase 2 [97]. La 3α -THP, es sintetizada principalmente en las gónadas y la corteza adrenal y el SNC.

La 3α -THP entonces, es un producto del catabolismo de la P4 que comienza con el paso de la reducción irreversible de la P4 a 5α -Dihidroprogesterona (5α -DHP). Este paso metabólico está regulado por la una enzima perteneciente a las SDR, la enzima 5α -reductasa (5α -R, también denominada 3-oxo- 5α -esteroide deshidrogenasa). En el genoma humano hay tres isoenzimas de la 5α -R con alta homología codificadas por los genes *SRD5A1* (5α -R1), *SRD5A2* (5α -R2) y *SRD5A3* (5α -R3). Sin embargo, sólo las isoenzimas 5α -R1 y 5α -R2 están involucradas en la reducción de la P4, mientras que la 5α -R3 participa en la glicosilación de proteínas [98,99].

Cabe mencionar que la P4 no es el único sustrato de la 5α -R. Los sustratos de la 5α -R son moléculas con estructura de 3-oxo (3-ceto), $\Delta^{4,5}$ C 19/21 esteroides, es decir, esteroides de 19 a 21 átomos de carbono con un grupo radical en C3 –preferentemente un grupo cetona– y un doble enlace entre C4 y C5. Algunos ejemplos de esteroides con dichas características moleculares son la testosterona, el cortisol y la aldosterona [98]. En la **Figura 6** se presenta un esquema de la síntesis de la 3α -THP a partir del colesterol.

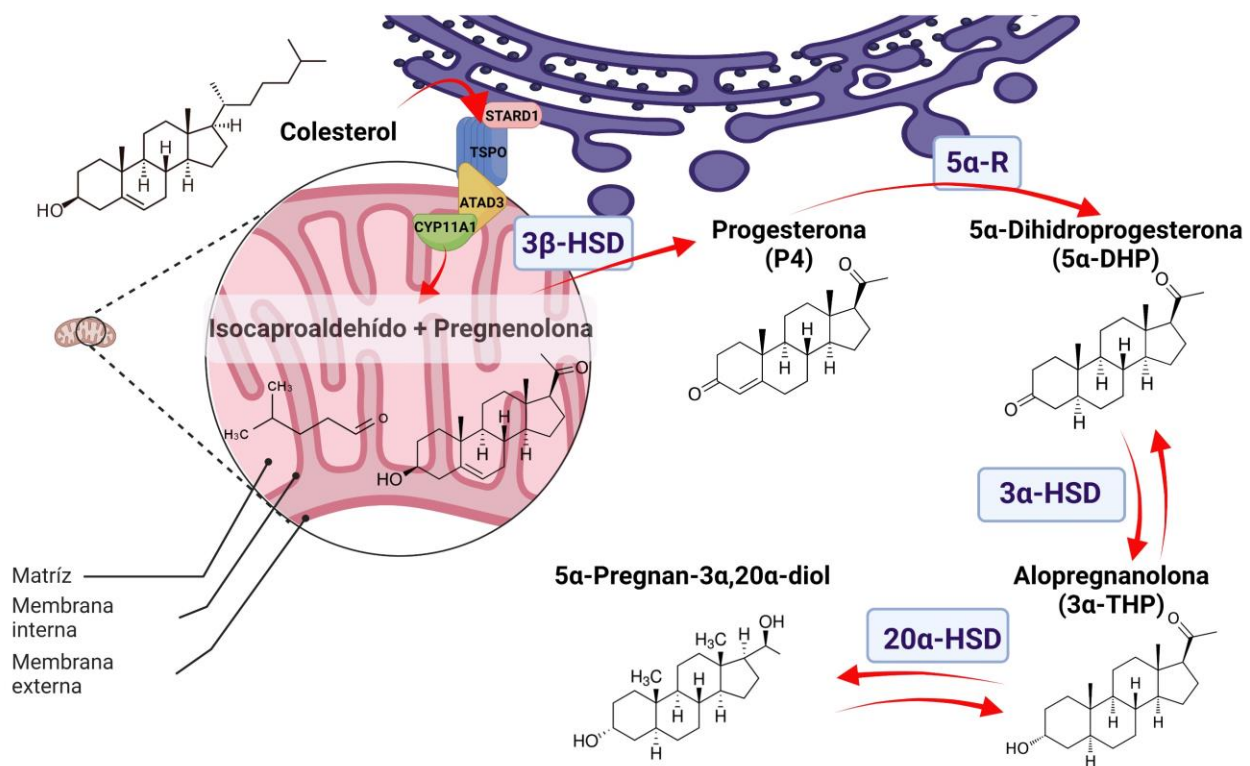


Figura 6. Síntesis de la 3α-THP a partir del colesterol. La síntesis comienza con el ingreso del colesterol a la matriz mitocondrial a través de un complejo proteico en íntimo contacto entre las gotas lipídicas del retículo endoplasmático con la mitocondria. Aunque el complejo suele variar de forma dependiente al tipo celular, algunos de los componentes comúnmente encontrados son: la proteína reguladora de la esteroidogénesis aguda (STARD1), la proteína traslocadora de 18 kDa (TSPO) y ATAD3A (ATPase family AAA-domain-containing protein A3, por sus siglas en inglés). Este complejo se encuentra unido o cercano al CYP11A1: el citocromo P450 encargado de la ruptura de la cadena lateral del colesterol para generar isocaproaldehído y pregnenolona. La pregnenolona, generada en la matriz mitocondrial es deshidrogenada e isomerizada a P4 por la 3β-hidroxiesteroide deshidrogenasa (3β-HSD). La P4 difunde hacia el retículo endoplasmático donde es reducida a 5α-dihidroprogesterona (5α-DHP) por la enzima 5α-Reductasa (5α-R). En el citoplasma, la 5α-DHP es reducida a alopregnanolona (3α-THP) por las enzimas con actividad de 3α-hidroxiesteroide deshidrogenasas (3α-HSD). Además, la 3α-THP puede ser reducida a 5α-pregnan-3α,20α-diol a través de enzimas con actividad de 20α-hidroxiesteroide deshidrogenasas (20α-HSD). Imagen modificada de Zamora-Sánchez *et al.*, 2022 [104].

Las isoenzimas 5α-R1 y 5α-R2 catalizan una reacción irreversible, por lo tanto, reguladora del catabolismo de la P4. La reacción que regulan es la reducción del doble enlace entre el C4 y el C5 ($\Delta^{4,5}$) de la estructura de la P4 utilizando como cofactor una molécula de NADPH. Ocurrida la ruptura del doble enlace, un ion de hidrógeno (H⁻) es insertado en la posición α del C5, mientras que un protón (H⁺) es insertado en la cara β

del C4 [98]. Esta reacción se lleva a cabo en el retículo endoplasmático liso, dado que la 5α -R presenta alto contenido de aminoácidos hidrofóbicos organizados en una estructura rica en α -hélices que la mantienen anclada y estable en dicha membrana [100,101].

A pesar de que las dos isoenzimas catalizan la misma reacción, su localización tisular y su pH óptimo de reacción son diferentes. Además, la 5α -R1 presenta una afinidad por sus sustratos de orden milimolar, mientras que la 5α -R2 presenta una afinidad en el rango de concentraciones nanomolares [102]. En la **Tabla 4** se presentan las características de las dos isoenzimas. Cabe destacar que, en el SNC, la 5α -R1 juega un papel muy importante en la síntesis de esteroides neuroactivos, como la 5α -DHP y la 3α -THP.

Tabla 4. Características de las isoenzimas 5α -R1 y 5α -R2 involucradas en la reducción de P4 a 5α -DHP

Características	5α -R1	5α -R2
Gen/Localización	<i>SDR5A1/5p15.31</i>	<i>SRD5A2/2p23.1</i>
Número de exones	7	9
Peso de la proteína	29.4 kDa	28.4 kDa
pH óptimo	6-8.5	~5
Localización tisular	Cerebro (en adultos), tracto gastrointestinal, hígado, piel	Casi exclusivo de sistema reproductor masculino, hígado, pulmones, cerebro (durante periodo embrionario y recién nacidos), y piel

Tabla modificada de Zamora-Sánchez *et al.*, 2022 [104].

En la línea celular C6 derivada de un glioma de rata, así como en cultivos primarios de neuronas y astrocitos derivados de ratas recién nacidas, se observó una mayor síntesis de metabolitos de la P4 con respecto a los niveles de metabolitos de la testosterona, como la dihidrotestosterona, mientras que la 5α -R2 parece jugar un papel más importante en la próstata y testículos para la producción mayoritaria de metabolitos de la testosterona [103].

En el SNC adulto, hay una mayor expresión de la isoenzima 5α -R1 con respecto a la 5α -R2. En roedores, se ha reportado mayor expresión de dicha enzima en tractos cerebrales ricos en mielina con respecto a otras áreas cerebrales –mesencéfalo, cuerpo calloso, comisura anterior y quiasma óptico, por ejemplo– [105]. Además, está presente principalmente en oligodendrocitos, neuronas, microglía y en células troncales [105,106].

Con respecto a las células de GB, también se ha reportado la expresión de dichas enzimas. En la línea celular U87 se reportó una expresión significativamente mayor del Mrna de la 5α -R1 con respecto a la 5α -R2 [12]. Mientras que los niveles de proteína fueron detectados en las células U87 y LN229, ambas de GB humanos, además de la línea celular C6 de glioma de rata [107]. Además, la funcionalidad de la 5α -R ha sido demostrada en la línea celular U87 por Pinacho-García y colaboradores, quienes confirmaron que el tratamiento farmacológico con finasterida y dutasterida, ambos inhibidores de la 5α -R, disminuyeron la síntesis de metabolitos 5α -reducidos de la testosterona, y corticosteroides [108].

Por otro lado, la 5α -DHP producida por la 5α -R, es interconvertida a 3α -THP a través de las enzimas con actividad de 3α -hidroxiesteroide deshidrogenasas (3α -HSD). En el genoma humano existen cuatro miembros de la superfamilia de aldo-ceto reductasas (AKR, por sus siglas en inglés) subfamilia 1C (*AKR1C1-AKR1C4*), con actividad de 3α -HSD [109]. El mecanismo catalítico de dichas enzimas está altamente conservado a lo largo de la evolución, a pesar de que la cinética y/o afinidad de los sustratos de cada enzima sea diferente. Las AKR1C1-4 catalizan reacciones reversibles de oxido-reducción en las posiciones C3, C5, C11, C17 y C2 del núcleo esteroide o sus cadenas laterales. Esto lo hace de manera dependiente de NAD(P)(H), de la reacción química preferente de cada isoforma y de la afinidad por su sustrato.

Algunos de los sustratos naturales de las AKR1C1-4 incluyen andrógenos, estrógenos y progestágenos, además de metabolizar algunos xenobióticos,

prostaglandinas y retinaldehído [97]. En la **Tabla 5** se presentan las características de cada isoenzima.

Tabla 5. Características de las diferentes isoformas de la 3 α -HSD.

Isoenzima:	<i>AKR1C1</i>	<i>AKR1C2</i>	<i>AKR1C3</i>	<i>AKR1C4</i>
Locus (no. de exones)	10p15.1 (9)	10p15.1 (14)	10p15.1 (10)	10p15.1 (9)
Nombre de la proteína	20 α -(3 α)-HSD	3 α -HSD tipo 3	3 α -(17 β)-HSD tipo 2	3 α -HSD tipo 1
Actividad preferente	1. 3 β -cetoreductasa 2. 20 α -cetoreductasa 3. 3 α -cetoreductasa 4. 17 β -cetoreductasa	3 α -cetoreductasa	1. 3 α -cetoreductasa 2. 17 β -cetoreductasa 3. 20 α -cetoreductasa	3 α -cetoreductasa
Localización tisular	SN, pulmón, hígado, glándulas mamarias, testículos	SN, pulmón, próstata, testículos, útero, glándulas mamarias	Próstata, pulmón, hígado, glándulas mamarias, útero, SN	Hígado

HSD = Hidroxiesteroide deshidrogenasa; SN = sistema nervioso. Tabla modificada de Zamora-Sánchez et al., 2022 [104].

Las enzimas de la familia AKR1C tienen una estructura terciaria de barril (α/β)₈ – de manera alterna, α -hélices y láminas- β que se repiten 8 veces hasta formar el barril—. En la parte trasera del barril se localizan 3 giros largos que definen la especificidad de cada enzima por diferentes sustratos [109,110]. Las isoenzimas que se expresan principalmente en el SNC son las AKR1C1-2. Por años se ha considerado a la *AKR1C2* como la isoenzima más importante responsable de la síntesis de 3 α -THP en el cerebro, mientras que la *AKR1C4* se encarga del mismo proceso con alta eficiencia casi exclusivamente en hígado [11]. A pesar de que la isoenzima *AKR1C3* también se expresa de manera significativa en el SNC, presenta mayor afinidad por andrógenos y estrógenos que por la reducción de progestágenos. Además, las isoenzimas con actividad de 20 α -hidroxiesteroide deshidrogenasa (*AKR1C1* y *AKR1C3*) pueden reducir

a la 3α -THP en el grupo cetona del C20 para producir 5α -pregnan- $3\alpha,20\alpha$ -diol, un metabolito menos activo y de desecho [111,112].

Más recientemente se ha detectado también la síntesis de 3α -THP en el colon de rata [113]. Se ha hipotetizado que la síntesis de dicho metabolito en intestino participa en la regulación de las funciones del SN a través del eje intestino-cerebro. Hasta el momento, Liang y colaboradores han hipotetizado las posibles proteínas a nivel sérico involucradas en el transporte de 3α -THP a través del torrente sanguíneo con base en su estructura química. Las proteínas propuestas son: la albúmina, la transcortina o globulina de unión a corticosteroides y la globulina fijadora de hormonas sexuales [96].

Con respecto a la presencia de las AKR1C1-4 en GB aún se sabe poco. La presencia y funcionalidad de dichas enzimas fue indirectamente demostrada en la línea celular U87 por Pinacho-García y colaboradores al detectar la síntesis de progestágenos como la 3α -THP, andrógenos y corticosteroides a partir del colesterol [108]. Además de participar en el metabolismo de los esteroides en GB, las AKR1C1-4 podrían favorecer la resistencia a la temozolomida. En un modelo de resistencia a temozolomida con las líneas U373 y T98G se observó la sobreexpresión de la *AKR1C3* en las células resistentes con respecto a las células no resistentes [114].

5.7 Mecanismos de acción de la 3α -THP

Los mecanismos de acción de la 3α -THP pueden ser agrupados en mecanismos genómicos y no genómicos. Si bien los mecanismos no genómicos son mecanismos rápidos que desencadenan la regulación de diversas vías de señalización, debe considerarse que a largo plazo también pueden inducir la expresión de genes tal como los mecanismos genómicos. Cabe destacar también que los mecanismos descritos en esta sección han sido descritos en diversas células del SNC tanto en condiciones fisiológicas como fisiopatológicas.

A nivel genómico, la 3α -THP es un ligando del Receptor X de Pregnano (PXR, también llamado Receptor de Esteroides y Xenobióticos [SXR]). El PXR es un factor de transcripción activado por ligando que presenta diversas variantes. Cada variante tiene diferencias en la afinidad por ligandos, dimerización y actividad transcripcional [115]. Este receptor presenta mayor flexibilidad estructural en el dominio de unión a ligando con respecto a otros receptores nucleares, lo cual le confiere mayor promiscuidad por ligandos hidrofóbicos como los esteroides, entre los que destaca la 3α -THP.

La activación del PXR a través de su interacción con la 3α -THP se ha demostrado por ensayos de actividad de la luciferasa. En dichos ensayos, los efectos de la 3α -THP fueron significativamente mayores con respecto a la actividad inducida por la deshidroepiandrosterona, un andrógeno que también ha sido identificado como ligando del PXR [115]. Además, en el modelo murino 3xTgAD de la enfermedad de Alzheimer, la 3α -THP incrementó la expresión de PXR a los 9 meses del establecimiento de la enfermedad, sin embargo, se desconoce a través de qué mecanismo de acción se debe dicho efecto [116].

Una vez que el PXR es activado, y localizado en el núcleo celular, se une a elementos de respuesta a xenobióticos en la región promotora de sus genes blanco. Además, recluta a coactivadores o correpresores de la transcripción. Algunos de los genes blanco del PXR, están involucrados en el metabolismo del colesterol o forman parte de sistemas de detoxificación de xenobióticos, tales como genes de las subfamilias de citocromos P450: *CYP3A*, *CYP2B* y *CYP20*, así como transportadores del tipo ATP-binding cassette (por su nombre en inglés) [117,118].

Se sabe que dicho receptor participa en la regulación de procesos fisiológicos como también en cáncer. El PXR se expresa en diversos órganos: hígado, tracto gastrointestinal, gónadas, útero, glándulas mamarias y adrenales, cerebro y piel [115,119]. Su expresión también ha sido reportada en diversas líneas celulares

cancerosas como en adenocarcinoma gástrico (células SNU719), adenocarcinoma de colon (células SW403), adenocarcinoma ductal pancreático (ASPC1) y hepatoblastoma (Células HepG2) [119]. Asimismo, se ha visto implicado tanto en procesos de carcinogénesis como de promoción y progresión del cáncer y resistencia a la terapia [119].

Los mecanismos no genómicos activados por la 3α -THP, tienen efectos rápidos sobre las células. Sin embargo, a tiempos largos (de horas a días), estos mecanismos también pueden llevar a la regulación de la transcripción. Los mecanismos rápidos que son activados por la 3α -THP, el mejor caracterizado hasta el momento es mediado por el receptor A del ácido γ -aminobutírico ($GABA_A$ R).

El $GABA_A$ R es un canal ionotrópico activado por ligando. Para ser funcional, éste está constituido como un canal pentamérico. Este se puede formar de 19 posibles subunidades: α (1-6), β (1-3), γ (1-3), δ , ϵ , θ , π , y ρ (1-3). Todas las subunidades están conformadas por un dominio extracelular largo, cuatro dominios transmembranales (TMD1-4), un loop largo entre TMD3 y TMD4, a través del cual interactúa con proteínas intracelulares y un dominio extracelular corto en el extremo C-terminal de la proteína [120]. La mayoría de los receptores $GABA_A$ R están formados por dos subunidades α , dos β y una adicional de la cual depende la función y localización del receptor [121]. Los $GABA_A$ R sinápticos generalmente están constituidos por subunidades γ , y los receptores extrasinápticos comúnmente presentan una subunidad δ .

La 3α -THP es un modulador alostérico del receptor $GABA_A$ R y presenta mayor afinidad por los receptores que contienen subunidades δ o $\gamma 1$ [122]. Además, la presencia de la subunidad $\alpha 1$ también parece ser determinante para los efectos de la 3α -THP [120]. Chen y colaboradores en 2018 demostraron que, aunque existen hasta cuatro sitios de unión de la 3α -THP en el receptor $GABA_A$ R conformado sólo por subunidades $\alpha 1$ y $\beta 3$, no todos están involucrados en la modulación alostérica positiva o activación

del mismo [120]. Existen dos sitios de unión de la 3α -THP en el receptor a través de los cuales dicho esteroide modula positivamente la $\text{GABA}_{\text{A}}\text{R}$. Esto quiere decir que en presencia de la 3α -THP, el ligando natural de $\text{GABA}_{\text{A}}\text{R}$, el GABA, activa de forma con mayor potencia al receptor en con respecto a cuando la 3α -THP se encuentra ausente. Dichos sitios alostéricos se localizan entre las subunidades α y β en la región transmembranal adyacente a los dominios extracelulares de ambas subunidades [120]. Además, un sitio de unión de 3α -THP ha sido identificado en $\alpha 1$, entre los dominios transmembranales TM1 y TM4 de dicha subunidad. La unión de la 3α -THP con estos tres sitios alostéricos aumentan la potencia de GABA al promover la estabilización del canal en su forma activa, es decir, abierta [123].

El efecto de la 3α -THP sobre los $\text{GABA}_{\text{A}}\text{R}$ depende de la concentración. Estudios electrofisiológicos indican que a concentraciones de orden nanomolar (100 nM), la 3α -THP actúa como modulador alostérico positivo del receptor. Mientras que a concentraciones micromolares (1-10 μM), la 3α -THP promueve la activación directa del $\text{GABA}_{\text{A}}\text{R}$ sin embargo, se desconoce cuál, o cuáles sitios de unión de la 3α -THP están involucrados en este efecto independiente del GABA [123,124]. Ambos efectos tienen consecuencias inmediatas en las células blanco. El tratamiento con otro esteroide con una estructura química y afinidad por el $\text{GABA}_{\text{A}}\text{R}$ muy similar a la 3α -THP, la tetrahydrodesoxicorticosterona (THDOC), promueve la fosforilación mediada por la cinasa PKC, de la subunidad $\alpha 4$ de $\text{GABA}_{\text{A}}\text{R}$, lo que favorece su permanencia en la membrana celular y promueve su señalización [125,126].

El efecto de la 3α -THP mediado a través de los $\text{GABA}_{\text{A}}\text{R}$ depende del tipo celular y la expresión de cotransportadores como SLC12A2. En células maduras y con baja o nula expresión de SLC12A2, la activación o modulación positiva de $\text{GABA}_{\text{A}}\text{R}$ promueve el influjo de iones cloruro (Cl^-). Esto provoca la hiperpolarización de la membrana, una señal de inhibición celular. Sin embargo, en células troncales neurales o pre-

progenitoras de oligodendrocitos con alta expresión del cotransportador SLC12A2, la concentración basal de Cl⁻ intracelular es elevada. En ellas, se promueve la despolarización de la membrana al activarse GABA_AR [124]. Lo anterior, activa a canales de calcio tipo L dependientes de voltaje e incrementa los niveles de los segundos mensajeros: Ca²⁺ y adenosín monofosfato cíclico (AMPc). El incremento en los niveles de AMPc promueve la activación de la proteína cinasa A (PKA) con la consecuente activación de la proteína 1 de unión a elementos de respuesta a AMPc (CREB1), un factor de transcripción [94,127]. CREB1 regula la transcripción de genes que promueven la síntesis de DNA y la proliferación celular [94], así como genes que promueven la síntesis de GABA [128].

Con respecto a la migración celular, se ha visto que el neurotransmisor GABA, a concentraciones de orden femtomolar induce la migración celular en neuronas de rata entre los días E15 y E20 del desarrollo embrionario a través del GABA_AR [129]. Sin embargo, también se ha reportado el incremento de la migración neuronal en la corteza parietal de ratas recién nacidas en un modelo *in vitro* con el tratamiento de metiodido de bicuculina, un antagonista del GABA_AR, lo cual implica que dicho receptor puede tener efectos dependientes del tipo celular en el SNC durante el desarrollo [130]. El efecto positivo del GABA_AR sobre la migración celular también parece estar mediado por la presencia del cotransportador SLC12A2 en neuroblastos de ratón [131]. Sin embargo, no se han descrito qué cascada de señalización regulada por GABA_AR promueve la migración de dichos tipos celulares. En GB, una alta expresión de SLC12A2 correlaciona con un fenotipo más invasivo e induce la transición epitelio a mesénquima en la línea celular U87 [132].

En células completamente diferenciadas, la 3 α -THP induce cambios en el citoesqueleto de actina y el aumento de la migración celular, a través de activación de las proteínas cinasas en los complejos de adhesión focal. Melfi y colaboradores

reportaron en las células Schwann de rata, que la 3α -THP promueve la migración celular y el rearrreglo del citoesqueleto de actina. Estos efectos dependen de la actividad de cSrc, ya que el inhibidor farmacológico de cSrc, el PP2, bloqueado la migración celular inducida por la 3α -THP a las 2, 6 y 24 h de tratamiento. Además, el tratamiento con 3α -THP 1 μ M indujo una disminución seguida de un incremento en los niveles de cSrc y FAK fosforiladas a los 30 y 60 min de tratamiento [14]. De manera interesante, el tratamiento conjunto de 3α -THP y bicuculina, un antagonista de los GABA_AR indujo un aumento significativo de los niveles de FAK fosforilada [14]. La 3α -THP además, induce la proliferación, angiogénesis y el aumento de la actividad de las 3α -HSD de manera dependiente del GABA_AR en un modelo de rata del plexo ovárico [133,134].

La 3α -THP también puede activar la transducción de señales mediada por los receptores membranales de progesterona (mPR). Los mPR son cinco proteínas que forman parte de la familia del receptor de progestinas y adipoQ: mPR α (PAQR7), mPR β (PAQR8), mPR γ (PAQR5), mPR δ (PAQR7) y mPR ϵ (PAQR9). Todos presentan de 7 a 8 dominios transmembranales [135,136]. Aún no está del todo dilucidado su mecanismo de acción, algunos autores proponen que estos receptores actúan como enzimas activadas por ligando con actividad de ceramidasa y producen como segundos mensajeros bases esfingoides que activan a proteínas G [136,137]. Otros estudios indican que los receptores están directamente acoplados a proteínas G: mPR α , mPR β y mPR γ están acoplados a proteínas de tipo G inhibitorias (G_i) en humanos y a proteínas G olfatorias (G_{olf}) en teleósteos, mientras que los mPR δ y mPR ϵ están acoplados a proteínas G estimuladoras (G_s) [138,139].

La afinidad de la 3α -THP por los mPR se ha determinado a través de ensayos de unión en los que se ha observado el papel de la 3α -THP como agonista de mPR δ (100 nM), y mPR α y mPR β (~400-500 nM) [139]. Por lo anterior, el efecto de la 3α -THP depende de la presencia de los mPRs. La expresión de los mPR δ y mPR β es

particularmente alta en algunas áreas cerebrales como el hipotálamo, hipocampo, amígdala y corteza cerebral, zonas donde también son comunes los GB. Asimismo, la expresión de los cinco receptores membranales también ha sido reportada en las líneas celulares U251 y U87 de GB humano [140,141].

En neuronas hipocampales, el tratamiento de 3α -THP (20 y 100 nM) por 15 min incrementó los niveles de AMPc en las células, lo cual correlaciona con la activación de proteínas G_s [139]. En este mismo estudio, se sobreexpresó al mPR δ en células MDA-MB-231 de adenocarcinoma mamario. Cuando las células fueron tratadas con 3α -THP durante 20 min, se observó el aumento de AMPc y la activación de la cinasa ERK, junto con la disminución de la apoptosis celular [139]. Por otro lado, en las células inmortalizadas de hipotálamo de rata GnRH GT1-7 se observó una alta expresión de mPR α y mPR β con respecto a los demás mPR. En ellas, el tratamiento con 3α -THP disminuyó los niveles de AMPc y la muerte celular [142].

Se ha propuesto una interrelación entre los mecanismos de acción de la 3α -THP. Melfi y colaboradores reportaron que la 3α -THP induce cambios en el citoesqueleto y un aumento en la migración celular a través de la activación de cSrc y FAK, como ya se mencionó [14]. Sin embargo, cuando las células fueron tratadas con 3α -THP y bicuculina, un inhibidor de GABA $_A$ R, la fosforilación de dichas cinasas aumentó significativamente con respecto al tratamiento sólo de 3α -THP o el agonista de GABA $_A$ R, muscimol sólo. Otro estudio con el agonista de los mPR, el ORG-02-0, también demostró un aumento en la fosforilación de cSrc [143]. Lo anterior puede indicar que los efectos de la 3α -THP son el resultado de la activación de múltiples mecanismos que pueden compensarse entre sí cuando alguno de ellos está bloqueado. En la **Figura 7** se presentan resumidos, los mecanismos de la 3α -THP más estudiados hasta el momento.

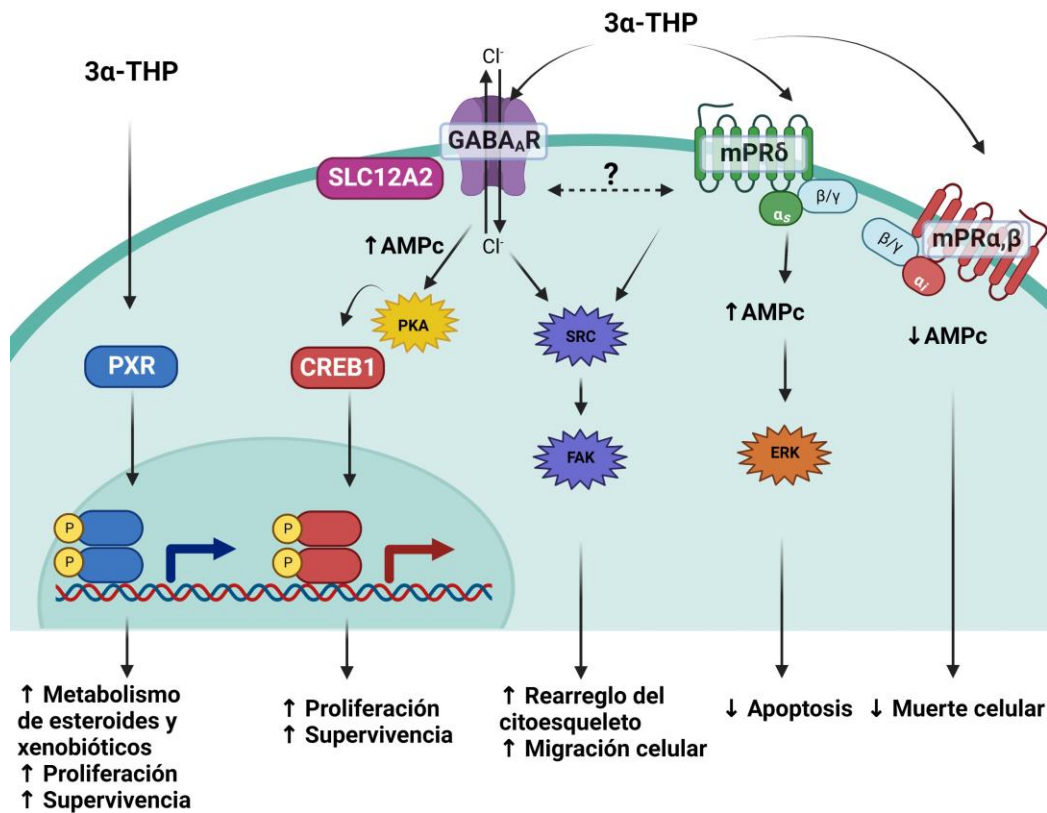


Figura 7. Mecanismos de acción y efectos de la 3 α -THP. Por sus características hidrofóbicas, la 3 α -THP atraviesa la membrana celular por difusión y activa al PXR, un factor de transcripción. A nivel de membrana, la 3 α -THP modula positivamente al canal ionotrópico GABA_AR. En células que conjuntamente expresan GABA_AR y el cotransportador SLC12A2, se activa una vía de señalización dependiente del segundo mensajero adenosín monofosfato cíclico (AMPc) para activar al factor de transcripción CREB1. En células completamente diferenciadas, la 3 α -THP induce la activación de las cinasas cSrc y FAK a través de GABA_AR. Además, la 3 α -THP es un agonista de los mPRs, a través de los cuales induce cambios en los niveles de AMPc y la activación de cSrc/FAK y ERK. Imagen modificada de Zamora-Sánchez *et al.*, 2022: [104].

Además de los mecanismos anteriormente descritos, hay otros receptores de neurotransmisores que también son modulados por la 3 α -THP, tales como los receptores dopaminérgicos D1 [144] y los receptores glutamatérgicos de N-metil-D-aspartato (NMDA)[145].

Adicionalmente, hay autores que hipotetizan que la 3 α -THP indirectamente puede activar al receptor a progesterona (RP). Lo anterior, a través de la interconversión de la

3 α -THP a 5 α -DHP a través de las AKR1C1-4 [11,146]. Se ha reportado la alta afinidad de la P4 (0.35 nM) y la 5 α -DHP (22 nM) por el RP. Sin embargo, por ensayos de unión y de gen reportero, se ha visto que la 3 α -THP presenta muy baja afinidad directa por dicho receptor (>500 nM por el RP de pollo y no detectable en humanos) [146]. El RP es un factor de transcripción que pertenece a la superfamilia de receptores nucleares [147]. Además de su función como regulador de la transcripción de genes específicos, también se sabe que a nivel citoplasmático regula la activación de vías de señalización rápidas en el citoplasma a través de su interacción con proteínas que reconocen los motivos ricos en poliprolina localizados en el NTD del RP. Un ejemplo de este tipo de proteínas es la cinasa cSrc [83,148].

5.8 Efectos de la 3 α -THP en cáncer

Hasta el momento hay pocos estudios sobre el papel que tiene la 3 α -THP en la fisiopatología del cáncer. En la línea celular U87 de GB humano, previamente se reportó que la 3 α -THP (10 nM – 1 μ M) induce un aumento en el número de células a través de un ensayo dosis-respuesta durante 6 días, así como la proliferación a los 3 días de tratamiento. De manera interesante en este estudio, el tratamiento con P4 y la finasterida, un inhibidor farmacológico de las 5 α -R, disminuyó significativamente el efecto de la P4 sobre el aumento en el número de células [12]. Lo anterior fue uno de los primeros indicios de que no sólo la P4, sino sus metabolitos, pueden promover la malignidad de los GB. En otro estudio, a través de microarreglos en la línea celular U87, se demostró que la 3 α -THP (10 nM) promueve la sobreexpresión de genes relacionados con la proliferación celular, reparación del DNA y el rearrreglo del citoesqueleto [13].

Además, en otros modelos de cáncer, la 3 α -THP también promovió la malignidad tumoral a bajas concentraciones. En células PC12 derivadas de un feocromocitoma de rata y que no expresan al GABA_AR ni a receptores NMDA, la 3 α -THP indujo un

aumento en la expresión de proteínas anti-apoptóticas como Bcl-2 y Bcl-xl, así como un aumento en activación de la cinasa PKC, involucrada también en la regulación de diversas vías de señalización y una disminución en la apoptosis celular [149]. Por otro lado, en la línea celular de cáncer ovárico humano IGROV-1, la 3 α -THP indujo la proliferación, migración, invasión y la clonogenicidad a bajas concentraciones (10 pM- 1 μ M) [150].

Contrario a lo anterior, se ha visto que altas concentraciones de 3 α -THP inducen la muerte celular o una disminución de procesos relacionados con la progresión del cáncer. En las líneas celulares de cáncer de mama MCF-7 y T47D, la 3 α -THP (50 μ M) disminuyó la viabilidad celular igual que la P4 y la 5 α -DHP, mientras que concentraciones relativamente bajas de 10 μ M estimularon la supervivencia celular [151]. En las líneas celulares T98G y A172 de GB humanos, la 3 α -THP (20 – 60 μ M) promovió la muerte celular por sí sola y potenció el efecto de la temozolomida sobre la muerte celular, la migración, invasión y la disminución de la expresión de genes relacionados con la proliferación celular y la señalización mediada por integrinas [152]. Todos estos estudios indican que la 3 α -THP a concentraciones que van de 1 nM a 10 μ M, inducen la malignidad de diferentes modelos cancerosos in vitro. Mientras que concentraciones mayores a 20 μ M inducen la muerte celular y la disminución de la migración e invasión de las células cancerosas.

Además de la 3 α -THP, también sus análogos han sido estudiados en el contexto del cáncer. La ganaxolona es un análogo 3-metilado de la 3 α -THP que fue aprobado recientemente por la Food and Drugs Administration de Estados Unidos para el tratamiento de epilepsia. Este fármaco tiene alta afinidad por el GABA_AR y también presenta cierta afinidad por los mPRs [153]. La ganaxolona disminuyó la apoptosis y muerte celular de la línea de cáncer de mama MDA-MB-231 que no expresan al GABA_AR. En estas células utilizadas como modelo para sobreexpresar al mPR δ , la

ganaxolona y la 3α -THP (100 nM) indujeron un aumento en la fosforilación de la cinasa ERK [153].

Taleb y colaboradores, en la búsqueda de análogos de la 3α -THP sin efectos proliferativos, sintetizaron diversos compuestos. Estos autores reportaron que la 3α -THP y sus análogos sintéticos BR351 (O-alil-alopregnanolona) y BR338 (12-oxo-alopregnanolona), a concentraciones de 250 nM a 1 μ M aumentaron la viabilidad celular en las células SH-SY5Y de neuroblastoma humano [154]. Mientras que el análogo BR297 (O-alil-epi-alopregnanolona) no presentó dichos efectos. Todos los esteroides evaluados por dichos autores presentaron efectos neuroprotectores y aumentaron la conductancia de GABA [154,155]. En la **Figura 8** se presentan algunas de las estructuras químicas de los análogos de la 3α -THP.

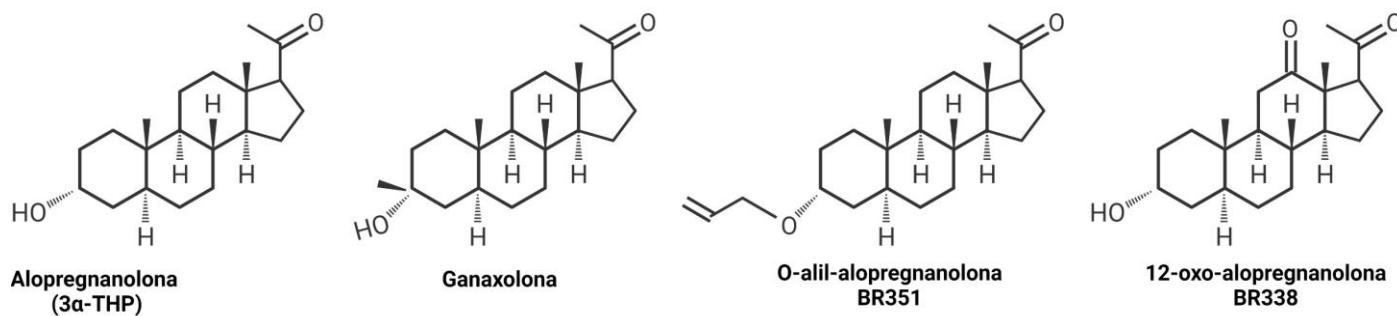


Figura 8. Estructura química de los análogos sintéticos de la 3α -THP. Se presenta la estructura base de la 3α -THP, así como de sus análogos sintéticos con modificaciones: La ganaxolona presenta un metilo como grupo sustituyente en el C3. El análogo BR351 presenta grupo alilo como sustituyente en oxígeno del C3, mientras que BR338 presenta un grupo cetona en el C12.

6 PLANTEAMIENTO DEL PROBLEMA

Se sabe que los metabolitos de la P4, como la 3α -THP, promueven la proliferación y la expresión de genes clave para el crecimiento de los GB. La 3α -THP, además, induce cambios en el citoesqueleto y la migración de células del SNC. Sin embargo, se desconocen los efectos de la 3α -THP, así como la repercusión de su metabolismo a través de las 3α -HSD sobre la migración e invasión de células de GB humanos y las vías de señalización implicadas en la regulación de estos procesos.

7 HIPÓTESIS

La 3α -THP promoverá la migración e invasión, así como cambios en la activación de la cinasa cSrc en células derivadas de GB humanos, independientemente de su metabolismo a través de las 3α -HSD.

8 OBJETIVOS

8.1 OBJETIVO GENERAL

Conocer el papel de la 3α -THP y de su metabolismo mediado por las 3α -HSD en la migración e invasión de células derivadas de GB humanos y determinar si el efecto de la 3α -THP sobre la migración e invasión está regulado a través de la activación de la proteína cinasa cSrc.

8.2 OBJETIVOS PARTICULARES

- a) Determinar el efecto de la 3α -THP sobre la migración e invasión de células derivadas de GB humanos.
- b) Caracterizar la expresión de las 3α -HSD.
- c) Determinar el efecto de la 3α -THP sobre la migración e invasión de las células de GB con la expresión de las 3α -HSD silenciada.
- d) Estudiar el efecto de la 3α -THP sobre los niveles de la proteína cinasa cSrc fosforilada en el residuo Y416 en las células de GB.
- e) Evaluar si el efecto de la 3α -THP sobre la migración e invasión está mediado por la cinasa cSrc.

9 METODOLOGÍA

9.1 *Cultivo celular*

Las líneas celulares U87, U251 y LN229 derivadas de GB humanos se obtuvieron de la American Type Culture Collection (ATCC). Las tres líneas celulares son IDH WT, la cual corresponde con una característica genotípica de GB. Además, las tres líneas presentan una firma génica que corresponde con los subtipos proneural/mesenquimal [156,157]. Las líneas celulares U251 y U87 provienen de GB extirpados de hombres caucásicos, mientras que la línea celular LN229 proviene de una mujer blanca. Algunas otras de sus características particulares se presentan en las Tablas 7 y 8 de la sección de 14.1 de Anexos. Las células de GB fueron cultivadas en medio Eagle Modificado Dulbecco (DMEM) alto en glucosa, con rojo fenol y suplementado con suero fetal bovino (SFB, 10 %), piruvato y aminoácidos no esenciales y en condiciones de CO₂ al 5 % y a 37 °C. El medio fue cambiado cada 48 h hasta obtener una confluencia de 70 – 80 %. A las 24 h previas a comenzar con los diferentes ensayos, el medio de cultivo fue reemplazado por DMEM sin rojo fenol y suplementado con SFB sin hormonas (10 %).

9.2 *Ensayos de migración*

Para determinar el efecto de la 3 α -THP sobre la migración de células derivadas de GB, se realizaron ensayos de cierre de herida. Para ello, se sembraron 3.5 x 10⁵ células por pozo en cajas de 6 pozos de las líneas celulares U251, U87 y LN229. El día del ensayo, se realizó una herida lineal sobre la monocapa del cultivo celular con una punta de pipeta de 200 μ l. Se eliminaron el medio de cultivo (DMEM sin rojo de fenol y SFB sin hormonas) y las células despegadas de la monocapa con 700 μ l de PBS. El medio se reemplazó y se agregó arabinósido de citocina (AraC, 10 Mm) 1 h antes de agregar los tratamientos hormonales, con el fin de inhibir la progresión del ciclo celular.

- Tratamientos utilizados para determinar el efecto de la 3 α -THP sobre la migración celular: vehículo (V; etanol [EtOH] a una concentración en el medio de cultivo de 0.1 %), P4 (10 nM) y 3 α -THP (10, 100 nM y 1 μ M). La concentración de P4 utilizada previamente demostró promover la migración de las células de GB por artículos del laboratorio [158,159].
- Tratamientos para determinar el efecto del silenciamiento de las 3 α -HSD sobre la migración de células de GB inducida con 3 α -THP: vehículo (V; etanol [EtOH] 0.1%) y 3 α -THP 100 nM. Éstos fueron agregados a los cultivos celulares 24 h después de realizado el protocolo de transfección y silenciamiento de las 3 α -HSD descrito en la sección 8.4.
- Tratamientos para evaluar si el efecto de la 3 α -THP sobre la migración celular está mediado por la cinasa cSrc: V (EtOH 0.1 %), V (dimetilsulfóxido [DMSO] 0.001 % como concentración final en el medio de cultivo), 3 α -THP 100 nM, el inhibidor farmacológico de cSrc, 1-tert-Butil-3-(4-clorofenil)-1H-pirazolo[3,4-d]pirimidin-4-amina (PP2, 1 μ M), y el tratamiento conjunto de 3 α -THP+PP2 a las mismas concentraciones.

Posteriormente, se tomaron fotografías del área de la herida con la cámara Infinity 1-2C (Lumenera) acoplada al microscopio invertido Olympus CKX41 a un aumento de 10x a las 0, 6, 12 y 24 h de tratamiento. El procesamiento de las imágenes de migración se realizó con el macro MRI Wound Healing Tool del software ImageJ versión 1.15r. Los datos se analizaron con la fórmula del porcentaje de cierre de herida, que considera el área inicial (0 h de tratamiento) como 0% de migración y el área de los tiempos consecutivos evaluados (6, 12 y 24 h) como un porcentaje del cierre del área inicial. Se realizó un mínimo de 3 experimentos por línea celular y se analizaron estadísticamente con el software GraphPad Prism 5 (ANOVA de una vía seguido de una prueba de Tukey).

9.3 Ensayos de invasión

Para determinar el efecto de la 3 α -THP sobre la capacidad de invasión de las células U251, U87 y LN229, se utilizó una modificación de la cámara de Boyden: Se colocó un inserto con una membrana porosa de policarbonato (tamaño de poro = 8.0 μ m) sobre la que se agregó Matrigel® (Sigma Aldrich), un gel de proteínas de matriz extracelular derivado de células de sarcoma murino Engelbreth-Holm-Swarn. Cuando la matriz se gelifica, las células cultivadas en medio DMEM sin SFB y los tratamientos, se colocan en el compartimento superior de la cámara. En la parte inferior se coloca medio DMEM con SFB, como agente quimioatrayente. Después de 24 h de cultivo con los tratamientos, el Matrigel es retirado y las células con capacidad de invadir, es decir, aquellas que atravesaron la membrana porosa, son teñidas y cuantificadas.

Las células fueron cultivadas en cajas de 40 mm. Al obtener una confluencia de 80 %, el medio se reemplazó por DMEM sin rojo fenol y suplementado con 10 % SFB sin hormonas. El Matrigel se descongeló a 4°C una noche antes de comenzar el ensayo. Se realizó la dilución del Matrigel (2 mg/ml) en medio DMEM sin rojo fenol y sin SFB. Posteriormente, 100 ml de Matrigel se colocaron sobre los insertos y se dejaron gelificar a 37 °C durante 3 h en una atmósfera con 5 % CO₂. A continuación, en el compartimento inferior de la cámara se agregó 600 ml de medio DMEM sin rojo fenol con 10 % SFB sin hormonas. En el compartimento superior se colocaron 3x10⁴ células en medio DMEM sin rojo fenol y sin SFB, AraC (10 Mm), y los tratamientos de interés en un volumen de 150 ml.

- Tratamientos para determinar el efecto de la 3 α -THP sobre la invasión celular: vehículo (V; EtOH, 0.1%), P4 (10 nM) y 3 α -THP (100 nM).
- Tratamientos para evaluar el efecto del silenciamiento de las 3 α -HSD sobre la invasión celular inducida con 3 α -THP: V (EtOH, 0.1%) y 3 α -THP 100 nM. Estos tratamientos fueron agregados a los cultivos 24 h después de

realizado el protocolo de transfección y silenciamiento de las 3 α -HSD descrito en la sección 8.4.

- Tratamientos para evaluar si el efecto de la 3 α -THP sobre la migración celular está mediado por la cinasa cSrc: V (EtOH, 0.1 %), V (DMSO, 0.001 %), 3 α -THP 100 nM, PP2 1 μ M, y 3 α -THP+PP2 a las mismas concentraciones.

Transcurridas 24 h de cultivo se eliminaron los medios de cultivo y el inserto se lavó suavemente con PBS para retirar el Matrigel. Después, las células en el inserto fueron fijadas con paraformaldehído (PFA, 4 %) durante 20 min a temperatura ambiente. Posteriormente se realizaron 3 lavados de 5 min cada uno con PBS en agitación moderada. Las células fueron teñidas con cristal violeta al 1 % durante 20 min, nuevamente se realizaron 3 lavados con PBS (10 min cada lavado) y se dejaron secar.

Los insertos ya secos, se observaron al microscopio. Se tomaron imágenes representativas de cada experimento con la cámara Infinity 1-2C acoplada al microscopio invertido a un aumento de 10x. Se determinó el número de células que atravesaron el matrigel con el software ImageJ versión 1.15r. Los datos obtenidos se analizaron en el programa GraphPad Prism 5. El análisis estadístico realizado fue un ANOVA seguido de una prueba *post hoc* Tukey. Todos los resultados mostrados se expresan como la media \pm el Error Estándar de la Media (E.E.M).

9.4 *Transfección y silenciamiento de las 3 α -HSD*

A fin de determinar si el efecto observado de la 3 α -THP sobre la migración e invasión celulares se debe a la 3 α -THP *per se* y no a su interconversión a 5 α -DHP, la expresión de las 3 α -HSD se silenció de forma transitoria en la línea celular U251 utilizando un siRNA comercial diseñado para las isoenzimas AKR1C1-3 considerando que en el SNC se ha reportado una baja expresión de la isoenzima AKR1C4.

Un número de 2×10^5 células U251 por pozo fueron cultivadas en cajas de 6 pozos en medio DMEM con rojo fenol y suplementado. Transcurridas las 24 h, el medio de cultivo fue reemplazado por DMEM sin rojo fenol y sin suplementar para evitar cualquier posible interferencia de las proteínas contenidas en el SFB con la formación del complejo lipofectamina-siRNAs, así como la acción de posibles RNAasas en el SFB, y se realizó la transfección. El agente de transfección utilizado fue lipofectamina 7.5 % (Lipofectamine RNAiMAX; Thermo Fisher Scientific) diluida en medio DMEM sin rojo fenol y sin suplementar. Una vez preparado el agente de transfección, se realizó la dilución de los siRNA comerciales:

- Como control del silenciamiento (siRNA control): Silencer Select Negative Control #1 (no. de catálogo: 4390844, Thermo Fisher Scientific) a una concentración de 100 nM, diluido en DMEM sin rojo fenol y sin suplementos.
- siRNA que reconoce a las isoenzimas AKR1C1-3 (sAKR1C1-3): siRNA comercial (no. de catálogo 4392420; ID: s3988, Thermo Fisher Scientific), a una concentración de 100 nM y diluido en DMEM sin rojo fenol sin suplementos.

Los siRNA utilizados y el agente de transfección fueron incorporados por medio de agitación e incubados a temperatura ambiente durante 20 min antes de ser agregados a los cultivos celulares. Las células U251 fueron incubadas durante 12 h con los agentes de transfección. Después, las células se cultivaron durante 24 h en el medio de recuperación: DMEM sin rojo fenol suplementado como se indica en la sección de Cultivo celular. Posteriormente, se evaluó a través de Western blot la eficiencia del silenciamiento y se realizaron los correspondientes ensayos de migración o invasión.

9.5 Extracción de RNA total y RT-qPCR

Para determinar la expresión de las 3 α -HSD en las células de GB humano, 2.5x10⁵ células de las líneas U87, U251, y LN229 fueron cultivadas en pozos de 40 mm. Transcurridas 24 h de cultivo, las células fueron lavadas con 600 μ L de PBS y lisadas con 600 μ L de TRIzol (fenol, ácido tiocianico y guanidina; Ambion). Se incubaron a -20°C por 5 min y se transfirieron a un tubo Eppendorf donde se les agregó cloroformo (200 μ L). Después de homogenizar las muestras durante 20 s en el vórtex, se centrifugó a 14,000 rpm a 4 °C por 15 min y se obtuvieron 2 fases.

A la fase acuosa se le agregó isopropanol en un volumen equivalente. El RNA se precipitó a -20 °C durante toda la noche. Posteriormente, colectó por centrifugación 15 min a 14,000 rpm a 4 °C. La pastilla color blanco de RNA se observó en el fondo del tubo. El sobrenadante se decantó y el pellet fue lavado dos veces: con etanol al 75 % en agua grado biología molecular y con etanol al 80 %, entre cada lavado se centrifugó a 7500 rpm a 4 °C durante 8 min. Se dejó secar la pastilla de RNA y se resuspendió en 30 μ L de agua.

La cantidad y pureza del RNA se cuantificó en el espectrofotómetro NanoDrop 2000 (Thermo Scientific, MA, USA). Su integridad se determinó por electroforesis en un gel de agarosa al 1.5 % en buffer TB 0.5x (Tris base, ácido bórico), donde se observaron las bandas correspondientes a los RNAr 28 y 18S, así como su intensidad y la ausencia de barrido que indicara degradación de los ácidos ribonucleicos.

Para la síntesis de cDNA se utilizó 1 μ g del RNA total extraído, la enzima M-MLV Reverse Transcriptase (ThermoFisher Scientific, MA, USA) y oligo dT (500 μ g/mL) de acuerdo con las recomendaciones del fabricante: 20 μ L de reacción se incubaron por 50 min a 37 °C para la síntesis de cDNA y 15 min a 70 °C para la inactivación de la enzima. 2 μ L de la reacción anterior se utilizaron para realizar una qPCR para

determinar la expresión de las isoformas de la 3 α -HSD (AKR1C1 y AKR1C2, por los nombres de los genes). En la **Tabla 6** se presentan la secuencia de los oligonucleótidos diseñados para este trabajo.

Tabla 6. Secuencia de los oligonucleótidos diseñados y tamaño del producto de qPCR a amplificar por cada par utilizado.

Gen	Oligonucleótidos (5'→3')	Fragmento amplificado (pb)
AKR1C1-2	FW: GTTGCCAGCTCATTGCTCTT	165
	RV: CTTTTAGGAACCTCTGCAGGC	
	RV: AGTCCAACCTGCTCCTCATT	
AKR1C3-4	FW: ACCTCCAGAGGTTCCGAG	114
	RV: AGTCCAACCTGCTCCTCATT	
18S	FW: AGTGAAACTGCGAATGGCTC	167
	RV: CTGACCGGGTTGGTTTTGAT	

Para obtener una reacción de 20 μ L se utilizó el kit LightCycler FastStart DNA Master SYBR Green I (Versión 18, Roche) y el equipo LightCycler 1.5 (Roche). Las condiciones de reacción para la determinación de las AKR1C1-2 fueron: desnaturalización a 95 °C por 10 min, 45 ciclos de: 10 s a 95 °C, 10 s a 62 °C y 10 s a 72 °C. Las condiciones de amplificación para determinar la expresión de AKR1C3-4 fueron: desnaturalización a 95 °C por 10 min, 45 ciclos de: 10 s a 95 °C, 10 s a 58 °C y 10 s a 72 °C. Como control negativo de la reacción se adicionó agua grado Biología Molecular en lugar del volumen de cDNA. Los resultados se presentan como expresión relativa los transcritos de interés con respecto a la expresión del RNAr 18S calculada por el método de $2^{-\Delta CT}$ [160]. Todos los resultados mostrados se expresan como la media \pm E.E.M. Para el análisis de resultados se realizó un ANOVA seguido de una prueba de Tukey.

9.6 Extracción de proteína y Western Blot

Las células U87, U251 y LN229 se sembraron en cajas 100 mm (2×10^6 células), bajo las condiciones mencionadas en la sección de Cultivo Celular. Para determinar los niveles

basales de las 3 α -HSD o la eficiencia del silenciamiento de las mismas, los cultivos celulares se mantuvieron 24 h en medio DMEM sin rojo fenol y suplementado.

Transcurrido el tiempo de cultivo, las células fueron colectadas y homogenizadas con buffer RIPA con inhibidores de proteasas (AEBSF, aprotinina, clorhidrato de bestatina, E-64, leupeptina, dilución 1:100) y 1 mM de EDTA. Las muestras se mantuvieron en agitación a 4 °C durante toda la noche, posteriormente se centrifugaron a 14,000 rpm durante 15 min. El sobrenadante con las proteínas totales fue colectado. La cantidad de proteínas se determinó con el ensayo colorimétrico de Pierce, detectado a 660 nm utilizando el espectrofotómetro NanoDrop 2000. Después, 20 μ g de proteína se llevaron a ebullición durante 5 minutos con buffer de Laemlie (1 μ L de buffer de Laemlie por cada 10 μ L de muestra). A fin de comparar los niveles de las 3 α -HSD en las líneas celulares de GB con respecto a un linaje celular sano del SNC, se cargaron 20 μ g de proteínas totales de un cultivo primario de astrocitos humanos (número de catálogo: 1806, ScienCell, Carlsbad, CA, USA).

Las proteínas se separaron por electroforesis en un gel SDS-PAGE (12 %) a 80 V. Posteriormente, fueron transferidas a una membrana de nitrocelulosa en una cámara de transferencia semihúmeda a 30 mA durante 1:30 h. La membrana se incubó con solución de bloqueo (3 % albumina sérica bovina y 3 % leche libre de grasa en buffer TBS-tween 0.1 %) durante 1:30 h a 37 °C. Dicha solución se retiró y después se incubó el anticuerpo primario a una dilución 1:1000 del anticuerpo monoclonal de ratón anti-3 α HSD (sc-390419, Santa Cruz, CA, USA) a 4°C durante toda la noche. Se realizaron 3 lavados de 5 minutos cada uno con buffer TBS-Tween 0.1 %. Posteriormente, se incubó con el anticuerpo secundario acoplado a peroxidasa (IgG de cabra anti-ratón; Santa Cruz, CA, USA) en una dilución 1:5000, a temperatura ambiente durante 50 min. Nuevamente se realizaron lavados y se detectó a las proteínas de interés por quimioluminiscencia, mismas que fueron reveladas en placas sensibles a quimioluminiscencia. Después, el

anticuerpo primario se eliminó de la membrana con un buffer de glicina (0.1 M, pH 2.5) durante 30 min a 50 °C, se realizaron 5 lavados de 4 min cada uno con buffer TBS. Posteriormente, se incubó con solución de bloqueo y se repitió el protocolo anterior para la detección de la proteína α -tubulina como control de carga. El anticuerpo primario monoclonal para la detección de la α -tubulina fue agregado en una dilución 1:1000 (T9026, Sigma Aldrich, St. Louis, MO, USA) e incubado durante 24 h a 4 °C.

Para determinar el efecto de la 3 α -THP sobre los niveles de la proteína cSrc fosforilada en el residuo Y416, mismo que se asocia a un estado activo de la cinasa cSrc, se cargaron 30 μ g de proteína total por muestra. La separación de las proteínas se realizó por electroforesis de SDS-PAGE (8.5 %), a 80 V. Las proteínas fueron transferidas a una membrana de nitrocelulosa en una cámara de transferencia semihúmeda a condiciones de 25 V durante 30 min. Después, la membrana se incubó con solución de bloqueo (albúmina sérica bovina [BSA] al 5 % a 37 °C durante 2 h). Se utilizó un anticuerpo primario para el residuo fosforilado Y-416 de cSrc (1:1000; Ref. 2101; Cell Signaling, Massachusetts, MA, USA) que fue incubado durante 48 h a 4 °C. El anticuerpo secundario acoplado a peroxidasa para la detección del anticuerpo primario fue un IgG de cabra anti-conejo a una dilución 1:10,000. Una vez revelada la señal de la proteína buscada, los anticuerpos fueron retirados de la membrana con una solución de Tris-HCl (pH 6.8 a 0.06 M), SDS al 2 % y β -mercaptoetanol al 0.7 % durante 30 min a 50 °C en agitación. Posteriormente, las membranas fueron incubadas nuevamente con la solución de bloqueo: BSA 5 % durante 2h a 37 °C. Para determinar los niveles de cSrc total se utilizó la dilución 1:1000 de anticuerpo primario (Ref. 2108, Cell Signaling, Massachusetts, MA, USA). Se utilizó el anticuerpo secundario de cabra anti-conejo a una dilución 1:10,000 para la determinación de cSrc fosforilada.

La densidad de las bandas obtenidas se cuantificó a través de su análisis densitométrico en el programa ImageJ versión 1.15r. Los datos obtenidos de los

experimentos de Western blot para medir los niveles de las AKR1C1-4 se analizaron estadísticamente por un ANOVA de una vía seguida de una prueba Tukey utilizando el programa GraphPad Prism 5. Los datos de los niveles de la proteína cSrc fosforilada se analizaron estadísticamente con una t de Student, se presentan como la media \pm el E.E.M.

10 RESULTADOS

10.1 Efecto de la 3 α -THP sobre la migración de las células de GB

Se determinó el efecto de la 3 α -THP (10 nM, 100 nM y 1 μ M) sobre la migración de las células U251, U87 y LN229 derivadas de GB humanos. Las características de cada línea celular se pueden localizar en la sección de Anexos (14.1). Los efectos de la 3 α -THP fueron comparados con respecto a los de la P4 (10 nM), cuyos efectos promotores de la migración celular en GB se reportó anteriormente en otros trabajos del laboratorio [158,159].

La P4 indujo la migración significativamente sólo en la línea celular U251 a partir de las 12 h de tratamiento (**Figura 9**). En esta misma línea celular, la 3 α -THP a la concentración de 100 nM también indujo la migración a partir de las 12 h, mientras que las concentraciones de 10 nM y 1 μ M aumentaron significativamente la migración hasta las 24 h de tratamiento. En la línea celular U87 todas las concentraciones de 3 α -THP indujeron la migración celular hasta las 24 h de tratamiento (**Figura 10**). En esta línea celular, la P4 presenta una tendencia a aumentar la migración celular, aunque dicho valor no fue estadísticamente significativo. En las células LN229, las concentraciones de 10 nM y 1 μ M de 3 α -THP disminuyeron significativamente la migración a las 12 h de tratamiento, sin embargo, dicho efecto no se mantuvo hasta las 24 h de tratamiento. En estas células, sólo la concentración de 100 nM indujo significativamente la migración a las 24 h de tratamiento (**Figura 11**).

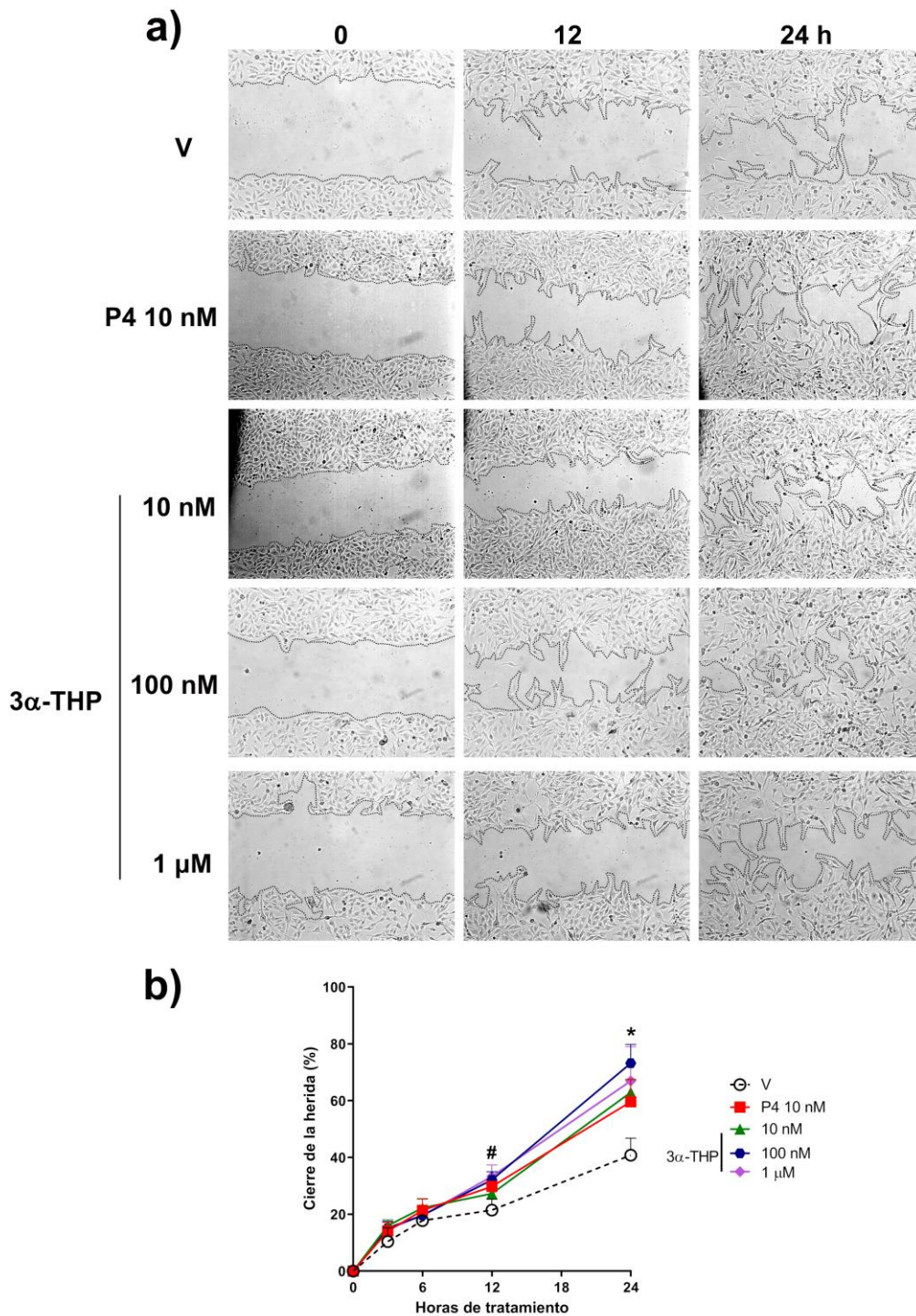


Figura 9. Efecto de la 3 α -THP sobre la migración de la línea celular U251. Las células fueron tratadas con el vehículo (V; EtOH, 0.01 %), P4 (10 nM) y 3 α -THP (10, 100 nM, and 1 μ M). **a)** Imágenes representativas de los ensayos de cierre de herida realizados en la línea celular U251 a las 0, 12 y 24 h. **b)** Gráfica del porcentaje de cierre de herida de las células U251. # $p < 0.05$ P4 y 3 α -THP 100 nM vs. V; * $p < 0.05$ P4 10 nM, 3 α -THP 10 nM, 100 nM y 1 μ M vs. V. Cada punto representa la media \pm el error estándar de la media (E.E.M.); $n = 3$.

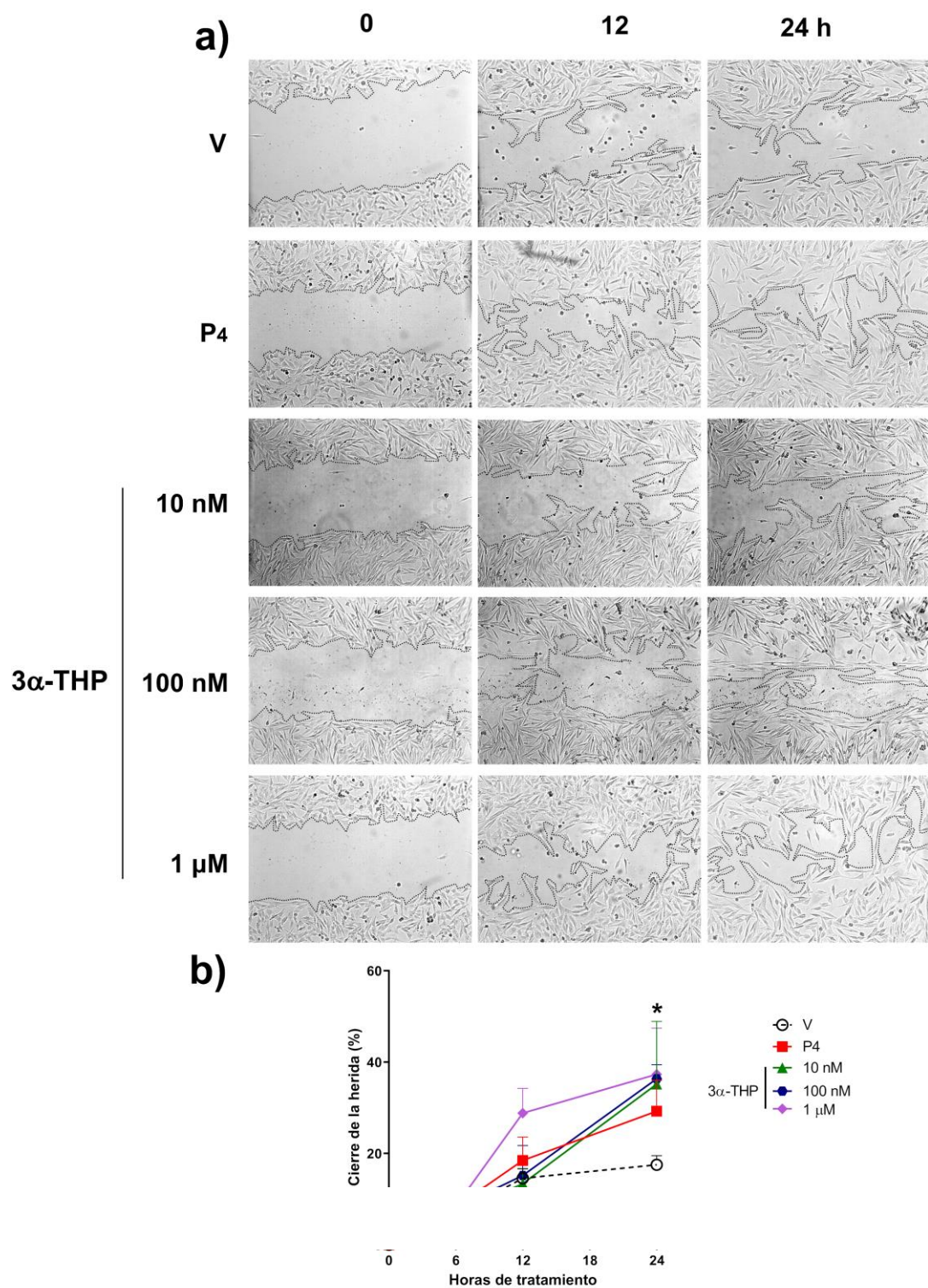


Figura 10. Efecto de la 3α-THP sobre la migración de la línea celular U87. Las células fueron tratadas con el vehículo (V; EtOH, 0.01 %), P4 (10 nM) y 3α-THP (10, 100 nM, and 1 μM). **a)** Imágenes representativas de los ensayos de cierre de herida realizados en la línea celular U87 a las 0, 12 y 24 h. **b)** Gráfica del porcentaje de cierre de herida de las células U87. * $p < 0.05$ 3α-THP 10 nM, 100 nM y 1 μM vs. V. Cada punto representa la media ± E.E.M.; $n = 3$.

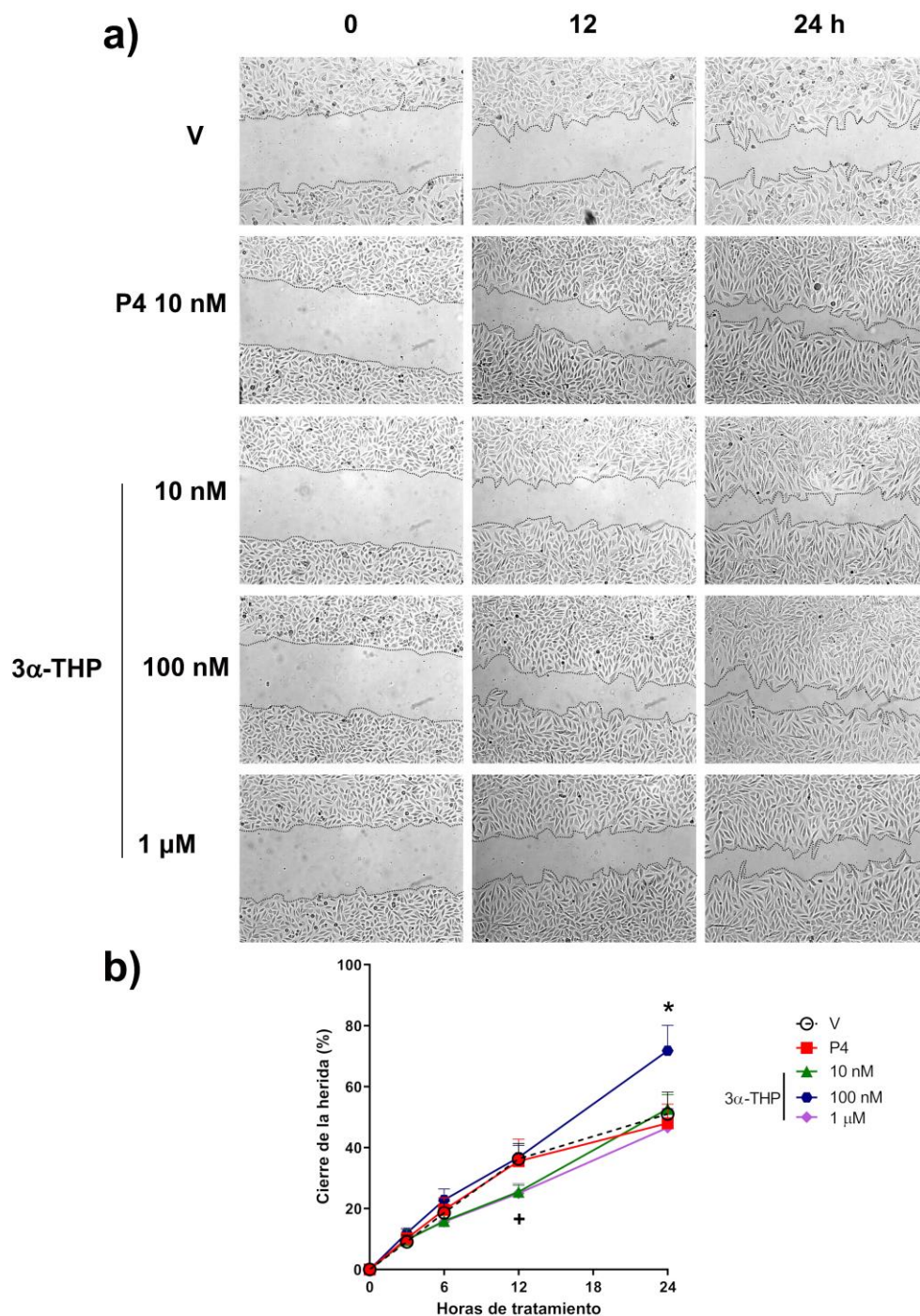


Figura 11. Efecto de la 3α-THP sobre la migración de la línea celular LN229. Las células fueron tratadas con el vehículo (V; EtOH, 0.01 %), P4 (10 nM) y 3α-THP (10, 100 nM, and 1 μM). **a)** Imágenes representativas de los ensayos de cierre de herida realizados en la línea celular LN229 a las 0, 6, 12 y 24 h. **b)** Gráfica del porcentaje de cierre de herida de las células LN229. + $p < 0.05$ 3α-THP 10 nM y 1 μM vs. V; * $p < 0.05$ 3α-THP 100 nM vs. V. Cada punto representa la media ± E.E.M.; n = 4.

Dado que la concentración de 3 α -THP 100 nM indujo la migración en todos los modelos celulares, ésta fue utilizada en subsecuentes experimentos de migración e invasión. Cabe destacar que los experimentos anteriores demuestran que la 3 α -THP a concentraciones de orden nanomolar, induce la migración de las células de GB.

10.2 Efecto de la 3 α -THP sobre la capacidad de invasión de las células de GB

Posteriormente, se evaluó el efecto de la 3 α -THP 100 nM sobre la capacidad de invasión de las líneas celulares U251, U87 y LN229 a las 24 horas de tratamiento. Nuevamente se utilizó la P4 10 nM como control positivo por su efecto previamente determinado sobre la invasión de las células de GB. La P4 incrementó significativamente la invasión de las células U251 y LN229 (**Figura 12**), mientras que la 3 α -THP indujo la invasión celular en las tres líneas celulares (**Figura 12**).

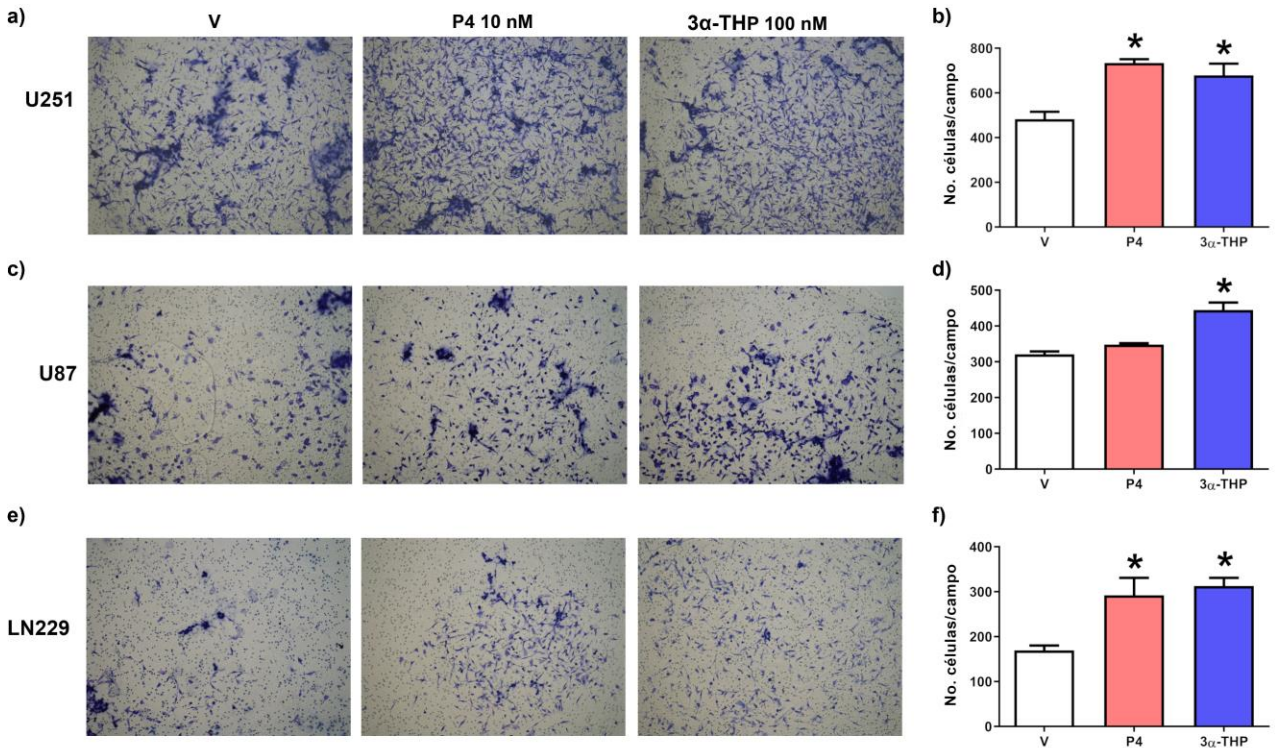


Figura 12. Efecto de la 3 α -THP sobre la invasión de las células de GB. Las células fueron tratadas con el vehículo (V; EtOH, 0.01 %), P4 (10 nM) y 3 α -THP (100 nM) durante 24 h. Imágenes representativas de los ensayos de invasión realizados en las células: a) U251, c) U87, y e) LN229. Todas las imágenes fueron tomadas a un aumento de 10x. Gráficos del número de células que invadieron por campo para las líneas celulares: b) U251, d) U87, y f) LN229. Cada columna representa la media \pm el error estándar de la media (E.E.M.); n = 3 para todas las líneas celulares. * p < 0.05 P4 o 3 α -THP vs. V.

10.3 Caracterización de las 3 α -HSD (AKR1C1-4) en las líneas celulares de GB

Considerando que la 5 α -DHP producto del metabolismo de la 3 α -THP puede inducir la migración e invasión, se determinó la presencia de los transcritos para las 3 α -HSD. Éstas son codificadas por cuatro genes diferentes (AKR1C1-4). En este trabajo, los niveles del mRNA y la proteína de dichas enzimas en las líneas celulares de GB se comparó con los niveles en muestras comerciales de RNA total y proteína de astrocitos humanos. Debido a la homología que tienen, se diseñaron dos pares de oligonucleótidos. Cada uno reconoce específicamente a dos isoenzimas (AKR1C1-2 y AKR1C3-4). Por ello no se determinó individualmente la expresión de las AKR1C1-4. Al evaluar la expresión de dichas enzimas a nivel de mRNA se encontró que las células U251 presentaron una amplificación significativamente mayor de transcritos detectados con los oligonucleótidos para las AKR1C1-2 y AKR1C3-4 con respecto a los astrocitos. Las células LN229 presentan una amplificación significativa de los transcritos detectados AKR1C3-4 con respecto a los astrocitos humanos. La línea celular U87 no presentó diferencias significativas en los niveles de las AKR1C1-4 con respecto a las células

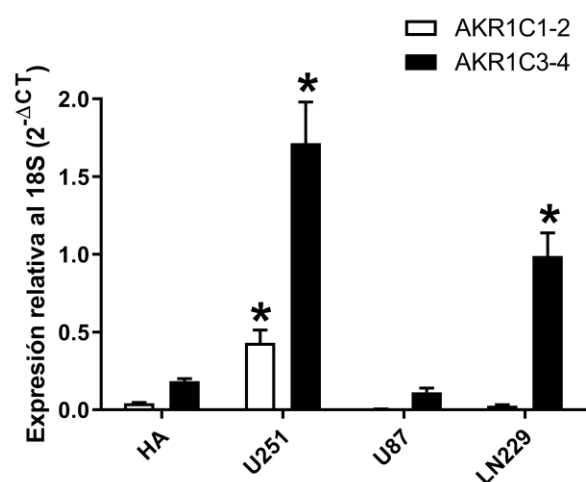


Figura 13. Expresión diferencial de las AKR1C1-4 en astrocitos y células de GB humano. El RNA total de las células de GB fue extraído después de 24 h de cultivo en medio DMEM sin rojo fenol y suplementado con 10 % de SFB libre de hormonas. La técnica de determinación fue RT-qPCR. La expresión de las AKR1C1-4 en las líneas celulares se comparó con la de una muestra comercial del RNA total de astrocitos humanos (HA). Las columnas representan la media \pm E.E.M. n = 3; * p < 0.05 vs. HA y U87.

normales (**Figura 13**).

Para evaluar los niveles de la proteína, se utilizó un anticuerpo monoclonal que reconoce a los aminoácidos 1-78 de la región N-terminal de las cuatro isoenzimas. Nuevamente, las líneas celulares U251 y LN229 presentaron niveles significativamente mayores de las 3 α -HSD con respecto a la muestra de astrocitos y a la línea celular U87 (**Figura 14**). Cabe destacar que con los resultados actuales no se puede determinar cuál o cuáles de las 4 isoenzimas son las sobreexpresadas en cada una de las líneas celulares utilizadas en este proyecto.

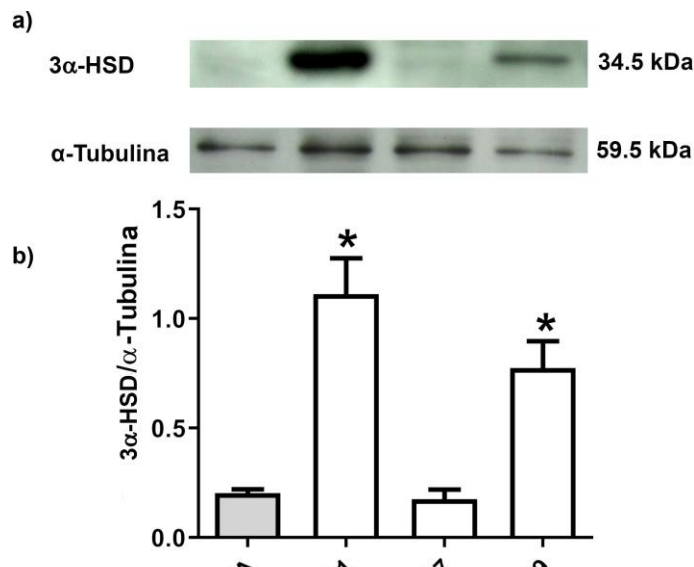


Figura 14. Niveles protéicos de las 3 α -HSD en astrocitos y las líneas celulares de GB. Las 3 α -HSD fueron detectadas a partir de la extracción de proteínas totales de astrocitos humanos (HA), y de las líneas celulares de GB humanos: U251, U87 y LN229. **a)** Western blot representativo de 3 α -HSD y de α -Tubulina detectada como control de cambio. **b)** Gráfica del análisis densitométrico de los experimentos de Western blot. Cada columna representa la media \pm E.E.M. n = 3; * p < 0.05 U251 y LN229 vs. HA y U87.

10.4 Efecto del silenciamiento de las 3 α -HSD sobre la migración de células de GB tratadas con 3 α -THP

Para determinar el efecto del metabolismo de la 3 α -THP a través de las 3 α -HSD, se silenció la expresión de dichas enzimas en la línea celular U251 y se evaluó la migración celular mediante los ensayos de cierre de herida. Primero se determinó el silenciamiento

de tres de las isoenzimas al momento de comenzar los ensayos de migración mediante el uso de un siRNA comercial diseñado para el silenciamiento de AKR1C1, AKR1C2 y AKR1C3 (AKR1C1-3). Se consideró el uso de dicho siRNA ya que la isoenzima AKR1C4 no se expresa en el SNC (**Figura 15a**). Bajo esta condición de silenciamiento, la 3 α -THP indujo significativamente la migración celular, tanto en las células que fueron tratadas con un SiRNA control (Control siRNA), como en las células U251 con la expresión de las AKR1C1-3 silenciada (sAKR1C1-3) a las 24 h de tratamiento (**Figura 15**). Con lo anterior se demuestra que el efecto de la 3 α -THP no depende de los productos de su metabolismo para inducir la migración de las células de GB.

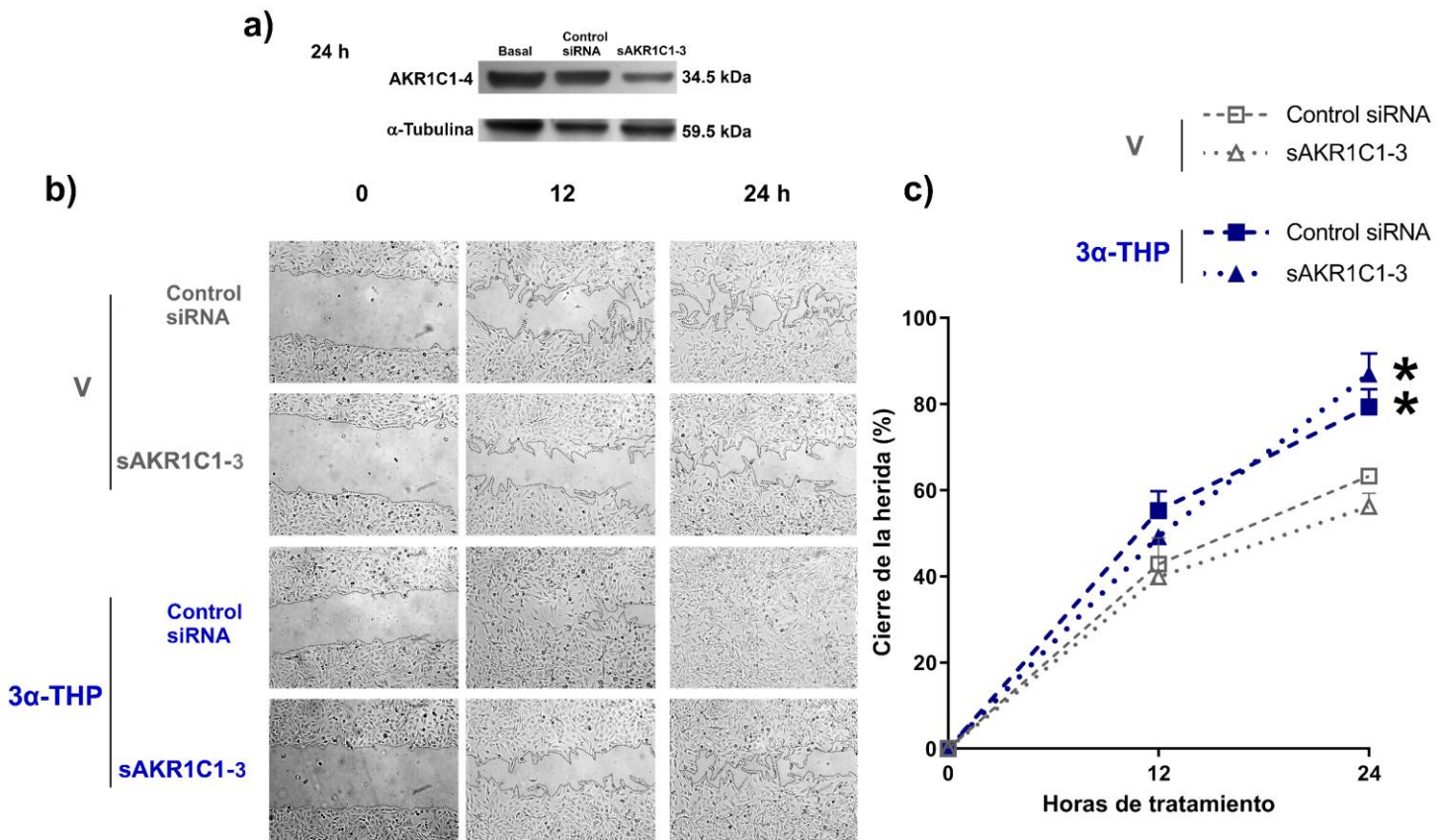


Figura 15. Efecto de la 3 α -THP y el silenciamiento de las AKR1C1-3 sobre la migración de la línea celular U251. *a)* Western blot representativo del silenciamiento de las AKR1C1-3 al inicio de los experimentos de migración. *b)* Imágenes representativas de los ensayos de migración con las células transfectadas con un siRNA control del silenciamiento (Control siRNA) o con el siRNA para las AKR1C1-3 (sAKR1C1-3). Las células fueron tratadas con V (EtOH) y 3 α -THP. Fotos tomadas a un aumento de 10x. *c)* Gráfica del porcentaje del cierre de la herida de las células U251. Cada punto representa la media \pm E.E.M. * $p < 0.05$ 3 α -THP (Control siRNA y sAKR1C1-3) vs. V (Control siRNA y sAKR1C1-3); $n = 3$.

10.5 Efecto del silenciamiento de las 3 α -HSD sobre la invasión de células de GB tratadas con 3 α -THP

Bajo las mismas condiciones de silenciamiento anteriores, se determinó el efecto de la 3 α -THP sobre la capacidad de invasión de las células U251. Nuevamente la 3 α -THP indujo significativamente la invasión tanto en las células tratadas con el SiRNA control como en las células donde las AKR1C1-3 fueron silenciadas (**Figura 16**). Lo anterior indica que la 3 α -THP induce la capacidad de invasión independientemente de la expresión de las AKR1C1-3.

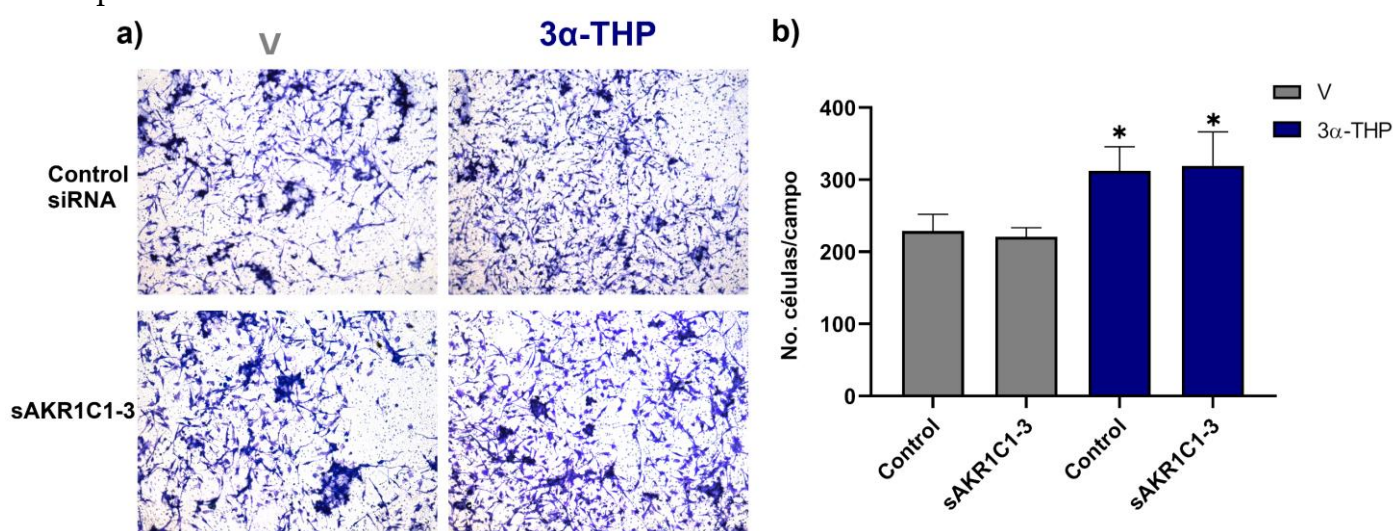


Figura 16. Efecto de la 3 α -THP y el silenciamiento de las AKR1C1-3 sobre la invasión de la línea celular U251. a) Imágenes representativas de los ensayos de invasión de las células U251 transfectadas con un siRNA control negativo (Control siRNA) o con el siRNA específico para las AKR1C1-3 (sAKR1C1-3) y tratadas con 3 α -THP (100 nM) o V (EtOH, 0.01 %). Fotos tomadas a un aumento de 10x b) Gráfica del número de células que invadieron por campo. Cada punto representa la media \pm E.E.M. * $p < 0.05$ 3 α -THP (Control siRNA y sAKR1C1-3) vs. V (Control siRNA y sAKR1C1-3).

10.6 Efecto de la 3 α -THP sobre la activación de la cinasa cSrc

La participación de la cinasa cSrc en la transducción de señales inducida por la 3 α -THP ha sido reportada por diversos autores anteriormente [14,153]. Además, la marca de fosforilación del residuo Y416 de cSrc se asocia al estado activo de la proteína. Para determinar la participación de dicha enzima en los efectos de la 3 α -THP sobre la migración e invasión de las células de GB, se determinó por Western blot, la

fosforilación del residuo Y416 de cSrc a los 5, 10, 15 y 30 min de tratamiento con 3α -THP en las líneas celulares U251, U87 y LN229. Bajo las condiciones anteriormente descritas, se observó un aumento significativo en la fosforilación de cSrc a los 10 min de tratamiento con 3α -THP con respecto al vehículo (V) en las células U251 (**Figura 17**) y a los 15 min de tratamiento en las líneas celulares U87 (**Figura 18**) y LN229 (**Figura 19**).

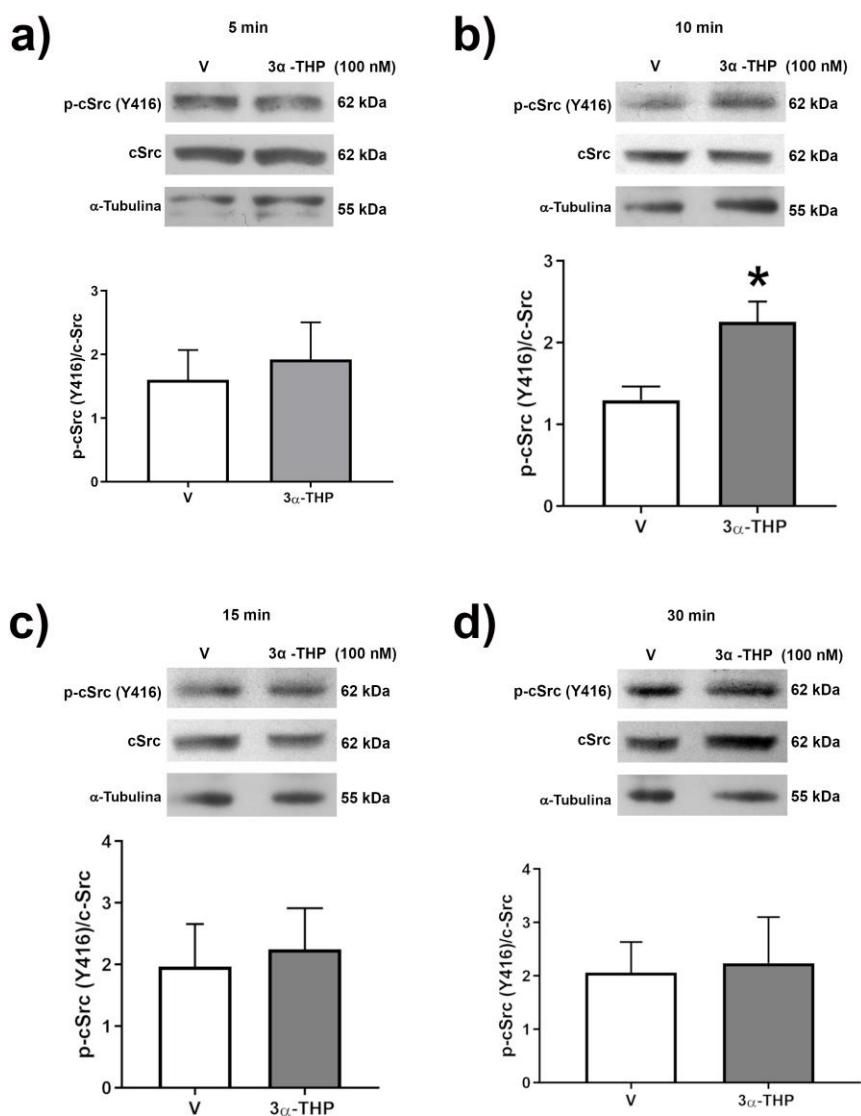


Figura 17. Efecto de la 3α -THP sobre los niveles de cSrc fosforilada (Y416) en las células U251. La fosforilación de cSrc (Y416) fue determinada mediante Western blot con los tratamientos de V (EtOH; 0.01 %) y 3α -THP (100 nM) a: **a)** 5 min, **b)** 10 min, **c)** 15 min y **d)** 30 min de tratamiento. En cada inciso se muestran los Western blots representativos de la cSrc fosforilada [p-cSrc (Y416)], cSrc total y α -Tubulina, junto con la gráfica del análisis densitométrico de p-Src/cSrc total. Cada columna representa la media \pm E.E.M. * p < 0.05

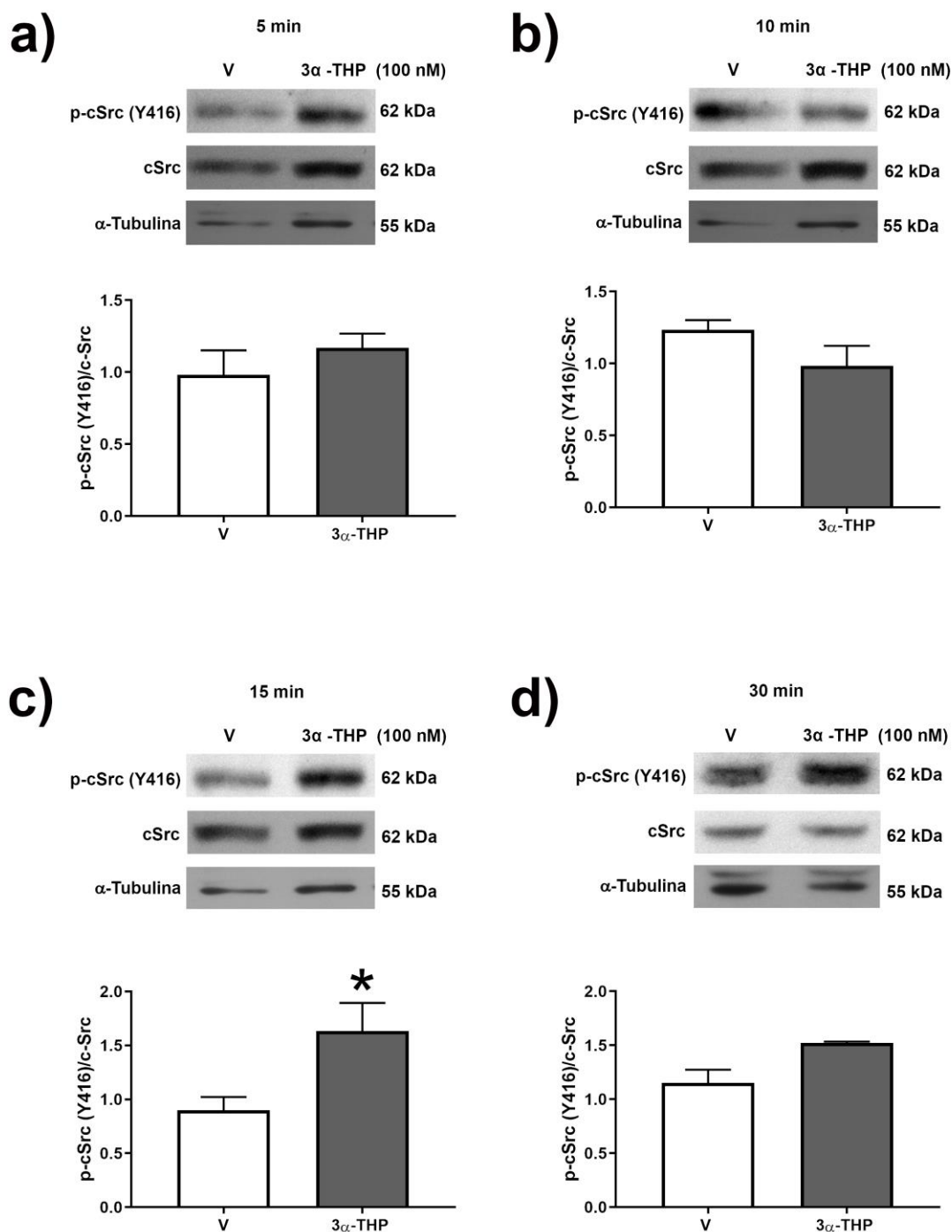


Figura 18. Efecto de la 3α-THP sobre los niveles de cSrc fosforilada (416) en la línea celular U73. La fosforilación de cSrc (Y416) fue determinada mediante Western blot con los tratamientos de V (EtOH; 0.01 %) y 3α THP (100 nM) a: **a)** 5 min, **b)** 10 min, **c)** 15 min y **d)** 30 min de tratamiento. En cada inciso se muestran los Western blots representativos de la cSrc fosforilada [p-cSrc (Y416)], cSrc total y α-Tubulina, junto con la gráfica del análisis densitométrico de p-Src/cSrc total. Cada columna representa la media ± E.E.M. * $p < 0.05$ 3α-THP vs. V; $n = 3$.

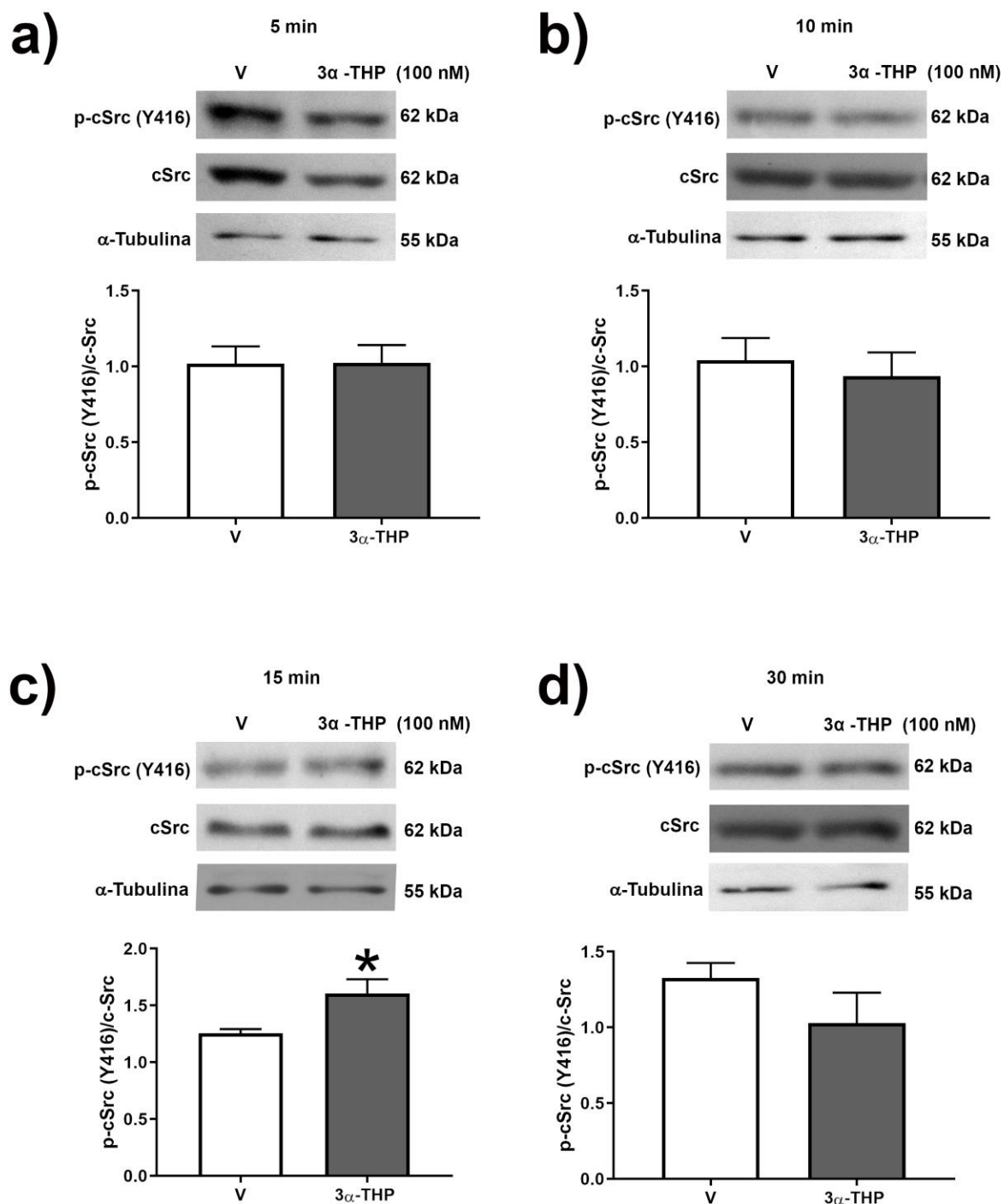


Figura 19. Efecto de la 3α-THP sobre los niveles de cSrc fosforilada (Y416) en la línea celular LN229. La fosforilación de cSrc (Y416) fue determinada mediante Western blot con los tratamientos de V (EtOH; 0.01 %) y 3α THP (100 nM) a: **a)** 5 min, **b)** 10 min, **c)** 15 min y **d)** 30 min de tratamiento. En cada inciso se muestran los Western blots representativos de la cSrc fosforilada [p-cSrc (Y416)], cSrc total y α-Tubulina, junto con la gráfica del análisis densitométrico de p-Src/cSrc total. Cada columna representa la media ± E.E.M. * p < 0.05 3α-THP vs. V; n = 3.

10.7 Efecto de la 3 α -THP y el PP2 sobre la migración de las líneas celulares de GB

Dado que la 3 α -THP induce cambios en la activación de cSrc en las células de GB, se evaluó si el efecto de la 3 α -THP sobre la migración también está mediado por cSrc. Para ello se llevaron a cabo ensayos de migración con 3 α -THP, el inhibidor farmacológico de cSrc, el PP2 (1-tert-Butil-3-(4-clorofenil)-1H-pirazolo[3,4-d]pirimidin-4-amina), y el tratamiento conjunto de 3 α -THP+PP2. Dichos ensayos fueron realizados en las líneas celulares U251 y U87.

En la línea celular U251, la 3 α -THP indujo la migración a partir de las 12 h de tratamiento (**Figura 20**). El tratamiento conjunto (3 α -THP+PP2), aumentó la migración a partir de las 12 h de tratamiento con respecto al vehículo EtOH. Además, mostró diferencias estadísticamente significativas con respecto al tratamiento con 3 α -THP. Mientras que el PP2 sólo no tuvo efecto sobre la migración celular en la línea U251 (**Figura 20**). Lo anterior indica que el efecto de la 3 α -THP sobre la migración de las células U251 está mediado de manera parcial por la cinasa cSrc.

En las células U87, la 3 α -THP indujo la migración celular a partir de las 12 h de tratamiento (**Figura 21**). El tratamiento conjunto disminuyó completamente el efecto de la 3 α -THP. Además, tanto el PP2 como el tratamiento de 3 α -THP+PP2 disminuyeron significativamente la migración celular con respecto al vehículo (**Figura 21**). Lo anterior indica que el efecto de la 3 α -THP sobre la migración de la línea celular U87 sí está mediado por la cinasa cSrc.

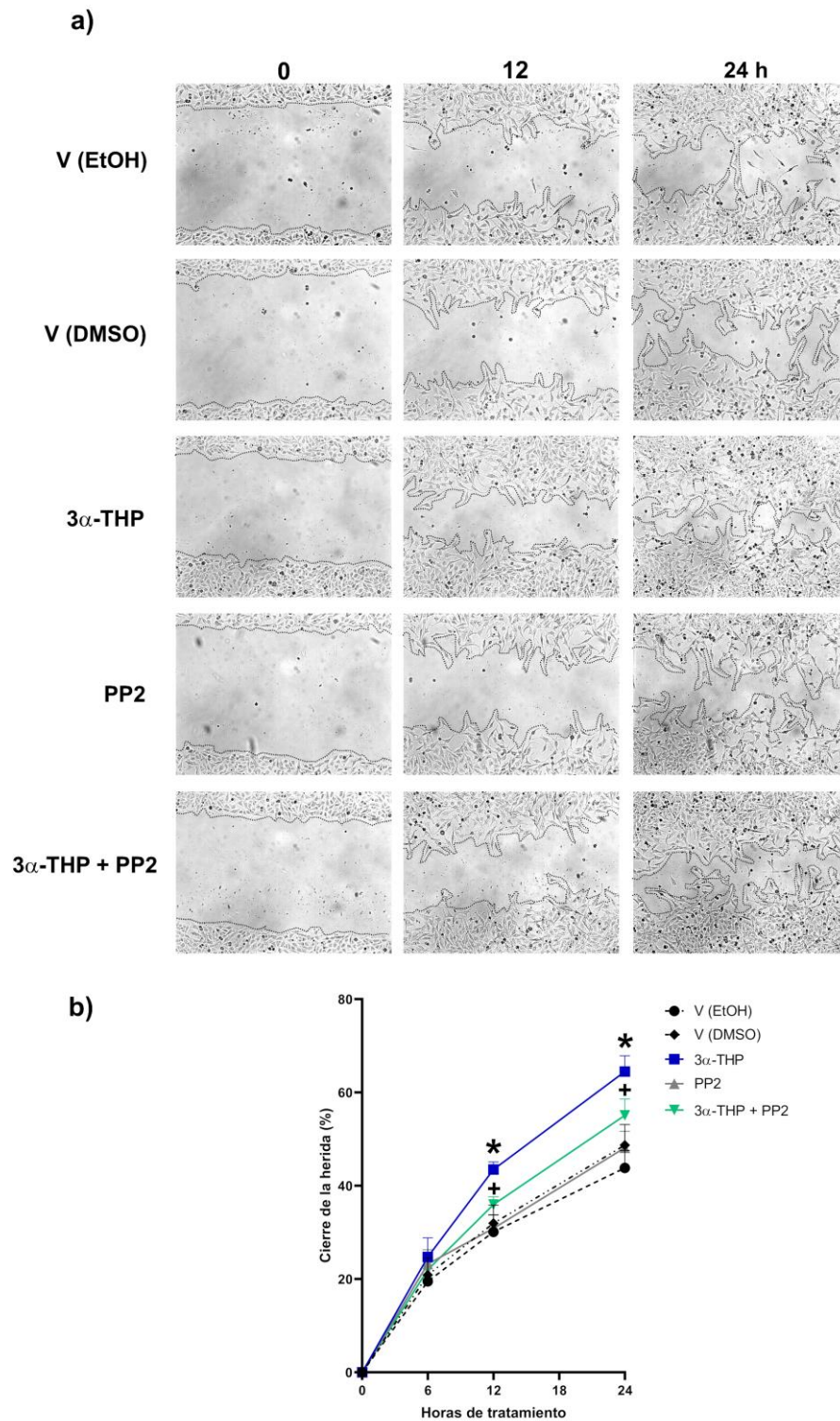


Figura 20. Efecto de la 3 α -THP y el inhibidor farmacológico de cSrc, el PP2, sobre la migración de las células U251. **a)** Imágenes representativas de las células U251 tratadas con 3 α -THP (100 nM), PP2 (1 μ M), 3 α -THP+PP2, y los vehículos V (EtOH 0.01 % y DMSO 0.001 %) a las 0, 12 y 24 h de tratamiento. **b)** Gráfica del porcentaje de cierre de herida con la línea celular U251. Cada punto representa la media \pm E.E.M.; n = 3. * p < 0.05 3 α -THP vs. Todos los demás tratamientos; + p < 0.05 3 α -THP+PP2 vs V (EtOH) y 3 α -THP+PP2 vs. 3 α -THP.

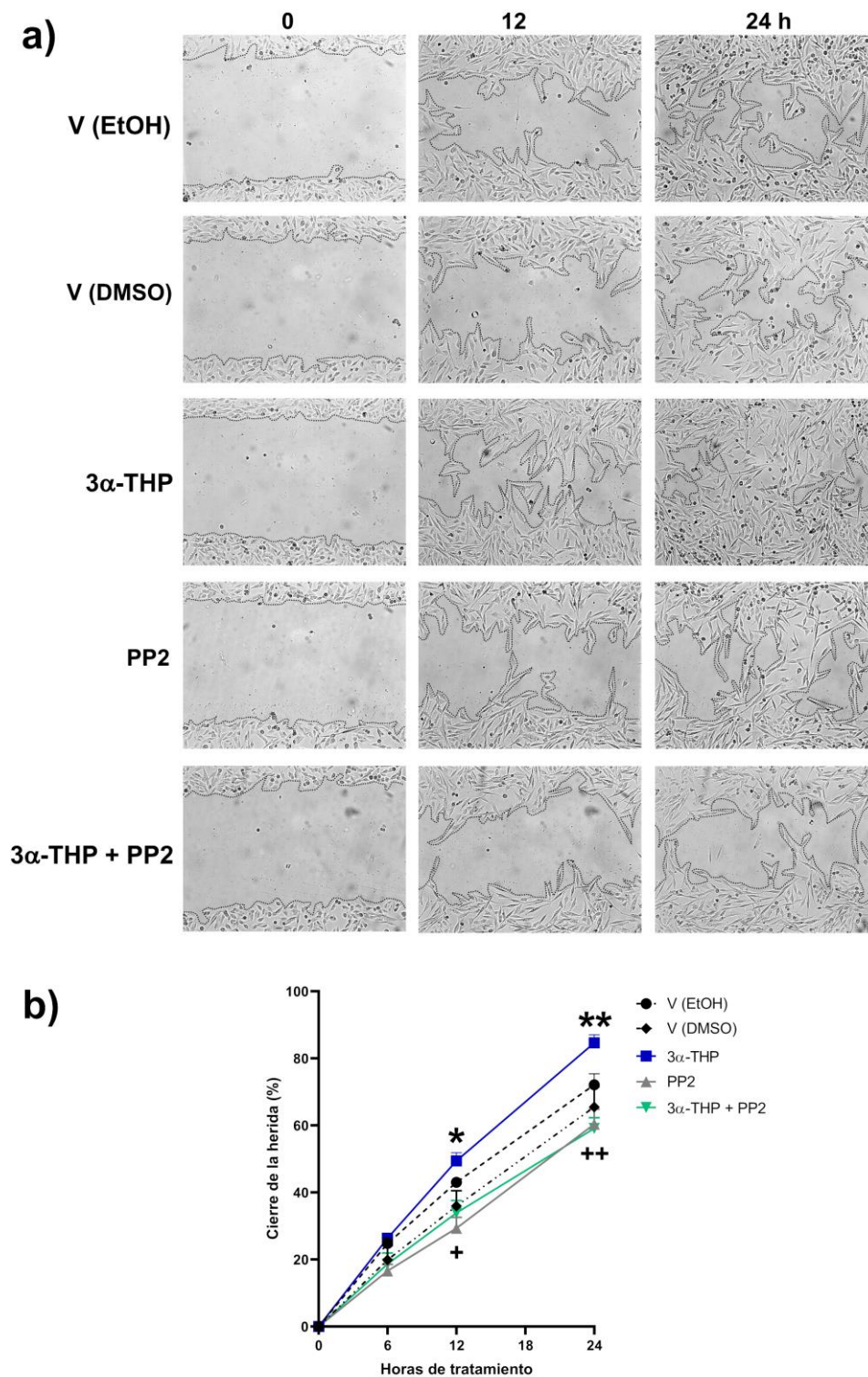


Figura 21. Efecto de la 3α-THP y el inhibidor farmacológico de cSrc, el PP2, sobre la migración de las células U87. **a)** Imágenes representativas de las células U87 tratadas con 3α-THP (100 nM), PP2 (1 μM), 3α-THP+PP2, y los vehículos V (EtOH 0.01 % y DMSO 0.001 %) a las 0, 12 y 24 h de tratamiento. **b)** Gráfica del porcentaje de cierre de la herida. Cada punto representa la media ± E.E.M.; n = 4. * p < 0.05 3α-THP vs. V (DMSO), 3α-THP+PP2 y PP2; ** p < 0.05 3α-THP vs. todos los demás tratamientos; + p < 0.05 PP2 y 3α-THP + PP2 vs. V (EtOH); ++ p < 0.05 PP2 vs V (EtOH) y 3α-THP+PP2 vs V (EtOH).

10.8 Efecto de la 3 α -THP y el PP2 sobre la invasión de las líneas celulares de GB

Dada la estrecha relación entre los mecanismos de migración e invasión celular, y que los efectos de la 3 α -THP sobre la migración están mediados por la cinasa cSrc, se realizaron ensayos de invasión con 3 α -THP, el inhibidor farmacológico de cSrc, el PP2, y el tratamiento conjunto (3 α -THP+PP2). Estos ensayos se realizaron en las líneas celulares U251 y U87.

En la línea celular U251 y U87, la 3 α -THP indujo significativamente la invasión celular. El tratamiento conjunto 3 α -THP+PP2 abatió completamente el efecto de la 3 α -THP (**Figura 22 y 23**). Además, el PP2 no tuvo efecto sobre la invasión celular. Lo anterior indica que el efecto de la 3 α -THP sobre la invasión de las células de GB también está mediado por la cinasa cSrc.

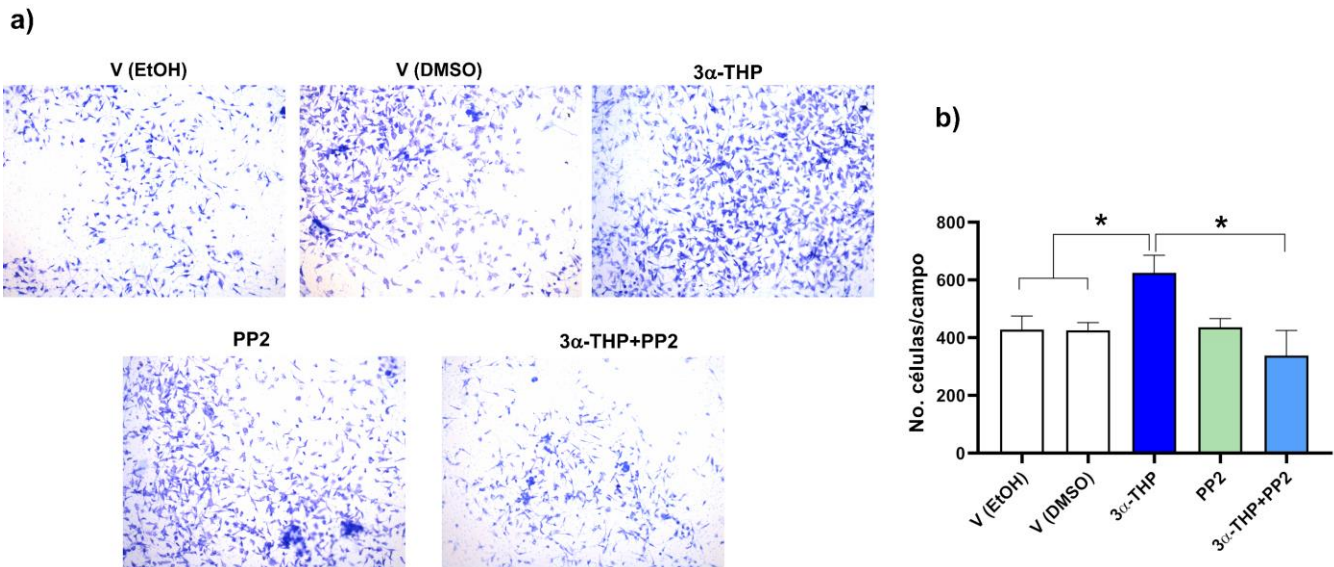


Figura 22. Efecto de la 3 α -THP y el inhibidor farmacológico de cSrc, el PP2, sobre la invasión de la línea celular U251. Las células fueron tratadas con V (EtOH, 0.01 %), V (DMSO 0.001 %), 3 α -THP (100 nM), PP2 (1 μ M), o el tratamiento conjunto (3 α -THP+PP2) durante 24 h de tratamiento. **a)** Imágenes representativas de los ensayos de invasión con las células U251, tomadas a un aumento de 10x. **b)** Gráfico del número de células que invadieron por campo. Cada columna representa la media \pm E.E.M. * $p < 0.05$ 3 α -THP vs. V (EtOH, DMSO), y 3 α -THP+PP2; $n = 3$.

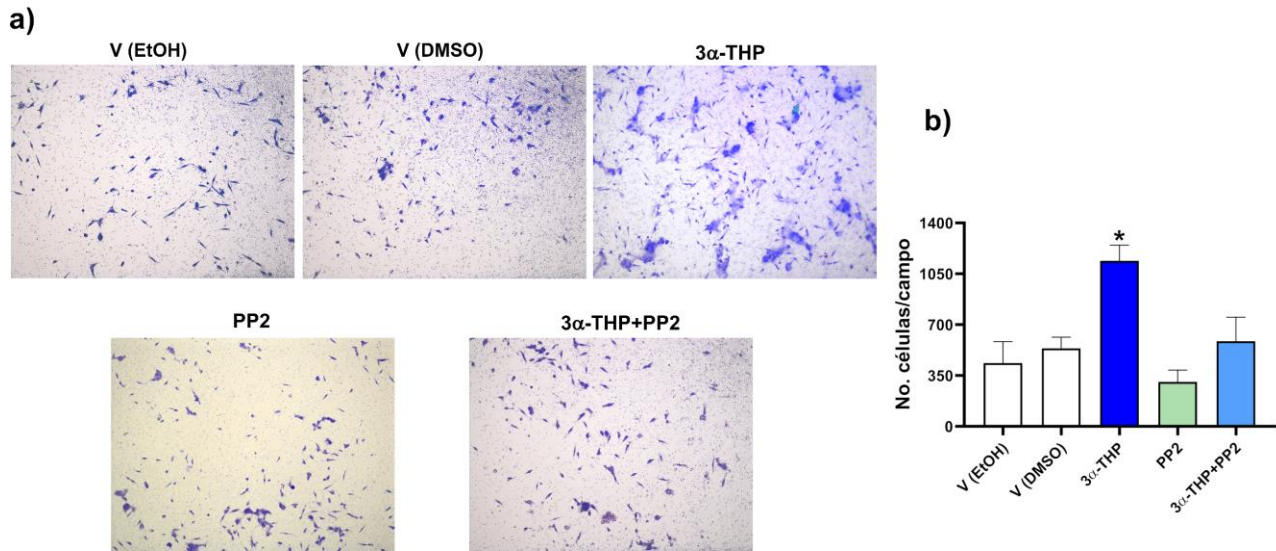


Figura 23. Efecto de la 3α-THP y el inhibidor farmacológico de cSrc, el PP2, sobre la invasión de la línea celular U87. Las células fueron tratadas con V (EtOH, 0.01 %), V (DMSO 0.001 %), 3α-THP (100 nM), PP2 (1 μM), o el tratamiento conjunto (3α-THP+PP2) durante 24 h de tratamiento. **a)** Imágenes representativas de los ensayos de invasión con las células U87, tomadas a un aumento de 10x. **b)** Gráfico del número de células que invadieron por campo. Cada columna representa la media ± E.E.M. * $p < 0.05$ 3α-THP vs. todos los demás tratamientos; $n = 4$.

11 DISCUSIÓN

Si bien es cierto que el papel de los metabolitos de la P4 en el desarrollo del cáncer se ha estudiado poco, particularmente en los GB, sí hay algunos estudios que revelan su importancia en diferentes modelos. En tejido tumoral mamario, por ejemplo, se ha visto una mayor concentración de metabolitos 5α-reducidos (como la 5α-DHP y la 3α-THP), con respecto al tejido no tumoral de los mismos pacientes [161]. Lo anterior sugiere que dichos esteroides pueden tener relevancia en la fisiopatología de este tipo de enfermedades. En líneas celulares de cáncer de mama receptor a estrógenos (ER)-/PR-, los 5α-pregnanos promueven un aumento en la viabilidad celular, lo cual indica que en dichos modelos, no sólo el PR juega un papel importante en la malignidad tumoral, sino también la activación de otros mecanismos independientes del PR y mediados, posiblemente, por más de un progestágeno [162,163].

Aunque los GB no son considerados tumores dependientes de hormonas sexuales, se ha visto que éstas, a concentraciones bajas, influyen en el desarrollo de la enfermedad [27]. Esto cobra relevancia al considerar que el cerebro es un órgano esteroideogénico cuyo proceso de síntesis es independiente de la esteroidogénesis en las gónadas. Lo anterior ha sido demostrado en modelos de roedores gonadectomizados donde los niveles de hormonas sexuales y sus metabolitos son detectables a largo plazo después de la resección de las gónadas [164].

Con respecto a los GB, previamente se reportó el aumento de la viabilidad y la proliferación de líneas celulares con el tratamiento de P4, 5 α -DHP y 3 α -THP [12,15,165]. En el presente trabajo, se comprobó que la 3 α -THP a concentraciones de orden nanomolar induce la migración e invasión de las células de GB humanos, lo cual puede promover la rápida progresión de este tipo de tumores. Además, estos resultados concuerdan con el trabajo de Pelegrina y colaboradores, quienes reportaron que a concentraciones que van del rango picomolar al nanomolar, la 3 α -THP induce la migración e invasión de la línea celular IGROV-1 de cáncer ovárico [150]. Lo anterior corresponde con los niveles de 3 α -THP en el cerebro reportados en la literatura. Bixo y colaboradores indicaron que la concentración de 3 α -THP y en general de progestágenos varía dependiendo del área cerebral, sin embargo, la concentración de 3 α -THP se encuentra en rangos de 40 – 100 nM en el tejido cerebral de mujeres de diferentes edades, siendo más alta en el hipotálamo y ganglios basales [166]. Mientras que en otro se reportó en la corteza prefrontal de hombres sin déficits cognitivos, una concentración de 105 nM con respecto a 47 nM en la misma zona en individuos con Alzheimer [167,168].

En contraste con lo anterior, otros autores reportaron que la 3 α -THP a altas concentraciones (20-60 μ M) disminuye la expresión de proteínas que participan en la tumorigénesis de diversos tipos de cáncer cerebral (DPYSL3, S100A11 y S100A4), e

induce apoptosis *per se*. Además, la 3 α -THP incrementó el efecto que tiene la temozolomida sobre la inhibición de la migración en las líneas celulares T98G y A172, también derivadas de GB humanos [152]. Lo anterior apunta a que la 3 α -THP presenta un comportamiento similar al previamente descrito para la P4 por Atif y colaboradores. Dichos autores han demostrado que altas concentraciones de P4 promueve la senescencia y muerte de las células de GB [169,170].

La 5 α -R y la 3 α -HSD regulan la disponibilidad de metabolitos de la P4 en las células. La 5 α -R regula irreversiblemente la reducción de P4 a 5 α -DHP. En un estudio previo en la línea celular U87, la inhibición farmacológica de la enzima 5 α -R bloqueó el efecto de la P4 sobre el aumento en el número de células inducido por la P4, lo que apunta a la importancia del estudio de los metabolitos 5 α -reducidos en los GB [12]. Por otro lado, la reducción de la 5 α -DHP a 3 α -THP mediante las 3 α -HSD es un proceso reversible que puede ocurrir en las células de GB. En este trabajo se observó que las células U251, LN229 y en menores niveles, las U87 expresan a dichas enzimas. Además, se comprobó que los niveles de la proteína son consecuentes con los niveles del RNAm de las diferentes isoenzimas. Otros autores también han reportado la presencia de dichas enzimas en la línea celular C6 de glioma (de rata), las células 1231N1 (astrocitoma humano), las células U373 y T98G (astrocitoma grado 3 y GB, respectivamente) y en las U87 [103,108,114].

En este proyecto se observó que la expresión de dichas enzimas es baja en astrocitos humanos con respecto a las líneas celulares de GB, lo cual era esperado considerando que en general, se ha visto que la expresión de las isoenzimas AKR1C1-4 es baja en SNC con respecto a otros órganos como el hígado y pulmones [171]. Otro punto en consideración es que se sabe que la expresión de dichas enzimas es heterogénea en el SNC. Por datos colectados a través de microarreglos, se ha reportado una expresión significativamente menor de las AKR1C1-4 en biopsias de GB con respecto a tejido

cerebral normal [114]. Sin embargo, otros autores también han reportado diferencias entre sus hallazgos con respecto a los niveles de RNAm y proteína de las AKR1C1-4 [172], por lo que el estudio de dichas enzimas en cáncer debe ser monitoreada a través del uso de diferentes estrategias metodológicas. Además, cabe destacar que la sobreexpresión de las AKR1C1-4 generalmente correlaciona con un mal pronóstico en pacientes con cáncer [173].

Dado que las AKR1C1-4 regulan los niveles de 5α -DHP y 3α -THP, entonces, podrían modular indirectamente a los mecanismos que activan los progestágenos en las células de GB. Como ya se mencionó, tanto la P4 como la 5α -DHP presentan afinidad por el PR [146]. En células de GB ambos progestágenos regulan la proliferación y migración celular parcialmente a través de dicho receptor [15,158,159]. Sin embargo, por otro reporte, se sabe que la 3α -THP no presenta afinidad por dicho receptor [146].

Considerando que al realizar tratamientos con 3α -THP los efectos de ésta podrían ser mediados por su interconversión a 5α -DHP, en este proyecto se utilizó la estrategia del silenciamiento de las 3α -HSD antes de realizar el tratamiento con 3α -THP en las células U251. Asumiendo un fenotipo normal de las 3α -HSD en las células de GB, se esperaría que la oxidación de 3α -THP a 5α -DHP esté mediada principalmente por las isoenzimas AKR1C1-2, ya que se ha reportado que la isoenzima AKR1C3 tiene baja actividad de oxidación [171]. Sin embargo, el estado mutacional, así como la actividad de dichas enzimas en el caso particular de los GB puede ser un punto de partida para determinar el estado del metabolismo de esteroides en este tipo de cáncer. Además, la AKR1C1, podría reducir el grupo cetona del C20 de la 3α -THP para producir 5α -pregnano- $3\alpha,20\alpha$ -diol [174].

Este último esteroide, es un agonista parcial del GABA_AR y tiene menor afinidad por el sitio alostérico del receptor con respecto a la 3α -THP [112]. En este trabajo, el silenciamiento de las 3α -HSD no modificó el efecto inductor de la 3α -THP sobre la

migración e invasión, lo cual indica que este metabolito promueve la malignidad de los GB de forma independiente de su interconversión a 5 α -DHP, o 5 α -pregnano-3 α ,20 α -diol. Cabe destacar que existen otras enzimas que también pueden metabolizar a la 3 α -THP en el SNC. La 17 β -hidroxiesteroide deshidrogenasa 10 (17 β -HSD10) codificada por el gen *SRD5C1* (o *HSD17B10*) y localizada principalmente en la mitocondria, puede catalizar la oxidación de 3 α -THP a 5 α -DHP [175]. La expresión de dicha enzima en GB ha sido asociada a resistencia al tratamiento con bevacizumab un anticuerpo dirigido para el VEGF [176]. Sin embargo, se desconoce aún el papel que esta enzima puede desempeñar en el metabolismo de la 3 α -THP en GB. Dado que la 3 α -THP es un metabolito que tiene diferentes mecanismos de acción es necesario determinar en las células de GB, qué mecanismos activa y si éstos podrían ser regulados por otros metabolitos hormonales con una estructura química similar a la 3 α -THP.

Los mecanismos de acción de la 3 α -THP descritos en la literatura pueden tener efectos a corto plazo (segundos-minutos) o largo plazo (horas-días). Los mecanismos de acción a corto plazo de la 3 α -THP dependen de la modulación de receptores de membrana como GABA_AR y los mPR [14,139]. Mientras que los mecanismos de acción de la 3 α -THP a largo plazo dependen de la activación del factor de transcripción PXR [177], u otros mediados por los receptores membranales. El tipo de mecanismo activado depende de la expresión de los receptores y de sus efectores en las células de GB.

Además de modular positivamente al GABA_AR, la 3 α -THP modula otros aspectos de la transducción mediada por el neurotransmisor GABA. La 3 α -THP promueve la expresión de dos isoformas de la enzima glutamato descarboxilasa, la enzima reguladora de la síntesis de GABA [128]. Además, la expresión de las subunidades δ y $\gamma(2-3)$ del GABA_AR aumentan la afinidad de la 3 α -THP por el receptor [122]. A pesar de que la 3 α -THP no tiene afinidad por los receptores metabotrópicos del GABA (GABA_BR), la 3 α -THP aumenta la expresión de 3 de las isoformas de dicho receptor

[178]. Hay estudios que indican que la expresión de las subunidades de GABA_AR es baja en los GB [179]. Sin embargo, en la línea celular U251 se expresan diversas enzimas involucradas en el metabolismo de GABA y el tratamiento con este neurotransmisor aumenta significativamente la proliferación celular [180].

Además del GABA_AR, la 3 α -THP presenta afinidad por los mPR δ , mPR α y mPR β . El receptor mPR δ activa a proteínas de tipo G_s, mismas que promueven la activación de la enzima Adenilato Ciclasa y la producción del segundo mensajero AMPc [135]. En la línea celular de cáncer de mama MDA-MB-231, la activación de esta vía de señalización promueve la activación de la cinasa ERK, y en las células H19-7 (neuronas hipocámpales de rata), a través de este mismo mecanismo se disminuyó el porcentaje de células apoptóticas [139]. La 3 α -THP también tiene afinidad por los receptores mPR α y mPR β , mismos que activan a proteínas de tipo G_i y disminuyen la producción de AMPc [142]. Lo anterior activa a cSrc y la vía de PI3K-Akt junto con la migración e invasión de células humanas tipo Schwann diferenciadas a partir de células troncales adiposas [181].

En las células de GB se ha caracterizado la expresión y localización tanto a nivel membranal como citoplasmático de los cinco mPRs [140,141]. Asimismo, el tratamiento con el agonista del mPR α ORG-OD 02-0 en las líneas celulares U87 y U251 promovió la proliferación, migración e invasión celular. Dicho tratamiento además, promovió un aumento en la fosforilación de cSrc (Y416) y p-Akt (T-308), asociadas con un aumento en la actividad de dichas cinasas [182]. El mecanismo anterior podría ser activado por la 3 α -THP en dichas líneas celulares. Otros autores también se ha propuesto una interrelación entre los mecanismos regulados por GABA_AR y los mPRs, por lo que esta interrelación podría ocurrir también en las células de GB.

La 3 α -THP además regula la transcripción génica a través del factor de transcripción PXR. A través de la activación de este receptor, la 3 α -THP puede regular positivamente la expresión de enzimas esteroideogénicas, afectando su propia síntesis [177]. Se ha visto

que el tratamiento con dexametasona, un glucocorticoide administrado comúnmente para el tratamiento del dolor y del aumento de la presión intracraneal, podría estar aumentando la expresión de transportadores asociados a la resistencia a fármacos a través de su interacción no sólo con el receptor a glucocorticoides, sino también por la activación del PXR en cultivos primarios de células endoteliales [183]. Sin embargo, no se sabe si este mismo proceso ocurre en las células de GB.

En este proyecto, se observó que la 3α -THP indujo un aumento en la cantidad de cSrc fosforilada en el residuo Y416, a 10 y 15 minutos de tratamiento en las células de GB. La fosforilación del residuo Y416 se asocia con un aumento en la actividad de cinasa de cSrc [83]. Sin embargo, aún no hay evidencia experimental que indique a través de qué mecanismo, la 3α -THP induce la activación de dicha cinasa. Además, el tratamiento conjunto del inhibidor PP2 y la 3α -THP en las células U251 y U87 reveló que la migración e invasión inducida por la 3α -THP está mediado por la activación de la cinasa cSrc. En células Schwann de rata, la migración celular inducida por la 3α -THP también estuvo mediada por la cinasa cSrc y FAK [14]. En el área ventromedial del hipotálamo, la 3α -THP también induce la activación de MAPK y cSrc [184].

El efecto de la 3α -THP sobre la migración de línea celular U87 fue totalmente mediado por la cinasa cSrc, sin embargo, dicho efecto fue parcial en las células U251. Lo anterior nuevamente indica que el efecto de la 3α -THP depende de la expresión y estado de los efectores de los mecanismos de acción que regula la 3α -THP en las líneas celulares de GB. Los GB son tumores caracterizados por su alta heterogeneidad genómica intra- e inter-tumoral. Si bien la línea celular U87 presenta características fenotípicas de un GB neuronal y la U251 presenta características de un subtipo mesenquimal [184], es notable que en ellas, además de la línea celular LN229, la 3α -THP haya inducido los mismos efectos sobre la migración e invasión, por lo que se puede

hipotetizar que en un modelo in vivo de la misma patología, la 3α -THP tenga los mismos efectos.

12 CONCLUSIONES

1. A concentración fisiológica, de 100 nM, la 3α -THP promueve la migración e invasión de las células de GB humano.
2. Las células de GB expresan a las enzimas 3α -HSD, lo cual sugiere que estas células pueden metabolizar activamente a la 3α -THP.
3. Los efectos de la 3α -THP sobre la migración e invasión celulares son independientes del metabolismo de dicho esteroide a través de las 3α -HSD.
4. Los efectos de la 3α -THP, están mediados por la activación de la cinasa cSrc en las células de GB.

13 PERSPECTIVAS

1. Caracterizar el estado de las 3α -HSD en tejido tumoral de GB con respecto al tejido cerebral sano junto con los niveles de metabolitos de la P4 generados por ambos tejidos.
2. Establecer los mecanismos de acción de la 3α -THP a través de los cuales se induce la activación de cSrc en las células de GB.
3. Dilucidar qué proteínas regulan el efecto de la 3α -THP sobre la migración e invasión celulares.
4. Caracterizar el tipo de migración que es inducida por la 3α -THP en las células de GB.
5. Determinar el efecto de la 3α -THP sobre la expresión y actividad de las metaloproteasas en células de GB.
6. Evaluar el efecto de la inhibición farmacológica de las 3α -HSD y el tratamiento con P4 y 3α -THP sobre la proliferación, migración e invasión celular.

14 REFERENCIAS

1. Renault, I.Z.; Golgher, D. Molecular genetics of glioblastomas: defining subtypes and understanding the biology. *Neuroimaging Clin. N. Am.* **2015**, *25*, 97–103, doi:10.1016/j.nic.2014.09.007.
2. Ostrom, Q.T.; Price, M.; Neff, C.; Cioffi, G.; Waite, K.A.; Kruchko, C.; Barnholtz-Sloan, J.S. CBTRUS Statistical Report: Primary Brain and Other Central Nervous System Tumors Diagnosed in the United States in 2015-2019. *Neuro. Oncol.* **2022**, *24*, v1–v95, doi:10.1093/neuonc/noac202.
3. Meir, E.G. Van; Hadjipanayis, C.G.; Norden, A.D.; Shu, H.; Wen, P.Y.; Olson, J.J. Exciting new advances in neuro-oncology: The avenue to a cure for malignant glioma. *CA Cancer J Clin* **2010**, *60*, 166–193, doi:10.3322/caac.20069.
4. González-Agüero, G.; Gutiérrez, A. a; González-Espinosa, D.; Solano, J.D.; Morales, R.; González-Arenas, A.; Cabrera-Muñoz, E.; Camacho-Arroyo, I. Progesterone effects on cell growth of U373 and D54 human astrocytoma cell lines. *Endocrine* **2007**, *32*, 129–135, doi:10.1007/s12020-007-9023-0.
5. Rodríguez-Lozano, D.C.; Piña-Medina, A.G.; Hansberg-Pastor, V.; Bello-Alvarez, C.; Camacho-Arroyo, I. Testosterone Promotes Glioblastoma Cell Proliferation, Migration, and Invasion Through Androgen Receptor Activation. *Front. Endocrinol. (Lausanne)*. **2019**, *10*, 16, doi:10.3389/fendo.2019.00016.
6. González-Arenas, A.; Hansberg-Pastor, V.; Hernández-Hernández, O.T.; González-García, T.K.; Henderson-Villalpando, J.; Lemus-Hernández, D.; Cruz-Barrios, A.; Rivas-Suárez, M.; Camacho-Arroyo, I. Estradiol increases cell growth in human astrocytoma cell lines through ER α activation and its interaction with SRC-1 and SRC-3 coactivators. *Biochim. Biophys. Acta - Mol. Cell Res.* **2012**, *1823*, 379–386, doi:10.1016/j.bbamcr.2011.11.004.
7. Melcangi, R.C.; Giatti, S.; Calabrese, D.; Pesaresi, M.; Cermenati, G.; Mitro, N.; Viviani, B.; Garcia-Segura, L.M.; Caruso, D. Levels and actions of progesterone and its metabolites in the nervous system during physiological and pathological conditions. *Prog. Neurobiol.* **2014**, *113*, 56–69, doi:10.1016/j.pneurobio.2013.07.006.
8. Wiebe, J.P. Progesterone metabolites in breast cancer. *Endocr. Relat. Cancer* **2006**, *13*, 717–38, doi:10.1677/erc.1.01010.
9. Pinna, G. Allopregnanolone (1938–2019): A trajectory of 80 years of outstanding scientific achievements. *Neurobiol. Stress* **2020**, *13*, 13–16, doi:10.1016/j.ynstr.2020.100246.
10. Paul, S.M.; Pinna, G.; Guidotti, A. Allopregnanolone: From molecular pathophysiology to therapeutics. A historical perspective. *Neurobiol. Stress* **2020**, *12*, 100215, doi:10.1016/j.ynstr.2020.100215.
11. Diviccaro, S.; Cioffi, L.; Falvo, E.; Giatti, S.; Melcangi, R.C. Allopregnanolone: An overview on its synthesis and effects. *J. Neuroendocrinol.* **2022**, *34*, e12996,

- doi:10.1111/jne.12996.
12. Zamora-Sánchez, C.J.; Hansberg-Pastor, V.; Salido-Guadarrama, I.; Rodríguez-Dorantes, M.; Camacho-Arroyo, I. Allopregnanolone promotes proliferation and differential gene expression in human glioblastoma cells. *Steroids* **2017**, *119*, doi:10.1016/j.steroids.2017.01.004.
 13. Zamora-Sánchez, C.C.J.; del Moral-Morales, A.; Hernández-Vega, A.A.M.; Hansberg-Pastor, V.; Salido-Guadarrama, I.; Rodríguez-Dorantes, M.; Camacho-Arroyo, I. Allopregnanolone Alters the Gene Expression Profile of Human Glioblastoma Cells. *Int. J. Mol. Sci.* **2018**, *19*, 864, doi:10.3390/ijms19030864.
 14. Melfi, S.; Montt Guevara, M.M.; Bonalume, V.; Ruscica, M.; Colciago, A.; Simoncini, T.; Magnaghi, V. Src and phospho-FAK kinases are activated by allopregnanolone promoting Schwann cell motility, morphology and myelination. *J. Neurochem.* **2017**, *141*, 165–178, doi:10.1111/jnc.13951.
 15. Zamora-Sánchez, C.J.; Hernández-Vega, A.M.; Gaona-Domínguez, S.; Rodríguez-Dorantes, M.; Camacho-Arroyo, I. 5alpha-dihydroprogesterone promotes proliferation and migration of human glioblastoma cells. *Steroids* **2020**, *163*, 108708, doi:10.1016/j.steroids.2020.108708.
 16. Phillips, J.J. Brain Tumors; Biology. *Encycl. Neurol. Sci.* **2014**, *1*, 525–526, doi:10.1016/B978-0-12-385157-4.00483-8.
 17. Louis, D.N.; Perry, A.; Reifenberger, G.; von Deimling, A.; Figarella-Branger, D.; Cavenee, W.K.; Ohgaki, H.; Wiestler, O.D.; Kleihues, P.; Ellison, D.W. The 2016 World Health Organization Classification of Tumors of the Central Nervous System: a summary. *Acta Neuropathol.* **2016**, *131*, 803–820, doi:10.1007/s00401-016-1545-1.
 18. Louis, D.N.; Perry, A.; Wesseling, P.; Brat, D.J.; Cree, I.A.; Figarella-Branger, D.; Hawkins, C.; Ng, H.K.; Pfister, S.M.; Reifenberger, G.; et al. The 2021 WHO Classification of Tumors of the Central Nervous System: a summary. *Neuro. Oncol.* **2021**, *23*, 1231–1251, doi:10.1093/neuonc/noab106.
 19. Merve, A.; Millner, T.O.; Marino, S. Integrated phenotype–genotype approach in diagnosis and classification of common central nervous system tumours. *Histopathology* **2019**, *75*, 299–311, doi:10.1111/his.13849.
 20. Antonelli, M.; Poliani, P.L. Adult type diffuse gliomas in the new 2021 WHO Classification. *Pathologica* **2022**, *114*, 397–409, doi:10.32074/1591-951X-823.
 21. Weller, M.; Wick, W.; Aldape, K.; Brada, M.; Berger, M.; Pfister, S.M.; Nishikawa, R.; Rosenthal, M.; Wen, P.Y.; Stupp, R.; et al. Glioma. *Nat. Rev. Dis. Prim.* **2015**, *1*, 15017, doi:10.1038/nrdp.2015.17.
 22. IARC Mexico Source: Globocan 2020. *Int. Agency Res. Cancer WHO* **2020**, *929*, 1–2.
 23. Sánchez-Barriga, J.J. Mortality trends from central nervous system tumors in the seven socioeconomic regions and thirty-two states of Mexico from 2000 until 2017. *Rev. Neurol.*

- 2022, 74, 315–324, doi:10.33588/rn.7410.2021398.
24. Davis, F.G.; Smith, T.R.; Gittleman, H.R.; Ostrom, Q.T.; Kruchko, C.; Barnholtz-Sloan, J.S. Glioblastoma incidence rate trends in Canada and the United States compared with England, 1995-2015. *Neuro. Oncol.* **2020**, *22*, 301–302, doi:10.1093/neuonc/noz203.
 25. Ober, C.; Loisel, D.A.; Gilad, Y. Sex-specific genetic architecture of human disease. *Nat. Rev. Genet.* **2008**, *9*, 911–922.
 26. Dunford, A.; Weinstock, D.M.; Savova, V.; Schumacher, S.E.; Cleary, J.P.; Yoda, A.; Sullivan, T.J.; Hess, J.M.; Gimelbrant, A.A.; Beroukhi, R.; et al. Tumor-suppressor genes that escape from X-inactivation contribute to cancer sex bias. *Nat. Genet.* **2017**, *49*, 10–16, doi:10.1038/ng.3726.
 27. Bello-Alvarez, C.; Camacho-Arroyo, I. Impact of sex in the prevalence and progression of glioblastomas: the role of gonadal steroid hormones. **2021**, *12*, 1–13.
 28. Molinaro, A.M.; Taylor, J.W.; Wiencke, J.K.; Wrensch, M.R. Genetic and molecular epidemiology of adult diffuse glioma. *Nat. Rev. Neurol.* **2019**, *15*, 405–417, doi:10.1038/s41582-019-0220-2.
 29. Bondy, M.L.; Scheurer, M.E.; Malmer, B.; Barnholtz-Sloan, J.S.; Davis, F.G.; Il'yasova, D.; Kruchko, C.; McCarthy, B.J.; Rajaraman, P.; Schwartzbaum, J.A.; et al. Brain tumor epidemiology: Consensus from the Brain Tumor Epidemiology Consortium. *Cancer* **2008**, *113*, 1953–1968, doi:10.1002/cncr.23741.
 30. Tonn, J.C.; Westphal, M.; Rutka, J.T. *Oncology of CNS tumors*; 2010; ISBN 9783642028731.
 31. Yoon, S.-J.J.; Park, J.; Jang, D.-S.S.; Kim, H.J.; Lee, J.H.J.H.; Jo, E.; Choi, R.J.; Shim, J.-K.K.; Moon, J.H.; Kim, E.-H.H.; et al. Glioblastoma cellular origin and the firework pattern of cancer genesis from the subventricular zone. *J. Korean Neurosurg. Soc.* **2020**, *63*, 26–33, doi:10.3340/jkns.2019.0129.
 32. Chesler, D.A.; Berger, M.S.; Quinones-Hinojosa, A. The potential origin of glioblastoma initiating cells. *Front. Biosci. - Sch.* **2012**, *4 S*, 190–205, doi:10.2741/261.
 33. Alcantara Llaguno, S.; Chen, J.; Kwon, C.-H.; Jackson, E.L.; Li, Y.; Burns, D.K.; Alvarez-Buylla, A.; Parada, L.F. Malignant astrocytomas originate from neural stem/progenitor cells in a somatic tumor suppressor mouse model. *Cancer Cell* **2009**, *15*, 45–56, doi:10.1016/j.ccr.2008.12.006.
 34. Alcantara Llaguno, S.R.; Wang, Z.; Sun, D.; Chen, J.; Xu, J.; Kim, E.; Hatanpaa, K.J.; Raisanen, J.M.; Burns, D.K.; Johnson, J.E.; et al. Adult Lineage-Restricted CNS Progenitors Specify Distinct Glioblastoma Subtypes. *Cancer Cell* **2015**, *28*, 429–440, doi:10.1016/j.ccell.2015.09.007.
 35. Alcantara Llaguno, S.; Sun, D.; Pedraza, A.M.; Vera, E.; Wang, Z.; Burns, D.K.; Parada, L.F. Cell-of-origin susceptibility to glioblastoma formation declines with neural lineage restriction. *Nat. Neurosci.* **2019**, *22*, 545–555, doi:10.1038/s41593-018-0333-8.

36. Larjavaara, S.; Mäntylä, R.; Salminen, T.; Haapasalo, H.; Raitanen, J.; Jääskeläinen, J.; Auvinen, A. Incidence of gliomas by anatomic location. *Neuro. Oncol.* **2007**, *9*, 319–325, doi:10.1215/15228517-2007-016.
37. Li, H.Y.; Sun, C.R.; He, M.; Yin, L.C.; Du, H.G.; Zhang, J.M. Correlation Between Tumor Location and Clinical Properties of Glioblastomas in Frontal and Temporal Lobes. *World Neurosurg.* **2018**, *112*, e407–e414, doi:10.1016/j.wneu.2018.01.055.
38. Bao, H.; Ren, P.; Yi, L.; Lv, Z.; Ding, W.; Li, C.; Li, S.; Li, Z.; Yang, X.; Liang, X.; et al. New Insights into Glioma Frequency Maps: From Genetic and Transcriptomic Correlate to Survival Prediction. *Int. J. Cancer* **2022**, 998–1012, doi:10.1002/ijc.34336.
39. Perry, A.; Wesseling, P. *Histologic classification of gliomas*; 1st ed.; Elsevier B.V., 2016; Vol. 134; ISBN 9780128029978.
40. Tan, A.C.; Ashley, D.M.; López, G.Y.; Malinzak, M.; Friedman, H.S.; Khasraw, M. Management of glioblastoma: State of the art and future directions. *CA. Cancer J. Clin.* **2020**, *70*, 299–312, doi:10.3322/caac.21613.
41. Verhaak, R.G.W.W.; Hoadley, K.A.; Purdom, E.; Wang, V.; Qi, Y.; Wilkerson, M.D.; Miller, C.R.; Ding, L.; Golub, T.; Mesirov, J.P.; et al. Integrated genomic analysis identifies clinically relevant subtypes of glioblastoma characterized by abnormalities in PDGFRA, IDH1, EGFR, and NF1. *Cancer Cell* **2010**, *17*, 98–110, doi:10.1016/j.ccr.2009.12.020.
42. Brennan, C.W.W.; Verhaak, R.G.W.G.W.; McKenna, A.; Campos, B.; Nounshmehr, H.; Salama, S.R.R.; Zheng, S.; Chakravarty, D.; Sanborn, J.Z.Z.; Berman, S.H.H.; et al. The somatic genomic landscape of glioblastoma. *Cell* **2013**, *155*, 462–77, doi:10.1016/j.cell.2013.09.034.
43. Wang, Q.; Hu, B.; Hu, X.; Kim, H.; Squatrito, M.; Scarpace, L.; deCarvalho, A.C.; Lyu, S.; Li, P.; Li, Y.; et al. Tumor Evolution of Glioma-Intrinsic Gene Expression Subtypes Associates with Immunological Changes in the Microenvironment. *Cancer Cell* **2017**, *32*, 42–56.e6, doi:10.1016/j.ccell.2017.06.003.
44. Teo, W.Y.; Sekar, K.; Seshachalam, P.; Shen, J.; Chow, W.Y.; Lau, C.C.; Yang, H.K.; Park, J.; Kang, S.G.; Li, X.; et al. Relevance of a TCGA-derived Glioblastoma Subtype Gene-Classifer among Patient Populations. *Sci. Rep.* **2019**, *9*, 1–10, doi:10.1038/s41598-019-43173-y.
45. Lah, T.T.; Novak, M.; Breznik, B. Brain malignancies: Glioblastoma and brain metastases. *Semin. Cancer Biol.* **2020**, *60*, 262–273.
46. Matteoni, S.; Abbruzzese, C.; Villani, V.; Malorni, W.; Pace, A.; Matarrese, P.; Paggi, M.G. The Influence of Patient Sex on Clinical Approaches to Malignant Glioma. *Cancer Lett.* **2019**, doi:10.1016/j.canlet.2019.10.012.
47. Stupp, R.; Mason, W.P.; van den Bent, M.J.; Weller, M.; Fisher, B.; Taphoorn, M.J.B.; Belanger, K.; Brandes, A.A.; Marosi, C.; Bogdahn, U.; et al. Radiotherapy plus concomitant and adjuvant temozolomide for glioblastoma. *N. Engl. J. Med.* **2005**, *352*, 987–

- 996, doi:10.1056/NEJMoa043330.
48. Stupp, R.; van den Bent, M.J.; Hegi, M.E. Optimal role of temozolomide in the treatment of malignant gliomas. *Curr. Neurol. Neurosci. Rep.* **2005**, *5*, 198–206, doi:10.1007/s11910-005-0047-7.
49. Woo, P.M.; Li, Y.; Chan, A.Y.; Ng, S.P.; Loong, H.F.; Chan, D.M.; Wong, G.C.; Poon, W.-S. A multifaceted review of temozolomide resistance mechanisms in glioblastoma beyond O-6-methylguanine-DNA methyltransferase. *Glioma* **2019**, *2*, 68, doi:10.4103/glioma.glioma_3_19.
50. Lee, S.Y. Temozolomide resistance in glioblastoma multiforme. *Genes Dis.* **2016**, *3*, 198–210, doi:10.1016/J.GENDIS.2016.04.007.
51. Dunn, J.; Baborie, A.; Alam, F.; Joyce, K.; Moxham, M.; Sibson, R.; Crooks, D.; Husband, D.; Shenoy, A.; Brodbelt, A.; et al. Extent of MGMT promoter methylation correlates with outcome in glioblastomas given temozolomide and radiotherapy. *Br. J. Cancer* **2009**, *101*, 124–131, doi:10.1038/sj.bjc.6605127.
52. Friedl, P.; Wolf, K. Tumour-cell invasion and migration: diversity and escape mechanisms. *Nat. Rev. Cancer* **2003**, *3*, 362–74, doi:10.1038/nrc1075.
53. Trepap, X.; Chen, Z.; Jacobson, K. Cell migration. *Compr. Physiol.* **2012**, *2*, 2369–2392, doi:10.1002/cphy.c110012.
54. Cuddapah, V.A.; Robel, S.; Watkins, S.; Sontheimer, H. A neurocentric perspective on glioma invasion. *Nat. Rev. Neurosci.* **2014**, *15*, 455–465.
55. Goodwin, C.R.; Liang, L.; Abu-Bonsrah, N.; Hdeib, A.; Elder, B.D.; Kosztowski, T.; Bettegowda, C.; Laterra, J.; Burger, P.; Sciubba, D.M. Extraneural Glioblastoma Multiforme Vertebral Metastasis. *World Neurosurg.* **2016**, *89*, 578-582.e3, doi:10.1016/j.wneu.2015.11.061.
56. Kumar, V.; Singh, D.; Singh, H.; Saran, R.K. A case report of pontine glioblastoma presenting as subcutaneous metastasis in nape of neck in a child. *J. Pediatr. Neurosci.* **2015**, *10*, 386–8, doi:10.4103/1817-1745.174458.
57. Mart, A.; P, C.L.A. Hypoxic Cell Waves around Necrotic Cores in Glioblastoma: A Biomathematical Model and its Therapeutic Implications.
58. Mughal, A.A.; Zhang, L.; Fayzullin, A.; Server, A.; Li, Y.; Wu, Y.; Glass, R.; Meling, T.; Langmoen, I.A.; Leergaard, T.B.; et al. Patterns of Invasive Growth in Malignant Gliomas—The Hippocampus Emerges as an Invasion-Spared Brain Region. *Neoplasia (United States)* **2018**, *20*, 643–656, doi:10.1016/j.neo.2018.04.001.
59. Kim, J.; Lee, I.H.; Cho, H.J.; Park, C.K.; Jung, Y.S.; Kim, Y.; Nam, S.H.; Kim, B.S.; Johnson, M.D.; Kong, D.S.; et al. Spatiotemporal Evolution of the Primary Glioblastoma Genome. *Cancer Cell* **2015**, *28*, 318–328, doi:10.1016/j.ccell.2015.07.013.
60. Claes, A.; Idema, A.J.; Wesseling, P. Diffuse glioma growth: A guerilla war. *Acta*

- Neuropathol.* 2007, 114, 443–458.
61. Scherer, H.J. the American Journal of Cancer Volume Xxxiv November, 1938 Number 3 Structural Development in Gliomas. **1938**, XXXIV, doi:10.1158/ajc.1938.333.
 62. Vollmann-Zwerenz, A.; Leidgens, V.; Feliciello, G.; Klein, C.A.; Hau, P. Tumor cell invasion in glioblastoma. *Int. J. Mol. Sci.* **2020**, 21, 1–21, doi:10.3390/ijms21061932.
 63. Friedl, P.; Locker, J.; Sahai, E.; Segall, J.E. Classifying collective cancer cell invasion. *Nat. Cell Biol.* 2012, 14, 777–783.
 64. Friedl, P.; Gilmour, D. Collective cell migration in morphogenesis, regeneration and cancer. *Nat. Rev. Mol. Cell Biol.* 2009, 10, 445–457.
 65. te Boekhorst, V.; Friedl, P. Plasticity of Cancer Cell Invasion—Mechanisms and Implications for Therapy. In *Advances in Cancer Research*; Elsevier Inc., 2016; Vol. 132, pp. 209–264 ISBN 0065-230X.
 66. Machesky, L.M. Lamellipodia and filopodia in metastasis and invasion. *FEBS Lett.* **2008**, 582, 2102–2111, doi:10.1016/j.febslet.2008.03.039.
 67. Raftopoulou, M.; Hall, A. Cell migration: Rho GTPases lead the way. *Dev. Biol.* **2004**, 265, 23–32, doi:10.1016/j.ydbio.2003.06.003.
 68. Gritsenko, P.G.; Friedl, P. Adaptive adhesion systems mediate glioma cell invasion in complex environments. *J. Cell Sci.* **2018**, 131, doi:10.1242/jcs.216382.
 69. Serafim, R.B.; da Silva, P.; Cardoso, C.; Di Cristofaro, L.F.M.; Netto, R.P.; de Almeida, R.; Navegante, G.; Storti, C.B.; de Sousa, J.F.; de Souza, F.C.; et al. Expression Profiling of Glioblastoma Cell Lines Reveals Novel Extracellular Matrix-Receptor Genes Correlated With the Responsiveness of Glioma Patients to Ionizing Radiation. *Front. Oncol.* **2021**, 11, 1–14, doi:10.3389/fonc.2021.668090.
 70. Hagemann, C.; Anacker, J.; Ernestus, R.-I.; Vince, G.H. A complete compilation of matrix metalloproteinase expression in human malignant gliomas. *World J. Clin. Oncol.* **2012**, 3, 67–79, doi:10.5306/wjco.v3.i5.67.
 71. Seals, D.F.; Courtneidge, S.A. The ADAMs family of metalloproteases: Multidomain proteins with multiple functions. *Genes Dev.* **2003**, 17, 7–30, doi:10.1101/gad.1039703.
 72. Mentlein, R.; Hattermann, K.; Held-Feindt, J. Lost in disruption: Role of proteases in glioma invasion and progression. *Biochim. Biophys. Acta - Rev. Cancer* **2012**, 1825, 178–185, doi:10.1016/j.bbcan.2011.12.001.
 73. Guarino, M. Src signaling in cancer invasion. *J. Cell. Physiol.* **2010**, 223, 14–26, doi:10.1002/jcp.22011.
 74. McLendon, R.; Friedman, A.; Bigner, D.; Van Meir, E.G.; Brat, D.J.; Mastrogiannakis, G.M.; Olson, J.J.; Mikkelsen, T.; Lehman, N.; Aldape, K.; et al. Comprehensive genomic characterization defines human glioblastoma genes and core pathways. *Nature* **2008**, 455, 1061–1068, doi:10.1038/nature07385.

75. Du, J.; Bernasconi, P.; Clauser, K.R.; Mani, D.R.; Finn, S.P.; Beroukhir, R.; Burns, M.; Julian, B.; Peng, X.P.; Hieronymus, H.; et al. Bead-based profiling of tyrosine kinase phosphorylation identifies SRC as a potential target for glioblastoma therapy. *Nat. Biotechnol.* **2009**, *27*, 77–83, doi:10.1038/nbt.1513.
76. Ahluwalia, M.S.; Groot, J. de; Liu, W.M.; Gladson, C.L. Targeting SRC in glioblastoma tumors and brain metastases: Rationale and preclinical studies. *Cancer Lett.* **2010**, *298*, 139–149, doi:10.1016/J.CANLET.2010.08.014.
77. Fajer, M.; Meng, Y.; Roux, B. The Activation of c-Src Tyrosine Kinase: Conformational Transition Pathway and Free Energy Landscape. *J. Phys. Chem. B* **2017**, *121*, 3352–3363, doi:10.1021/acs.jpcc.6b08409.
78. Kurochkina, N.; Guha, U. SH3 domains: Modules of protein-protein interactions. *Biophys. Rev.* **2013**, *5*, 29–39, doi:10.1007/s12551-012-0081-z.
79. Bjorge, J.D.; Pang, A.; Fujita, D.J. Identification of protein-tyrosine phosphatase 1B as the major tyrosine phosphatase activity capable of dephosphorylating and activating c-Src in several human breast cancer cell lines. *J. Biol. Chem.* **2000**, *275*, 41439–41446, doi:10.1074/jbc.M004852200.
80. Pallen, C. Protein Tyrosine Phosphatase α (PTP α): A Src Family Kinase Activator and Mediator of Multiple Biological Effects. *Curr. Top. Med. Chem.* **2003**, *3*, 821–835, doi:10.2174/1568026033452320.
81. Sieg, D.J.; Hauck, C.R.; Schlaepfer, D.D. Required role of focal adhesion kinase (FAK) for integrin-stimulated cell migration. *J. Cell Sci.* **1999**, *112*, 2677–2691, doi:10.1242/JCS.112.16.2677.
82. Anand-Apte, B.; Zetter, B.R.; Viswanathan, A.; Qiu, R.G.; Chen, J.; Ruggieri, R.; Symons, M. Platelet-derived growth factor and fibronectin-stimulated migration are differentially regulated by the Rac and extracellular signal-regulated kinase pathways. *J. Biol. Chem.* **1997**, *272*, 30688–30692, doi:10.1074/JBC.272.49.30688.
83. Bello-Alvarez, C.; Zamora-Sánchez, C.J.; Camacho-Arroyo, I. Rapid Actions of the Nuclear Progesterone Receptor through cSrc in Cancer. *Cells* **2022**, *11*, 1964, doi:10.3390/cells11121964.
84. Mitra, S.K.; Hanson, D.A.; Schlaepfer, D.D. Focal adhesion kinase: In command and control of cell motility. *Nat. Rev. Mol. Cell Biol.* **2005**, *6*, 56–68, doi:10.1038/nrm1549.
85. Weaver, A.M. Invadopodia: Specialized cell structures for cancer invasion. *Clin. Exp. Metastasis* **2006**, *23*, 97–105, doi:10.1007/s10585-006-9014-1.
86. Di Renzo, G.C.; Tosto, V.; Tsibizova, V. Progesterone: History, facts, and artifacts. *Best Pract. Res. Clin. Obstet. Gynaecol.* **2020**, *69*, 2–12, doi:10.1016/j.bpobgyn.2020.07.012.
87. Marker, R.E.; Kamm, O. Sterols. IX. Isolation of epi-Pregnanol-3-one-20 from Human Pregnancy Urine. *J. Am. Chem. Soc.* **1937**, *59*, 616–618, doi:10.1021/ja01283a006.

88. Mellon, S.H. Neurosteroid regulation of central nervous system development. *Pharmacol. Ther.* **2007**, *116*, 107–124, doi:10.1016/J.PHARMTHERA.2007.04.011.
89. Paris, J.J.; Brunton, P.J.; Russell, J.A.; Walf, A.A.; Frye, C.A. Inhibition of 5 α -reductase activity in late pregnancy decreases gestational length and fecundity and impairs object memory and central progesterone milieu of juvenile rat offspring. *J. Neuroendocrinol.* **2011**, *23*, 1079–1090, doi:10.1111/j.1365-2826.2011.02219.x.
90. Brunton, P.J.; Russell, J.A.; Hirst, J.J. *Allopregnanolone in the brain: Protecting pregnancy and birth outcomes*; Elsevier Ltd, 2014; Vol. 113; ISBN 3154511277783.
91. Balan, I.; Aurelian, L.; Schleicher, R.; Boero, G.; O'Buckley, T.; Morrow, A.L. Neurosteroid allopregnanolone (3 α ,5 α -THP) inhibits inflammatory signals induced by activated MyD88-dependent toll-like receptors. *Transl. Psychiatry* **2021**, *11*, 1–11, doi:10.1038/s41398-021-01266-1.
92. He, J.; Evans, C.-O.; Hoffman, S.W.; Oyesiku, N.M.; Stein, D.G. Progesterone and allopregnanolone reduce inflammatory cytokines after traumatic brain injury. *Exp. Neurol.* **2004**, *189*, 404–12, doi:10.1016/j.expneurol.2004.06.008.
93. González-Orozco, J.C.; Camacho-Arroyo, I. Progesterone Actions During Central Nervous System Development. *Front. Neurosci.* **2019**, *13*, 503, doi:10.3389/fnins.2019.00503.
94. Wang, J.M.; Johnston, P.B.; Ball, B.G.; Brinton, R.D. The neurosteroid allopregnanolone promotes proliferation of rodent and human neural progenitor cells and regulates cell-cycle gene and protein expression. *J. Neurosci.* **2005**, *25*, 4706–4718, doi:10.1523/JNEUROSCI.4520-04.2005.
95. Falvo, E.; Diviccaro, S.; Melcangi, R.C.; Giatti, S. Physiopathological role of neuroactive steroids in the peripheral nervous system. *Int. J. Mol. Sci.* **2020**, *21*, 1–26, doi:10.3390/ijms21239000.
96. Liang, J.J.; Rasmusson, A.M. Overview of the Molecular Steps in Steroidogenesis of the GABAergic Neurosteroids Allopregnanolone and Pregnanolone. *Chronic Stress* **2018**, *2*, 247054701881855, doi:10.1177/2470547018818555.
97. Rižner, T.L.; Penning, T.M. Role of aldo-keto reductase family 1 (AKR1) enzymes in human steroid metabolism. *Steroids* **2014**, *79*, 49–63, doi:10.1016/j.steroids.2013.10.012.
98. Azzouni, F.; Godoy, A.; Li, Y.; Mohler, J. The 5 alpha-reductase isozyme family: a review of basic biology and their role in human diseases. *Adv. Urol.* **2012**, *2012*, 530121, doi:10.1155/2012/530121.
99. Stiles, A.R.; Russell, D.W. SRD5A3: A surprising role in glycosylation. *Cell* **2010**, *142*, 196–8, doi:10.1016/j.cell.2010.07.003.
100. Andersson, S.; Russell, D.W. Structural and biochemical properties of cloned and expressed human and rat steroid 5 α -reductases. *Proc. Natl. Acad. Sci. U. S. A.* **1990**, *87*, 3640–3644, doi:10.1073/pnas.87.10.3640.

101. Xiao, Q.; Wang, L.; Supekar, S.; Shen, T.; Liu, H.; Ye, F.; Huang, J.; Fan, H.; Wei, Z.; Zhang, C. Structure of human steroid 5 α -reductase 2 with the anti-androgen drug finasteride. *Nat. Commun.* 2020 111 **2020**, 11, 1–11, doi:10.1038/s41467-020-19249-z.
102. Russell, D.W.; Wilson, J.D. Steroid 5 α -Reductase: Two Genes/Two Enzymes. *Annu. Rev. Biochem.* **1994**, 63, 25–61, doi:10.1146/annurev.bi.63.070194.000325.
103. Melcangi, R.C.; Cavarretta, I.; Magnaghi, V.; Ballabio, M.; Martini, L.; Motta, M. Crosstalk between normal and tumoral brain cells. Effect on sex steroid metabolism. *Endocrine* **1998**, 8, 65–71, doi:10.1385/ENDO:8:1:65.
104. Zamora-Sánchez, C.J.; Camacho-Arroyo, I. Allopregnanolone: Metabolism, Mechanisms of Action, and Its Role in Cancer. *Int. J. Mol. Sci.* **2023**, 24, doi:10.3390/ijms24010560.
105. Melcangi, R.C.; Poletti, A.; Cavarretta, I.; Celotti, F.; Colciago, A.; Magnaghi, V.; Motta, M.; Negri-Cesi, P.; Martini, L. The 5 α -reductase in the central nervous system: expression and modes of control. *J. Steroid Biochem. Mol. Biol.* **1998**, 65, 295–299, doi:10.1016/S0960-0760(98)00030-2.
106. Melcangi, R.C.; Froelichsthal, P.; Martini, L.; Vescovi, A.L. Steroid metabolizing enzymes in pluripotential progenitor central nervous system cells: Effect of differentiation and maturation. *Neuroscience* **1996**, 72, 467–475, doi:10.1016/0306-4522(95)00522-6.
107. Mondragón, J.A.; Serrano, Y.; Torres, A.; Orozco, M.; Segovia, J.; Manjarrez, G.; Romano, M.C. Glioblastoma cells express crucial enzymes involved in androgen synthesis: 3 β -hydroxysteroid dehydrogenase, 17-20 α -hydroxylase, 17 β -hydroxysteroid dehydrogenase and 5 α -reductase. *Endocrinol. Diabetes Metab.* **2021**, 4, 1–9, doi:10.1002/edm2.289.
108. Pinacho-Garcia, L.M.; Valdez, R.A.; Navarrete, A.; Cabeza, M.; Segovia, J.; Romano, M.C. The effect of finasteride and dutasteride on the synthesis of neurosteroids by glioblastoma cells. *Steroids* **2020**, 155, 108556, doi:10.1016/j.steroids.2019.108556.
109. Penning, T.M.; Drury, J.E. Human aldo-keto reductases: Function, gene regulation, and single nucleotide polymorphisms. *Arch. Biochem. Biophys.* **2007**, 464, 241–250, doi:10.1016/j.abb.2007.04.024.
110. Penning, T.M.; Burczynski, M.E.; Jez, J.M.; Lin, H.-K.; Ma, H.; Moore, M.; Ratnam, K.; Palackal, N. Structure-function aspects and inhibitor design of type 5 17 β -hydroxysteroid dehydrogenase (AKR1C3). *Mol. Cell. Endocrinol.* **2001**, 171, 137–149, doi:10.1016/S0303-7207(00)00426-3.
111. Karavolas, H.J.; Hodges, D.; O'brien, D. Uptake of [3H]progesterone and [3H]5 α -dihydroprogesterone by rat tissues in vivo and analysis of accumulated radioactivity: Accumulation of 5 α -dihydroprogesterone by pituitary and hypothalamic tissues. *Endocrinology* **1976**, 98, 164–175, doi:10.1210/endo-98-1-164.
112. Belelli, D.; Gee, K.W. 5 α -pregnan-3 α ,20 α -diol behaves like a partial agonist in the modulation of GABA-stimulated chloride ion uptake by synaptoneuroosomes. *Eur. J. Pharmacol.* **1989**, 167, 173–176, doi:10.1016/0014-2999(89)90760-7.

113. Diviccaro, S.; Giatti, S.; Borgo, F.; Falvo, E.; Caruso, D.; Garcia-Segura, L.M.; Melcangi, R.C. Steroidogenic machinery in the adult rat colon. *J. Steroid Biochem. Mol. Biol.* **2020**, *203*, 105732, doi:10.1016/J.JSBMB.2020.105732.
114. Le Calvé, B.; Rynkowski, M.; Le Mercier, M.; Bruyère, C.; Lonez, C.; Gras, T.; Haibe-Kains, B.; Bontempi, G.; Decaestecker, C.; Ruyschaert, J.-M.; et al. Long-term In Vitro Treatment of Human Glioblastoma Cells with Temozolomide Increases Resistance In Vivo through Up-regulation of GLUT Transporter and Aldo-Keto Reductase Enzyme AKR1C Expression. *Neoplasia* **2010**, *12*, 727–739, doi:10.1593/neo.10526.
115. Lamba, V.; Yasuda, K.; Lamba, J.K.; Assem, M.; Davila, J.; Strom, S.; Schuetz, E.G. PXR (NR1I2): splice variants in human tissues, including brain, and identification of neurosteroids and nicotine as PXR activators. *Toxicol. Appl. Pharmacol.* **2004**, *199*, 251–265, doi:10.1016/J.TAAP.2003.12.027.
116. Chen, S.; Wang, J.M.; Irwin, R.W.; Yao, J.; Liu, L.; Brinton, R.D. Allopregnanolone Promotes Regeneration and Reduces β -Amyloid Burden in a Preclinical Model of Alzheimer's Disease. *PLoS One* **2011**, *6*, e24293, doi:10.1371/journal.pone.0024293.
117. Skandalaki, A.; Sarantis, P.; Theocharis, S. Pregnane x receptor (Pxr) polymorphisms and cancer treatment. *Biomolecules* **2021**, *11*, doi:10.3390/biom11081142.
118. Rigalli, J.P.; Tocchetti, G.N.; Weiss, J. Modulation of ABC Transporters by Nuclear Receptors: Physiological, Pathological and Pharmacological Aspects. *Curr. Med. Chem.* **2018**, *26*, 1079–1112, doi:10.2174/0929867324666170920141707.
119. Xing, Y.; Yan, J.; Niu, Y. PXR: a center of transcriptional regulation in cancer. *Acta Pharm. Sin. B* **2020**, *10*, 197–206, doi:10.1016/j.apsb.2019.06.012.
120. Chen, Z.W.; Bracamontes, J.R.; Budelier, M.M.; Germann, A.L.; Shin, D.J.; Kathiresan, K.; Qian, M.X.; Manion, B.; Cheng, W.W.L.; Reichert, D.E.; et al. Multiple functional neurosteroid binding sites on gabaa receptors. *PLoS Biol.* **2019**, *17*, 1–27, doi:10.1371/journal.pbio.3000157.
121. Kim, J.J.; Hibbs, R.E. Direct Structural Insights into GABAA Receptor Pharmacology. *Trends Biochem. Sci.* **2021**, *46*, 502–517, doi:10.1016/j.tibs.2021.01.011.
122. Hosie, A.M.; Wilkins, M.E.; Da Silva, H.M.A. a; Smart, T.G. Endogenous neurosteroids regulate GABAA receptors through two discrete transmembrane sites. *Nature* **2006**, *444*, 486–489, doi:10.1038/nature05324.
123. Sugasawa, Y.; Cheng, W.W.L.; Bracamontes, J.R.; Chen, Z.W.; Wang, L.; Germann, A.L.; Pierce, S.R.; Senneff, T.C.; Krishnan, K.; Reichert, D.E.; et al. Site-specific effects of neurosteroids on gabaa receptor activation and desensitization. *Elife* **2020**, *9*, 1–32, doi:10.7554/ELIFE.55331.
124. Liu, Q.-Y.; Chang, Y.H.; Schaffner, A.E.; Smith, S. V.; Barker, J.L. Allopregnanolone Activates GABA_A Receptor/Cl⁻ Channels in a Multiphasic Manner in Embryonic Rat Hippocampal Neurons. *J. Neurophysiol.* **2002**, *88*, 1147–1158, doi:10.1152/jn.00942.2001.

125. Hosie, A.M.; Wilkins, M.E.; Smart, T.G. Neurosteroid binding sites on GABAA receptors. *Pharmacol. Ther.* **2007**, *116*, 7–19, doi:10.1016/j.pharmthera.2007.03.011.
126. Abramian, A.M.; Comenencia-Ortiz, E.; Modgil, A.; Vien, T.N.; Nakamura, Y.; Moore, Y.E.; Maguire, J.L.; Terunuma, M.; Davies, P.A.; Moss, S.J. Neurosteroids promote phosphorylation and membrane insertion of extrasynaptic GABAA receptors. *Proc. Natl. Acad. Sci. U. S. A.* **2014**, *111*, 7132–7137, doi:10.1073/pnas.1403285111.
127. Brinton, R.D. Neurosteroids as regenerative agents in the brain: therapeutic implications. *Nat. Rev. Endocrinol.* **2013**, *9*, 241–50, doi:10.1038/nrendo.2013.31.
128. Magnaghi, V.; Parducz, A.; Frasca, A.; Ballabio, M.; Procacci, P.; Racagni, G.; Bonanno, G.; Fumagalli, F. GABA synthesis in Schwann cells is induced by the neuroactive steroid allopregnanolone. *J. Neurochem.* **2010**, *112*, 980–990, doi:10.1111/j.1471-4159.2009.06512.x.
129. Behar, T.N.; Li, Y.X.; Tran, H.T.; Ma, W.; Dunlap, V.; Scott, C.; Barker, J.L. GABA stimulates chemotaxis and chemokinesis of embryonic cortical neurons via calcium-dependent mechanisms. *J. Neurosci.* **1996**, *16*, 1808–1818, doi:10.1523/jneurosci.16-05-01808.1996.
130. Heck, N.; Kilb, W.; Reiprich, P.; Kubota, H.; Furukawa, T.; Fukuda, A.; Luhmann, H.J. GABA-A receptors regulate neocortical neuronal migration in vitro and in vivo. *Cereb. Cortex* **2007**, *17*, 138–148, doi:10.1093/cercor/bhj135.
131. Mejia-Gervacio, S.; Murray, K.; Lledo, P.M. NKCC1 controls GABAergic signaling and neuroblast migration in the postnatal forebrain. *Neural Dev.* **2011**, *6*, 24–27, doi:10.1186/1749-8104-6-4.
132. Ma, H.; Li, T.; Tao, Z.; Hai, L.; Tong, L.; Yi, L.; Abeysekera, I.R.; Liu, P.; Xie, Y.; Li, J.; et al. NKCC1 promotes EMT-like process in GBM via RhoA and Rac1 signaling pathways. *J. Cell. Physiol.* **2019**, *234*, 1630–1642, doi:10.1002/jcp.27033.
133. Cáceres, A.R.R.; Vega Orozco, A.S.; Cabrera, R.J.; Laconi, M.R. Rapid actions of the neurosteroid allopregnanolone on ovarian and hypothalamic steroidogenesis: Central and peripheral modulation. *J. Neuroendocrinol.* **2020**, *32*, 1–13, doi:10.1111/jne.12836.
134. Cáceres, A.R.R.; Campo Verde Arboccó, F.; Cardone, D.A.; Sanhueza, M. de los Á.; Casais, M.; Vega Orozco, A.S.; Laconi, M.R. Superior mesenteric ganglion neural modulation of ovarian angiogenesis, apoptosis and proliferation by the neuroactive steroid allopregnanolone. *J. Neuroendocrinol.* **2022**, *34*, e13056, doi:10.1111/JNE.13056.
135. Valadez-Cosmes, P.; Vázquez-Martínez, E.R.; Cerbón, M.; Camacho-Arroyo, I. Membrane progesterone receptors in reproduction and cancer. *Mol. Cell. Endocrinol.* **2016**, *434*, 166–175, doi:10.1016/j.mce.2016.06.027.
136. Thomas, P. Membrane Progesterone Receptors (mPRs, PAQRs): Review of Structural and Signaling Characteristics. *Cells* **2022**, *11*, 1785, doi:10.3390/cells11111785.
137. Moussatche, P.; Lyons, T.J. Non-genomic progesterone signalling and its non-canonical receptor. *Biochem. Soc. Trans.* **2012**, *40*, 200–204, doi:10.1042/BST20110638.

138. Thomas, P.; Pang, Y.; Dong, J.; Groenen, P.; Kelder, J.; de Vlieg, J.; Zhu, Y.; Tubbs, C. Steroid and G protein binding characteristics of the seatrout and human progesterin membrane receptor α subtypes and their evolutionary origins. *Endocrinology* **2007**, *148*, 705–718, doi:10.1210/en.2006-0974.
139. Pang, Y.; Dong, J.; Thomas, P. Characterization, neurosteroid binding and brain distribution of human membrane progesterone receptors δ and ϵ (mPR δ and mPR ϵ) and mPR δ involvement in neurosteroid inhibition of apoptosis. *Endocrinology* **2013**, *154*, 283–295, doi:10.1210/en.2012-1772.
140. Valadez-Cosmes, P.; Germán-Castelán, L.; González-Arenas, A.; Velasco-Velázquez, M.A.; Hansberg-Pastor, V.; Camacho-Arroyo, I. Expression and hormonal regulation of membrane progesterone receptors in human astrocytoma cells. *J. Steroid Biochem. Mol. Biol.* **2015**, *154*, 176–185, doi:10.1016/j.jsbmb.2015.08.006.
141. Del Moral-Morales, A.; González-Orozco, J.C.; Capetillo-Velázquez, J.M.; Piña-Medina, A.G.; Camacho-Arroyo, I. The Role of mPR δ and mPR ϵ in Human Glioblastoma Cells: Expression, Hormonal Regulation, and Possible Clinical Outcome. *Horm. Cancer* **2020**, *11*, 117–127, doi:10.1007/s12672-020-00381-7.
142. Thomas, P.; Pang, Y. Membrane progesterone receptors: evidence for neuroprotective, neurosteroid signaling and neuroendocrine functions in neuronal cells. *Neuroendocrinology* **2012**, *96*, 162–171, doi:10.1159/000339822.
143. Castelnovo, L.F.; Caffino, L.; Bonalume, V.; Fumagalli, F.; Thomas, P.; Magnaghi, V. Membrane Progesterone Receptors (mPRs/PAQRs) Differently Regulate Migration, Proliferation, and Differentiation in Rat Schwann Cells. *J. Mol. Neurosci.* **2020**, *70*, 433–448, doi:10.1007/S12031-019-01433-6/FIGURES/9.
144. Mosher, L.J.; Cadeddu, R.; Yen, S.; Staudinger, J.L.; Traccis, F.; Fowler, S.C.; Maguire, J.L.; Bortolato, M. Allopregnanolone is required for prepulse inhibition deficits induced by D1 dopamine receptor activation. *Psychoneuroendocrinology* **2019**, *108*, 53–61, doi:10.1016/j.psyneuen.2019.06.009.
145. Giuliani, F.A.; Yunes, R.; Mohn, C.E.; Laconi, M.; Rettori, V.; Cabrera, R. Allopregnanolone induces LHRH and glutamate release through NMDA receptor modulation. *Endocrine* **2011**, *40*, 21–26, doi:10.1007/s12020-011-9451-8.
146. Rupprecht, R.; Reul, J.M.H.M.; Trapp, T.; Steensel, B. van; Wetzel, C.; Damm, K.; Ziegglänsberger, W.; Holsboer, F. Progesterone receptor-mediated effects of neuroactive steroids. *Neuron* **1993**, *11*, 523–530, doi:10.1016/0896-6273(93)90156-L.
147. Ignacio Camacho-Arroyo, Valeria Hansberg-Pastor, Edgar Ricardo Vázquez-Martínez, M.C. Mechanism of Progesterone Action in the Brain. In *Hormones, Brain and Behavior*; 2017; Vol. 3, pp. 181–214 ISBN 9780128035924.
148. Bello-Alvarez, C.; Moral-Morales, A. Del; González-Arenas, A.; Camacho-Arroyo, I. Intracellular Progesterone Receptor and cSrc Protein Working Together to Regulate the Activity of Proteins Involved in Migration and Invasion of Human Glioblastoma Cells.

- Front. Endocrinol. (Lausanne)*. **2021**, *12*, 1, doi:10.3389/fendo.2021.640298.
149. Charalampopoulos, I.; Tsatsanis, C.; Dermitzaki, E.; Alexaki, V.I.; Castanas, E.; Margioris, A.N.; Gravanis, A. Dehydroepiandrosterone and allopregnanolone protect sympathoadrenal medulla cells against apoptosis via antiapoptotic Bcl-2 proteins. *Proc. Natl. Acad. Sci. U. S. A.* **2004**, *101*, 8209–8214, doi:10.1073/pnas.0306631101.
150. Pelegrina, L.T.; de los Ángeles Sanhueza, M.; Ramona Cáceres, A.R.; Cuello-Carrión, D.; Rodríguez, C.E.; Laconi, M.R. Effect of progesterone and first evidence about allopregnanolone action on the progression of epithelial human ovarian cancer cell lines. *J. Steroid Biochem. Mol. Biol.* **2020**, *196*, 105492, doi:10.1016/j.jsbmb.2019.105492.
151. Tserfas, M.O.; Levina, I.S.; Kuznetsov, Y. V.; Scherbakov, A.M.; Mikhaevich, E.I.; Zavarzin, I. V. Selective synthesis of the two main progesterone metabolites, 3 α -hydroxy-5 α -pregnanolone (allopregnanolone) and 3 α -hydroxypregn-4-en-20-one, and an assessment of their effect on proliferation of hormone-dependent human breast cancer cells. *Russ. Chem. Bull.* **2020**, *69*, 552–557, doi:10.1007/s11172-020-2797-4.
152. Feng, Y.-H.; Lim, S.-W.; Lin, H.-Y.; Wang, S.-A.; Hsu, S.-P.; Kao, T.-J.; Ko, C.-Y.; Hsu, T.-I. Allopregnanolone suppresses glioblastoma survival through decreasing DPYSL3 and S100A11 expression. *J. Steroid Biochem. Mol. Biol.* **2022**, *219*, 106067, doi:10.1016/j.jsbmb.2022.106067.
153. Thomas, P.; Pang, Y. Anti-apoptotic Actions of Allopregnanolone and Ganaxolone Mediated Through Membrane Progesterone Receptors (PAQRs) in Neuronal Cells. *Front. Endocrinol. (Lausanne)*. **2020**, *11*, 1–9, doi:10.3389/fendo.2020.00417.
154. Taleb, O.; Patte-Mensah, C.; Meyer, L.; Kemmel, V.; Geoffroy, P.; Miesch, M.; Mensah-Nyagan, A. -G.; Patte-Mensah, C.; Meyer, L.; Kemmel, V.; et al. Evidence for effective structure-based neuromodulatory effects of new analogues of neurosteroid allopregnanolone. *J. Neuroendocrinol.* **2018**, *30*, e12568, doi:10.1111/jne.12568.
155. Karout, M.; Miesch, M.; Geoffroy, P.; Kraft, S.; Hofmann, H.D.; Mensah-Nyagan, A.G.; Kirsch, M. Novel analogs of allopregnanolone show improved efficiency and specificity in neuroprotection and stimulation of proliferation. *J. Neurochem.* **2016**, *139*, 782–794, doi:10.1111/jnc.13693.
156. Motaln, H.; Koren, A.; Gruden, K.; Ramšak, Ž.; Schichor, C.; Lah, T.T. Heterogeneous glioblastoma cell cross-talk promotes phenotype alterations and enhanced drug resistance. *Oncotarget* **2015**, *6*, 40998–41017, doi:10.18632/oncotarget.5701.
157. Wu, Y.; Fletcher, M.; Gu, Z.; Wang, Q.; Costa, B.; Bertoni, A.; Man, K.H.; Schlotter, M.; Felsberg, J.; Mangei, J.; et al. Glioblastoma epigenome profiling identifies SOX10 as a master regulator of molecular tumour subtype. *Nat. Commun.* **2020**, *11*, doi:10.1038/s41467-020-20225-w.
158. Piña-Medina, A.G.; Hansberg-Pastor, V.; González-Arenas, A.; Cerbón, M.; Camacho-Arroyo, I. Progesterone promotes cell migration, invasion and cofilin activation in human astrocytoma cells. *Steroids* **2016**, *105*, 19–25, doi:10.1016/j.steroids.2015.11.008.

159. Germán-Castelán, L.; Manjarrez-Marmolejo, J.; González-Arenas, A.; González-Morán, M.G.; Camacho-Arroyo, I. Progesterone induces the growth and infiltration of human astrocytoma cells implanted in the cerebral cortex of the rat. *Biomed Res. Int.* **2014**, *2014*, 393174, doi:10.1155/2014/393174.
160. Schmittgen, T.D.; Livak, K.J. Analyzing real-time PCR data by the comparative CT method. *Nat. Protoc.* **2008**, *3*, 1101–1108, doi:10.1038/nprot.2008.73.
161. Wiebe, J.P.; Beausoleil, M.; Zhang, G.; Cialacu, V. Opposing actions of the progesterone metabolites, 5 α -dihydroprogesterone (5 α P) and 3 α -dihydroprogesterone (3 α HP) on mitosis, apoptosis, and expression of Bcl-2, Bax and p21 in human breast cell lines. *J. Steroid Biochem. Mol. Biol.* **2010**, *118*, 125–132, doi:10.1016/j.jsbmb.2009.11.005.
162. Wiebe, J.P.; Lewis, M.J. Activity and expression of progesterone metabolizing 5 α -reductase, 20 α -hydroxysteroid oxidoreductase and 3 α 9(β -hydroxysteroid oxidoreductase in tumorigenic (MCF-7, MDA-MB-231, T-47D) and nontumorigenic (MCF-10A) human breast cancer cells. *BMC Cancer* **2003**, *3*, 9, doi:10.1186/1471-2407-3-9.
163. Wiebe, J.P.; Rivas, M.A.; Mercogliano, M.F.; Elizalde, P. V.; Schillaci, R. Progesterone-induced stimulation of mammary tumorigenesis is due to the progesterone metabolite, 5 α -dihydroprogesterone (5 α P) and can be suppressed by the 5 α -reductase inhibitor, finasteride. *J. Steroid Biochem. Mol. Biol.* **2015**, *149*, 27–34, doi:10.1016/j.jsbmb.2015.01.004.
164. Corpéchet, C.; Synguelakis, M.; Talha, S.; Axelson, M.; Sjövall, J.; Vihko, R.; Baulieu, E.E.; Robel, P. Pregnenolone and its sulfate ester in the rat brain. *Brain Res.* **1983**, *270*, 119–125, doi:10.1016/0006-8993(83)90797-7.
165. Germán-Castelán, L.; Manjarrez-Marmolejo, J.; González-Arenas, A.; Camacho-Arroyo, I. Intracellular Progesterone Receptor Mediates the Increase in Glioblastoma Growth Induced by Progesterone in the Rat Brain. *Arch. Med. Res.* **2016**, *47*, 419–426, doi:10.1016/j.arcmed.2016.10.002.
166. Bixo, M.; Andersson, A.; Winblad, B.; Purdy, R.H.; Bäckström, T. Progesterone, 5 α -pregnane-3,20-dione and 3 α -hydroxy-5 α -pregnane-20-one in specific regions of the human female brain in different endocrine states. *Brain Res.* **1997**, *764*, 173–178, doi:10.1016/S0006-8993(97)00455-1.
167. Marx, C.E.; Trost, W.T.; Shampine, L.J.; Stevens, R.D.; Hulette, C.M.; Steffens, D.C.; Ervin, J.F.; Butterfield, M.I.; Blazer, D.G.; Massing, M.W.; et al. The Neurosteroid Allopregnanolone Is Reduced in Prefrontal Cortex in Alzheimer's Disease. *Biol. Psychiatry* **2006**, *60*, 1287–1294, doi:10.1016/J.BIOPSYCH.2006.06.017.
168. Naylor, J.C.; Kilts, J.D.; Hulette, C.M.; Steffens, D.C.; Blazer, D.G.; Ervin, J.F.; Strauss, J.L.; Allen, T.B.; Massing, M.W.; Payne, V.M.; et al. Allopregnanolone levels are reduced in temporal cortex in patients with Alzheimer's disease compared to cognitively intact control subjects. *Biochim. Biophys. Acta - Mol. Cell Biol. Lipids* **2010**, *1801*, 951–959, doi:10.1016/J.BBALIP.2010.05.006.
169. Atif, F.; Yousuf, S.; Stein, D.G. Anti-tumor effects of progesterone in human glioblastoma

- multiforme: Role of PI3K/Akt/mTOR signaling. *J. Steroid Biochem. Mol. Biol.* **2015**, *146*, doi:10.1016/j.jsbmb.2014.04.007.
170. Atif, F.; Patel, N.R.; Yousuf, S.; Stein, D.G. The synergistic effect of combination progesterone and temozolomide on human glioblastoma cells. *PLoS One* **2015**, *10*, doi:10.1371/journal.pone.0131441.
171. Penning, T.M.; Burczynski, M.E.; JEZ, J.M.; HUNG, C.-F.F.; Lin, H.-K.K.; MA, H.; MOORE, M.; PALACKAL, N.; Ratnam, K. Human 3 α -hydroxysteroid dehydrogenase isoforms (AKR1C1-AKR1C4) of the aldo-keto reductase superfamily: Functional plasticity and tissue distribution reveals roles in the inactivation and formation of male and female sex hormones. *Biochem. J.* **2000**, *351*, 67–77, doi:10.1042/0264-6021:3510067.
172. Yang, L.; Zhang, J.; Zhang, S.; Dong, W.; Lou, X.; Liu, S. Quantitative evaluation of aldo-keto reductase expression in hepatocellular carcinoma (HCC) cell lines. *Genomics. Proteomics Bioinformatics* **2013**, *11*, 230–40, doi:10.1016/j.gpb.2013.04.001.
173. Zeng, C.-M.M.; Chang, L.-L.L.; Ying, M.-D.D.; Cao, J.; He, Q.-J.J.; Zhu, H.; Yang, B. Aldo-keto reductase AKR1C1-AKR1C4: Functions, regulation, and intervention for anti-cancer therapy. *Front. Pharmacol.* **2017**, *8*, 1–9, doi:10.3389/fphar.2017.00119.
174. Sinreih, M.; Anko, M.; Zukunft, S.; Adamski, J.; Rižner, T.L. Important roles of the AKR1C2 and SRD5A1 enzymes in progesterone metabolism in endometrial cancer model cell lines. *Chem. Biol. Interact.* **2015**, *234*, 297–308, doi:10.1016/j.cbi.2014.11.012.
175. Yang, S.Y.; He, X.Y.; Isaacs, C.; Dobkin, C.; Miller, D.; Philipp, M. Roles of 17 β -hydroxysteroid dehydrogenase type 10 in neurodegenerative disorders. *J. Steroid Biochem. Mol. Biol.* **2014**, *143*, 460–472, doi:10.1016/j.jsbmb.2014.07.001.
176. Hermawan, A.; Putri, H. Systematic analysis of potential targets of the curcumin analog pentagamavunon-1 (PGV-1) in overcoming resistance of glioblastoma cells to bevacizumab. *Saudi Pharm. J.* **2021**, *29*, 1289–1302, doi:10.1016/j.jsps.2021.09.015.
177. Frye, C.A.; Koonce, C.J.; Walf, A.A. The pregnane xenobiotic receptor, a prominent liver factor, has actions in the midbrain for neurosteroid synthesis and behavioral/neural plasticity of female rats. *Front. Syst. Neurosci.* **2014**, *8*, 1–12, doi:10.3389/fnsys.2014.00060.
178. Magnaghi, V.; Ballabio, M.; Consoli, A.; Lambert, J.J.; Roglio, I.; Melcangi, R.C. GABA receptor-mediated effects in the peripheral nervous system. *J. Mol. Neurosci.* **2006**, *281*, 2006, *28*, 89–102, doi:10.1385/JMN:28:1:89.
179. Cucchiara, F.; Pasqualetti, F.; Giorgi, F.S.; Danesi, R.; Bocci, G. Epileptogenesis and oncogenesis: An antineoplastic role for antiepileptic drugs in brain tumours? *Pharmacol. Res.* **2020**, *156*, doi:10.1016/J.PHRS.2020.104786.
180. Hujber, Z.; Horváth, G.; Petovári, G.; Krencz, I.; Dankó, T.; Mészáros, K.; Rajnai, H.; Szoboszlai, N.; Leenders, W.P.J.; Jeney, A.; et al. GABA, glutamine, glutamate oxidation and succinic semialdehyde dehydrogenase expression in human gliomas. *J. Exp. Clin. Cancer Res.* **2018**, *37*, 1–12, doi:10.1186/s13046-018-0946-5.

181. Castelnovo, L.F.; Thomas, P. Membrane progesterone receptor α (mPR α /PAQR7) promotes migration, proliferation and BDNF release in human Schwann cell-like differentiated adipose stem cells. *Mol. Cell. Endocrinol.* **2021**, *531*, 111298, doi:10.1016/j.mce.2021.111298.
182. González-Orozco, J.C.; Hansberg-Pastor, V.; Valadez-Cosmes, P.; Nicolas-Ortega, W.; Bastida-Beristain, Y.; Fuente-Granada, M.D. La; González-Arenas, A.; Camacho-Arroyo, I. Activation of membrane progesterone receptor-alpha increases proliferation, migration, and invasion of human glioblastoma cells. *Mol. Cell. Endocrinol.* **2018**, *477*, 81–89, doi:10.1016/J.MCE.2018.06.004.
183. Narang, V.S.; Fraga, C.; Kumar, N.; Shen, J.; Throm, S.; Stewart, C.F.; Waters, C.M. Dexamethasone increases expression and activity of multidrug resistance transporters at the rat blood-brain barrier. *Am. J. Physiol. - Cell Physiol.* **2008**, *295*, 440–450, doi:10.1152/ajpcell.00491.2007.
184. González-Flores, O.; Beyer, C.; Gómora-Arrati, P.; García-Juárez, M.; Lima-Hernández, F.J.; Soto-Sánchez, A.; Etgen, A.M. A role for Src kinase in progestin facilitation of estrous behavior in estradiol-primed female rats. *Horm. Behav.* **2010**, *58*, 223–229, doi:10.1016/J.YHBEH.2010.03.014.

15 ANEXOS

15.1 Características de las líneas celulares utilizadas

Tabla 7. Origen y características generales de las líneas celulares utilizadas.

No. ATCC	Línea celular	Origen del tumor	Etnia/Sexo	Edad	Fecha de aislamiento
	U251	Cerebro	Caucásico/M	75	Obtenidas de paciente en 1973
HTB-14™	U87	Cerebro	Caucásico/M	44	Depositadas en 1966; Clasificadas como tipo- GB en 2007
CRL-2611™	LN229	Cerebro/corteza derecha frontal parieto-occipital	Blanco /F	60	Obtenidas de paciente en 1979

M: Masculino; F: Femenino

Tabla 8. Características morfológicas y genéticas de las células utilizadas.

Línea celular	Morfología (Tiempo de duplicación)	Subtipo de GB más parecido	Características genéticas
U251	Tipo fibroblasto; adherentes	Proneural/ Mesenquimal	CDKN2A delección homocigota Amplificación del locus de EGFR PTEN mutada p16 deletado p14ARF deletado
U87	Epiteliales; adherentes	Proneural	Hipodiplide. Numero modal de cromosomas: 44 en el 48 % de las células. CDKN2A mutada (471del471) PTEN mutada (+1G > T, codón 209) CDKN2C mutada (507del507)
LN229	Epiteliales; adherentes	Proneural/ Mesenquimal	p53 + mutada (CCT [Pro] > CTT [Leu], codón 98) PTEN + silvestre p16 deletado p14ARF deletado

15.2 Artículos derivados del proyecto de doctorado



5 α -dihydroprogesterone promotes proliferation and migration of human glioblastoma cells



Carmen J. Zamora-Sánchez^a, Ana M. Hernández-Vega^a, Saúl Gaona-Domínguez^a,
Mauricio Rodríguez-Dorantes^b, Ignacio Camacho-Arroyo^{a,*}

^a Unidad de Investigación en Reproducción Humana, Instituto Nacional de Perinatología-Facultad de Química, Universidad Nacional Autónoma de México (UNAM), Mexico

^b Instituto Nacional de Medicina Genómica (INMEGEN), Periférico Sur No. 4809, Col. Arenal Tepepan, Delegación Tlalpan, C.P. 14610 Ciudad de Mexico, Mexico

ARTICLE INFO

Keywords:

Progesterone metabolites
Dihydroprogesterone
Cancer
Mifepristone
Glioblastoma
Progesterone receptor

ABSTRACT

Glioblastomas (GBMs) are the most common and deadliest intracranial tumors. Steroid hormones, such as progesterone (P4), at physiological concentrations, promote proliferation, and migration of human GBM cells in vivo and in vitro. Neuronal and glial cells, but also GBMs, metabolize P4 and synthesize different active metabolites such as 5 α -dihydroprogesterone (5 α -DHP). However, their contribution to GBM malignancy remains unknown. Here, we determined the 5 α -DHP effects on the number of cells, proliferation, and migration of the U87 and U251 human GBM-derived cell lines. Of the tested concentrations (1 nM–1 μ M), 5 α -DHP 10 nM significantly increased the number of U87 and U251 cells from day 2 of treatment, and proliferation (at day 3) in a similar manner as P4 (10 nM). The treatment with the progesterone receptor (PR) antagonist RU486 (mifepristone), blocked the effects of 5 α -DHP on the number of cells and proliferation. Besides, in U251 and LN229 GBM cells, 5 α -DHP promoted cell migration (from 12 to 24 h). We also determined that GBM cells expressed the 3 α -hydroxysteroid oxidoreductases (3 α -HSOR), which reversibly reduce 5 α -DHP to allopregnanolone (3 α -THP). These data indicate that 5 α -DHP induces proliferation and migration of human GBM through the activation of PR.

1. Introduction

High-grade astrocytomas (WHO grade IV), also known as glioblastomas (GBMs) are the most common primary malignant brain tumors [1]. Progesterone (P4) has been considered as a vital steroid hormone involved in the maintenance of GBMs because it promotes proliferation, migration, and invasion at physiological concentrations [2–5].

Neuronal and glial cells have steroidogenic activity. In the central nervous system (CNS), steroid hormones are synthesized from intermediaries present in the circulation such as pregnenolone, or by de novo biosynthesis from cholesterol [6–8]. P4 is formed throughout the brain tissue and metabolized in neuroactive steroids such as 5 α -dihydroprogesterone (5 α -DHP), and 3 α , 5 α -tetrahydroprogesterone (3 α -THP, allopregnanolone) [8–11]. Such metabolites participate in a wide variety of physiological and pathological processes within brain tissue, due to the regulation of different mechanisms of action [12,13].

5 α -DHP is a C21-steroid with two ketone groups at C3 and C20. It is synthesized by the 5 α -reductase (5 α R) by neurons and glial cells [14].

5 α R reduces the double bond between the C4 and C5 of P4, giving rise to 5 α -DHP. Besides, 5 α -DHP is reversibly reduced to 3 α -THP by the enzymes 3 α -hydroxysteroid oxidoreductases (3 α -HSOR) [15]. During menstrual cycle and pregnancy, the levels of 5 α -DHP present fluctuations similar to those of P4 in plasma and the brain tissue [16–18], and both steroids accumulate in brain areas such as hypothalamus and cortex [19,20]. Although the function of 5 α -DHP has been less studied than that of P4 or 3 α -THP, there are reports indicating that 5 α -DHP promotes the expression of myelination proteins [21], and exhibits anti-seizure actions [22]. In a study conducted in 1998 by Melcangi et al., the formation of 5 α -DHP in rat C6 glioma cells and 1321 N1, a subclone of the human GBM cell line U-118MG, was significantly greater than in rat astrocytes and neurons [11]. Nevertheless, the influence of P4 metabolites in such malignancies is understudied until now.

Little is known about the role of 5 α -DHP in the regulation of intracellular signaling pathways and gene expression in the CNS, neither its effects on brain malignant tumors. 5 α -DHP binds with a high affinity to the intracellular progesterone receptor (PR) [23,24], a ligand-activated transcription factor, which also has extranuclear effects by

* Corresponding author.

E-mail addresses: mrodriguez@inmegen.gob.mx (M. Rodríguez-Dorantes), camachoarroyo@gmail.com (I. Camacho-Arroyo).

<https://doi.org/10.1016/j.steroids.2020.108708>

Received 10 April 2020; Received in revised form 12 July 2020; Accepted 22 July 2020

Available online 28 July 2020

0039-128X/ © 2020 Elsevier Inc. All rights reserved.

activating transduction pathways as Src/Ras/MEK/ERK and Rho/Rho-associated kinase complexes [25–28]. Moreover, 5 α -DHP binds to the membrane progesterone receptor α (mPR α), which regulates the activation of different signaling pathways by the generation of second messengers that act through transactivation of coactivators and transcription factors [29,30]. There is evidence about PR expression in high-grade astrocytomas, suggesting that PR-positive tumors have a high proliferative potential [31,32]. We have reported the content of PR-B and PR-A proteins as well as their transcriptional activity at 48 h of treatment with P4, besides, such activity was correlated with an augment in PR phosphorylation by PKC [33]. We also have reported the expression of mPRs in human GBM cell lines [34,35], and the involvement of the mPR α in promoting cell proliferation, migration and invasion along with the activation of Src and Akt [36]. Considering that 5 α -DHP also binds to both PR and mPR, it is likely that this metabolite has effects on the malignancy progression of GBM. In this study, we determined the impact of 5 α -DHP via PR, on the number of cells, proliferation, and migration of human GBM cells.

2. Material and methods

2.1. Cell culture and treatments

The human glioblastoma cell lines U251, U87, LN229, and T98G (ATCC, VA, USA) were cultured in Dulbecco's Modified Eagle's medium (DMEM) High Glucose (In vitro, Mexico City), supplemented with 10% fetal bovine serum (FBS), one mM pyruvate, two mM glutamine, and 0.1 mM of non-essential amino acids, at 37 °C in a humidified 5% CO₂ atmosphere. A different number of cells was plated, as indicated in each performed method. Twenty four h before steroid treatments, the culture medium was replaced with DMEM high glucose phenol red-free medium supplemented with 10% charcoal-stripped FBS. Treatments for cell growth experiments were: P4 (10 nM), 5 α -DHP (1, 10, 100 nM, and 1 μ M), and vehicle (ethanol 0.1%). Treatments for cell proliferation, and migration assays were: P4 (10 nM), 5 α -DHP (10 nM), RU486 (1 μ M), 5 α -DHP + RU486 (10 nM and 1 μ M, respectively), vehicle (ethanol 0.1%). When conjunct treatments were performed, RU486 was added one h before to the 5 α -DHP stimulus. All steroids were purchased from Sigma Aldrich (St. Louis, MO, USA), whereas ethanol was purchased from AMPEX CHEMICALS (NL, Mexico).

2.2. Cell growth

10 \times 10⁴ cells of each line were plated in 24-well plates. Cells were harvested with 1 mL PBS-EDTA 1 mM every day during five consecutive days of treatment. After resuspension, ten μ L of 0.4% trypan blue solution was added to each well. We determined the number of live and dead cells by the trypan blue dye exclusion assay with a hemocytometer and the microscope Olympus BX41 (Olympus, PA, USA).

2.3. Cell proliferation assays

3 \times 10³ cells of each line were plated in 4-well glass slides. Cells were treated during 72 h with: P4 (10 nM), 5 α -DHP (10 nM), RU 486 (1 μ M), 5 α -DHP + RU486, and vehicle (V, ethanol 0.1%). Cell proliferation was determined with the 5-Bromo-2'-deoxyuridine (BrdU) incorporation kit (11296736001 Roche, IN, USA) according to the manufacturer's recommendations. Besides, nuclei were stained with Hoechst 33342 solution (1 μ g/mL). The fluorescence signal of Hoechst 33342 and positive BrdU cells was observed in the Olympus Bx43F microscope (Olympus, PA, USA). Cell counting of total and BrdU positive cells was done with the ImageJ software 1.455 (National Institutes of Health, USA).

2.4. Migration

The wound-healing assay was performed to determine cell migration in U251, U87, and LN229 glioblastoma cells. In 6-well slides 2x10⁵ were plated in each well. After 24 h of cell culture in phenol red-free DMEM supplemented with 10% charcoal-stripped FBS. The scratch was performed with a 200 μ L pipette tip, and the removed cells were washed with PBS. Before cells were treated with P4 (10 nM), 5 α -DHP (10 nM), RU486 (1 μ M), 5 α -DHP + RU486, and vehicle (V, ethanol 0.1%), a pre-treatment with cytosine β -D-arabinofuranoside hydrochloride (AraC, ten μ M, Sigma Aldrich) during 1 h was added to inhibit cell proliferation. Four random fields were chosen per treatment to determine the cell migration after 0, 3, 6, 12, and 24 h of treatment. Photographs of each area were taken with an Infinity 1-2C camera (Lumenera, CA) attached to the inverted microscope Olympus CKX41 (Olympus, JPN).

2.5. RT-qPCR

To characterize the expression of aldo-ketoreductase isoforms (AKR1C1-4) involved in the metabolism of 5 α -DHP and allopregnanolone, we performed the cell culture of U251, U87, LN229, and T98G cells as described in the cell culture section. 24 h before total RNA extraction, cells were cultured in DMEM phenol red-free medium supplemented with 10% charcoal-stripped FBS. To compare the expression of AKR1C1-4 in GBM cell lines and normal astrocytic cells, total RNA from normal human astrocytes was purchased (ScienCell Research Laboratories, CA, USA). Total RNA of the cell lines, was extracted with TRIzol[®] LS Reagent (Invitrogen, CA, USA) by the phenol-guanidine isothiocyanate-chloroform according to the manufacturer's recommendations. The quantity of total RNA was determined with a NanoDrop 2000 Spectrophotometer (Thermo Fisher Scientific, MA, USA), and the purity and integrity were determined by electrophoresis on a 1% agarose gel in 0.5 X TB buffer. cDNA was synthesized with 1 μ g of the samples with the M – MLV Reverse Transcriptase (Invitrogen, CA, USA), and oligonucleotides (dT)12–18 Primer (Invitrogen, MA, USA). 2 μ L of such reaction were employed to perform qPCR with the LightCycler[®] FastStar DNA Master SYBR Green I, and the LightCycler 1.5 (Roche Molecular Systems, IN, USA) as manufacturer's recommendation. Due to their high homology, each pair of designed primers recognize two isoforms of AKR1C1-4, also the expression of the 18S ribosomal gene was detected as an expression control. The oligonucleotide sequences for AKR1C1-2 (165 bp) were: 5'-GTTGCCAGCTC ATTGCTCTT-3' forward primer; 5'-CTTTTAGGAACCTCTGCAGGC-3' reverse primer. The oligonucleotides for AKR1C3-4 (114 bp) were: 5'-ACCTCCAGAGGTTCCGAG-3' forward primer; 5'-AGTCCAACCTGCTCC TCATT-3' reverse primer. The oligonucleotides for 18S (167 bp) were: 5'-AGTGAAACTGCAATGGCTC-3' forward primer; 5'-CTGACCGGGTTG GTTTTGAT-3' reverse primer. As a negative control, a reaction without RT was performed. The relative expression of AKR1C1-4 was calculated with the 2^{- Δ CT} method [37,38].

2.6. Statistical analysis

All statistical analysis of the obtained data was performed and plotted in the GraphPad Prism 5.0 software for Windows XP (GraphPad Software, CA, USA). All assays were performed at least by triplicate, the number of experiments made is indicated in each figure legend. The statistical analysis was one-way ANOVA, followed by a Tukey post hoc test. Values of $p < 0.05$ were considered statistically significant.

3. Results

3.1. 5 α -DHP increases the number of human GBM cells

To establish if there are differences in the number of human GBM

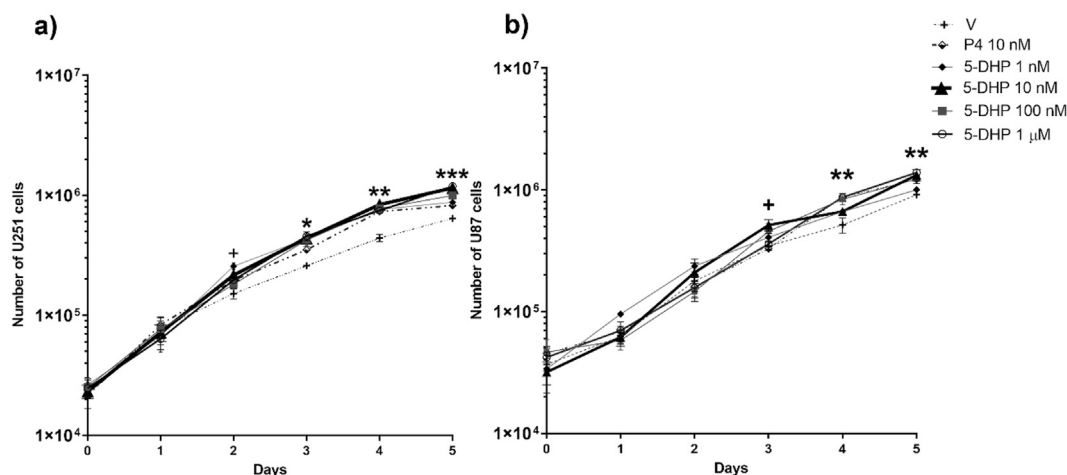


Fig. 1. Effects of 5 α -DHP on the U251 and U87 number of cells. a) The number of U251 human GBM cells treated with different concentrations of 5 α -DHP. $n = 5 + p < 0.05$ 5 α -DHP (1 nM) vs V; $*p < 0.05$ 5 α -DHP (10 nM) vs V; $**p < 0.05$ P4 and 5 α -DHP (1–100 nM and 1 μ M) vs V; $***p < 0.05$ P4 and 5 α -DHP (1–100 nM and 1 μ M) vs V, and P4 vs 5 α -DHP (1–100 nM and 1 μ M). b) The number of U87 human GBM cells treated with different concentrations of 5 α -DHP. $n = 4$; $+p < 0.05$ 5 α -DHP 10 nM vs V; $**p < 0.05$ 5 α -DHP (10–100 nM, 1 μ M) and P4 vs V. All data are expressed as the mean \pm SEM.

cells when they are exposed to 5 α DHP, we treated GBM cells with different concentrations of this steroid (1, 10, 100 nM, 1 μ M), and compared them with P4 10 nM, whose positive effect over cell number has been described [2,39]. In the U251 cell line, 5 α -DHP 1 nM significantly increased the number of cells at day two of treatment, and 5 α -DHP 10 nM did it on day 3. P4 and all the 5 α -DHP tested concentrations increased the number of cells since day 4 (Fig. 1a). In U87 cells, 5 α -DHP 10 nM significantly increased the number of cells since day 3. P4 10 nM and 5 α -DHP (100 nM and 1 μ M) augmented the number of cells until day 4 (Fig. 1b), while 5 α -DHP 1 nM had no effect on the number of cells. The lowest concentration of 5 α -DHP that showed the most consistent effect on the number of both cell lines was 10 nM therefore, subsequent experiments were performed with this concentration.

3.2. The effect of 5 α -DHP on the number of cells and proliferation is mediated by PR

It has been reported that 5 α -DHP exerts some of its effects through the PR. In this line, we determined the effect of 5 α -DHP combined with a PR antagonist (RU486, 1 μ M) in time-course experiments. 5 α DHP 10 nM significantly increased the number of U251 and U87 cells since day 2, and 3 of treatment, respectively. Such effect was blocked by RU486, as seen in the conjunct treatment (5 α -DHP + RU486) in U251 cell line since day 2 of treatment (Fig. 2a). Remarkably, 5 α -DHP increased the number of cells even more than P4 at days 4 and 5 in the U251 cell line (Fig. 2a). In U87 cells, 5 α DHP had a very similar effect to that of P4, but RU486 blocked their effect only at day 3 of treatment (Fig. 2b).

Then, we decided to test if the effect at day 3 of 5 α -DHP alone or with RU486 was due to changes in cell proliferation. BrdU incorporation assay was done to determine cell proliferation. In such experiments, P4 and 5 α -DHP similarly increased the cell proliferation of the evaluated cell lines, and RU486 also blocked the effect of 5 α -DHP. RU486 alone presented a tendency to increase cell proliferation in U251 cells (Fig. 3a, b) and significantly increased it in the U87 cell line (Fig. 3c).

3.3. 5 α -DHP promotes migration of human GBM cell lines

We determined the effect of 5 α -DHP and the blockage of PR on the migration capacity of the human GBM cell lines U251, U87, and LN229. The percentage of wound closure was measured after 3, 6, 12, and 24 h

of treatment with 5 α -DHP, P4, RU486, and 5 α -DHP + RU486. P4 significantly promoted migration of the U251 and U87 cell lines since 12 h of treatment, while it presented a non-significant tendency to do so at 12 h in LN229 cells. 5 α -DHP significantly augmented cell migration of the three cell lines at 24 h of treatment. RU486 showed a tendency to block the effect of 5 α -DHP, although this blockage was significant just in the LN229 cell line (Fig. 4a-d).

3.4. Expression of 3 α -HSOR in GBM cell lines

To investigate if human GBM cells could reversibly reduce 5 α -DHP to 3 α -THP, we determined the expression of 3 α -HSOR. In humans, there have been characterized four isoforms, AKR1C1-4. Due to the high homology of sequences, we could only design oligonucleotides which identified each pair of two of the isoforms. Only U251 cells expressed higher levels of AKR1C1-2 isoforms than those of human normal astrocytic cells. The U251 cell line presented the highest expression of AKR1C1-2 enzymes of all the evaluated GBM cell lines. Interestingly, U251, T98G and LN229 cell lines expressed higher levels of AKR1C1-4 than normal astrocytes. The U87 cell line was the only one which a similar AKR1C1-4 expression profile as that of normal human astrocytes. All GBM cells exhibited different expression levels of AKR1C1-4.

4. Discussion

About 48% of malignant brain tumors in the United States are GBMs. Such tumors are more common in middle to old age, and have a higher incidence in men than in women with a 1.6:1 (men: women) odds ratio, which is accentuated in patients with more than 50 years old [1]. Besides, women present better survival and response to therapy [40,41]. Regarding sex steroid hormones, Huang et al. reported the risk factor for reproductive hormones. This study reveals that women are more susceptible to developing GBMs after menarche, however, this risk decreases after menopause [42]. Also, one study reported that 44% of women with high-grade gliomas shows cancer progression during pregnancy, when progesterone levels are very high [43]. These data suggest that progestins participate in GBM pathophysiology. Here, we reported the relevance of 5 α -DHP in the of proliferation and cell migration of GBMs. Until now, there is no information about plasmatic levels of progestins in GBM patients nor in tumor biopsies, despite this, it is known that the brain is a steroidogenic organ that produces neuroactive P4 metabolites such as 5 α -DHP during all life stages (for

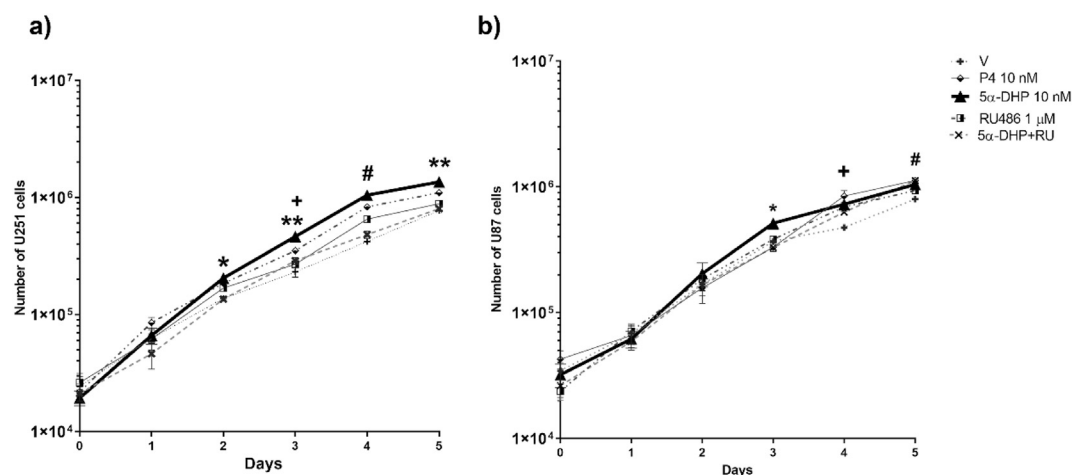


Fig. 2. Effects of 5 α -DHP and RU486 on the U251 and U87 number of cells. a) Number of U251 cells: $n = 4$; * $p < 0.05$ 5 α -DHP vs V and 5 α -DHP + RU486; ** $p < 0.05$ 5 α -DHP vs all other treatments (Day 3), or P4 and 5 α -DHP vs all other treatments (Day 5); + $p < 0.05$ P4 vs V (Day 3); # $p < 0.05$ P4, 5 α -DHP, or RU486 vs all other treatments; b) Number of U87 cells: $n = 4$; * $p < 0.05$ 5 α -DHP vs. V, P4, and 5 α -DHP + RU486; + $p < 0.05$ P4, 5 α -DHP, or RU486 vs V; # $p < 0.05$ P4, 5 α -DHP, and 5 α -DHP + RU486 vs V. All data are expressed as the mean \pm SEM.

review see [13,44]). GBM cells also express the enzymatic machinery to do so, opening the possibility that once initiated cancer, P4 and its metabolites promote GBM progression. Moreover, beyond sex hormones, different genomic profiles associated to sex has been identified, suggesting that other differences inherent to each sex, are involved in glioma pathogenesis, such as epigenetic regulation [40,45].

Beyond reproductive functions, P4 exerts essential functions involved in the maintenance of glial and neuronal cells, such as the control of myelination, or neural plasticity [13,46]. Besides, such effects are also regulated by its metabolites. Although 5 α -DHP is one of the main P4 metabolites produced in the brain, little attention has been paid to it [47]. 5 α -DHP is accumulated in the medial basal hypothalamus, the pituitary, and the cerebral cortex of rats even more than in uterus or plasma, which suggests its relevance in regulating progesterin

effects in hormonal axis regulation areas [19]. Few evidences remark the relevance of studying the physiopathology of P4 metabolism in GBMs until now. Von Schoultz et al., reported lower levels of P4 in brain tumors (mostly astrocytomas grades III and IV) than in normal brain tissue, hypothesizing the high metabolism of this steroid in brain tumors [48]. Melcangi and collaborators showed that rat glioma C6 cells and the subclone 1321N1 derived from the U-118MG, a human glioblastoma cell line, produce higher levels of 5 α -DHP rather than normal rat astrocytes. Besides, the reduction of P4 by 5 α R was greater than that of testosterone to dihydrotestosterone [11], which is in line with von Schoultz hypothesis. In addition, we have reported the presence of the 5 α R enzyme in U87 cells, which suggests that such cells metabolize P4 to its 5 α -reduced metabolites. In such study, we found that in GBM cells, the 5 α R-inhibitor, finasteride, blocked the effects of

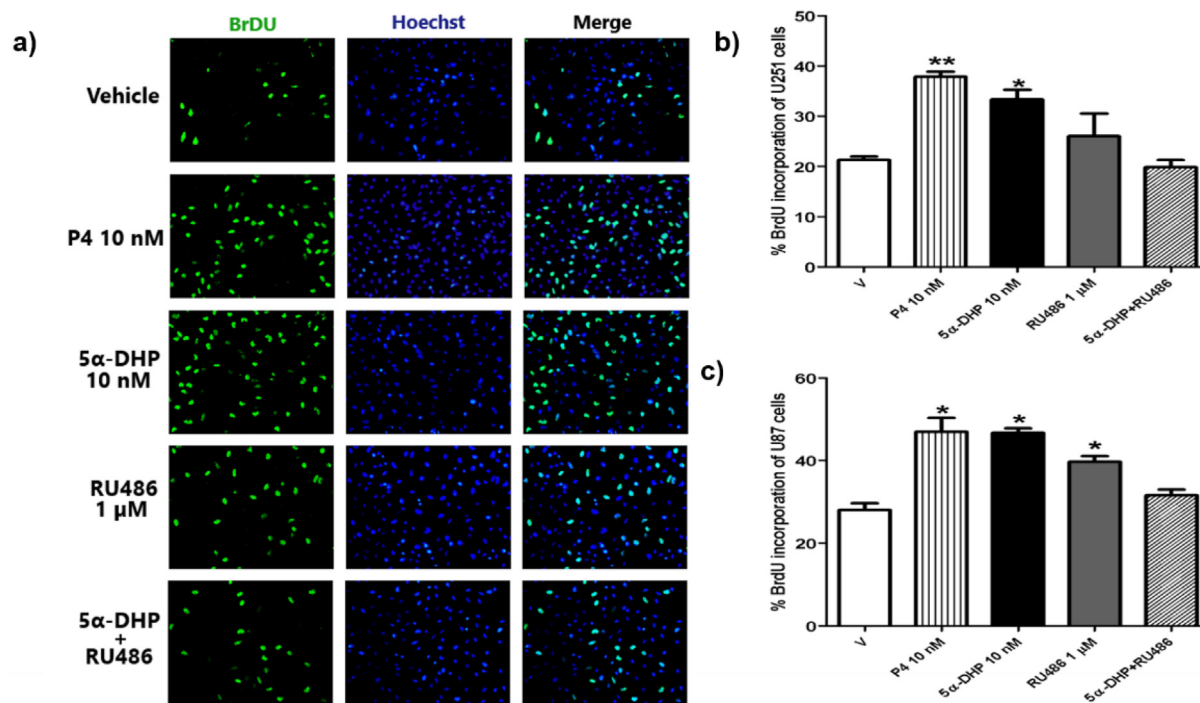


Fig. 3. Effects of 5 α -DHP in the BrdU incorporation of the U251 and U87 cells. a) Representative images of BrdU incorporation assays in the U251 cell line. b) U251 cells: * $p < 0.05$ 5 α -DHP vs V and 5 α -DHP + RU486, ** $p < 0.05$ P4 vs V, RU486 and 5 α -DHP + RU486; c) U87 cells: * $p < 0.05$ P4, 5 α -DHP, and RU486 vs V and 5 α -DHP + RU486. All data are expressed as the mean \pm SEM; $n = 3$.

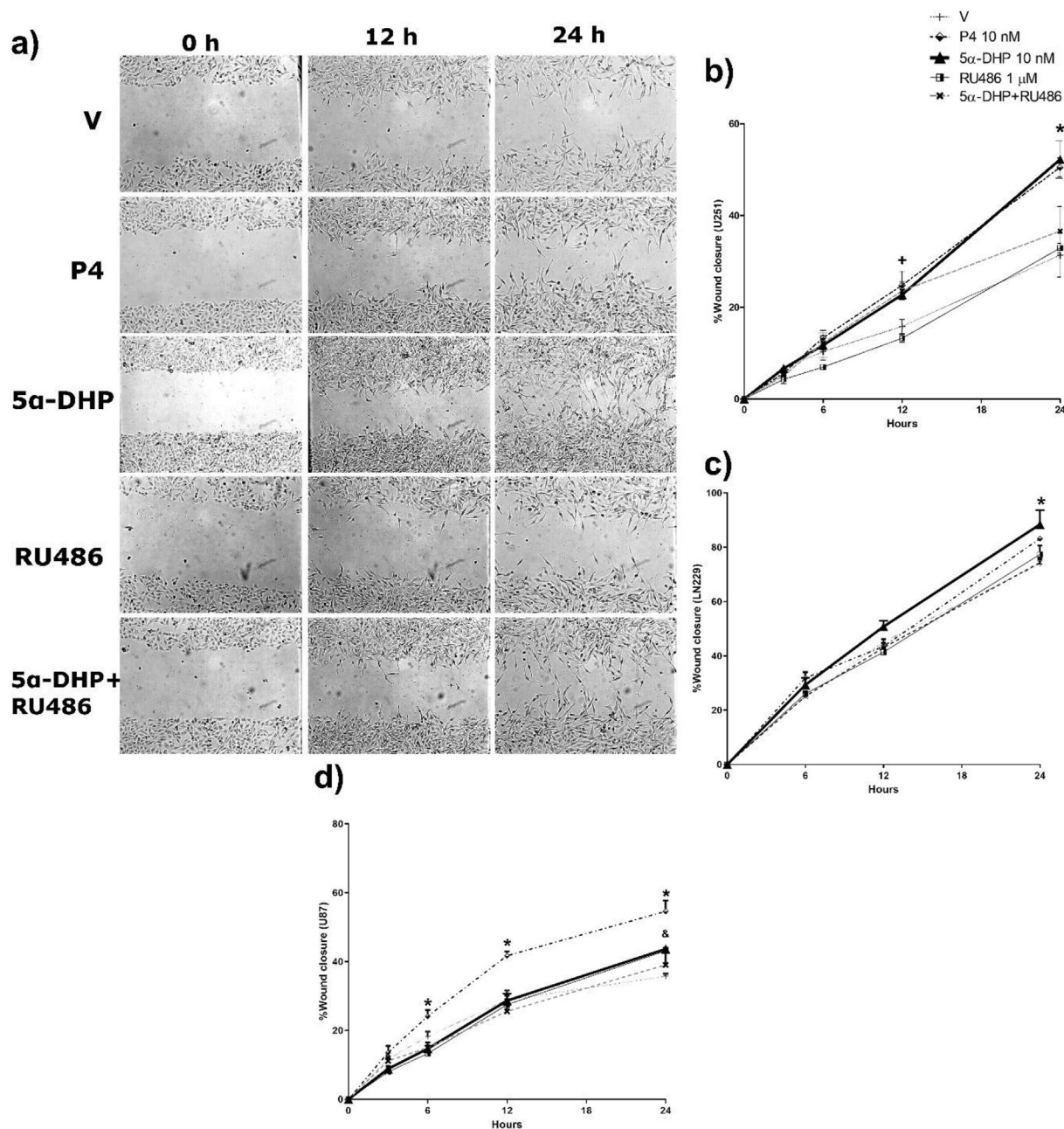


Fig. 4. Effect of 5 α -DHP on the migration of the human GBM cells. a) Representative images of wound healing assays in the U251 cell line after 12 and 24 h of treatment with P4 10 nM, 5 α -DHP 10 nM, RU486 1 μ M, 5 α -DHP + RU486, and V. b) Percentage of wound healing assay closure (U251 cells): n = 5; +p < 0.05 P4 vs. V and RU486; *p < 0.05 5 α -DHP and P4 vs. V and RU486. c) Percentage of wound healing assay closure in the LN229 cells; n = 3; *p < 0.05 5 α -DHP vs all other treatments. d) Percentage of wound healing assay closure (U87 cells): n = 5; *p < 0.05 P4 vs. all other treatments; &p < 0.05 5 α -DHP vs. V. All data are expressed as the mean \pm SEM.

P4 on the number of cells and proliferation [39]. Wiebe et al., found similar results when breast cancer cells were treated with P4 and finasteride or dutasteride, another 5 α R-inhibitor. Interestingly, the effect of P4 was reestablished when 5 α -DHP was added to the cells [49,50]. The relevance of P4 metabolites in the maintenance of other cancer types has been reported. Wiebe and collaborators were pioneers in determining differences between the levels and the opposite effects of P4 metabolites in normal vs. breast cancer biopsies [51]. They found that P4 metabolites with a chemical structure of 4-pregnene, promotes the inhibition of cancer cell growth, while 5 α -pregnanes, such as 5 α -DHP, promotes growth and cell proliferation [52]. Other studies demonstrate the relevance of 5 α -DHP in initiating tumor in breast cancer models, since the treatment with finasteride, blocked the effects of P4

on promoting tumor formation [50,53]. More recently, other authors reported the levels of P4 and 5 α -pregnanes in prostate cancer cell lines, which were even higher than those of androgens, also when cells were treated with 5 α -pregnanes, they promoted cell proliferation [54]. In concordance with such results, here, we demonstrate that 5 α -DHP at different concentrations augments the number of U251 and U87 cells, derived from two different human GBMs (Fig. 1).

Since 2017 when we described the expression of 5 α R in the U87 cell line, we did not discard the importance of the endogenous metabolism of P4, however, we started very recently to investigate the role of P4 metabolites in GBM cell lines. We chose the tested concentrations of 5 α -DHP in this study because they are very similar to those reported by other authors evaluating normal levels of P4 metabolites in the brain or

in cell lines [16,18,19,55,56], which means that chosen concentrations are at physiological levels. We did not evaluate the levels of 5 α -DHP or other progesterone metabolites since we assume that the levels of 5 α -DHP or steroids in general, are low since before performing the experiments, cells were cultured in DMEM phenol-red medium supplemented with charcoal/dextran filtered fetal bovine serum for 24 h. Also, it is inferred that steroid levels are around picomoles according to Cheney DL and cols [57], and our control groups reflect the endogenous low levels of P4 or 5 α -DHP. Interestingly, Pinacho-García et al., have reported this year that U87 cell line synthesizes steroids, particularly, P4 rather than testosterone, when cells are supplemented with 3H-cholesterol for 24 h or 48 h, however, due to the employed technique, it was not possible to quantitatively determine the amount of P4 or its metabolites when a precursor is present in the cell culture medium [58]. The effect on the number of cells is tightly related with an augment of cell proliferation determined in this study at day 3 of treatment (Fig. 3). These results are in line with our previous reports, where we demonstrated that the positive effect of P4 10 nM on the number of cells and proliferation is promoted not only by P4 but by its metabolites, as seen when the effect of P4 on the number of cells was blocked by the 5 α R inhibitor, finasteride [39,59]. In U251 cells, it seems that even the lowest concentration of 5 α -DHP tested, induces a significant augment in the number of cells. Besides, in both cell lines, the effect of 5 α -DHP on the number of cells appear at least one day before that of P4, which could be related with the differences in the mechanisms of action of the two steroids. Here, we focused our study on the effects of 5 α -DHP through PR because 3 α -THP does not have affinity to this receptor. We demonstrated the expression of 3 α -HSOR. There have been characterized four isoforms of such enzymes of the aldo-keto reductases (AKR1C1-4) family which function as 3-, 17- and 20-ketosteroid reductases and 3 α -17 β - and 20 α -hydroxysteroid oxidases, although they have different kinetic constants [60]. Owing to the fact that U87 cells present a very low expression of such enzymes, the effects of 5 α -DHP on cell proliferation and migration are mostly due to this steroid. Almost all the results in the U87 cell line were very similar in the studied cell lines, however, more studies are necessary to fully understand the implication of P4 and its metabolites in GBMs etiology.

Little is known about the mechanism of action of 5 α -DHP. Its interaction with PR has been determined in many species [23,24]. In humans, 5 α -DHP has a high affinity to PR [23,61,62]. In this study, the effect of 5 α -DHP on the number of cells and proliferation seems to be entirely mediated by the PR, since the effects of 5 α -DHP were blocked by RU486 when the conjunct treatments were performed (Figs. 2 and 3). We decided to use a relatively high dose of RU486 due to the duration of cell viability and proliferation assays (5 and 3 days). We observed an increase in cell viability in U87 cells, and proliferation at day 3 of treatment with RU486 which is an agonist-antagonist drug that has a greater affinity for PR than for glucocorticoid and estrogen receptors, thus, it can modulate the activation of these receptors [63,64]. This could explain the effect of RU486 alone on the number of cells and proliferation. This led us to consider the dose-dependent agonist-antagonist function of 5 α -DHP and RU486 on the activation of the PR and its relevance in inducing the proliferation of both cell lines (Figs. 2 and 3) when compared with the effect of 5 α -DHP alone. Such phenomenon was also reported in different models [65,66]. Since the observed effects of 5 α -DHP were almost totally blocked by RU486, we propose that in GBM cells, 5 α -DHP effects are mainly mediated by PR. With the presented experimental data, we cannot discard the participation of both genomic and non-genomic mechanisms mediated by PR activation when cells are treated by 5 α -DHP. In rat astrocytes, there have been reported changes in gene expression after 2 h of treatment with 5 α -DHP [67]. Moreover, the activation of ERK1/2 5 α -DHP has also been reported in the rat brain [68]. To determine which is the predominant effect of 5 α -DHP in promoting genomic or non-genomic mechanisms through PR, and to establish a better model of progestins, more functional assays are needed. Our research group has reported the

role of steroid hormones in the regulation of gene transcription in human GBM cells [39,59,69,70]. P4 and estradiol induce the expression of the vascular endothelial growth factor (VEGF), epidermal growth factor receptor (EGFR), and cyclin D1 through the recruitment of coactivators such as those of the steroid receptor coactivator (SRC) family [69,70]. Besides, we have reported that P4 and 3 α -THP regulate the expression of different sets of genes involved in cell cycle promotion, DNA repair and changes in actin cytoskeleton which correlates with an augment in cell viability and proliferation [39,59]. Regarding other types of cancer, it has been reported that 5 α -DHP promotes the expression of Bcl-2, which is correlated with an antiapoptotic effect in breast cancer cell lines [71]. Whereas in brain tissue, it has been reported that P4, 5 α -DHP, and 3 α -THP promote the gene expression of relevant genes for the neural cytoskeleton in certain areas [28]. In the Central Nervous System, it has been reported the relevance of such progestins in promoting cell proliferation and myelination. In such studies, the authors identified some genes which expression is regulated by 3 α -THP and P4 through the activation of different mechanisms [13]. Given the present data, and the broad spectrum of mechanisms activated by P4 metabolites, it is possible that they regulate the expression of different sets of genes involved in cell proliferation and migration, specially 3 α -THP with respect to P4 and 5 α -DHP.

Interestingly, the migration process induced by 5 α -DHP was partially regulated by PR since RU486 presented a clear tendency to diminish the increase in migration induced by 5 α -DHP in U251 and U87 cell lines, and significantly decreased 5 α -DHP effect in LN229 cells. (Fig. 4a-d). Piña-Medina also reported a partial decrease in migration and invasion processes when PR expression was diminished in the human GBM cell line D54 [5]. These data indicate that different mechanisms regulate the effects of progestins, such as P4 or 5 α -DHP on migration and invasion. There are reports that progestins could promote cancer progression in either PR-positive or -negative cancer cells. In PR-negative non-tumorous breast cell lines (MCF10A and MCF12A) expressing mPRs, treatment with mPRs agonists, or 5 α -DHP, promoted activation of the ERK, JNK, and p38 kinases [72]. While in the PR-negative breast cancer cell lines SKBR3 and MDA-MB-468, expressing mPR α , mPR β , and mPR γ , the mPR agonist ORG-02-0 has antiapoptotic effects [73]. Recently, we have reported the role of mPRs subtypes in GBM progression [35,36,74]. Our group also reported that the agonist ORG-02-0 promotes proliferation, migration, and invasion of U87 and U251 cell lines [36]. In ovarian cancer cells lacking PR, activation of JNK172 and p38 signaling was reported along with the expression of mPRs [75]. It would be interesting to determine the contribution of such receptors in 5 α -DHP positive effects on the migration and invasion of GBM cells. Also, it has been reported the relatively high affinity of 5 α -DHP for mPR α [30]. So, we consider as a perspective of the present study, to evaluate the possible involvement of mPRs in 5 α -DHP effects through different genetic and pharmacological strategies.

Interestingly, in PR-positive T47D breast cancer cell lines, PR has fast effects due to its interaction with Src, leading to the positive regulation of the MAPK signaling pathway [25,26]. Also, in T47D cells PR induces the fast rearrangement of the actin cytoskeleton by the activation of FAK in a dependent manner of the Src/PI3K pathway, along with the activation of the Rho/ROCK pathway [27,28]. Finally, in the Central Nervous System, there has been hypothesized a crosstalk between the genomic and non-genomic mechanisms of P4 and its metabolites 5 α -DHP, and allopregnanolone [76,77]. Although there is information about 5 α -DHP and its interaction with mPRs, more research is needed to understand how P4 metabolites, such as 5 α -DHP, maintains the malignancy of GBMs or if interrupting their metabolism, an improvement in GBM therapy could be obtained.

We focused our study on P4 metabolites since many authors had described the potential of glioma cells for synthesizing P4 metabolites rather than testosterone metabolites due to the same enzymatic complex (5 α -R-3 α -HSOR) [11,58]. There is no evidence about the conversion of 3 α -THP to 5 α -DHP in glioma cells, however, it is known that

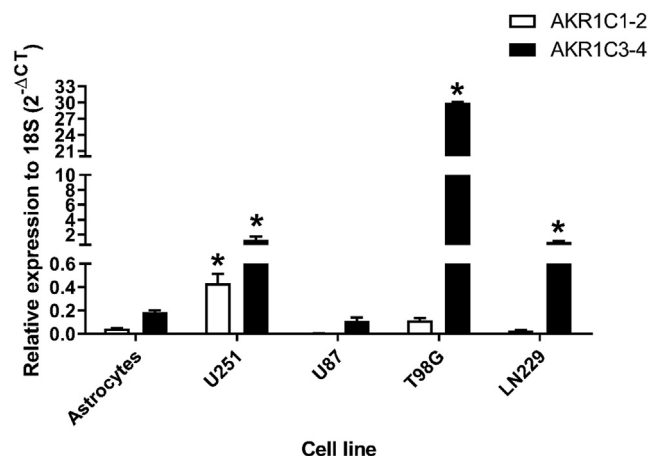


Fig. 5. Characterization of AKR1C1-4 in GBM cell lines. Total RNA of human GBM cells was extracted after 24 h of culture in DMEM red-free medium supplemented with 10% charcoal-stripped FBS. * $p < 0.05$ vs human astrocytes and all other GBM cells. All data are expressed as the mean \pm SEM; $n = 3$.

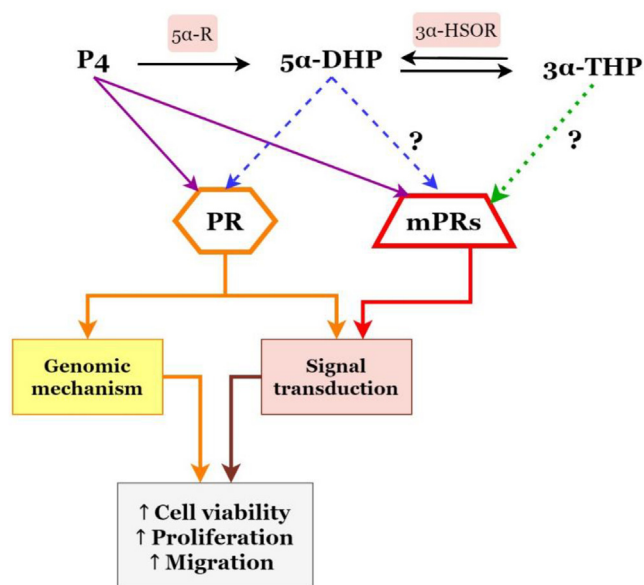


Fig. 6. General mechanisms of action of P4 and its metabolites in human GBM cell lines. In black arrows it is indicated the irreversible reduction of P4 to 5 α -DHP and the reversible reduction of 5 α -DHP to 3 α -THP. Purple, blue, and green arrows indicate the mechanisms of actions of P4, 5 α -DHP, and 3 α -THP, respectively. PR promotes the expression of target genes participating in the regulation of cell proliferation and migration, through its genomic mechanism, while in the cytoplasm, it induces the activation of signal transduction pathways involved in cell migration and invasion. Also, in GBM cells, the presence of mPR has been detected. Particularly, mPR α activation promotes cell viability, proliferation, invasion, and migration.

their oxidative potential is inhibited by NADPH [15]. In the Central Nervous System it has been described the preferential oxidative activity of 3 α -HSOR under pharmacological conditions or availability of substrates [78,79]. Now, we have added to our manuscript the characterization of 3 α -HSOR in human GBM cell lines (Fig. 5). We found a high expression of 3 α -HSOR in our cell lines except in U87 cells. We cannot discard that GBM cells actively interconvert 5 α -DHP and 3 α -THP to sustain a juxtacrine/autocrine loop that promotes proliferation and migration through different mechanisms of action. In the Fig. 6 is summarized all the findings we have performed about P4 metabolism and the effect of P4 metabolites in human GBM cell lines. Another interesting finding reported by Melcangi and collaborators is that neurons

change their P4 metabolic profile when they are exposed to the culture media of glioma cells [11]. Thus, a more detailed study of P4 metabolism in the microenvironment of GBM cells is needed.

Together, in this study, we show that 5 α -DHP contributes to GBM malignancy by increasing the number of cells proliferation, and migration through the PR. With this study, we wanted to point out the relevance of P4 metabolites in the pathophysiology of GBMs. We have reported that P4, 5 α -DHP, 3 α -THP at physiological concentrations, influence the growth of GBMs through different mechanisms of action. Nowadays, some clinical studies with RU486 prove to have positive effects on patients with such malignancy. However, due to the multiple mechanisms of action of P4 and their metabolites, more integral strategies have to be planned. Regarding P4 metabolism, 3 α -HSOR reversibly reduces 5 α -DHP to 3 α -THP which is involved in maintaining proliferation and migration of different types of cancer, such as prostate and lung [80–82]. 3 α -HSOR has also been detected in different brain tumors and in GBM cells its high expression is associated with resistance to temozolomide, such agent is the standard treatment for such tumors [83]. A plausible alternative that needs to be investigated is the regulation of PR by 5 α -DHP, and P4 metabolites.

Declaration of Competing Interest

The authors declare that they have no known competing financial interests or personal relationships that could have appeared to influence the work reported in this paper.

Acknowledgments

This work was supported by Programa de Apoyo de Investigación e Innovación Tecnológica (PAPIIT) project IN217120, DGAPA-UNAM, México.

References

- [1] Q.T. Ostrom, G. Cioffi, H. Gittleman, N. Patil, K. Waite, C. Kruchko, J.S. Barnholtz-Sloan, CBTRUS statistical report: primary brain and other central nervous system tumors diagnosed in the United States in 2012–2016, *Neuro. Oncol.* 21 (2019) v1–v100, <https://doi.org/10.1093/neuonc/noz150>.
- [2] G. González-Aguero, A.a. Gutiérrez, D. González-Espinosa, J.D. Solano, R. Morales, A. González-Arenas, E. Cabrera-Muñoz, I. Camacho-Arroyo, Progesterone effects on cell growth of U373 and D54 human astrocytoma cell lines, *Endocrine*. 32 (2007) 129–135. doi: 10.1007/s12020-007-9023-0.
- [3] E. Cabrera-Muñoz, O.T. Hernández-Hernández, I. Camacho-Arroyo, Role of progesterone in human astrocytomas growth, *Curr. Top. Med. Chem.* 11 (2011) 1663–1667 (accessed April 7, 2015), <http://www.ncbi.nlm.nih.gov/pubmed/21463255>.
- [4] L. Germán-Castelán, J. Manjarrez-Marmolejo, A. González-Arenas, M.G. González-Morán, I. Camacho-Arroyo, Progesterone induces the growth and infiltration of human astrocytoma cells implanted in the cerebral cortex of the rat, *Biomed Res. Int.* 2014 (2014) 393174, <https://doi.org/10.1155/2014/393174>.
- [5] A.G. Piña-Medina, V. Hansberg-Pastor, A. González-Arenas, M. Cerbón, I. Camacho-Arroyo, Progesterone promotes cell migration, invasion and cofilin activation in human astrocytoma cells, *Steroids* 105 (2016) 19–25, <https://doi.org/10.1016/j.steroids.2015.11.008>.
- [6] C. Corpéchet, M. Synguelakis, S. Talha, M. Axelson, J. Sjövall, R. Vihko, E.E. Baulieu, P. Robel, Pregnenolone and its sulfate ester in the rat brain, *Brain Res.* 270 (1983) 119–125, [https://doi.org/10.1016/0006-8993\(83\)90797-7](https://doi.org/10.1016/0006-8993(83)90797-7).
- [7] S.E. Abdelgadir, C.E. Roselli, J.V.A. Choate, J.A. Resko, Distribution of aromatase cytochrome P450 messenger ribonucleic acid in adult rhesus monkey brains1, *Biol. Reprod.* 57 (1997) 772–777, <https://doi.org/10.1095/biolreprod57.4.772>.
- [8] J.L. Do Rego, J.Y. Seong, D. Burel, J. Leprince, V. Luu-The, K. Tsutsui, M.C. Tonon, G. Pelletier, H. Vaudry, Neurosteroid biosynthesis: Enzymatic pathways and neuroendocrine regulation by neurotransmitters and neuropeptides, *Front. Neuroendocrinol.* 30 (2009) 259–301, <https://doi.org/10.1016/j.ymrne.2009.05.006>.
- [9] G. Pelletier, Steroidogenic enzymes in the brain: morphological aspects, *Prog. Brain Res.* 181 (2010) 193–207, [https://doi.org/10.1016/S0079-6123\(08\)81011-4](https://doi.org/10.1016/S0079-6123(08)81011-4).
- [10] Y. Tsuruo, K. Ishimura, K. Morita, Influence of serum-free culture conditions on subcellular localization of steroid 5 α -reductase in rat C6 glioma cells, *Brain Res.* 801 (1998) 130–136, [https://doi.org/10.1016/S0006-8993\(98\)00555-1](https://doi.org/10.1016/S0006-8993(98)00555-1).
- [11] R.C. Melcangi, I. Cavarretta, V. Magnaghi, M. Ballabio, L. Martini, M. Motta, Crosstalk between normal and tumoral brain cells. Effect on sex steroid metabolism, *Endocrine* 8 (1998) 65–71, <https://doi.org/10.1385/ENDO:8:1.65>.
- [12] M. Schumacher, C. Mattern, A. Ghomari, J.P. Oudinet, P. Liere, F. Labombarda,

- R. Sitruk-Ware, a.F. De Nicola, R. Guennoun, Revisiting the roles of progesterone and allopregnanolone in the nervous system: resurgence of the progesterone receptors, *Prog. Neurobiol.* 113 (2014) 6–39, <https://doi.org/10.1016/j.pneurobio.2013.09.004>.
- [13] R.C. Melcangi, S. Giatti, D. Calabrese, M. Pesaresi, G. Cermenati, N. Mitro, B. Viviani, L.M. Garcia-Segura, D. Caruso, Levels and actions of progesterone and its metabolites in the nervous system during physiological and pathological conditions, *Prog. Neurobiol.* 113 (2014) 56–69, <https://doi.org/10.1016/j.pneurobio.2013.07.006>.
- [14] R.C. Melcangi, F. Celotti, L. Martini, Progesterone 5- α -reduction in neuronal and in different types of glial cell cultures: type 1 and 2 astrocytes and oligodendrocytes, 1994. doi: 10.1016/0006-8993(94)91731-0.
- [15] T.M. Penning, Y. Jin, S. Steckelbroeck, T.L. Rizner, M. Lewis, Structure-function of human 3 α -hydroxysteroid dehydrogenases: genes and proteins, *Mol. Cell. Endocrinol.* 215 (2004) 63–72, <https://doi.org/10.1016/j.mce.2003.11.006>.
- [16] B.E. Pearson Murphy, S.I. Steinberg, F.-Y. Hu, C.M. Allison, Neuroactive ring A-reduced metabolites of progesterone in human plasma during pregnancy: elevated levels of 5 α -dihydroprogesterone in depressed patients during the latter half of pregnancy, *J. Clin. Endocrinol. Metab.* 86 (2001) 5981–5987, <https://doi.org/10.1210/jcem.86.12.8122>.
- [17] R.A. Dombroski, M.L. Casey, P.C. MacDonald, The metabolic disposition of plasma 5 alpha-dihydroprogesterone (5 alpha-pregnane-3,20-dione) in women and men, *J. Clin. Endocrinol. Metab.* 77 (1993) 944–948, <https://doi.org/10.1210/jcem.77.4.8408469>.
- [18] M. Bixo, A. Andersson, B. Winblad, R.H. Purdy, T. Bäckström, Progesterone, 5 α -pregnane-3,20-dione and 3 α -hydroxy-5 α -pregnane-20-one in specific regions of the human female brain in different endocrine states, *Brain Res.* 764 (1997) 173–178, [https://doi.org/10.1016/S0006-8993\(97\)00455-1](https://doi.org/10.1016/S0006-8993(97)00455-1).
- [19] H.J. Karavolas, D. Hodges, D. O'Brien, Uptake of [3H]progesterone and [3H]5 α -dihydroprogesterone by rat tissues in vivo and analysis of accumulated radioactivity: accumulation of 5 α -dihydroprogesterone by pituitary and hypothalamic tissues, *Endocrinology.* 98 (1976) 164–175, <https://doi.org/10.1210/endo-98-1-164>.
- [20] A. Nechmad, R. Maayan, B. Spivak, E. Ramadan, M. Poyurovsky, A. Weizman, Brain neurosteroid changes after paroxetine administration in mice, *Eur. Neuropsychopharmacol.* 13 (2003) 327–332, [https://doi.org/10.1016/S0924-977X\(03\)00015-4](https://doi.org/10.1016/S0924-977X(03)00015-4).
- [21] R.C. Melcangi, I.T.R. Cavarretta, M. Ballabio, E. Leonelli, A. Schenone, I. Azcoitia, L.M. Garcia-Segura, V. Magnaghi, Peripheral nerves: A target for the action of neuroactive steroids, in *Brain Res. Rev.*, Elsevier (2005) 328–338, <https://doi.org/10.1016/j.brainresrev.2004.12.021>.
- [22] Y.V. Wu, W.M. Burnham, The anti-seizure effects of IV 5 α -dihydroprogesterone on amygdala-kindled seizures in rats, *Epilepsy Res.* 146 (2018) 132–136, <https://doi.org/10.1016/j.eplepsyres.2018.07.022>.
- [23] K. Jewgenow, H.H.D. Meyer, Comparative binding affinity study of progestins to the cytosol progesterin receptor of endometrium in different mammals, *Gen. Comp. Endocrinol.* 110 (1998) 118–124, <https://doi.org/10.1006/genen.1997.7054>.
- [24] M.F. Pichon, E. Milgrom, Characterization and assay of progesterone receptor in human mammary carcinoma, *Cancer Res.* 37 (1977) 464–471 (accessed December 9, 2019), <http://www.ncbi.nlm.nih.gov/pubmed/832270>.
- [25] A. Migliaccio, D. Piccolo, G. Castoria, M. Di Domenico, A. Bilancio, M. Lombardi, W. Gong, M. Beato, F. Auricchio, Activation of the Src/p21(ras)/Erk pathway by progesterone receptor via cross-talk with estrogen receptor, *EMBO J.* 17 (1998) 2008–2018, <https://doi.org/10.1093/emboj/17.7.2008>.
- [26] A. Migliaccio, G. Castoria, M. Domenico, A. Falco, A. Bilancio, F. Auricchio, Src is an initial target of sex steroid hormone action, *Ann. N. Y. Acad. Sci.* 963 (2006) 185–190, <https://doi.org/10.1111/j.1749-6632.2002.tb04109.x>.
- [27] X. Fu, M.S. Giretti, C. Baldacci, S. Garibaldi, M. Flamini, A. Matias, A. Gadducci, A.R. Genazzani, T. Simoncini, Extra-nuclear signaling of progesterone receptor to breast cancer cell movement and invasion through the actin cytoskeleton, *PLoS One* 3 (2008) 1–14, <https://doi.org/10.1371/journal.pone.0002790>.
- [28] X.D. Fu, L. Goglia, A.M. Sanchez, M. Flamini, M.S. Giretti, V. Tosi, A.R. Genazzani, T. Simoncini, Progesterone receptor enhances breast cancer cell motility and invasion via extranuclear activation of focal adhesion kinase, *Endocr. Relat. Cancer.* 17 (2010) 431–443, <https://doi.org/10.1677/ERC-09-0258>.
- [29] G.E. Dressing, P. Thomas, Identification of membrane progesterin receptors in human breast cancer cell lines and biopsies and their potential involvement in breast cancer, *Steroids* 72 (2007) 111–116, <https://doi.org/10.1016/j.steroids.2006.10.006>.
- [30] P. Thomas, Y. Pang, J. Dong, P. Groenen, J. Kelder, J. De Vlieg, Y. Zhu, C. Tubbs, Steroid and G protein binding characteristics of the seatrout and human progesterin membrane receptor α subtypes and their evolutionary origins, *Endocrinology* 148 (2007) 705–718, <https://doi.org/10.1210/en.2006-0974>.
- [31] R.S. Carroll, J. Zhang, K. Dashner, M. Sar, P.M. Black, Steroid hormone receptors in astrocytic neoplasms, *Neurosurgery* 37 (1995) 496–504, <https://doi.org/10.1227/00006123-199509000-00019>.
- [32] W. Berny, A. Weiser, W. Jarmundowicz, A. Markowska-Woyciechowska, R. Załuski, W. Zub, [Analysis of expression of estrogen (ER) and progesterone receptors (PR) in brain glial tumors and its correlation with expression of p53 protein and proliferating cell nuclear antigen (PCNA)], *Neurol. Neurochir. Pol.* 38 (n.d.) 367–71. <http://www.ncbi.nlm.nih.gov/pubmed/15565522> (accessed December 9, 2019).
- [33] A. González-Arenas, M.Á. Peña-Ortiz, V. Hansberg-Pastor, B. Marquina-Sánchez, N. Baranda-Ávila, K. Nava-Castro, A. Cabrera-Wrooman, J. González-Jorge, I. Camacho-Arroyo, PKC α and PKC δ Activation Regulates Transcriptional Activity and Degradation of Progesterone Receptor in Human Astrocytoma Cells, *Endocrinology* 156 (2015) 1010–1022, <https://doi.org/10.1210/en.2014-1137>.
- [34] P. Valadez-Cosmes, L. Germán-Castelán, A. González-Arenas, M.A. Velasco-Velázquez, V. Hansberg-Pastor, I. Camacho-Arroyo, Expression and hormonal regulation of membrane progesterone receptors in human astrocytoma cells, *J. Steroid Biochem. Mol. Biol.* 154 (2015) 176–185, <https://doi.org/10.1016/j.jsbmb.2015.08.006>.
- [35] A. Del Moral-Morales, J.C. González-Orozco, J.M. Capetillo-Velázquez, A.G. Piña-Medina, I. Camacho-Arroyo, The role of mpr δ and mpr ϵ in human glioblastoma cells: expression, hormonal regulation, and possible clinical outcome, *Horm. Cancer* (2020) 1–11, <https://doi.org/10.1007/s12672-020-00381-7>.
- [36] J.C. González-Orozco, V. Hansberg-Pastor, P. Valadez-Cosmes, W. Nicolas-Ortega, Y. Bastida-Beristain, M.D. La Fuente-Granada, A. González-Arenas, I. Camacho-Arroyo, Activation of membrane progesterone receptor-alpha increases proliferation, migration, and invasion of human glioblastoma cells, *Mol. Cell. Endocrinol.* 477 (2018) 81–89, <https://doi.org/10.1016/j.mce.2018.06.004>.
- [37] M.W. Pfaffl, A new mathematical model for relative quantification in real-time RT-PCR, 45e 45e, *Nucl. Acids Res.* 29 (2001), <https://doi.org/10.1093/nar/29.9.e45>.
- [38] T.D. Schmittgen, K.J. Livak, Analyzing real-time PCR data by the comparative CT method, *Nat. Protoc.* 3 (2008) 1101–1108, <https://doi.org/10.1038/nprot.2008.73>.
- [39] C.J. Zamora-Sánchez, V. Hansberg-Pastor, I. Salido-Guadarrama, M. Rodríguez-Dorantes, I. Camacho-Arroyo, Allopregnanolone promotes proliferation and differential gene expression in human glioblastoma cells, *Steroids* 119 (2017) 36–42, <https://doi.org/10.1016/j.steroids.2017.01.004>.
- [40] W. Yang, N.M. Warrington, S.J. Taylor, P. Whitmire, E. Carrasco, K.W. Singleton, N. Wu, J.D. Lathia, M.E. Berens, A.H. Kim, J.S. Barnholtz-Sloan, K.R. Swanson, J. Luo, J.B. Rubin, Sex differences in GBM revealed by analysis of patient imaging, transcriptome, and survival data, *Sci. Transl. Med.* 11 (2019) 5253. doi: 10.1126/scitranslmed.aao5253.
- [41] M. Tian, W. Ma, Y. Chen, Y. Yu, D. Zhu, J. Shi, Y. Zhang, Impact of gender on the survival of patients with glioblastoma, *Biosci. Rep.* 38 (2018) BSR20180752. doi: 10.1042/BSR20180752.
- [42] K. Huang, E.A. Whelan, A.M. Ruder, E.M. Ward, J.A. Deddens, K.E. Davis-King, T. Carreón, M.A. Waters, M.A. Butler, G.M. Calvert, P.A. Schulte, Z. Zivkovich, E.F. Heineman, J.S. Mandel, R.F. Morton, D.J. Reding, K.D. Rosenman, Reproductive factors and risk of glioma in women, *Cancer Epidemiol. Biomarkers Prev.* 13 (2004) 1583–1588.
- [43] S. Yust-Katz, J.F. de Groot, D. Liu, J. Wu, Y. Yuan, M.D. Anderson, C.A. Conrad, A. Milbourne, M.R. Gilbert, T.S. Armstrong, Pregnancy and glial brain tumors, *Neuro. Oncol.* 16 (2014) 1289–1294, <https://doi.org/10.1093/neuonc/nou019>.
- [44] P.J. Brunton, J.A. Russell, J.J. Hirst, Allopregnanolone in the brain: protecting pregnancy and birth outcomes, Elsevier Ltd, 2014. doi: 10.1016/j.pneurobio.2013.08.005.
- [45] T. Sun, A. Plutynski, S. Ward, J.B. Rubin, An integrative view on sex differences in brain tumors, *Cell. Mol. Life Sci.* 72 (2015) 3323–3342, <https://doi.org/10.1007/s00018-015-930-2>.
- [46] V. Hansberg-Pastor, A. González-Arenas, A.G. Piña-Medina, I. Camacho-Arroyo, Sex hormones regulate cytoskeletal proteins involved in brain plasticity, *Front. Psychiatry* 6 (2015), <https://doi.org/10.3389/fpsy.2015.00165>.
- [47] Y.V. Wu, W.M. Burnham, Progesterone, 5 α -dihydroprogesterone and allopregnanolone's effects on seizures: a review of animal and clinical studies, *Seizure* 63 (2018) 26–36, <https://doi.org/10.1016/j.seizure.2018.10.012>.
- [48] E. Von Schoultz, R. Henriksson, M. Bixo, T. Bäckström, H. Silfvenius, N. Wilking, Sex steroids in human brain tumors and breast cancer, *Cancer* 65 (1990) 949–952, [https://doi.org/10.1002/1097-0142\(19900215\)65:4<949::AID-CNCR2820650421>3.0.CO;2-2](https://doi.org/10.1002/1097-0142(19900215)65:4<949::AID-CNCR2820650421>3.0.CO;2-2).
- [49] J.P. Wiebe, L. Souter, G. Zhang, Dutasteride affects progesterone metabolizing enzyme activity/expression in human breast cell lines resulting in suppression of cell proliferation and detachment, *J. Steroid Biochem. Mol. Biol.* 100 (2006) 129–140, <https://doi.org/10.1016/j.jsbmb.2006.03.010>.
- [50] J.P. Wiebe, M.A. Rivas, M.F. Mercogliano, P.V. Elizalde, R. Schillaci, Progesterone-induced stimulation of mammary tumorigenesis is due to the progesterone metabolite, 5 α -dihydroprogesterone (5 α P) and can be suppressed by the 5 α -reductase inhibitor, finasteride, *J. Steroid Biochem. Mol. Biol.* 149 (2015) 27–34, <https://doi.org/10.1016/j.jsbmb.2015.01.004>.
- [51] J.P. Wiebe, Progesterone metabolites in breast cancer, *Endocr. Relat. Cancer* 13 (2006) 717–738, <https://doi.org/10.1677/erc.1.01010>.
- [52] J.P. Wiebe, D. Muzia, J. Hu, D. Sz wajcer, S.A. Hill, J.L. Seachrist, The 4-pregnene and 5 α -pregnane progesterone metabolites formed in nontumorous and tumorous breast tissue have opposite effects on breast cell proliferation and adhesion, *Cancer Res.* 60 (2000) 936–943 (accessed November 24, 2014), <http://www.ncbi.nlm.nih.gov/pubmed/10706108>.
- [53] J.P. Wiebe, G. Zhang, I. Welch, H.-A.T. Cadieux-Pitre, Progesterone metabolites regulate induction, growth, and suppression of estrogen- and progesterone receptor-negative human breast cell tumors, *Breast Cancer Res.* 15 (2013) R38, <https://doi.org/10.1186/bcr3422>.
- [54] T. Ando, T. Nishiyama, I. Takizawa, Y. Miyashiro, N. Hara, Y. Tomita, A carbon 21 steroidal metabolite from progesterin, 20 β -hydroxy-5 α -dihydroprogesterone, stimulates the androgen receptor in prostate cancer cells, *Prostate.* 78 (2018) 222–232, <https://doi.org/10.1002/pros.23460>.
- [55] R.B. Billiar, B. Little, I. Kline, P. Reier, Y. Takaoka, R.J. White, The metabolic clearance rate, head and brain extractions, and brain distribution and metabolism of progesterone in the anesthetized, female monkey (Macaca Mulatta), *Brain Res.* 94 (1975) 99–113, [https://doi.org/10.1016/0006-8993\(75\)90880-X](https://doi.org/10.1016/0006-8993(75)90880-X).
- [56] X.Y. He, J. Wegiel, S.Y. Yang, Intracellular oxidation of allopregnanolone by human brain type 10 17 β -hydroxysteroid dehydrogenase, *Brain Res.* 1040 (2005) 29–35, <https://doi.org/10.1016/j.brainres.2005.01.022>.
- [57] D.L. Cheney, D. Uzunov, E. Costa, A. Guidotti, Gas chromatographic-mass

- fragmentographic quantitation of 3 α -hydroxy- 5 α -pregnan-20-one (allopregnanolone) and its precursors in blood and brain of adrenalectomized and castrated rats, *J. Neurosci.* 15 (1995) 4641–4650, <https://doi.org/10.1523/jneurosci.15-06-04641.1995>.
- [58] L.M. Pinacho-García, R.A. Valdez, A. Navarrete, M. Cabeza, J. Segovia, M.C. Romano, The effect of finasteride and dutasteride on the synthesis of neurosteroids by glioblastoma cells, *Steroids* 155 (2020), <https://doi.org/10.1016/j.steroids.2019.108556>.
- [59] C. Zamora-Sánchez, A. del Moral-Morales, A. Hernández-Vega, V. Hansberg-Pastor, I. Salido-Guadarrama, M. Rodríguez-Dorantes, I. Camacho-Arroyo, Allopregnanolone alters the gene expression profile of human glioblastoma cells, *Int. J. Mol. Sci.* 19 (2018) 864, <https://doi.org/10.3390/ijms19030864>.
- [60] S. Steckelbroeck, Y. Jin, S. Gopishetty, B. Oyesanmi, T.M. Penning, Human cytosolic 3 α -hydroxysteroid dehydrogenases of the aldo-keto reductase superfamily display significant 3 β -hydroxysteroid dehydrogenase activity: implications for steroid hormone metabolism and action, *J. Biol. Chem.* 279 (2004) 10784–10795, <https://doi.org/10.1074/jbc.M313308200>.
- [61] R. Rupprecht, F. Holsboer, Neuroactive steroids: mechanisms of action and neuropsychopharmacological perspectives, *Trends Neurosci.* 22 (1999) 410–416, [https://doi.org/10.1016/S0166-2236\(99\)01399-5](https://doi.org/10.1016/S0166-2236(99)01399-5).
- [62] R. Rupprecht, J.M.H.M. Reul, T. Trapp, B. van Steensel, C. Wetzel, K. Damm, W. Zieglgänsberger, F. Holsboer, Progesterone receptor-mediated effects of neuroactive steroids, *Neuron* 11 (1993) 523–530, [https://doi.org/10.1016/0896-6273\(93\)90156-L](https://doi.org/10.1016/0896-6273(93)90156-L).
- [63] A.J.J. Wood, I.M. Spitz, C.W. Bardin, Mifepristone (RU 486) – a modulator of progestin and glucocorticoid action, *N. Engl. J. Med.* 329 (1993) 404–412, <https://doi.org/10.1056/NEJM199308053290607>.
- [64] L.M. Ramondetta, A.J. Johnson, C.C. Sun, N. Atkinson, J.A. Smith, M.S. Jung, R. Broaddus, R.B. Iyer, T. Burke, Phase 2 trial of mifepristone (RU-486) in advanced or recurrent endometrioid adenocarcinoma or low-grade endometrial stromal sarcoma, *Cancer*. 115 (2009) 1867–1874, <https://doi.org/10.1002/cncr.24197>.
- [65] S. Zhang, J. Jonklaas, M. Danielsen, The glucocorticoid agonist activities of mifepristone (RU486) and progesterone are dependent on glucocorticoid receptor levels but not on EC50 values, *Steroids* 72 (2007) 600–608, <https://doi.org/10.1016/j.steroids.2007.03.012>.
- [66] S.M. Grunberg, M.H. Weiss, C.A. Russell, I.M. Spitz, J. Ahmadi, A. Sadun, R. Sitruk-Ware, Long-term administration of mifepristone (RU486): clinical tolerance during extended treatment of meningioma, *Cancer Invest.* 24 (2006) 727–733, <https://doi.org/10.1080/07357900601062339>.
- [67] R.C. Melcangi, M.A. Riva, F. Fumagalli, V. Magnaghi, G. Racagni, L. Martini, Effect of progesterone, testosterone and their 5 α -reduced metabolites on GFAP gene expression in type 1 astrocytes, *Brain Res.* 711 (1996) 10–15, [https://doi.org/10.1016/0006-8993\(95\)01302-4](https://doi.org/10.1016/0006-8993(95)01302-4).
- [68] C. Guerra-Araiza, M.A.R. Amorim, R. Pinto-Almazán, A. González-Arenas, M.G. Campos, L.M. García-Segura, Regulation of the phosphoinositide-3 kinase and mitogen-activated protein kinase signaling pathways by progesterone and its reduced metabolites in the rat brain, *J. Neurosci. Res.* 87 (2009) 470–481, <https://doi.org/10.1002/jnr.21848>.
- [69] O.T. Hernández-Hernández, T.K. González-García, I. Camacho-Arroyo, Progesterone receptor and SRC-1 participate in the regulation of VEGF, EGFR and Cyclin D1 expression in human astrocytoma cell lines, *J. Steroid Biochem. Mol. Biol.* 132 (2012) 127–134, <https://doi.org/10.1016/j.jsbmb.2012.04.005>.
- [70] A. González-Arenas, V. Hansberg-Pastor, O.T. Hernández-Hernández, T.K. González-García, J. Henderson-Villalpando, D. Lemus-Hernández, A. Cruz-Barrios, M. Rivas-Suárez, I. Camacho-Arroyo, Estradiol increases cell growth in human astrocytoma cell lines through ER α activation and its interaction with SRC-1 and SRC-3 coactivators, *Biochim. Biophys. Acta – Mol. Cell Res.* 2012 (1823) 379–386, <https://doi.org/10.1016/j.bbamcr.2011.11.004>.
- [71] J.P. Wiebe, M. Beausoleil, G. Zhang, V. Cialacu, Opposing actions of the progesterone metabolites, 5 α -dihydroprogesterone (5 α P) and 3 α -dihydroprogesterone (3 α HP) on mitosis, apoptosis, and expression of Bcl-2, Bax and p21 in human breast cell lines, *J. Steroid Biochem. Mol. Biol.* 118 (2010) 125–132, <https://doi.org/10.1016/j.jsbmb.2009.11.005>.
- [72] M. Salazar, A. Lerma-Ortiz, G.M. Hooks, A.K. Ashley, R.L. Ashley, Progesterone-mediated activation of MAPK and AKT in nuclear progesterone receptor negative breast epithelial cells: the role of membrane progesterone receptors, *Gene*. 591 (2016) 6–13, <https://doi.org/10.1016/j.gene.2016.06.044>.
- [73] G.E. Dressing, R. Alyea, Y. Pang, P. Thomas, Membrane progesterone receptors (mPRs) mediate progestin induced antimorbidity in breast cancer cells and are expressed in human breast tumors, *Horm. Cancer* 3 (2012) 101–112, <https://doi.org/10.1007/s12672-012-0106-x>.
- [74] P. Valadez-Cosmes, E.R. Vázquez-Martínez, M. Cerbón, I. Camacho-Arroyo, Membrane progesterone receptors in reproduction and cancer, *Mol. Cell. Endocrinol.* 434 (2016) 166–175, <https://doi.org/10.1016/j.mce.2016.06.027>.
- [75] N.J. Charles, P. Thomas, C.A. Lange, Expression of membrane progesterone receptors (mPR/PAQR) in ovarian cancer cells: implications for progesterone-induced signaling events, *Horm. Cancer*. 1 (2010) 167–176, <https://doi.org/10.1007/s12672-010-0023-9>.
- [76] L.F. Castelnovo, L. Caffino, V. Bonalume, F. Fumagalli, P. Thomas, V. Magnaghi, Membrane progesterone receptors (mPRs/PAQRs) differently regulate migration, proliferation, and differentiation in rat schwann cells, *J. Mol. Neurosci.* (2019), <https://doi.org/10.1007/s12031-019-01433-6>.
- [77] P. Thomas, Y. Pang, Membrane progesterone receptors: evidence for neuroprotective, neurosteroid signaling and neuroendocrine functions in neuronal cells, *Neuroendocrinology*. 96 (2012) 162–171, <https://doi.org/10.1159/000339822>.
- [78] L. Meyer, C. Venard, V. Schaeffer, C. Patte-Mensah, A.G. Mensah-Nyagan, The biological activity of 3 α -hydroxysteroid oxidoreductase in the spinal cord regulates thermal and mechanical pain thresholds after sciatic nerve injury, *Neurobiol. Dis.* 30 (2008) 30–41, <https://doi.org/10.1016/j.nbd.2007.12.001>.
- [79] O.V. Belyaeva, S.V. Chetyrkin, A.L. Clark, N.V. Kostereva, K.S. SantaCruz, B.M. Chronwall, N.Y. Kedishvili, Role of microsomal retinol/sterol dehydrogenase-like short-chain dehydrogenases/reductases in the oxidation and epimerization of 3 α -hydroxysteroids in human tissues, *Endocrinology* 148 (2007) 2148–2156, <https://doi.org/10.1210/en.2006-1491>.
- [80] H. Tian, X. Li, W. Jiang, C. Lv, W. Sun, C. Huang, R. Chen, High expression of AKR1C1 is associated with proliferation and migration of small-cell lung cancer cells, *Lung Cancer (Auckland, N.Z.)*. 7 (2016) 53–61. doi: 10.2147/LCTT.S90694.
- [81] S. Wang, Q. Yang, K.M. Fung, H.K. Lin, AKR1C2 and AKR1C3 mediated prostaglandin D2 metabolism augments the PI3K/Akt proliferative signaling pathway in human prostate cancer cells, *Mol. Cell. Endocrinol.* 289 (2008) 60–66, <https://doi.org/10.1016/j.mce.2008.04.004>.
- [82] A.L. Park, H.-K. Lin, Q. Yang, C.W. Sing, M. Fan, T.B. Mapstone, N.L. Gross, M.K. Gumerlock, M.D. Martin, C.H. Rabb, K.-M. Fung, Differential expression of type 2 3 α /type 5 17 β -hydroxysteroid dehydrogenase (AKR1C3) in tumors of the central nervous system, *Int. J. Clin. Exp. Pathol.* 3 (2010) 743–754 (accessed July 31, 2018), <http://www.ncbi.nlm.nih.gov/pubmed/21151387>.
- [83] B. Le Calvé, M. Rynkowski, M. Le Mercier, C. Bruyère, C. Lonzé, T. Gras, B. Haibe-Kains, G. Bontempi, C. Decaestecker, J.-M. Ruyschaert, R. Kiss, F. Lefranc, Long-term in vitro treatment of human glioblastoma cells with temozolomide increases resistance in vivo through up-regulation of GLUT transporter and aldo-keto reductase enzyme AKR1C expression, *Neoplasia* 12 (2010) 727–739, <https://doi.org/10.1593/neo.10526>.



Article

Allopregnanolone Promotes Migration and Invasion of Human Glioblastoma Cells through the Protein Tyrosine Kinase c-Src Activation

Carmen J. Zamora-Sánchez ¹, Claudia Bello-Alvarez ¹, Mauricio Rodríguez-Dorantes ² and Ignacio Camacho-Arroyo ^{1,*}

¹ Unidad de Investigación en Reproducción Humana, Instituto Nacional de Perinatología-Facultad de Química, Universidad Nacional Autónoma de México, Ciudad de México 04510, Mexico; carmenzamora@gmail.com (C.J.Z.-S.); clautus.bello@gmail.com (C.B.-A.)

² Laboratorio de Oncogenómica, Instituto Nacional de Medicina Genómica, Ciudad de México 14610, Mexico; mrodriguez@inmegen.gob.mx

* Correspondence: camachoarroyo@gmail.com

Abstract: Glioblastomas (GBs) are the most aggressive and common primary malignant brain tumors. Steroid hormone progesterone (P4) and its neuroactive metabolites, such as allopregnanolone (3 α -THP) are synthesized by neural, glial, and malignant GB cells. P4 promotes cellular proliferation, migration, and invasion of human GB cells at physiological concentrations. It has been reported that 3 α -THP promotes GB cell proliferation. Here we investigated the effects of 3 α -THP on GB cell migration and invasion, the participation of the enzymes involved in its metabolism (AKR1C1-4), and the role of the c-Src kinase in 3 α -THP effects in GBs. 3 α -THP 100 nM promoted migration and invasion of U251, U87, and LN229 human-derived GB cell lines. We observed that U251, LN229, and T98G cell lines exhibited a higher protein content of AKR1C1-4 than normal human astrocytes. AKR1C1-4 silencing did not modify 3 α -THP effects on migration and invasion. 3 α -THP activated c-Src protein at 10 min (U251 cells) and 15 min (U87 and LN229 cells). Interestingly, the pharmacological inhibition of c-Src decreases the promoting effects of 3 α -THP on cell migration and invasion. Together, these data indicate that 3 α -THP promotes GB migration and invasion through c-Src activation.

Keywords: allopregnanolone; progesterone; neurosteroid; steroidogenesis; Aldo-keto reductase; c-Src; glioblastoma; glioma; cancer progression



Citation: Zamora-Sánchez, C.J.; Bello-Alvarez, C.; Rodríguez-Dorantes, M.; Camacho-Arroyo, I. Allopregnanolone Promotes Migration and Invasion of Human Glioblastoma Cells through the Protein Tyrosine Kinase c-Src Activation. *Int. J. Mol. Sci.* **2022**, *23*, 4996. <https://doi.org/10.3390/ijms23094996>

Academic Editor: Ahmad R. Safa

Received: 12 April 2022

Accepted: 27 April 2022

Published: 30 April 2022

Publisher's Note: MDPI stays neutral with regard to jurisdictional claims in published maps and institutional affiliations.



Copyright: © 2022 by the authors. Licensee MDPI, Basel, Switzerland. This article is an open access article distributed under the terms and conditions of the Creative Commons Attribution (CC BY) license (<https://creativecommons.org/licenses/by/4.0/>).

1. Introduction

Glioblastomas (GBs) are the most common tumors in the central nervous system (CNS) malignancies and have the worst overall survival, which makes them clinically relevant. GBs are often diagnosed at 50–65 years old [1]. According to data between 1995 and 2021, they have an incidence of 3–7 per 100,000 inhabitants depending on the nation, even though their frequency rises in many countries [2–4]. The survival time of patients with GBs is about 2–4 months without treatment [4,5] due to the highly proliferative and invasive capacity of GB cells [1]. GBs present a higher incidence in men than in women at 1.60:1, which remain unchanged for years [3,4]. This datum has brought attention to the study of sex-specific components that contribute to GB development, such as steroid hormones [6]. Gonadal steroids, like progesterone (P4), participate in the progression of GBs. At physiological concentrations, P4 promotes proliferation, migration, and invasion of GB cells, and it also augments the number of primary gliomaspheres [7–11]. In addition, it has been reported that GB cells actively metabolize P4 [12–14], although the effects of its reduced metabolites have been scarcely studied in cancer. Regarding the effects of 5 α -reduced P4 metabolites, only a few studies on breast and ovarian cancers have been made [15–17].

The first step in the synthesis of active P4 metabolites is the irreversible reduction of P4 to 5 α -dihydroprogesterone (5 α -DHP) through the enzyme 5 α -reductase (5 α R) [12,13,18]. Then, 5 α -DHP is reversibly reduced to allopregnanolone (3 α -THP) by the 3 α -hydroxysteroid dehydrogenases (3 α -HSD), whose activity has been reported in four members of the Aldo-keto reductase enzyme superfamily (AKR1C1-4 by their coding genes) [19,20].

The steroid 3 α -THP has been, by far, the most studied neuroactive metabolite of P4. 3 α -THP is synthesized in the CNS by glial progenitors, neurons, and glial cells in different brain regions such as the cortex, olfactory bulb, hippocampus, thalamus, cerebellum, and amygdala [13,19,21–23]. 3 α -THP increases the expression of proliferating markers, along with the cellular proliferation of rat and human neural progenitor cells [24]. Besides, it has cytoprotective properties against cytotoxic insults in oligodendrocytes [25]. Interestingly, it promotes migration and changes in the morphology of rat Schwann cells through the activation of kinases like c-Src and FAK [26]. 3 α -THP also promotes proliferation and the expression of different cell cycle and cytoskeleton regulators, such as the Rho-associated protein kinase (ROCK) in the U87 human GB cell line [18,27].

P4 metabolism enzymes and the active production of 3 α -THP have been reported in GB cells [12,14,18,28]. In human-derived GB cell lines, it has been reported that P4, 5 α -DHP, and 3 α -THP promote GB malignancy by increasing cell proliferation. Moreover, this effect could be independent of the classical P4 receptor (PR), particularly in the case of 3 α -THP, since it has a very low affinity to PR [18,27,28].

The proto-oncogene non-receptor tyrosine kinase c-Src is a hub protein involved in many cell transduction signals, promoting inflammation, cell survival, proliferation, migration, invasion, and tumor resistance to treatment in GB [29–31]. As we have mentioned, some of the effects of 3 α -THP are mediated by c-Src. However, the 3 α -THP effect on GBs progression is poorly known. Here, we report the effects of 3 α -THP on cell migration and invasion of different human-derived GB cell lines, the relevance of its metabolism, and the interplay between c-Src and 3 α -THP in GB progression. Consult the abbreviations of this manuscript to see a list of the most used abbreviations in this study.

2. Results

2.1. 3 α -THP Promotes Migration and Invasion of Human GB Cells

First, we determined the effect of different concentrations of 3 α -THP (10 nM, 100 nM, and 1 μ M) on cell migration of the three human GB cell lines U251, U87, and LN229. The effect of 3 α -THP was compared to P4 10 nM, due to its previously reported promotion of migration in these cells [8]. In Figure 1, we show that P4 10 nM promoted the migration of U251 cells after 12 h of treatment. Also, we observed that all concentrations of 3 α -THP promoted the migration in U251 and U87 cells at 24 h (Figures 1a–c and S1). In LN229 cells, only 3 α -THP 100 nM increased migration at 24 h of treatment (Figures 1d and S1). In all cell lines, 3 α -THP 100 nM promoted cell migration; therefore, we used this concentration in the subsequent experiments.

Then, we evaluated the invasion capacity of the different human GB cell lines treated with 3 α -THP 100 nM for 24 h. The invasion assays showed that P4 10 nM significantly increased the number of invading cells in U251 and LN229 lines but not in U87 cells (Figure 2), whereas 3 α -THP 100 nM significantly increased the number of invading cells in the three evaluated cell lines (Figure 2a–f). In U251 and LN229 cells, the effect of 3 α -THP was similar to that of P4 (Figure 2a,b,e,f).

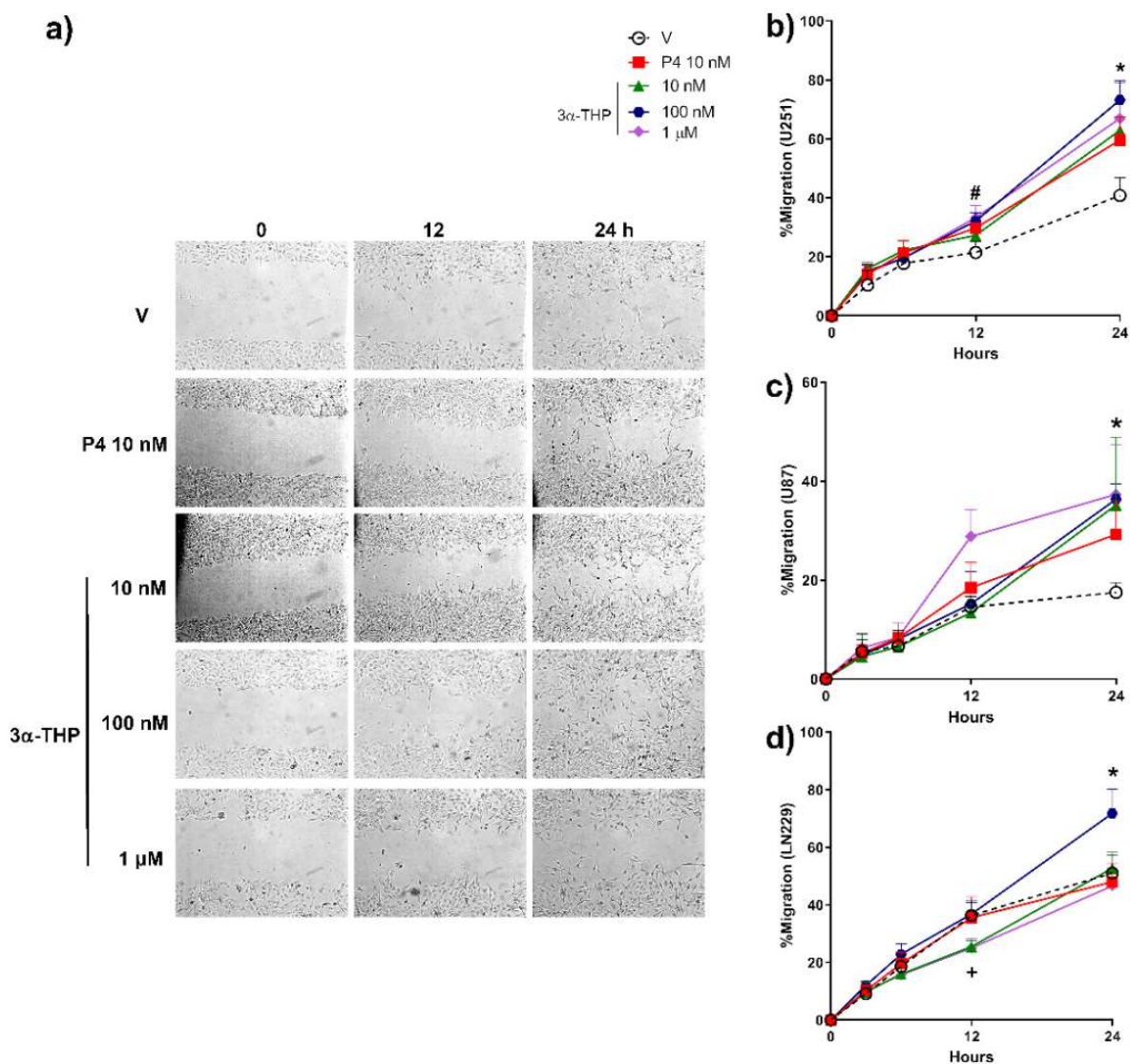


Figure 1. Effect of 3α-THP on human GB cell migration. (a) Representative images of the scratch area from U251 cells treated with vehicle (V, ethanol 0.1% in the medium), progesterone (P4; 10 nM), or allopregnanolone (3α-THP; 10, 100 nM and 1 μM). Percentage migration graphs of (b) U251, (c) U87, and (d) LN229 human GB cell lines. Each point represents the mean ± SEM. U251 (Graph b): # $p < 0.05$ for P4 and 3α-THP 100 nM vs. V; * $p < 0.05$ for P4 and all concentrations of 3α-THP vs. V. U87 (Graph c): * $p < 0.05$ for 3α-THP 10 nM, 100 nM and 1 μM vs. V. LN229 (Graph d): + $p < 0.05$ 3α-THP 10 nM and 1 μM vs. V; * $p < 0.05$ for 3α-THP 100 nM vs. all other treatments. $n = 3$ for U251 and U87 cells; $n = 4$ for LN229 cell line.

2.2. Human GB Cell Lines Express 3α-THP Metabolism Enzymes

3α-HSD are necessary for 3α-THP metabolism. Previously, we have reported, the expression of the Aldo-keto reductases at the mRNA level, called AKR1C1-4 by the name of their genes (35): AKR1C1 (20αHSD), AKR1C2 (3α-HSD type 3), AKR1C3 (3α-HSD type 2), AKR1C4 (3α-HSD type 1) [32,33]. They have a high amino-acid sequence identity, and a similar weight (32–46 kDa) [34]. Here, we determined the protein content of such enzymes in human GB cell lines and compared it with that of normal human astrocytes (HA). All of them were detected as a single Western blot band with a primary antibody designed for the 1–78 amino acids at their N-terminus. The content of AKR1C1-4 enzymes of the HA lysate and U87 cells was low and nearly detected (Figure 3), whereas their content was significantly higher in U251, LN229, and T98G cells when compared with HA (Figure 3).

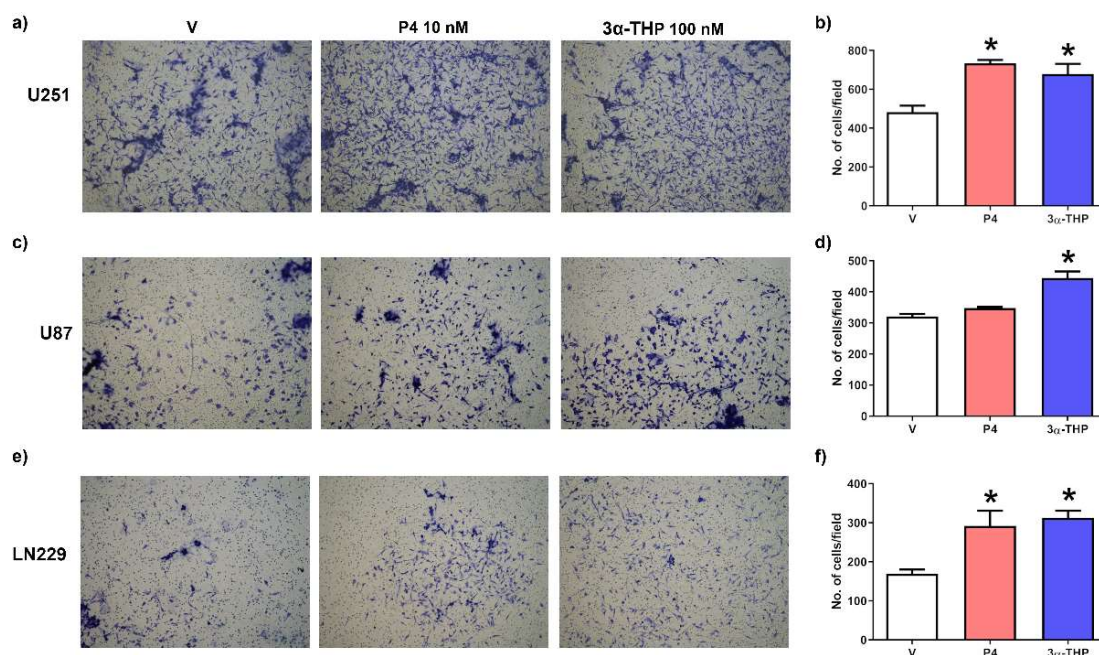


Figure 2. Effect of 3α-THP on the invasion of human GB cell lines. Cells were treated with vehicle (V; ethanol, 0.1% in the medium), P4 (10 nM), and 3α-THP (100 nM) for 24 h. Representative images of (a) U251; (c) U87, and (e) LN229 invasion assays. All photographs were taken at 10× augment. Graphs of the invading cells number per field: (b) U251; (d) U87; and (f) LN229 cell lines. Each column represents the mean ± SEM. $n = 3$ for all cell lines evaluated; * $p < 0.05$ vs. V.

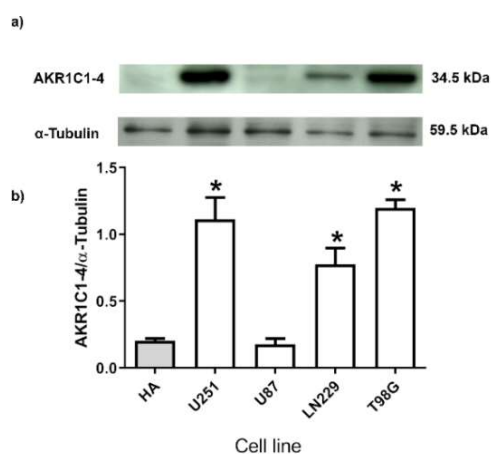


Figure 3. AKR1C1-4 are differentially expressed in GB cells. The expression of AKR1C1-4 was detected in a total protein extract from normal human astrocytes (HA) and different human GB cell lines. (a) Representative Western blots of AKR1C1-4 and α-Tubulin, which was used as a loading control. (b) Densitometric analysis graph. Each column represents the mean ± SEM. $n = 3$; * $p < 0.05$ U251, T98G, and LN229 vs. HA and U87 cell lines.

2.3. Role of AKR1C1-3 Silencing in the Effect of 3α-THP on GB Cell Migration and Invasion

To determine the effect of 3α-THP metabolism in the migration of human GB cells in the U251 cell line, we silenced the expression of the Aldo-keto reductases AKR1C1-3, which mainly participates in metabolizing 3α-THP in the brain. First, we ensured that AKR1C1-3 isozymes were silenced during the wound healing assays (Figure 4a). 3α-THP promoted cell migration in the sAKR1C1-3 U251 cells and the Control siRNA group compared to the V sAKR1C1-3 and Control siRNA groups (Figure 4b,c); this indicates that 3α-THP promotes cell migration of U251 cell line independently of its metabolism by the enzymes AKR1C1-3.

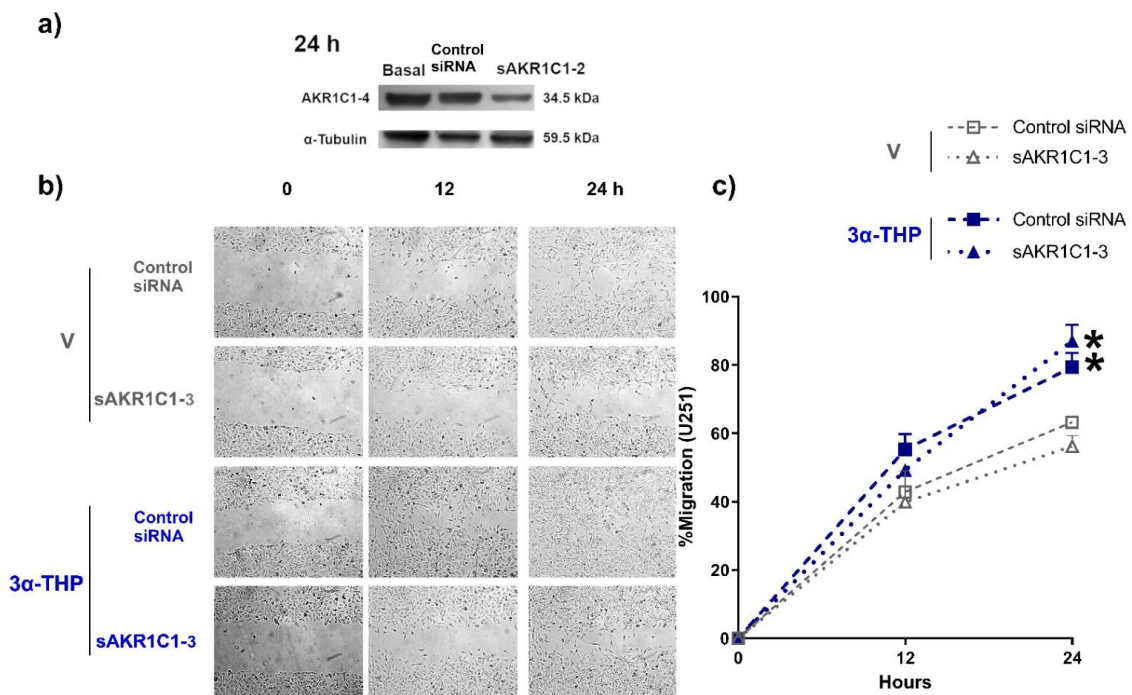


Figure 4. Effect of 3α-THP and the silencing of AKR1Cs on the migration of U251 cells. (a) AKR1C1-3 silencing for 24 h and at the beginning of migration assays. (b) Representative images of U251 cells without transfection, transfected with the negative control siRNA (Control siRNA), and transfected with de the siRNA against AKR1C1-3 (sAKR1C1-3). Cells were treated with V or 3α-THP. (c) Graph of the percentage of U251 migrating cells. Each point represents the mean ± SEM. * $p < 0.05$ 3α-THP (control siRNA, and sAKR1C1-3) vs. V (control siRNA, and sAKR1C1-3); $n = 3$.

Next, we determined the effect of 3α-THP metabolism on the human GB U251 cell line invasion. 3α-THP promoted the invasion of the U251 cell line in Control siRNA, and sAKR1C1-3 groups when compared with V (Control siRNA and sAKR1C1-3). We did not find any significant differences in cell invasion between groups treated with V (Control siRNA and sAKR1C1-3), nor between those treated with 3α-THP (Control siRNA and sAKR1C1-3) (Figure 5a,b). This points out that 3α-THP promotes cell invasion per se and not by generating other progesterin products from AKR1C1-3 activity in GB cells.

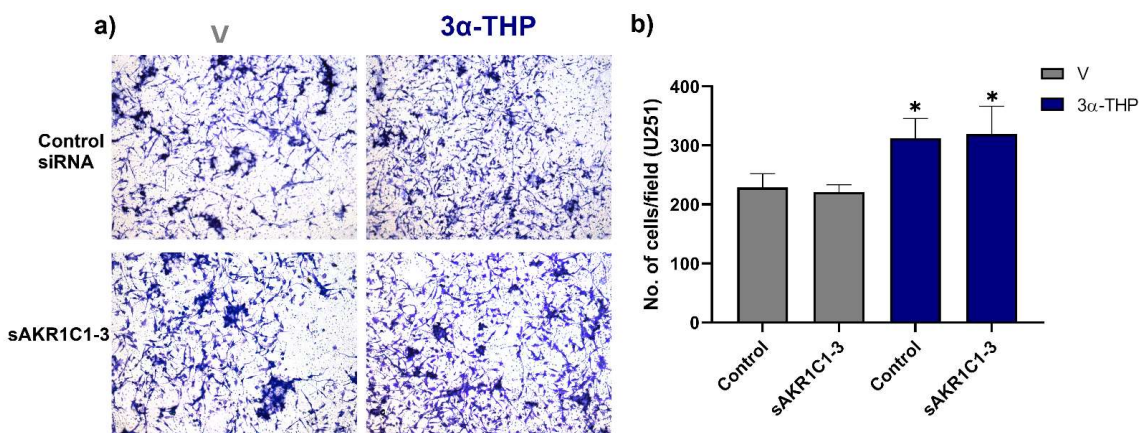


Figure 5. Effect of 3α-THP and the silencing of AKR1Cs on the invasion of U251 cells. (a) Representative images of U251 cells transfected with the negative control siRNA (Control siRNA), the siRNA against AKR1C1-3 (sAKR1C1-3) and treated with V or 3α-THP. (b) Graph of the number of invading U251 cells per field. Each point represents the mean ± SEM. * $p < 0.05$ THP (control SiRNA and sAKR1C1-3) vs. V (control siRNA and sAKR1C1-3) $n = 4$.

2.4. 3α -THP Promotes c-Src Activation in Human GB Cell Lines

The involvement of c-Src in the transduction signals induced by 3α -THP has been reported [26]. To elucidate the participation of c-Src in the effects of 3α -THP on human GB cells, we first determined the phosphorylation of Y416 residue of c-Src at (5–60 min). Phosphorylation increased at Y416 of c-Src residue was correlated with an augment of c-Src activity. We found a significant augment in Y416 phosphorylated c-Src after 10 min of 3α -THP 100 nM treatment in U251 cells compared to V (Figure 6). We also observed a significant increase in Y416 phosphorylated c-Src with 3α -THP treatment at 15 min in U87 and LN299 cells (Supplementary Figures S2 and S3).

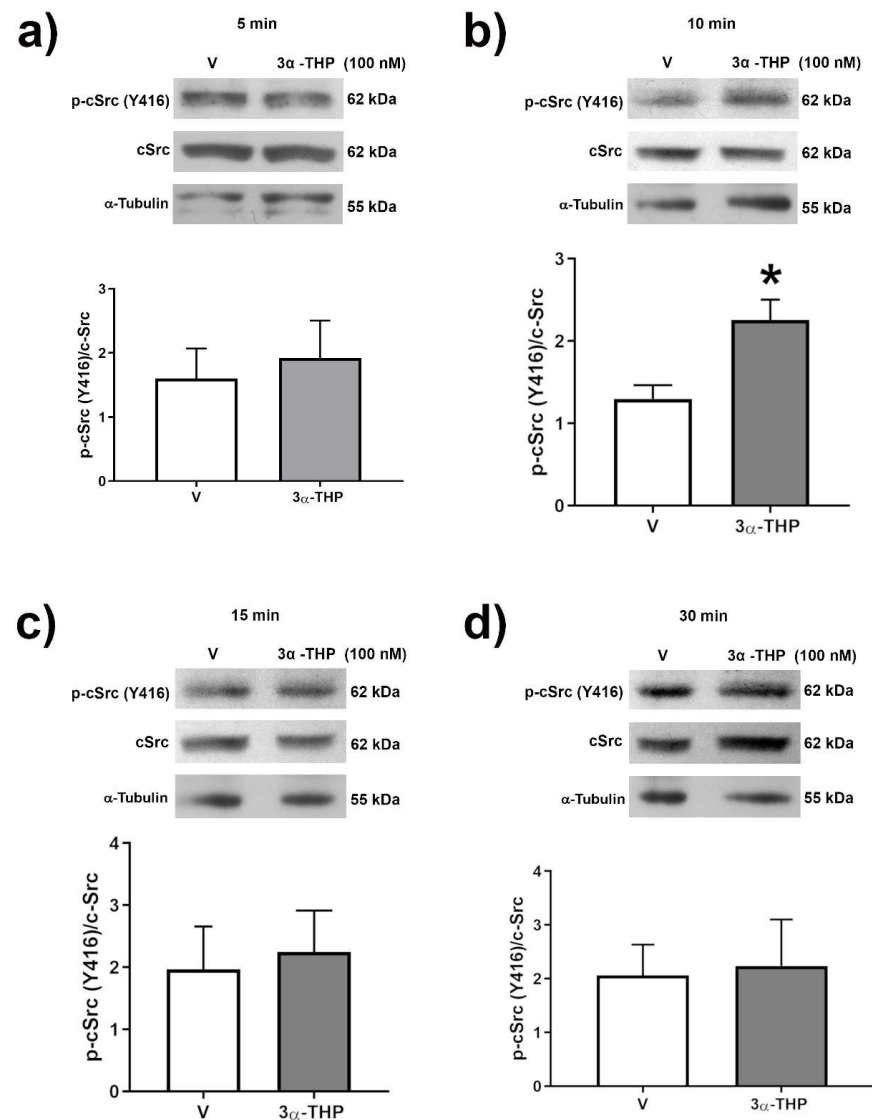


Figure 6. Effect of 3α -THP on c-Src activation in U251 GB cells in time-course experiments. The phosphorylation of c-Src (Y416) was determined under the treatments of 3α -THP 100 nM or Vehicle (V, EtOH 0.01%) at (a) 5 min; (b) 10 min; (c) 15 min; (d) 30 min by Western blot. The upper panel of each section shows a representative Western blot experiment of p-c-Src, total c-Src, and α -Tubulin as a loading control. Each lower panel presents the densitometric analysis of p-c-Src/c-Src. Each column represents the mean \pm SEM, $n = 3$; * $p < 0.05$ 3α -THP vs. V.

2.5. Influence of c-Src Inhibition in the Effect of 3α -THP on Cell Invasion

Since we observed changes in c-Src phosphorylation, then we evaluated if 3α -THP effects on invasion were mediated by this enzyme. We performed invasion assays with the

c-Src pharmacological inhibitor PP2 1 μM , alone or in combination (3 α -THP + PP2). Again, we showed that 3 α -THP promoted invasion in U251 and U87 cell lines. Interestingly, the effect of 3 α -THP was significantly decreased by PP2 (Figures 7 and S4).

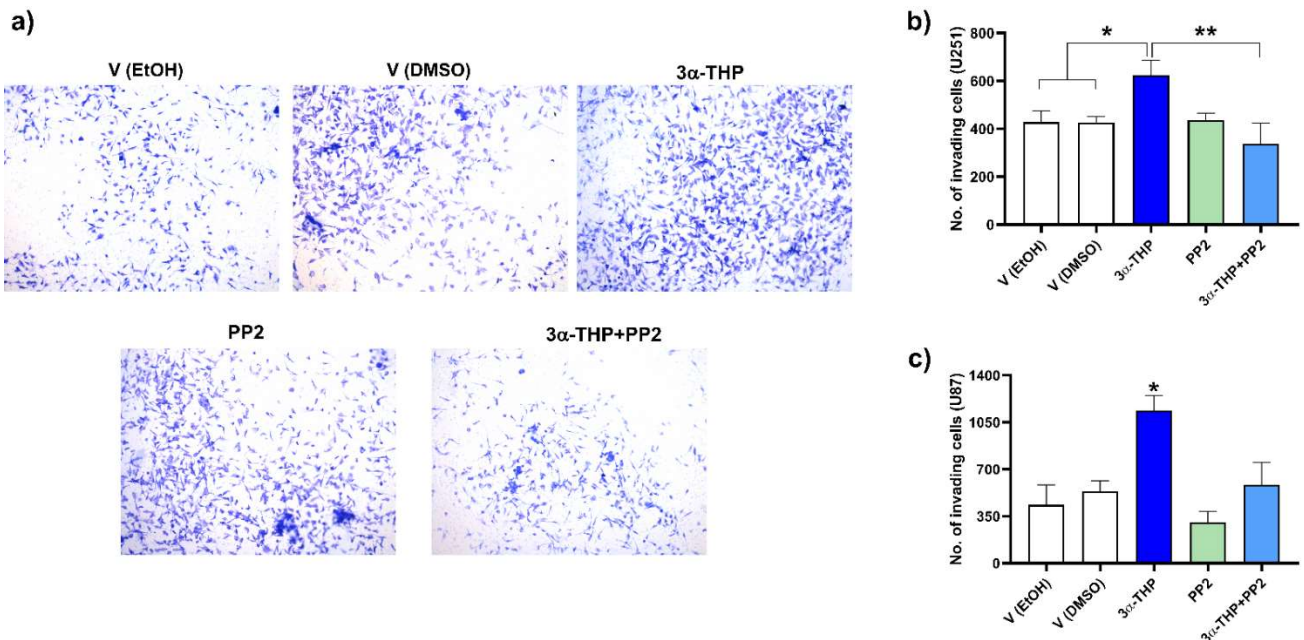


Figure 7. Effect of 3 α -THP and the pharmacological inhibitor of c-SRC PP2 on U251 and U87 cell invasion. (a) Representative images of U251 cell invasion assays. All photographs were taken at 10 \times augment. (b) Graph of the number of invading U251 cells per field. Each column represents the mean \pm SEM., $n = 4$; * $p < 0.05$ 3 α -THP vs. V (EtOH, and DMSO); ** $p < 0.005$ 3 α -THP vs. 3 α -THP + PP2. (c) Graph of the number of invading U87 cells per field. Each column represents the mean \pm SEM., $n = 4$; * $p < 0.05$ 3 α -THP vs. all other treatments.

3. Discussion

In recent years the evidence of sexual dimorphism and gonadal steroids participation in the GB pathophysiology has substantially increased (for review, see [6,35]). Moreover, it has been reported that such hormones are actively metabolized in GB cells [14], and by neural and glial cells in the CNS [19]. This is important because GBs are more frequent in aging patients when the gonadal steroidogenesis is practically null. However, many studies point out that steroidogenic enzymes expression is maintained in different brain areas during aging [36]. Recently, a study based on the transcriptomic information of nearly 900 GB isocitrate dehydrogenase (IDH)-wt patients included in four databases showed that the expression of steroidogenic enzymes by the cells in the core tumor correlates with poor prognostic of GB patients [37].

Despite this, the relevance of many steroid metabolites has been poorly studied in cancer, particularly in glioblastomas. In breast cancer, higher levels of 5 α -pregnanes than in normal tissue have been reported, suggesting that progestins like 5 α -DHP and 3 α -THP have relevance in cancer pathophysiology [38]. In breast cancer cell lines, 5 α -pregnanes promote an augment in the cell viability, even in an estrogen receptor (ER)-/PR-cell line, suggesting that such metabolites exert their actions independently of PR [16,39]. Regarding GB, we have reported that P4, 5 α -DHP, and 3 α -THP promote cell viability and proliferation of human GB cell lines [27,28,40]. Here we report that 3 α -THP promotes migration and invasion in three human GB cell lines (Figures 1 and 2). It is important to notice that the concentrations used in this protocol are relatively low and in concordance with physiological concentrations. Our results are similar to those in the human ovarian cancer cell line IGROV-1, where 3 α -THP promotes cell migration and invasion [17]. In contrast, other authors have recently reported that high concentrations of 3 α -THP (20–60 μM) in-

creased temozolomide-inhibited migration in human T98G and A172 GB cells [41]. This points out that 3 α -THP, similar to P4, differently affect GB progression depending on the concentration, at least in vitro [42].

The Aldo-keto reductases AKR1C1-4 modulate the catabolism of many drugs and gonadal steroids. Along with the 5 α R, Aldo-keto reductases regulate the levels of many steroids, and therefore, their local availability. In the particular case of P4 metabolism, the reduction to 5 α -DHP through the action of 5 α R is irreversible. However, the catabolism of 5 α -DHP to 3 α -THP is reversible. Besides their 3 α -HSD activity, AKR1C1-3 isozymes also have 17 β - and 20 α -HSD activity. We have reported before that GB cell lines express 5 α R and AKR1C1-4 at a transcriptional level [18,28]. Since a tiny band was found in the Western blot for either HA or U87 cells, we cannot discard their presence (Figure 3). In a previous work, we have evaluated the expression of such isozymes by RT-qPCR, and we found concordant results between them and those reported in the present study: both HA and U87 cells present the lower expression levels of such enzymes. When compared with other steroidogenic tissues, the expression of all isozymes in the human brain is low, so we expect that the levels of such enzymes, were also low in human astrocytes [32]. It has been reported that the activity of such enzymes is highly cell type dependent in the CNS. In rat-derived cells, greater significant activity of 3 α -HSD was detected in a very particular subtype of astrocytes (type 1 astrocytes), rather than in type 2 astrocytes or neurons [43]. We consider these results cannot be entirely extrapolated or compared to humans, because until now, only one AKR1C family member with 3 α -HSD activity has been characterized in rats [44]. Besides, many authors determined the activity of such enzymes on different glioma cell lines such as C6 (rat origin), 1231N1 (human astrocytoma), and U87 cells [12,14]. Here we report AKR1C1-4 protein levels in four human GB cell lines compared with those of human astrocyte lysate (Figure 3). Remarkably, the levels of such enzymes were higher in GB cells than in the normal human astrocyte lysate, except for the U87 cell line. Some microarrays analyses suggest that the expression of AKR1C1-3 transcripts levels are significantly lower in GB biopsies compared to normal brain tissue [45]. Discrepancies between AKR1C1-4 mRNA and protein levels have been reported, and they emphasize the importance of better strategies to detect and determine the functional status of such enzymes [46]. The expression of AKR1C1-4 commonly is correlated with a poor prognostic in patients with different types of cancer [34].

As we mentioned, AKR1C1-4 regulates the availability of P4 and its metabolites to activate different signaling pathways. While P4 and 5 α -DHP promote the activation of intracellular PR, 3 α -THP has no affinity to such receptors [18,27,28]. Previously, the role of PR in migration and invasion has been described [8,40]. Here, the silencing of AKR1C1-3 isozymes was necessary to ensure a low conversion of 3 α -THP to metabolites like 5 α -DHP with different mechanisms of action from that of 3 α -THP. Considering a normal phenotype of AKR1C1-4 enzymes in the GB cell lines, it is expected that isozymes AKR1C1-2 are the main involved in the oxidation of 3 α -THP to 5 α -DHP. It has been reported that AKR1C3 isozyme has low oxidation activity of 3 α -THP [32]. Additionally, 3 α -THP is catabolized to 5 α -pregnane-3 α ,20-diol (5 α -pregnanediol) by AKR1C1 enzymes [47]. This metabolite possesses activity as a partial agonist of the γ -aminobutyric acid (GABA) receptor type A (GABA_AR), although with less affinity for the same allosteric site than that of 3 α -THP [48]. In this study, we found that AKR1C1-3 silencing did not alter the effect of 3 α -THP on GB cell migration and invasion (Figures 4 and 5), which indicates that 3 α -THP promotes cell migration and invasion independently of its interconversion to 5 α -DHP or other P4 metabolites such as 5 α -pregnanediol. Since many mechanisms of action have been detected for 3 α -THP, it is important to determine them in glioblastoma.

The most described mechanisms of 3 α -THP so far can be divided into rapid mechanisms mediated by membrane receptors or genomic and slow ones, which depend on the activation of transcription factors. The first implies the modulatory function of neurotransmitters receptors and the activation of membrane P4 receptors (mPR). Regarding rapid mechanisms, 3 α -THP is a positive allosteric modulator of the ionotropic receptor type A of

GABA neurotransmitter (GABA_AR); such effect is enhanced in extra-synaptic GABA_AR containing δ and γ 2-3 subunits [49]. Besides, the physiological concentration of 3 α -THP regulates other aspects of GABA neurotransmission by promoting the expression of three isoforms of the metabotropic GABA receptor type B (GABA_BR) in rat Schwann cells from 4 to 24 h of treatment [50]. Also, 3 α -THP promotes GABA metabolism by upregulating the expression of two isoforms of the glutamate decarboxylase, the rate-limiting step enzyme of GABA synthesis [51]. It has been suggested that GABA_AR levels in GB are lower than in low-grade gliomas [52]. 3 α -THP also has a high affinity to mPR δ and α subtypes. Such receptors are members of the progestin and adipoQ receptor family. mPR δ is coupled to G_s proteins that activate adenylyl cyclase (AC) and favors the increase of AMPc and the activation of ERK in MDA-MB-231 human breast adenocarcinoma cells [53]. With a lesser affinity to that of mPR δ , 3 α -THP also binds to mPR α and mPR β , which are coupled to G_i proteins that promote a decrease in AMPc in GT1-7, a mouse hypothalamic GnRH neuronal immortalized cell line [54]. Also, these mechanisms involve the activation of rapid signaling pathways, particularly of c-Src, and PI3K-Akt signaling to promote cell proliferation and migration of human Schwann cell-like differentiated from adipose stem cells [55].

As indicated before, 3 α -THP also modulates gene transcription due to the activation of the pregnane xenobiotic receptor (PXR). Such receptors mainly promote the expression of transporters and metabolic enzymes, affecting the biosynthesis of 3 α -THP itself [56]. Here, we observed that 3 α -THP (100 nM) treatment induced the rapid phosphorylation of c-Src at 10 and 15 min in U251, U87, and LN229 cell lines (Figures 6, S2 and S3), although it remains unclear which component of the described 3 α -THP mechanisms of action promote the rapid activation of the non-receptor tyrosine kinase c-Src in human GB cell lines. Moreover, when U87 and U251 cell lines were treated with the c-Src inhibitor PP2, the effect of 3 α -THP on GB cell invasion was suppressed and dependent on c-Src activation (Figures 7 and S4). This suggests that 3 α -THP effect depends on the expression status of its possible effectors. Regarding the normal SNC cells, Melfi and cols. reported that low 3 α -THP concentrations promote migration in Schwann rat cells due to activation of c-Src and FAK activation [26].

4. Materials and Methods

4.1. Cell Culture and Treatments

Human GB cell lines U251, LN229, T98G, and U87 (unknown origin) were purchased from ATCC. U251 and U87 cells were authenticated before by STR profiling. All cell lines were cultured in high glucose phenol red Dulbecco's Modified Eagle Medium (DMEM, Biowest, FRA) supplemented with 10% Fetal Bovine Serum (FBS, Biowest, FRA), pyruvate 1 mM (InVitro SA, MEX), non-essential amino acids 0.1 mM (InVitro SA, MEX), and 10 mL/L of antibiotic-antimycotic (Catalog number: L0010; Amphotericin B, Penicillin G Sodium Salt, and Streptomycin Sulfate; Biowest, FRA). Cells were maintained in a 5% CO₂ humidified atmosphere at 37 °C. Before steroid treatments, the medium was replaced by DMEM supplemented with charcoal dextran filtered 10% FBS (without steroid hormones) for 24 h. Cells were treated with vehicle (V; 0.1% ethanol), progesterone (P4; 10 nM), and different concentrations of 3 α -THP (10, 100 nM, and 1 μ M), or as indicated in each section. P4 was purchased from Sigma Aldrich (St. Louis, MO, USA), and 3 α -THP was purchased from MP Biomedicals (Santa Ana, CA, USA). To evaluate the involvement of c-Src in the 3 α -THP effects on migration and invasion, c-Src was pharmacologically inhibited with pyrazolopyrimidine (PP2, 1 μ M) (Sigma Aldrich, MO, USA).

4.2. Migration Assays

To determine the effects of 3 α -THP on GB cell migration, wound-healing assays were performed. 3.5×10^5 U251 or U87 cells, and 2.5×10^5 LN229 cells were seeded in 6-well plates. After 24 h of culture in the red-free DMEM supplemented as indicated in the Cell Culture section, the wound was made in the cell monolayer with a 200 μ L fine pipette tip. The culture medium and the detached cells were washed out with PBS. The cell

culture medium was replaced, and 10 μM of cytosine β -D-arabinofuranoside (AraC) was added 1 h before vehicle and steroid treatments to inhibit cell cycle progression. First, we tested different concentrations of 3 α -THP: 10 nM, 100 nM, and 1 μM to determine the concentration with effect on cell migration. For subsequent experiments, the chosen concentration of 3 α -THP was 100 nM.

To determine the participation of AKR1C1-4 in 3 α -THP on cell migration, the silencing was performed first as indicated in the siRNA Silencing of AKR1C1-3 section. 24 h after the silencing protocol, the migration assays with V, and 3 α -THP 100 nM, were carried out.

Immediately after adding treatments, photographs of four different fields were taken with an Infinity 1-2C camera (Lumenera, Ottawa, ON, Canada) coupled to the inverted microscope Olympus CKX41. Then, images of the previously selected fields were taken at 0, 6, 12, and 24 h. Images were processed in the ImageJ software with the MRI Would Healing Tool macro.

4.3. Invasion Assays

To determine the effects of 3 α -THP on GB cell invasion, we used a modified Boyden chamber assay. Matrigel (1 mg/mL; extracellular matrix of Engelbreth-Holm-Swarm murine sarcoma, Sigma-Aldrich, St. Louis, MO, USA) diluted in phenol red-free DMEM without supplements were added to the membrane inserts (pore: 8.0 μm ; Corning, New York, NY, USA) and incubated at 37 $^{\circ}\text{C}$ and 5% CO_2 atmosphere for 2 h. Phenol red-free DMEM supplemented with 10% FBS was added as a chemoattractant in the lower chamber, and 2×10^4 U251, U87, or LN229 were incubated on the top of the inserts in phenol red-free DMEM without supplements, with cytosine β -D-arabinofuranoside (AraC; 10 μM), and the pharmacological treatments (V, and 3 α -THP 100 nM).

To determine the effect of the pharmacological inhibition of c-Src on the 3 α -THP effect on cell invasion, cells were treated with V, 3 α -THP 100 nM, the c-Src inhibitor PP2 (1 μM), and the conjunct treatments of 3 α -THP + PP2.

Silencing of Aldo-keto reductases AKR1C1-3 was performed as indicated in the siRNA Silencing of AKR1C1-3 section before the invasion assays with the pharmacological treatments were performed.

After 24 h of culture at 37 $^{\circ}\text{C}$ and 5% CO_2 atmosphere, the cell culture medium was retired, and the inserts were gently washed with PBS to eliminate Matrigel and uninvaded cells. Invading cells were fixed to the membrane in the insert with 4% paraformaldehyde for 5 min and stained with crystal violet 1%. After mounting samples with synthetic resin, four fields per treatment were photographed in the Olympus Bx43F microscope (Olympus, Center Valley, PA, USA). Invading cells were counted in the ImageJ software (National Institute of Health, Seattle, WA, USA).

4.4. siRNA Silencing of AKR1C1-3

To determine if the effect of 3 α -THP on cell migration and invasion is mediated through the Tyrosine-Protein Kinase c-SRC, its expression was silenced with one siRNA. To determine the influence of 3 α -THP metabolism on GB cell migration and invasion, AKR1C1-3 were silenced using one siRNA. 2×10^5 U251, U87, or LN229 cells were plated per well in 6-well plates. Cells were grown in phenol red-free DMEM without supplements to perform the transfection. Separately, cells were transfected with a negative control siRNA (control siRNA, 100 nM; Silencer Select Negative Control #1 siRNA1, catalog number: 4390844; Thermo Fisher Scientific, Bannockburn, IL, USA), and the sAKR1C1-3 (100 nM; catalog number: 4392420; ID: s3988; Thermo Fisher Scientific, Bannockburn, IL, USA). The transfection agent was Lipofectamine RNAiMAX (7.5%; Thermo Fisher Scientific, IL, USA); siRNAs were incubated with the transfection agent at room temperature before transfection for 20 min. Then, cells were incubated with siRNA dilutions for 12 h. After transfection, cells were cultured with supplemented phenol red-free DMEM for 24 h. Western blot verification of silencing was performed for the migration or invasion assays.

4.5. Protein Extraction and Western Blotting

To determine the protein content of the Aldo-keto reductases AKR1C1-4 in the human GB cell lines, 2×10^6 U251, U87, LN229, and T98G cells were cultured in 100 mm cell culture plates, as mentioned in the cell culture and treatments section. Before the cellular lysis, cells were cultured in red phenol-free DMEM supplemented with 10% charcoal dextran-filtered SFB for 24 h. Cells were collected and homogenized in RIPA buffer (50 mM Tris-HCl pH 7.5, 150 mM NaCl, 1% Triton, 0.01% SDS, and ethylenediaminetetraacetic acid EDTA, 0.5M, 1 mL) with a protease inhibitors mixture (p8340, Sigma-Aldrich, St. Louis, MO, USA). Samples were maintained in agitation at 4 °C for 1 h, and then centrifuged at 14,000 rpm for 15 min. The supernatant was obtained and stored at -20 °C until quantification with the Pierce Protein Assay reagent (Thermo Scientific, Waltham, MA, USA) according to manufacturer's instructions, and the NanoDrop 2000 spectrophotometer (Thermo Fisher Scientific, IL, USA) at 660 nm. For Western blot determination of AKR1C1-4 (37 kDa), 20 µg of normal human primary astrocytes lysate (HA; 1806, ScienCell, Carlsbad, CA, USA), and 20 µg of protein lysate of the cell lines were mixed with Laemmli 2X buffer (100 mM Tris-base pH 6.8, 20% glycerol, 4% SDS, 10% β-mercaptoethanol, and bromophenol blue) were boiled for 5 min and separated in a 12% SDS-PAGE gels at 80 V. The separated proteins were then transferred to nitrocellulose membranes (Millipore, Burlington, MA, USA) by electrophoresis in semi-dry conditions at 30 mA per membrane for 2 h. Membranes were blocked in agitation at 37 °C with a blocking solution (TBS buffer-0.1% Tween with 5% bovine serum albumin; InVitro, MEX) for 2 h; then, membranes were incubated with a mouse monoclonal AKR1C1-4 antibody (1:1000; sc-390419, Santa Cruz, CA, USA) overnight. Also, blots were incubated with the conjugated to horseradish peroxidase secondary antibody (1:10,000; goat anti-mouse IgG, Santa Cruz, CA, USA) for 45 min. To correct the protein amount loaded in each line, the content of AKR1C1-4 was normalized to that of α-Tubulin. Blots were stripped with a glycine solution (0.1 M, pH 2.5, 0.5% SDS) in agitation for 30 min at 50 °C, and incubated with a mouse anti-α-Tubulin monoclonal primary antibody (T9026, Sigma Aldrich, St. Louis, MO, USA) overnight, and with the goat anti-mouse secondary antibody in agitation for 45 min. For AKR1C1-4 silencing, the same Western Blot conditions were used.

To determine c-Src in GB cell lines, 30 µg of total protein were separated in 8.5% SDS-PAGE gels at 80 V, transference to a nitrocellulose membrane was performed at semi-dry conditions at 25 V for 30 min. When c-Src activation was evaluated, the membranes were first incubated with the primary antibodies for the phosphorylated or total forms of c-Src: phospho c-Src Tyr-416 (1:1000; Ref. 2101; Cell Signaling, Massachusetts, MA, USA), and c-Src (1:1000; Ref. 2108, Cell Signaling, Massachusetts, MA, USA). In both cases, blots were incubated with the conjugated to horseradish peroxidase secondary antibody (1:10,000; Ref: 1858415, goat anti-rabbit IgG, Thermo Scientific, Waltham, MA, USA). The total content of proteins was normalized to that of α-Tubulin.

Chemiluminescence signals of the membranes were detected with the SuperSignal West Femto Maximum Sensitivity (Thermo Scientific, Waltham, MA, USA) kit, according to the manufacturer's instructions, and in Kodak Biomax Light Films (Sigma-Aldrich, St. Louis, MO, USA). Western blot images were captured with a digital camera (SD1400IS, Canon), and densitometric analysis was performed in the ImageJ software (National Institute of Health, Seattle, WA, USA).

4.6. Statistical Analysis

All graphs and statistical analysis were performed in GraphPad Prism 8 Software (GraphPad Software Inc., La Jolla, CA, USA). Each experiment was performed at least in triplicate or as indicated in each figure legend. A one-way ANOVA and the post hoc Bonferroni test with a confidence interval of 95% were performed. A value of $p < 0.05$ was considered significant and was indicated in each figure.

5. Conclusions

Our work indicates that 3α -THP at low concentration participates in the regulation of glioblastoma (GB) malignancy by promoting cell migration and invasion. Such effects are mediated by the rapid activation of c-Src. Besides, GB cells express AKR1C1-4 isozymes, involved in the metabolism of 3α -THP and other steroids, which indicate that such metabolites are actively generated by GB. These data point out the relevance of P4 metabolites in the pathophysiology of GB since they promote the rapid progression of GB through different mechanisms from that of P4.

Supplementary Materials: The following supporting information can be downloaded at: <https://www.mdpi.com/article/10.3390/ijms23094996/s1>.

Author Contributions: Conceptualization, C.J.Z.-S., M.R.-D. and I.C.-A.; methodology, C.J.Z.-S. and C.B.-A.; writing—original draft preparation, C.J.Z.-S.; writing—review and editing, C.J.Z.-S., C.B.-A., M.R.-D. and I.C.-A.; visualization, C.J.Z.-S. and C.B.-A.; supervision, M.R.-D. and I.C.-A.; funding acquisition, I.C.-A. and M.R.-D. All authors have read and agreed to the published version of the manuscript.

Funding: This work, CJZS, and CBA were funded by the Programa de Apoyo a Proyectos de Investigación e Innovación Tecnológica (PAPIIT), project number: IN217120, DGAPA-UNAM, México.

Conflicts of Interest: The authors declare no conflict of interest.

Abbreviations

3α -HSD	3α -Hydroxysteroid dehydrogenase
20α -HSD	20α -Hydroxysteroid dehydrogenase
3α -THP	Allopregnanolone
5α -DHP	Dihydroprogesterone
5α R	5α -Reductase
AKR1C1	Aldo-keto reductase family 1 member C1 (also $20\alpha(3\alpha)$ -HSD)
AKR1C2	Aldo-keto reductase family 1 member C2 (also 3α -HSD type 3)
AKR1C3	Aldo-keto reductase family 1 member C3 (also $3\alpha(17\beta)$ -HSD type 2)
AKR1C4	Aldo-keto reductase family 1 member C4 (also 3α -HSD type 1)
AraC	cytosine β -D-arabinofuranoside
c-Src	SRC Proto-Oncogene, Non-Receptor Tyrosine Kinase
ERK	Mitogen-activated protein kinase
FAK	Focal adhesion kinase
GABA	γ -aminobutyric acid
GABA _A R	γ -aminobutyric acid type A receptor
GABA _B R	γ -aminobutyric acid type B receptor
GB	Glioblastoma
HA	Human astrocytes
mPR α	Membrane progesterone receptor α (PAQR-7)
mPR β	Membrane progesterone receptor β (PAQR-8)
mPR γ	Membrane progesterone receptor γ (PAQR-5)
mPR δ	Membrane progesterone receptor δ (PAQR-6)
mPR ϵ	Membrane progesterone receptor ϵ (PAQR-9)
P4	Progesterone
PR	Progesterone receptor
sAKR1C1-3	GB cells with silenced expression of the Aldo-keto reductase family 1 member C1-3
V	Vehicle, ethanol 0.1% in the medium

References

1. Wen, P.Y.; Weller, M.; Lee, E.Q.; Alexander, B.M.; Barnholtz-Sloan, J.S.; Barthel, F.P.; Batchelor, T.T.; Bindra, R.S.; Chang, S.M.; Chiocca, E.A.; et al. Glioblastoma in adults: A Society for Neuro-Oncology (SNO) and European Society of Neuro-Oncology (EANO) consensus review on current management and future directions. *Neuro-Oncology* **2020**, *22*, 1073–1113. [[CrossRef](#)] [[PubMed](#)]
2. Davis, F.G.; Smith, T.R.; Gittleman, H.R.; Ostrom, Q.T.; Kruchko, C.; Barnholtz-Sloan, J.S. Glioblastoma incidence rate trends in Canada and the United States compared with England, 1995–2015. *Neuro-Oncology* **2020**, *22*, 301–302. [[CrossRef](#)] [[PubMed](#)]
3. Simińska, D.; Korbecki, J.; Kojder, K.; Kapczuk, P.; Fabiańska, M.; Gutowska, I.; Machoy-Mokrzyńska, A.; Chlubek, D.; Baranowska-Bosiacka, I. Epidemiology of anthropometric factors in glioblastoma multiforme—Literature review. *Brain Sci.* **2021**, *11*, 116. [[CrossRef](#)] [[PubMed](#)]
4. Ostrom, Q.T.; Patil, N.; Cioffi, G.; Waite, K.; Kruchko, C.; Barnholtz-Sloan, J.S. CBTRUS Statistical Report: Primary Brain and Other Central Nervous System Tumors Diagnosed in the United States in 2013–2017. *Neuro-Oncology* **2020**, *22*, iv1–iv96. [[CrossRef](#)]
5. Ohgaki, H. Epidemiology of brain tumors. *Methods Mol. Biol.* **2009**, *472*, 323–342.
6. Bello-Alvarez, C.; Camacho-Arroyo, I. Impact of sex in the prevalence and progression of glioblastomas: The role of gonadal steroid hormones. *Biol. Sex Differ.* **2021**, *12*, 28. [[CrossRef](#)]
7. Germán-Castelán, L.; Manjarrez-Marmolejo, J.; González-Arenas, A.; Camacho-Arroyo, I. Intracellular Progesterone Receptor Mediates the Increase in Glioblastoma Growth Induced by Progesterone in the Rat Brain. *Arch. Med. Res.* **2016**, *47*, 419–426. [[CrossRef](#)]
8. Piña-Medina, A.G.; Hansberg-Pastor, V.; González-Arenas, A.; Cerbón, M.; Camacho-Arroyo, I. Progesterone promotes cell migration, invasion and cofilin activation in human astrocytoma cells. *Steroids* **2016**, *105*, 19–25. [[CrossRef](#)]
9. Del Moral-Morales, A.; González-Orozco, J.C.; Capetillo-Velázquez, J.M.; Piña-Medina, A.G.; Camacho-Arroyo, I. The Role of mPR δ and mPR ϵ in Human Glioblastoma Cells: Expression, Hormonal Regulation, and Possible Clinical Outcome. *Horm. Cancer* **2020**, *11*, 117–127. [[CrossRef](#)]
10. Piña-Medina, A.G.; Díaz, N.F.; Molina-Hernández, A.; Mancilla-Herrera, I.; Camacho-Arroyo, I. Effects of progesterone on the cell number of gliomaspheres derived from human glioblastoma cell lines. *Life Sci.* **2020**, *249*, 117536. [[CrossRef](#)]
11. Bello-Alvarez, C.; Moral-Morales, A.D.; González-Arenas, A.; Camacho-Arroyo, I. Intracellular Progesterone Receptor and cSrc Protein Working Together to Regulate the Activity of Proteins Involved in Migration and Invasion of Human Glioblastoma Cells. *Front. Endocrinol.* **2021**, *12*, 286. [[CrossRef](#)]
12. Melcangi, R.C.; Cavarretta, I.; Magnaghi, V.; Ballabio, M.; Martini, L.; Motta, M. Crosstalk between normal and tumoral brain cells. Effect on sex steroid metabolism. *Endocrine* **1998**, *8*, 65–71. [[CrossRef](#)]
13. Garcia, L.M.P.; Valdez, R.A.; Navarrete, A.; Cabeza, M.; Segovia, J.; Romano, M.C. Cell line derived from glioblastoma synthesizes steroid hormone. Effect of enzyme inhibitors. *Endocr. Abstr.* **2018**, *56*, 136. [[CrossRef](#)]
14. Pinacho-Garcia, L.M.; Valdez, R.A.; Navarrete, A.; Cabeza, M.; Segovia, J.; Romano, M.C. The effect of finasteride and dutasteride on the synthesis of neurosteroids by glioblastoma cells. *Steroids* **2020**, *155*, 108556. [[CrossRef](#)]
15. Wiebe, J.P.; Muzia, D.; Hu, J.; Szwajcer, D.; Hill, S.A.; Seachrist, J.L. The 4-pregnene and 5 α -pregnane progesterone metabolites formed in nontumorous and tumorous breast tissue have opposite effects on breast cell proliferation and adhesion. *Cancer Res.* **2000**, *60*, 936–943.
16. Wiebe, J.P.; Zhang, G.; Welch, I.; Cadieux-Pitre, H.-A.T. Progesterone metabolites regulate induction, growth, and suppression of estrogen- and progesterone receptor-negative human breast cell tumors. *Breast Cancer Res.* **2013**, *15*, R38. [[CrossRef](#)]
17. Pelegrina, L.T.; de los Ángeles Sanhueza, M.; Ramona Cáceres, A.R.; Cuello-Carrión, D.; Rodríguez, C.E.; Laconi, M.R. Effect of progesterone and first evidence about allopregnanolone action on the progression of epithelial human ovarian cancer cell lines. *J. Steroid Biochem. Mol. Biol.* **2020**, *196*, 105492. [[CrossRef](#)]
18. Zamora-Sánchez, C.J.; Hansberg-Pastor, V.; Salido-Guadarrama, I.; Rodríguez-Dorantes, M.; Camacho-Arroyo, I. Allopregnanolone promotes proliferation and differential gene expression in human glioblastoma cells. *Steroids* **2017**, *119*, 36–42. [[CrossRef](#)]
19. Gago, N.; Akwa, Y.; Sananès, N.; Guennoun, R.; Baulieu, E.E.; El-Etr, M.; Schumacher, M. Progesterone and the oligodendroglial lineage: Stage-dependent biosynthesis and metabolism. *Glia* **2001**, *36*, 295–308. [[CrossRef](#)]
20. Penning, T.M. Human hydroxysteroid dehydrogenases and pre-receptor regulation: Insights into inhibitor design and evaluation. *J. Steroid Biochem. Mol. Biol.* **2011**, *125*, 46–56. [[CrossRef](#)]
21. Bixo, M.; Andersson, A.; Winblad, B.; Purdy, R.H.; Bäckström, T. Progesterone, 5 α -pregnane-3,20-dione and 3 α -hydroxy-5 α -pregnane-20-one in specific regions of the human female brain in different endocrine states. *Brain Res.* **1997**, *764*, 173–178. [[CrossRef](#)]
22. Agis-Balboa, R.C.; Pinna, G.; Zhubi, A.; Maloku, E.; Veldic, M.; Costa, E.; Guidotti, A. Characterization of brain neurons that express enzymes mediating neurosteroid biosynthesis. *Proc. Natl. Acad. Sci. USA* **2006**, *103*, 14602–14607. [[CrossRef](#)] [[PubMed](#)]
23. Melcangi, R.C.; Poletti, A.; Cavarretta, I.; Celotti, F.; Colciago, A.; Magnaghi, V.; Motta, M.; Negri-Cesi, P.; Martini, L. The 5 α -reductase in the central nervous system: Expression and modes of control. *J. Steroid Biochem. Mol. Biol.* **1998**, *65*, 295–299. [[CrossRef](#)]
24. Wang, J.M.; Johnston, P.B.; Ball, B.G.; Brinton, R.D. The neurosteroid allopregnanolone promotes proliferation of rodent and human neural progenitor cells and regulates cell-cycle gene and protein expression. *J. Neurosci.* **2005**, *25*, 4706–4718. [[CrossRef](#)]

25. Noorbakhsh, F.; Ellestad, K.K.; Maingat, F.; Warren, K.G.; Han, M.H.; Steinman, L.; Baker, G.B.; Power, C. Impaired neurosteroid synthesis in multiple sclerosis. *Brain* **2011**, *134*, 2703–2721. [[CrossRef](#)]
26. Melfi, S.; Guevara, M.; Bonalume, V.; Ruscica, M.; Colciago, A.; Simoncini, T.; Magnaghi, V. Src and phospho-FAK kinases are activated by allopregnanolone promoting Schwann cell motility, morphology and myelination. *J. Neurochem.* **2017**, *141*, 165–178. [[CrossRef](#)]
27. Zamora-Sánchez, C.; del Moral-Morales, A.; Hernández-Vega, A.; Hansberg-Pastor, V.; Salido-Guadarrama, I.; Rodríguez-Dorantes, M.; Camacho-Arroyo, I. Allopregnanolone Alters the Gene Expression Profile of Human Glioblastoma Cells. *Int. J. Mol. Sci.* **2018**, *19*, 864. [[CrossRef](#)]
28. Zamora-Sánchez, C.J.; Hernández-Vega, A.M.; Gaona-Domínguez, S.; Rodríguez-Dorantes, M.; Camacho-Arroyo, I. 5 α -dihydroprogesterone promotes proliferation and migration of human glioblastoma cells. *Steroids* **2020**, *163*, 108708. [[CrossRef](#)]
29. Torrisi, F.; Vicario, N.; Spitale, F.M.; Cammarata, F.P.; Minafra, L.; Salvatorelli, L.; Russo, G.; Cuttone, G.; Valable, S.; Gulino, R.; et al. The Role of Hypoxia and SRC Tyrosine Kinase in Glioblastoma Invasiveness and Radioresistance. *Cancers* **2020**, *12*, 2860. [[CrossRef](#)]
30. Li, Y.; Min, W.; Li, M.; Han, G.; Dai, D.; Zhang, L.; Chen, X.; Wang, X.; Zhang, Y.; Yue, Z.; et al. Identification of hub genes and regulatory factors of glioblastoma multiforme subgroups by RNA-seq data analysis. *Int. J. Mol. Med.* **2016**, *38*, 1170. [[CrossRef](#)]
31. Cirotti, C.; Contadini, C.; Barilà, D. SRC Kinase in Glioblastoma: News from an Old Acquaintance. *Cancers* **2020**, *12*, 1558. [[CrossRef](#)]
32. Penning, T.M.; Burczynski, M.E.; Jez, J.M.; Hung, C.F.; Lin, H.K.; Ma, H.; Moore, M.; Palackal, N.; Ratnam, K. Human 3 α -hydroxysteroid dehydrogenase isoforms (AKR1C1-AKR1C4) of the aldo-keto reductase superfamily: Functional plasticity and tissue distribution reveals roles in the inactivation and formation of male and female sex hormones. *Biochem. J.* **2000**, *351*, 67–77. [[CrossRef](#)]
33. Jez, J.M.; Bennett, M.J.; Schlegel, B.P.; Lewis, M.; Penning, T.M. Comparative anatomy of the aldo-keto reductase superfamily. *Biochem. J.* **1997**, *326*, 625–636. [[CrossRef](#)]
34. Zeng, C.-M.; Chang, L.-L.; Ying, M.-D.; Cao, J.; He, Q.-J.; Zhu, H.; Yang, B. Aldo-Keto Reductase AKR1C1-AKR1C4: Functions, Regulation, and Intervention for Anti-cancer Therapy. *Front. Pharmacol.* **2017**, *8*, 119. [[CrossRef](#)]
35. Carrano, A.; Juarez, J.J.; Incontri, D.; Ibarra, A.; Guerrero Cazares, H. Sex-Specific Differences in Glioblastoma. *Cells* **2021**, *10*, 1783. [[CrossRef](#)]
36. Zwain, I.H.; Yen, S.S.C. Neurosteroidogenesis in Astrocytes, Oligodendrocytes, and Neurons of Cerebral Cortex of Rat Brain. *Endocrinology* **1999**, *140*, 3843–3852. [[CrossRef](#)]
37. Sharpe, M.A.; Baskin, D.S.; Jenson, A.V.; Baskin, A.M. Hijacking Sexual Immuno-Privilege in GBM—An Immuno-Evasion Strategy. *Int. J. Mol. Sci.* **2021**, *22*, 10983. [[CrossRef](#)]
38. Wiebe, J.P.; Beausoleil, M.; Zhang, G.; Cialacu, V. Opposing actions of the progesterone metabolites, 5 α -dihydroprogesterone (5 α P) and 3 α -dihydroprogesterone (3 α HP) on mitosis, apoptosis, and expression of Bcl-2, Bax and p21 in human breast cell lines. *J. Steroid Biochem. Mol. Biol.* **2010**, *118*, 125–132. [[CrossRef](#)]
39. Wiebe, J.P.; Rivas, M.A.; Mercogliano, M.F.; Elizalde, P.V.; Schillaci, R. Progesterone-induced stimulation of mammary tumorigenesis is due to the progesterone metabolite, 5 α -dihydroprogesterone (5 α P) and can be suppressed by the 5 α -reductase inhibitor, finasteride. *J. Steroid Biochem. Mol. Biol.* **2015**, *149*, 27–34. [[CrossRef](#)]
40. Germán-Castelán, L.; Manjarrez-Marmolejo, J.; González-Arenas, A.; González-Morán, M.G.; Camacho-Arroyo, I. Progesterone induces the growth and infiltration of human astrocytoma cells implanted in the cerebral cortex of the rat. *BioMed Res. Int.* **2014**, *2014*, 393174. [[CrossRef](#)]
41. Feng, Y.-H.; Lim, S.-W.; Lin, H.-Y.; Wang, S.-A.; Hsu, S.-P.; Kao, T.-J.; Ko, C.-Y.; Hsu, T.-I. Allopregnanolone suppresses glioblastoma survival through decreasing DPYSL3 and S100A11 expression. *J. Steroid Biochem. Mol. Biol.* **2022**, *219*, 106067. [[CrossRef](#)] [[PubMed](#)]
42. Atif, F.; Yousuf, S.; Stein, D.G. Anti-tumor effects of progesterone in human glioblastoma multiforme: Role of PI3K/Akt/mTOR signaling. *J. Steroid Biochem. Mol. Biol.* **2015**, *146*, 62–73. [[CrossRef](#)] [[PubMed](#)]
43. Melcangi, R.C.; Celotti, F.; Castano, P.; Martini, L. Differential localization of the 5 α -reductase and the 3 α -hydroxysteroid dehydrogenase in neuronal and glial cultures. *Endocrinology* **1993**, *132*, 1252–1259. [[CrossRef](#)] [[PubMed](#)]
44. Patil, V.; Pal, J.; Somasundaram, K. Elucidating the cancer-specific genetic alteration spectrum of glioblastoma derived cell lines from whole exome and RNA sequencing. *Oncotarget* **2015**, *6*, 43452–43471. [[CrossRef](#)]
45. Le Calvé, B.; Rynkowski, M.; Le Mercier, M.; Bruyère, C.; Lonzec, C.; Gras, T.; Haibe-Kains, B.; Bontempi, G.; Decaestecker, C.; Ruyschaert, J.-M.; et al. Long-term In Vitro Treatment of Human Glioblastoma Cells with Temozolomide Increases Resistance In Vivo through Up-regulation of GLUT Transporter and Aldo-Keto Reductase Enzyme AKR1C1 Expression. *Neoplasia* **2010**, *12*, 727–739. [[CrossRef](#)]
46. Yang, L.; Zhang, J.; Zhang, S.; Dong, W.; Lou, X.; Liu, S. Quantitative Evaluation of Aldo-keto Reductase Expression in Hepatocellular Carcinoma (HCC) Cell Lines. *Genomics. Proteom. Bioinform.* **2013**, *11*, 230–240. [[CrossRef](#)]
47. Sinreih, M.; Anko, M.; Zukunft, S.; Adamski, J.; Rižner, T.L. Important roles of the AKR1C2 and SRD5A1 enzymes in progesterone metabolism in endometrial cancer model cell lines. *Chem. Biol. Interact.* **2015**, *234*, 297–308. [[CrossRef](#)]
48. Belelli, D.; Gee, K.W. 5 α -pregnan-3 α ,20 α -diol behaves like a partial agonist in the modulation of GABA-stimulated chloride ion uptake by synaptoneurosome. *Eur. J. Pharmacol.* **1989**, *167*, 173–176. [[CrossRef](#)]

49. Hosie, A.M.; Wilkins, M.E.; Da Silva, H.M.A.; Smart, T.G. Endogenous neurosteroids regulate GABAA receptors through two discrete transmembrane sites. *Nature* **2006**, *444*, 486–489. [[CrossRef](#)]
50. Magnaghi, V.; Ballabio, M.; Consoli, A.; Lambert, J.J.; Roglio, I.; Melcangi, R.C. GABA receptor-mediated effects in the peripheral nervous system. *J. Mol. Neurosci.* **2006**, *28*, 89–102. [[CrossRef](#)]
51. Magnaghi, V.; Parducz, A.; Frasca, A.; Ballabio, M.; Procacci, P.; Racagni, G.; Bonanno, G.; Fumagalli, F. GABA synthesis in Schwann cells is induced by the neuroactive steroid allopregnanolone. *J. Neurochem.* **2010**, *112*, 980–990. [[CrossRef](#)]
52. Cucchiara, F.; Pasqualetti, F.; Giorgi, F.S.; Danesi, R.; Bocci, G. Epileptogenesis and oncogenesis: An antineoplastic role for antiepileptic drugs in brain tumours? *Pharmacol. Res.* **2020**, *156*, 104786. [[CrossRef](#)]
53. Pang, Y.; Dong, J.; Thomas, P. Characterization, neurosteroid binding and brain distribution of human membrane progesterone receptors δ and ϵ (mPR δ and mPR ϵ) and mPR δ involvement in neurosteroid inhibition of apoptosis. *Endocrinology* **2013**, *154*, 283–295. [[CrossRef](#)]
54. Thomas, P.; Pang, Y. Membrane progesterone receptors: Evidence for neuroprotective, neurosteroid signaling and neuroendocrine functions in neuronal cells. *Neuroendocrinology* **2012**, *96*, 162–171. [[CrossRef](#)]
55. Castelnovo, L.F.; Thomas, P. Membrane progesterone receptor α (mPR α /PAQR7) promotes migration, proliferation and BDNF release in human Schwann cell-like differentiated adipose stem cells. *Mol. Cell. Endocrinol.* **2021**, *531*, 111298. [[CrossRef](#)]
56. Frye, C.A.; Koonce, C.J.; Walf, A.A. The pregnane xenobiotic receptor, a prominent liver factor, has actions in the midbrain for neurosteroid synthesis and behavioral/neural plasticity of female rats. *Front. Syst. Neurosci.* **2014**, *8*, 60. [[CrossRef](#)]



Review

Allopregnanolone: Metabolism, Mechanisms of Action, and Its Role in Cancer

Carmen J. Zamora-Sánchez  and Ignacio Camacho-Arroyo *

Unidad de Investigación en Reproducción Humana, Instituto Nacional de Perinatología-Facultad de Química, Universidad Nacional Autónoma de México, Ciudad de México 04510, Mexico

* Correspondence: camachoarroyo@gmail.com; Tel.: +52-55-5622-3732

Abstract: Allopregnanolone (3α -THP) has been one of the most studied progesterone metabolites for decades. 3α -THP and its synthetic analogs have been evaluated as therapeutic agents for pathologies such as anxiety and depression. Enzymes involved in the metabolism of 3α -THP are expressed in classical and nonclassical steroidogenic tissues. Additionally, due to its chemical structure, 3α -THP presents high affinity and agonist activity for nuclear and membrane receptors of neuroactive steroids and neurotransmitters, such as the Pregnane X Receptor (PXR), membrane progesterone receptors (mPR) and the ionotropic GABA_A receptor, among others. 3α -THP has immunomodulator and antiapoptotic properties. It also induces cell proliferation and migration, all of which are critical processes involved in cancer progression. Recently the study of 3α -THP has indicated that low physiological concentrations of this metabolite induce the progression of several types of cancer, such as breast, ovarian, and glioblastoma, while high concentrations inhibit it. In this review, we explore current knowledge on the metabolism and mechanisms of action of 3α -THP in normal and tumor cells.

Keywords: allopregnanolone; pregnanolone; progesterone; neuroactive steroids; cancer; glioblastoma; membrane progesterone receptor (mPR); PXR; GABA_A receptor



Citation: Zamora-Sánchez, C.J.; Camacho-Arroyo, I. Allopregnanolone: Metabolism, Mechanisms of Action, and Its Role in Cancer. *Int. J. Mol. Sci.* **2023**, *24*, 560. <https://doi.org/10.3390/ijms24010560>

Academic Editor: Daniela Grimm

Received: 23 November 2022

Revised: 17 December 2022

Accepted: 17 December 2022

Published: 29 December 2022



Copyright: © 2022 by the authors. Licensee MDPI, Basel, Switzerland. This article is an open access article distributed under the terms and conditions of the Creative Commons Attribution (CC BY) license (<https://creativecommons.org/licenses/by/4.0/>).

1. Introduction

Allopregnanolone (3α -THP) is a 5α -reduced metabolite of the steroid hormone progesterone (P4), which was the first hormone characterized in the corpus luteum to maintain pregnancy in mammals [1]. The P4 metabolite 3α -THP and its isomer pregnanolone were isolated from the urine of pregnant women in 1934 [2]. Later, a correlation between the chemical structure and sedative effects of 3α -THP and other steroids was determined [3]. Since then, the synthesis of P4 metabolites, the consequences of their impairing synthesis, and their widely diverse mechanisms of action have been described as a never-ending story in both physiological and pathological conditions [4].

The 5α -reduced P4 metabolites were first described as central regulators of female reproductive function, gestation maintenance, and lactation [5–7]. However, other relevant actions of these metabolites, particularly 3α -THP, have been described in females and males. 3α -THP has anti-inflammatory effects [8–10] and, in the central nervous system (CNS), it induces cell proliferation and migration of neural and glial cells [11,12] and promotes neurodevelopment in different vertebrates like rodents and sheep [13]. The impairment of 3α -THP synthesis in the CNS has been associated with pathologies such as Parkinson's and Alzheimer's diseases, anxiety, and depression [14]. Significantly, such effects are mediated through different mechanisms of action from those of P4.

The pioneering work of Wiebe and coworkers in 2000 indicated that levels of 5α -reduced metabolites of P4 are increased in breast cancer [15,16]. Moreover, such steroids promote tumor progression through different mechanisms of action [17]. Along with this, knowledge of 3α -THP's effects on neuroprotection and as a proliferative agent in

the CNS leads to its study in cancer pathophysiology. In this review, we will focus on the synthesis and mechanisms of action described for the P4 metabolite 3 α -THP and summarize evidence of the 3 α -THP effects, or their impaired synthesis and mechanisms of action, on the progression of diverse cancer types, particularly glioblastomas. We wrote our literature review according to guidelines proposed by Marco Pautasso in 2013 [18] and the IJMS guidelines.

2. Allopregnanolone Metabolism in Normal Tissues

The synthesis of 3 α -THP depends on P4 availability in steroidogenic cells. The first rate-limiting step of P4 synthesis is the transport of cholesterol from the endoplasmic reticulum or the cytoplasm to the outer mitochondrial membrane, and then to the inner mitochondrial membrane. In the latter, the P450 side chain cleavage (CYP11A1) catalyzes, as indicated by its name, the cleavage of the C20–C22 side chain from cholesterol to produce pregnenolone and isocaproaldehyde [19]. The mechanism and the proteins involved in the cholesterol transport to the mitochondria are not well defined. Some studies point to a huge complex of proteins that maintain close contact between the membranes of the endoplasmic reticulum and mitochondrial membranes of steroidogenic cells.

Although the mitochondrial cholesterol transport complex differs between steroidogenic tissues, some essential proteins have been identified in tight contact with CYP11A1. Examples of this are the steroidogenic acute regulatory protein (StAR) and the translocator protein of 18 kDa (TSPO) [20,21]. Diverse StAR-related lipid transfer domain-containing proteins have been identified. However, in humans, only two bind sterols: STARD1 and STARD3 [22,23]. In this review, we will focus on STARD1, which is a hydrophobic ~37 kDa protein. Although STARD1 has been broadly detected in the whole mitochondria, studies in the mouse MA-10 tumoral Leydig cell line suggest that STARD1 imports cholesterol only when it is located at the outer mitochondrial membrane [24]. To be functional, STARD1 first enters from the intermembrane space to the mitochondrial matrix to be processed into a ~30 kDa shorter form [25,26]. The structural analysis of such proteins indicates that their N-terminal includes a mitochondrial localization sequence, seconded by the classical α/β grip domain from StAR proteins, and a C-terminal, which comprises the cholesterol-binding pocket [27]. STARD1 is highly hydrophobic and conformationally labile, so deciphering its structural changes for importing cholesterol from the endoplasmic reticulum or cytoplasm to the outer mitochondrial membrane has been difficult. However, its interaction with the oligomerized TSPO channel at the outer mitochondrial membrane and the ATPase family AAA-domain-containing protein 3A (ATAD3A), the link between TSPO, STARD1, and CYP11A1, which is located at the inner mitochondrial membrane, have been described [20].

As a monomer, TSPO is abundantly expressed in steroidogenic cells. It has a five α -helix structure with a cholesterol recognition sequence at its C-Terminal. Its location has been detected as a polymer either at the outer or the inner mitochondrial membrane [22,28]. Besides cholesterol transport, levels of TSPO correlate with changes in fatty acid metabolism in steroidogenic cells [29]. Moreover, the inhibition of TSPO directly decreases 3 α -THP levels in the Ventral Tegmental Area of female rodents' brains [30]. ATAD3A also participates in the complex of cholesterol transport. It contains two transmembrane domains (TM): TM1 (a.a. 225–242), involved in its spanning in the outer mitochondrial membrane, and TM2 (a.a. 264–274), for its transmembrane location at the inner mitochondrial membrane, and colocalizes with CYP11A1 [31].

Once cholesterol is transported to the inner mitochondrial membrane, its C20–C22 side chain is cleaved by the CYP11A1. CYP11A1 depends on NADPH as a cofactor to produce pregnenolone and isocaproaldehyde through the catalysis of three subsequent reactions. The first and limiting step in steroid synthesis is the 22-hydroxylation of cholesterol, seconded by its 20-hydroxylation to finally produce pregnenolone as the product of oxidative cleavage [32,33]. Although we focused on cholesterol catabolism, some of its derivatives have also been identified as substrates of CYP11A1 for synthesizing pregnenolone [33]. In addition, in tissues and cells with a barely detected expression of CYP11A1, like brain

and glial cells, pregnenolone production is detectable and secreted to the culture medium. In such tissues, pregnenolone production was attributed to the metabolic activity of P450 cytochrome other than CYP11A1 [34].

Then, pregnenolone is isomerized to P4 by the 3β -hydroxysteroid dehydrogenase (3β -HSD), which presents two 3β -HSD isozymes: 3β -HSD1 and 3β -HSD2. They are located in the smooth endoplasmic reticulum and the mitochondria [35]. 3β -HSD has been found at the transmembrane inner mitochondrial membrane and in the intermembrane space, where it could be more active due to its structural configuration being sensitive to the pH conditions [36]. P4 is mainly synthesized in the classical steroidogenic tissues: adrenal glands, testis, ovaries, and placenta [35,37,38], although the presence of P4 metabolism machinery has also been reported in tissues such as lungs, skin, and colon, among others, in humans, rodents and monkeys [39–41]. Notably, the 3β -HSD2 isozyme has less affinity for its substrates. In addition, 3β -HSD2 is mainly located in steroidogenic tissues, while 3β -HSD1, which presents high substrate affinity, is mainly expressed in other tissues such as the CNS [19].

The synthesis of 3α -THP from P4 begins with the regulatory step of the reduction of P4 hormone to 5α -Dihydroprogesterone (5α -DHP) by the 5α -reductase enzymes (5α -R), also named 3-oxo-5-alpha-steroid 4-dehydrogenases. In humans, three 5α -R isozymes present homology and are expressed in different tissues (Table 1). However, only 5α -R1 and 5α -R2 have a well-described activity of 5α -reductases, whereas 5α -R3 participates in the N-glycosylation of asparagine residues of membrane proteins [42,43]. In addition, two other proteins have been reported with 5α -reductase activity: the glycoprotein synaptic 2 (GSPN2) and the GSPN2-like. However, less is known about such proteins [44]. Here we will focus on the relevance of 5α -R in 5α -DHP synthesis.

Table 1. Comparative characteristics of the 5α -R isozymes involved in the 5α -reduction of steroids.

Isozyme:	5α -R1	5α -R2
Gen/localization	SRD5A1/5p15.31	SRD5A2/2p23.1
Exons number	7	9
Protein weight	29.4 kDa	28.4 kDa
Optimum pH	6–8.5	~5
Human tissue localization	Brain (mainly in adulthood), gastrointestinal tract, liver, and skin.	Almost exclusive in the male reproductive system, liver, and lungs. It is also reported in the brain (mainly in developmental stages: fetal and newborns), and skin.

The data summarized in this table are from the references [45–47].

The 5α -Rs have an α -rich structure due to their highly hydrophobic amino acid content. They are embedded in the endoplasmic reticulum [48,49]. 5α -R enzymes catalyze the 5α -reduction of the double bond between C4 and C5 of P4 ($\Delta 4,5$ -ene position), using NADPH as a cofactor and introducing a hydrogen atom with 5 alpha stereochemistry into the C5 of P4 [48,50]. Besides P4, other steroid hormones, such as testosterone and corticosteroids, are substrates for these isozymes. The two main differences in the biochemical properties of 5α -Rs are their optimum pH for synthesizing 5α -reduced steroids (Table 1) [51] and their affinity for substrates. While 5α -R1 presents a substrate affinity in micromolar ranges, the 5α -R2 presents a significantly higher affinity in a nanomolar range. Additionally, 5α -Rs have a preferred affinity for P4 over testosterone and corticosteroids [52]. According to some authors, such isozymes present tissue specificity, which could explain the relevance of the preferred synthesis of some hormone metabolites over others in specific tissues. For example, the role of 5α -DHP and 3α -THP on the CNS has been broadly investigated. They maintain neural function and inflammation in males and females throughout life, and their synthesis is mainly attributed to 5α -R1 in adulthood [45]. In contrast, the sexual maturation and function of the reproductive system in males are maintained by testosterone and its

most potent metabolite in humans, the 5 α -dihydrotestosterone, whose synthesis is favored by 5 α -R2 [46].

Once the 5 α -DHP is synthesized, it is then interconverted to 3 α -THP by 3 α -hydroxysteroid dehydrogenases (3 α -HSD). Isozymes with 3 α -HSD activity are members of the Aldo-keto reductases family (AKR), subfamily 1C, which in humans comprises four members (AKR1C1-4) with a protein length of ~37 kDa. They all have a highly conserved structure composed of (α / β)8-barrels with three loops conferring their substrate specificity. They are all coded at the same chromosome by different adjacent genes and share a very high sequence identity [53,54]. The reaction directionality of these enzymes depends on the levels of NAD(P)(H), their cofactor, and the availability of substrates. The AKR1C1-4 isozymes act mainly as reductases because the NAD(P)H is usually higher than the NAD(P)⁺ in the cells. It has also been demonstrated that NAD(P)H inhibits the oxidative reaction of AKR1C2 [55]. Additionally, it has been reported that AKR1C3 has very little oxidative activity [56]. The reduction of 5 α -DHP to 3 α -THP is mainly promoted by AKR1C1-2 and AKR1C4, as indicated by kinetic analyses [57]. Figure 1 presents the pathway of the 3 α -THP metabolism in most steroidogenic human cells.

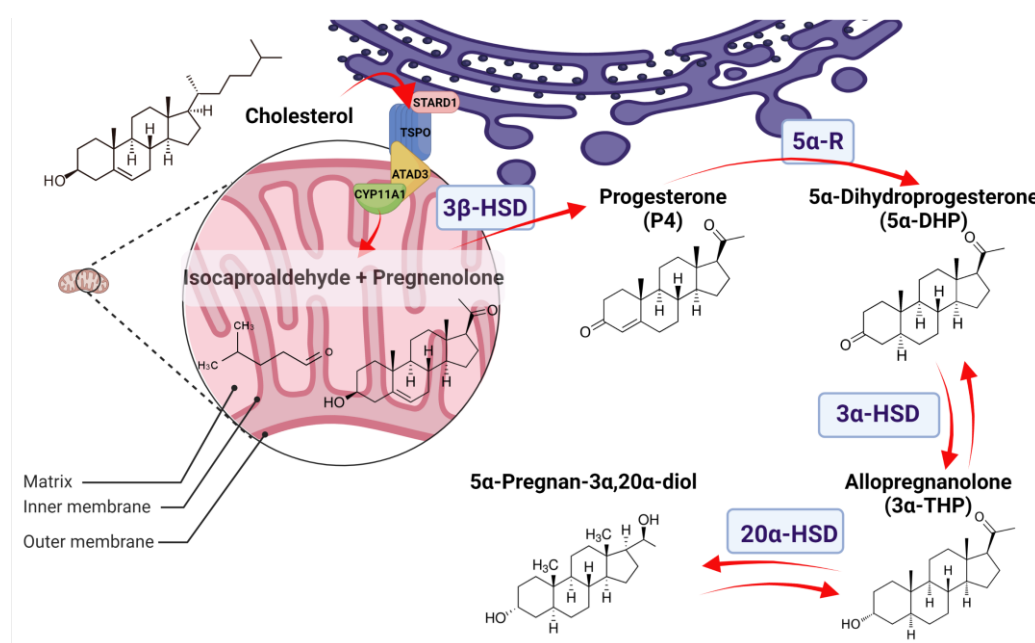


Figure 1. Allopregnanolone (3 α -THP) synthesis in normal tissues. The 3 α -THP synthesis begins when cholesterol is imported from the cytoplasm or the endoplasmic reticulum (purple) to the mitochondrion (pink) by a protein complex formed by the steroidogenic acute regulatory protein (StARD1), the translocator protein of 18 kDa (TSPO), and the ATPase family AAA-domain-containing protein 3A (ATAD3A), which are in close contact with the P450 side chain cleavage (CYP11A1). CYP11A1, at the inner mitochondrial membrane, catalyzes the cleavage of cholesterol to pregnenolone and isocaproaldehyde. Pregnenolone, either in the inner mitochondrial membrane or at the endoplasmic reticulum, is then isomerized to progesterone (P4) by the 3 β -hydroxysteroid dehydrogenase (3 β -HSD). At the endoplasmic reticulum, P4 is irreversibly reduced to 5 α -Dihydroprogesterone (5 α -DHP) by the isozymes 5 α -reductases (5 α -R). At the cytoplasm, 5 α -DHP is reversibly reduced to allopregnanolone (3 α -THP) by 3 α -hydroxysteroid dehydrogenases (3 α -HSD) coded by the AKR1C1-4 genes. Finally, 3 α -THP can be a substrate of the 20 α -hydroxysteroid dehydrogenase (20 α -HSD), coded by AKR1C1, to produce 5 α -Pregnan-3 α ,20 α -diol.

AKR1C1-4 isozymes regulate the metabolism of many steroids (androgens and prostaglandins) and xenobiotics. As well as their 3 α -HSD activity at the C3 carbonyl group of 5 α -DHP, they also promote the reduction or oxidation of other carbonyl groups in the C17 and C20 of the cyclopentanoperhydrophenanthrene structure or at the side chain

of steroid substrates. They also have different preferred activities for reducing the other mentioned carbonyl groups (Table 2). Under normal conditions, the AKR1C4 isozyme is the most active, and its expression is restricted to the liver; however, this differs in certain cancers, as will be discussed in the next section [58]. AKR1C1-3, in contrast, presents a wider distribution in classical steroidogenic and nonclassical steroidogenic tissues. In human lymphatic endothelial cells, the synthesis pathway of 3 α -THP is favored due to a high expression of the involved enzymes [59].

Table 2. Comparative characteristics of the AKR1C1-4 isozymes involved in the 3 α -reduction of steroids.

Isozyme (Gene Name):	AKR1C1	AKR1C2	AKR1C3	AKR1C4
Gene location (exon number)	10p15.1 (9)	10p15.1 (14)	10p15.1 (10)	10p15.1 (9)
Protein name	20 α -(3 α)-HSD	3 α -HSD type 3	3 α -(17 β)-HSD type 2	3 α -HSD type 1
Preferred activity	1. 3 β -keto reductase 2. 20 α -keto reductase 3. 3 α -keto reductase 4. 17 β -keto reductase	3 α -keto reductase	1. 3 α -keto reductase 2. 17 β -keto reductase 3. 20 α -keto reductase	3 α -keto reductase
Human tissue localization	NS, lungs, liver, mammary glands, testis	NS, lungs, prostate, testis, uterus, mammary glands	Prostate, lungs, liver, prostate, mammary glands, uterus, NS	Liver

The data summarized in this table are from references [58,60,61]. NS: Nervous system.

Once 3 α -THP is synthesized, it also serves as a substrate for AKR1C1. 3 α -THP has a ketone group at C20, reduced by AKR1C1, the isoenzyme with the most significant activity of 20 α -keto reductase. The produced metabolite 5 α -Pregnan-3 α ,20 α -diol is much less active than 3 α -THP and comprises the first step before conjugation to be excreted [62,63]. Additionally, 3 α -THP also serves as a substrate for CYP17A1 to produce androsterone as part of the called “backdoor pathway” to promote the synthesis of the potent androgen 5 α -dihydrotestosterone [64].

3. Allopregnanolone Metabolism in Cancer

One of the best-described phenomena that differentiate normal from malignant tissues is the Warburg effect, which is also considered one of the classic hallmarks of cancer [65,66]. The Warburg effect is characterized by the enhanced processing of glucose as the principal energy source through glycolysis and lactate production, even in the presence of normal levels of oxygen. In such conditions, normal cells produce pyruvate for further oxidative phosphorylation [67]. It is still under discussion when such a metabolic shift in cancer cells occurs: in the carcinogenesis process, or the progression of cancer. However, overexpression of glycolytic enzymes and glucose transporters has been reported in cancer tissues. In addition, several metabolite regulators of glycolysis, such as fructose 2,6-biphosphate, are overproduced to evade the inhibition mechanisms of glycolysis [68]. It has been described that several changes in the mitochondrial function in cancer cells are essential to this process [69,70].

As mentioned in the first section above, the mitochondria are involved in several limiting steps of steroidogenesis. One of the main changes identified in tumoral mitochondria is the overproduction of reactive oxygen species, which leads to carcinogenesis when they reach the cellular nucleus and cause DNA damage. One important source of reactive oxygen species is the deregulated expression of the respiratory chain complexes [70].

Regarding cholesterol, in the 1950s, cholesterol was studied as a carcinogen [71]. It is now accepted that hypercholesterolemia and a high-cholesterol diet promote cancer development. Additionally, high levels of lipoproteins involved in cholesterol transport are associated with the worst survival rates in gastric cancer, among others [72]. The synthesis de novo of cholesterol is enhanced in the cancer context. Cholesterol is needed

as a cellular membrane component in highly proliferative cells and for steroidogenesis. Besides, cholesterol is the precursor of all steroid hormones involved in the progression of endocrine and nonendocrine cancers. This section describes current data about alterations in 3α -THP synthesis during cancer. However, it is essential to add that 3α -THP could also regulate the transcription of several enzymes involved in cholesterol processing and steroidogenesis, as will be reviewed in subsequent sections.

As previously mentioned, a rate-limiting step in the 3α -THP synthesis is cholesterol transport to the mitochondria, along with the expression and correct function of CYP11A1. Regarding CYP11A1, the presence of specific single nucleotide polymorphisms in its gene has been associated with a higher risk of endometrial cancer [73]. Moreover, Fan et al. reported that expression of CYP11A1 was downregulated in 2754 samples of different types of cancer, such as prostate and colon adenocarcinoma, renal clear cell, hepatocellular, lung squamous cell, and uterine corpus endometrial carcinoma, all of them located at The Cancer Gene Atlas (TCGA) repository [74]. However, even if the level expression of CYP11A1 is low, pregnenolone synthesis could also occur in tumor cells independently of the CYP11A1. It must be considered that the recent work of Christina Lin et al. included both immortalized and glioblastoma cell lines, so that pregnenolone synthesis could be carried out not just in normal but tumor cells as well. Lin and colleagues found the production of pregnenolone in two cell lines (MGM-1 and MGM-3) of glioblastoma, the most common primary malignant brain tumor. In these models, levels of CYP11A1 were low. However, the production of pregnenolone was observed and associated with the activity of a different CYP family protein [34]. In the MA-10 mouse tumoral Leydig cells, the synthesis of pregnenolone and P4 was significantly decreased when ATAD3A was silenced [75]. Together, this evidence indicates that the P4 metabolism is active in different types of cancer, even when the well-characterized enzymes involved in P4 synthesis, such as CYP11A1, have not been detectable. This points to the relevance of a better characterization of the cholesterol transport and its cleavage to pregnenolone, especially in nonclassical steroidogenic tissues. Additionally, in MGM-1 and MGM-3 human glioblastoma cells, 3β -HSD, 5α -R1, 5α -R2, and AKR1C1-3 expression were observed, indicating that besides pregnenolone, other steroids could be synthesized by these cancer cells. Another study in MGM-3 cells reported the production of P4. However, 3α -THP levels were not measured [76].

Significantly, steroidogenesis in the cancer context could be altered in tumor cells but also in the tumor microenvironment components, such as immune cells. In the B16-F10 melanoma and the orthotopic EO771 breast cancer models in mice, Mahata et al. reported that interleukins commonly found in tumor cells and their environment, such as IL-4, promote Cyp11a1 upregulation and an increase in pregnenolone synthesis in tumor-infiltrating immunosuppressive Th2 lymphocytes. The silencing of Cyp11a1 in such cells was correlated with significant tumor growth inhibition [77].

Regarding 3β -HSD, its expression and involvement in many malignancies have been reported. In ovarian cancer, the protective effects of P4 have been reported, and the StAR, CYP11A1, and 3β -HSD expression have been correlated with better patient prognosis [78]. In a breast cancer study with a cohort of 161 patient samples, 3β -HSD1 expression was correlated with breast cancer ER-positive tumors. Interestingly, the expression of 3β -HSD1 was positively associated with a better prognosis and low risk of cancer recurrence. However, such data must be taken cautiously because the cohort is too small [79]. In breast cancer cell lines, positive feedback was reported between the upregulated expression of 3β -HSD1 and the expression of IL-4 in ER-positive and ER-negative breast cancer cells [80]. In patients with hepatocellular cancer, 3β -HSD expression is higher than in the normal liver. Additionally, the expression of 3β -HSD1 and 3β -HSD2 isozymes is present in hepatocellular human cancer cell lines. By functional assays, 3β -HSD silencing diminishes the clonogenicity of such cells [81]. In prostate and testis cancer, its activity is enhanced, and it is even considered as a therapeutic approach in treating prostate and breast cancer [82]. Despite this, in such types of cancer, little is known about the relationships between 3β -HSD expression, the synthesis or levels of 3α -THP in plasma or tumoral tissue, and their

pathophysiological relevance. The expression of StAR, CYP11A1 and 3β HSD has also been reported in human endometrial cancer cell lines HHUA (estrogen (ER) and intracellular progesterone receptors (PR) positive; differentiated phenotype) and HOUA-1 (ER and PR negative, undifferentiated phenotype). In both cell lines, the production of pregnenolone and P4 was evident [83]. P4 detection in the cell culture medium appears earlier in HHUA than in HOUA-1 cells. This could be explained by differences in P4 metabolism.

Besides the production of 5α -DHP, the 5α -R isozymes are responsible for synthesizing the potent androgen 5α -dihydrotestosterone. In this sense, the relevance of such isozymes in prostate cancer has been evaluated as a therapeutic target [84,85]. However, 5α -R inhibitor treatment has been associated with the decreased synthesis of 5α -DHP and 3α -THP in the CNS, favoring some cases of depression and the risk of high-grade prostate cancer and decreased libido [86]. Interestingly, it has been reported that P4 promotes the transactivation of the androgen receptor in prostate cancer [87], which cannot discard other P4 metabolites that could activate and exert actions in such types of cancer. The role of 5α -reduced progesterone metabolites in malignancies has been mainly reported in breast cancer by Wiebe and collaborators. These authors reported an augmented synthesis of 5α -DHP and 3α -THP levels in infiltrating ductal breast carcinoma, compared with nontumoral tissue from the same patients [15]. Such data could indicate that 5α -R expression or its activity differs in cancerous versus normal tissue. Comparing the human breast cancer cells MCF-7, T47-D, and MDA-MB-231 with the nontumorigenic breast epithelial MCF-10A cells, the expression of 5α -R and AKR1C1-3 isozymes were higher, and lower respectively in the breast cancer cell lines [88]. Interestingly, subcutaneous administration of 5α -DHP promoted tumor growth in a MDA-MB-231 ER-/PR- breast cancer model implanted into mice [89]. This indicates that P4 metabolites could act through other mechanisms apart from activating PR.

As mentioned above, glioblastoma cells also express 5α -R and AKR1C1-3 isozymes. Their functionality was assumed to be due to the high steroid metabolite levels produced when cells are incubated with cholesterol, testosterone, pregnenolone, or P4. The presence of 3α -THP has also been reported among other steroid metabolites [90–92]. In human U87 and U251 glioblastoma-derived cells, 5α -DHP induced cell proliferation and migration through the PR [93]. Additionally, in colorectal cancer biopsies and cell lines, the expression of 5α -R1 is significantly elevated compared with that in normal tissue. Such data correlate the high expression of 5α -R1 with the worst prognosis in patients [94]. The levels of P4 metabolites synthesized by colorectal tissue in humans are yet unknown. However, high 5α -DHP and 3α -THP levels were observed in the adult rat colon. In such tissue, the levels of P4 metabolites were superior to those of testosterone [95]. Figure 2 summarizes the correlation between the overexpression of enzymes involved in 3α -THP synthesis and the prognosis detected in different kinds of cancer patients.

AKR1C1-4 involvement in cancer has been reported, although its association with 5α -DHP to 3α -THP conversion has been poorly studied. AKR1C1 levels are higher in small-cell and other lung cancers in stages I to III than in the adjacent nontumoral tissue. In such contexts, overexpression of AKR1C1 induced an increase in cell viability, migration, invasion, and overexpression of metalloproteases MMP2 and MMP9, involved in extracellular matrix degradation and invasion in the human small-cell lung cancer cell line H446 [96]. In breast cancer samples, the expression levels of AKR1C1-2 were lower when compared with the paired nontumoral tissue of the same patients [16].

Interestingly, AKR1C1 and AKR1C1-2 silencing in the T47-D breast cancer cell line enhanced the effect of P4 on decreasing cell numbers, which indicates that P4 metabolism could affect cellular death or proliferation processes in such cells [97]. AKR1C2 in esophageal squamous cell carcinoma is overexpressed relative to paired normal tissue, and its high expression was related to a reduced survival time. AKR1C2 silencing in the KYSE410 and EC109 esophageal cancer cell lines diminished cell migration and viability, along with decreasing tumor growth, when cells were subcutaneously injected in a nude mice model [98]. In prostate cancer, 3α -THP conversion to 5α -DHT has been hypothesized, but yet, un-

confirmed [99]. In the human glioblastoma T98G and U373 cell lines, a temozolomide resistance model—the standard chemotherapeutic agent for such types of cancer—has been developed. AKR1C3 overexpression was observed here and proposed as one of the mechanisms involved in the temozolomide resistance [100]. AKR1C4 was also highly expressed in 58% of a cohort of nasopharyngeal carcinoma, which is associated with a high possibility of relapse [101].

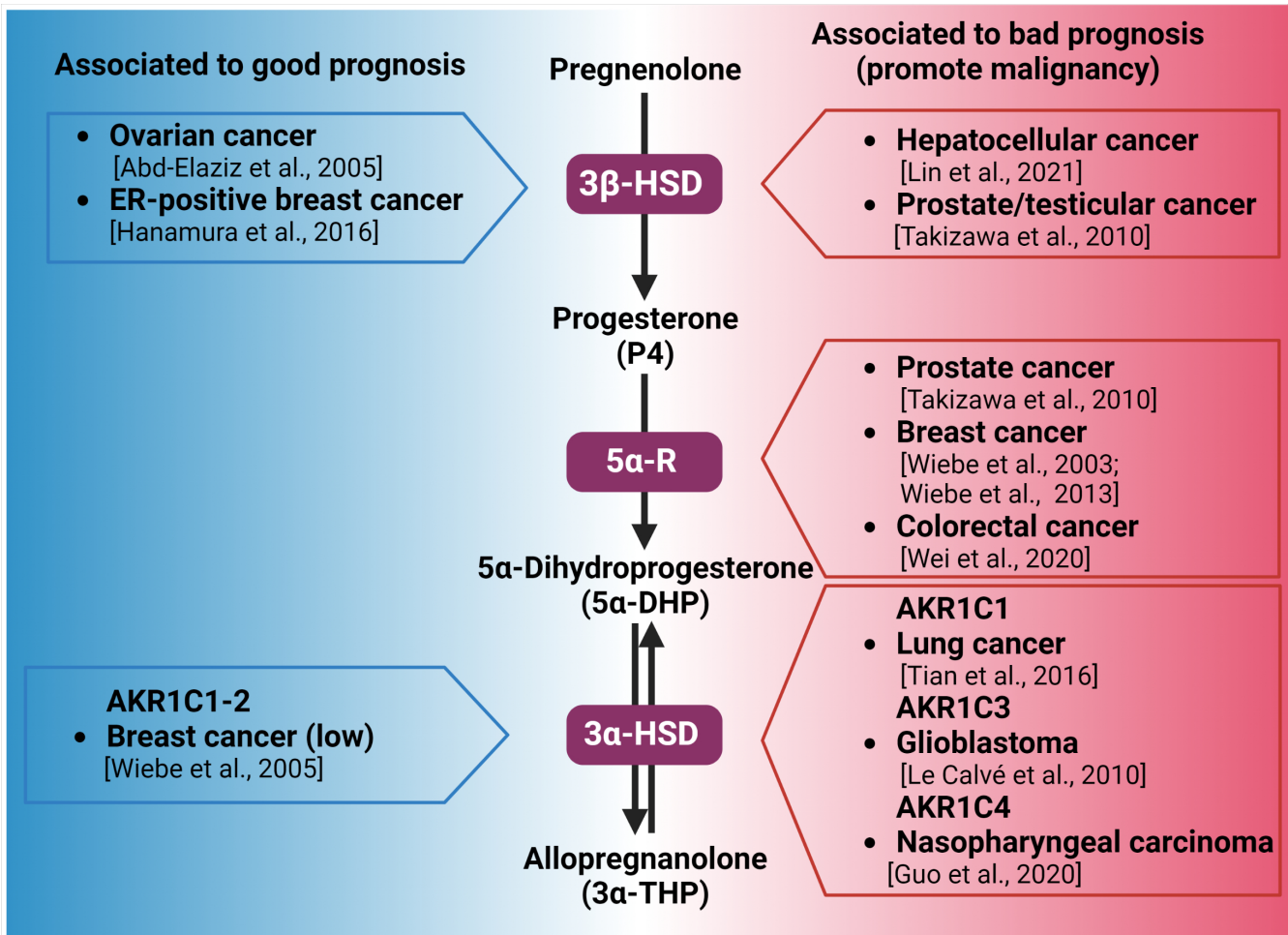


Figure 2. Synthesis of 3 α -THP from pregnenolone and the alteration of the expression of the involved enzymes in different types of cancer. Enzymes participating in each metabolic step are indicated by purple squares. On the left side (blue), the association between the high expression of 3 β -HSD, 3 α -HSD, and good prognosis of patients with different types of cancer is indicated. In the right side (red space), the different types of cancer in which the high expression of 3 β -HSD, 3 α -HSD, and 3 α -HSD isozymes are related to poor prognosis and cancer progression are presented [16,78,79,81,82,88,89,94,96,100,101].

Regarding the study of AKR1C1-4, some considerations must be taken to study the role of such isozymes in the metabolism of cancer. First, some animal models, especially rodents, do not accurately represent AKR1C1-4 activity in humans, because aldo-keto reductase murine isozymes have different preferred substrates and activities [102]. Additionally, some discrepancies have been reported between the expression levels of the AKR1C1-4 mRNA and their protein content [103]. Some other catalytic-independent activities for such enzymes have been described [104].

4. Allopregnanolone Mechanisms of Action

The mechanisms of action described for 3α -THP could be grouped into genomic or nongenomic due to the nature of its binding receptor in different cells. It is also important to mention that such effects and mechanisms have mostly been described in the context of neurodevelopment and pathologies of the CNS [105,106].

The PR is a transcription factor of the nuclear receptor superfamily, coded by the PGR gene (also named NR3C3). Two main PR isoforms, coded by such gen under the control of two different promoter sequences, have been reported [107,108]. In addition to its function as a transcription factor, PR interacts with other cytoplasm proteins through the polyproline-rich motifs at their N-terminal domains. An example of this is its interaction with the kinase cSrc [109].

One of the most notable differences between progestogens is their PR affinity, which has been described for P4 (0.35 nM) and 5α -DHP (22 nM). However, binding and gene-reporter assays showed that 3α -THP presents a low direct affinity (>500 nM for the chicken PR, and nondetectable in humans) for PR [110]. Despite this, it has been hypothesized that 3α -THP could regulate the effects of PR due to its interconversion to 5α -DHP in tissues expressing 5α -R and AKR1C1-4 [106,110]. In this section, other reported mechanisms directly activated by 3α -THP will be described.

At the genomic level, 3α -THP has been proposed as a ligand for the Pregnane X Receptor (PXR, also known as Steroid and Xenobiotic Receptor, SXR). PXR is a ligand-activated transcription factor of the nuclear receptors superfamily, coded by the gene NR1I2 [111]. Some variants of PXR have been reported, with different influences on their ligand affinity, dimerization, and transcriptional activity [112]. Although it is constituted by a DNA-binding Domain (DBD) at its N-terminal, and a hinge region, which connects the DBD with the Ligand Binding Domain (LBD) at the C-terminal, its LBD is more flexible than those of other nuclear receptors. Due to its unique pocket binding site, PXR is highly promiscuous to hydrophobic ligands such as steroids. The expression of PXR has been detected by RT-qPCR and RNAseq or microarrays in many tissues, mainly the liver. It has also been detected in the gastrointestinal tract, gonads, uterus, breast, adrenals, bone marrow, smooth muscle, brain, and skin [112,113].

To be functional, PXR forms homodimers and heterodimers, mainly with the retinoic acid receptor (RXR). However, other interactions of PXR with nuclear receptors such as the androgen receptor (AR) have been proposed to promote gene silencing [113,114]. Once activated and in the cellular nuclei, PXR dimers bind to xenobiotic response elements in the promoter or regulator regions of target genes. They recruit coactivators or corepressors for regulating transcription. Many of PXR's classic targets are involved in cholesterol metabolism and the detoxification of xenobiotics, such as the CYP3A, CYP2B, and CYP20 gene subfamilies [115]. Other targets of PXR are ATP-binding cassette drug transporters [116]. Moreover, it also regulates inflammatory responses and the cell cycle, which are undoubtedly essential processes in the physiopathology of cancer [117]. RNAseq data indicate that PXR is highly expressed in some human cancer cell lines: gastric tubular adenocarcinoma SNU719 cells, colon adenocarcinoma SW403 cells, pancreatic ductal adenocarcinoma ASPC1 cells, and the hepatoblastoma HepG2 cell line [113]. PXR has been implicated in all steps, from carcinogenesis to cancer progress and resistance to therapy [113]. In cancer stem cells from colon cancer, it is overexpressed, and its high levels correlate with the worst survival time and probability of cancer relapse [118]. The expression of PXR was reported in the human ovarian cancer cell lines SKOV-3 and OVCAR-8. When activated, classic PXR targets are overexpressed, along with augmented cell proliferation and tumor weight, in mouse xenografts [119].

The transcription factor function of PXR is activated by 3α -THP, as demonstrated by luciferase activity assays. Interestingly, 3α -THP effects were more significant than those of dehydroepiandrosterone, one androgen metabolite which is a PXR ligand and has similar reported effects to those of 3α -THP in the CNS [112]. This was also observed by Langmade et al. in the cerebellar tissue of the mouse Niemann–Pick C disease npc1–/–

model and Chinese hamster ovary cells [120]. It is worth mentioning that Niemann–Pick C disease is characterized by the impairment of cholesterol metabolism and accumulation, in which 3α -THP treatment improved animal survival and reduced inflammatory mediators in a GABA_A receptor-independent way [120]. This study clarifies the broad actions of 3α -THP other than the GABA_A receptor, which is by far the most characterized mechanism described for 3α -THP, as reviewed below. To our knowledge, there have been no affinity studies performed for 3α -THP to PXR so far.

Moreover, positive feedback between PXR and 3α -THP has been reported. Frye et al. reported that in the Ventral Tegmental Area of female rodents, silencing of PXR with antisense oligonucleotides decreases the levels of 5α -DHP and 3α -THP measured in other brain areas such as the hippocampus [121]. Additionally, in the mice 3xTgAD model of Alzheimer's disease, 3α -THP significantly increased the expression of PXR and the Liver X receptor (LXR) after 9 months of the establishment of pathology, but decreased it at month 12 [122]. There is no evidence, to date, that 3α -THP could also bind LXR.

3α -THP could rapidly activate or modulate membrane receptors. Although these mechanisms are considered nongenomic, as their primary effects are to modify ion conductance, second messengers, and diverse signaling pathways, they ultimately modify gene expression in a relatively more extended lapse. 3α -THP modulates gamma-aminobutyric acid (GABA) neurotransmission through its GABA_A receptor. Notably, neither P4 nor 5α -DHP present affinity for GABA_A receptors, as determined by binding assays [123]. The GABA_A receptor is a ligand-gated ionotropic channel. A functional GABA_A receptor comprises a pentameric channel constituted of five from 19 possible different subunits: α 1-6, β 1-3, γ 1-3, δ , ϵ , θ , π , and ρ 1-3. Most receptors are composed of two α , two β , and a fifth subunit which depends on the function and location of the receptor [124]. The subunit composition of the receptor impacts its functional and pharmacological properties. While the γ subunit is most often located in synaptic GABA_A receptors, δ subunits are commonly part of extrasynaptic GABA_A receptors, for example, in astrocyte cells. Notably, the presence of δ or γ 1 subunits favors 3α -THP affinity for the receptor. However, 3α -THP and other pregnanes bind it allosterically into two putative steroid binding sites in the transmembrane space between the α and β subunits of the receptor [125].

The effects of 3α -THP on such receptors depend on its concentration. At nanomolar concentration (100 nM), 3α -THP is a positive allosteric modulator of the GABA_A receptor, while micromolar concentrations (1 to 10 μ M) directly activate it [126]. Such effects have immediate consequences in the cells, due to the activation of different signaling pathways and the production of second messengers. The neuroactive steroid tetrahydrodeoxycorticosterone (THDOC), which presents a similar structure and affinity for the GABA_A receptor as 3α -THP, promotes the phosphorylation of the common extrasynaptic subunit α 4 in its residue S443 depending on the protein kinase PKC activity. Importantly, this favors the membrane localization of the GABA_A receptor [125,127].

Once 3α -THP binds to GABA_A receptors, the cellular response depends on the expression and activity of effectors, modulators, and cotransporters such as SLC12A2. In mature cells of the CNS, activation or positive modulation of GABA_A receptors promotes the influx of Cl⁻ ions, and thus, hyperpolarization, which is an inhibitory signal. This has been the most exploited mechanism of 3α -THP and its pharmacological analogs to induce anxiolytic, anticonvulsive, and sedative effects [123,128]. However, in neural stem cells and pre-progenitor oligodendrocytes, which express cotransporter SLC12A2 that triggers high basal intracellular levels of Cl⁻, 3α -THP leads to an efflux of Cl⁻ ions when it activates GABA_A receptors, and thereby promotes cell depolarization [126]. This effect leads to the activation of voltage-dependent L-type calcium channels, and thus, an increase in the intracellular levels of Ca²⁺ and cyclic-AMP, promoting the activation of protein kinase a (PKA) and, thus, the activation of transcription factor cyclic AMP-responsive element-binding protein 1 (CREB1) [12,129]. CREB1 regulates the expression of target genes involved in promoting DNA synthesis and cell proliferation [12]. In human Schwann cells, 3α -THP also increases the phosphorylation of CREB, and the expression of glutamate

decarboxylase, an enzyme involved in the synthesis of GABA. This is also correlated with an increase in GABA levels [130]. Melfi et al. have reported in the same model that 3α -THP treatment induces a rearrangement of the actin cytoskeleton and cell migration in a GABA_A receptor-dependent way and through the activation of Src/p-FAK [11]. Besides this mechanism, 3α -THP also favors the release of gonadotropin-releasing hormone (GnRH) in mouse-immortalized GnRH GT1-1 cells [131]. In physiological conditions, in the rat ovarian nerve plexus–ovary system, these authors also demonstrated that 3α -THP induces the proliferation, angiogenesis, and enhanced activity of the 3-HSD through the GABA_A receptor [132,133]. Besides the CNS, GABA_A receptors are also expressed in several tissues in physiologic conditions. They are particularly relevant in controlling the liberation of cytokines by immune cells, along with their proliferation and migration [134]. In murine glioma models and human glioblastoma cell lines, GABA_A receptors are functional. When treated with its antagonist bicuculine, cell proliferation is highly promoted, compared with cells treated with the agonist muscimol or vehicle conditions [135]. This suggests that GABA_A receptors negatively regulate glioblastoma growth.

Importantly, 3α -THP presents a high affinity for membrane P4 receptors (mPRs). The mPRs are membrane proteins of the progestin and adipoQ receptor family (PAQR) with five members: mPR α (PAQR7), mPR β (PAQR8), mPR γ (PAQR5), mPR δ (PAQR7), and mPR ϵ (PAQR9) with a similar weight of ~40 kDa. Although they are not part of the G protein-coupled receptors family, mPRs present a structure of transmembrane domains [136,137]. To date, modeling and experimentally determining their structure has been complex. However, it is proposed that they are constituted of seven to eight transmembrane domains with a large C-Terminal domain involved in activating G proteins. Moreover, some studies have suggested that some progestogens' and progestins' effects mediated by mPRs could also be independent of the activation of G proteins, and they could act more as ligand-activated enzymes with ceramidase activity that produce sphingoid bases as second messengers capable of secondly activating GPCRs [137,138]. Several studies indicate that mPR α , mPR β , and mPR γ are coupled to inhibitory G-proteins (G_i) in human cells or olfactory stimulatory G-proteins (G_{olf}) in teleost, while mPR δ and mPR ϵ seem to be coupled to stimulatory G-proteins (G_s) [139,140].

By binding assays, the affinity of 3α -THP for mPR δ (100 nM) and, to a lesser extent, mPR α and mPR β has been demonstrated (~400 to 500 nM) [140]. 3α -THP is an agonist of mPR δ , mPR α , and mPR β , and some of its effects depend on mPRs expression levels. The expression of mPR δ and mPR β is particularly high in several CNS areas such as the hypothalamus, hippocampus, amygdala, and cerebral cortex. In hippocampal neuronal cells, 3α -THP treatment for 15 min increases cAMP levels, which are correlated with the positive modulation of adenylyl cyclase by G_s proteins. When triple-negative MDA-MB-231 breast adenocarcinoma cells were transfected with mPR δ and treated with 3α -THP for 20 min, the activation of ERK kinase was observed along with a decrease in apoptosis [140]. In GT1-7 hypothalamic mouse GnRH cells, where mPR α and mPR β are the most expressed receptors, treatment with 3α -THP in concordance with the activation of G_i proteins decreases cAMP levels and cell death [141]. In Figure 3, the most studied mechanisms of 3α -THP to date are presented.

Additionally, crosstalk among the three mechanisms activated by 3α -THP has been proposed. When Melfi et al. reported the effects of 3α -THP on cell migration, a correlation between augmented migration and a dynamic change in the levels of Src and Fak kinases phosphorylation was observed. Interestingly, cotreatment with 3α -THP and the GABA_A inhibitor bicuculine promotes higher phosphorylation levels of such kinases than 3α -THP alone or the GABA_A agonist muscimol [11]. Additionally, when mPRs were stimulated with the agonist ORG-02-0, migration was promoted in Schwann cells, along with increased activation of Src [142]; this could indicate a complicated activation of several mechanisms involved in the effects of 3α -THP that could compensate each other when one of them is blocked.

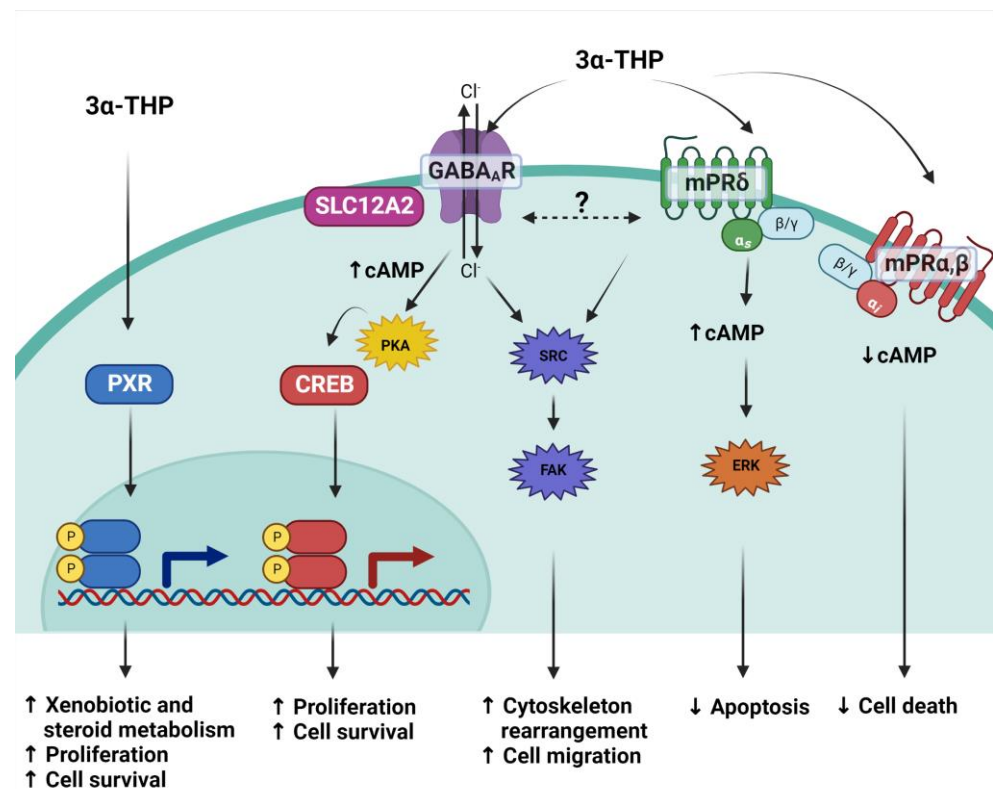


Figure 3. 3 α -THP mechanisms of action. Due to its lipophilic structure, 3 α -THP crosses the cellular membrane and directly activates the Pregnane X receptor (PXR), a transcription factor. It also modulates to the ionotropic pentamer GABA_A receptor, which, depending on the expression of the cotransporter SLC12A2, induces changes in the current of chloride ions (Cl⁻), augments cAMP levels and promotes the activation of the PKA kinase and the subsequent activation of the transcription factor CREB. 3 α -THP is also a ligand of the membrane P4 receptor mPR δ (green membrane receptor), a transmembrane receptor coupled to G_s proteins that augments cAMP. It is hypothesized that both the latter mechanisms interact and regulate the activation of the Src/FAK pathway. Additionally, 3 α -THP also binds mPR α and mPR β (red membrane receptor), which are coupled to G_i proteins, and their activation with 3 α -THP decreases cAMP levels.

Moreover, 3 α -THP, but not 5 α -DHP or 5 α -reduced androgen metabolites, could modulate other neurotransmitter receptors. 3 α -THP enhances the activation of dopamine D1 receptors. This was analyzed in a mice model of prepulse inhibition of startle, which is helpful in determining the function of the dopamine receptor. It was reported that D1 receptor agonists, like SKF-82958, impair the prepulse inhibition of startle, and cotreatment with 3 α -THP potentiates the effect of SKF-82958. The effect of SKF-82958 was not modified by the pharmacological antagonist of the GABA_A receptor bicuculine, or the PXR silencing, suggesting that 3 α -THP effects are produced directly through the regulation of the D1 receptor [143]. 3 α -THP could also act through glutamate N-methyl-D-aspartate (NMDA) receptors. The release of GnRH and glutamate was induced by a micromolar concentration of 3 α -THP in the medium basal hypothalamus and the anterior preoptic area slices of ovariectomized rats. In this study, the NMDA receptor antagonist AP-7 decreased the 3 α -THP effect of inducing GnRH and glutamate release, suggesting that the effect of 3 α -THP is mediated by its interaction with NMDA receptors [144].

5. Effects of Allopregnanolone on Cancer Models

In some *in vitro* models, the effects of 3 α -THP have been determined. In the human U87 glioblastoma-like cells, the metabolite 3 α -THP significantly increases the number of cells over 6 days of treatment and promotes proliferation at 72 h of treatment. Interestingly,

in such studies, cotreatment with P4 and the 5 α R inhibitor, finasteride, almost completely inhibits the effect of P4 [92]. This indicates that besides P4, its metabolites contribute to glioblastoma progression. Using microarrays in the U87 cell line, changes in the gene expression profile under 3 α -THP were also assessed. 3 α -THP at nanomolar concentration promotes the overexpression of proliferation, DNA repair, and cytoskeleton rearrangement genes [145]. In addition, in U87 and other glioblastoma cell lines such as U251 and LN229, 3 α -THP promotes Src-mediated migration and invasion [146], although the mechanism by which 3 α -THP induces Src activation in this model needs to be elucidated. In PC12 rat pheochromocytoma cells, which lack GABA_A or NMDA receptors, 3 α -THP decreases apoptosis through overexpression of the antiapoptotic proteins Bcl-2 and Bcl-xl. It also induces the activation of PKC [147]. In the breast cancer cell lines MCF-7 and T47D, high concentrations (50 μ M) of 3-THP decreased cell viability, while lower concentration (12 μ M) stimulated the augmentation of cell numbers, similar to P4 or 5 α -DHP [148].

Conversely, in T98G and A172 human glioblastoma cell lines, high micromolar concentrations of 3 α -THP alone promote cell death and potentiate the effect of temozolomide, the standard chemotherapeutic agent used for glioblastoma treatment. Such cotreatment also diminished cell migration and invasion through the downregulation of proteins involved in proliferation and integrin signaling [149].

The effects of 3 α -THP have been reported in other cancer models. In the human ovarian cancer cell line IGROV-1, 3 α -THP promotes proliferation, migration, and clonogenicity at low concentrations [150]. However, the 3 α -THP-activated mechanisms in these models are still understudied. Together, the cited *in vitro* studies analyzed in this review indicate that 1 nM to 20 μ M 3 α -THP concentrations could induce cancer progression, while higher concentrations inhibit it. Furthermore, changes in the *in vivo* levels of 3 α -THP, and specifically, plasmatic levels of 3 α -THP, are not necessarily related to or the cause of cancer. However, the local expression or activity of many enzymes involved in the 3 α -THP metabolism is altered in different types of cancer. This could be translated in an altered synthesis (and levels) of such metabolites in cancer tissues. To state specific concentrations of 3 α -THP and their real impact on the tumoral microenvironment, more studies are needed.

In addition to 3 α -THP, its synthetic analogs have also been studied in the cancer context. As in the case of 3 α -THP, these studies point out that Ganaxolone, a 3-methylated analog, and others promote cell proliferation in different cancer cell lines. Ganaxolone has been proposed as a therapeutic agent for epilepsy because of its high affinity to GABA_A receptors, although it also activates mPRs. Ganaxolone has a similar affinity to mPR δ to that reported for 3 α -THP (~100 nM) [140,151]. In MDA-MB-231 breast cancer cells (with no expression of GABA_A receptors) transfected with mPR δ , Ganaxolone decreased apoptosis and cell death at the same concentration as 3 α -THP. In the same model, Ganaxolone also activated the same signaling pathways as 3 α -THP: increasing cAMP and activating ERK kinase [151]. Taleb et al. propose the synthesis of 3 α -THP analogs with GABA_A receptor-agonist effects, but low pro-proliferative action. These authors reported that low concentrations (250 nm to 1 μ M) of 3 α -THP and its synthetic analogs, BR351 (O-allyl-Allopregnanolone) and BR338 (12-oxo-Allopregnanolone), increase cell viability of the human neuroblastoma cell line SH-SY5Y. The analog BR297 (O-allyl-epi-Allopregnanolone) lacks pro-proliferative activity. All tested steroids, however, present neuroprotective effects and augment GABA conductance [152]. A similar effect for these analogs was observed in primary cultures of mice neural stem cells [153].

To our knowledge, there are no specific reports about sexually dimorphic 3 α -THP levels and cancer. However, there are sex differences in cancer prevalence and in neurosteroids, specifically, 3 α -THP levels and actions. Although these aspects are not necessarily related, it would be interesting to study them. Regarding many types of cancers, including glioblastomas, their overall incidence is higher in men than women in a proportion of 3:2 (men: women) [154]. Cancer's aggressiveness, response to treatment, and prognosis are unequal due to the sex effect. It has been reported that genetic sexual differences related to autosomic and sexually specific gene expression influence cancer [155]. However, differ-

ences between males and females regarding long-lasting levels of exposure to the endogenous sexual hormones and synthetic progestins throughout life in cancer prevalence have been broadly studied. At least in the case of glioblastoma, the most common primary malignant brain tumor, sex hormones impact cancer differently [156–158]. While androgens induce glioblastoma progression, the effect of estrogens and progestins depends on their levels, receptor expression, and long-lasting exposure to the hormonal stimulus [156]. Regarding 3α -THP in humans, its plasmatic levels in fertile females vary similarly to P4 and 5α -DHP according to the menstrual cycle phase. The 3α -THP plasmatic levels of females at the follicular phase of the menstrual cycle are similar to those found in healthy adult males (~1 nM). Interestingly, Genazzani et al. evaluated 3α -THP plasmatic levels in males and females of different age ranges (19–39, 40–49, 50–59, and >60 years old). They found that the 3α -THP plasmatic levels of males proportionally decrease as men age. However, female 3α -THP levels at the follicular phase of the menstrual cycle do not vary with age [159].

The evidence presented in this article shows that tumoral cells display very similar responses to those of normal cells when they are exposed to 3α -THP or its analogs at nanomolar to low micromolar concentrations: an increase in cell proliferation, protection against insults, and migration. Although such effects could be beneficial for patients in neurodegenerative states [14,106], cancer cases have to be studied vigilantly [152]. It is worth mentioning that estrogens, and progestins act as inductors of cancer progression and not as carcinogens, at least in glioblastoma, as recently reviewed by Bello-Alvarez et al. [156]. In this line, the P4 metabolite 3α -THP and its analog Ganaxolone display very similar effects to progestins once tumoral growth is established. Moreover, neurological diseases like epilepsy require chronic treatments to improve symptoms and patient quality of life [160]. Under such treatment conditions, the local levels of Ganaxolone could be higher than those needed to induce cancer cell proliferation, although this needs to be investigated.

6. Conclusions and Perspectives

State-of-the-art evidence about 3α -THP synthesis and its mechanisms of action in cancer was presented in this review. 3α -THP has been one of the most studied neuroactive steroids with broad actions in neuroprotection, proliferation induction, and immunomodulation. Such characteristics could be exploited by cancer cells. To date, the synthesis of 3α -THP and other P4 metabolites has been confirmed in patient tissue of breast cancer, colon, ovarian, and glioblastoma cell lines, among others. These data suggest an altered synthesis of P4 metabolites in at least some types of cancer, which points to the urgency of generating more data on the P4 metabolism in cancer patients. Moreover, there is little information about the role of other P4 metabolites, 3α -THP, and its analogs, as agents that favor the initiation, promotion, and progression of cancer. This is particularly relevant because analogs of 3α -THP, like Ganaxolone, are approved by the FDA for the long-lasting treatment of epilepsy [160].

To date, few studies about 3α -THP's role in cancer progression exist. Additionally, 3α -THP presents affinity for a broad class of receptors that could be simultaneously expressed in the same cell or tissue, which makes it difficult to study them. There are plenty of data about 3α -THP effects mediated by its binding to $GABA_A$ receptors. However, the crosstalk between $GABA_A$ receptors and other mechanisms, like mPRs or PXR activation along with their signaling pathways, needs to be clarified. Additionally, in models where physiological concentrations of P4 induce cancer progression, such as glioblastoma and ovarian cancer, 3α -THP also promotes cellular malignancy, which could reinforce the possible crosstalk between P4, and its 5α -reduced metabolites previously described in breast cancer. Together, these data point to the urgency of illuminating 3α -THP's effects in cancer pathophysiology by measuring steroid metabolites in cancer patients and studying the potential role of 3α -THP in the progression of cancer malignancy.

Author Contributions: Conceptualization and first draft was done by C.J.Z.-S. and I.C.-A. Commentaries and correction of the manuscript was done by both authors. All authors have read and agreed to the published version of the manuscript.

Funding: This research was funded by DGAPA-PAPIIT, grant number: IN217120, UNAM, México and by a scholarship to Carmen J. Zamora-Sánchez from Consejo Nacional de Ciencia y Tecnología, México, and by DGAPA-PAPIIT, UNAM, México.

Institutional Review Board Statement: Not applicable.

Informed Consent Statement: Not applicable.

Data Availability Statement: Not applicable.

Acknowledgments: All figures were created with [BioRender.com](https://www.biorender.com), accessed on 17 November 2022.

Conflicts of Interest: The authors declare no conflict of interest.

References

1. Di Renzo, G.C.; Tosto, V.; Tsibizova, V. Progesterone: History, facts, and artifacts. *Best Pract. Res. Clin. Obstet. Gynaecol.* **2020**, *69*, 2–12. [[CrossRef](#)] [[PubMed](#)]
2. Marker, R.E.; Kamm, O.; McGrew, R.V. Sterols. IX. Isolation of epi-Pregnanol-3-one-20 from Human Pregnancy Urine. *J. Am. Chem. Soc.* **1937**, *59*, 616–618. [[CrossRef](#)]
3. Selye, H. Correlations between the chemical structure and the pharmacological actions of the steroids. *Endocrinology* **1942**, *30*, 437–453. [[CrossRef](#)]
4. Piette, P. The history of natural progesterone, the never-ending story. *Climacteric* **2018**, *21*, 308–314. [[CrossRef](#)] [[PubMed](#)]
5. Hill, M.; Pařízek, A.; Kancheva, R.; Jirásek, J.E. Reduced progesterone metabolites in human late pregnancy. *Physiol. Res.* **2011**, *60*, 225–241. [[CrossRef](#)]
6. Brunton, P.J.; Russell, J.A.; Hirst, J.J. *Allopregnanolone in the Brain: Protecting Pregnancy and Birth Outcomes*; Elsevier Ltd.: Amsterdam, The Netherlands, 2014; Volume 113, ISBN 3154511277783.
7. Paris, J.J.; Brunton, P.J.; Russell, J.A.; Walf, A.A.; Frye, C.A. Inhibition of 5 α -reductase activity in late pregnancy decreases gestational length and fecundity and impairs object memory and central progesterone milieu of juvenile rat offspring. *J. Neuroendocrinol.* **2011**, *23*, 1079–1090. [[CrossRef](#)]
8. Parks, E.E.; Logan, S.; Yeganeh, A.; Farley, J.A.; Owen, D.B.; Sonntag, W.E. Interleukin 6 reduces allopregnanolone synthesis in the brain and contributes to age-related cognitive decline in mice. *J. Lipid Res.* **2020**, *61*, 1308–1319. [[CrossRef](#)]
9. Balan, I.; Aurelian, L.; Schleicher, R.; Boero, G.; O’ Buckley, T.; Morrow, A.L. Neurosteroid allopregnanolone (3 α ,5 α -THP) inhibits inflammatory signals induced by activated MyD88-dependent toll-like receptors. *Transl. Psychiatry* **2021**, *11*, 145. [[CrossRef](#)]
10. He, J.; Evans, C.-O.; Hoffman, S.W.; Oyesiku, N.M.; Stein, D.G. Progesterone and allopregnanolone reduce inflammatory cytokines after traumatic brain injury. *Exp. Neurol.* **2004**, *189*, 404–412. [[CrossRef](#)]
11. Melfi, S.; Montt Guevara, M.M.; Bonalume, V.; Ruscica, M.; Colciago, A.; Simoncini, T.; Magnaghi, V. Src and phospho-FAK kinases are activated by allopregnanolone promoting Schwann cell motility, morphology and myelination. *J. Neurochem.* **2017**, *141*, 165–178. [[CrossRef](#)]
12. Wang, J.M.; Johnston, P.B.; Ball, B.G.; Brinton, R.D. The neurosteroid allopregnanolone promotes proliferation of rodent and human neural progenitor cells and regulates cell-cycle gene and protein expression. *J. Neurosci.* **2005**, *25*, 4706–4718. [[CrossRef](#)] [[PubMed](#)]
13. González-Orozco, J.C.; Camacho-Arroyo, I. Progesterone actions during central nervous system development. *Front. Neurosci.* **2019**, *13*, 503. [[CrossRef](#)] [[PubMed](#)]
14. Falvo, E.; Diviccaro, S.; Melcangi, R.C.; Giatti, S. Physiopathological role of neuroactive steroids in the peripheral nervous system. *Int. J. Mol. Sci.* **2020**, *21*, 9000. [[CrossRef](#)] [[PubMed](#)]
15. Wiebe, J.P.; Muzia, D.; Hu, J.; Szwajcer, D.; Hill, S.A.; Seachrist, J.L. The 4-pregnene and 5 α -pregnane progesterone metabolites formed in nontumorous and tumorous breast tissue have opposite effects on breast cell proliferation and adhesion. *Cancer Res.* **2000**, *60*, 936–943. [[PubMed](#)]
16. Wiebe, J.P.; Lewis, M.J.; Cialacu, V.; Pawlak, K.J.; Zhang, G. The role of progesterone metabolites in breast cancer: Potential for new diagnostics and therapeutics. *J. Steroid Biochem. Mol. Biol.* **2005**, *93*, 201–208. [[CrossRef](#)]
17. Wiebe, J.P.; Beausoleil, M.; Zhang, G.; Cialacu, V. Opposing actions of the progesterone metabolites, 5 α -dihydroprogesterone (5 α P) and 3 α -dihydroprogesterone (3 α HP) on mitosis, apoptosis, and expression of Bcl-2, Bax and p21 in human breast cell lines. *J. Steroid Biochem. Mol. Biol.* **2010**, *118*, 125–132. [[CrossRef](#)]
18. Pautasso, M. Ten Simple Rules for Writing a Literature Review. *PLoS Comput. Biol.* **2013**, *9*, 7–10. [[CrossRef](#)]
19. Liang, J.J.; Rasmuson, A.M. Overview of the Molecular Steps in Steroidogenesis of the GABAergic Neurosteroids Allopregnanolone and Pregnanolone. *Chronic Stress* **2018**, *2*, 247054701881855. [[CrossRef](#)]

20. Rone, M.B.; Midzak, A.S.; Issop, L.; Rammouz, G.; Jagannathan, S.; Fan, J.; Ye, X.; Blonder, J.; Veenstra, T.; Papadopoulos, V. Identification of a dynamic mitochondrial protein complex driving cholesterol import, trafficking, and metabolism to steroid hormones. *Mol. Endocrinol.* **2012**, *26*, 1868–1882. [[CrossRef](#)]
21. Morel, Y.; Roucher, F.; Plotton, I.; Goursaud, C.; Tardy, V.; Mallet, D. Evolution of steroids during pregnancy: Maternal, placental and fetal synthesis. *Ann. Endocrinol.* **2016**, *77*, 82–89. [[CrossRef](#)]
22. Elustondo, P.; Martin, L.A.; Karten, B. Mitochondrial cholesterol import. *Biochim. Biophys. Acta-Mol. Cell Biol. Lipids* **2017**, *1862*, 90–101. [[CrossRef](#)] [[PubMed](#)]
23. Clark, B.J. The mammalian START domain protein family in lipid transport in health and disease. *J. Endocrinol.* **2012**, *212*, 257–275. [[CrossRef](#)] [[PubMed](#)]
24. Bose, H.S.; Lingappa, V.R.; Miller, W.L. The steroidogenic acute regulatory protein, StAR, works only at the outer mitochondrial membrane. *Endocr. Res.* **2002**, *28*, 295–308. [[CrossRef](#)]
25. Gatta, A.T.; Wong, L.H.; Sere, Y.Y.; Calder, D.M.; Cockcroft, S.; Menon, A.K.; Levine, T.P. A new family of StART domain proteins at membrane contact sites has a role in ER-PM sterol transport. *eLife* **2015**, *4*, e07253. [[CrossRef](#)] [[PubMed](#)]
26. Artemenko, I.P.; Zhao, D.; Hales, D.B.; Hales, K.H.; Jefcoate, C.R. Mitochondrial Processing of Newly Synthesized Steroidogenic Acute Regulatory Protein (StAR), but Not Total StAR, Mediates Cholesterol Transfer to Cytochrome P450 Side Chain Cleavage Enzyme in Adrenal Cells. *J. Biol. Chem.* **2001**, *276*, 46583–46596. [[CrossRef](#)] [[PubMed](#)]
27. Sluchanko, N.N.; Tugaeva, K.V.; Maksimov, E.G. Solution structure of human steroidogenic acute regulatory protein STARD1 studied by small-angle X-ray scattering. *Biochem. Biophys. Res. Commun.* **2017**, *489*, 445–450. [[CrossRef](#)]
28. Li, H.; Papadopoulos, V. Peripheral-type benzodiazepine receptor function in cholesterol transport. Identification of a putative cholesterol recognition/interaction amino acid sequence and consensus pattern. *Endocrinology* **1998**, *139*, 4991–4997. [[CrossRef](#)] [[PubMed](#)]
29. Tu, L.N.; Zhao, A.H.; Hussein, M.; Stocco, D.M.; Selvaraj, V. Translocator Protein (TSPO) Affects Mitochondrial Fatty Acid Oxidation in Steroidogenic Cells. *Endocrinology* **2016**, *157*, 1110–1121. [[CrossRef](#)] [[PubMed](#)]
30. Frye, C.A.; Koonce, C.J.; Walf, A.A. The pregnane xenobiotic receptor, a prominent liver factor, has actions in the midbrain for neurosteroid synthesis and behavioral/neural plasticity of female rats. *Front. Syst. Neurosci.* **2014**, *8*, 60. [[CrossRef](#)]
31. Lang, L.; Loveless, R.; Teng, Y. Emerging links between control of mitochondrial protein atad3a and cancer. *Int. J. Mol. Sci.* **2020**, *21*, 7917. [[CrossRef](#)]
32. Burstein, S.; Middleditch, B.S.; Gut, M. Mass spectrometric study of the enzymatic conversion of cholesterol to (22R) 22 hydroxycholesterol, (20R,22R) 20,22 dihydroxycholesterol, and pregnenolone, and of (22R) 22 hydroxycholesterol to the glycerol and pregnenolone in bovine adrenocortical prepar. *J. Biol. Chem.* **1975**, *250*, 9028–9037. [[CrossRef](#)] [[PubMed](#)]
33. Slominski, A.T.; Li, W.; Kim, T.K.; Semak, I.; Wang, J.; Zjawiony, J.K.; Tuckey, R.C. Novel activities of CYP11A1 and their potential physiological significance. *J. Steroid Biochem. Mol. Biol.* **2015**, *151*, 25–37. [[CrossRef](#)] [[PubMed](#)]
34. Lin, Y.C.; Cheung, G.; Porter, E.; Papadopoulos, V. The neurosteroid pregnenolone is synthesized by a mitochondrial P450 enzyme other than CYP11A1 in human glial cells. *J. Biol. Chem.* **2022**, *298*, 102110. [[CrossRef](#)] [[PubMed](#)]
35. Berchtold, J.P. Ultracytochemical demonstration and probable localization of 3 β -hydroxysteroid dehydrogenase activity with a ferricyanide technique. *Histochemistry* **1977**, *50*, 175–190. [[CrossRef](#)] [[PubMed](#)]
36. Prasad, M.; Thomas, J.L.; Whittal, R.M.; Bose, H.S. Mitochondrial 3 β -hydroxysteroid dehydrogenase enzyme activity requires reversible pH-dependent conformational change at the intermembrane space. *J. Biol. Chem.* **2012**, *287*, 9534–9546. [[CrossRef](#)]
37. McNatty, K.P.; Makris, A.; Degrazia, C.; Osathanondh, R.; Ryan, K.J. The production of progesterone, androgens, and estrogens by granulosa cells, thecal tissue, and stromal tissue from human ovaries in vitro. *J. Clin. Endocrinol. Metab.* **1979**, *49*, 687–699. [[CrossRef](#)]
38. Lachance, Y.; Luu-The, V.; Labrie, C.; Simard, J.; Dumont, M.; De Launoit, Y.; Guerin, S.; Leblanc, G.; Labrie, F. Characterization of human 3 β -hydroxysteroid dehydrogenase/ Δ 5- Δ 4-isomerase gene and its expression in mammalian cells. *J. Biol. Chem.* **1990**, *265*, 20469–20475. [[CrossRef](#)] [[PubMed](#)]
39. Labrie, F.; Simard, J.; Luu-The, V.; Bélanger, A.; Pelletier, G. Structure, function and tissue-specific gene expression of 3 β -hydroxysteroid dehydrogenase/5-ene-4-ene isomerase enzymes in classical and peripheral intracrine steroidogenic tissues. *J. Steroid Biochem. Mol. Biol.* **1992**, *43*, 805–826. [[CrossRef](#)]
40. Milewich, L.; Shaw, C.E.; Ian Mason, J.; Carr, B.R.; Blomquist, C.H.; Thomas, J.L. 3 β -Hydroxysteroid Dehydrogenase Activity in Tissues of the Human Fetus Determined with 5 α -Androstane-3 β ,17 β -Diol and Dehydroepiandrosterone As Substrates. *J. Steroid Biochem. Mol. Biol.* **1993**, *45*, 525–537. [[CrossRef](#)]
41. Martel, C.; Meiner, M.H.; Gagné, D.; Simarda, J.; Labrie, F. Widespread tissue distribution of steroid sulfatase, 3 β -hydroxysteroid dehydrogenase/ Δ 5- Δ 4 isomerase (3 β -HSD), 17 β -HSD 5 α -reductase and aromatase activities in the rhesus monkey. *Mol. Cell. Endocrinol.* **1994**, *104*, 103–111. [[CrossRef](#)]
42. Cantagrel, V.; Lefeber, D.J.; Ng, B.G.; Guan, Z.; Silhavy, J.L.; Bielas, S.L.; Lehle, L.; Hombauer, H.; Adamowicz, M.; Swiezewska, E.; et al. SRD5A3 is required for converting polyprenol to dolichol and is mutated in a congenital glycosylation disorder. *Cell* **2010**, *142*, 203–217. [[CrossRef](#)] [[PubMed](#)]
43. Stiles, A.R.; Russell, D.W. SRD5A3: A surprising role in glycosylation. *Cell* **2010**, *142*, 196–198. [[CrossRef](#)] [[PubMed](#)]
44. Azzouni, F.; Godoy, A.; Li, Y.; Mohler, J. The 5 alpha-reductase isozyme family: A review of basic biology and their role in human diseases. *Adv. Urol.* **2012**, *2012*, 530121. [[CrossRef](#)] [[PubMed](#)]

45. Silvia, G.; Silvia, D.; Cosimo, M.R. Key players in progesterone and testosterone action: The metabolizing enzymes. *Curr. Opin. Endocr. Metab. Res.* **2022**, *23*, 100319. [[CrossRef](#)]
46. Robitaille, J.; Langlois, V.S. Consequences of steroid-5 α -reductase deficiency and inhibition in vertebrates. *Gen. Comp. Endocrinol.* **2020**, *290*, 113400. [[CrossRef](#)]
47. Chetyrkin, S.V.; Hu, J.; Gough, W.H.; Dumauval, N.; Kedishvili, N.Y. Further characterization of human microsomal 3 α -hydroxysteroid dehydrogenase. *Arch. Biochem. Biophys.* **2001**, *386*, 1–10. [[CrossRef](#)]
48. Andersson, S.; Russell, D.W. Structural and biochemical properties of cloned and expressed human and rat steroid 5 α -reductases. *Proc. Natl. Acad. Sci. USA* **1990**, *87*, 3640–3644. [[CrossRef](#)]
49. Xiao, Q.; Wang, L.; Supekar, S.; Shen, T.; Liu, H.; Ye, F.; Huang, J.; Fan, H.; Wei, Z.; Zhang, C. Structure of human steroid 5 α -reductase 2 with the anti-androgen drug finasteride. *Nat. Commun.* **2020**, *11*, 5430. [[CrossRef](#)]
50. Makridakis, N.M.; Di Salle, E.; Reichardt, J.K.V. Biochemical and pharmacogenetic dissection of human steroid 5 α -reductase type II. *Pharmacogenetics* **2000**, *10*, 407–413. [[CrossRef](#)]
51. Russell, D.W.; Wilson, J.D. Steroid 5 α -Reductase: Two Genes/Two Enzymes. *Annu. Rev. Biochem.* **1994**, *63*, 25–61. [[CrossRef](#)]
52. Normington, K.; Russell, D.W. Tissue distribution and kinetic characteristics of rat steroid 5 α -reductase isozymes. Evidence for distinct physiological functions. *J. Biol. Chem.* **1992**, *267*, 19548–19554. [[CrossRef](#)] [[PubMed](#)]
53. Nonneman, D.J.; Wise, T.H.; Ford, J.J.; Kuehn, L.A.; Rohrer, G.A. Characterization of the aldoketo reductase 1C gene cluster on pig chromosome 10: Possible associations with reproductive traits. *BMC Vet. Res.* **2006**, *2*, 28. [[CrossRef](#)] [[PubMed](#)]
54. Penning, T.M.; Drury, J.E. Human aldoketo reductases: Function, gene regulation, and single nucleotide polymorphisms. *Arch. Biochem. Biophys.* **2007**, *464*, 241–250. [[CrossRef](#)] [[PubMed](#)]
55. Rižner, T.L.; Lin, H.K.; Peehl, D.M.; Steckelbroeck, S.; Bauman, D.R.; Penning, T.M. Human type 3 3 α -hydroxysteroid dehydrogenase (aldoketo reductase 1C2) and androgen metabolism in prostate cells. *Endocrinology* **2003**, *144*, 2922–2932. [[CrossRef](#)] [[PubMed](#)]
56. Beranič, N.; Lanišnik Rižner, T. Progestin effects on expression of AKR1C1-AKR1C3, SRD5A1 and PGR in the Z-12 endometriotic epithelial cell line. *Chem. Biol. Interact.* **2013**, *202*, 218–225. [[CrossRef](#)] [[PubMed](#)]
57. Higaki, Y.; Usami, N.; Shintani, S.; Ishikura, S.; El-Kabbani, O.; Hara, A. Selective and potent inhibitors of human 20 α -hydroxysteroid dehydrogenase (AKR1C1) that metabolizes neurosteroids derived from progesterone. *Chem. Biol. Interact.* **2003**, *143–144*, 503–513. [[CrossRef](#)] [[PubMed](#)]
58. Penning, T.M.; Sharp, R.B.; Krieger, N.R. Purification and properties of 3 α -hydroxysteroid dehydrogenase from rat brain cytosol. Inhibition by nonsteroidal anti-inflammatory drugs and progestins. *J. Biol. Chem.* **1985**, *260*, 15266–15272. [[CrossRef](#)] [[PubMed](#)]
59. Klossner, R.; Groessl, M.; Schumacher, N.; Fux, M.; Escher, G.; Verouti, S.; Jamin, H.; Vogt, B.; Mohaupt, M.G.; Gennari-Moser, C. Steroid hormone bioavailability is controlled by the lymphatic system. *Sci. Rep.* **2021**, *11*, 9666. [[CrossRef](#)]
60. Penning, T.M.; Burczynski, M.E.; Jez, J.M.; Hung, C.F.; Lin, H.K.; Ma, H.; Moore, M.; Palackal, N.; Ratnam, K. Human 3 α -hydroxysteroid dehydrogenase isoforms (AKR1C1-AKR1C4) of the aldoketo reductase superfamily: Functional plasticity and tissue distribution reveals roles in the inactivation and formation of male and female sex hormones. *Biochem. J.* **2000**, *351*, 67–77. [[CrossRef](#)]
61. Steckelbroeck, S.; Jin, Y.; Gopishetty, S.; Oyesanmi, B.; Penning, T.M. Human cytosolic 3 α -hydroxysteroid dehydrogenases of the aldoketo reductase superfamily display significant 3 β -hydroxysteroid dehydrogenase activity: Implications for steroid hormone metabolism and action. *J. Biol. Chem.* **2004**, *279*, 10784–10795. [[CrossRef](#)]
62. Karavolas, H.J.; Hodges, D.; O'Brien, D. Uptake of [3H]progesterone and [3H]5 α -dihydroprogesterone by rat tissues in vivo and analysis of accumulated radioactivity: Accumulation of 5 α -dihydroprogesterone by pituitary and hypothalamic tissues. *Endocrinology* **1976**, *98*, 164–175. [[CrossRef](#)] [[PubMed](#)]
63. Belelli, D.; Gee, K.W. 5 α -pregnan-3 α ,20 α -diol behaves like a partial agonist in the modulation of GABA-stimulated chloride ion uptake by synaptoneuroosomes. *Eur. J. Pharmacol.* **1989**, *167*, 173–176. [[CrossRef](#)] [[PubMed](#)]
64. Gupta, M.K.; Guryev, O.L.; Auchus, R.J. 5 α -reduced C21 steroids are substrates for human cytochrome P450c17. *Arch. Biochem. Biophys.* **2003**, *418*, 151–160. [[CrossRef](#)] [[PubMed](#)]
65. Hanahan, D.; Weinberg, R.A. Hallmarks of cancer: The next generation. *Cell* **2011**, *144*, 646–674. [[CrossRef](#)] [[PubMed](#)]
66. Hanahan, D. Hallmarks of Cancer: New Dimensions. *Cancer Discov.* **2022**, *12*, 31–46. [[CrossRef](#)] [[PubMed](#)]
67. Warburg, O. On the origin of cancer cells. *Science* **1956**, *123*, 309–314. [[CrossRef](#)]
68. Collier, H.A. Is Cancer a Metabolic Disease? *Am. J. Pathol.* **2014**, *184*, 4–17. [[CrossRef](#)]
69. Seth Nanda, C.; Venkateswaran, S.V.; Patani, N.; Yuneva, M. Defining a metabolic landscape of tumours: Genome meets metabolism. *Br. J. Cancer* **2020**, *122*, 136–149. [[CrossRef](#)]
70. Grasso, D.; Zampieri, L.X.; Capelôa, T.; Van De Velde, J.A.; Sonveaux, P. Mitochondria in cancer. *Cell Stress* **2020**, *4*, 114–146. [[CrossRef](#)]
71. Hieger, I. Carcinogenesis by cholesterol. *Br. J. Cancer* **1959**, *13*, 439–451. [[CrossRef](#)]
72. Chang, W.C.; Huang, S.F.; Lee, Y.M.; Lai, H.C.; Cheng, B.H.; Cheng, W.C.; Ho, J.Y.P.; Jeng, L.B.; Ma, W.L. Cholesterol import and steroidogenesis are biosignatures for gastric cancer patient survival. *Oncotarget* **2017**, *8*, 692–704. [[CrossRef](#)] [[PubMed](#)]
73. Terry, K.; McGrath, M.; Lee, I.M.; Buring, J.; De Vivo, I. Genetic variation in CYP11A1 and StAR in relation to endometrial cancer risk. *Gynecol. Oncol.* **2010**, *117*, 255–259. [[CrossRef](#)] [[PubMed](#)]

74. Fan, Z.; Wang, Z.; Chen, W.; Cao, Z.; Li, Y. Association between the CYP11 family and six cancer types. *Oncol. Lett.* **2016**, *12*, 35–40. [[CrossRef](#)] [[PubMed](#)]
75. Issop, L.; Fan, J.; Lee, S.; Rone, M.B.; Basu, K.; Mui, J.; Papadopoulos, V. Mitochondria-Associated membrane formation in hormone-stimulated leydig cell steroidogenesis: Role of ATAD3. *Endocrinology* **2015**, *156*, 334–345. [[CrossRef](#)] [[PubMed](#)]
76. Brown, R.C.; Cascio, C.; Papadopoulos, V. Pathways of neurosteroid biosynthesis in cell lines from human brain: Regulation of dehydroepiandrosterone formation by oxidative stress and β - amyloid peptide. *J. Neurochem.* **2000**, *74*, 847–859. [[CrossRef](#)]
77. Mahata, B.; Pramanik, J.; van der Weyden, L.; Polanski, K.; Kar, G.; Riedel, A.; Chen, X.; Fonseca, N.A.; Kundu, K.; Campos, L.S.; et al. Tumors induce de novo steroid biosynthesis in T cells to evade immunity. *Nat. Commun.* **2020**, *11*, 3588. [[CrossRef](#)]
78. Abd-Elaziz, M.; Moriya, T.; Akahira, J.I.; Suzuki, T.; Sasano, H. StAR and progesterone producing enzymes (3 β -hydroxysteroid dehydrogenase and cholesterol side-chain cleavage cytochromes P450) in human epithelial ovarian carcinoma: Immunohistochemical and real-time PCR studies. *Cancer Sci.* **2005**, *96*, 232–239. [[CrossRef](#)]
79. Hanamura, T.; Ito, T.; Kanai, T.; Maeno, K.; Shimojo, Y.; Uehara, T.; Suzuki, T.; Hayashi, S.I.; Ito, K.I. Human 3 β -hydroxysteroid dehydrogenase type 1 in human breast cancer: Clinical significance and prognostic associations. *Cancer Med.* **2016**, *5*, 1405–1415. [[CrossRef](#)]
80. Gingras, S.; Moriggl, R.; Groner, B.; Simard, J. Induction of 3 β -hydroxysteroid dehydrogenase/ Δ 5- Δ 4 isomerase type I gene transcription in human breast cancer cell lines and in normal mammary epithelial cells by interleukin-4 and interleukin-13. *Mol. Endocrinol.* **1999**, *13*, 66–81. [[CrossRef](#)]
81. Lin, J.C.; Liu, C.L.; Chang, Y.C.; Cheng, S.P.; Huang, W.C.; Lin, C.H.; Wu, C.Y.; Chen, M.J. Trilostane, a 3 β -hydroxysteroid dehydrogenase inhibitor, suppresses growth of hepatocellular carcinoma and enhances anti-cancer effects of sorafenib. *Investig. New Drugs* **2021**, *39*, 1493–1506. [[CrossRef](#)]
82. Takizawa, I.; Nishiyama, T.; Hara, N.; Hoshii, T.; Ishizaki, F.; Miyashiro, Y.; Takahashi, K. Trilostane, an inhibitor of 3 β -hydroxysteroid dehydrogenase, has an agonistic activity on androgen receptor in human prostate cancer cells. *Cancer Lett.* **2010**, *297*, 226–230. [[CrossRef](#)] [[PubMed](#)]
83. Sugawara, T.; Nomura, E.; Fujimoto, S. Expression of enzyme associated with steroid hormone synthesis and local production of steroid hormone in endometrial carcinoma cells. *J. Endocrinol.* **2004**, *180*, 135–144. [[CrossRef](#)]
84. Labrie, F. Blockade of testicular and adrenal androgens in prostate cancer treatment. *Nat. Rev. Urol.* **2011**, *8*, 73–80. [[CrossRef](#)] [[PubMed](#)]
85. Fang, Q.; Chen, P.; Du, N.; Nandakumar, K.S. Analysis of Data From Breast Diseases Treated With 5-Alpha Reductase Inhibitors for Benign Prostatic Hyperplasia. *Clin. Breast Cancer* **2019**, *19*, e624–e636. [[CrossRef](#)]
86. Hirshburg, J.M.; Kelsey, P.A.; Therrien, C.A.; Gavino, A.C.; Reichenberg, J.S. Adverse effects and safety of 5-alpha reductase inhibitors (finasteride, dutasteride): A systematic review. *J. Clin. Aesthet. Dermatol.* **2016**, *9*, 56–62. [[PubMed](#)]
87. Culig, Z.; Hobisch, A.; Cronauer, M.V.; Cato, A.C.B.; Hittmair, A.; Radmayr, C.; Eberle, J.; Bartsch, G.; Klocker, H. Mutant androgen receptor detected in an advanced-stage prostatic carcinoma is activated by adrenal androgens and progesterone. *Mol. Endocrinol.* **1993**, *7*, 1541–1550. [[CrossRef](#)]
88. Wiebe, J.P.; Lewis, M.J. Activity and expression of progesterone metabolizing 5 α -reductase, 20 α -hydroxysteroid oxidoreductase and 3 α 9(β -hydroxysteroid oxidoreductase in tumorigenic (MCF-7, MDA-MB-231, T-47D) and nontumorigenic (MCF-10A) human breast cancer cells. *BMC Cancer* **2003**, *3*, 9. [[CrossRef](#)]
89. Wiebe, J.P.; Zhang, G.; Welch, I.; Cadioux-Pitre, H.-A.T. Progesterone metabolites regulate induction, growth, and suppression of estrogen- and progesterone receptor-negative human breast cell tumors. *Breast Cancer Res.* **2013**, *15*, R38. [[CrossRef](#)]
90. Garcia, L.M.P.; Valdez, R.A.; Navarrete, A.; Cabeza, M.; Segovia, J.; Romano, M.C. Cell line derived from glioblastoma synthesizes steroid hormone. Effect of enzyme inhibitors. *Endocr. Abstr.* **2018**, *56*, P136. [[CrossRef](#)]
91. Pinacho-Garcia, L.M.; Valdez, R.A.; Navarrete, A.; Cabeza, M.; Segovia, J.; Romano, M.C. The effect of finasteride and dutasteride on the synthesis of neurosteroids by glioblastoma cells. *Steroids* **2020**, *155*, 108556. [[CrossRef](#)]
92. Zamora-Sánchez, C.J.; Hansberg-Pastor, V.; Salido-Guadarrama, I.; Rodríguez-Dorantes, M.; Camacho-Arroyo, I. Allopregnanolone promotes proliferation and differential gene expression in human glioblastoma cells. *Steroids* **2017**, *119*, 36–42. [[CrossRef](#)] [[PubMed](#)]
93. Zamora-Sánchez, C.J.; Hernández-Vega, A.M.; Gaona-Domínguez, S.; Rodríguez-Dorantes, M.; Camacho-Arroyo, I. 5alpha-dihydroprogesterone promotes proliferation and migration of human glioblastoma cells. *Steroids* **2020**, *163*, 108708. [[CrossRef](#)] [[PubMed](#)]
94. Wei, R.; Zhong, S.; Qiao, L.; Guo, M.; Shao, M.; Wang, S.; Jiang, B.; Yang, Y.; Gu, C. Steroid 5 α -Reductase Type I Induces Cell Viability and Migration via Nuclear Factor- κ B/Vascular Endothelial Growth Factor Signaling Pathway in Colorectal Cancer. *Front. Oncol.* **2020**, *10*, 1501. [[CrossRef](#)]
95. Diviccaro, S.; Giatti, S.; Borgo, F.; Falvo, E.; Caruso, D.; Garcia-Segura, L.M.; Melcangi, R.C. Steroidogenic machinery in the adult rat colon. *J. Steroid Biochem. Mol. Biol.* **2020**, *203*, 105732. [[CrossRef](#)] [[PubMed](#)]
96. Tian, H.; Li, X.; Jiang, W.; Lv, C.; Sun, W.; Huang, C.; Chen, R. High expression of AKR1C1 is associated with proliferation and migration of small-cell lung cancer cells. *Lung Cancer* **2016**, *7*, 53–61. [[CrossRef](#)] [[PubMed](#)]
97. Ji, Q.; Aoyama, C.; Nien, Y.D.; Liu, P.I.; Chen, P.K.; Chang, L.; Stanczyk, F.Z.; Stolz, A. Selective loss of AKR1C1 and AKR1C2 in breast cancer and their potential effect on progesterone signaling. *Cancer Res.* **2004**, *64*, 7610–7617. [[CrossRef](#)] [[PubMed](#)]

98. Zhang, Z.F.; Huang, T.J.; Zhang, X.K.; Xie, Y.J.; Lin, S.T.; Luo, F.F.; Meng, D.F.; Hu, H.; Wang, J.; Peng, L.X.; et al. AKR1C2 acts as a targetable oncogene in esophageal squamous cell carcinoma via activating PI3K/AKT signaling pathway. *J. Cell. Mol. Med.* **2020**, *24*, 9999–10012. [[CrossRef](#)]
99. Snaterse, G.; Visser, J.A.; Arlt, W.; Hofland, J. Circulating steroid hormone variations throughout different stages of prostate cancer. *Endocr. Relat. Cancer* **2017**, *24*, R403–R420. [[CrossRef](#)]
100. Le Calvé, B.; Rynkowski, M.; Le Mercier, M.; Bruyère, C.; Lonez, C.; Gras, T.; Haibe-Kains, B.; Bontempi, G.; Decaestecker, C.; Ruyschaert, J.-M.; et al. Long-term In Vitro Treatment of Human Glioblastoma Cells with Temozolomide Increases Resistance In Vivo through Up-regulation of GLUT Transporter and Aldo-Keto Reductase Enzyme AKR1C Expression. *Neoplasia* **2010**, *12*, 727–739. [[CrossRef](#)]
101. Guo, S.S.; Chen, Y.Z.; Liu, L.T.; Liu, R.P.; Liang, Y.J.; Wen, D.X.; Jin, J.; Tang, L.Q.; Mai, H.Q.; Chen, Q.Y. Prognostic significance of AKR1C4 and the advantage of combining EBV DNA to stratify patients at high risk of locoregional recurrence of nasopharyngeal carcinoma. *BMC Cancer* **2022**, *22*, 880. [[CrossRef](#)]
102. Veliça, P.; Davies, N.J.; Rocha, P.P.; Schrewe, H.; Ride, J.P.; Bunce, C.M. Lack of functional and expression homology between human and mouse aldo-keto reductase 1C enzymes: Implications for modelling human cancers. *Mol. Cancer* **2009**, *8*, 121. [[CrossRef](#)] [[PubMed](#)]
103. Yang, L.; Zhang, J.; Zhang, S.; Dong, W.; Lou, X.; Liu, S. Quantitative evaluation of aldo-keto reductase expression in hepatocellular carcinoma (HCC) cell lines. *Genomics. Proteom. Bioinform.* **2013**, *11*, 230–240. [[CrossRef](#)] [[PubMed](#)]
104. Zeng, C.-M.; Chang, L.-L.; Ying, M.-D.; Cao, J.; He, Q.-J.; Zhu, H.; Yang, B. Aldo-Keto Reductase AKR1C1-AKR1C4: Functions, Regulation, and Intervention for Anti-cancer Therapy. *Front. Pharmacol.* **2017**, *8*, 119. [[CrossRef](#)] [[PubMed](#)]
105. González-Orozco, J.C.; Hansberg-Pastor, V.; Valadez-Cosmes, P.; Nicolas-Ortega, W.; Bastida-Beristain, Y.; De La Fuente-Granada, M.; González-Arenas, A.; Camacho-Arroyo, I. Activation of membrane progesterone receptor-alpha increases proliferation, migration, and invasion of human glioblastoma cells. *Mol. Cell. Endocrinol.* **2018**, *477*, 81–89. [[CrossRef](#)] [[PubMed](#)]
106. Diviccaro, S.; Cioffi, L.; Falvo, E.; Giatti, S.; Melcangi, R.C. Allopregnanolone: An overview on its synthesis and effects. *J. Neuroendocrinol.* **2022**, *34*, 1–17. [[CrossRef](#)] [[PubMed](#)]
107. Bonéy-Montoya, J.; Ziegler, Y.S.; Curtis, C.D.; Montoya, J.A.; Nardulli, A.M. Long-range transcriptional control of progesterone receptor gene expression. *Mol. Endocrinol.* **2010**, *24*, 346–358. [[CrossRef](#)]
108. Kastner, P.; Krust, A.; Turcotte, B.; Stropp, U.; Tora, L.; Gronemeyer, H.; Chambon, P. Two distinct estrogen-regulated promoters generate transcripts encoding the two functionally different human progesterone receptor forms A and B. *EMBO J.* **1990**, *9*, 1603–1614. [[CrossRef](#)]
109. Bello-Alvarez, C.; Zamora-Sánchez, C.J.; Camacho-Arroyo, I. Rapid Actions of the Nuclear Progesterone Receptor through cSrc in Cancer. *Cells* **2022**, *11*, 1964. [[CrossRef](#)]
110. Rupperecht, R.; Reul, J.M.H.M.; Trapp, T.; van Steensel, B.; Wetzel, C.; Damm, K.; Zieglgänsberger, W.; Holsboer, F. Progesterone receptor-mediated effects of neuroactive steroids. *Neuron* **1993**, *11*, 523–530. [[CrossRef](#)]
111. Kliewer, S.A.; Goodwin, B.; Willson, T.M. The nuclear pregnane X receptor: A key regulator of xenobiotic metabolism. *Endocr. Rev.* **2002**, *23*, 687–702. [[CrossRef](#)]
112. Lamba, V.; Yasuda, K.; Lamba, J.K.; Assem, M.; Davila, J.; Strom, S.; Schuetz, E.G. PXR (NR1I2): Splice variants in human tissues, including brain, and identification of neurosteroids and nicotine as PXR activators. *Toxicol. Appl. Pharmacol.* **2004**, *199*, 251–265. [[CrossRef](#)] [[PubMed](#)]
113. Xing, Y.; Yan, J.; Niu, Y. PXR: A center of transcriptional regulation in cancer. *Acta Pharm. Sin. B* **2020**, *10*, 197–206. [[CrossRef](#)] [[PubMed](#)]
114. Xiang, E.; Guo, Q.; Dai, Y.G.; Sun, X.X.; Liu, J.; Fan, C.P.; Wang, Y.Q.; Qiu, S.K.; Wang, H.; Guo, Y. Female-specific activation of pregnane X receptor mediates sex difference in fetal hepatotoxicity by prenatal monocrotaline exposure. *Toxicol. Appl. Pharmacol.* **2020**, *406*, 115137. [[CrossRef](#)] [[PubMed](#)]
115. Skandalaki, A.; Sarantis, P.; Theocharis, S. Pregnane x receptor (Pxr) polymorphisms and cancer treatment. *Biomolecules* **2021**, *11*, 1142. [[CrossRef](#)]
116. Rigalli, J.P.; Tocchetti, G.N.; Weiss, J. Modulation of ABC Transporters by Nuclear Receptors: Physiological, Pathological and Pharmacological Aspects. *Curr. Med. Chem.* **2018**, *26*, 1079–1112. [[CrossRef](#)]
117. Rigalli, J.P.; Theile, D.; Nilles, J.; Weiss, J. Regulation of pxxr function by coactivator and corepressor proteins: Ligand binding is just the beginning. *Cells* **2021**, *10*, 3137. [[CrossRef](#)]
118. Planque, C.; Rajabi, F.; Grillet, F.; Finetti, P.; Bertucci, F.; Gironella, M.; Lozano, J.J.; Beucher, B.; Giraud, J.; Garambois, V.; et al. Pregnane X-receptor promotes stem cell-mediated colon cancer relapse. *Oncotarget* **2016**, *7*, 56558–56573. [[CrossRef](#)]
119. Gupta, D.; Venkatesh, M.; Wang, H.; Kim, S.; Sinz, M.; Goldberg, G.L.; Whitney, K.; Longley, C.; Mani, S. Expanding the roles for pregnane X receptor in cancer: Proliferation and drug resistance in ovarian cancer. *Clin. Cancer Res.* **2008**, *14*, 5332–5340. [[CrossRef](#)]
120. Langmade, S.J.; Gale, S.E.; Frolov, A.; Mohri, I.; Suzuki, K.; Mellon, S.H.; Walkley, S.U.; Covey, D.F.; Schaffer, J.E.; Ory, D.S. Pregnane X receptor (PXR) activation: A mechanism for neuroprotection in a mouse model of Niemann-Pick C disease. *Proc. Natl. Acad. Sci. USA* **2006**, *103*, 13807–13812. [[CrossRef](#)]

121. Frye, C.A.; Koonce, C.J.; Walf, A.A. Involvement of pregnane xenobiotic receptor in mating-induced allopregnanolone formation in the midbrain and hippocampus and brain-derived neurotrophic factor in the hippocampus among female rats. *Psychopharmacology* **2014**, *231*, 3375–3390. [[CrossRef](#)]
122. Chen, S.; Wang, J.M.; Irwin, R.W.; Yao, J.; Liu, L.; Brinton, R.D. Allopregnanolone Promotes Regeneration and Reduces β -Amyloid Burden in a Preclinical Model of Alzheimer's Disease. *PLoS ONE* **2011**, *6*, e24293. [[CrossRef](#)] [[PubMed](#)]
123. Majewska, M.D.; Harrison, N.L.; Schwartz, R.D.; Barker, J.L.; Paul, S.M. Steroid Hormone Metabolites Are Barbiturate-Like Modulators of the GABA Receptor. *Science* **1986**, *232*, 1004–1007. [[CrossRef](#)] [[PubMed](#)]
124. Kim, J.J.; Hibbs, R.E. Direct Structural Insights into GABAA Receptor Pharmacology. *Trends Biochem. Sci.* **2021**, *46*, 502–517. [[CrossRef](#)] [[PubMed](#)]
125. Hosie, A.M.; Wilkins, M.E.; Smart, T.G. Neurosteroid binding sites on GABAA receptors. *Pharmacol. Ther.* **2007**, *116*, 7–19. [[CrossRef](#)]
126. Liu, Q.-Y.; Chang, Y.H.; Schaffner, A.E.; Smith, S.V.; Barker, J.L. Allopregnanolone Activates GABA_A Receptor/Cl⁻ Channels in a Multiphasic Manner in Embryonic Rat Hippocampal Neurons. *J. Neurophysiol.* **2002**, *88*, 1147–1158. [[CrossRef](#)]
127. Abramian, A.M.; Comenencia-Ortiz, E.; Modgil, A.; Vien, T.N.; Nakamura, Y.; Moore, Y.E.; Maguire, J.L.; Terunuma, M.; Davies, P.A.; Moss, S.J. Neurosteroids promote phosphorylation and membrane insertion of extrasynaptic GABAA receptors. *Proc. Natl. Acad. Sci. USA* **2014**, *111*, 7132–7137. [[CrossRef](#)]
128. Almeida, F.B.; Nin, M.S.; Barros, H.M.T. The role of allopregnanolone in depressive-like behaviors: Focus on neurotrophic proteins. *Neurobiol. Stress* **2020**, *12*, 100218. [[CrossRef](#)]
129. Brinton, R.D. Neurosteroids as regenerative agents in the brain: Therapeutic implications. *Nat. Rev. Endocrinol.* **2013**, *9*, 241–250. [[CrossRef](#)]
130. Magnaghi, V.; Parducz, A.; Frasca, A.; Ballabio, M.; Procacci, P.; Racagni, G.; Bonanno, G.; Fumagalli, F. GABA synthesis in Schwann cells is induced by the neuroactive steroid allopregnanolone. *J. Neurochem.* **2010**, *112*, 980–990. [[CrossRef](#)]
131. El-Etr, M.; Akwa, Y.; Fiddes, R.J.; Robel, P.; Baulieu, E.E. A progesterone metabolite stimulates the release of gonadotropin-releasing hormone from GT1-1 hypothalamic neurons via the γ -aminobutyric acid type A receptor. *Proc. Natl. Acad. Sci. USA* **1995**, *92*, 3769–3773. [[CrossRef](#)]
132. Cáceres, A.R.R.; Vega Orozco, A.S.; Cabrera, R.J.; Laconi, M.R. Rapid actions of the neurosteroid allopregnanolone on ovarian and hypothalamic steroidogenesis: Central and peripheral modulation. *J. Neuroendocrinol.* **2020**, *32*, e12836. [[CrossRef](#)] [[PubMed](#)]
133. Cáceres, A.R.R.; Campo Verde Arboccó, F.; Cardone, D.A.; de los, Á.; Sanhueza, M.; Casais, M.; Vega Orozco, A.S.; Laconi, M.R. Superior mesenteric ganglion neural modulation of ovarian angiogenesis, apoptosis and proliferation by the neuroactive steroid allopregnanolone. *J. Neuroendocrinol.* **2022**, *34*, e13056. [[CrossRef](#)] [[PubMed](#)]
134. Bhattacharya, D.; Gawali, V.S.; Kallay, L.; Toukam, D.K.; Koehler, A.; Stambrook, P.; Krummel, D.P.; Sengupta, S. Therapeutically leveraging GABAA receptors in cancer. *Exp. Biol. Med.* **2021**, *246*, 2128–2135. [[CrossRef](#)] [[PubMed](#)]
135. Blanchart, A.; Fernando, R.; Häring, M.; Assaife-Lopes, N.; Romanov, R.A.; Andäng, M.; Harkany, T.; Ernfors, P. Endogenous GABA_{AA} receptor activity suppresses glioma growth. *Oncogene* **2017**, *36*, 777–786. [[CrossRef](#)]
136. Valadez-Cosmes, P.; Vázquez-Martínez, E.R.; Cerbón, M.; Camacho-Arroyo, I. Membrane progesterone receptors in reproduction and cancer. *Mol. Cell. Endocrinol.* **2016**, *434*, 166–175. [[CrossRef](#)]
137. Thomas, P. Membrane Progesterone Receptors (mPRs, PAQRs): Review of Structural and Signaling Characteristics. *Cells* **2022**, *11*, 1785. [[CrossRef](#)]
138. Moussatche, P.; Lyons, T.J. Non-genomic progesterone signalling and its non-canonical receptor. *Biochem. Soc. Trans.* **2012**, *40*, 200–204. [[CrossRef](#)]
139. Thomas, P.; Pang, Y.; Dong, J.; Groenen, P.; Kelder, J.; de Vlieg, J.; Zhu, Y.; Tubbs, C. Steroid and G Protein Binding Characteristics of the Seatrout and Human Progesterin Membrane Receptor α Subtypes and Their Evolutionary Origins. *Endocrinology* **2007**, *148*, 705–718. [[CrossRef](#)]
140. Pang, Y.; Dong, J.; Thomas, P. Characterization, Neurosteroid Binding and Brain Distribution of Human Membrane Progesterone Receptors δ and ϵ (mPR δ and mPR ϵ) and mPR δ Involvement in Neurosteroid Inhibition of Apoptosis. *Endocrinology* **2013**, *154*, 283–295. [[CrossRef](#)]
141. Thomas, P.; Pang, Y. Membrane progesterone receptors: Evidence for neuroprotective, neurosteroid signaling and neuroendocrine functions in neuronal cells. *Neuroendocrinology* **2012**, *96*, 162–171. [[CrossRef](#)]
142. Castelnovo, L.F.; Caffino, L.; Bonalume, V.; Fumagalli, F.; Thomas, P.; Magnaghi, V. Membrane Progesterone Receptors (mPRs/PAQRs) Differently Regulate Migration, Proliferation, and Differentiation in Rat Schwann Cells. *J. Mol. Neurosci.* **2020**, *70*, 433–448. [[CrossRef](#)] [[PubMed](#)]
143. Mosher, L.J.; Cadeddu, R.; Yen, S.; Staudinger, J.L.; Traccis, F.; Fowler, S.C.; Maguire, J.L.; Bortolato, M. Allopregnanolone is required for prepulse inhibition deficits induced by D1 dopamine receptor activation. *Psychoneuroendocrinology* **2019**, *108*, 53–61. [[CrossRef](#)] [[PubMed](#)]
144. Giuliani, F.A.; Yunes, R.; Mohn, C.E.; Laconi, M.; Rettori, V.; Cabrera, R. Allopregnanolone induces LHRH and glutamate release through NMDA receptor modulation. *Endocrine* **2011**, *40*, 21–26. [[CrossRef](#)] [[PubMed](#)]
145. Zamora-Sánchez, C.; del Moral-Morales, A.; Hernández-Vega, A.; Hansberg-Pastor, V.; Salido-Guadarrama, I.; Rodríguez-Dorantes, M.; Camacho-Arroyo, I. Allopregnanolone Alters the Gene Expression Profile of Human Glioblastoma Cells. *Int. J. Mol. Sci.* **2018**, *19*, 864. [[CrossRef](#)] [[PubMed](#)]

146. Zamora-Sánchez, C.J.; Bello-Alvarez, C.; Rodríguez-Dorantes, M.; Camacho-Arroyo, I. Allopregnanolone Promotes Migration and Invasion of Human Glioblastoma Cells through the Protein Tyrosine Kinase c-Src Activation. *Int. J. Mol. Sci.* **2022**, *23*, 4996. [[CrossRef](#)] [[PubMed](#)]
147. Charalampopoulos, I.; Tsatsanis, C.; Dermitzaki, E.; Alexaki, V.I.; Castanas, E.; Margioris, A.N.; Gravanis, A. Dehydroepiandrosterone and allopregnanolone protect sympathoadrenal medulla cells against apoptosis via antiapoptotic Bcl-2 proteins. *Proc. Natl. Acad. Sci. USA* **2004**, *101*, 8209–8214. [[CrossRef](#)] [[PubMed](#)]
148. Tserfas, M.O.; Levina, I.S.; Kuznetsov, Y.V.; Scherbakov, A.M.; Mikhaevich, E.I.; Zavarzin, I.V. Selective synthesis of the two main progesterone metabolites, 3 α -hydroxy-5 α -pregnanolone (allopregnanolone) and 3 α -hydroxypregn-4-en-20-one, and an assessment of their effect on proliferation of hormone-dependent human breast cancer cells. *Russ. Chem. Bull.* **2020**, *69*, 552–557. [[CrossRef](#)]
149. Feng, Y.-H.; Lim, S.-W.; Lin, H.-Y.; Wang, S.-A.; Hsu, S.-P.; Kao, T.-J.; Ko, C.-Y.; Hsu, T.-I. Allopregnanolone suppresses glioblastoma survival through decreasing DPYSL3 and S100A11 expression. *J. Steroid Biochem. Mol. Biol.* **2022**, *219*, 106067. [[CrossRef](#)]
150. Pelegrina, L.T.; de los Angeles Sanhueza, M.; Ramona Cáceres, A.R.; Cuello-Carrión, D.; Rodríguez, C.E.; Laconi, M.R. Effect of progesterone and first evidence about allopregnanolone action on the progression of epithelial human ovarian cancer cell lines. *J. Steroid Biochem. Mol. Biol.* **2020**, *196*, 105492. [[CrossRef](#)]
151. Thomas, P.; Pang, Y. Anti-apoptotic Actions of Allopregnanolone and Ganaxolone Mediated Through Membrane Progesterone Receptors (PAQRs) in Neuronal Cells. *Front. Endocrinol.* **2020**, *11*, 417. [[CrossRef](#)]
152. Taleb, O.; Patte-Mensah, C.; Meyer, L.; Kemmel, V.; Geoffroy, P.; Miesch, M.; Mensah-Nyagan, A.-G. Evidence for effective structure-based neuromodulatory effects of new analogues of neurosteroid allopregnanolone. *J. Neuroendocrinol.* **2018**, *30*, e12568. [[CrossRef](#)] [[PubMed](#)]
153. Karout, M.; Miesch, M.; Geoffroy, P.; Kraft, S.; Hofmann, H.D.; Mensah-Nyagan, A.G.; Kirsch, M. Novel analogs of allopregnanolone show improved efficiency and specificity in neuroprotection and stimulation of proliferation. *J. Neurochem.* **2016**, *139*, 782–794. [[CrossRef](#)] [[PubMed](#)]
154. Siegel, R.L.; Miller, K.D.; Fuchs, H.E.; Jemal, A. Cancer statistics, 2022. *CA Cancer J. Clin.* **2022**, *72*, 7–33. [[CrossRef](#)] [[PubMed](#)]
155. Yuan, Y.; Liu, L.; Chen, H.; Wang, Y.; Xu, Y.; Mao, H.; Li, J.; Mills, G.B.; Shu, Y.; Li, L.; et al. Comprehensive Characterization of Molecular Differences in Cancer between Male and Female Patients. *Cancer Cell* **2016**, *29*, 711–722. [[CrossRef](#)]
156. Bello-Alvarez, C.; Camacho-Arroyo, I. Impact of sex in the prevalence and progression of glioblastomas: The role of gonadal steroid hormones. *Biol. Sex Differ.* **2021**, *12*, 28. [[CrossRef](#)]
157. Yang, W.; Warrington, N.M.; Taylor, S.J.; Whitmire, P.; Carrasco, E.; Singleton, K.W.; Wu, N.; Lathia, J.D.; Berens, M.E.; Kim, A.H.; et al. Sex differences in GBM revealed by analysis of patient imaging, transcriptome, and survival data. *Sci. Transl. Med.* **2019**, *11*, eaao5253. [[CrossRef](#)]
158. Yang, W.; Warrington, N.M.; Taylor, S.J.; Carrasco, E.; Singleton, K.W.; Wu, N.; Lathia, J.D.; Berens, M.E.; Kim, A.H.; Barnholtz-Sloan, J.S.; et al. Clinically Important sex differences in GBM biology revealed by analysis of male and female imaging, transcriptome and survival data. *bioRxiv* **2017**. [[CrossRef](#)]
159. Genazzani, A.R.; Petraglia, F.; Bernardi, F.; Casarosa, E.; Salvestroni, C.; Tonetti, A.; Nappi, R.E.; Luisi, S.; Palumbo, M.; Purdy, R.H.; et al. Circulating levels of allopregnanolone in humans: Gender, age, and endocrine influences. *J. Clin. Endocrinol. Metab.* **1998**, *83*, 2099–2103. [[CrossRef](#)]
160. Lamb, Y.N. Ganaxolone: First Approval. *Drugs* **2022**, *82*, 933–940. [[CrossRef](#)]

Disclaimer/Publisher’s Note: The statements, opinions and data contained in all publications are solely those of the individual author(s) and contributor(s) and not of MDPI and/or the editor(s). MDPI and/or the editor(s) disclaim responsibility for any injury to people or property resulting from any ideas, methods, instructions or products referred to in the content.

Progesterone and its metabolite allopregnanolone promote invasion of human glioblastoma cells through metalloproteinase-9 and cSrc kinase

CLAUDIA BELLO-ALVAREZ*, CARMEN J. ZAMORA-SÁNCHEZ*,
KARLA M. PEÑA-GUTIÉRREZ and IGNACIO CAMACHO-ARROYO

Unidad de Investigación en Reproducción Humana, Instituto Nacional de Perinatología-Facultad de Química,
Universidad Nacional Autónoma de México, Mexico City 04510, Mexico

Received July 1, 2022; Accepted January 26, 2023

DOI: 10.3892/ol.2023.13809

Abstract. Glioblastomas are the most aggressive and common primary brain tumors in adults. Glioblastoma cells have a great capacity to migrate and invade the brain parenchyma, often reaching the contralateral hemisphere. Progesterone (P4) and its metabolite, allopregnanolone (3 α -THP), promote the migration and invasion of human glioblastoma-derived cells. P4 induces migration in glioblastoma cells by the activation of the proto-oncogene tyrosine-protein kinase Src (cSrc) and focal adhesion kinase (Fak). In breast cancer cells, cSrc and Fak promote invasion by increasing the expression and activation of extracellular matrix metalloproteinases (MMPs). However, the mechanism of action by which P4 and 3 α -THP promote invasion in glioblastoma cells remains unclear. The effects of P4 and 3 α -THP on the protein expression levels of MMP-2 and -9 and the participation of cSrc in progestin effects in U251 and U87 human glioblastoma-derived cells were evaluated. It was determined by western blotting that the P4 increased the protein expression level of MMP-9 in U251 and U87 cells, and 3 α -THP increased the protein expression level of MMP-9 in U87 cells. None of these progestins modified MMP-2 protein expression levels. The increase in MMP-9 expression was reduced when the intracellular progesterone receptor and cSrc expression were blocked with small interfering RNAs. Cell invasion induced by P4 and 3 α -THP was also blocked by inhibiting cSrc activity with PP2 or by cSrc gene silencing. These results suggest that P4

and its metabolite 3 α -THP induce the invasion of glioblastoma cells by increasing MMP-9 expression through the cSrc kinase family. The results of this study provide information of interest in the context of targeted therapies against molecular pathways involved in glioblastoma invasion.

Introduction

Glioblastomas are the primary tumors of the central nervous system that cause the most deaths and therefore have the highest fatality rate. The median survival time of patients with this disease is <15 months, and this statistic has not changed for more than two decades (1). Glioblastoma cells' high migration and invasion capacity into areas of the brain parenchyma adjacent to the tumor, even reaching the contralateral hemisphere, makes it impossible to perform a complete surgical resection, resulting in tumor recurrence (2).

Proto-oncogene tyrosine-protein kinase Src (cSrc) is a non-receptor tyrosine kinase that participates in diverse biological activities, including cell migration. Furthermore, it has been broadly associated with controlling the expression of metalloproteinases (MMPs) and tumor invasiveness (3). cSrc and focal adhesion kinase (Fak) kinase activity inhibition in the breast cancer MCF-7 cell line, was reported to have blocked MMP-9 secretion (4). Gautam *et al* (5) reported that, in triple-negative MDA-MB-231 breast cancer cells, the inhibition of cSrc activity decreased MMP-9 levels and cell invasion. Within the high molecular complexity of the mechanisms that regulate invasion in glioblastomas, MMPs serve a fundamental role in degrading the extracellular matrix (ECM). Upregulation of MMP-2 and -9 in glioblastomas is associated with poor prognosis (6). The involvement of MMP-2 and -9 in the progression of glioblastomas has been studied for >20 years. In 1999, Forsyth *et al* (7) reported that the levels and activity of MMP-2 and -9 were higher in glioblastomas than in normal brain tissue. The expression level of MMP-9 also showed a strong correlation with the tumor grade in gliomas. Later, Kondraganti *et al* (8) reported that impaired expression of MMP-9 reduced glioblastoma cells' invasiveness. More recently, in 2019, Zhou *et al* (6) reported that MMP-2 and -9 expression was higher in recurrent glioma than in primary glioma.

Correspondence to: Dr Ignacio Camacho-Arroyo, Unidad de Investigación en Reproducción Humana, Instituto Nacional de Perinatología-Facultad de Química, Universidad Nacional Autónoma de México, Ciudad Universitaria, Avenue Universidad 3000, Coyoacán, Mexico City 04510, Mexico
E-mail: camachoarroyo@gmail.com

*Contributed equally

Key words: glioblastoma, progesterone, allopregnanolone, cSrc, invasion, MMP-9

Progesterone (P4) has been associated with increased invasiveness capacity in numerous malignant processes (9-11). In breast cancer cells, P4 increases the formation of the protrusions associated with focal adhesion complex, and migration and invasion processes through cSrc kinase activation (12). Although glioblastoma is not a cancer of the reproductive system, it is sex-dependent since there is a higher prevalence in men than in women, as evidenced by epidemiological data (13). In the context of P4, the results of previous studies indicate that this hormone induces glioblastoma progression when administered at 10-50 nM (14,15). Notably, in terms of glioblastoma, Piña-Medina *et al* (16) reported that P4 increased the number of invasive and migrating cells. More recently, Bello-Alvarez *et al* (15) demonstrated that P4 activates cSrc kinase and Fak, which are fundamental components of focal adhesion complexes. It has also been reported that 3 α -tetrahydroprogesterone (3 α -THP), an active P4 reduced metabolite, increased cell proliferation of glioblastoma cells. In addition, finasteride, an inhibitor of 5 α -reductase, the rate-limiting enzyme for the P4 transformation to 3 α -THP, partially inhibited this effect (17). Moreover, 3 α -THP regulates migration in glioblastoma cells, and this effect is dependent on the activation of cSrc (18). In rat Schwann cells, the 3 α -THP induction of cell migration is regulated by cSrc and Fak (19). However, it is not known whether P4 and 3 α -THP regulate MMP-2 and -9 expression through cSrc activity and whether this effect is reflected in the migration and invasiveness of glioblastoma cells.

Materials and methods

Cell culture and treatments. U251 (astrocytoma cell line) and U87 (HTB-14; glioblastoma of unknown origin) cells were purchased from the American Type Culture Collection (ATCC) and were previously authenticated by STR profiling using an AmpFISTR® Identifiler™ kit (cat. no. 4322288) and Genetic Analyzer 3130xl (Applied Biosystems; Thermo Fisher Scientific, Inc.). Mycoplasma contamination was routinely monitored using a Universal Mycoplasma Detection Kit (cat. no. 30-1012K; ATCC). Cells were plated in 35 mm culture dishes and maintained in DMEM medium (Vitro SA) supplemented with 10% fetal bovine serum (FBS; Biowest), 1 mM pyruvate, 2 mM glutamine, 0.1 mM MEM Non-Essential Amino Acids Solution (Gibco; Thermo Fisher Scientific) and 1 mM antibiotic (streptomycin 10 g/l; penicillin G 6.028 g/l; and amphotericin B 0.025 g/l, Biowest, cat. no. L0010) at conditions of 37°C and 5% CO₂. Culture medium was replaced by DMEM phenol red-free (Biowest) and supplemented with 10% charcoal-stripped serum FBS (sFBS; HyClone; Cytiva), to avoid additional hormone supplementation, ~24 h before treatment. On the day of treatment, cells were treated with 50 nM P4 (0.001% DMSO vehicle; cat. no. P-8783; MilliporeSigma) or 100 nM 3 α -THP (0.01% ethanol vehicle; cat. no. 195886; MP Biomedicals, LLC) for 3 or 6 h at 37°C to assess the protein expression levels of MMP-2 and MMP-9.

Cell migration (wound healing assays). For evaluating cell migration, wound healing assays were performed. A total of 3.5x10⁵ U251 or U87 cells were seeded per well in 6-well

plates and cultured as aforementioned. After 24 h of culture conditions free of phenol red and 10% sFBS (20), a scratch wound was made in the 90% confluent cells with a fine pipette tip. After washing the detached cells with 1X PBS (137 mM NaCl, 2.7 mM KCl, 1.8 mM KH₂PO₄ and 10 mM NaHPO₄), the cell cultures were treated with 10 μ M cytosine β -D-arabinofuranoside (Ara-C; Sigma-Aldrich; Merck KGaA) to inhibit cell proliferation 1 h before adding either 50 nM P4 (0.001% DMSO vehicle), 1 μ M 1-tert-Butyl-3-(4-chlorophenyl)-1H-pyrazolo[3,4-d] pyrimidin-4-amine (PP2, a Src family kinase inhibitor; 0.001% DMSO vehicle), P4 + PP2 at the aforementioned concentrations, 100 nM 3 α -THP (0.01% ethanol vehicle) or 3 α -THP + PP2 at the aforementioned concentrations. To determine the percentage of cell migration, images of four fields of view per treatment condition were taken at 0, 6, 12 and 24 h with an Infinity 1-2C camera attached to an Olympus CKX41 inverted microscope. Image processing was performed using the macro-MRI Wound Healing Tool in ImageJ 1.45S software (National Institutes of Health).

Invasion assays. Cells were grown according to the aforementioned method. The invasion assays were performed using Transwell inserts (8.0 μ m membrane; Corning, Inc.) and 6-well plates with Matrigel (2 mg/ml; Engelbreth-Holm-Swann murine sarcoma extract; MilliporeSigma) diluted in DMEM phenol red-free without FBS or antibiotics. This dilution was incubated in the inserts at conditions of 37°C and 5% CO₂ atmosphere for 2 h. In the upper insert, 3x10⁴ cells suspended in DMEM without phenol red, FBS or antibiotics but with 10 μ M Ara-C were seeded. DMEM supplemented with 10% FBS (Biowest) as a chemoattractant was added to the lower wells. Cells in the upper Transwell inserts received the following steroid treatments: 50 nM P4, 100 nM 3 α -THP or 1 μ M PP2. The incubation conditions were 37°C and 5% CO₂ atmosphere for 24 h. To evaluate the specific role of cSrc on cell invasion, cSrc expression was first downregulated as described in the small interfering (siRNA) transfection subsection of this manuscript, followed by vehicle, P4 or 3 α -THP treatments. After incubation, the non-invading cells were washed from the upper surface of the insert. Invasive cells at the membrane were fixed, stained, visualized and quantified as described previously by Piña-Medina *et al* (16).

Senescence assays. Based on preliminary results, growth pattern and cell size, a total of 5x10⁴ U87 cells or 3x10⁴ U251 cells were plated per well in 6-well plates with phenol red-free DMEM and 10% sFBS for 24 h at 37°C. After 24 h, the following treatments were added: 50 nM P4, 1 μ M PP2, 50 nM P4 + 1 μ M PP2, 100 nM 3 α -THP, 100 nM 3 α -THP + 1 μ M PP2 or vehicle (0.01% DMSO for PP2 and P4 or 0.01% ethanol for 3 α -THP). After a further 24 h, cells were washed with PBS and senescence was evaluated using the Senescent Cells Staining Kit (cat. no. CS0030-1KT; MilliporeSigma), according to the manufacturer's instructions, to determine the expression of β -galactosidase in senescent cells. Incubation with β -galactosidase staining solution was performed overnight at 37°C. A total of three independent experiments were performed for each cell line. After staining, images of four fields of view per treatment condition were taken with an Infinity 1-2C camera attached to an Olympus CKX41 inverted

microscope. ImageJ 1.45S software (National Institutes of Health) was used to perform the image processing and counting of β -galactosidase positive cells to determine the proportion of senescent cells.

siRNA transfection. A total of 2.5×10^5 U251 cells were plated in 35-mm culture dishes with DMEM and 10% FBS for 24 h. After incubation, the medium was replaced with DMEM without phenol red, FBS, or antibiotics. Transfection was performed with 100 nM commercial cSrc siRNA (cat. no. 4392420; ID, s13412; Thermo Fisher Scientific, Inc.) or with 100 nM control siRNA (Silencer Select Negative Control #1; cat. no. 4390844; Thermo Fisher Scientific, Inc.), an aleatory sequence that did not recognize a specific target in the cell, using Lipofectamine RNAiMAX (Thermo Fisher Scientific, Inc.) for 48 h at 37°C. This commercial cSrc siRNA was also used to evaluate the effect of P4 on MMP-2 and MMP-9 expression promoted by cSrc. After transfection with the cSrc siRNA or control siRNA, the medium was refreshed for 12 h. Cells were harvested for protein extraction to evaluate transfection efficiency 48 h after the addition of siRNAs, and the wound healing assays were performed. Commercial siRNA against progesterone receptor (PR) (Ambion, PGR Silencer Select, Pre-designed; cat. no. 4392420) and control siRNA (Silencer Select Negative Control #1; cat. no. 4390844) (both Thermo Fisher Scientific, Inc.) was used to evaluate the effect of PR on MMP-2 and -9 expression 48 h after the addition of siRNAs. The transfection protocol was performed as previously described (15,18).

Protein extraction and western blotting. The protein expression levels of MMP-2, MMP-9, cSrc and PR were determined by western blotting. After any hormone treatment or transfection procedure described above was performed, cells were homogenized in RIPA buffer with protease inhibitors (cat. no. P8340; Sigma-Aldrich; Merck KGaA). Proteins were obtained as described by Bello-Alvarez *et al* (15). For protein electrophoresis, 40 μ g of total extracted proteins were loaded on an 8.5% SDS-PAGE gel. Proteins were transferred to nitrocellulose membranes in semi-dry conditions (Bio-Rad Laboratories, Inc.) at 25 V for 1 h (MMP-2, MMP-9 and cSrc) or 2 h (PR). Membranes were blocked with 5% bovine serum albumin (cat. no. A-420-100; Gold Biotechnology) in Tris-buffered saline with 0.1% Tween, at 37°C for 2 h. Membranes were then incubated with primary antibodies against MMP-2 (cat. no. 4042; Cell Signaling Technology, Inc.), MMP-9 (cat. no. 3852; Cell Signaling Technology, Inc.), cSrc (cat. no. 2108; Cell Signaling Technology, Inc.), PR (cat. no. B-30 sc-811; Santa Cruz Biotechnology, Inc.) or the α -tubulin loading control (cat. no. sc-398103; Santa Cruz Biotechnology, Inc.). The dilution of all primary antibodies was 1:1,000 and antibodies were incubated for 24 h at 4°C. Secondary antibodies were against rabbit (cat. no. 1858415; Thermo Fisher Scientific, Inc.) or mouse (cat. no. sc-516102; Santa Cruz Biotechnology, Inc.), and were incubated at a dilution of 1:10,000 at room temperature for 45 min. Finally the signal was detected with Super Signal West Femto Maximum Sensitivity Substrate (Thermo Fisher Scientific, Inc.) (15). Densitometric analysis was performed with ImageJ 1.45S software (National Institutes of Health). To determine changes in the protein expression levels of MMP-2 and MMP-9, the same

membrane was re-probed three times, alongside the α -tubulin loading control.

Statistical analysis. All statistical analyses were performed using Graph Pad Prism 5 software (GraphPad Software; Dotmatics). A one-way ANOVA and Bonferroni post hoc test, or unpaired Student's t-test were used to analyze differences between comparable groups. $P < 0.05$ was considered to indicate a statistically significant difference.

Results

P4 and 3 α -THP enhance cell migration through activation of the Src family of kinases. The impact of the Src kinase family on the actions of P4 and 3 α -THP in cell migration using the kinase inhibitor, PP2, which has a high affinity for many members of the Src kinase family, was evaluated. Both progestins (P4 and 3 α -THP) induced cell migration (Figs. 1 and 2). The effect of P4 in the U251 and U87 cell lines was significant compared to the vehicle following 24 h of treatment (Figs. 1A-C and S1). 3 α -THP also promoted cell migration but significance compared with vehicle was only demonstrated at 12 and 24 h of treatment in both cell lines (Figs. 2A-C and S2). The inhibitor PP2 completely blocked the effect of P4 in U251 cells and significantly blocked the effect of P4 in U87 cells (Fig. 1A-C). PP2 significantly, partially blocked the effect of 3 α -THP at 12 and 24 h of treatment in U251 cells (Fig. 2A and B); whereas in U87 cells, PP2 completely blocked its effect (Fig. 2C). No marked changes in cell migration were observed for any treatments at 6 h (Figs. 1, 2, S1 and S2).

Furthermore, the potential of any of the treatment conditions to induce senescence was evaluated in both cell lines using a β -galactosidase staining assay (β -galactosidase catalyzes the hydrolysis of β -galactosidase only in senescent cells). In U251 cells, the proportion of β -galactosidase positive cells was 0% for any treatment (Figs. S3 and S4). In U87 cells, the proportion of β -galactosidase positive cells in each treatment was 0.88-1.5%. However, no significant differences between treatments were demonstrated (Figs. S5 and S6).

cSrc activity participates in the invasion induced by P4 and 3 α -THP in human glioblastoma-derived cells. Considering that the addition of P4 increased cell migration, the effect of cSrc on the invasiveness of P4-stimulated human glioblastoma-derived cells was evaluated. A Transwell invasion assay was performed to determine whether inhibiting Src kinase family activity with PP2 altered the invasion triggered by P4 in U251 and U87 cells. In P4-treated cells, a significant enhancement of invasion compared with the vehicle group was observed at 24 h in both U251 (Fig. 3A and B) and U87 cells (Fig. 3C and D). This enhancement was significantly suppressed by PP2 in U87 cells (Fig. 3D). In U251 cells, the effect of PP2 on invasiveness was not significant; however, there was a marked trend towards a decrease in invasion (Fig. 3B). This result demonstrated that the Src kinase family modulates the invasion of glioblastoma cells triggered by P4.

The effect of cSrc silencing on the invasiveness of U251 cells after treatment with P4 or 3 α -THP was also assessed. Silencing in U87 was not performed due to limited siRNA availability). As with the PP2 experiments, P4 significantly induced U251

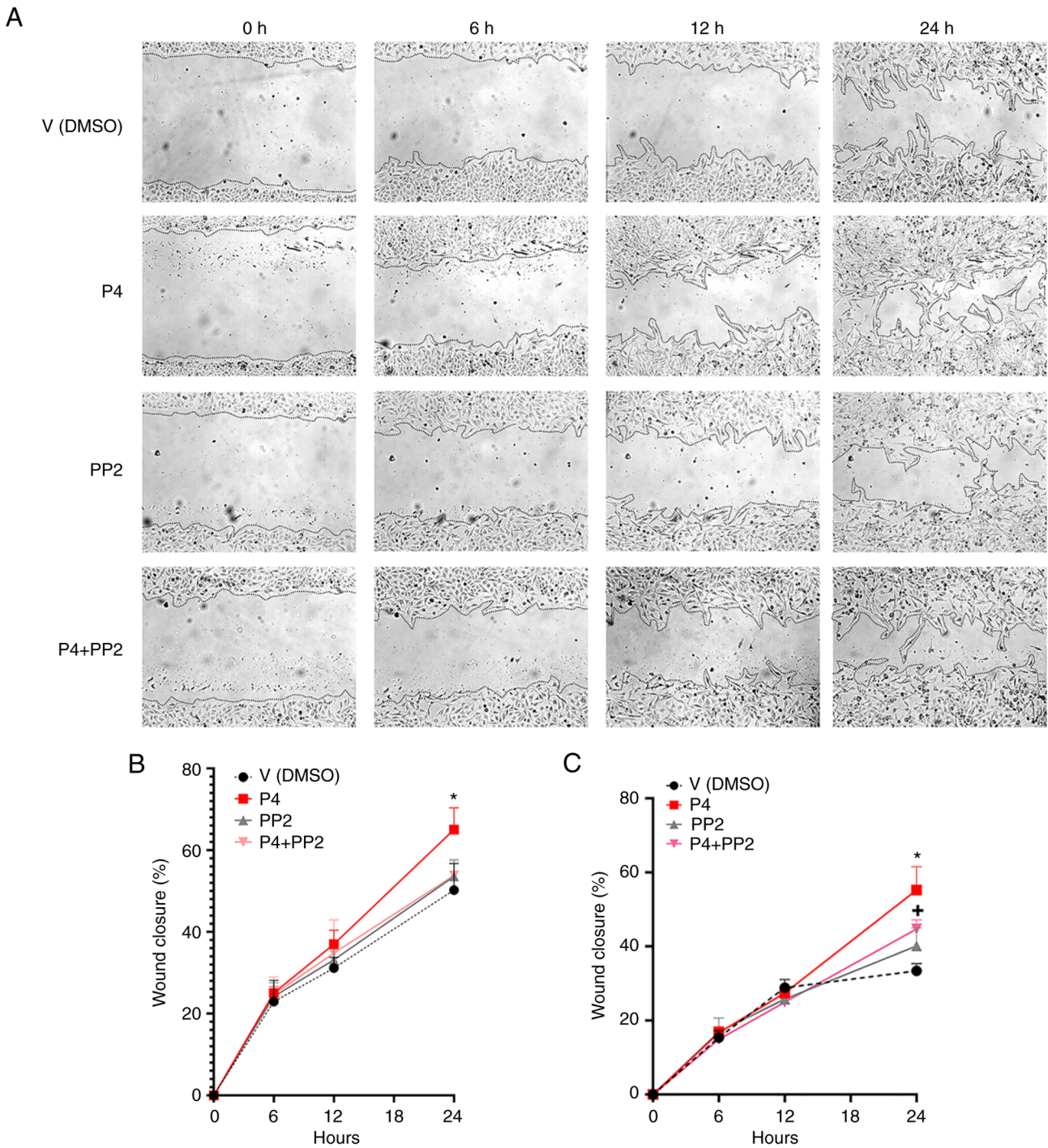


Figure 1. The pharmacological inhibition of cSrc interferes with the effect of P4 on glioblastoma cell migration. (A) Representative images of U251 cells treated with P4 (50 nM), PP2 (1 μM) and the P4 + PP2 conjunct treatment at 0, 6, 12 and 24 h. Percentage cell migration graphs of (B) U251 (*P<0.05, P4 vs. V at 24 h) and (C) U87 cells (*P<0.05, P4 vs. all other treatments at 24 h; +P<0.05, P4 + PP2 vs. V at 24 h). Each point represents the mean ± SEM, n=4. All images were taken using a 10X magnification lens. P4, progesterone; V, vehicle; PP2, 1-tert-Butyl-3-(4-chlorophenyl)-1H-pyrazolo[3,4-d] pyrimidin-4-amine.

cell invasion compared with the untreated group and this effect was significantly reduced by cSrc silencing (Fig. 4A and B) compared with the siRNA control. 3α-THP also significantly promoted cell invasion compared with the untreated group and this effect decreased significantly when cSrc was silenced compared with the siRNA control (Fig. 4C and D). Notably, marked inhibition of cell invasion by cSrc silencing was evident in vehicle-treated cells (Fig. 4D). When treatment with 3α-THP was administered to the cells, invasion returned to basal levels.

P4 and 3α-THP increase the protein expression level of MMP-9 in human glioblastoma-derived cells. MMPs perform a vital role in ECM degradation to promote cell invasion and are frequently upregulated in malignant tumors (21). MMP-2 and MMP-9 are upregulated in glioblastomas and are associated with poor prognosis (6). Therefore, the effect of P4 and 3α-THP on MMP-2 and MMP-9 protein expression levels in human glioblastoma-derived cell lines was evaluated. U87 and U251 cells were treated with 50 nM P4 and 100 nM 3α-THP

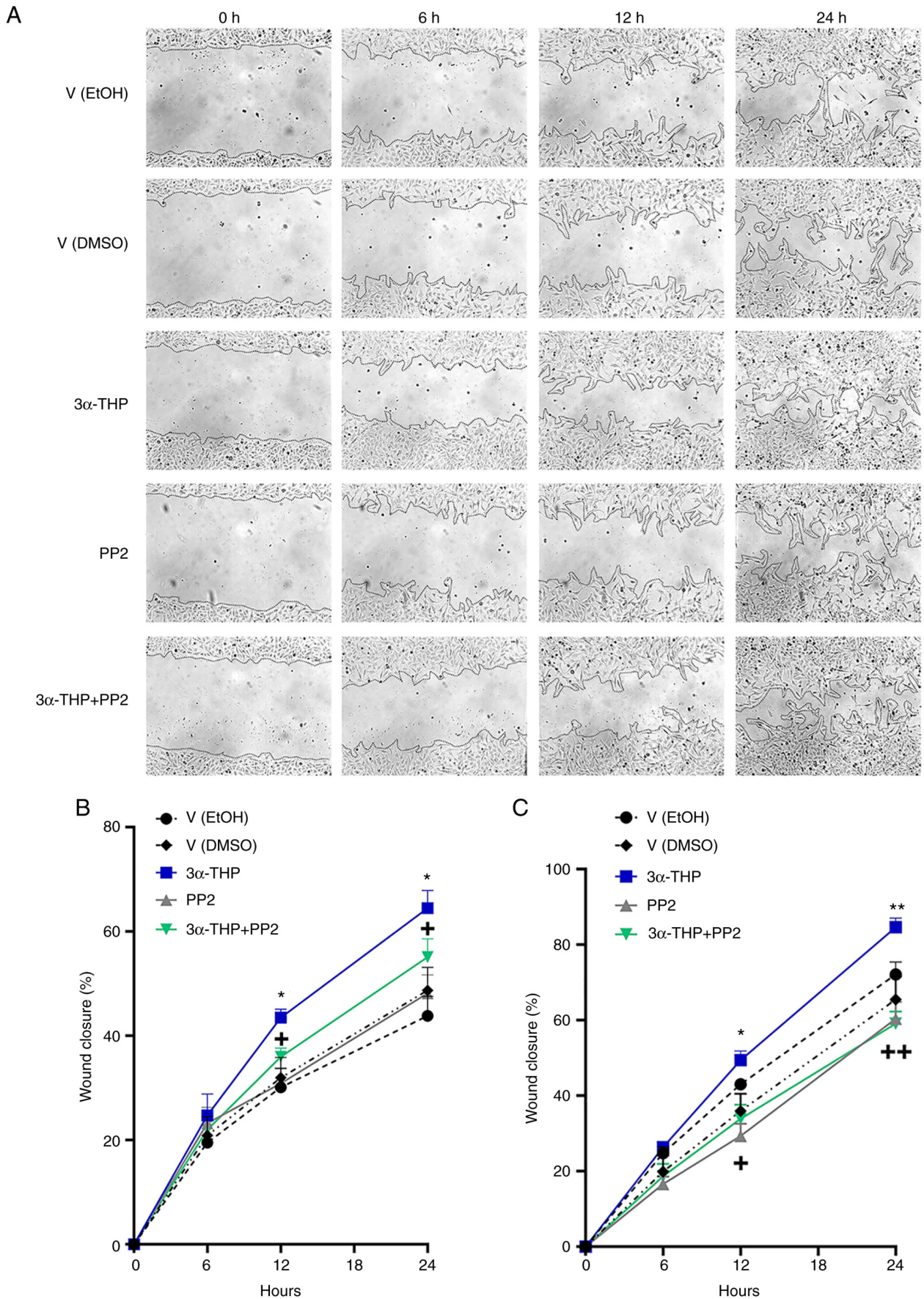


Figure 2. cSrc inhibition blocks the effect of 3 α -THP on glioblastoma cell migration. (A) Representative images of U251 cells treated with 3 α -THP (100 nM), PP2 (1 μ M) and the 3 α -THP + PP2 conjunct treatment at 0, 6, 12 and 24 h. Percentage migration graph of (B) U251 cells [$P < 0.05$, 3 α -THP vs. all other treatments; $^*P < 0.05$, 3 α -THP + PP2 vs. V (EtOH); n=3] and (C) U87 cells [$P < 0.05$, 3 α -THP vs. V (DMSO 0.001%), 3 α -THP + PP2, and PP2; $^{**}P < 0.05$, 3 α -THP vs. all other treatments; $^*P < 0.05$, PP2 and 3 α -THP + PP2 vs. V (EtOH 0.01%); $^{**}P < 0.05$, PP2 vs. V (EtOH), and 3 α -THP + PP2 vs. V (EtOH)]; n=4. Each point represents the mean \pm SEM. EtOH, ethanol; V, vehicle; PP2, 1-tert-Butyl-3-(4-chlorophenyl)-1H-pyrazolo[3,4-d] pyrimidin-4-amine; 3 α -THP, allopregnanolone.

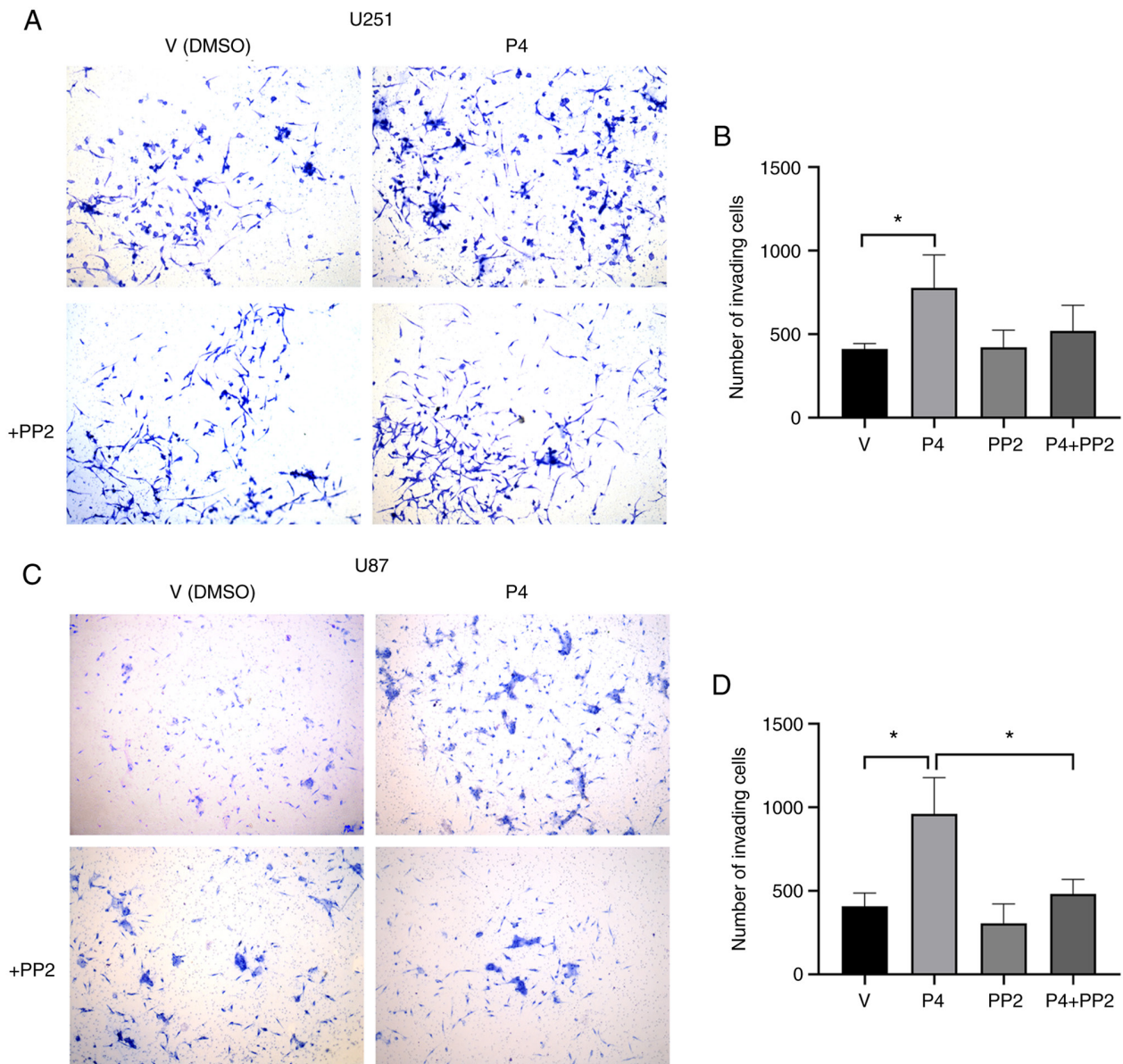


Figure 3. The pharmacological inhibition of cSrc reduces cell invasion induced by P4 in glioblastoma cells. (A) U251 and (C) U87 cells treated with V (0.001% DMSO), P4 (50 nM), PP2 (1 μ M) or the P4 + PP2 conjunct treatment for 24 h. Representative images of the Transwell invasion assay are shown. Graphs presented the number of invasive (B) U251 and (D) U87 cells. Data are presented as the mean \pm SEM; n=4. *P<0.05. P4, progesterone; V, vehicle.

for 3 or 6 h (Figs. 5 and 6). P4 and 3 α -THP did not significantly increase MMP-2 protein expression levels compared with the control in U251 and U87 cells (Figs. 5A and B, and 6A and B). However, P4 significantly increased MMP-9 protein expression levels compared with the control at 3 and 6 h in U251 cells and at 6 h in U87 cells (Fig. 5C and D). 3 α -THP significantly increased MMP-9 protein expression levels compared with the control in U87 cells at 3 h (Fig. 6D).

cSrc is involved in the regulation of MMP-9 expression in human glioblastoma-derived cells treated with P4. It has previously been reported that the inactivation of cSrc inhibits triple-negative breast cancer progression through the downregulation of MMP-9 expression (5). Therefore, the role of cSrc in the expression of MMP-9 in P4-treated glioblastoma cells was evaluated. A commercial siRNA against cSrc or a control siRNA were used to transfect U251 and U87 cells. After transfection, cells were

treated with 100 nM 3 α -THP or 50 nM P4 for 6 h, respectively (Fig. 7). cSrc silencing caused a significant reduction in cSrc protein expression levels compared with the siRNA control (Fig. 7A and B). In cells transfected with siRNA against cSrc, the increase in MMP-9 expression triggered by P4 was significantly reduced compared with cells that received the control siRNA. This result suggested that, at least partially, cSrc participated in the induction of MMP-9 expression by P4 (Fig. 7C and D).

PR regulates the expression of MMP-9. Bello-Alvarez *et al* (15) previously reported that P4 promoted interaction between the PR and cSrc, which led to the activation of cSrc. To assess the effect of PR on MMP-2 and MMP-9 expression, cells were transfected with an siRNA against PR (Fig. 8). MMP-9 protein expression levels were significantly reduced upon PR silencing compared with control siRNA, whereas no significant change was demonstrated for MMP-2 (Fig. 8B and C).

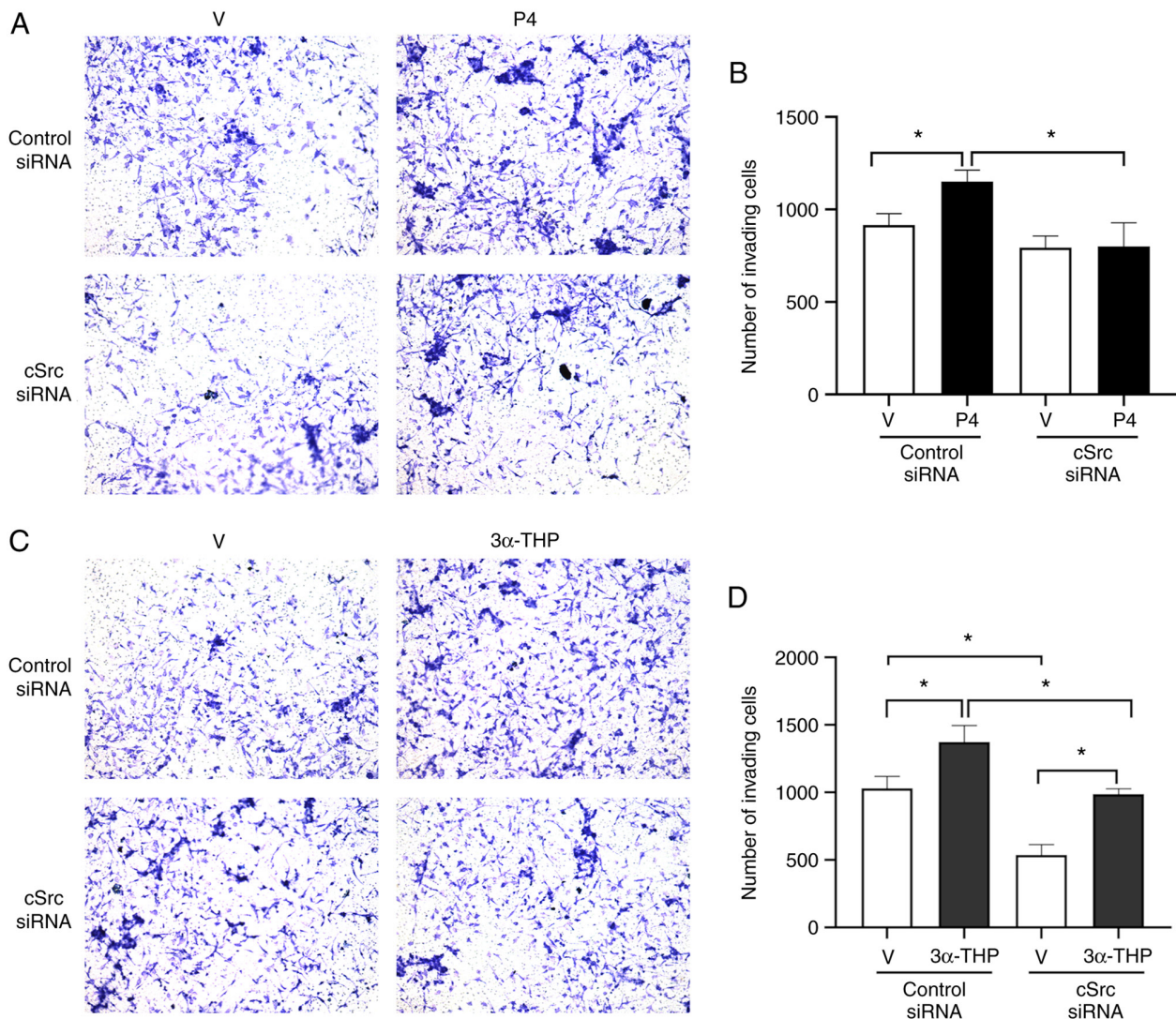


Figure 4. cSrc expression mediates invasion induced by P4 and 3 α -THP in U251 cells. cSrc was silenced in the U251 cell line and was treated with P4 (50 nM), 3 α -THP (100 nM) or their respective vehicles (0.001% DMSO or 0.01% ethanol) for 24 h. Representative images of cell invasion assays of transfected U251 cells treated with (A) P4 or (C) 3 α -THP. Graphs representing the number of invasive U251 cells treated with (B) P4 or (D) 3 α -THP. Data are presented as the mean \pm SEM; n=3. *P<0.05. P4, progesterone; siRNA, small interfering RNA; V, vehicle; 3 α -THP, allopregnanolone.

Discussion

According to the Global Cancer Observatory database (<https://gco.iarc.fr/>) (22), central nervous system tumors are the 13th leading cause of mortality among all known types of cancer. Glioblastoma is the most malignant and frequent entity among adult brain tumors (1). Due to glioblastoma's migratory and invasive nature, the treatments available are insufficient and tumor recurrence is invariably manifested (23). The migration and subsequent degradation of the ECM is one of the critical events for a malignant cell to colonize areas distant from the tumor's site of origin (24). Proteases are members of the group of molecules that, in a coordinated manner, orchestrate this event to gain cancer aggressiveness (25). MMPs are among the most relevant families of proteases in glioblastoma invasion. The expression of 11 members (MMP-1, -2, -7, -8, -9, -10, -11, -14, -15, -19 and -23) of this group have been reported to be elevated in glioblastomas (26). However, according to the results of several studies (6,27-29), MMP-2 and MMP-9 are essential in the progression of glioblastomas. The expression

of these proteins are increased in recurrent gliomas compared with primary gliomas (6). In addition, the expression of both of these MMPs correlates with the tumor grade (7). In the case of MMP-9, its low expression is related to an improved prognosis and response to Temozolomide (30).

The role of P4 at physiological concentrations (10-100 nM) in the development of glioblastomas has been extensively reported. In addition to inducing glioblastoma cell proliferation (23-25), P4 promotes migration and invasion in both *in vitro* and *in vivo* models (15,16,31-33). P4 is one of the most prominent examples of the hormesis effect, a dose-response phenomenon in which stimulation occurs at low concentrations and inhibition at high concentrations (34). In the context of glioblastomas, it has been reported that P4 concentrations >20 μ M promoted apoptosis and decreased tumor growth, while concentrations <10 μ M promoted the opposite effect (35). Previous results published by our laboratory support this observation as concentrations of 10 and 50 nM promoted glioblastoma cell progression by increasing proliferation, migration and invasion (14-16).

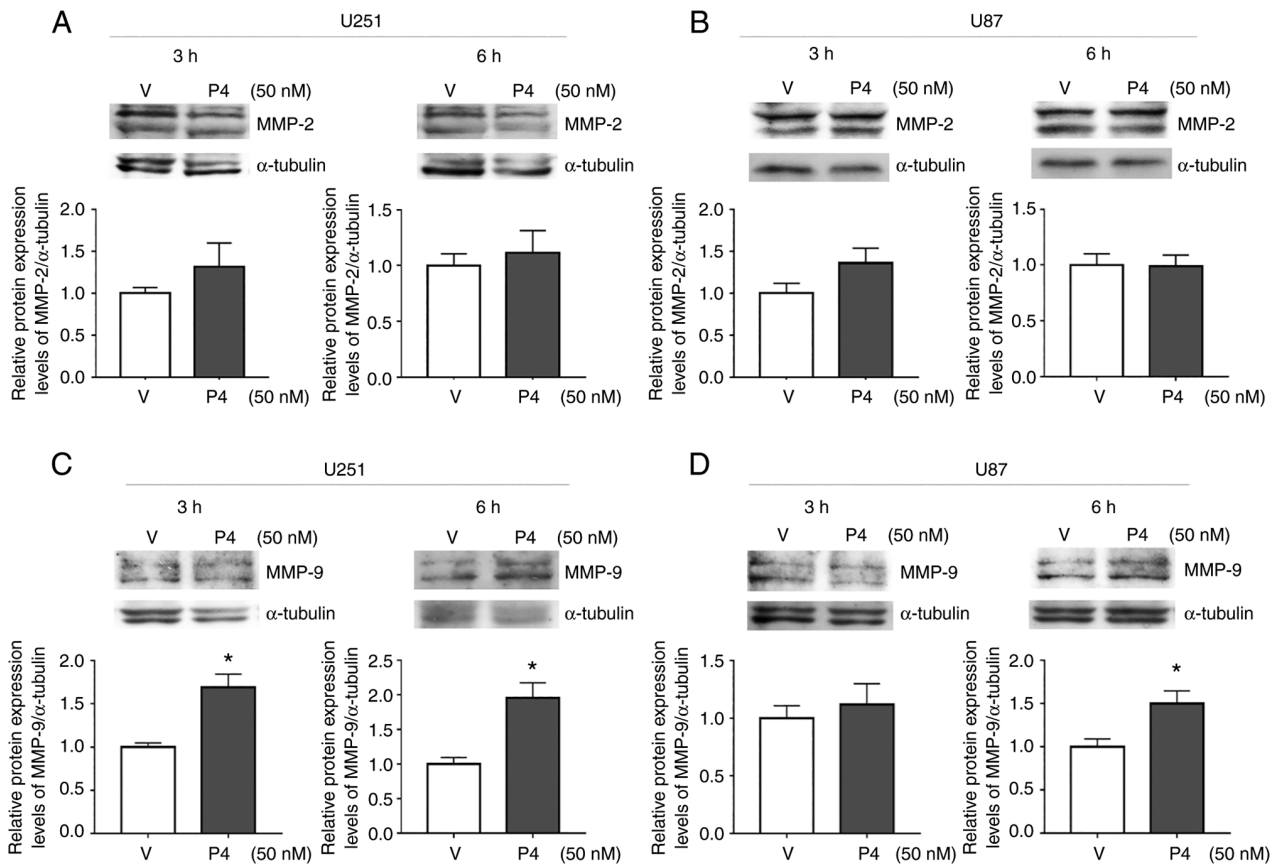


Figure 5. The effect of P4 on MMP-2 and MMP-9 protein expression levels in human glioblastoma-derived cell lines. U251 and U87 cells were treated with P4 (50 nM) or V (0.001% DMSO) for 3 and 6 h. The upper panels show the representative western blots for MMP-2 (proenzyme, 72 kDa; active enzyme, 64 kDa) in (A) U251 and (B) U87 cells, and for MMP-9 (proenzyme, 92 kDa; active enzyme, 84 kDa) in (C) U251 and (D) U87 cells. α -tubulin (55 kDa) was used as the loading control. The lower panels show the densitometric analysis. Data were normalized with respect to V and are presented as the mean \pm SEM; n=4. *P<0.05. MMP, metalloproteinase; P4, progesterone; V, vehicle.

The previous study by Piña Medina *et al* (16), from our laboratory, reported that PR was partially implicated in the induction of migration and invasion processes in glioblastoma cells, which suggested alternative activation of other regulatory mechanisms mediated by P4 or its metabolites. In that study, when P4 were added to cells treated with antisense oligonucleotides against PR expression, the P4-induced effect was partially reduced. Recently, Bello-Alvarez *et al* (15) reported that, in glioblastoma cells, P4 promoted PR-cSrc interaction, which led to cSrc autophosphorylation and subsequent Fak activation and migration.

Notably, 3 α -THP possesses different mechanisms of action than those reported for P4. One of the main differences between these progestins is that 3 α -THP lacks affinity for the classical PR (36). This metabolite induces rapid cellular changes by activating membrane PR (mPR) δ and mPR α (37,38). At the genomic level, 3 α -THP activates the pregnane X receptor, which is a transcription factor (39,40). The progestin 3 α -THP also modulates the action of neurotransmitters due to its interaction with their receptors, such as the ionotropic channel receptor, GABA $_A$ R (41). It has recently been reported that 3 α -THP promotes the migration of glioblastoma cells independently of the oxidation of other P4 metabolites with high binding affinity from the PR. In addition, the activation of cSrc kinase by 3 α -THP has been reported (18,42). Melfi *et al* (19) reported that, in rat Schwann cells, induced cell migration was dependent on cSrc activation. An additional study reported

that 3 α -THP promoted cSrc activation at the ventromedial hypothalamus, although the mechanism involved in this activation has not been fully elucidated (43). In the present study, an increase in glioblastoma cell migration induced by P4 is reported. This effect was completely blocked with the addition of the cSrc kinase family inhibitor, PP2, in U251 cells and partially blocked in U87 cells. Glioblastomas are among the tumors with the greatest intra- and inter-tumor heterogeneity (44,45). Therefore, it can be assumed that the established cell lines derived from these tumors have significant differences in their genetic signature. The U87 cell line has a neuronal-like phenotype with a high proliferative capacity, while the U251 cell line has a mesenchymal-like phenotype with a lower proliferative activity (46). The results in the present study demonstrated a difference in the migration rate of both cell lines, which may be related to the aforementioned differences. Considering that, despite the differences in migration rate, the results showed the same trend in both cell lines, it can be hypothesized that the effects of P4, in general, not cell line-dependent but pathology-dependent.

Regarding 3 α -THP, in the present study, an increase in cell migration partially blocked by PP2 in U251 and U87 cells was demonstrated. Considering that PP2 is not a specific inhibitor of cSrc, but of the entire Src family, this result suggested that, in addition to cSrc, other members of the Src kinase family may interact with P4 or 3 α -THP effectors. For example, the

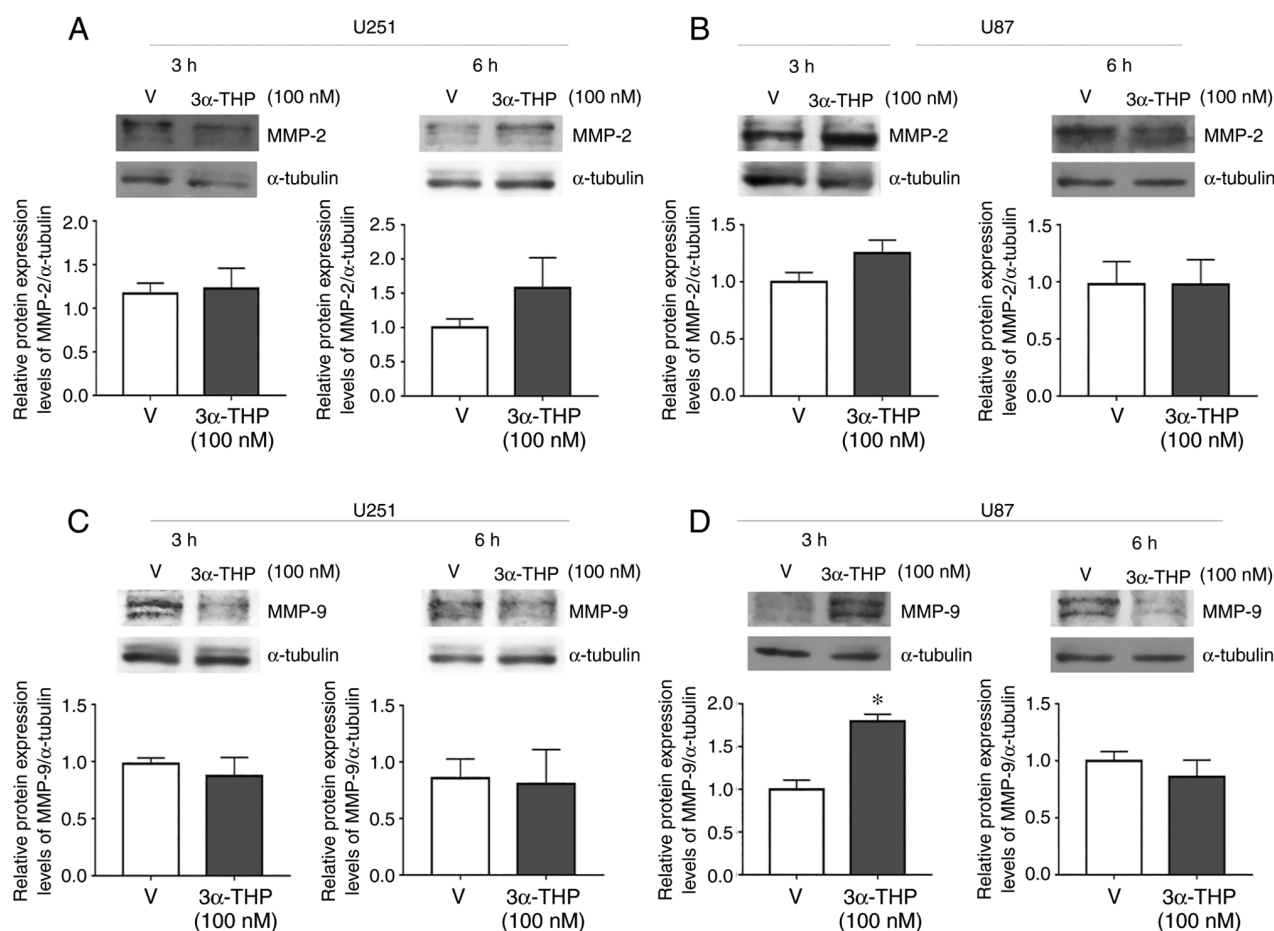


Figure 6. The effect of 3 α -THP on MMP-2 and MMP-9 protein expression levels in human glioblastoma-derived cell lines. U251 and U87 cells were treated with 3 α -THP (100 nM) or V (0.01% ethanol) for 3 and 6 h. The upper panels show the representative western blots for MMP-2 (proenzyme, 72 kDa; active enzyme, 64 kDa) in (A) U251 and (B) U87 cells, and for MMP-9 (proenzyme, 92 kDa; active enzyme, 84 kDa) in (C) U251 and (D) U87 cells. α -tubulin (55 kDa) was used as the loading control. The lower panels show the densitometric analysis. Data were normalized with respect to V and are presented as the mean \pm SEM; n=4. *P<0.05. MMP, metalloproteinase; V, vehicle; 3 α -THP, allopregnanolone.

high expression of Lyn, a member of cSrc kinase family, has been reported in glioblastoma cells and is linked to increased tumor progression (47).

The invasiveness of glioblastoma cells depends on the dynamic activation of at least two essential processes: Cell migration and ECM degradation. Until recently, no information on the role of cSrc in the regulation of proteins directly involved in ECM degradation in glioblastoma cells treated with P4 or any of its metabolites was available. In the present study, the effect of P4 and 3 α -THP on the expression of MMP-2 and MMP-9 was evaluated. The results demonstrated that in P4-treated cells, the protein expression level of MMP-9 was increased in U251 and U87 cells, and in 3 α -THP-treated cells, the protein expression level of MMP-9 was increased in U87 cells. These results indicated that increased MMP-9 expression may be one of the mechanisms implicated in P4- and 3 α -THP-induced invasion of glioblastoma cells. MMP-2 upregulation is also associated with poor prognosis and progression of glioblastoma (48). Notably, no significant changes in MMP-2 expression were demonstrated with P4 and 3 α -THP treatments. In fibroblast cells, the increase in the protein expression levels of MMP-9 but not MMP-2 were reported to be dependent on the activation of the cSrc-Fak signaling pathway (49). In MCF-7 breast cancer cells, cSrc and Fak activity inhibition blocked MMP-9 secretion (4). A recent

article reported the anti-inflammatory property of quercetin that, through the inhibition of TNF- α , decreased MMP-9 expression and activity in the gastric mucosa epithelial GES-1 cell line. This study also reported that the addition of PP1 (a Src family kinase inhibitor) decreased the activity of MMP-9 but not MMP-2 (50). The occurrence of this phenomenon in cells of different lineages suggests that it is independent of cellular context and that it is regulated by highly conserved molecular mechanisms.

Interactions between cSrc and Fak have been widely reported. It is known that cSrc phosphorylates residues Y576 and Y577 of Fak, which are indispensable for full activation of the latter (51,52). Sex steroid receptors are primarily known for their function as transcription factors. However, PR and the androgen receptor are also known to function in the activation of signaling cascades in the cytoplasm through the interaction of their polyproline motifs with the SH3 domains of cytoplasmic molecules, such as cSrc (53). In a recent publication by Bello-Alvarez *et al* (15), it was demonstrated that P4 activates cSrc kinase through the PR, for the first time in glioblastoma-derived cells. This, in turn, induces the phosphorylation of Fak at residues Y397, Y576 and Y577, which provided evidence of the non-genomic function of the PR in this brain tumor.

In the present study to assess the role of cSrc in the regulation of MMP-9 expression by P4 and 3 α -THP, an siRNA against

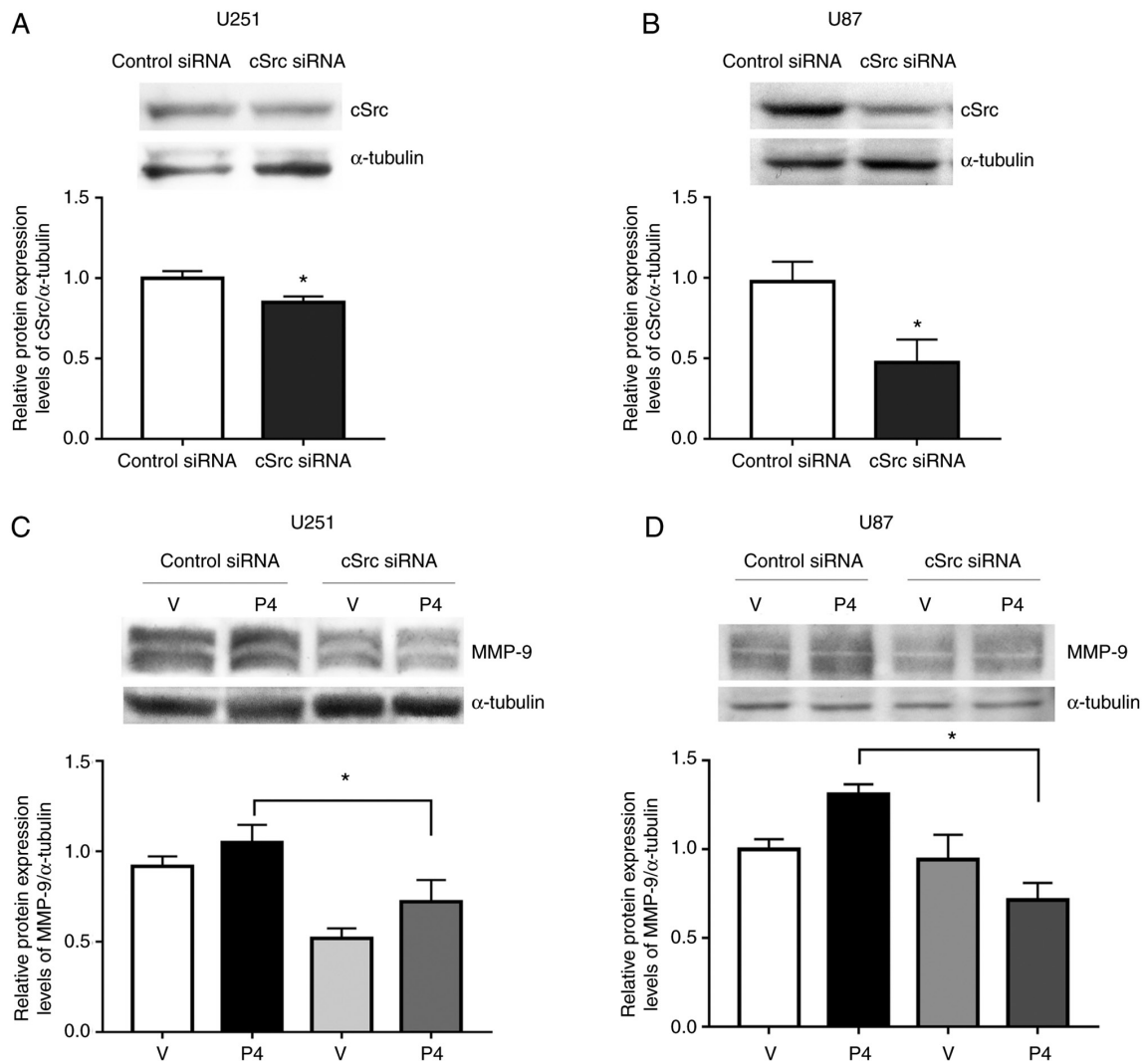


Figure 7. cSrc is involved in the regulation of MMP-9 expression by P4 in glioblastoma cells. (A) U251 and (B) U87 cells were transfected with cSrc siRNA and control siRNA. Transfected cells were treated with (C) P4 (50 nM) or (D) V (0.001% DMSO) for 6 h. The upper panels show the representative western blots for cSrc (60 kDa), MMP-9 (proenzyme, 92 kDa; active enzyme, 84 kDa) and α -tubulin (55 kDa; loading control). The lower panels show the densitometric analysis. Data were normalized with respect to V and are presented as the mean \pm SEM; n=4. *P<0.05. MMP, metalloproteinase; P4, progesterone; siRNA, small interfering RNA; V, vehicle.

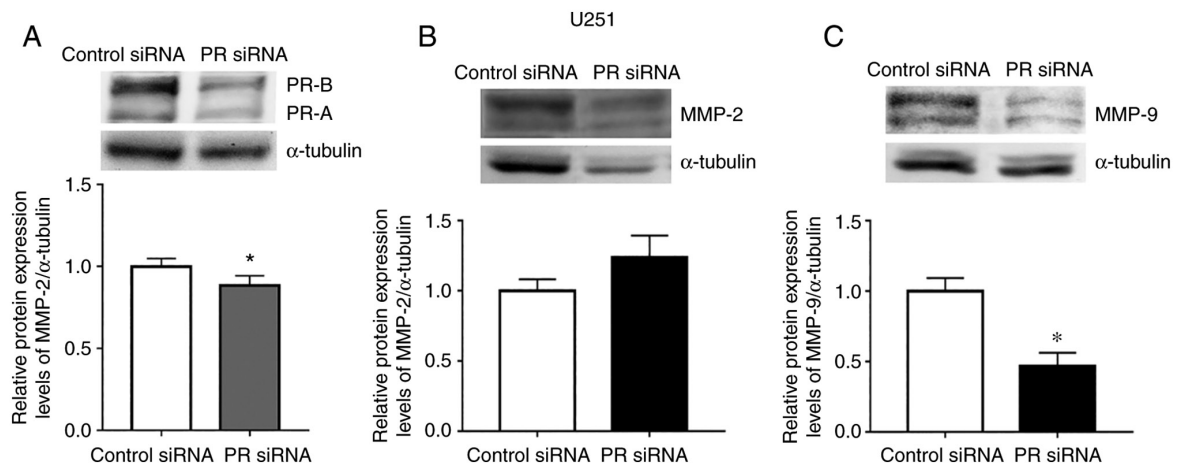


Figure 8. PR silencing reduces the protein expression levels of MMP-9 but not MMP-2. (A) U251 cells were transfected with a PR siRNA and a control siRNA (100 nM). (B) MMP-2 and (C) MMP-9 protein expression levels were determined in cells transfected with PR siRNA at 6 h. The upper panels show the representative western blots for PR (PR-B 110 kDa, 90 PR-A kDa), MMP-2 (proenzyme, 72 kDa; active enzyme, 64 kDa), MMP-9 (proenzyme, 92 kDa; active enzyme, 84 kDa), and α -tubulin (55 kDa, loading control). The lower panels show the densitometric analysis. Data were normalized with respect to control siRNA and are presented as the mean \pm SEM; n=3. *P<0.05. MMP, metalloproteinase; P4, progesterone; PR, progesterone receptor; siRNA, small interfering RNA; V, vehicle.

cSrc expression was used. The silencing of cSrc blocked the increase in MMP-9 protein expression levels induced by P4 in U251 and U87 cells. Only a partial effect was demonstrated in U251 cells, possibly due to lower efficiency of the silencing. These results indicated that cSrc mediates P4-induced MMP-9 expression and suggest that, in the context of glioblastoma cells, P4 treatment activates the cSrc-Fak signaling pathway, which modifies the expression of MMP-9 but not that of MMP-2.

Notably, Liu *et al* (54) reported that the PR^{-/-} condition in zebrafish follicular cells decreased the expression of MMP-9 but not MMP-2. In the present study, transfection with an siRNA against the PR decreased MMP-9 but not MMP-2 protein expression levels, which suggested that the difference in the effect of P4 on the regulation of MMP-9 and MMP-2 also involved the PR. However, another study reported that, in a rat model of blood-brain barrier breakdown, P4 and 3 α -THP downregulated the expression of MMP-9 and MMP-2 (55); this could be related to differences in the progesterone concentration. At the level of transcriptional regulation, these differences could be related to the composition of the MMP-2 and MMP-9 promoters (56).

In the present study, PP2 was used to evaluate the effect of the cSrc family of kinases on P4-induced invasion in human glioblastoma-derived cells. The results of the present study demonstrated that inhibition of cSrc activity decreased invasiveness in both U251 and U87 cell lines, as measured using a Matrigel Boyden chamber assay. A similar effect of 3 α -THP has also been recently reported by our laboratory (18).

In conclusion, the results of the present study suggest that the effect of P4 and 3 α -THP on the invasion of human glioblastoma-derived cells involves the activation of cSrc and its regulatory role in MMP-9 expression. Experimentation on cell lines is an important limitation of this study since it implies a study model that is far from reality. However, the results obtained broaden the knowledge for the future development of targeted therapies against migration and invasion processes in an underestimated area in the study of glioblastomas, namely, signaling through sex hormones and their receptors.

Acknowledgements

Not applicable.

Funding

The present study was supported by the Programa de Apoyo a Proyectos de Investigación e Innovación Tecnológica (PAPIIT; project no. PAPIIT IN217120), DGAPA-UNAM, México, and Programa de Apoyo a la Investigación y el Posgrado (PAIP) 5000-9107.

Availability of data and materials

The datasets used and/or analyzed during the current study are available from the corresponding author on reasonable request.

Authors' contributions

CBA, CJZS and ICA conceptualized the study. CBA, CJZS and KMPG performed the experiments. CBA and CJZS prepared the first draft of the manuscript and ICA contributed

to the revision and editing of the manuscript. ICA obtained the funding. CBA, CJZS, KMPG and ICA confirm the authenticity of all the raw data. All authors read and approved the final version of the manuscript.

Ethics approval and consent to participate

Not applicable.

Patient consent for publication

Not applicable.

Competing interests

The authors declare that they have no competing interests.

References

- Ostrom QT, Gittleman H, Truitt G, Boscia A, Kruchko C and Barnholtz-Sloan JS: CBTRUS statistical report: Primary brain and other central nervous system tumors diagnosed in the United States in 2011-2015. *Neuro Oncol* 20: iv1-iv86, 2018.
- Giese A, Bjerkvig R, Berens ME and Westphal M: Cost of migration: Invasion of malignant gliomas and implications for treatment. *J Clin Oncol* 21: 1624-1636, 2003.
- Patel A, Sabbini H, Clarke A and Somanath PR: Novel roles of Src in cancer cell epithelial-to-mesenchymal transition, vascular permeability, microinvasion and metastasis. *Life Sci* 157: 52-61, 2016.
- Cortes-Reynosa P, Robledo T, Macias-Silva M, Wu SV and Salazar EP: Src kinase regulates metalloproteinase-9 secretion induced by type IV collagen in MCF-7 human breast cancer cells. *Matrix Biol* 27: 220-231, 2008.
- Gautam J, Banskota S, Lee H, Lee YJ, Jeon YH, Kim JA and Jeong BS: Down-regulation of cathepsin S and matrix metalloproteinase-9 via Src, a non-receptor tyrosine kinase, suppresses triple-negative breast cancer growth and metastasis. *Exp Mol Med* 50: 1-14, 2018.
- Zhou W, Yu X, Sun S, Zhang X, Yang W, Zhang J, Zhang X and Jiang Z: Increased expression of MMP-2 and MMP-9 indicates poor prognosis in glioma recurrence. *Biomed Pharmacother* 118: 109369, 2019.
- Forsyth PA, Wong H, Laing TD, Rewcastle NB, Morris DG, Muzik H, Leco KJ, Johnston RN, Brasher PM, Sutherland G and Edwards DR: Gelatinase-A (MMP-2), gelatinase-B (MMP-9) and membrane type matrix metalloproteinase-1 (MT1-MMP) are involved in different aspects of the pathophysiology of malignant gliomas. *Br J Cancer* 79: 1828-1835, 1999.
- Kondraganti S, Mohanam S, Chintala SK, Kin Y, Jasti SL, Nirmala C, Lakka SS, Adachi Y, Kyritsis AP, Ali-Osman F, *et al*: Selective suppression of matrix metalloproteinase-9 in human glioblastoma cells by antisense gene transfer impairs glioblastoma cell invasion. *Cancer Res* 60: 6851-6855, 2000.
- Trabert B, Sherman ME, Kannan N and Stanczyk FZ: Progesterone and breast cancer. *Endocr Rev* 41: 320-344, 2020.
- Grindstad T, Richardsen E, Andersen S, Skjefstad K, Khanekhenari MR, Donnem T, Ness N, Nordby Y, Bremnes RM, Al-Saad S and Busund LT: Progesterone receptors in prostate cancer: Progesterone receptor B is the isoform associated with disease progression. *Sci Rep* 8: 1-11, 2018.
- Bello-Alvarez C and Camacho-Arroyo I: Impact of sex in the prevalence and progression of glioblastomas: The role of gonadal steroid hormones. *Biol Sex Differ* 12: 28, 2021.
- Fu XD, Goglia L, Sanchez AM, Flamini M, Giretti MS, Tosi V, Genazzani AR and Simoncini T: Progesterone receptor enhances breast cancer cell motility and invasion via extranuclear activation of focal adhesion kinase. *Endocr Relat Cancer* 17: 431-443, 2010.
- Grochans S, Cybulska AM, Simińska D, Korbecki J, Kojder K, Chlubek D and Baranowska-Bosiacka I: Epidemiology of glioblastoma multiforme-literature review. *Cancers (Basel)* 14: 2412, 2022.
- Germán-Castelán L, Manjarrez-Marmolejo J, González-Arenas A and Camacho-Arroyo I: Intracellular progesterone receptor mediates the increase in glioblastoma growth induced by progesterone in the rat brain. *Arch Med Res* 47: 419-426, 2016.

15. Bello-Alvarez C, Moral-Morales AD, González-Arenas A and Camacho-Arroyo I: Intracellular progesterone receptor and cSrc protein working together to regulate the activity of proteins involved in migration and invasion of human glioblastoma cells. *Front Endocrinol (Lausanne)* 12: 640298, 2021.
16. Piña-Medina AG, Hansberg-Pastor V, González-Arenas A, Cerbón M and Camacho-Arroyo I: Progesterone promotes cell migration, invasion and cofilin activation in human astrocytoma cells. *Steroids* 105: 19-25, 2016.
17. Zamora-Sánchez CJ, Hansberg-Pastor V, Salido-Guadarrama I, Rodríguez-Dorantes M and Camacho-Arroyo I: Allopregnanolone promotes proliferation and differential gene expression in human glioblastoma cells. *Steroids* 119: 36-42, 2017.
18. Zamora-Sánchez CJ, Bello-Alvarez C, Rodríguez-Dorantes M and Camacho-Arroyo I: Allopregnanolone promotes migration and invasion of human glioblastoma cells through the protein tyrosine kinase c-Src activation. *Int J Mol Sci* 23: 4996, 2022.
19. Melfi S, Guevara MM, Bonalume V, Ruscica M, Colciago A, Simoncini T and Magnaghi V: Src and phospho-FAK kinases are activated by allopregnanolone promoting Schwann cell motility, morphology and myelination. *J Neurochem* 141: 165-178, 2017.
20. Pirkmajer S and Chibalin AV: Serum starvation: Caveat emptor. *Am J Physiol Cell Physiol* 301: C272-C279, 2011.
21. Jabłońska-Trypuć A, Matejczyk M and Rosochacki S: Matrix metalloproteinases (MMPs), the main extracellular matrix (ECM) enzymes in collagen degradation, as a target for anti-cancer drugs. *J Enzyme Inhib Med Chem* 31: 177-183, 2016.
22. Global Cancer Observatory.
23. van Linde ME, Brahm CG, de Witt Hamer PC, Reijneveld JC, Bruynzeel AME, Vandertop WP, van de Ven PM, Wagemakers M, van der Weide HL, Enting RH, *et al*: Treatment outcome of patients with recurrent glioblastoma multiforme: A retrospective multicenter analysis. *J Neurooncol* 135: 183-192, 2017.
24. Gkretsi V and Stylianopoulos T: Cell adhesion and matrix stiffness: Coordinating cancer cell invasion and metastasis. *Front Oncol* 8: 145, 2018.
25. Quintero-Fabián S, Arreola R, Becerril-Villanueva E, Torres-Romero JC, Arana-Argáez V, Lara-Riegos J, Ramírez-Camacho MA and Alvarez-Sánchez ME: Role of matrix metalloproteinases in angiogenesis and cancer. *Front Oncol* 9: 1370, 2019.
26. Quesnel A, Karagiannis GS and Filippou PS: Extracellular proteolysis in glioblastoma progression and therapeutics. *Biochim Biophys Acta Rev Cancer* 1874: 188428, 2020.
27. Cai HP, Wang J, Xi SY, Ni XR, Chen YS, Yu YJ, Cen ZW, Yu ZH, Chen FR, Guo CC, *et al*: Tenascin-c mediated vasculogenic mimicry formation via regulation of MMP2/MMP9 in glioma. *Cell Death Dis* 10: 1-14, 2019.
28. Mirabdaly S, Komi DE, Shakiba Y, Moini A and Kiani A: Effects of temozolomide on U87MG glioblastoma cell expression of CXCR4, MMP2, MMP9, VEGF, anti-proliferatory cytotoxic and apoptotic properties. *Mol Biol Rep* 47: 1187-1197, 2020.
29. Chen CJ, Shang HS, Huang YL, Tien N, Chen YL, Hsu SY, Wu RSC, Tang CL, Lien JC, Lee MH, *et al*: Bisdemethoxycurcumin suppresses human brain glioblastoma multiforme GBM 8401 cell migration and invasion via affecting NF- κ B and MMP-2 and MMP-9 signaling pathway in vitro. *Environ Toxicol* 37: 2388-2397, 2022.
30. Li Q, Chen B, Cai J, Sun Y, Wang G, Li Y, Li R, Feng Y, Han B, Li J, *et al*: Comparative analysis of matrix metalloproteinase family members reveals that MMP9 predicts survival and response to temozolomide in patients with primary glioblastoma. *PLoS One* 11: e0151815, 2016.
31. González-Agüero G, Gutiérrez AA, González-Espinosa D, Solano JD, Morales R, González-Arenas A, Cabrera-Muñoz E and Camacho-Arroyo I: Progesterone effects on cell growth of U373 and D54 human astrocytoma cell lines. *Endocrine* 32: 129-135, 2007.
32. Hernández-Hernández OT, González-García TK and Camacho-Arroyo I: Progesterone receptor and SRC-1 participate in the regulation of VEGF, EGFR and cyclin D1 expression in human astrocytoma cell lines. *J Steroid Biochem Mol Biol* 132: 127-134, 2012.
33. González-Arenas A, Valadez-Cosmes P, Jiménez-Arellano C, López-Sánchez M and Camacho-Arroyo I: Progesterone-induced blocking factor is hormonally regulated in human astrocytoma cells, and increases their growth through the IL-4R/JAK1/STAT6 pathway. *J Steroid Biochem Mol Biol* 144: 463-470, 2014.
34. Strom JO, Theodorsson A and Theodorsson E: Hormesis and female sex hormones. *Pharmaceuticals (Basel)* 4: 726-740, 2011.
35. Atif F, Yousuf S and Stein DG: Anti-tumor effects of progesterone in human glioblastoma multiforme: Role of PI3K/Akt/mTOR signaling. *J Steroid Biochem Mol Biol* 146: 62-73, 2015.
36. Diviccaro S, Cioffi L, Falvo E, Giatti S and Melcangi RC: Allopregnanolone: An overview on its synthesis and effects. *J Neuroendocrinol* 34: e12996, 2022.
37. Thomas P and Pang Y: Membrane progesterone receptors: Evidence for neuroprotective, neurosteroid signaling and neuroendocrine functions in neuronal cells. *Neuroendocrinology* 96: 162-71, 2012.
38. Pang Y, Dong J and Thomas P: Characterization, neurosteroid binding and brain distribution of human membrane progesterone receptors δ and $\{\epsilon\}$ (mPR δ and mPR $\{\epsilon\}$) and mPR δ involvement in neurosteroid inhibition of apoptosis. *Endocrinology* 154: 283-295, 2013.
39. Lamba V, Yasuda K, Lamba JK, Assem M, Davila J, Strom S and Schuetz EG: PXR (NR1I2): Splice variants in human tissues, including brain, and identification of neurosteroids and nicotine as PXR activators. *Toxicol Appl Pharmacol* 199: 251-265, 2004.
40. Frye CA, Koonce CJ and Wolf AA: The pregnane xenobiotic receptor, a prominent liver factor, has actions in the midbrain for neurosteroid synthesis and behavioral/neural plasticity of female rats. *Front Syst Neurosci* 8: 60, 2014.
41. Belelli D and Gee KW: 5 α -pregnan-3 α ,20 α -diol behaves like a partial agonist in the modulation of GABA-stimulated chloride ion uptake by synaptosomes. *Eur J Pharmacol* 167: 173-176, 1989.
42. Zamora-Sánchez CJ, Hernández-Vega AM, Gaona-Domínguez S, Rodríguez-Dorantes M and Camacho-Arroyo I: 5 α -dihydroprogesterone promotes proliferation and migration of human glioblastoma cells. *Steroids* 163: 108708, 2020.
43. González-Flores O, Beyer C, Gómora-Arrati P, García-Juárez M, Lima-Hernández FJ, Soto-Sánchez A and Etgen AM: A role for Src kinase in progestin facilitation of estrous behavior in estradiol-primed female rats. *Horm Behav* 58: 223-229, 2010.
44. Bergmann N, Delbridge C, Gempt J, Feuchtinger A, Walch A, Schirmer L, Bunk W, Aschenbrenner T, Liesche-Starnecker F and Schlegel J: The intratumoral heterogeneity reflects the intertumoral subtypes of glioblastoma multiforme: A regional immunohistochemistry analysis. *Front Oncol* 10: 494, 2020.
45. Becker AP, Sells BE, Haque SJ and Chakravarti A: Tumor heterogeneity in glioblastomas: From light microscopy to molecular pathology. *Cancers (Basel)* 13: 1-25, 2021.
46. Motaln H, Koren A, Gruden K, Ramšak Ž, Schichor C and Lah TT: Heterogeneous glioblastoma cell cross-talk promotes phenotype alterations and enhanced drug resistance. *Oncotarget* 6: 40998-41017, 2015.
47. Stettner MR, Wang W, Nabors LB, Bharara S, Flynn DC, Grammer JR, Gillespie GY and Gladson CL: Lyn kinase activity is the predominant cellular Src kinase activity in glioblastoma tumor cells. *Cancer Res* 65: 5535-5543, 2005.
48. Ramachandran RK, Sørensen MD, Aaberg-Jessen C, Hermansen SK and Kristensen BW: Expression and prognostic impact of matrix metalloproteinase-2 (MMP-2) in astrocytomas. *PLoS One* 12: e0172234, 2017.
49. Hsia DA, Mitra SK, Hauck CR, Streblov DN, Nelson JA, Ilic D, Huang S, Li E, Nemerow GR, Leng J, *et al*: Differential regulation of cell motility and invasion by FAK. *J Cell Biol* 160: 753-767, 2003.
50. Hsieh HL, Yu MC, Cheng LC, Chu MY, Huang TH, Yeh TS and Tsai MM: Quercetin exerts anti-inflammatory effects via inhibiting tumor necrosis factor- α -induced matrix metalloproteinase-9 expression in normal human gastric epithelial cells. *World J Gastroenterol* 28: 1139-1158, 2022.
51. Yeatman TJ: A renaissance for SRC. *Nat Rev Cancer* 4: 470-480, 2004.
52. Mitra SK and Schlaepfer DD: Integrin-regulated FAK-Src signaling in normal and cancer cells. *Curr Opin Cell Biol* 18: 516-523, 2006.
53. Boonyaratankornkit V and Edwards DP: Receptor mechanisms mediating non-genomic actions of sex steroids. *Semin Reprod Med* 25: 139-153, 2007.
54. Liu DT, Carter NJ, Wu XJ, Hong WS, Chen SX and Zhu Y: Progesterin and nuclear progesterin receptor are essential for upregulation of metalloproteinase in zebrafish preovulatory follicles. *Front Endocrinol (Lausanne)* 9: 517, 2018.
55. Ishrat T, Sayeed I, Atif F, Hua F and Stein DG: Progesterone and allopregnanolone attenuate blood-brain barrier dysfunction following permanent focal ischemia by regulating the expression of matrix metalloproteinases. *Exp Neurol* 226: 183-190, 2010.
56. Yan C and Boyd DD: Regulation of matrix metalloproteinase gene expression. *J Cell Physiol* 211: 19-26, 2007.



15.3 Otras publicaciones



ELSEVIER



BIOMEDICAL

Tibolone Effects on Human Glioblastoma Cell Lines

Aliesha González-Arenas,^a Marisol De la Fuente-Granada,^a Ignacio Camacho-Arroyo,^b
Carmen J. Zamora-Sánchez,^b Ana Gabriela Piña-Medina,^c Julia Segura-Uribe,^d and
Christian Guerra-Araiza^e

^aDepartamento de Medicina Genómica y Toxicología Ambiental, Instituto de Investigaciones Biomédicas, Universidad Nacional Autónoma de México, Ciudad Universitaria, Ciudad de México, México

^bUnidad de Investigación en Reproducción Humana, Instituto Nacional de Perinatología-Facultad de Química, Universidad Nacional Autónoma de México, Ciudad de México, México

^cFacultad de Química, Departamento de Biología, Universidad Nacional Autónoma de México, Ciudad de México, México

^dUnidad de Investigación Médica en Enfermedades Neurológicas, Centro Médico Nacional Siglo XXI, Instituto Mexicano del Seguro Social, Ciudad de México, México

^eUnidad de Investigación Médica en Farmacología, Hospital de Especialidades, Centro Médico Nacional Siglo XXI, Instituto Mexicano del Seguro Social, Ciudad de México, México

Received for publication August 27, 2018; accepted August 5, 2019 (ARCMED_2019_310).

Background. Ovarian steroid hormones are involved in modulating the growth of glioblastomas (the most common, aggressive, and lethal brain tumor) through the interaction with their intracellular receptors. Activation of sex hormone receptors is involved in glioblastomas progression. Tibolone (TIB) is a selective tissue estrogenic activity regulator widely prescribed to treat menopausal symptoms and to prevent bone loss. The effects of TIB on the growth of glioblastoma are unknown.

Aim of the study. To evaluate the effects of TIB on cell number, migration, and invasion of two derived human glioblastoma cell lines (U251 MG and U87), as well as the role of this steroid in estrogen and progesterone receptors activity and content.

Methods. U251-MG and U87 human glioblastoma cell lines were grown with different doses of TIB. The number of cells was determined and migration and invasion tests were carried out. Protein expression was performed by Western blot.

Results. We observed that TIB (10 nM) increased the number of cells by inducing proliferation with no effects on cell migration or invasion. The increase in cell proliferation induced by TIB was blocked by estrogen (ERs) or progesterone receptor (PRs) antagonists, ICI 162,780 and RU 486, suggesting that these receptors mediate proliferating actions of TIB; TIB also modified the content of ERs and PRs by increasing ER- α , ER- β , and PR-B, while decreased PR-A.

Conclusion. Our results suggest that TIB increases cell number and proliferation of human glioblastoma cells through the regulation of ERs and PRs actions and content. © 2019 IMSS. Published by Elsevier Inc.

Key Words: Tibolone, Human glioblastoma, Estrogen receptor, Progesterone receptor, U251-MG cells, U87 cells.

Address reprint requests to: Christian Guerra-Araiza, Unidad de Investigación Médica en Farmacología, Hospital de Especialidades, Centro Médico Nacional Siglo XXI, Instituto Mexicano del Seguro Social, Av.

Cuauhtémoc 330, Colonia Doctores, Delegación Cuauhtémoc, 06720 Ciudad de México, Mexico; Phone: +52 55 5627-6900 ext. 21367; E-mail: christianguerre2001@gmail.com

Introduction

Glioblastomas (GBM) are a kind of astrocytoma and represent the most common and aggressive primary intracerebral tumors that are derived from astrocytes, glial progenitor cells or cancer stem cells (1–5). Chemotherapy, radiotherapy, as well as neurosurgery, are currently used in the treatment of glioblastomas, obtaining very poor results in the survival and quality of life of patients, which have a mean survival of 15 months (6–8).

Several studies indicate that sex steroid hormones, progesterone (P4), estradiol (E2) and dihydrotestosterone (DHT), are involved in the regulation of several physiological and pathological processes in the brain including tumor cell growth (9–13). These hormones exert many effects through the interaction with their intracellular receptors (PR, ER, and AR, respectively) which are ligand-activated transcription factors (14,15). After binding to their ligands, steroid receptors enter cell nucleus to interact with sequences called hormone response elements in the promoter regions of target genes to initiate their transcription. ER is synthesized as two protein subtypes, ER α and ER β (14,15), while PR and AR are each expressed as two isoforms (A and B) with different functions (16,17).

It has been shown that 2-hydroxyestradiol treatment increased cell proliferation of U373 MG astrocytoma cell line and that the treatment with PPT (ER α agonist) but not DPN (ER β agonist) increased the number of U373 cells (18) PR isoforms have been detected in several cell lines and biopsies derived from human astrocytomas (19–23). In astrocytoma cell lines (U373 and D54), P4 increased proliferation, migration, and invasion through its intracellular receptor (11,22). Interestingly, a direct relation between the content of PR and the tumor grade has been reported (23). Moreover, the administration of the PR antagonist, RU486, or antisense oligonucleotides against PR blocks P4 effects in *in vivo* experiments in U373 cells implanted in the motor cerebral cortex of the rat. In these studies, the P4 administration significantly increased both the area and the infiltration length of the tumor (24,25). It has also been reported that RU486 improves the efficacy of chemoradiotherapy in glioblastoma xenografts in mice (26). As in the case of PR, AR expression is increased in tumor tissue of astrocytoma patients according to the progressing WHO grades. 5 α -DHT significantly blocked the inhibitory effect of TGF β 1 on GBM growth (27). Moreover, AR antagonist inhibited proliferation *in vitro* and *in vivo* of U87 cells derived from glioblastoma (28), and gene silencing and pharmacological inhibition of this receptor induced GBM cell death *in vivo* and *in vitro* (28,29).

Tibolone (TIB) is a selective tissue estrogenic activity regulator that is widely prescribed to treat menopausal symptoms and to prevent bone loss (30). TIB is metabolized into three biologically active metabolites, the 3- α -hydroxyestrogenic metabolite, the 3- β -hydroxyestrogenic metabolite,

and the Δ 4-keto isomer. The 3-hydroxy-metabolites bind ERs while the Δ 4-isomer shows an affinity for PRs and AR (31). Previous reports have indicated that the 3 α - and 3 β -hydroxy-TIB are the predominant free metabolites in the brain of ovariectomized (OVX) cynomolgus monkeys (32). A randomized, placebo-controlled, double-blind trial demonstrated that TIB increased breast cancer recurrence (33) and a literature review points out that this synthetic hormone increases the risk of endometrial cancer, even when the treatment lasts less than 5 years (34,35). These data suggest that TIB participates in tumor progression processes; however, the participation of TIB in the progression of glioblastomas is unknown. In this work, we studied the effects of TIB on cell number, migration, and invasion, as well as on the content of ERs, PRs, and ARs in cell lines derived from human glioblastomas.

Experimental

Cell Cultures

U251-MG and U87 human glioblastoma cell lines were used. Cells were grown in 10 cm dishes and maintained in Dulbecco's modification of Eagle's medium (DMEM), supplemented with 10% fetal bovine serum (FBS), 1 mmol pyruvate, 2 mmol glutamine, 0.1 mmol nonessential amino acids (GIBCO, NY) at 37°C under a 95% air, 5% CO₂ atmosphere.

Cell Number and Treatments

Cells were grown on 48 well plates (5 × 10³ cells) and maintained as indicated in the Cell cultures section. Twenty-four hours before treatments, medium was changed by DMEM phenol red free medium supplemented with 10% FBS without steroid hormones (Hyclone, UT, USA), 1 mmol pyruvate, 2 mmol glutamine, 0.1 mmol nonessential amino acids (GIBCO, NY, USA) at 37°C under a 95% air, 5% CO₂ atmosphere. The following treatments were applied on day 0: (1) vehicle (0.02% cyclodextrin in sterile water); (2) TIB (10 nM); (3) TIB (100 nM); (4) TIB (1 μ M); (5) TIB (10 μ M); (6) RU 486 (1 μ M, RU); (7) TIB (10 nM) +RU; (8) ICI 182, 780 (2 μ M, ICI); and (9) TIB (10 nM) +ICI. Each experiment was performed in four independent cultures. Cyclodextrin and TIB were purchased from Sigma-Aldrich, MO, USA. Cells were harvested from incubation every day during six consecutive days with PBS 1X + EDTA (1 mmol). The number of living cells, evaluated by a blind observer, was measured by trypan blue dye exclusion using an inverted microscope (Olympus CKX41, PA, USA).

BrdU Incorporation Assay

5-Bromo-2'-deoxyuridine (BrdU) incorporation kit (11296736001 Roche, IN, USA) was used according to the manufacturer's recommendations to determine U251 MG cell line proliferation. Cells cultured in four-well glass slides were treated for 24 h and afterward cell culture medium was replaced by the BrdU labeling medium for

45 min. After cell fixation, BrdU incorporation was detected by immunofluorescence using a monoclonal antibody against it and a fluorochrome-conjugated secondary antibody. Additionally, nuclei were stained with Hoechst 33342 solution (1 $\mu\text{g}/\text{mL}$). Cell nuclei stained with Hoechst, and positive BrdU cells were visualized in an Olympus Bx43 F microscope (Olympus, PA, USA). Cell counting was done with the ImageJ software 1.45S (National Institutes of Health, USA).

Migration Assay

To evaluate whether TIB induces migration, we used the scratch-wound assay. Cells (300,000) were seeded with DMEM medium in six-well plates when the 70% of confluence was reached, the medium was changed for phenol red free DMEM medium supplemented with 10% FBS without hormones. After 24 h, the culture reached approximately 90% of confluence, and the formation of a uniform monolayer was observed. With a 200 μL pipet tip, two parallel scratches by well were made. The detached cells were washed by aspiration. Cells were incubated with phenol red-free DMEM medium with DNA synthesis inhibitor cytosine β -D-arabino-furanoside hydrochloride (10 μM , AraC; Sigma-Aldrich, MO, USA). One hour later, TIB (10 nM) was added, and images of the scratch area were taken with an AxioCam (Carl Zeiss, GER) attached to an inverted microscope Axio Vert A1 (Carl Zeiss, GER) at 100X magnification at 0, 12 and 24 h. The number of migrating cells in the scratch areas was counted from four random fields using the ImageJ software (National Institute of Health, WA, USA).

Invasion Assay

Invasion experiments were performed as described by Piña-Medina V, et al. (22). Briefly, Transwell chambers (Corning, NY) were covered with 2 mg/mL of Matrigel supplemented with the DNA synthesis inhibitor AraC (Sigma Aldrich, St. Louis, MO) and left at room temperature for gelation. U251 MG and U87 cells (300,000) were suspended in 1.5 mL serum-free medium and treatments were added to the upper chambers. The lower chambers were filled with 2 mL DMEM with 10% FBS. The chambers were incubated at 37°C, 5% CO₂ for 24 h. After incubation, the Matrigel with the non-invading cells was removed from the upper surface of the transwell membrane. The invading cells were fixed in 4% paraformaldehyde for 20 min and stained with 0.1% crystal violet for 20 min. The inserts were observed under an inverted microscope (Olympus CKX41) and the images of five randomly selected fields were captured with an Infinity1-2C camera at 20X magnification.

Western Blot

U251 MG cells (2×10^6 cells) were grown in 10 cm dishes and maintained as described in the Cell cultures section.

Twenty-four hours before treatments, the medium was changed by DMEM phenol red free medium at 37°C under a 95% air, 5% CO₂ atmosphere. Vehicle (cyclodextrin 0.02%) and TIB (10 nM) were applied for 24 h. Each experiment was performed in four independent cultures. After the treatments, cells were homogenized in 500 μL of RIPA lysis buffer with protease inhibitors (1 mM EDTA, 2 $\mu\text{g}/\text{mL}$ leupeptin, 2 $\mu\text{g}/\text{mL}$ aprotinin, 1 mM PMSF). Proteins were obtained by centrifugation at 20,000 \times g, at 4°C for 15 min, and quantified by the method of Bradford (Bio-Rad Laboratories, TX, USA). Proteins (70 μg) were separated by electrophoresis on 8% SDS-PAGE at 20 mA. Colored markers (Bio Rad, CA, USA) were included for size determination. Gels were transferred to nitrocellulose membranes (Amersham, NJ, USA) for 2 h at 60 mA to detect ER α , ER β , ARs, epidermal growth factor receptor (EGFR), insulin-like growth factor receptor (IGFR) and vascular endothelial growth factor (VEGF); the transfer for PRs detection was done for 7 h at 30 mA, at room temperature in semi-dry conditions. Membranes were blocked at room temperature with 3% nonfat dry milk and 1% bovine serum albumin for 2 h. Membranes were then incubated with 0.8 $\mu\text{g}/\text{mL}$ of antibodies against ER α (Santa Cruz sc-8002, TX, USA), ER β (Santa Cruz sc-, TX, USA), EGFR (Santa Cruz sc-003), VEGF (Santa Cruz sc-152), IGFR (Santa Cruz sc-81464, TX, USA), 3 $\mu\text{g}/\text{mL}$ of mouse anti-PR monoclonal antibody (ab58565, Abcam, Cambridge, ENG), 4 $\mu\text{g}/\text{mL}$ of mouse anti-AR monoclonal antibody (Santa Cruz sc-815, TX, USA), both recognize PR and AR isoforms, respectively, at 4°C overnight. Blots were then incubated with 400 $\mu\text{g}/\text{mL}$ of secondary antibody conjugated to horseradish peroxidase (Santa Cruz Biotechnology, TX, USA) for 45 min.

To correct for differences in the amount of total protein loaded in each lane, ER α , ER β , PRs, ARs, VEGF, EGFR, and IGFR content was normalized to that of α -tubulin. Blots were stripped with glycine (0.1 M, pH 2.5, 0.5% SDS) at 4°C overnight and at room temperature for 30 min, and reprobed with 0.2 $\mu\text{g}/\text{mL}$ of mouse anti- α -tubulin monoclonal antibody (sc-5286, Santa Cruz Biotechnology, TX, USA) at 4°C overnight. Blots were incubated with a 1:3000 dilution of goat anti-mouse IgG conjugated to horseradish peroxidase (Santa Cruz Biotechnology, TX, USA) at room temperature for 1 h. Enhanced chemiluminescence (ECL) signals were detected exposing membranes to Kodak Biomax Light Film (Sigma-Aldrich, MO, USA) using Supersignal West Femto as peroxidase substrate (Thermo Scientific, MA, USA). The antigen-antibody complex was detected as the area under a peak corresponding to a band density (the area is given in inches with a default scale of 72 pixels/inch) in a semiquantitative way using HP Scanjet G3110 apparatus (Hewlett-Packard Company, CA, USA) and the Image J 1.45S software (National Institutes of Health, USA). In order to minimize inter-assay variations, all Western blots were carried out in parallel.

Statistical Analysis

All data were analyzed and plotted using the GraphPad Prism 5.0 software for Windows XP (GraphPad Software, CA, USA). Statistical analysis between comparable groups was performed using a one-way ANOVA with a Bonferroni post-test. For invasion and western blot assays a t-student test was applied. A value of $p < 0.05$ was considered statistically significant.

Results

Effects of TIB on the Cell Number of Human Glioblastoma Cell Lines

To study the effects of TIB on cell number of U251-MG and U87 human glioblastoma cell lines, we performed a time-course study over a period of six days by using different concentrations of TIB (10 nM, 100 nM, 1 mmol, 10 mmol). In U251-MG and U87 cells, all TIB treatments increased the number of cells on the fifth and sixth day of culture (Figure 1).

Effect of ERs and PRs Inhibition on Glioblastoma Cell Proliferation Increase Induced by TIB

TIB and its metabolites have affinity for ERs and PRs (31). To study the role of ERs and PRs in cell proliferation induced by TIB (10 nM), we carried out a time-course study to count glioblastoma cells for six days and a BrdU incorporation assay with TIB. In U251-MG, TIB treatment increased the number of proliferating cells from the fourth to the sixth day of culture (Figure 2A). This increase was blocked by RU 486 (PRs antagonist) and ICI 182, 780 (ERs antagonist) applied 30 min before TIB treatment (Figure 2A). Interestingly, in BrdU assays, ICI 182, 780 treatment without TIB diminished cell proliferation under the vehicle value (Figures 2B and 2C).

Effects of TIB on Migration and Invasion of Glioblastoma Cell Lines

To assess whether treatment with TIB (10 nM, 24 h) modify the migration (Figure 3) and invasiveness (Figure 4) of U251 and U87 cells, we performed the scratch-wound and transwell assays. It was observed that there was a significant increase in the number of U251 cells in the scratch area of cells treated with TIB with respect to the vehicle, however, when cells were further treated with the inhibitor of DNA replication AraC, no significant differences in the number of migrating cells in the scratch area were observed. In U87 cells no differences were observed between TIB treatment and vehicle with or without AraC. These results demonstrate that TIB treatment increases cell number but has no effect on the motility of the U251 and U87 cells (Figure 3). Besides cell migration, we also evaluated cell invasion after TIB treatment, our results show that TIB did not modify the invading capabilities of both cell lines in comparison with vehicle (Figure 4).

TIB Specific Effect on the Content of Sex Steroid Hormone Receptors and Growth Factors Receptors in U251-MG Cell Line

To determine the effect of TIB on the content of PRs, and ERs, we performed Western blotting of total protein extracted from U251-MG cells after 24 h of treatment with 10 nM of TIB. We observed that in U251-MG cells, TIB treatment increased PR-B content meanwhile decreased PR-A (Figure 5A). ER α and ER β content increased after TIB treatment (Figures 5B and 5C). To evaluate whether TIB could regulate other proteins involved in glioblastoma progression such as androgen receptor (AR), VEGF, EGFR and IGFR-1, the content of these proteins was evaluated; we found that treatment with this steroid did not modify the content of these proteins (Supplementary Figure 1).

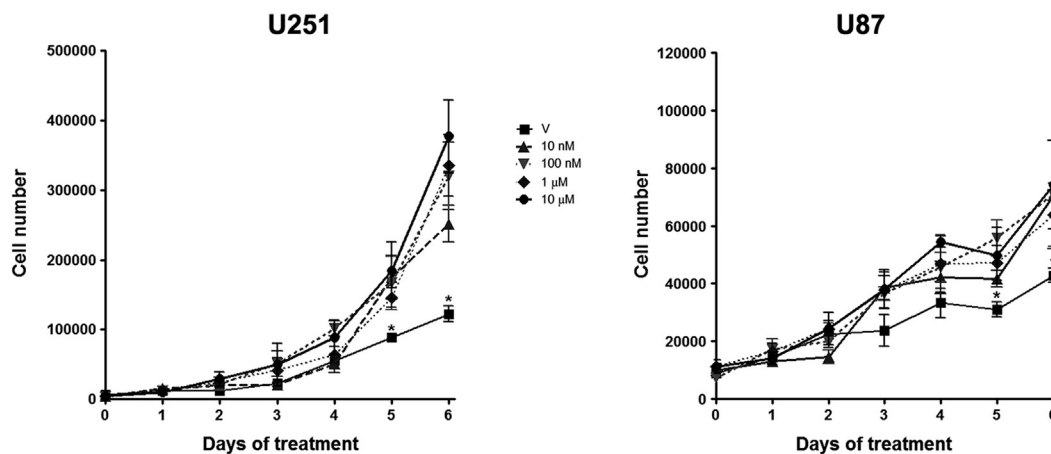


Figure 1. Effects of TIB on the number of human glioblastoma cells. U251-MG and U87 cell lines were treated with: (1) vehicle (V) (0.02% cyclodextrin in sterile water) (2) TIB (100 nM); (3) TIB (1 mmol); (4) TIB (10 mmol) and (5) TIB (10 nM) for six days. Every day cells were harvested, and the number of cells was determined by trypan blue dye exclusion using an inverted microscope. Data are mean \pm S.E.M. $n = 4$; * $p < 0.05$ vs. all TIB concentrations.

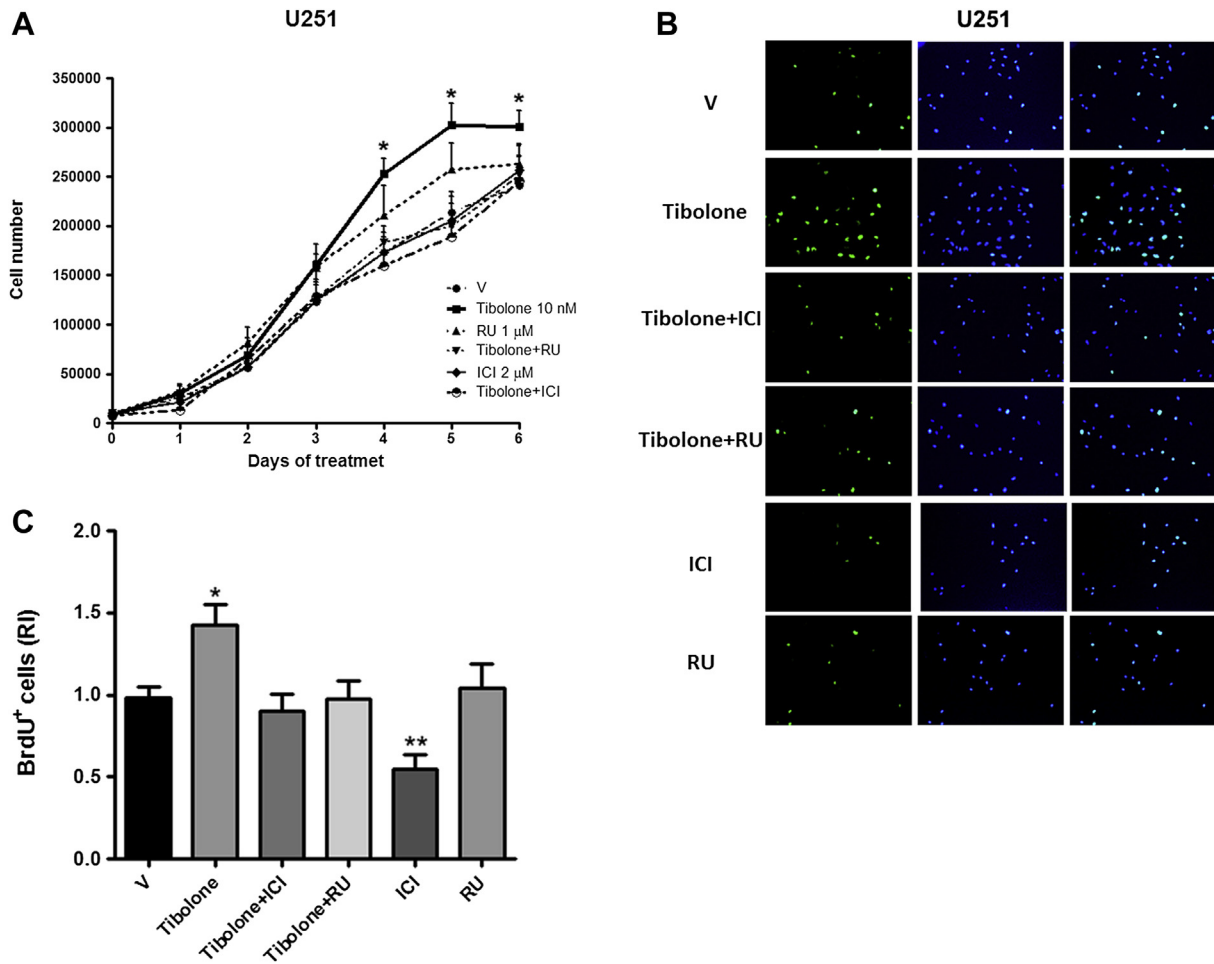


Figure 2. Effect of ERs and PRs inhibition on glioblastoma cell proliferation increase induced by TIB. (A) U251-MG with: (1) vehicle (V) (0.02% cyclodextrin in sterile water); (2) TIB (10 nM); (3) RU 486 (1 mmol, RU); (4) TIB + RU (5) ICI 182, 780 (2 mmol, ICI); and (6) TIB + ICI during 6 days. Every day cells were harvested, and cell number was determined by trypan blue dye exclusion using an inverted microscope. Data are mean \pm S.E.M. $n = 4$; * $p < 0.05$ vs. all treatments. (B,C) U251-MG were treated with V or TIB; Cell incorporating BrdU were determined as a percentage of the total number of cells stained with the nuclei dye Hoechst. Values were normalized to V = 1. Histograms represent the mean \pm SEM of the relative increase (RI) compared to V, $n = 4$. * $p < 0.05$ vs. all groups except RU; ** $p < 0.05$ vs. all groups.

Discussion

In the present study, we examined the effect of TIB on cell number, proliferation, migration, and invasion of the human glioblastoma cell lines: U251-MG and U87, as well as on the activation and content of sex steroid hormone receptors and other proteins involved in cancer progression. The results showed that TIB increased the number and proliferation of cells, with no effects on cell migration or invasion.

Previous reports indicate that E2 is involved in the regulation of several physiological and pathological processes in the brain and may play a role in the control of brain tumor growth (10,36). It has been reported that estrogen biosynthesis inhibition decreased the growth of C6 mouse glioma cells (37). Barone TA, et al. (36) found that E2 decreased tumor growth in nude rats intracerebrally implanted with U373 MG glioblastoma cell line; however, cell proliferation increased at 72 h after 10 nM of 2-hydroxyestradiol treatment

in *in vitro* experiments (38,39). Moreover, previous studies indicate that in U373 cell line, the number of cells significantly increased after PPT (ER α agonist) treatment but not after DPN (ER β agonist) treatment (37). All these data indicate a proliferative effect of E2 *in vitro*; however, the effects of this hormone *in vivo* are completely different. Some reports describe that estrogens could be related to the inhibition of tumor growth (38,39). Our results do not correlate with those obtained by Altinoz MA, et al. (37), who demonstrated an inhibitory effect of TIB on the cell number of rat C6 malignant glioma cells and primary cultures of glioblastoma tumors cultured *in vitro*. These discrepancies could be due to differences in the cell lines used in both works; U251 cell line shows several genetic alterations similar to human GBM tumor, including alterations in key tumor suppressors and oncogenic pathways. Furthermore, magnetic resonance imaging features of the U251 mouse model correlate with human GBM, including a necrotic center, poorly demarcated

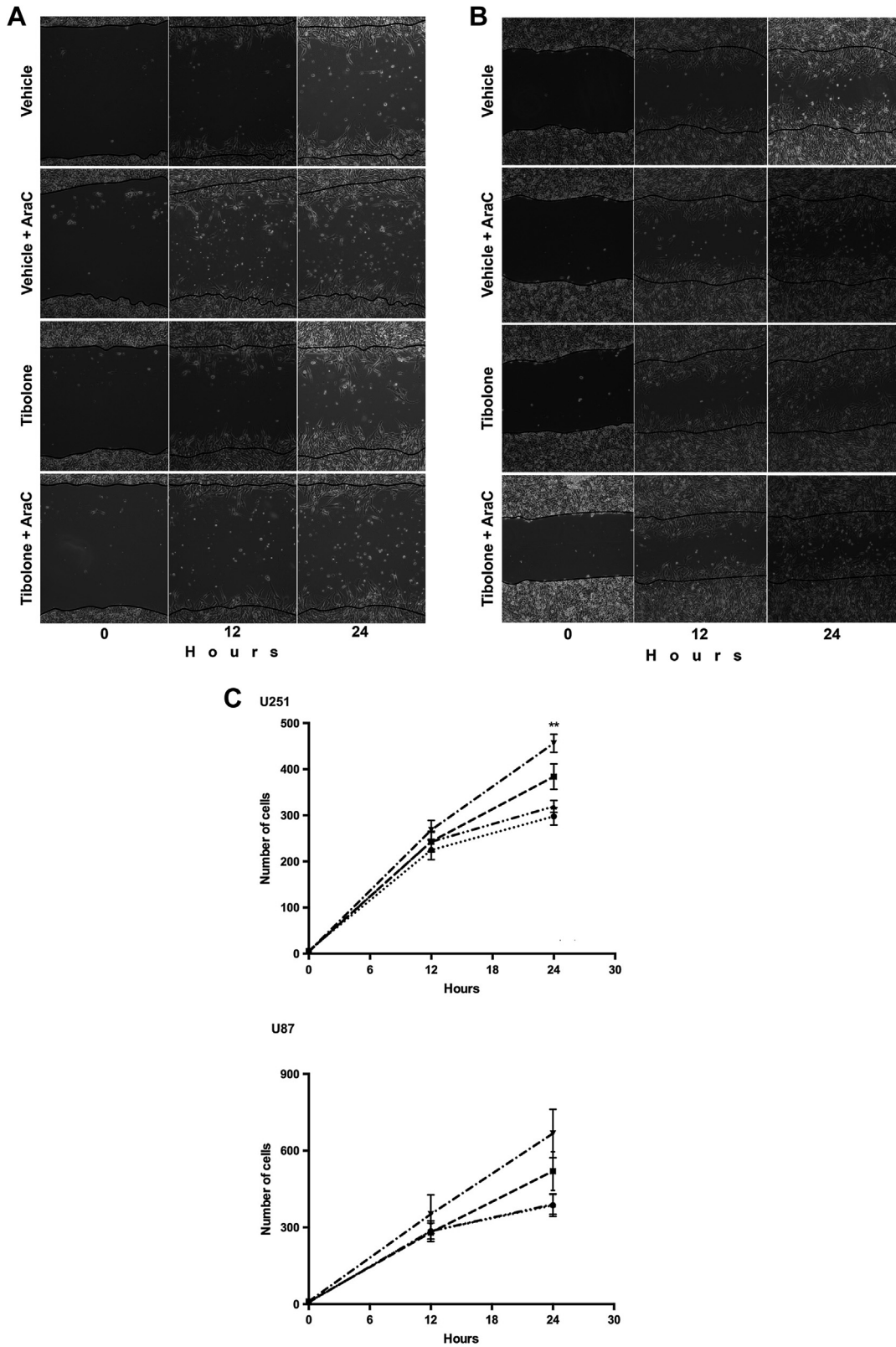


Figure 3. Effects of TIB on the migration of cells derived from human glioblastomas. U251-MG and U87 cells were treated with Tibolone (TIB 10 nM), Tibolone (10 nM) + AraC (10 μM), Vehicle (V) (DMSO 10%) or Vehicle (DMSO 10%) + AraC (10 μM), and photographs from the scratch area were taken at 0, 12 and 24 h. (A,B) representative photographs of the scratch area, (C) Graph of the number of cells counted in the scratch area. Data are mean ± S.E.M. *n* = 4; ***p* < 0.05 vs. V.

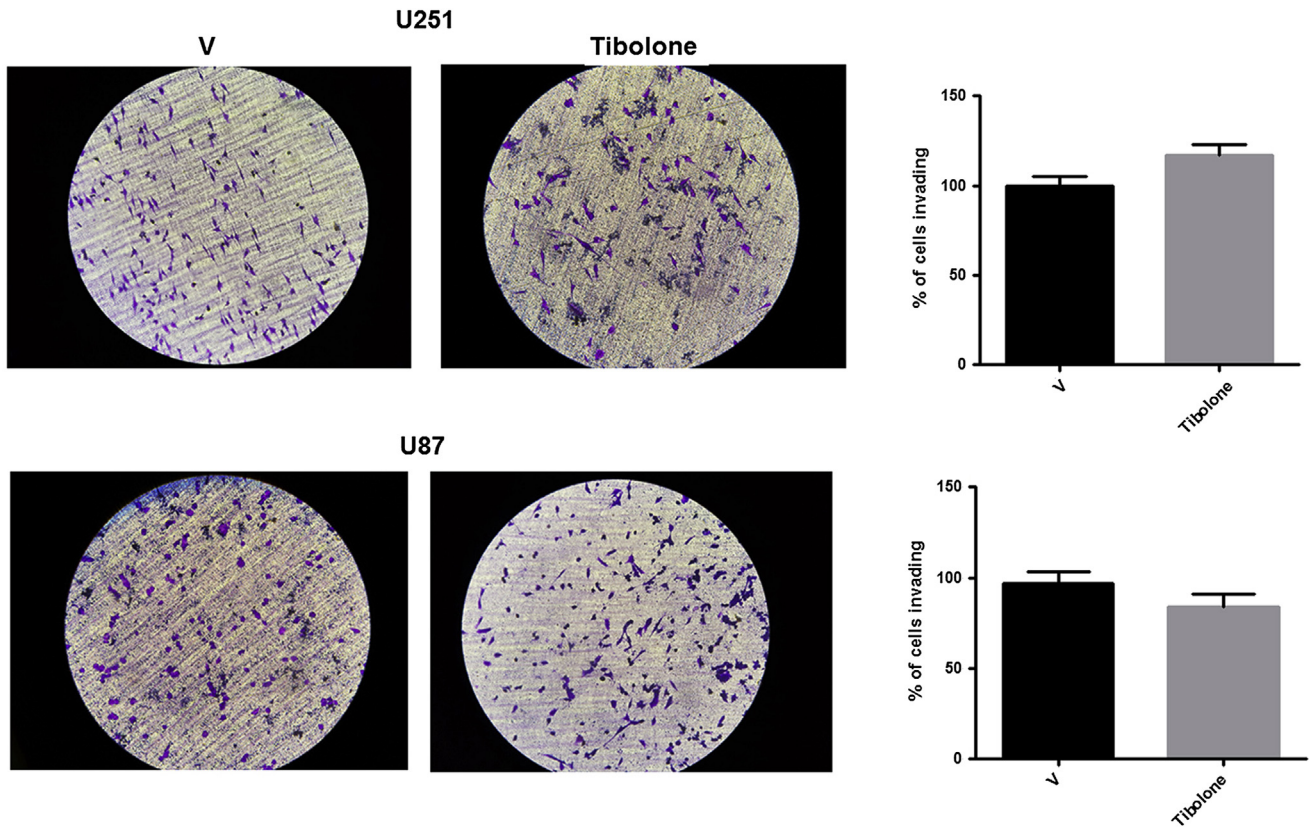


Figure 4. Effects of TIB on the invasion of cells derived from a human glioblastoma. Cells were treated with Tibolone (10 nM) or 0.02% cyclodextrin (Vehicle, V) for 24 h. (Left panels) Representative photographs of the transwell invasion assay. (Right panels) Graph representing the number of invasive cells. Data are mean \pm S.E.M. $n = 4$.

and infiltrative tumor borders (40). In contrast, in C6 cell line, some mutations in tumor suppressors as P53 and PTEN are missing (41); also, when these cells are implanted in Sprague–Dawley or Long–Evans rats, the tumor loses its invasive characteristics and grows encapsulated, no longer resembling the diffusely infiltrative nature of GBM (41). In primary cultures, many kind of cells, besides glioblastoma cells, could be present. Therefore, this heterogeneity could lead to different responses to TIB treatment. The present results were obtained in a homogeneous population of U251 immortalized cell line. These results together suggest that TIB effects will depend on the cell and tumor microenvironment.

Some studies report that the use of different compounds does not necessarily promote proliferation, invasion, and migration as a combo, but promote those effects independently (42,43). TIB promotes proliferation without effects on migration or invasion. This could be related to the fact that this steroid did not have effects over proteins involved in these processes that are overexpressed in glioblastomas, such as VEGF, EGFR or IGFR (44–46).

TIB and its metabolites have affinity for ERs and PRs (47); estradiol and progesterone treatments induce proliferation of glioblastoma cells and the inhibition of their

receptors blocked this effect (11,18,48). Our results showed that the inhibition of ERs and PRs blocked the proliferative effect of TIB in glioblastoma cells, suggesting that TIB exerts its effect on cell proliferation through these steroid receptors.

TIB decreases reactive gliosis and death after wound injury in neurons from the cerebral cortex in female mice (49), and in the T98 G cell line (derived from glioblastoma), by protecting them from glucose deprivation (50). These results suggest that TIB induces survival processes in normal or tumorigenic brain cells, which should explain its effect on the cell number and BrdU incorporation in U251 and U87 cell lines. Interestingly, this induction could be mediated by ERs and PRs. Also, it has been reported that estradiol prevents death induced by glucose deprivation through its interaction with ERs in cultured rat hippocampal neurons and after 8 weeks of progesterone treatment (51).

In a cell line derived from PC-3 (human prostate cancer) that was genetically modified to express AR stably, TIB modified this receptor activity through its metabolites: $\Delta 4$ -tibolone increased its transcriptional activity, while 3α -OH-tibolone diminished it (47). Although AR levels in glioblastomas are higher compared to periphery normal

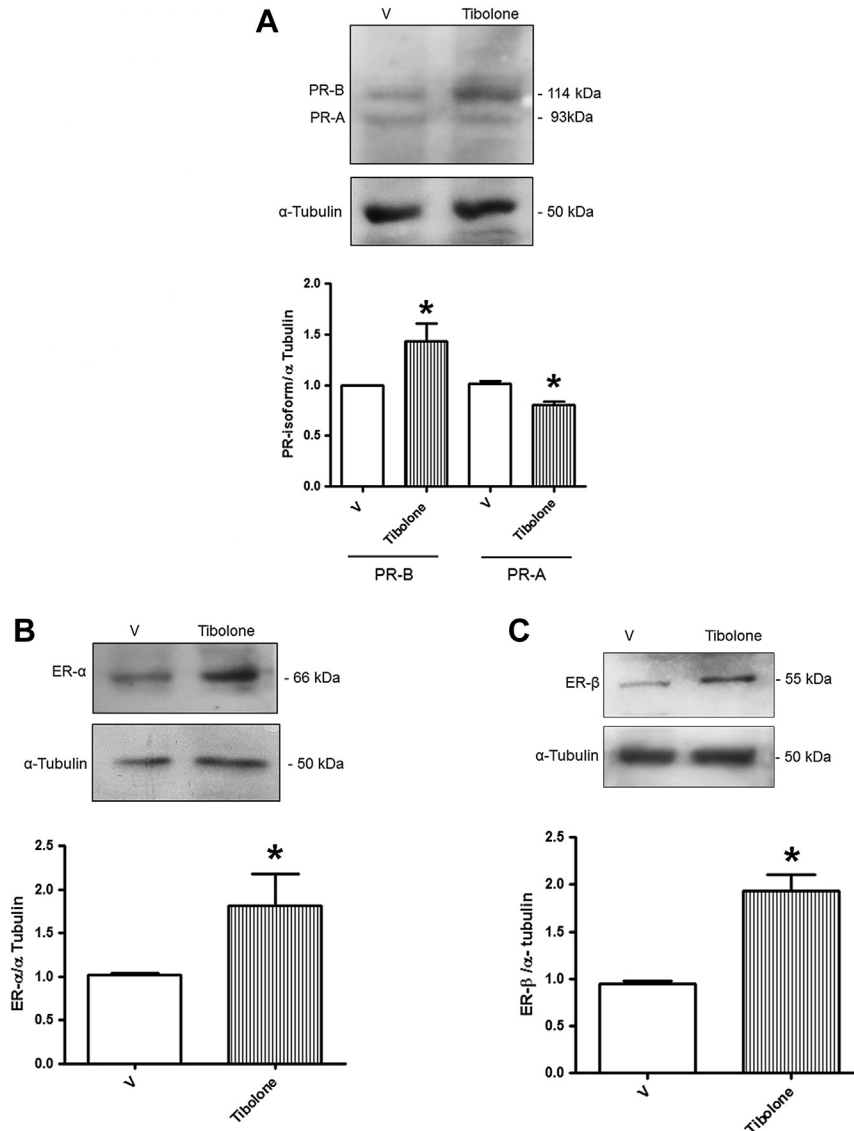


Figure 5. Effect of TIB on the content of AR, ER and PR isoforms on U251-MG cells. U251-MG cells were treated with TIB (10 nM) or vehicle (V) (0.02% cyclodextrin in sterile water); after 24 h, cells were lysed and proteins (70 μ g) were separated by electrophoresis on 10% SDS-PAGE. Gels were transferred to nitrocellulose membranes and then incubated with antibodies against PR isoforms (A), ER α (B) and ER β (C). The protein–antibody complexes were detected by ECL. The densitometric analysis was performed using the α -tubulin signal to correct for differences in the amount of total loaded protein. Representative blots (upper panel) and the densitometric analysis (lower panel) are shown. Data are normalized to V, bars represent mean \pm S.E.M. $n = 4$; * $p < 0.05$ vs. V.

brain tissue (52), our findings showed that TIB did not modify the content of ARs.

We observed that TIB increased ER α and ER β content in U251-MG cells. A study reported that 3-hydroxytibolone metabolites were stronger ligands and activators of estrogen receptors (ERs) with greater affinity for ER α than for ER β (53). Concomitantly with these data, it has been reported that U737 cell line expresses estrogen receptors, being ER α the predominant subtype, and that E2 and ICI 182,780 (ER antagonist) down-regulated the ER α content in this cell line (18). These results suggest that the effect of TIB and its metabolites could be mediated by their binding to

ERs. Although an estrogenic effect of TIB on the cell number could be suggested, a progestogenic effect cannot be excluded. A previous report indicates that P4 induces proliferation of cell lines derived from human astrocytomas grades III and IV (11). It has also been reported that PR isoforms are expressed both in human astrocytoma biopsies and glioblastoma cell lines (11,23), where PR-B was the predominant isoform (11). Moreover, PR-A overexpression in an astrocytoma cell line significantly diminished the increase in U373 cells number produced after progesterone treatment, suggesting that PR-A inhibits proliferation, while PR-B induces it (19). In this work, we observed that

TIB (10 nM) increased PR-B content but decreased that of PR-A in U251-MG cells.

We have reported that both estradiol (18) and progesterone (11,22) stimulate the proliferation, migration, invasiveness and expression of growth factors in these cell lines derived from human glioblastoma, while TIB has an effect only on the proliferation and the expression of hormone receptors. These *in vitro* results indicate that further *in vivo* studies are necessary to interpret the possible meaning of these findings and their clinical relevance for this type of tumors.

Our results suggest that TIB increases cell number and proliferation of human glioblastoma cells without affecting migration or invasion through the regulation of the content and activity of ERs and PRs.

Acknowledgments

Christian Guerra-Araiza received Beca de Excelencia en Investigación by Fundación IMSS A. C.

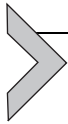
Supplementary Data

Supplementary data related to this article can be found at <https://doi.org/10.1016/j.arcmed.2019.08.001>.

References

- Ostrom QT, Gittleman H, Liao P, et al. CBTRUS Statistical Report: Primary brain and other central nervous system tumors diagnosed in the United States in 2010–2014. *Neuro Oncol* 2017;19(Suppl 5):v1–v88.
- Alcantara Llaguno S, Chen J, Kwon CH, et al. Malignant astrocytomas originate from neural stem/progenitor cells in a somatic tumor suppressor mouse model. *Cancer Cell* 2009;15:45–56.
- Cheng L, Bao S, Rich JN. Potential therapeutic implications of cancer stem cells in glioblastoma. *Biochem Pharmacol* 2010;80:654–665.
- Arko L, Katsyv I, Park GE, et al. Experimental approaches for the treatment of malignant gliomas. *Pharmacol Ther* 2010;128:1–36.
- Brandes AA, Tosoni A, Franceschi E, et al. Glioblastoma in adults. *Crit Rev Oncol Hematol* 2008;67:139–152.
- Osoba D, Brada M, Yung WK, et al. Health related quality of life in patients with anaplastic astrocytoma during treatment with temozolomide. *Eur J Cancer* 2000;36:1788–1795.
- Sahebjam S, McNamara M, Mason WP. Management of glioblastoma in the elderly. *Clin Adv Hematol Oncol* 2012;10:379–386.
- Anton K, Baehring JM, Mayer T. Glioblastoma multiforme: overview of current treatment and future perspectives. *Hematol Oncol Clin North Am* 2012;26:825–853.
- Grunberg SM, Weiss MH, Spitz IM, et al. Treatment of unresectable meningiomas with the antiprogestosterone agent mifepristone. *J Neurosurg* 1991;74:861–866.
- Schrell UM, Adams EF, Fahlbusch R, et al. Hormonal dependency of cerebral meningiomas. Part 1: Female sex steroid receptors and their significance as specific markers for adjuvant medical therapy. *J Neurosurg* 1990;73:743–749.
- González-Agüero G, Gutiérrez AA, González-Espinosa D, et al. Progesterone effects on cell growth of U373 and D54 human astrocytoma cell lines. *Endocrine* 2007;32:129–135.
- Hassanzadeh P, Arbabi E. The Effects of Progesterone on Glial Cell Line-derived Neurotrophic Factor Secretion from C6 Glioma Cells. *Iran J Basic Med Sci* 2012;15:1046–1052.
- Yu X, Jiang Y, Wei W, et al. Androgen receptor signaling regulates growth of glioblastoma multiforme in men. *Tumour Biol* 2015;36:967–972.
- Levine JE, Chappell PE, Schneider JS, et al. Progesterone receptors as neuroendocrine integrators. *Front Neuroendocrinol* 2001;22:69–106.
- Schumacher M, Guennoun R. Progesterone: Synthesis, Metabolism, Mechanisms of Action, and Effects in the Nervous System. An overview. In: Pfaff DW, Arnold AP, Etgen AM, Fahrbach SE, Rubin RT, eds. *Hormones, Brain and Behavior*. San Diego, CA: Elsevier: Academic Press; 2009. pp. 1505–1560.
- Liegibel UM, Sommer U, Boercoek I, et al. Androgen receptor isoforms AR-A and AR-B display functional differences in cultured human bone cells and genital skin fibroblasts. *Steroids* 2003;68:1179–1187.
- Xin QL, Qiu JT, Cui S, et al. Transcriptional activation of nuclear estrogen receptor and progesterone receptor and its regulation. *Sheng Li Xue Bao* 2016;68:435–454.
- González-Arenas A, Hansberg-Pastor V, Hernández-Hernández OT, et al. Estradiol increases cell growth in human astrocytoma cell lines through ER α activation and its interaction with SRC-1 and SRC-3 co-activators. *Biochim Biophys Acta* 2012;1823:379–386.
- Cabrera-Muñoz E, Gonzalez-Arenas A, Saqui-Salces M, et al. Regulation of progesterone receptor isoforms content in human astrocytoma cell lines. *J Steroid Biochem Mol Biol* 2009;113:80–84.
- Carroll RS, Zhang J, Dashner K, et al. Steroid hormone receptors in astrocytic neoplasms. *Neurosurgery* 1995;37:496–504.
- Hansberg-Pastor V, González-Arenas A, Camacho-Arroyo I. CCAAT/enhancer binding protein β negatively regulates progesterone receptor expression in human glioblastoma cells. *Mol Cell Endocrinol* 2017;439:317–327.
- Piña-Medina AG, Hansberg-Pastor V, González-Arenas A, et al. Progesterone promotes cell migration, invasion and cofilin activation in human astrocytoma cells. *Steroids* 2016;105:19–25.
- González-Agüero G, Ondarza R, Gamboa-Domínguez A, et al. Progesterone receptor isoforms expression pattern in human astrocytomas. *Brain Res Bull* 2001;56:43–48.
- Germán-Castelán L, Manjarrez-Marmolejo J, González-Arenas A, et al. Progesterone induces the growth and infiltration of human astrocytoma cells implanted in the cerebral cortex of the rat. *Biomed Res Int* 2014;2014:393174.
- Germán-Castelán L, Manjarrez-Marmolejo J, González-Arenas A, et al. Intracellular progesterone receptor mediates the increase in glioblastoma growth induced by progesterone in the rat brain. *Arch Med Res* 2016;47:419–426.
- Llaguno-Munive M, Medina LA, Jurado R, et al. Mifepristone improves chemo-radiation response in glioblastoma xenografts. *Cancer Cell Int* 2013;13:29.
- Zalcman N, Canello T, Ovadia H, et al. Androgen receptor: a potential therapeutic target for glioblastoma. *Oncotarget* 2018;9:19980–19993.
- Bao D, Cheng C, Lan X, et al. Regulation of p53wt glioma cell proliferation by androgen receptor-mediated inhibition of small VCP/p97-interacting protein expression. *Oncotarget* 2017;8:23142–23154.
- Rodríguez-Lozano DC, Piña-Medina AG, Hansberg-Pastor V, et al. Testosterone promotes glioblastoma cell proliferation, migration, and invasion through androgen receptor activation. *Front Endocrinol (Lausanne)* 2019;4:10–16.
- Campisi R, Marengo FD. Cardiovascular effects of tibolone: a selective tissue estrogenic activity regulator. *Cardiovasc Drug Rev* 2007;25:132–145.
- Kloosterboer HJ. Tibolone: A steroid with a tissue-specific mode of action. *J Steroid Biochem Mol Biol* 2001;76:231–238.
- Verheul HA, van Iersel ML, Delbressine LP, et al. Selective tissue distribution of tibolone metabolites in mature ovariectomized female

- cynomolgus monkeys after multiple doses of tibolone. *Drug Metab Dispos* 2007;35:1105–1111.
33. Bundred NJ, Kenemans P, Yip CH, et al. Tibolone increases bone mineral density but also relapse in breast cancer survivors: LIBERATE trial bone substudy. *Breast Cancer Res* 2012;14:R13.
 34. Sjögren LL, Mørch LS, Løkkegaard E. Hormone replacement therapy and the risk of endometrial cancer: A systematic review. *Maturitas* 2016;91:25–35.
 35. Kabat GC, Etgen AM, Rohan TE. Do steroid hormones play a role in the etiology of glioma? *Cancer Epidemiol Biomarkers Prev* 2010;19:2421–2427.
 36. Barone TA, Gorski JW, Greenberg SJ, et al. Estrogen increases survival in an orthotopic model of glioblastoma. *J Neurooncol* 2009;95:37–48.
 37. Altinoz MA, Albayrak SB, Karasu A, Sabanci PA, Imer M, Bilir A. The effects of tibolone on the human primary glioblastoma multiforme cell culture and the rat C6 glioma model. *Neurol Res* 2009;31:923–927.
 38. Qi ZY, Shao C, Zhang X, et al. Exogenous and endogenous hormones in relation to glioma in women: a meta-analysis of 11 case-control studies. *PLoS One* 2013;8:e68695.
 39. Plunkett RJ, Lis A, Barone TA, et al. Hormonal effects on glioblastoma multiforme in the nude rat model. *J Neurosurg* 1999;90:1072–1077.
 40. Radaelli E, Ceruti R, Patton V, et al. Immunohistopathological and neuroimaging characterization of murine orthotopic xenograft models of glioblastoma multiforme recapitulating the most salient features of human disease. *Histol Histopathol* 2009;24:879–891.
 41. Jacobs VL, Valdes PA, Hickey WF, et al. Current review of *in vivo* GBM rodent models: emphasis on the CNS-1 tumor model. *ASN Neuro* 2011;3:e00063.
 42. Andrade J, Potente M. New Q(ues) to keep blood vessels growing. *EMBO J* 2017;36:2315–2317.
 43. Velasco-Velázquez M, Pestell RG. The CCL5/CCR5 axis promotes metastasis in basal breast cancer. *Oncoimmunology* 2013;2:e23660.
 44. Deshpande A, Sicinski P, Hinds PW. Cyclins and cdks in development and cancer: a perspective. *Oncogene* 2005;24:2909–2915.
 45. Weathers SP, de Groot J. VEGF manipulation in glioblastoma. *Oncology (Williston Park)* 2015;29:720–727.
 46. Khajah MA, Al Saleh S, Mathew PM, et al. Differential effect of growth factors on invasion and proliferation of endocrine resistant breast cancer cells. *PLoS One* 2012;7:e41847.
 47. Escande A, Servant N, Rabenoelina F, et al. Regulation of activities of steroid hormone receptors by tibolone and its primary metabolites. *J Steroid Biochem Mol Biol* 2009;116:8–14.
 48. González-Arenas A, Peña-Ortiz MA, Hansberg-Pastor V, et al. PKC α and PKC δ activation regulates transcriptional activity and degradation of progesterone receptor in human astrocytoma cells. *Endocrinology* 2015;156:1010–1022.
 49. Crespo-Castrillo A, Yanguas-Casás N, Arevalo MA, et al. The synthetic steroid tibolone decreases reactive gliosis and neuronal death in the cerebral cortex of female mice after a stab wound injury. *Mol Neurobiol* 2018;55:8651–8667.
 50. Avila-Rodriguez M, Garcia-Segura LM, Hidalgo-Lanussa O, et al. Tibolone protects astrocytic cells from glucose deprivation through a mechanism involving estrogen receptor beta and the upregulation of neuroglobin expression. *Mol Cell Endocrinol* 2016;433:35–46.
 51. Hernández-Fonseca K, Massieu L, García de la Cadena S, et al. Neuroprotective role of estradiol against neuronal death induced by glucose deprivation in cultured rat hippocampal neurons. *Neuroendocrinology* 2012;96:41–50.
 52. Zhao N, Ahmed S, Wang F, et al. Targeting the androgen receptor as a novel therapeutic strategy for high-grade gliomas by suppressing glioma cancer stem cells. *J Clin Oncol* 2019;37(15_suppl):e13504.
 53. de Gooyer ME, Deckers GH, Schoonen WG, et al. Receptor profiling and endocrine interactions of tibolone. *Steroids* 2003;68:21–30.



Sex hormones and proteins involved in brain plasticity

Ignacio Camacho-Arroyo^{a,*}, Ana Gabriela Piña-Medina^b,
Claudia Bello-Alvarez^a, Carmen J. Zamora-Sánchez^a

^aUnidad de Investigación en Reproducción Humana, Instituto Nacional de Perinatología-Facultad de Química, Universidad Nacional Autónoma de México (UNAM), Mexico City, Mexico

^bFacultad de Química, Departamento de Biología, Universidad Nacional Autónoma de México (UNAM), Ciudad de México, México

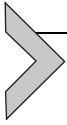
*Corresponding author: e-mail address: camachorroyo@gmail.com

Contents

1. Brain plasticity	146
1.1 What is brain plasticity?	146
1.2 Structural and chemical changes during brain plasticity	146
1.3 Brain plasticity during developmental stages	147
1.4 Brain plasticity during childhood and adulthood	147
1.5 Abnormalities in brain plasticity	148
2. Sex hormones and brain	148
2.1 General mechanisms of sex hormone actions	148
2.2 Actions of progesterone, estradiol, and testosterone in the brain	149
3. Sex hormones and brain plasticity	149
3.1 Progesterone in brain plasticity	149
3.2 Estrogens in the brain plasticity	152
3.3 Androgens in the brain plasticity	156
4. Conclusions and future directions	158
References	159

Abstract

It is well known that peripheral sex steroid hormones cross the blood-brain barrier and control a broad spectrum of reproductive behaviors. However, their role in other essential brain functions was investigated since the 1980s, when the accumulation of pregnenolone and dehydroepiandrosterone in the brain of mammalian species was determined. Since then, numerous studies have demonstrated the participation of sex hormones in brain plasticity processes. Sex hormones through both genomic and non-genomic mechanisms of action are capable of inducing gene transcription or activating signaling cascades that result in the promotion of different physiological and pathological events of brain plasticity, such as remodeling or formation of dendritic spines, neurogenesis, synaptogenesis or myelination. In this chapter, we will present the effects of sex hormones and proteins involved in brain plasticity.



1. Brain plasticity

1.1 What is brain plasticity?

The concept of brain plasticity (BP) is used to summarize the intrinsic abilities of the brain cells to change under physiologic or pathologic conditions in an adaptive way. Such processes occur at different timescales, from a few minutes to years. These changes involve molecular and structural characteristics of neurons and glial cells and their interactions. In this chapter, we will focus on the effects of sex steroid hormones over some plastic elements in brain synapses.

1.2 Structural and chemical changes during brain plasticity

The neural structure is continually changing. Cytoskeleton participates in regulating morphogenesis of neurons and the maintenance of mature synapses. The regulation of actin filaments (F-actin) and microtubules are essential for dendritic spines. F-actin are polymers of actin globular monomers (G-actin), their arrangement is carried out through dynamic events of polymerization and depolymerization of F-actin, which is controlled by the activity of proteins such as members of the Rho GTPases family and their effectors (Gonzalez-Billault et al., 2012; Jan & Jan, 2010), whereas microtubules are polymers of α - and β -tubulin. Besides, neuronal microtubules display a dynamic instability in neurites (Kuijpers & Hoogenraad, 2011).

The structures with more changes among life course are dendrites and axonal ends of neurons. Dendritic spines are small membranous protrusions of the neuronal surface connected to the cell by a thin neck; these can arise from the soma, dendrites, or axons, and contain the postsynaptic machinery necessary to respond to neurotransmitters (Rochefort & Konnerth, 2012).

Dendrites compute the information received from the axons of other cells. The number of dendrites, their length, diameter, and branches, limit the range and speed of information that a neuron can integrate. Moreover, dendritic spines are associated with the biochemical isolation of one synapse to another in the same dendrite (Nimchinsky, Sabatini, & Svoboda, 2002). These structures are critical because they can rapidly change their structure and even disappear due to changes in the F-actin content in a time-lapse of 2–3 min (Honkura, Matsuzaki, Noguchi, Ellis-Davies, & Kasai, 2008). Dendritic spines are of particular interest in neuroscience because they participate in synaptic plasticity and regulate mental processes such as cognition, learning, and memory (Bruehl-Jungerman, Davis, & Laroche, 2007).

1.3 Brain plasticity during developmental stages

Neurogenesis and gliogenesis are the two processes that originate mature neurons and glial cells, respectively, from neural stem cells (NSC). While neurogenesis occurs early during embryonic development and early postnatal life, gliogenesis starts at late embryo developmental states and continues in postnatal life. Neurogenesis begins when neuroepithelial cells are symmetrically divided, and numerous cell layers of them are formed. The neurogenesis switch at the ventricular zone where downregulates tight junction proteins such as occludin in embryo models of chick and mice (Aaku-Saraste, Hellwig, & Huttner, 1996). Then, neuroepithelial cells give rise to radial glial cells, which eventually originates neurons, astrocytes, and oligodendrocytes in humans (Howard, Chen, & Zecevic, 2006; Mo et al., 2007). Several transcription factors regulate the differentiation of NSC in both embryo telencephalon, and adult NSC population at subventricular zone such as Pax6 or Gsx2 in mice (Brill et al., 2008; Lopez-Juarez et al., 2013). Besides, it has been proposed that a quiescent state of the adult NSC is promoted by differences between neurogenic niches during embryo life (Fuentealba, Obernier, & Alvarez-Buylla, 2012).

1.4 Brain plasticity during childhood and adulthood

In the brain at the moment of birth, each neuron has 7500 connections, and these connections will reach the maximal number at 2 years old. Half of these synapses are pruning through programmed cell death. This phenomenon is explained by the Hebb Rule, which says that only synapses that have been constantly stimulated will be preserved (Mundkur, 2005). During childhood, BP is present through several mechanisms, including the persistence of neurogenesis, elimination of some neurons, refinement of synaptic connections, and proliferation and pruning of synapses (Johnston, 2004). During several years, BP had been seen only as an event predominantly in childhood, but nowadays, thanks to improvements in the field of imaging techniques is clear that BP takes place throughout the entire life (Pauwels, Chalavi, & Swinnen, 2018).

In a newborn, the brain is very immature, and in humans, this organ is entirely mature at 20 years old. All this period is known as “critical period” because all experiences have a significant impact on learning and development, which results in a healthy behavior accordingly to a particular environment in which an individual is exposed. For example, in the case of language acquisition, the critical period is during the first 6 years of life, this ability decreases drastically after 12 years old (Vaegan & Taylor, 1979).

Although BP is maximal in childhood, it does not disappear in adulthood, it rather decreases and is activated in a more specific context (Mundkur, 2005). The most convincing data about BP in adults comes from the fact that stroke patients with severe damage have shown the highest recovery after continuous therapy (Ramanathan, Conner, & Tuszyński, 2006).

Myelination is a mechanism of BP that has been underappreciated. The first steps in myelination begin at the last period of fetal development and continue during the first days of life and into early adult life. In the same way, the environment influences BP, and evidence of improvement of myelination in a context-dependent way has been documented (Fields, 2005).

1.5 Abnormalities in brain plasticity

BP is a fundamental event for the healthy development of cognitive and social activities. Dysfunctions in any of its molecular or structural elements lead to some neurological and psychiatric impairments. Neurodegenerative diseases such as Alzheimer's (AD), Parkinson's, and Huntington's disease or neuropsychiatric disorders like schizophrenia or major depression are closely related to synaptic dysfunction (Martella, Bonsi, Johnson, & Quartarone, 2018).

AD is the principal cause of dementia in older people, and it is characterized by the loss of cholinergic neurons in the basal forebrain. Although an effective treatment for AD is not yet available, some treatments consist in using agents that enhance the action of endogenous glutamate, nonsteroidal anti-inflammatory drugs, and estrogens (Gooch & Stennett, 1996).

Tuberous sclerosis, neurofibromatosis, Fragile X syndrome, or cerebral palsy are among neurological disorders that are a concern of pediatrics with frequency. Signaling pathways associated with processes like learning and memory are linked with most of these disorders. For example, Fragile X syndrome has been associated with a deficiency in the FMRP protein, implicated in the regulation of activity-dependent protein translation during synapsis. In mouse with Fragile X syndrome, dendritic spines present abnormalities in shape and size. These mice also show alterations in signaling through AMPA receptors and a more perdurable long-term depression (Comery et al., 1997).



2. Sex hormones and brain

2.1 General mechanisms of sex hormone actions

The sex hormones (SH) progestins, estrogens, and androgens exert their actions through a classic mechanism that involves the activation of nuclear

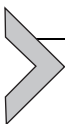
receptors, progesterone receptor (PR), estrogen receptor (ER) and androgen receptor (AR), respectively. Also, there are non-classic mechanisms that can be activated by SH modulating different signaling pathways. These mechanisms are mediated by specific membrane progesterone receptors (mPRs), membrane estrogen receptors (mERs), membrane androgen receptors (mARs), or some neurotransmitters receptors (Camacho-Arroyo, Hansberg-Pastor, Vázquez-Martínez, & Cerbón, 2017; Lai, Yu, Zhang, & Chen, 2017) (Fig. 1).

2.2 Actions of progesterone, estradiol, and testosterone in the brain

Actions of SH in the brain can be observed at different levels, such as cell differentiation, synaptogenesis, axon guidance, myelination, neurogenesis, cell migration, among others. Together, these actions result in changes in the number of cells, the cytoarchitecture, cellular activity, synaptic connectivity, and the content of neurotransmitters (Catenaccio, Mu, & Lipton, 2016; McEwen & Milner, 2017).

Progesterone (P4), estradiol (E2), and testosterone (T) are SH derived from cholesterol mainly synthesized in the adrenal gland and the gonads, also are synthesized within the brain, and their levels vary in different areas of the brain of males and females (Kato et al., 2013; Konkle & McCarthy, 2011). Changes in BP occur as a result of the action of SH produced by the gonads and adrenal glands, as well as by the local synthesis in the brain (Do Rego et al., 2009; Mellon & Griffin, 2002).

The effects of SH in the brain can be classified into two main groups: reproductive and non-reproductive. In the case of the reproductive effects, it is known that SH levels are differentially modified throughout life, resulting in various changes in the anatomy of the brain as well as in its physiology, and consequently in sexual behavior (Hillerer, Jacobs, Fischer, & Aigner, 2014; Nugent et al., 2012). Among the non-reproductive effects are neuroprotection, learning, and memory, sleep, the course of different mental and neurological diseases in response to physical damage, or the modulation of the immune system (Colciago, Casati, Negri-Cesi, & Celotti, 2015; Klein & Flanagan, 2016).



3. Sex hormones and brain plasticity

3.1 Progesterone in brain plasticity

P4 is known for its essential role in the reproductive process and the establishment and maintenance of pregnancy. However, since the discovery of P4

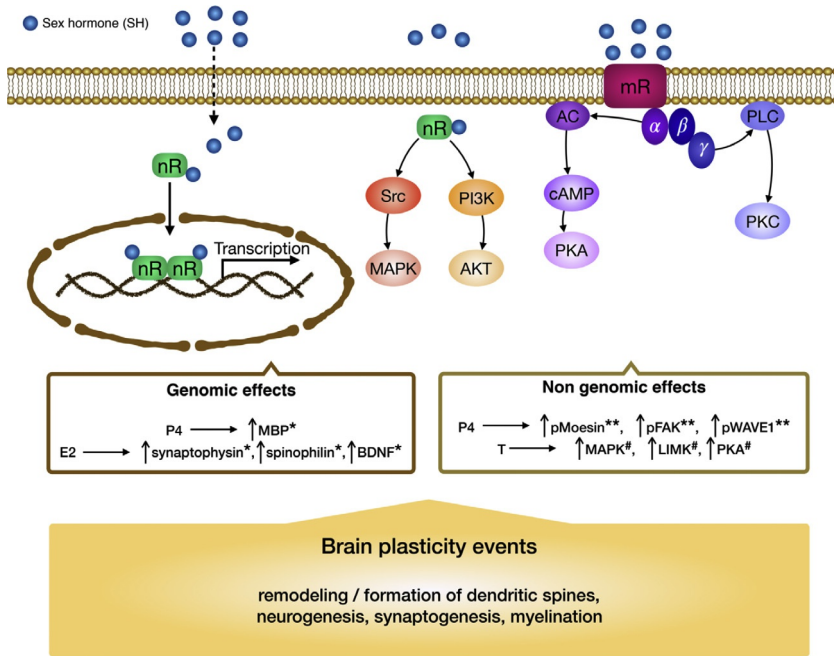


Fig. 1 General mechanism of sexual hormones action and brain plasticity. Sexual hormones such as progesterone (P4), estradiol (E2), and testosterone (T) can be synthesized *de novo* in the brain and exert a group of actions through their nuclear or membrane receptors (nR, mR, respectively). Once within the cell, these hormones can interact with their nR and activate the transcription of a group of genes related with specific processes of brain plasticity, for example, E2 induce the transcription of synaptophysin (synapse formation), spinophilin (formation and function of the dendritic spine) or BDNF (enhancement of dendritic spines and synaptogenesis). P4 induces the transcription of myelin basic protein (MPB; the protein component of the myelin sheat). Once activated by their respective hormones, nRs can also induce non-genomic effects through the activation of Src-MAPKs or PI3K-AKT signaling pathway. Besides, these hormones induce non-genomic effects trough their mRs, which are G-protein-coupled receptors, and therefore induce the activation of PKC or PKA. The activation of all these kinases finally conduces to the enhancement of FAK, Moesin, and WAVE phosphorylation (pFAK, pMoesin, pWAVE). All of these events lead up to the remodeling and formation of dendritic spines, neurogenesis, synaptogenesis, or myelination (* enhancement of expression, ** enhancement of phosphorylation, # signaling pathway activation).

metabolism in the CNS, plenty of studies determining its participation in BP processes has been made. Neurons and glial cells are capable of synthesizing P4 from cholesterol (Schumacher et al., 2012; Tsutsui, Ukena, Sakamoto, Okuyama, & Haraguchi, 2011). Several authors have reported the expression of PR-A/B receptors, mPRs, and PGRMC1 in neurons and glia

(Cabrera-Muñoz et al., 2009; Camacho-Arroyo, Hansberg-Pastor, Cabrera-Muñoz, Hernández-Hernández, & González-Arenas, 2012; González-Agüero, Ondarza, Gamboa-Domínguez, Cerbón, & Camacho-Arroyo, 2001; González-Orozco & Camacho-Arroyo, 2019; Valadez-Cosmes et al., 2015). The expression of PR has been associated with changes in the size and or formation of new dendritic spines, cytoskeleton reorganization, myelination, and neurogenesis (Ghoumari et al., 2003; Kato et al., 2013; Montes et al., 2019; Sanchez, Flamini, Genazzani, & Simoncini, 2013; Zhang et al., 2010).

Different research groups have studied the effect of hormones on dendritic spines. One of the most evident effects of P4 on dendritic spines has been observed during the estrous cycle in which a positive correlation between the levels of P4 in the hippocampus of rats and the density of dendritic spines has observed. Thus, when P4 locally reaches the highest levels, the highest density of dendritic spines is observed (Kato et al., 2013). Although the mechanisms by which these effects occur have not been described in detail, authors such as Sakamoto and collaborators have shown that in cerebellar Purkinje cells of newborn rats, P4 increases the number of dendritic spines in a dose-dependent manner, and the administration of a PR antagonist (RU486) blocked the effect of P4. These findings suggest that the mechanism by which these events occur is the genomic one (Sakamoto, Ukena, & Tsutsui, 2002). Besides, P4 administered for 2 h in hippocampus slices of adult male rats significantly increases the density of dendritic spines (Murakami et al., 2017), suggesting the participation of non-genomic mechanisms.

Morphological changes in dendritic spines depend on the cytoskeletal rearrangements, which can be dynamically regulated by hormones (Hansberg-Pastor, González-Arenas, Piña-Medina, & Camacho-Arroyo, 2015; Kaech, Parmar, Roelandse, Bornmann, & Matus, 2001). Although most of the SH effects on actin cytoskeleton remodeling have been observed with estrogens, P4 also induces cytoskeleton changes. Sanchez and collaborators demonstrated that P4 increases the phosphorylation as well as the distribution of the proteins moesin, focal adhesion kinase (FAK), and Wiskott-Aldrich syndrome protein family member 1 (WAVE1). Thus, promoting an increase in the density and the number of dendritic spines in primary cultures of rat cortical neurons (Sanchez et al., 2013) (Fig. 1). Another essential process in BP is myelination, in which P4 has been shown to have effects. In slices of rat cerebellum organotypic cultures, P4 by activating PR promotes in a dose-dependent manner, the expression of myelin basic protein (Ghoumari et al., 2003) (Fig. 1).

Finally, we cannot talk about P4 effects on BP without considering neurogenesis. Different groups have shown that P4 treatment improves neurogenesis during pathological conditions, such as cerebral ischemia. When P4 is administered to male mice after being subjected to an ischemia process, a higher density of new neurons in the dentate gyrus was observed (Zhang et al., 2010). These observations were confirmed by other groups. Recently by Montes and cols, they administered P4 to male rats after their induction of cerebral ischemia. It was observed a significant number of proliferating neurons in the dentate gyrus; additionally, these rats show a better performance in the Morris water maze test compared to rats that were treated with vehicle (Montes et al., 2019).

3.2 Estrogens in the brain plasticity

The first work about presence and activity of aromatase, the enzyme responsible for E2 synthesis, in the brain appeared beginning the 70s (Naftolin, Ryan, & Petro, 1971). Nowadays, it is known that E2 and aromatase have a vital role in physiological events during embryonic development such as sexual differentiation (Bakker & Baum, 2008) and through adulthood, on cognition, by its capacity to regulate synapses formation (Hara, Waters, McEwen, & Morrison, 2015). Also, E2 has been associated with neuroprotective functions in the context of some pathologic conditions such as perinatal asphyxia (Saraceno, Bellini, Garcia-Segura, & Capani, 2018).

E2 is in a sixfold higher concentration in the hippocampus than in plasma (Kretz et al., 2004). The main cells in which have been detected the aromatase expression are neurons (Yague et al., 2008). Some glial cells, including astrocytes in brain areas suffering different types of injuries, also present aromatase immunoreactivity (Azcoitia, Sierra, Veiga, & Garcia-Segura, 2003; Garcia-Segura et al., 1999).

There is a positive correlation between aromatase and expression of estrogen receptor alpha (ER α) and beta (ER β) (Azcoitia, Yague, & Garcia-Segura, 2011). ER α and ER β are widely distributed along human telencephalon, despite their different pattern of distribution. They are detected first during the fetal development, and their localization within the cell are different (González et al., 2007).

Neurogenesis has been mainly explored in the dentate gyrus of the hippocampus and the subventricular zone (Spalding et al., 2013). However, there are other areas such as the amygdala and hypothalamus, where newly proliferated neurons have been detected. In the hippocampus, treatments

with specific ER α (propyl-pyrazole triol) or ER β (diarylpropionitrile) agonists increased cell proliferation in adult ovariectomized Sprague-Dawley rats (Mazzucco et al., 2006). In the amygdala and hypothalamus of fetal rat, E2 induced the proliferation and survival of new neurons (Chowen, Torres-Alemán, & García-Segura, 1992). Various factors have been attributed to the role of E2 in the enhancement of neuronal proliferation. One of these factors is associated with the reduction of oxidative stress. In an Alzheimer's disease model, mice that received E2 during the initial stage of the disease exhibited a reduction in the levels of nitric oxide and reactive oxygen species. In addition, the treatment of E2 in these mice reduced the activation of the cytochrome-*c*/Bax/Bcl-2/caspase-3 pathway (Zheng et al., 2017). The effect of E2 in the neurogenesis has also been associated with its role through the activation of its nuclear receptors in changing the expression of genes related to different physiological processes (Aenlle, Kumar, Cui, Jackson, & Foster, 2009; Coyoy, Guerra-Araiza, & Camacho-Arroyo, 2016). Other authors have associated the proliferative effects of E2 with the activation of the extracellular ERK/MAPK signaling (Fig. 1) (Wang, Liu, & Brinton, 2008).

Synaptogenesis and synaptic plasticity are processes involving synapse formation, maintenance (stabilization), and activity-dependent refinement and elimination (Cohen-Cory, 2002). In the 90s, several studies demonstrated the role of E2 in synapses remodeling. Ovariectomy in rats for 6 days caused the decrease in density of dendritic spines (Gould, Woolley, Frankfurt, & McEwen, 1990): This effect was reverted by E2 replacement (Woolley & McEwen, 1993). E2 not only changes the density of the spine but also the shape of spines. For example, rats in the proestrus period (when E2 levels are the highest) showed more thin and fewer mushroom spines than rats in the estrus period (González-Burgos, Alejandre-Gómez, & Cervantes, 2005). Interestingly, E2 increased the frequency of multiple synapse boutons in CA1 neurons in the presynaptic terminal. These experiments were conducted in female ovariectomized rats (Woolley, Wenzel, & Schwartzkroin, 1996). Besides, other authors have demonstrated the relationship between E2 and proteins highly enriched in the presynaptic and postsynaptic areas such as synaptophysin I or spinophilin, respectively (Fig. 1). In both cases, immunoreactivity for the proteins was enhanced after E2 treatment, and this increase was reverted by ER antagonists (Rune et al., 2002). Synaptophysin is a synaptic vesicle protein ubiquitously expressed throughout the brain. Some pieces of evidence point to a role in synapse formation since the extent of synapses decreased in synaptophysin-mutant

cultured hippocampal neurons (Tarsa & Goda, 2002). Spinophilin is a dendritic spine protein closely related to the formation and function of the dendritic spine (Feng et al., 2000). E2 promotes the synthesis of neurotrophic factors such as insulin-like growth factor-1 (IGF-1) and brain-derived neurotrophic factor (BDNF) (Fig. 1). Both neurotrophic factors have been associated with the enhancement of dendritic spines (Luine & Frankfurt, 2013) and synaptogenesis (Sato, Akaishi, Matsuki, Ohno, & Nakazawa, 2007). Then, what are the molecular mechanism responsible for the rapid or non-genomic activation during events related to synaptogenesis? After binding to E2, ERs translocate to the plasma membrane. Once in the membrane, they interact with metabotropic glutamate receptors (mGluRs) and activate the ERK/MAPK pathway, which in turn induces the activation of the transcription factor cAMP response element-binding protein (CREB). These events have been associated with the increase in dendritic spines density in the rat somatosensory and prefrontal cortex (Khan, Dhandapani, Zhang, & Brann, 2013). In the hippocampus, non-genomic effects of E2 are associated with the stimulation of NMDA receptors (NMDAR), which activate PKA. Then, PKA induces the phosphorylation of ERK, finally resulting in the modulation of dendritic spines and synaptic functions (Lewis, Kerr, Orr, & Frick, 2008). Another kinase that has been linked to synapse formation by E2 action is mTOR. Once E2 interacts with its receptors, PI3K-mTOR pathway can be activated, inducing protein synthesis and actin polymerization (Briz & Baudry, 2014).

Long-term potentiation (LTP) and long-term depression (LTD) are necessary events to consolidate BP and, therefore, learning, and short and long-term memories. LTP is characterized by structural changes that let to enlargement of a thin spine while in LTD, the changes result in shrinkage of spines. E2 has been associated with LTP induction but not with LTD. Molecular events associated with LTP involve the activation of the NMDAR, followed by postsynaptic Ca²⁺ influx and actin polymerization. Several studies have proved the central role of E2 in the induction of LTP. Grassi and cols demonstrated that inhibition of aromatase or ER blockage decreases the high-frequency stimulation-induced LTP in male rat brainstem slices (Grassi, Frondaroli, Dieni, Scarduzio, & Pettorossi, 2009). PI3K/Akt pathway has been widely associated with LTP induction (Horwood, Dufour, Laroche, & Davis, 2006; Kelly & Lynch, 2000). In this way, E2 participates in the LTP regulation through the PI3K/Akt signaling and other kinases. Hasegawa and cols found that in the hypothalamus of young adult male Wistar rats, inhibitors of Erk MAPK, PKA, PKC, PI3K, NR2B, and CaMKII blocked the E2-LTP induction (Hasegawa et al., 2015).

In addition, the mechanism by which the E2 induces LTP implicates, first, the interaction with ER α or ER β , which in turn can activate to PI3K that stimulates ERK through Akt. Then, NMDAR is activated, and the influx of Ca²⁺ induces the phosphorylation of AMPA receptors and, finally, the enhancement of the LTP (Mannella, 2006). In 2004, it was demonstrated that E2 induces a lateral movement of NR1/NR2B along the synapsis in the aged hippocampus, specifically in the CA1 region of female Sprague-Dawley rats. This change in the distribution of NR1/NR2B was related to a more dynamic profile of this receptor, which is more similar to the physiologic state in a young rat (Adams, Fink, Janssen, Shah, & Morrison, 2004). Therefore, E2 can induce molecular changes not only related to expression or activation of proteins but also with their subcellular localization. As it was mentioned, the actin polymerization is an essential event for the formation and stabilization of LTP. Kramar and cols described one of the possible mechanisms by which E2 regulates the cytoskeletal remodeling in the LTP context. These authors found that latrunculin, a toxin that prevents F-actin assembly, inhibited the LTP induced by E2. Moreover, an antagonist of RhoA kinase was administered to acute hippocampal slices, and the previously plasticity effect induced by E2 was blocked. Besides, E2 induced the phosphorylation (inactivation) of cofilin, a protein that disassembles F-actin. These authors proposed that E2 can induce actin polymerization through the pathway: RhoA-ROCK-LIM kinase-cofilin (Kramar et al., 2009).

All these molecular and plastic changes allow the consolidation of a variety of physiological events fundamental to maintain a healthy status of cognitive processes. For example, in the prefrontal cortex and hypothalamus, modification in the pre-existing synapsis such as strengthening and weakening have been associated with the learning of new information (Bourne & Harris, 2007). Administration of E2 to Long-Evans hooded female rats, results in improvement of the working memory through the increase of NMDAR binding in CA1 neurons (Daniel & Dohanich, 2001). In the case of young and middle-aged females C57BL/6 mice, E2 enhanced the object recognition memory through the PI3K/Akt and ERK signaling (Fan et al., 2010). The enhancement of this kind of memory was observed in young and middle-aged but not in aged mice. What could be the causes of this difference? Aging is associated with the lowest expression of IGF-1, and the interaction between ER α and IGF-1 receptor is implicated in activating PI3K/Akt signaling pathway (Cardona-Gómez, DonCarlos, & Garcia-Segura, 2000). Thus, it has been proposed that young and middle-aged mice have a better response to E2 than aged mice.

The object recognition and memory consolidation are related to the activation of the classical Wnt signaling pathway by E2 (Fortress, Schram, Tuscher, & Frick, 2013). Zhang and cols demonstrated that E2 could stabilize the Wnt pathway through inhibition of dickkopf-1 (Dkk1), a negative regulator of the Wnt/beta-catenin pathway (Zhang, Wang, Khan, Mahesh, & Brann, 2008).

Many neurodegenerative diseases such as AD (Caricasole, 2004), Parkinson (Dun et al., 2012), stroke (Seifert-Held et al., 2011), and temporal lobe epilepsy (Busceti et al., 2007) are closely related to Dkk1 overexpression. As mentioned, E2 can stabilize the Wnt pathway through Dkk1 inhibition. Then, E2 might exert meaningful participation in neuroprotection. In a model of global cerebral ischemia, the treatment with E2 protected the hippocampus CA1 through the decrease in the expression of Dkk1, which induced the elevation of beta-catenin in the nucleus. In this study, E2 induced survivin expression after 24 and 48 h of cerebral ischemia and attenuated tau hyperphosphorylation (Zhang et al., 2008). Taking into account these facts, E2 could prevent the development of a group of neurodegenerative diseases or contribute to the recovery of patients.

3.3 Androgens in the brain plasticity

T is the most abundant male sex hormone, mainly produced in Leydig cells of the testis, in ovaries, and in the adrenal gland cortex. Conversion of T into dihydrotestosterone (DHT) is a clue in the modulation of the effects of androgens. T and its metabolite DHT are important androgens implicated in brain plasticity throughout human life. However, it is crucial to consider that some of the effects of T on learning, memory, and BP could be mediated by T aromatization to E2 by the aromatase enzyme (Bimonte-Nelson et al., 2003). In the previous section, it has been addressed the relevance of aromatase expression and the aromatization of T to E2. Effects of androgens on BP have been experimentally determined by using aromatase inhibitors or using the non-aromatizable androgen metabolite DHT. Other androgen metabolites, such as androstenediol (5 α -androstane-3 α ,17 β -diol), are considered neurosteroids (Reddy, 2008) because they are synthesized in the brain, and induce BP through different mechanisms of action. Androstenediol, for example, is a positive modulator of GABA-A receptors (Reddy & Jian, 2010).

The AR regulates the expression of target genes through their classic mechanism of action. AR also could interact with other intracellular

signaling molecules such as MAPKs (Foradori, Weiser, & Handa, 2008). T and DHT play a critical role during prenatal life, due to the activation of AR. Since prenatal life, AR is highly expressed in the hypothalamus, hippocampus, amygdala, olfactory bulb, and cortex (Genazzani, Pluchino, Freschi, Ninni, & Luisi, 2007). During fetal life of rodents, it has been reported that the dimorphic sex area of the preoptic area of females could present male characteristics, such as enhanced volume, due to T administration. This effect may be independent of proliferative events of such zone, since changes in POA/HA morphology begins after neurogenesis and at the same time of the beginning of T release from fetal testis (Clayton, Kogura, & Kraemer, 1970).

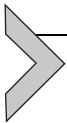
As the hippocampus is one of the most dimorphic brain areas in mammals, differences between androgenic and estrogenic effects in BP in both males and females have been broadly studied in this area. In adult male rats, T and DHT but not E2 could maintain neuronal survival in the hippocampus and dentate gyrus (Hamson et al., 2013; Spritzer & Galea, 2007), which suggest that both androgens actively participate in the survival and differentiation of neurons. Besides, AR promotes neurogenesis in the male rodent hippocampus (Okamoto et al., 2012).

Interestingly, there are reports that T or DHT but not E2, increase spine dendritic density in orchidectomized rodent males similar to that observed in intact animals. This finding contrasts with the fact that dendritic spines in females are highly augmented due to the effect of estrogens. In ovariectomized females, dendritic spines are induced by T. However, concomitant administration of T, with the aromatase inhibitor letrozole, abolish dendritic spines formation (MacLusky, Hajszan, Prange-Kiel, & Leranth, 2006; Okamoto et al., 2012). In female canaries, treatment with T increases the volume of the high vocal center (HVC), involved in the learning and control of song due to the enlargement of soma and the number of fusiform morphology of neurons. Interestingly, treatments with DHT or E2 alone did not exert similar results, although they do so when they are simultaneously administered (Yamamura, Barker, Balthazart, & Ball, 2011). All these data suggest that T or DHT actions in females or males are AR-dependent, and AR is highly expressed in the hippocampus. However, afferent inputs to the hippocampus need to be considered. For example, in female ovariectomized rats with contralateral transected fimbria/fornix area whose most afferences are located in the hippocampus, the subcutaneous treatment with E2 did not increase the dendritic spines number (Leranth, Shanabrough, & Horvath, 2000; Yamamura et al., 2011). Other reports demonstrate that

T modifies dendritic spines morphology in hippocampus slices between 0.5 and 2 h of treatment. This effect was due to the non-genomic mechanism of the AR, which involves the activation of signaling cascades of MAPKs, PKA, and LIMK (Fig. 1). DHT displays similar effects, however, within the time-lapse of 2 h, the metabolism of T to DHT or E2 did not contribute to the effects of T alone, as seen when this hormone was concomitantly administered with letrozole or the 5α R inhibitor, finasteride (Hatanaka et al., 2015).

It has been mentioned that the expression of 5α R is elevated in myelin-rich brain zones. T and DHT promote myelination in the cuprizone model of multiple sclerosis in rodents (Hussain et al., 2013). Also, in a ventral spinal cord demyelination model, T induces peripheral myelination through AR, and also promotes the recruitment of astrocytes into the demyelinated lesion and the recruitment and maturation of oligodendrocyte progenitors (Bielecki et al., 2016).

Other androgens such as dehydroepiandrosterone (DHEA) possess several mechanisms of actions additional to AR binding. DHEA is an allosteric modulator of the GABA-A receptor and thus, potentiating the antagonism of GABA in a long-term way in the hippocampus, which is related to learning and memory processes, remarkably in the older population (Wolf, Naumann, Hellhammer, & Kirschbaum, 1998).



4. Conclusions and future directions

After concluding this chapter, it is clear that sex hormones such as P4, E2, and T can be metabolized and exert a variety of functions in the CNS. Once in the brain, these hormones can interact with several kinds of receptors and activate a variety of signaling pathways, which included the regulation of gene transcription through their nuclear receptors or the activation of a plethora of signaling pathways through their mRs.

All of these actions are transcendental to confer the brain the capacity of remodeling and form dendritic spines, as well as regulate neurogenesis, synaptogenesis, or myelination. The specific mode of action of sex hormones on BP depends on sexual, age, and brain area. Based on the important role of sex hormones in the brain, they represent a promising field in the comprehension of BP, as well as in the therapeutic approach to the treatment of neurodegenerative diseases.

References

- Aaku-Saraste, E., Hellwig, A., & Huttner, W. B. (1996). Loss of occludin and functional tight junctions, but Not ZO-1, during neural tube closure-remodeling of the neuroepithelium prior to neurogenesis. *Developmental Biology*, *180*, 664–679.
- Adams, M. M., Fink, S. E., Janssen, W. G. M., Shah, R. A., & Morrison, J. H. (2004). Estrogen modulates synaptic N-methyl-D-aspartate receptor subunit distribution in the aged hippocampus. *The Journal of Comparative Neurology*, *474*(3), 419–426.
- Aenlle, K. K., Kumar, A., Cui, L., Jackson, T. C., & Foster, T. C. (2009). Estrogen effects on cognition and hippocampal transcription in middle-aged mice. *Neurobiology of Aging*, *30*(6), 932–945.
- Azcoitia, I., Sierra, A., Veiga, S., & Garcia-Segura, L. M. (2003). Aromatase expression by reactive astroglia is neuroprotective. *Annals of the New York Academy of Sciences*, *1007*, 298–305.
- Azcoitia, I., Yague, J. G., & Garcia-Segura, L. M. (2011). Estradiol synthesis within the human brain. *Neuroscience*, *191*, 139–147.
- Bakker, J., & Baum, M. J. (2008). Role for estradiol in female-typical brain and behavioral sexual differentiation. *Frontiers in Neuroendocrinology*, *29*, 1–16.
- Bielecki, B., Mattern, C., Ghomari, A. M., Javaid, S., Smietanka, K., Ghanem, C. A., et al. (2016). Unexpected central role of the androgen receptor in the spontaneous regeneration of myelin. *Proceedings of the National Academy of Sciences of the United States of America*, *113*, 14829–14834.
- Bimonte-Nelson, H. A., Singleton, R. S., Nelson, M. E., Eckman, C. B., Barber, J., Scott, T. Y., et al. (2003). Testosterone, but not nonaromatizable dihydrotestosterone, improves working memory and alters nerve growth factor levels in aged male rats. *Experimental Neurology*, *181*(2), 301–312.
- Bourne, J., & Harris, K. M. (2007). Do thin spines learn to be mushroom spines that remember? *Current Opinion in Neurobiology*, *17*(3), 381–386.
- Brill, M. S., Snappyan, M., Wohlfrom, H., Ninkovic, J., Jawerka, M., Mastick, G. S., et al. (2008). A Dlx2- and Pax6-dependent transcriptional code for periglomerular neuron specification in the adult olfactory bulb. *Journal of Neuroscience*, *28*, 6439–6452.
- Briz, V., & Baudry, M. (2014). Estrogen regulates protein synthesis and actin polymerization in hippocampal neurons through different molecular mechanisms. *Frontiers in Endocrinology*, *5*, 22.
- Bruel-Jungerman, E., Davis, S., & Laroche, S. (2007). Brain plasticity mechanisms and memory: A party of four. *The Neuroscientist*, *13*, 492–505.
- Busceti, C. L., Biagioni, F., Aronica, E., Rizzo, B., Storto, M., Battaglia, G., et al. (2007). Induction of the Wnt inhibitor, Dickkopf-1, is associated with neurodegeneration related to temporal lobe epilepsy. *Epilepsia*, *48*(4), 694–705.
- Cabrera-Muñoz, E., González-Arenas, A., Saqui-Salces, M., Camacho, J., Larrea, F., García-Becerra, R., et al. (2009). Regulation of progesterone receptor isoforms content in human astrocytoma cell lines. *The Journal of Steroid Biochemistry and Molecular Biology*, *113*(1–2), 80–84.
- Camacho-Arroyo, I., Hansberg-Pastor, V., Cabrera-Muñoz, E., Hernández-Hernández, O. T., & González-Arenas, A. (2012). Role of progesterone receptor isoforms in human astrocytomas growth. *Tumors of the Central Nervous System*, *5*, 57–63.
- Camacho-Arroyo, I., Hansberg-Pastor, V., Vázquez-Martínez, E. R., & Cerbón, M. (2017). Mechanism of progesterone action in the brain. In *Hormones, brain and behavior* (pp. 181–214). Elsevier.
- Cardona-Gómez, G. P., DonCarlos, L., & Garcia-Segura, L. M. (2000). Insulin-like growth factor I receptors and estrogen receptors colocalize in female rat brain. *Neuroscience*, *99*(4), 751–760.

- Caricasole, A. (2004). Induction of Dickkopf-1, a negative modulator of the Wnt pathway, is associated with neuronal degeneration in Alzheimer's brain. *Journal of Neuroscience*, *24*, 6021–6027.
- Catenaccio, E., Mu, W., & Lipton, M. L. (2016). Estrogen- and progesterone-mediated structural neuroplasticity in women: Evidence from neuroimaging. *Brain Structure & Function*, *221*(8), 3845–3867.
- Chowen, J. A., Torres-Alemán, I., & García-Segura, L. M. (1992). Trophic effects of estradiol on fetal rat hypothalamic neurons. *Neuroendocrinology*, *56*(6), 895–901.
- Clayton, R. B., Kogura, J., & Kraemer, H. C. (1970). Sexual differentiation of the brain: Effects of testosterone on brain RNA metabolism in newborn female rats. *Nature*, *226*(5248), 810–812.
- Cohen-Cory, S. (2002). The developing synapse: Construction and modulation of synaptic structures and circuits. *Science*, *298*(5594), 770–776.
- Colciago, A., Casati, L., Negri-Cesi, P., & Celotti, F. (2015). Learning and memory: Steroids and epigenetics. *The Journal of Steroid Biochemistry and Molecular Biology*, *150*, 64–85.
- Comery, T. A., Harris, J. B., Willems, P. J., Oostra, B. A., Irwin, S. A., Weiler, I. J., et al. (1997). Abnormal dendritic spines in fragile X knockout mice: Maturation and pruning deficits. *Proceedings of the National Academy of Sciences of the United States of America*, *94*(10), 5401–5404.
- Coyoy, A., Guerra-Araiza, C., & Camacho-Arroyo, I. (2016). Metabolism regulation by estrogens and their receptors in the central nervous system before and after menopause. *Hormone and Metabolic Research*, *48*(8), 489–496.
- Daniel, J. M., & Dohanich, G. P. (2001). Acetylcholine mediates the estrogen-induced increase in NMDA receptor binding in CA1 of the hippocampus and the associated improvement in working memory. *The Journal of Neuroscience: The Official Journal of the Society for Neuroscience*, *21*(17), 6949–6956.
- Do Rego, J. L., Seong, J. Y., Burel, D., Leprince, J., Luu-The, V., Tsutsui, K., et al. (2009). Neurosteroid biosynthesis: Enzymatic pathways and neuroendocrine regulation by neurotransmitters and neuropeptides. *Frontiers in Neuroendocrinology*, *30*(3), 259–301.
- Dun, Y., Li, G., Yang, Y., Xiong, Z., Feng, M., Wang, M., et al. (2012). Inhibition of the canonical Wnt pathway by Dickkopf-1 contributes to the neurodegeneration in 6-OHDA-lesioned rats. *Neuroscience Letters*, *525*(2), 83–88.
- Fan, L., Zhao, Z., Orr, P. T., Chambers, C. H., Lewis, M. C., & Frick, K. M. (2010). Estradiol-induced object memory consolidation in middle-aged female mice requires dorsal hippocampal extracellular signal-regulated kinase and phosphatidylinositol 3-kinase activation. *The Journal of Neuroscience: The Official Journal of the Society for Neuroscience*, *30*(12), 4390–4400.
- Feng, J., Yan, Z., Ferreira, A., Tomizawa, K., Liauw, J. A., Zhuo, M., et al. (2000). Spinophilin regulates the formation and function of dendritic spines. *Proceedings of the National Academy of Sciences of the United States of America*, *97*(16), 9287–9292.
- Fields, R. D. (2005). Myelination: An overlooked mechanism of synaptic plasticity? *The Neuroscientist: A Review Journal Bringing Neurobiology, Neurology and Psychiatry*, *11*(6), 528–531.
- Foradori, C. D., Weiser, M. J., & Handa, R. J. (2008). Non-genomic actions of androgens. *Frontiers in Neuroendocrinology*, *29*(2), 169–181.
- Fortress, A. M., Schram, S. L., Tuscher, J. J., & Frick, K. M. (2013). Canonical Wnt signaling is necessary for object recognition memory consolidation. *The Journal of Neuroscience: The Official Journal of the Society for Neuroscience*, *33*(31), 12619–12626.
- Fuentealba, L. C., Obernier, K., & Alvarez-Buylla, A. (2012). Adult neural stem cells bridge their niche. *Cell Stem Cell*, *10*, 698–708.
- García-Segura, L. M., Wozniak, A., Azcoitia, I., Rodríguez, J. R., Hutchison, R. E., & Hutchison, J. B. (1999). Aromatase expression by astrocytes after brain injury: Implications for local estrogen formation in brain repair. *Neuroscience*, *89*(2), 567–578.

- Genazzani, A. R., Pluchino, N., Freschi, L., Ninni, F., & Luisi, M. (2007). Androgens and the brain. *Maturitas*, *57*, 27–30.
- Ghoulari, A. M., Ibanez, C., El-Etr, M., Leclerc, P., Eychenne, B., O'Malley, B. W., et al. (2003). Progesterone and its metabolites increase myelin basic protein expression in organotypic slice cultures of rat cerebellum. *Journal of Neurochemistry*, *86*(4), 848–859.
- González, M., Cabrera-Socorro, A., Pérez-García, C. G., Fraser, J. D., López, F. J., Alonso, R., et al. (2007). Distribution patterns of estrogen receptor alpha and beta in the human cortex and hippocampus during development and adulthood. *The Journal of Comparative Neurology*, *503*(6), 790–802.
- González-Agüero, G., Ondarza, R., Gamboa-Domínguez, A., Cerbón, M. A., & Camacho-Arroyo, I. (2001). Progesterone receptor isoforms expression pattern in human astrocytomas. *Brain Research Bulletin*, *56*(1), 43–48.
- Gonzalez-Billault, C., Muñoz-Llancao, P., Henriquez, D. R., Wojnacki, J., Conde, C., & Caceres, A. (2012). The role of small GTPases in neuronal morphogenesis and polarity. *Cytoskeleton*, *69*(7), 464–485.
- González-Burgos, I., Alejandre-Gómez, M., & Cervantes, M. (2005). Spine-type densities of hippocampal CA1 neurons vary in proestrus and estrus rats. *Neuroscience Letters*, *379*(1), 52–54.
- González-Orozco, J. C., & Camacho-Arroyo, I. (2019). Progesterone actions during central nervous system development. *Frontiers in Neuroscience*, *13*, 503.
- Gooch, M. D., & Stennett, D. J. (1996). Molecular basis of Alzheimer's disease. *American Journal of Health-System Pharmacy*, *53*, 1545–1557.
- Gould, E., Woolley, C. S., Frankfurt, M., & McEwen, B. S. (1990). Gonadal steroids regulate dendritic spine density in hippocampal pyramidal cells in adulthood. *The Journal of Neuroscience: The Official Journal of the Society for Neuroscience*, *10*(4), 1286–1291.
- Grassi, S., Frondaroli, A., Dieni, C., Scarduzio, M., & Pettorossi, V. E. (2009). Long-term potentiation in the rat medial vestibular nuclei depends on locally synthesized 17 β -estradiol. *Journal of Neuroscience*, *29*, 10779–10783.
- Hamson, D. K., Wainwright, S. R., Taylor, J. R., Jones, B. A., Watson, N. V., & Galea, L. A. M. (2013). Androgens increase survival of adult-born neurons in the dentate gyrus by an androgen receptor-dependent mechanism in male rats. *Endocrinology*, *154*, 3294–3304.
- Hansberg-Pastor, V., González-Arenas, A., Piña-Medina, A. G., & Camacho-Arroyo, I. (2015). Sex hormones regulate cytoskeletal proteins involved in brain plasticity. *Frontiers in Psychiatry/Frontiers Research Foundation*, *6*, 165.
- Hara, Y., Waters, E. M., McEwen, B. S., & Morrison, J. H. (2015). Estrogen effects on cognitive and synaptic health over the lifecourse. *Physiological Reviews*, *95*, 785–807.
- Hasegawa, Y., Hojo, Y., Kojima, H., Ikeda, M., Hotta, K., Sato, R., et al. (2015). Estradiol rapidly modulates synaptic plasticity of hippocampal neurons: Involvement of kinase networks. *Brain Research*, *1621*, 147–161.
- Hatanaka, Y., Hojo, Y., Mukai, H., Murakami, G., Komatsuzaki, Y., Kim, J., et al. (2015). Rapid increase of spines by dihydrotestosterone and testosterone in hippocampal neurons: Dependence on synaptic androgen receptor and kinase networks. *Brain Research*, *1621*, 121–132.
- Hillner, K. M., Jacobs, V. R., Fischer, T., & Aigner, L. (2014). The maternal brain: An organ with peripartur plasticity. *Neural Plasticity*, *2014*, 1–20.
- Honkura, N., Matsuzaki, M., Noguchi, J., Ellis-Davies, G. C. R., & Kasai, H. (2008). The subsynaptic organization of actin fibers regulates the structure and plasticity of dendritic spines. *Neuron*, *57*, 719–729.
- Horwood, J. M., Dufour, F., Laroche, S., & Davis, S. (2006). Signalling mechanisms mediated by the phosphoinositide 3-kinase/Akt cascade in synaptic plasticity and memory in the rat. *The European Journal of Neuroscience*, *23*(12), 3375–3384.

- Howard, B., Chen, Y., & Zecevic, N. (2006). Cortical progenitor cells in the developing human telencephalon. *Glia*, *53*, 57–66. <https://doi.org/10.1002/glia.20259>.
- Hussain, R., Ghomari, A. M., Bielecki, B., Steibel, J., Boehm, N., Liere, P., et al. (2013). The neural androgen receptor: A therapeutic target for myelin repair in chronic demyelination. *Brain*, *136*, 132–146.
- Jan, Y.-N., & Jan, L. Y. (2010). Branching out: Mechanisms of dendritic arborization. *Nature Reviews Neuroscience*, *11*(5), 316–328.
- Johnston, M. V. (2004). Clinical disorders of brain plasticity. *Brain and Development*, *26*, 73–80.
- Kaech, S., Parmar, H., Roelandse, M., Bornmann, C., & Matus, A. (2001). Cytoskeletal microdifferentiation: A mechanism for organizing morphological plasticity in dendrites. *Proceedings of the National Academy of Sciences of the United States of America*, *98*(13), 7086–7092.
- Kato, A., Hojo, Y., Higo, S., Komatsuzaki, Y., Murakami, G., Yoshino, H., et al. (2013). Female hippocampal estrogens have a significant correlation with cyclic fluctuation of hippocampal spines. *Frontiers in Neural Circuits*, *7*, 149.
- Kelly, A., & Lynch, M. A. (2000). Long-term potentiation in dentate gyrus of the rat is inhibited by the phosphoinositide 3-kinase inhibitor, wortmannin. *Neuropharmacology*, *39*(4), 643–651.
- Khan, M. M., Dhandapani, K. M., Zhang, Q.-G., & Brann, D. W. (2013). Estrogen regulation of spine density and excitatory synapses in rat prefrontal and somatosensory cerebral cortex. *Steroids*, *78*(6), 614–623.
- Klein, S. L., & Flanagan, K. L. (2016). Sex differences in immune responses. *Nature Reviews Immunology*, *16*, 626–638.
- Konkle, A. T. M., & McCarthy, M. M. (2011). Developmental time course of estradiol, testosterone, and dihydrotestosterone levels in discrete regions of male and female rat brain. *Endocrinology*, *152*(1), 223–235.
- Kramer, E. A., Chen, L. Y., Brandon, N. J., Rex, C. S., Liu, F., Gall, C. M., et al. (2009). Cytoskeletal changes underlie estrogen's acute effects on synaptic transmission and plasticity. *Journal of Neuroscience*, *29*, 12982–12993.
- Kretz, O., Fester, L., Wehrenberg, U., Zhou, L., Brauckmann, S., Zhao, S., et al. (2004). Hippocampal synapses depend on hippocampal estrogen synthesis. *The Journal of Neuroscience: The Official Journal of the Society for Neuroscience*, *24*(26), 5913–5921.
- Kuijpers, M., & Hoogenraad, C. C. (2011). Centrosomes, microtubules and neuronal development. *Molecular and Cellular Neuroscience*, *48*, 349–358.
- Lai, Y.-J., Yu, D., Zhang, J. H., & Chen, G.-J. (2017). Cooperation of genomic and rapid nongenomic actions of estrogens in synaptic plasticity. *Molecular Neurobiology*, *54*(6), 4113–4126.
- Leranth, C., Shanabrough, M., & Horvath, T. L. (2000). Hormonal regulation of hippocampal spine synapse density involves subcortical mediation. *Neuroscience*, *101*(2), 349–356.
- Lewis, M. C., Kerr, K. M., Orr, P. T., & Frick, K. M. (2008). Estradiol-induced enhancement of object memory consolidation involves NMDA receptors and protein kinase A in the dorsal hippocampus of female C57BL/6 mice. *Behavioral Neuroscience*, *122*(3), 716–721.
- Lopez-Juarez, A., Howard, J., Ullom, K., Howard, L., Grande, A., Pardo, A., et al. (2013). Gsx2 controls region-specific activation of neural stem cells and injury-induced neurogenesis in the adult subventricular zone. *Genes & Development*, *27*, 1272–1287.
- Luine, V., & Frankfurt, M. (2013). Interactions between estradiol, BDNF and dendritic spines in promoting memory. *Neuroscience*, *239*, 34–45.
- MacLusky, N. J., Hajszan, T., Prange-Kiel, J., & Leranth, C. (2006). Androgen modulation of hippocampal synaptic plasticity. *Neuroscience*, *138*, 957–965.

- Mannella, P. (2006). Estrogen receptor protein interaction with phosphatidylinositol 3-kinase leads to activation of phosphorylated Akt and extracellular signal-regulated kinase 1/2 in the same population of cortical neurons: A unified mechanism of estrogen action. *Journal of Neuroscience*, *26*, 9439–9447.
- Martella, G., Bonsi, P., Johnson, S. W., & Quartarone, A. (2018). Synaptic plasticity changes: Hallmark for neurological and psychiatric disorders. *Neural Plasticity*, *2018*, 9230704.
- Mazzucco, C. A., Lieblich, S. E., Bingham, B. I., Williamson, M. A., Viau, V., & Galea, L. A. M. (2006). Both estrogen receptor alpha and estrogen receptor beta agonists enhance cell proliferation in the dentate gyrus of adult female rats. *Neuroscience*, *141*(4), 1793–1800.
- McEwen, B. S., & Milner, T. A. (2017). Understanding the broad influence of sex hormones and sex differences in the brain. *Journal of Neuroscience Research*, *95*(1–2), 24–39.
- Mellon, S. H., & Griffin, L. D. (2002). Neurosteroids: Biochemistry and clinical significance. *Trends in Endocrinology & Metabolism*, *13*, 35–43.
- Mo, Z., Moore, A. R., Filipovic, R., Ogawa, Y., Kazuhiro, I., Antic, S. D., et al. (2007). Human cortical neurons originate from radial glia and neuron-restricted progenitors. *Journal of Neuroscience*, *27*, 4132–4145.
- Montes, P., Viguera-Villaseñor, R. M., Rojas-Castañeda, J. C., Monfil, T., Cervantes, M., & Morali, G. (2019). Progesterone treatment in rats after severe global cerebral ischemia promotes hippocampal dentate gyrus neurogenesis and functional recovery. *Neurological Research*, *41*(5), 429–436.
- Mundkur, N. (2005). Neuroplasticity in children. *The Indian Journal of Pediatrics*, *72*, 855–857.
- Murakami, G., Hojo, Y., Kato, A., Komatsuzaki, Y., Horie, S., Soma, M., et al. (2017). Rapid nongenomic modulation by neurosteroids of dendritic spines in the hippocampus: Androgen, oestrogen and corticosteroid. *Journal of Neuroendocrinology*, *30*(2), e12561.
- Naftolin, F., Ryan, K. J., & Petro, Z. (1971). Aromatization of androstenedione by the diencephalon. *The Journal of Clinical Endocrinology and Metabolism*, *33*(2), 368–370.
- Nimchinsky, E. A., Sabatini, B. L., & Svoboda, K. (2002). Structure and function of dendritic spines. *Annual Review of Physiology*, *64*, 313–353.
- Nugent, B. M., Tobet, S. A., Lara, H. E., Lucion, A. B., Wilson, M. E., Recabarren, S. E., et al. (2012). Hormonal programming across the lifespan. *Hormone and Metabolic Research*, *44*(8), 577–586.
- Okamoto, M., Hojo, Y., Inoue, K., Matsui, T., Kawato, S., McEwen, B. S., et al. (2012). Mild exercise increases dihydrotestosterone in hippocampus providing evidence for androgenic mediation of neurogenesis. *Proceedings of the National Academy of Sciences of the United States of America*, *109*, 13100–13105.
- Pauwels, L., Chalavi, S., & Swinnen, S. P. (2018). Aging and brain plasticity. *Aging*, *10*, 1789–1790.
- Ramanathan, D., Conner, J. M., & Tuszynski, M. H. (2006). A form of motor cortical plasticity that correlates with recovery of function after brain injury. *Proceedings of the National Academy of Sciences of the United States of America*, *103*(30), 11370–11375.
- Reddy, D. S. (2008). Mass spectrometric assay and physiological–pharmacological activity of androgenic neurosteroids. *Neurochemistry International*, *52*, 541–553.
- Reddy, D. S., & Jian, K. (2010). The testosterone-derived neurosteroid androstanediol is a positive allosteric modulator of GABA_A receptors. *Journal of Pharmacology and Experimental Therapeutics*, *334*, 1031–1041.
- Rocheport, N. L., & Konnerth, A. (2012). Dendritic spines: From structure to in vivo function. *EMBO Reports*, *13*, 699–708.
- Rune, G. M., Wehrenberg, U., Prange-Kiel, J., Zhou, L., Adelman, G., & Frotscher, M. (2002). Estrogen up-regulates estrogen receptor alpha and synaptophysin in slice cultures of rat hippocampus. *Neuroscience*, *113*(1), 167–175.

- Sakamoto, H., Ukena, K., & Tsutsui, K. (2002). Dendritic spine formation in response to progesterone synthesized de novo in the developing Purkinje cell in rats. *Neuroscience Letters*, 322(2), 111–115.
- Sanchez, A. M., Flamini, M. I., Genazzani, A. R., & Simoncini, T. (2013). Effects of progesterone and medroxyprogesterone on actin remodeling and neuronal spine formation. *Molecular Endocrinology*, 27(4), 693–702.
- Saraceno, G. E., Bellini, M. J., Garcia-Segura, L. M., & Capani, F. (2018). Estradiol activates PI3K/Akt/GSK3 pathway under chronic neurodegenerative conditions triggered by perinatal asphyxia. *Frontiers in Pharmacology*, 9, 335.
- Sato, K., Akaishi, T., Matsuki, N., Ohno, Y., & Nakazawa, K. (2007). Beta-estradiol induces synaptogenesis in the hippocampus by enhancing brain-derived neurotrophic factor release from dentate gyrus granule cells. *Brain Research*, 1150, 108–120.
- Schumacher, M., Hussain, R., Gago, N., Oudinet, J.-P., Mattern, C., & Ghoumari, A. M. (2012). Progesterone synthesis in the nervous system: Implications for myelination and myelin repair. *Frontiers in Neuroscience*, 6, 10.
- Seifert-Held, T., Pekar, T., Gattringer, T., Simmet, N. E., Scharnagl, H., Stojakovic, T., et al. (2011). Circulating Dickkopf-1 in acute ischemic stroke and clinically stable cerebrovascular disease. *Atherosclerosis*, 218(1), 233–237.
- Spalding, K. L., Bergmann, O., Alkass, K., Bernard, S., Salehpour, M., Huttner, H. B., et al. (2013). Dynamics of hippocampal neurogenesis in adult humans. *Cell*, 153(6), 1219–1227.
- Spritzer, M. D., & Galea, L. A. M. (2007). Testosterone and dihydrotestosterone, but not estradiol, enhance survival of new hippocampal neurons in adult male rats. *Developmental Neurobiology*, 67, 1321–1333.
- Tarsa, L., & Goda, Y. (2002). Synaptophysin regulates activity-dependent synapse formation in cultured hippocampal neurons. *Proceedings of the National Academy of Sciences of the United States of America*, 99(2), 1012–1016.
- Tsutsui, K., Ukena, K., Sakamoto, H., Okuyama, S.-I., & Haraguchi, S. (2011). Biosynthesis, mode of action, and functional significance of neurosteroids in the Purkinje cell. *Frontiers in Endocrinology*, 2, 61.
- Vaegan, & Taylor, D. (1979). Critical period for deprivation amblyopia in children. *Transactions of the Ophthalmological Societies of the United Kingdom*, 99(3), 432–439.
- Valadez-Cosmes, P., Germán-Castelán, L., González-Arenas, A., Velasco-Velázquez, M. A., Hansberg-Pastor, V., & Camacho-Arroyo, I. (2015). Expression and hormonal regulation of membrane progesterone receptors in human astrocytoma cells. *The Journal of Steroid Biochemistry and Molecular Biology*, 154, 176–185.
- Wang, J. M., Liu, L., & Brinton, R. D. (2008). Estradiol-17 β -induced human neural progenitor cell proliferation is mediated by an estrogen receptor β -phosphorylated extracellularly regulated kinase pathway. *Endocrinology*, 149, 208–218.
- Wolf, O. T., Naumann, E., Hellhammer, D. H., & Kirschbaum, C. (1998). Effects of dehydroepiandrosterone replacement in elderly men on event-related potentials, memory, and well-being. *The Journals of Gerontology Series A: Biological Sciences and Medical Sciences*, 53A, M385–M390.
- Woolley, C. S., & McEwen, B. S. (1993). Roles of estradiol and progesterone in regulation of hippocampal dendritic spine density during the estrous cycle in the rat. *The Journal of Comparative Neurology*, 336, 293–306.
- Woolley, C. S., Wenzel, H. J., & Schwartzkroin, P. A. (1996). Estradiol increases the frequency of multiple synapse boutons in the hippocampal CA1 region of the adult female rat. *The Journal of Comparative Neurology*, 373(1), 108–117.
- Yague, J. G., Wang, A. C.-J., Janssen, W. G. M., Hof, P. R., Garcia-Segura, L. M., Azcoitia, I., et al. (2008). Aromatase distribution in the monkey temporal neocortex and hippocampus. *Brain Research*, 1209, 115–127.

- Yamamura, T., Barker, J. M., Balthazart, J., & Ball, G. F. (2011). Androgens and estrogens synergistically regulate the expression of doublecortin and enhance neuronal recruitment in the song system of adult female canaries. *Journal of Neuroscience*, *31*, 9649–9657.
- Zhang, Q.-G., Wang, R., Khan, M., Mahesh, V., & Brann, D. W. (2008). Role of Dickkopf-1, an antagonist of the Wnt/beta-catenin signaling pathway, in estrogen-induced neuroprotection and attenuation of tau phosphorylation. *The Journal of Neuroscience: The Official Journal of the Society for Neuroscience*, *28*(34), 8430–8441.
- Zhang, Z., Yang, R., Cai, W., Bai, Y., Sokabe, M., & Chen, L. (2010). Treatment with progesterone after focal cerebral ischemia suppresses proliferation of progenitor cells but enhances survival of newborn neurons in adult male mice. *Neuropharmacology*, *58*(6), 930–939.
- Zheng, J.-Y., Liang, K.-S., Wang, X.-J., Zhou, X.-Y., Sun, J., & Zhou, S.-N. (2017). Chronic estradiol administration during the early stage of Alzheimer's disease pathology rescues adult hippocampal neurogenesis and ameliorates cognitive deficits in A β 1-42 mice. *Molecular Neurobiology*, *54*, 7656–7669.

Article

Estradiol Induces Epithelial to Mesenchymal Transition of Human Glioblastoma Cells

Ana M. Hernández-Vega ¹, Aylin Del Moral-Morales ¹, Carmen J. Zamora-Sánchez ¹,
Ana G. Piña-Medina ², Aliesha González-Arenas ³ and Ignacio Camacho-Arroyo ^{1,*}

¹ Unidad de Investigación en Reproducción Humana, Instituto Nacional de Perinatología-Facultad de Química, Universidad Nacional Autónoma de México, México City CP 11000, Mexico; anahdzvg@gmail.com (A.M.H.-V.); aybindmm@gmail.com (A.D.M.-M.); carmenjaninzamora@comunidad.unam.mx (C.J.Z.-S.)

² Departamento de Biología, Facultad de Química, Universidad Nacional Autónoma de México, México City CP 04510, Mexico; a.gabriela.pime@gmail.com

³ Departamento de Medicina Genómica y Toxicología Ambiental, Instituto de Investigaciones Biomédicas, Universidad Nacional Autónoma de México, México City CP 04510, Mexico; alieshag@iibiomedicas.unam.mx

* Correspondence: camachoarroyo@gmail.com; Tel.: +52-55-5622-3732

Received: 4 July 2020; Accepted: 11 August 2020; Published: 21 August 2020



Abstract: The mesenchymal phenotype of glioblastoma multiforme (GBM), the most frequent and malignant brain tumor, is associated with the worst prognosis. The epithelial–mesenchymal transition (EMT) is a cell plasticity mechanism involved in GBM malignancy. In this study, we determined 17 β -estradiol (E2)-induced EMT by changes in cell morphology, expression of EMT markers, and cell migration and invasion assays in human GBM-derived cell lines. E2 (10 nM) modified the shape and size of GBM cells due to a reorganization of actin filaments. We evaluated EMT markers expression by RT-qPCR, Western blot, and immunofluorescence. We found that E2 upregulated the expression of the mesenchymal markers, vimentin, and N-cadherin. Scratch and transwell assays showed that E2 increased migration and invasion of GBM cells. The estrogen receptor- α (ER- α)-selective agonist 4,4',4''-(4-propyl-[1H]-pyrazole-1,3,5-triyl)trisphenol (PPT, 10 nM) affected similarly to E2 in terms of the expression of EMT markers and cell migration, and the treatment with the ER- α antagonist methyl-piperidino-pyrazole (MPP, 1 μ M) blocked E2 and PPT effects. ER- β -selective agonist diarylpropionitrile (DNP, 10 nM) and antagonist 4-[2-phenyl-5,7-bis(trifluoromethyl)pyrazole[1,5-a]pyrimidin-3-yl]phenol (PHTPP, 1 μ M) showed no effects on EMT marker expression. These data suggest that E2 induces EMT activation through ER- α in human GBM-derived cells.

Keywords: epithelial–mesenchymal transition (EMT); glioblastoma multiforme (GBM); 17 β -estradiol (E2); estrogen receptors (ERs)

1. Introduction

Malignant tumors of the central nervous system (CNS) are among the cancers with the worst prognosis. Glioblastoma multiforme (GBM) comprises approximately half of the malignant primary brain tumors and causes 3–4% of cancer-related deaths [1]. The World Health Organization defines GBM as a grade IV astrocytoma tumor characterized by uncontrolled proliferation, necrosis propensity, angiogenesis, deep infiltration, apoptosis resistance, genomic instability, and extensive heterogeneity at the cellular and molecular levels [2,3]. The Cancer Genome Atlas (TCGA) network identified four molecular subtypes of GBM on the basis of the gene expression profile of neural progenitor cells (proneural, PN), neurons (neural, N), proliferative cells with activation of the tyrosine kinase receptor (classical, CL), and mesenchymal tissue (mesenchymal, MES) [4]. The mesenchymal phenotype of

GBM tends to have the worst survival rates compared to the other subtypes, and it is associated with a highly invasive behavior [5–7].

Epithelial-to-mesenchymal transition (EMT) is a mechanism of cellular plasticity that regulates a set of transient states between the epithelial and mesenchymal phenotype. During EMT, epithelial cells lose their junctions with other cells and the apicobasal polarity while they acquire a mesenchymal phenotype with migratory and invasive properties [8]. EMT is a highly dynamic and transient mechanism induced by diverse signals and orchestrated by EMT-inducing transcription factors (EMT-TFs), which act in close association with the epigenetic machinery by repressing epithelial genes and activating mesenchymal genes [9]. The reverse process is the mesenchymal–epithelial transition (MET) [10]. EMT is essential in diverse physiological and pathological processes [11]. This mechanism is associated with embryogenesis [12–14], heart regeneration [15], wound healing, fibrosis, and organ repair [16]. In tumor cells, the activation of EMT-TFs promotes the mechanisms of migration, invasion, metastasis, apoptosis inhibition, resistance to radio- and chemotherapy, as well as maintenance of the plasticity of cancer stem cells [17].

Although EMT is typical in epithelial tumors, evidence suggests that EMT-TFs also lead to a gain in mesenchymal properties and the promotion of malignancy of non-epithelial tumors, including brain tumors, hematopoietic malignancies, and sarcomas [18,19]. Currently, the classic description of EMT as a process of change between two alternative states (epithelial and mesenchymal) has been replaced by a new concept of cellular plasticity and transient states, which proposes that cells move through a spectrum of various intermediate phases, which means that cells can carry out partial EMT programs [20]. Several studies have shown the role of EMT in GBM progression. Large-scale expression analysis of 85 highly diffuse glioma tumors revealed a set of genes associated with mesenchymal tissue overexpressed in GBM biopsies [21]. Tso et al. showed that a subset of primary GBM tumors expresses cellular and molecular markers associated with mesenchymal stem cells [22]. Then, the definition of the GBM mesenchymal subtype convincingly showed the clinical importance of the EMT program in tumor diagnosis and treatment [4,5]. Molecular profile analysis of the four GBM subtypes demonstrated that the mesenchymal subtype, unlike the other subtypes, presents the molecular characteristics of EMT [23].

Determination of the complete molecular network of the EMT program, as well as the fundamental mechanisms necessary to activate it, could provide new therapeutic approaches for GBM treatment. Autocrine and paracrine interactions within the GBM microenvironment induce EMT through intracellular signaling pathways that activate EMT-TFs. Although different studies have described several signaling pathways that induce EMT in GBM, the role of the different factors within the tumor microenvironment, as well as all the interactions that coordinate this cellular program, is still not understood.

Sex steroid hormones such as estrogens participate in a wide variety of functions throughout the nervous system. These hormones are mainly synthesized in the gonads and the adrenal glands, but they can also be produced *de novo* within the brain [24,25]. Estrogens include estrone (E1), 17 β -estradiol (E2), and estriol (E3). E2 is involved in many brain functions, such as brain development during sexual differentiation [26], differentiation of neurons and glial cells [27,28], and regulation of neurite growth and synaptic patterns [29,30], and it interacts with the glutamatergic, dopaminergic, and serotonergic neurotransmission pathways that influence the generation of memory, learning, and emotional state [31–33]. Estrogens act by binding specific intracellular and membrane receptors. There are two estrogen-specific intracellular receptor subtypes, estrogen receptors α and β (ER α and ER β), which are ligand-activated transcription factors that directly regulate gene expression. Moreover, these receptors are associated with the plasma membrane, where they activate intracellular signaling pathways [34].

E2 concentrations, as well as ERs expression and activity, are determinant in the malignant progression of tumors growing in estrogen-sensitive tissues [35–38]. On the basis of these studies, ER- α promotes cell proliferation, whereas ER- β has anti-proliferative effects [39]. ER expression status

in GBM is controversial. Some studies have reported the absence of ER in GBM [40,41], while other researchers have determined that ER expression varies according to malignancy degree, suggesting that these receptors are involved in GBM malignant progression [42–50]. ER subtypes have shown different effects in GBMs. E2 and 4,4',4''-(4-propyl-[1H]-pyrazole-1,3,5-triyl)trisphenol (PPT), a selective agonist of ER- α , increased the number of cells derived from human GBM [45], while ER- β -specific agonists decreased GBM cell proliferation [44]. However, the molecular mechanisms of E2 related to GBM malignant progression are still unclear.

E2-promoted signaling is known to be related to EMT induction in estrogen-responsive tissues. In ovarian and prostate cancer, E2 treatment induces ER- α -dependent EMT, while receptor silencing inhibits EMT [51–53]. Nevertheless, loss of ER- α expression in breast and endometrial cancer promotes morphological changes, motility, and improved invasion, as well as increased expression of EMT markers [54–58]. These investigations demonstrate the importance of specific cell context in the E2-induced EMT. However, E2 involvement in the EMT program in GBM is unknown.

To increase the knowledge regarding the EMT program of GBM, in this study, we investigated the participation of E2 on EMT induction in human GBM-derived cells expressing both ER subtypes. Our results showed that the treatment with E2 (10 nM) promoted: (1) changes in cell morphology and the structure of the actin cytoskeleton, (2) increased expression of mesenchymal markers such as vimentin and N-cadherin, and (3) increased migratory and invasive capacity of GBM cells. These effects were dependent on ER- α , since the treatment with its agonist, PPT (10 nM), produced similar results to E2, while the treatment with its antagonist methyl-piperidino-pyrazole (MPP, 1 μ M), blocked the effects of E2 and PPT.

2. Materials and Methods

2.1. TCGA Data Analysis

Ribonucleic acid sequencing (RNA-Seq) counts were obtained from low-grade gliomas (LGG, $n = 167$) and glioblastoma (GBM, $n = 155$) projects of The Cancer Genome Atlas (TCGA) repository (<https://portal.gdc.cancer.gov/>). The data were downloaded and processed using TCGAbiolinks package version 2.12.6 for R [59]. Additionally, expression profiles were obtained from healthy brain cortex samples ($n = 249$) in the GTEx database (<https://gtexportal.org/home/>). Data were normalized by DESeq2 version 1.22.2 [60] and plotted. TCGA_analyse_survival utility from the TCGAbiolinks package for R performed survival analysis.

2.2. Cell Cultures

Human GBM-derived cell lines U87, U251, T98, and LN229 (American Type Culture Collection, ATCC, Manassas, VA, USA) were cultivated in Dulbecco's modified Eagle's medium (DMEM, L0107-500) high glucose supplemented with 10% fetal bovine serum (FBS; S1650), 1.0 mM pyruvate (L0642-100), 1.0 mM antibiotic (streptomycin 10 g/L; penicillin G 6.028 g/L; and amphotericin B 0.025 g/L, L0010), and 0.1 mM non-essential amino acids (X0557-100, Biowest, Nuaille, PDL, France). Cell cultures were maintained at 37 °C in a humidified atmosphere with 5% CO₂. At 60% confluence (24 h before treatments), cells were culture in DMEM no phenol red (ME-019 Thermo Fisher Scientific, Waltham, MA, USA) supplemented with 10% charcoal/dextran-treated FBS (SH30068.03, Thermo Fisher Scientific), 1.0 mM pyruvate, 1.0 mM antibiotics, and 0.1 mM non-essential amino acids. When indicated, cells were treated with E2 (10 nM, E4389, Sigma-Aldrich, St. Louis, MO, USA), ER- α -selective agonist PPT (10 nM, 1426, Tocris, Bristol, UK, England), ER- β -selective agonist diarylpropionitrile (DNP, 10 nM, 1494, Tocris), ER- α -selective antagonist MPP (1 μ M, 1991, Tocris), and ER- β -selective antagonist 4-[2-phenyl-5,7-bis(trifluoromethyl)pyrazole[1,5-a]pyrimidin-3-yl]phenol (PHTPP, 1 μ M, 2662, Tocris). In combined treatments, antagonists MPP and PHTPP were added 2 h before the addition of agonist.

2.3. Cell Morphology Analysis

The epithelial phenotype is characterized by a polygonal shape, while the mesenchymal phenotype is spindle-shaped. Therefore, the geometric characteristics of both phenotypes differ from each other. Geometric characteristics can be quantified using high-performance software for the analysis of cell images [61–64]. The morphological changes of the U251, U87, T98G, and LN229 cells treated with vehicle and E2 at 0, 48, and 72 h were determined by phase contrast microscopy (IX71, inverted microscope Olympus, Shinjuku, TY, Japan), digitally capturing six arbitrary fields with a 400X magnification for each of the treatments. Adobe Photoshop CS6 software (Adobe Systems Inc., San Jose, CA, USA) was used to process the background correction and illumination of the captured images. Subsequently, the orientation, shape, and position of each of the cells in each image was determined to segment them with the Image-Pro software 10.0.6 (Media Cybernetics Inc., Rockville, MD, USA), which has automated algorithms to identify, separate, and quantify each of the cells that appear in the image. This quantification allows the extraction of various geometric characteristics that determine morphological parameters of the cells segmented in the two-dimensional plane.

2.4. RT-qPCR

Total RNA was extracted from cells by guanidine–thiocyanate–phenol–chloroform method with TRIzol LS Reagent (10296028, Thermo Fisher Scientific, Waltham, MA, USA), following the supplier's protocol, and was measured by spectrophotometry (Nanodrop 2000 spectrophotometer, Thermo Fisher Scientific). RNA integrity was checked by electrophoresis with 1.5% agarose gel in Tris-Borate-ethylenediaminetetraacetic acid (EDTA) buffer (TBE: 89 mM Tris, 89 mM boric acid, 2.0 mM EDTA (pH 8.3)) detected by fluorescence with GreenSafe (MB13201, NZYTech, Lisboa, PT, Portugal). Human astrocyte RNA was purchased from ScienCell Research Laboratories (1805, Carlsbad, CA, USA). Moloney Murine Leukemia Virus Reverse Transcriptase (M-MLV RT, 28025013, Thermo Fisher Scientific) was used to obtain the complementary DNA (cDNA) from one microgram of extracted RNA following the protocol recommended by the provider. Gene expression relative to the 18S ribosomal RNA (rRNA) gene was quantified through the quantitative polymerase chain reaction (qPCR) using standardized primers for each gene: ESR1 (estrogen receptor 1/ α) (FW-5'-agcaccctgaagtctctgga-3', RV-5'-gatgtgggagaggatgagga-3'); ESR2 (estrogen receptor 2/ β) (FW-5'-aagaagattcccggctttgt-3', RV-5'-tctacgcatttcccctcatc-3'); VIM (vimentin) (FW-5'-ggaccagtaaccaacgaca-3', RV-5'-aaggtcaagacgtgccagag-3'); CDH2 (cadherin-2/N-cadherin) (FW-5'-ctggagacattggggacttc-3', RV-5'-gagcactgccttcatagt-3'); TJP1 (tight junction protein 1/zonula occludens 1 (ZO-1)) (FW-5'-gccattcccgaaggagtga-3', RV-5'-atcacagtgtggaagcg-3'); rRNA18S (FW-5'-agtgaaactgcgaa tggctc-3', RV-5'-ctgaccgggtggtttgat-3'). FastStart DNA Master SYBR Green I kit (12239264001, Roche, Basel, Switzerland) was used to perform gene amplification in a LightCycler 2.0 instrument (03531414001, Roche). Relative expression was quantified by the comparative $2^{-\Delta\Delta C_t}$ method [65,66].

2.5. Western Blot

U251, U87, T98G, and LN229 cells were detached from culture plates using cold phosphate-buffered saline (PBS: 137 mM NaCl, 2.7 mM KCl, 10.0 mM Na₂HPO₄, 1.8 mM KH₂PO₄ (pH 7.4)) and cell scraper. The pellet obtained from the centrifuged cells at 45 × g for 3 min were lysed with radioimmunoprecipitation assay buffer (RIPA: 50 mM Tris-HCl, 150 mM NaCl, 1% Triton X-100, 0.1% sodium dodecyl sulfate (SDS) (pH 8.0)) supplemented with protease inhibitor cocktail (P8340, Sigma-Aldrich, St. Louis, MO, USA). Total proteins were extracted by centrifugation at 20,817 × g at 4 °C for 15 min and quantified by spectrophotometry (NanoDrop 2000 spectrophotometer, Thermo Fisher Scientific, Waltham, MA, USA) using the Pierce 660 nm protein assay reagent (22660, Thermo Fisher Scientific). Thirty µg of total protein was separated on 10% SDS-polyacrylamide gel electrophoresis (PAGE) at 80 V for 4 h and then transferred to a polyvinylidene fluoride (PVDF) membrane (IPVH00010, Merck, Kenilworth, NY, USA) at 20 V in semidry conditions at room temperature for 45 min. Membranes were blocked with 5% bovine serum albumin (BSA, A9418, Sigma-Aldrich) in Tris-buffered saline-Tween

(TBST: 150 mM NaCl, 50 mM Tris-HCl, 0.1% Tween (pH 7.6)) with constant agitation at 37 °C for 2 h, and then incubated with primary antibodies: anti-ER α (2 μ g/mL, rabbit polyclonal, ab3575, Abcam, Cambridge, UK, England), anti-ER β (0.4 μ g/mL, mouse monoclonal 1531: sc-53494), anti-ZO-1 (0.6 μ g/mL, rat monoclonal R40.76: sc-33725), anti-N-cadherin (0.8 μ g/mL, mouse monoclonal D-4: sc-8424), anti-vimentin (0.4 μ g/mL, mouse monoclonal V9: sc-6260), and α -tubulin (0.4 μ g/mL, mouse monoclonal A-6: sc-398103) (Santa Cruz Biotechnology, Dallas, TX, USA), diluted with 5% BSA in TBST at 4 °C for 48 h. Subsequently, the membranes were washed with TBST three times every 5 min and incubated with secondary antibodies conjugated to horseradish peroxidase (HRP): anti-rabbit (0.06 μ g/mL, goat polyclonal Immunoglobulin G (IgG) containing two heavy chains (H) and two light chains (L) (H+L), 65-6120; Thermo Fisher Scientific), anti-mouse (0.013 μ g/mL, purified recombinant mouse IgG κ light chain: sc-516102; Santa Cruz Biotechnology), and anti-rat (0.06 μ g/mL, goat polyclonal IgG (H+L), ab97057, Abcam) at room temperature and constant agitation for 45 min, and again washed with TBST three times every 5 min. Finally, Super Signal West Femto Maximum Sensitivity Substrate reagent (34096, Thermo Fisher Scientific) was incubated in the membranes, and immunoreactive bands were detected by chemiluminescence exposing blots to Kodak Biomax Light Film (Z370371, Sigma-Aldrich) captured by a digital camera of 14.1 megapixels (SD1400IS, Canon Inc., Ota, TY, Japan). ImageJ software (1.52u, National Institutes of Health, NIH, Bethesda, MD, USA) performed the densitometric analysis of blot images.

2.6. Immunofluorescence

U251 and U87 cells were fixed with 4% paraformaldehyde (4% PFA) at room temperature for 20 min, washed with PBS, and then incubated in permeabilizing blocking solution (1% BSA, 1% glycine, 0.2% Triton X-100, diluted in PBS) at room temperature for 90 min. Subsequently, cells were incubated with primary antibodies: anti-Actin (4 μ g/mL, goat polyclonal C-11, sc-1615), anti-ZO-1 (8 μ g/mL, rat monoclonal R40.76: sc-33725), anti-N-cadherin (8 μ g/mL, mouse monoclonal D-4: sc-8424), and anti-vimentin (4 μ g/mL, mouse monoclonal V9: sc-6260) (Santa Cruz Biotechnology, Dallas, TX, USA) at 4 °C overnight, and then rinsed three times every 5 min with PBST (PBS with 0.05% Tween). Later, cells were incubated with secondary antibodies: anti-mouse (4 μ g/mL, goat polyclonal IgG (H+L) Alexa Fluor 488: A11001, Thermo Fisher Scientific, Waltham, MA, USA), anti-rat (4 μ g/mL, goat polyclonal IgG (H+L) Alexa Fluor 488: ab150157, Abcam, Cambridge, UK, England), and anti-goat (8 μ g/mL, donkey IgG-FITC: sc-2024, Santa Cruz Biotechnology) at room temperature for 90 min, and again rinsed with PBST three times every 5 min. Nuclei were stained with Hoechst 33,342 (1 mg/mL, 62249, Thermo Fisher Scientific) at room temperature for 7 min and rinsed three times every 5 min with PBST. Finally, cells were coverslipped with mounting medium (18606-20, Polysciences, Warrington, PA, USA) and visualized by fluorescence microscopy (Bx43, light microscope, Olympus, Shinjuku, TY, Japan), digitally capturing six arbitrary fields with a 400 \times magnification. Fluorescence density was measured as integrated density from the *Analyze* menu of ImageJ software.

2.7. Migration Assay

Wound healing assays were performed to determine the migratory capacity of cells. U251 and U87 cells grew in DMEM high glucose supplemented until reaching 70% confluence. Then, the medium was changed to DMEM no phenol red supplemented 10% charcoal/dextran-treated FBS, 1.0 mM pyruvate, 1.0 mM antibiotics, and 0.1 mM non-essential amino acids, and incubated at 37 °C in a humidified atmosphere with 5% CO₂. Upon 90% confluence, a scratch was made using a 200 μ L pipette tip. Cells floating were rinsed with PBS and DMEM no phenol red-supplemented 10% charcoal/dextran treated-FBS, 1.0 mM pyruvate, 1.0 mM antibiotics, and 0.1 mM non-essential amino acids were added again. One hour before adding the experimental treatments, we incubated the cells with cytosine β -D-arabinofuranoside hydrochloride (10 μ M, Ara-C, C1768, Sigma-Aldrich, St. Louis, MO, USA), a selective inhibitor of DNA synthesis. Images of the wound area captured at 100 \times magnification with an Infinity 1-2C camera (Lumenera, Ottawa, ON, Canada) connected to an inverted microscope (CKX41,

Olympus, Shinjuku, TY, Japan) at 0, 12, and 24 h of treatment were analyzed using the MRI Wound Healing Tool plugins of Image J software.

2.8. Invasion Assay

Transwell assay determined the invasion potential of cells. Transwell inserts with 10 μm membrane thickness and 8 μm pore size (3422, Corning, Corning, NY, USA) were placed in 24-well plates, and each well was covered with 50 μL of ECM Gel from Engelbreth-Holm-Swarm murine sarcoma (2 mg/mL, matrigel E1270, Sigma-Aldrich, St. Louis, MO, USA) diluted in DMEM no phenol red without supplement, and immediately incubated at 37 °C for 2 hours. Then, 15,000 U87 cells or 10,000 U251 cells suspended in 150 μL DMEM no phenol red and without supplement with 10 μM Ara-C and treatments (vehicle or E2 10 nM) were added to the upper insert, while the lower wells were filled with 500 μL DMEM supplemented with 10% FBS as a chemoattractant were incubated in a humidified atmosphere with 5% CO₂ at 37 °C for 24 h. Transwell inserts were rinsed with PBS, fixed with 4% PFA for 20 min, and stained with 0.1% crystal violet dye for an additional 20 min. Inserts were washed three times with PBS for each 15 min in order to remove excess dye. Finally, images of invasive cells captured at 100 \times magnification with an Infinity 1-2C camera (Lumenera, Ottawa, ON, Canada) connected to an inverted microscope (CKX41, Olympus, Shinjuku, TY, Japan) were analyzed using the Cell Counter plugin in the ImageJ software.

2.9. Statistical Analysis

Data were analyzed and plotted with the GraphPad Prism 5.0 software (GraphPad, San Diego, CA, USA). Statistical analysis between comparable groups was performed using a one-way ANOVA with a Tukey post hoc-test. Time course analysis was performed using a two-way ANOVA test followed by Bonferroni post-test to compare replicate means by row. Values of $p < 0.05$ were considered statistically significant. Plotted data are representative of three independent experiments for each treatment.

3. Results

3.1. Differential Expression of ER α and ER β Subtypes in Human GBM-Derived Cells

We evaluated the mRNA expression levels of ESR1 (ER- α) and ESR2 (ER- β) genes in astrocytoma samples with different histological grades from the data obtained of the low-grade gliomas (LGG) and glioblastoma (GBM) projects from the TCGA repository, as well as samples of healthy cerebral cortex in the GTEx database. Low ESR1 expression levels were observed in GBM and LGG when compared to healthy tissue. A slight but significant increase was found in ESR1 expression in GBM as compared with LGG. These data highlight two critical points: (1) ESR1 expression was lower in gliomas compared to healthy tissue, (2) but also was higher in GBM compared to LGG, suggesting an important oncogenic role of ER- α in development of low- and high-grade gliomas. In contrast, ESR2 expression levels were higher in GBM as compared with LGG and healthy tissue (Figure 1A). Next, we compared ESR1 and ESR2 expression among the four GBM subtypes defined by Verhaak et al. [4]. The mesenchymal subtype showed higher levels of ESR1 mRNA expression compared to the classical and neural subtypes, without significant differences when compared with the proneural subtype. ESR2 expression in the mesenchymal subtype showed a tendency to be the highest, although it was only significantly higher when compared with the neural subtype ($p < 0.05$) (Figure 1B). It is interesting to highlight that our results showed that expression of both ER subtypes was enriched in the mesenchymal subtype. Analysis of expression in cell lines showed a similar trend to the TCGA data: the expression of both ESR1 and ESR2 in four cell lines derived from human GBM (U251, U87, T98G, and LN229) was found to be lower compared to the expression of normal human astrocytes (NHA). Among GBM cells, the ESR1 gene was expressed in a higher proportion in U251 cells, while ESR2 had a higher expression in U87 cells (Figure 1C). We evaluated the expression of both ERs subtypes at the protein level in GBM cells, and a higher content of ER- α than that of ER- β was observed in all cell lines. Moreover, we found two

isoforms of ER- β (ER- β_1 and ER- β_5) expressed in GBM cells; ER- β_1 was more abundant than ER- β_5 (Figure 1D). An analysis of the clinical outcome of ER expression in GBM patients showed that the higher expression of ER- α and ER- β was correlated with a poor prognosis. Therefore, patients with a low expression of both ER subtypes live longer than those with higher levels of expression (Figure 1E). Importantly, although lower ER- α expression was observed in GBM TCGA data compared to healthy tissue, survival analysis showed that high ER- α expression is a poor prognostic factor for the patients, which suggests that ER- α expression levels in GBM may not always be proportional to its oncogenic activity. These results suggest that ER- α and ER- β expression differentially changes among healthy tissue, LGG, and GBM, both in vivo and in vitro, and it also varies among GBM subtypes.

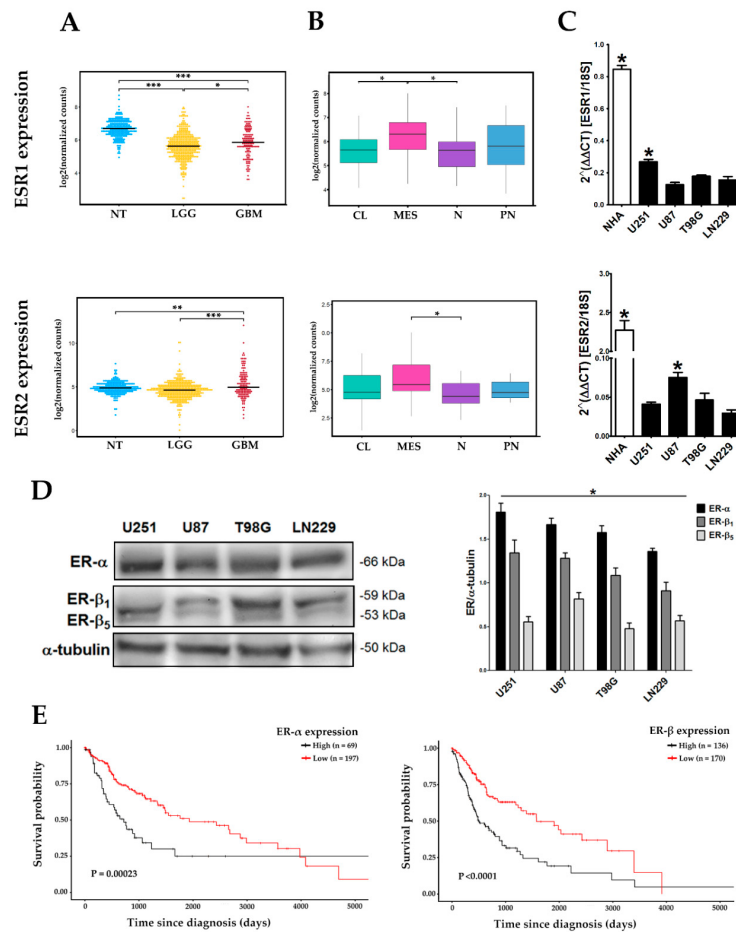


Figure 1. The estrogen receptor- α (ER- α) and estrogen receptor- β (ER- β) subtype gene expressions in human glioblastoma multiforme (GBM). **(A)** Ribonucleic acid sequencing (RNA-Seq) counts obtained from low-grade gliomas (LGG, $n = 167$) and GBM ($n = 155$) projects from The Cancer Genome Atlas (TCGA) and expression profiles obtained from healthy brain cortex samples (normal tissue, NT; $n = 249$) in the GTEx database. LGG includes grade I, II, and III gliomas. * $p < 0.05$; ** $p < 0.01$; *** $p < 0.001$. **(B)** RNA-Seq counts from GBM subtypes: classical (CL), mesenchymal (MES), neural (N), and proneural (PN) obtained from TCGA. * $p < 0.05$. **(C)** RT-qPCR quantified gene expression of estrogen receptor 1/ α (ESR1) and estrogen receptor 2/ β (ESR2) relative to the reference gene 18S ribosomal RNA (rRNA) using the comparative $2^{-\Delta\Delta C_t}$ method in total RNA from normal human astrocyte (NHA) and U251, U87, T98G, and LN229 human GBM-derived cells. Both receptor subtypes were less expressed in GBM cells than in NHAs. * $p < 0.05$ vs. all other groups; mean \pm standard error of the mean (SEM), $n = 3$. **(D)** ER- α and ER- β content analyzed by Western blot using α -tubulin as load control. The two main isoforms of ER- β expressed in GBM are shown: ER- β_1 and ER- β_5 . Representative blot image and the corresponding densitometric analysis for ER α and ER β expression in human GBM-derived cells. * $p < 0.05$ ER- α vs. ER- β and ER- β_1 vs. ER- β_5 ; mean \pm SEM, $n = 3$. **(E)** Survival analysis for ER- α and ER- β expression in GBM using TCGA data.

3.2. Changes in Cell Morphology During E2-Induced EMT

Morphological changes associated with EMT in U251 and U87 cells were evaluated after E2 (10 nM) treatment. At the beginning of the treatments, U251 cells presented a typical star-like morphology, and U87 cells a polygonal shape. Interestingly, the cells treated with E2 showed a spindle-shape and the typical features of mesenchymal cells at 48 and 72 h (Figure 2). Table 1 details the geometric parameters quantified in this work. Values close to the unity of the circularity and box XY (width/height) measurements are characteristic of a polygonal shape, while a high aspect (major/minor axis) and perimeter denote a fusiform shape. Plots show that E2 decreased circularity and box XY, while increased aspect and perimeter (Figure 2). This effect on the cellular morphology was consistent in T98G and LN229 cells (Figures S1 and S2). These results show that E2 promotes morphological changes associated with EMT.

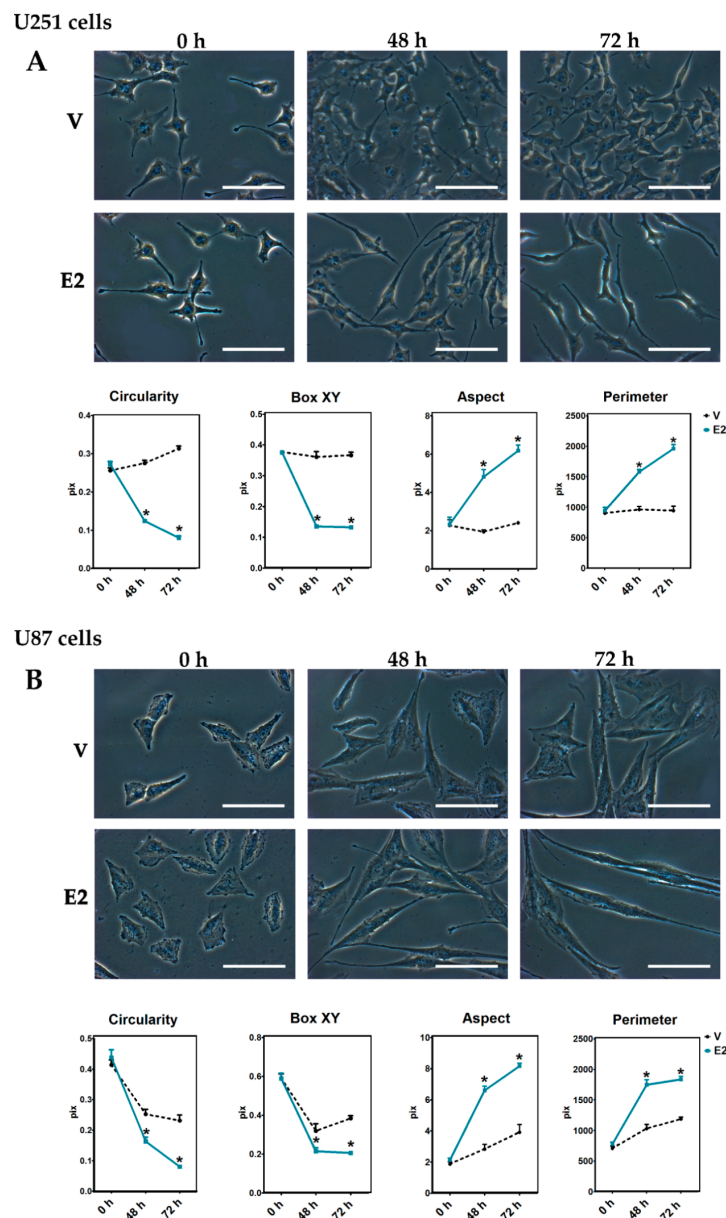


Figure 2. 17 β -Estradiol (E2)-induced morphological changes in human GBM-derived cells. (A) U251 and (B) U87 cells observed by phase-contrast microscopy with a magnification of 400 \times at 0, 48, and 72 h after adding 17 β -estradiol (E2, 10 nM) and the vehicle (V, 0.01% cyclodextrin). Magnification white bar = 100 μ m. Plots represent the quantification of the geometric parameters (circularity, box XY, aspect, perimeter) in this study. Results are expressed as the mean \pm standard error of the mean (SEM); $n = 3$; * $p < 0.05$ vs. V.

Table 1. Geometric parameters of Image-Pro software.

Parameter	Description	Image
Area	The area included in the polygon that defines the figure contour	
Axis major	Major axis length of an imaginary ellipse surrounding figure	
Axis minor	Minor axis length of an imaginary ellipse surrounding figure	
Aspect	The ratio between the major and minor axis of an ellipse	
Bound box height	Bounding box height of the figure	
Bound box width	Bounding box width of the figure	
Box XY	The ratio of width to height of bounding box	
Circularity	The ratio of figure area to the diameter of a circle around it	
Perimeter	Length of the region surrounding the figure	

3.3. E2-Induced Reorganization of Actin Filaments

To determine whether the morphological changes observed above were related to changes in the arrangement of actin filaments, we performed immunofluorescence assays in U251 and U87 cells. In U251 cells treated with vehicle, the actin filaments were predominantly organized into bundles of dense reticulated mesh, characteristic of cortical actin. In contrast, in cells treated with E2 (10 nM), the actin filaments assembled in parallel along the ventral surface of the cell, forming long projections towards the leading edge, which in the extreme showed focal sites with a high concentration of actin (Figure 3). In U87 cells, we observed a higher proportion of concentrated actin focal points, both in vehicle and E2 treated cells. However, cells incubated with E2 showed long parallel filament projections with a high concentration of actin around the edge (Figure 3). Thereby, the morphological changes induced by E2 in GBM cells were related to a reorganization of the actin filaments.

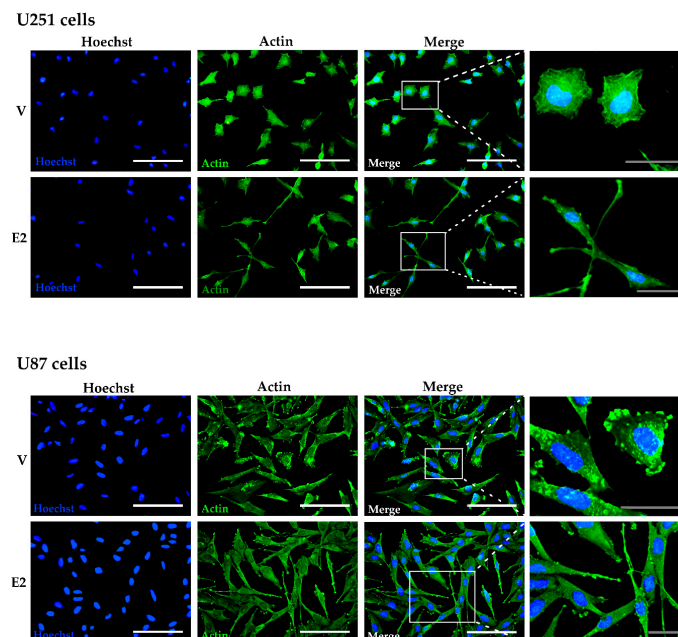


Figure 3. E2 rearranged the actin cytoskeleton of human GBM-derived cells. Actin immunostaining in U251 and U87 cells treated with 17 β -estradiol (E2, 10 nM) and vehicle (V, 0.01% cyclodextrin) for 48 h. Representative images captured under a fluorescence microscope at a magnification of 400 \times . Magnification white bar = 100 μ m and gray bar = 30 μ m.

3.4. E2 Regulated EMT Marker Expression

We analyzed the effects of E2 on EMT marker expression and distribution in GBM cells by RT-qPCR, Western blot, and immunofluorescence. We evaluated the peripheral membrane protein zonula occludens 1 (ZO-1, encoded by the TJP1 gene) as an epithelial marker, and the evaluated mesenchymal phenotype markers were N-cadherin (encoded by the CDH2 gene) and vimentin (encoded by the VIM gene). In U251 cells, E2 increased TJP1 expression only at 48 h, CDH2 expression from 24 to 72 h, and VIM expression from 48 h (Figure 4A). Importantly, ZO-1 protein content showed no changes due to E2 treatment, while the hormone increased the content of N-cadherin and vimentin proteins at 72 h (Figure 4B). E2 effects on U87 cells were like those of U251 cells. E2 upregulated TJP1 and ZO-1 expression from 48 h, CDH2 expression from 24 h, and N-cadherin expression from 48 h; VIM expression increased at 24 h, and decreased at 72 h, while the vimentin protein content increased at 72 h (Figure 4C,D).

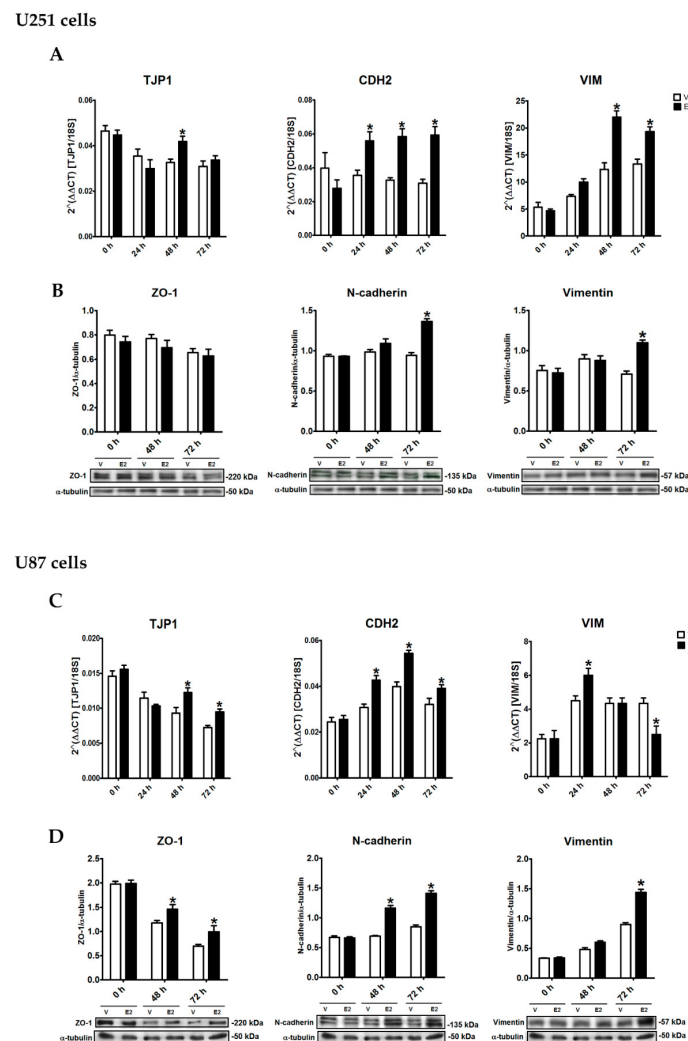


Figure 4. E2-regulated epithelial-to-mesenchymal transition (EMT) marker expression of human GBM-derived cells. (A,B) U251 and (C,D) U87 cells were treated with 17β-estradiol (E2, 10 nM) and vehicle (V, 0.01% cyclodextrin) for 24, 48, and 72 h. (A,C) Epithelial gene (tight junction protein 1 (TJP1)) and mesenchymal genes (vimentin (VIM) and cadherin-2/N-cadherin (CDH2)) expression was quantified by RT-qPCR using the comparative method 2^{-ΔΔCt} concerning the reference gene 18S rRNA. (B,D) Zonula occludens 1 (ZO-1), N-cadherin, and vimentin content was determined by Western blot. Densitometric analysis of EMT marker expression with their respective representative bands using α-tubulin as a load control showed that E2 increased EMT marker expression with different temporal dynamics. Results are expressed as the mean ± standard error of the mean (SEM); n = 3; * p < 0.05 vs. V.

The analysis of EMT markers by immunofluorescence showed that in U251 and U87 cells treated with the vehicle, ZO-1, and N-cadherin proteins were expressed in localized regions of the plasmatic membrane, particularly at cell-binding sites. In contrast, in E2-treated cells, these proteins were shown along the entire cell surface, especially in long projections at the cell ends (Figure 5A,B). Vimentin filaments formed a network within the cytoplasm in cells without E2, whereas in E2-incubated cells, vimentin filaments were arranged in parallel along the ventral surface of the cell, particularly at the borders, similar to actin filaments (Figure 5A,B). Overall, the fluorescence intensity of EMT markers significantly increased in E2-treated U251 and U87 cells (Figure 5C). These results show that E2 induces EMT marker expression and its redistribution in GBM cells.

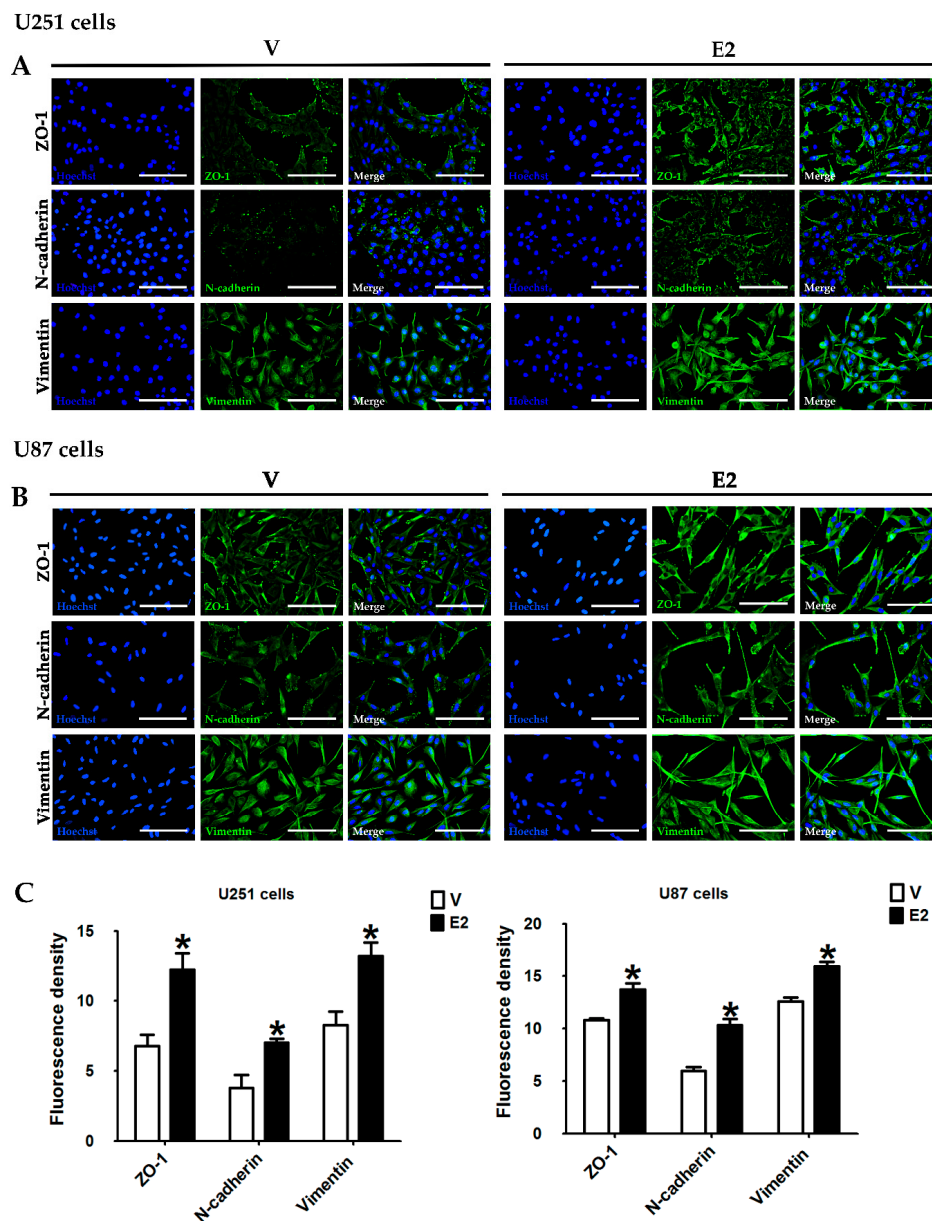


Figure 5. E2 modified EMT marker distribution and immunoreactivity in human GBM-derived cells. ZO-1, N-cadherin, and vimentin immunostaining in (A) U251 and (B) U87 cells treated with 17 β -estradiol (E2, 10 nM) and vehicle (V, 0.01% cyclodextrin) for 48 h. Representative images were captured under a fluorescence microscope at a magnification of 400 \times . (C) EMT marker expression measured as a fluorescence density. Results are expressed as the mean \pm standard error of the mean (SEM); $n = 3$; * $p < 0.05$ vs. V.

Furthermore, the increase in both epithelial and mesenchymal markers suggests that E2 promotes the induction of a partial EMT, which expresses both phenotypes. Nevertheless, the increase in ZO-1 in U251 cells was not as evident as in U87 cells, and thus these results are not sufficient to determine the status of E2-induced EMT. However, these results showed that E2 significantly induced the expression of mesenchymal markers, promoting the mesenchymal phenotype of cells derived from GBM.

3.5. E2 Promoted Migration and Invasion of Human GBM-Derived Cells

We evaluated cell migration by wound healing assay, and we observed that E2-treated U251 and U87 cells showed a higher migratory capacity by rapidly closing the wound compared to cells without E2 (Figure 6A,B). We also evaluated invasive capacity through transwell assay. E2 increased the number of invading U251 and U87 cells as compared with the vehicle (Figure 6C,D). These data show that E2, in addition to changing cell morphology and regulating EMT marker expression, also increased the migratory and invasive capacity of GBM-derived cells.

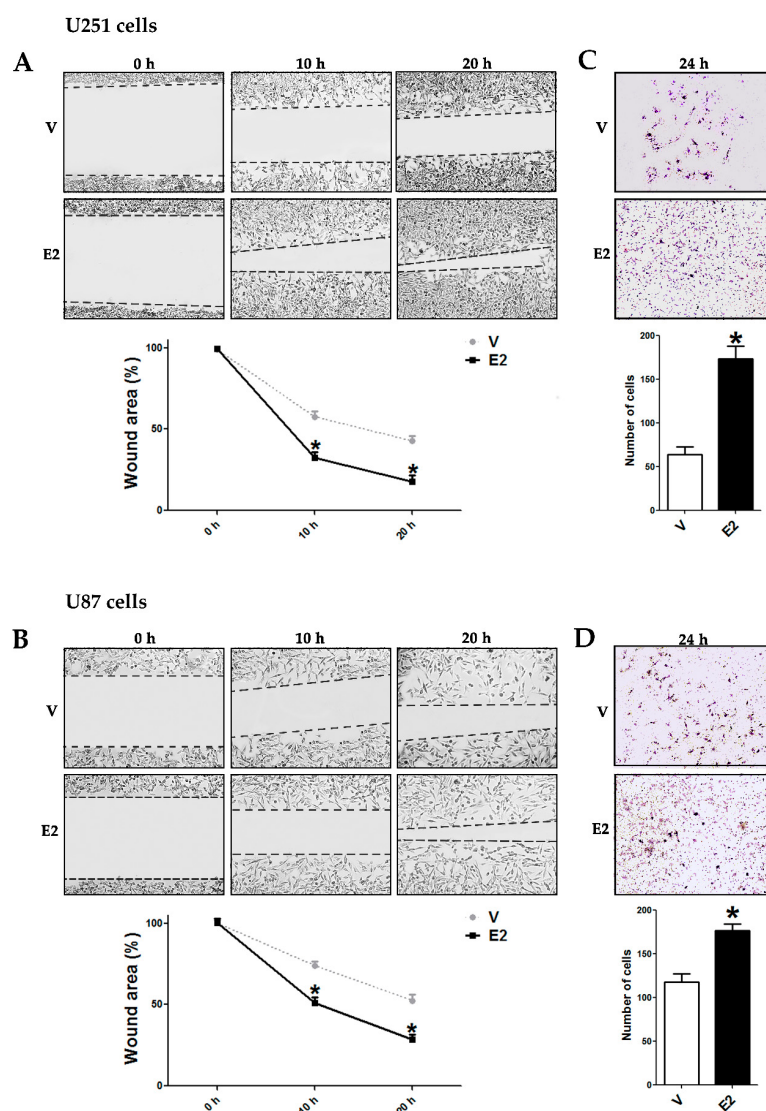


Figure 6. E2 increased migration and invasion of human GBM-derived cells. (A,B) Wound healing assays were performed in U251 and U87 cells treated with 17 β -estradiol (E2, 10 nM) and vehicle (V, cyclodextrin 0.01%). Representative images of wound closure at 0, 10, and 20 h and quantification of the wound area are shown. (C,D) Transwell assays were carried out in both cell lines. Quantification of cells staining with 0.1% crystal violet dye shows the number of invasive cells. Results are expressed as the mean \pm standard error of the mean (SEM); $n = 3$; * $p < 0.05$ vs. V.

3.6. ER- α Mediated E2 Effects on EMT

To determine the intracellular receptor subtype involved in E2 effects, we used specific agonists and antagonists' ER subtypes and assessed the expression of EMT markers. PPT, a selective ER- α agonist, increased TJP1, CDH2, and VIM gene expression in a similar way to E2 in U251 and U87 cells, and ER- α antagonist MPP blocked E2 effects in both cell types (Figure 7A,B). Treatment with antagonist alone did not show a significant effect on the expression of EMT markers, consistent with characterization of the effects of MPP in vitro, which showed that the antagonist does not behave as a partial or inverse agonist when administered in absence of an agonist. Treatments with the ER- β -selective agonist DPN and the antagonist PHTPP did not show any significant statistical effect on the regulation of EMT marker expression in either U251 or U87 cells (Figure 7A,B). These data suggest that E2 regulates EMT marker expression through the ER- α subtype. To functionally assess the role of ER- α in the EMT process, we performed wound healing assays using PPT and MPP. PPT-treated U251 cells rapidly closed the wound compared to cells treated with the vehicle, while the antagonist MPP blocked the PPT effect. Similarly, PPT increased the wound closure rate of U87 cells, and MPP blocked the agonist effect (Figure 8).

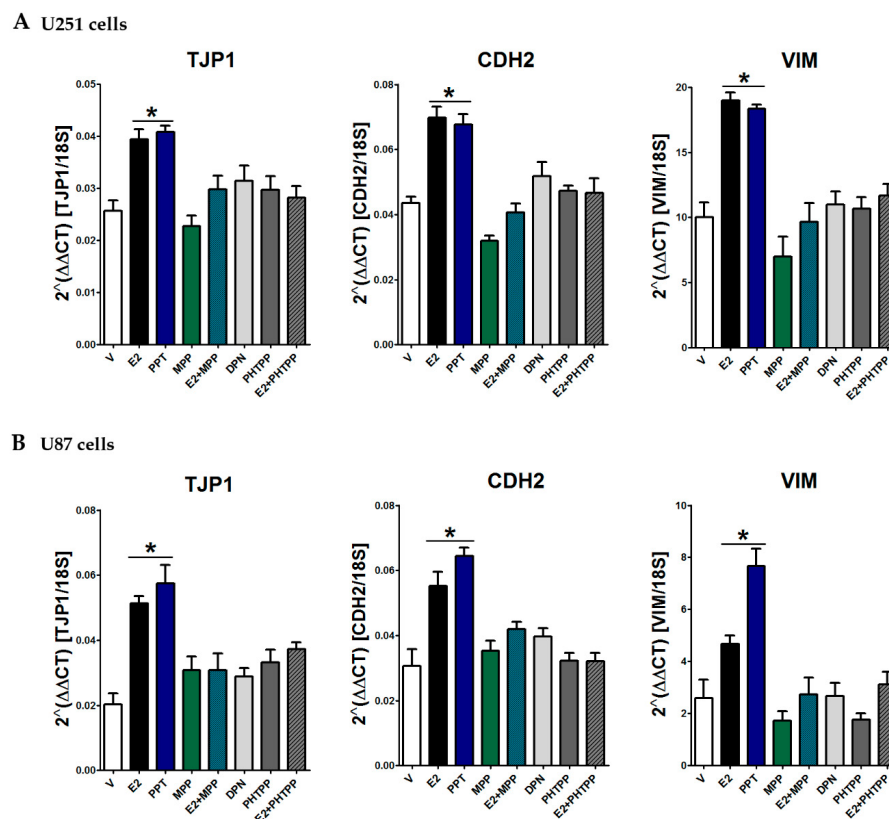


Figure 7. Effect of selective ER- α and ER- β agonists and antagonists on the EMT marker expression in GBM cells. U251 (A) and U87 (B) cells were treated with vehicle (V, 0.01% cyclodextrin + 0.01% DMSO), 17 β -estradiol (E2, 10 nM), 4,4',4''-(4-propyl-[1H]-pyrazole-1,3,5-triyl)trisphenol (PPT, 10 nM, selective ER- α agonist), methyl-piperidino-pyrazole (MPP, 1 μ M, selective ER- α antagonist), E2 + MPP, diarylpropionitrile (DPN, 10 nM, selective ER- β agonist), 4-[2-phenyl-5,7-bis(trifluoromethyl)pyrazole[1,5-a]pyrimidin-3-yl]phenol (PHTPP, 1 μ M, selective ER- β antagonist), and E2 + PHTPP for 48 h. Epithelial gene (TJP1) and mesenchymal gene (VIM and CDH2) expression were quantified by RT-qPCR using the comparative method $2^{-\Delta\Delta C_t}$ concerning the reference gene 18S rRNA. Results are expressed as the mean \pm standard error of the mean (SEM); $n = 3$; * $p < 0.05$ vs. all other groups.

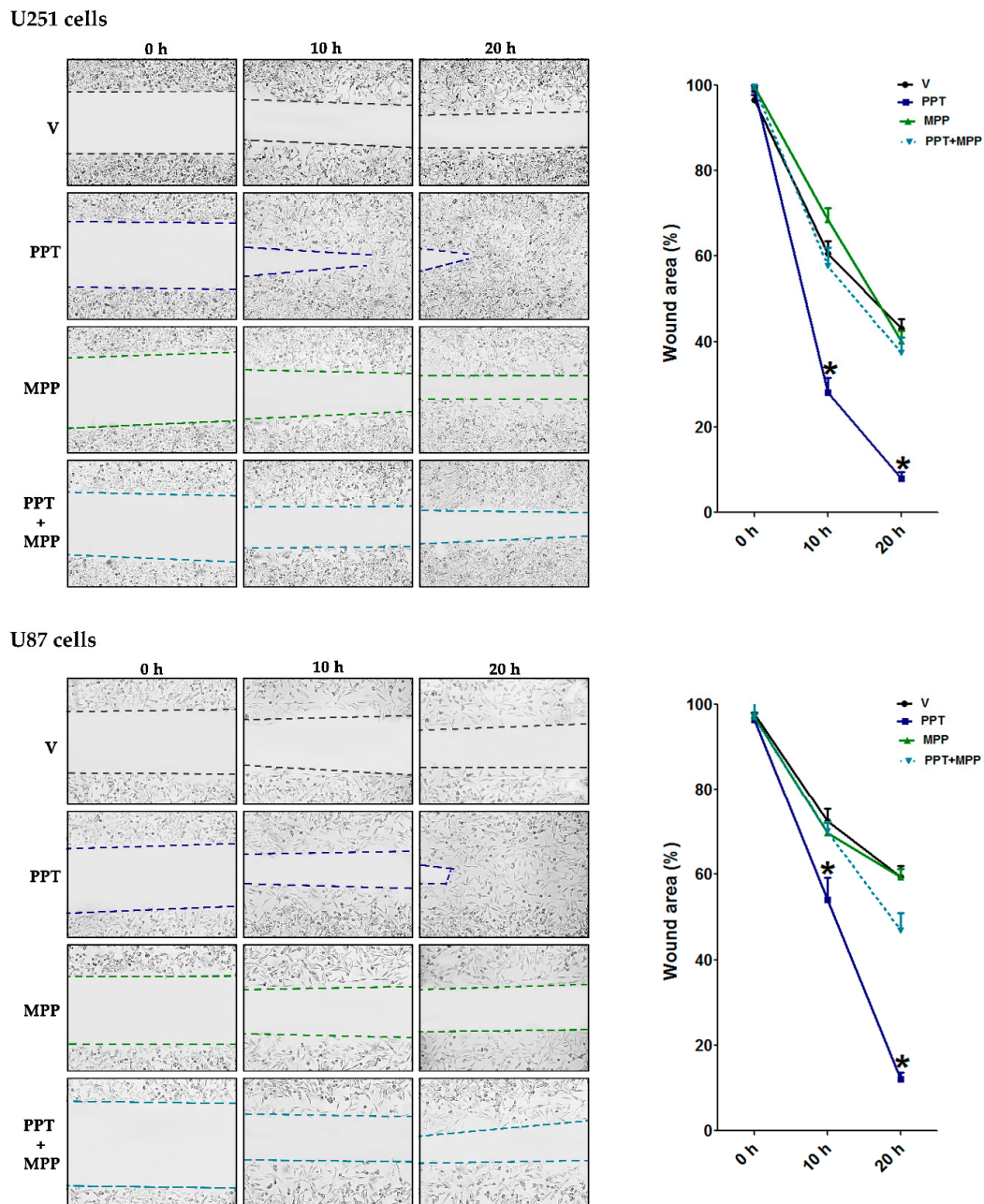


Figure 8. Effect of the selective ER- α agonist and antagonist on the migration of GBM cells. (A) U251 and (B) U87 cells that were treated for 20 h, with PPT (10 nM, selective ER- α agonist), MPP (1 μ M, selective ER- α antagonist), PPT + MPP, and vehicle (V, DMSO 0.01%). Wound healing assays determined the migratory capacity of the U251 and U87 cells. Representative images show wound closure at 0, 10, and 20 h and quantification of the wound area. Results are expressed as the mean \pm standard error of the mean (SEM); $n = 3$; * $p < 0.05$ vs. all other groups.

4. Discussion

The present study provides evidence of E2 effects on EMT-related molecular and cellular processes in human GBM-derived cells. EMT comprises a set of states between the epithelial and mesenchymal phenotypes, and its activation could be closely related to the high degree of phenotypic heterogeneity of GBM.

GBM is a highly heterogeneous tumor at both the molecular and cellular levels. The TCGA determined the existence of four main subtypes with different molecular expression profiles [4],

and some studies have shown the simultaneous presence of these subtypes within the same tumor [67,68]. GBM cells with proneural and mesenchymal expression are the most consistent subtypes in the literature. The proneural subtype is related to a more favorable prognosis, and the mesenchymal subtype tends to have the worst survival rate [5,69,70]. It has been shown that recurring GBM tumors that initially showed proneural expression presented mesenchymal expression profile after radiotherapy and chemotherapy [6,71,72], which has led to the proposal of a proneural–mesenchymal transition (PMT), whose molecular events are equivalent to those of EMT [7,73]. The transition between the two molecular subtypes is closely related to an enrichment of cells of the immune system within the GBM tumor microenvironment, which activate various signaling pathways that promote PMT/EMT [74–76]. The data shown in these studies highlight the importance of the factors found within the tumor microenvironment that promote phenotypic transitions between GBM subtypes. Immune system cells produce chemokines, cytokines, growth and angiogenic factors, immunosuppressive molecules, and extracellular matrix-modifying enzymes, which make the surroundings favorable for tumor progression [77]. Among the many factors found within the GBM tumor microenvironment, in this work, we focused on E2, which is produced by microglial cells, astrocytes, and GBM cells [78–81]. In this study, we evaluated E2 effects on the mesenchymal transition of human GBM-derived cells.

Both ER subtypes are predominantly expressed through healthy CNS; however, in human astrocytomas, both ER- α [45,47–49] and ER- β [44] expression decreases as the grade of tumor malignancy increases. Therefore, different researchers have proposed that ER expression may be reduced or lost during tumor development, although it is not clear if this represents a cause or consequence of tumor development. Much remains to be investigated on this topic, since determining the mechanisms underlying ER decrease during the development of gliomas could better understand the malignant tumor progression. Our results regarding the decrease of ER- α expression in gliomas compared with healthy tissue show agreement with that observed in other investigations. Likewise, we showed that ER- α subtype expression is higher in GBM than LGG (Figure 1A), which suggests an important oncogenic role of such receptor in the development of low- and high-grade gliomas. Among gliomas, a higher expression of ER- α could be involved in developing a high-grade glioma (GBM), while lower ER- α expression is associated with LGG development. The decrease or loss of ER expression during tumor development supposes the homeostatic imbalance of the normal functions of ERs in cells. Although this topic is not yet well studied in GBM, in breast cancer, it has been determined in more detail that in the most malignant tumors with multiple metastases, the nuclear factor kappa-light-chain-enhancer of activated B cells (NF- κ B) represses ER- α transcription through the enhancer of zeste homolog2 (EZH2), which negatively regulates ER- α transcription [82]. However, NF- κ B also improves the recruitment of ER- α to estrogen response elements (EREs) of its target promoters and increases its transcriptional activity [83,84]. The change in ER- α functions may also be due to other factors, such as altered structural conformations that increase interaction with transcriptional coactivators, point mutations that promote active forms of the receptor in the absence of an agonist, or variations by alternative splicing that change receptor transactivation mechanisms [85–87]. These data suggest that ER- α expression levels may not always be proportional to its activity. The positive correlation of ER- β expression concerning the GBM malignancy grade observed in this work does not correspond to other studies that find the opposite. However, we must consider that these studies do not specify the brain region of the used healthy tissue. We used expression data from the cerebral cortex, but there are other regions with a higher abundance of ESR2, such as the pons, cerebellum, thalamus, basal ganglia, and hypothalamus. Nevertheless, ESR1 and ESR2 expression on human GBM-derived cell lines were lower compared to healthy astrocytes, reinforcing the hypothesis of the studies above, which establish that the expression of both ER subtypes is inversely proportional to the tumor evolution degree. Different actions have been observed between ER subtypes in GBM. E2 (10 nM) and PPT (1 nM), the selective ER- α agonist, increased the number of cells derived from GBM [45], while treatment with different ER- β -specific agonists decreased GBM cell proliferation [44]. Within the cancer context, a positive correlation has been determined between EMT activation and

increased cell proliferation [88–91]. Previously, our group determined in GBM-derived cells that E2 induces cell growth and the expression of vascular endothelial growth factor (VEGF), epidermal growth factor receptor (EGFR), and cyclin D1 genes, which are involved in cell proliferation. These effects depended on ER- α activation [45]. This previous study represents the primary antecedent of our work. Once we demonstrated that E2 induces cell growth in GBM cells, we decided to investigate the relationship between E2 and canonical cellular processes of EMT activation, such as morphological and actin cytoskeleton organization changes, EMT marker expression, as well as cellular migration and invasion, which represent the main functional consequences of cells that undergo EMT. Additionally, it is worth mentioning that recently Castruccio et al. demonstrated that E2 significantly increases cell proliferation in U87 cells [92], which is consistent with our previously published results [45]. Still, our survival analysis showed that both ER- α and ER- β expression was positively correlated with a poor prognosis. It is interesting to highlight that our results showed that expression of both ER subtypes was enriched in the mesenchymal subtype concerning the other subtypes since this data led us to investigate the role of ERs on the induction of the mesenchymal phenotype.

EMT is a transition process between cellular phenotypes; therefore, it involves cellular morphological changes. To characterize the effects of E2 on EMT-related processes, in this study, we first evaluated changes in the morphology of cells treated with E2. Our results showed that E2 significantly changed the morphology of the four GBM-derived cells, towards an elongated mesenchymal phenotype. Moreover, these changes were correlated with an actin filament rearrangement. E2 regulates the reorganization of actin filaments through phosphorylation of actin-binding proteins such as cofilin and moesin in neurons, fibroblasts, and breast and endometrial cancer cells [93–96]. During EMT, actin filaments progressively reorganize from thin cortical bundles to thick contractile filaments that withstand stress fibers. The mesenchymal phenotype presents distribution of actin filaments in a front–rear polarization, with a network of short actin filaments branched at the leading edge, and long filaments arranged in different types of fibers behind the leading edge, which are associated with adhesion structures. This arrangement of the mesenchymal actin network allows cells to carry out migratory and invasive processes [97–99]. Thus, in this study, we demonstrated that E2 promotes a morphology change in GBM cells towards a mesenchymal phenotype due to the rearrangement of actin filaments, which were assembled in parallel along the ventral surface with long projections toward the leading edge. These changes in cellular morphology and reorganization of actin filaments suggest that E2 provides GBM-derived cells migratory and invasive capabilities.

All molecular events that occur during EMT are spatially and temporally coordinated during the transition. Therefore, the reorganization of the actin filaments is coupled with the expression changes that modify the cellular phenotype. Previously, the EMT definition described a complete transition between two different states, the epithelial and mesenchymal phenotype. Therefore, the primary experimental model for EMT evaluated the decrease in epithelial markers and the increase in mesenchymal markers. However, this perspective has generated extensive debate about the presence of EMT in certain circumstances, such as in cancer progression, which tends to create hybrid epithelial/mesenchymal (E/M) phenotypes that exhibit both epithelial and mesenchymal characteristics in a process known as partial EMT. Hybrid E/M phenotypes in cancer cells present better migratory and invasive capacities, as well as higher resistance to therapy [100–102].

We showed that E2 increased the expression of the epithelial marker ZO-1 and the mesenchymal markers N-cadherin and vimentin in U251 and U87 cells. However, the ZO-1 expression regulation was variable between cell lines, since in U251 cells, it only was increased by E2 at the mRNA level at 48 h, while in U87 cells, the expression increased both at the mRNA and protein levels at 48 and 72 h. ZO-1 marker is an adapter protein that binds to multiple components, such as integral proteins of the plasma membrane [103,104], and its presence is essential for assembly of tight and adherent junctions of epithelial cells [105,106]. Therefore, tumor cells from epithelial tissues decrease ZO-1 expression by activating EMT. The implications that ZO-1 expression may have on GBM have not yet been studied. Furthermore, our results showed that the regulation of E2 on ZO-1 expression varies

between different human GBM-derived cell lines, possibly due to the different expression profiles among these cells [107,108].

N-cadherin is a transmembrane protein that belongs to the calcium-dependent cell adhesion molecule (CAMs) family that is characteristic of mesenchymal tissue. Increased N-cadherin expression promotes cells to form elongated multicellular chains that migrate faster and more persistently, with a higher proportion of actin stress fibers that provide contractile forces during cell migration [109–111]. EMT activation in GBM cells leads to increased expression of N-cadherin, which is associated with increased migratory and invasive capacities. Vimentin is a type III intermediate filament protein that has an essential role in integrity maintaining of mesenchymal cells by providing support and anchorage to organelles, in addition to offering flexibility to cells by stabilizing dynamic interactions of the cytoskeleton during cell migration [112–114]. During EMT, there is an extensive change in the composition of intermediate filaments of epithelial cells, which generally express cytokeratin and initiates the expression of vimentin when they differentiate towards the mesenchymal phenotype. Our results showed that E2 promotes the mesenchymal phenotype by increasing the expression of N-cadherin and vimentin both at the mRNA and protein levels in two different human GBM cell lines. Although it was observed that E2 increased the expression of both epithelial and mesenchymal markers, we cannot affirm the induction of a partial EMT, since doing so requires the analysis of more epithelial and mesenchymal markers. However, our results open new perspectives regarding the determination of the status of E2-induced EMT in cells derived from GBM, since estradiol may promote partial EMT. Regardless of the status of EMT induced by E2, our results convincingly showed the acquisition of mesenchymal characteristics in GBM cells by E2 effect, since the changes in the expression of N-cadherin and vimentin are sufficiently forceful in the two cell lines studied.

Taken together, the effects promoted by E2 on GBM cells, such as reorganization of actin filaments as well as increased expression of N-cadherin and vimentin, are related to increased migratory and invasive capacities of U251 and U87 cells. These effects, associated with EMT activation, were replicated with PPT, a selective ER- α agonist that has a 410-fold relative binding affinity for ER- α over ER- β [115], suggesting that the E2 effects on EMT are regulated through ER- α . The latter was verified when using a highly selective ER- α antagonist (MPP, $K_i = 2.7$) [116], which blocked effects produced by E2 on EMT marker expression, as well as the increase of the migratory capacity provided by PPT. Furthermore, neither agonist DNP nor antagonist PHTPP, both selective for ER- β [117], showed significant effects on the expression of EMT markers. Therefore, we conclude that E2 effects observed on the expression of EMT markers are mainly produced by ER- α activation. Much remains to be known about the actions of both ER subtypes during the GBM's malignant progression. A more in-depth study of the molecular mechanisms of E2 signaling on GBM and its interaction with other signaling factors in specific cellular contexts is necessary for understanding E2 effects on this tumor, which could provide new strategies in GBM treatment.

In this work, we characterized E2-induced EMT in human GBM-derived cells. We found that E2 induces changes in cell morphology through actin filament reorganization and by increased expression of mesenchymal markers. These effects are related to the increased migratory and invasive capacities of GBM cells. Furthermore, E2 effects were mediated by ER- α , since the treatment with its agonist PPT produced similar results to E2, while the treatment with its antagonist MPP blocked these effects. Thus, E2 induces a mesenchymal phenotype through ER- α in cells derived from human GBM.

Supplementary Materials: The following are available online at <http://www.mdpi.com/2073-4409/9/9/1930/s1>, Figure S1: E2-induced morphological changes in human GBM-derived T98G cells. Figure S2: E2-induced morphological changes in human GBM-derived LN229 cells.

Author Contributions: A.M.H.-V., A.D.M.-M., C.J.Z.-S., and A.G.P.-M. contributed to carrying out the experiments and data analysis. A.M.H.-V., A.G.-A., and I.C.-A. conceived and managed experiments. A.M.H.-V. and I.C.-A. contributed to writing the manuscript. All authors have read and agreed to the published version of the manuscript.

Funding: This work was financially supported by *Programa de Apoyo a Proyectos de Investigación e Innovación Tecnológica (PAPIIT)*, project IN217120, DGAPA-UNAM, Mexico.

Acknowledgments: We would like to thank Marisol De La Fuente-Granada (Departamento de Medicina Genómica y Toxicología Ambiental, Instituto de Investigaciones Biomédicas, UNAM, Mexico) for the facilitation of cell culture during morphology analysis.

Conflicts of Interest: The authors declare no conflict of interest.

References

- Ostrom, Q.T.; Cioffi, G.; Gittleman, H.; Patil, N.; Waite, K.; Kruchko, C.; Barnholtz-Sloan, J.S. CBTRUS Statistical Report: Primary Brain and Other Central Nervous System Tumors Diagnosed in the United States in 2012–2016. *Neuro Oncol.* **2019**, *21*, v1–v100. [[CrossRef](#)] [[PubMed](#)]
- Furnari, F.B.; Fenton, T.; Bachoo, R.M.; Mukasa, A.; Stommel, J.M.; Stegh, A.; Hahn, W.C.; Ligon, K.L.; Louis, D.N.; Brennan, C.; et al. Malignant astrocytic glioma: Genetics, biology, and paths to treatment. *Genes Dev.* **2007**, *21*, 2683–2710. [[CrossRef](#)] [[PubMed](#)]
- Louis, D.N.; Perry, A.; Reifenberger, G.; von Deimling, A.; Figarella-Branger, D.; Cavenee, W.K.; Ohgaki, H.; Wiestler, O.D.; Kleihues, P.; Ellison, D.W. The 2016 World Health Organization Classification of Tumors of the Central Nervous System: A summary. *Acta Neuropathol.* **2016**, *131*, 803–820. [[CrossRef](#)] [[PubMed](#)]
- Verhaak, R.G.W.; Hoadley, K.A.; Purdom, E.; Wang, V.; Qi, Y.; Wilkerson, M.D.; Miller, C.R.; Ding, L.; Golub, T.; Mesirov, J.P.; et al. Integrated Genomic Analysis Identifies Clinically Relevant Subtypes of Glioblastoma Characterized. *Cancer Cell* **2010**, *17*, 98–110. [[CrossRef](#)] [[PubMed](#)]
- Phillips, H.S.; Kharbanda, S.; Chen, R.; Forrester, W.F.; Soriano, R.H.; Wu, T.D.; Misra, A.; Nigro, J.M.; Colman, H.; Soroceanu, L.; et al. Molecular subclasses of high-grade glioma predict prognosis, delineate a pattern of disease progression, and resemble stages in neurogenesis. *Cancer Cell* **2006**, *9*, 157–173. [[CrossRef](#)]
- Bhat, K.P.L.; Balasubramanian, V.; Vaillant, B.; Ezhilarasan, R.; Hummelink, K.; Hollingsworth, F.; Wani, K.; Heathcock, L.; James, J.D.; Goodman, L.D.; et al. Mesenchymal Differentiation Mediated by NF- κ B Promotes Radiation Resistance in Glioblastoma. *Cancer Cell* **2013**, *24*, 331–346. [[CrossRef](#)]
- Behnan, J.; Finocchiaro, G.; Hanna, G. The landscape of the mesenchymal signature in brain tumours. *Brain* **2019**, *142*, 847–866. [[CrossRef](#)]
- Nieto, M.A.; Huang, R.Y.J.; Jackson, R.A.; Thiery, J.P. EMT: 2016. *Cell* **2016**, *166*, 21–45. [[CrossRef](#)]
- Skrypek, N.; Goossens, S.; De Smedt, E.; Vandamme, N.; Berox, G. Epithelial-to-Mesenchymal Transition: Epigenetic Reprogramming Driving Cellular Plasticity. *Trends Genet.* **2017**, *33*, 943–959. [[CrossRef](#)]
- Lamouille, S.; Xu, J.; Derynck, R. Molecular mechanisms of epithelial–mesenchymal transition. *Nat. Rev. Mol. Cell Biol.* **2014**, *15*, 178–196. [[CrossRef](#)]
- Thiery, J.P.; Huang, R.Y.J.; Nieto, M.A. Epithelial-Mesenchymal Transitions in Development and Disease. *Cell* **2009**, *139*, 1–13. [[CrossRef](#)] [[PubMed](#)]
- Trelstad, R.L.; Hay, E.D.; Revel, J.D. Cell contact during early morphogenesis in the chick embryo. *Dev. Biol.* **1967**, *16*, 78–106. [[CrossRef](#)]
- Nieto, M.A.; Sargent, M.; Wilkinson, D.; Cooke, J. Control of cell behavior during vertebrate development by Slug, a zinc finger gene. *Science* **1994**, *6*, 835–839. [[CrossRef](#)] [[PubMed](#)]
- Lim, J.; Thiery, J.P. Epithelial-mesenchymal transitions: Insights from development. *Development* **2012**, *139*, 3471–3486. [[CrossRef](#)] [[PubMed](#)]
- Lepilina, A.; Coon, A.N.; Kikuchi, K.; Holdway, J.E.; Roberts, R.W.; Burns, C.G.; Poss, K.D. A Dynamic Epicardial Injury Response Supports Progenitor Cell Activity during Zebrafish Heart Regeneration. *Cell* **2006**, *127*, 607–619. [[CrossRef](#)] [[PubMed](#)]
- Stone, R.C.; Pastar, I.; Ojeh, N.; Chen, V.; Liu, S.; Garzon, K.I.; Tomic-Canic, M. Epithelial-mesenchymal transition in tissue repair and fibrosis. *Cell Tissue Res.* **2016**, *365*, 495–506. [[CrossRef](#)]
- Dongre, A.; Weinberg, R.A. New insights into the mechanisms of epithelial–mesenchymal transition and implications for cancer. *Nat. Rev. Mol. Cell Biol.* **2019**, *20*, 69–84. [[CrossRef](#)]
- Kahlert, U.D.; Joseph, J.V.; Kruyt, F.A.E. EMT- and MET-related processes in non-epithelial tumors: Importance for disease progression, prognosis, and therapeutic opportunities. *Mol. Oncol.* **2017**, *11*, 860–877. [[CrossRef](#)]
- Kahlert, U.D.; Nikkhah, G.; Maciaczyk, J. Epithelial-to-mesenchymal (-like) transition as a relevant molecular event in malignant gliomas. *Cancer Lett.* **2013**, *331*, 131–138. [[CrossRef](#)]

20. Brabletz, T.; Kalluri, R.; Nieto, M.A.; Weinberg, R.A. EMT in cancer. *Nat. Rev. Cancer* **2018**, *18*, 128–134. [[CrossRef](#)]
21. Freije, W.A.; Castro-Vargas, F.E.; Fang, Z.; Horvath, S.; Cloughesy, T.; Liao, L.M.; Mischel, P.S.; Nelson, S.F. Gene Expression Profiling of Gliomas Strongly Predicts Survival. *Cancer Res.* **2004**, *15*, 6503–6510. [[CrossRef](#)] [[PubMed](#)]
22. Tso, C.L.; Shintaku, P.; Chen, J.; Liu, Q.; Liu, J.; Chen, Z.; Yoshimoto, K.; Mischel, P.S.; Cloughesy, T.F.; Liao, L.M.; et al. Primary Glioblastomas Express Mesenchymal Stem-Like Properties. *Mol. Cancer Res.* **2006**, *4*, 607–619. [[CrossRef](#)] [[PubMed](#)]
23. Zarkoob, H.; Taube, J.H.; Singh, S.K.; Mani, S.A.; Kohandel, M. Investigating the Link between Molecular Subtypes of Glioblastoma, Epithelial-Mesenchymal Transition, and CD133 Cell Surface Protein. *PLoS ONE* **2013**, *8*, e64169. [[CrossRef](#)] [[PubMed](#)]
24. Azcoitia, I.; Yague, J.G.; Garcia-Segura, L.M. Estradiol synthesis within the human brain. *Neuroscience* **2011**, *191*, 139–147. [[CrossRef](#)]
25. Barakat, R.; Oakley, O.; Kim, H.; Jin, J.; Ko, C.M.J. Extra-gonadal sites of estrogen biosynthesis and function. *BMB Rep.* **2016**, *49*, 488–496. [[CrossRef](#)]
26. Toran-allerand, C.D. Sex steroids and the development of the newborn mouse hypothalamus and preoptic area In Vitro: Implications for sexual differentiation. *Brain Res.* **1976**, *106*, 407–412. [[CrossRef](#)]
27. Díaz, N.F.; Guerra-Arraiza, C.; Díaz-Martínez, N.E.; Salazar, P.; Molina-Hernández, A.; Camacho-Arroyo, I.; Velasco, I. Changes in the content of estrogen α and progesterone receptors during differentiation of mouse embryonic stem cells to dopamine neurons. *Brain Res. Bull.* **2007**, *73*, 75–80. [[CrossRef](#)]
28. Denley, M.C.S.; Gattford, N.J.F.; Sellers, K.J.; Srivastava, D.P. Estradiol and the development of the cerebral cortex: An unexpected role? *Front. Neurosci.* **2018**, *12*, 245. [[CrossRef](#)]
29. Díaz, H.; Lorenzo, A.; Carrer, H.F.; Cáceres, A. Time lapse study of neurite growth in hypothalamic dissociated neurons in culture: Sex differences and estrogen effects. *J. Neurosci. Res.* **1992**, *33*, 266–281. [[CrossRef](#)]
30. Pérez, J.; Naftolin, F.; García-Segura, L.M. Sexual differentiation of synaptic connectivity and neuronal plasma membrane in the arcuate nucleus of the rat hypothalamus. *Brain Res.* **1990**, *527*, 116–122. [[CrossRef](#)]
31. Sugiyama, N.; Andersson, S.; Lathe, R.; Fan, X.; Schwend, T.; Nalvarte, I. Spatiotemporal dynamics of the expression of estrogen receptors in the postnatal mouse brain. *Mol. Psychiatry* **2009**, *14*, 223–232. [[CrossRef](#)] [[PubMed](#)]
32. Barth, C.; Villringer, A.; Sacher, J. Sex hormones affect neurotransmitters and shape the adult female brain during hormonal transition periods. *Front. Neurosci.* **2015**, *9*, 37. [[CrossRef](#)] [[PubMed](#)]
33. Hansberg-Pastor, V.; González-Arenas, A.; Piña-Medina, A.G.; Camacho-Arroyo, I. Sex hormones regulate cytoskeletal proteins involved in brain plasticity. *Front. Psychiatry* **2015**, *6*, 165. [[CrossRef](#)] [[PubMed](#)]
34. Kuiper, G.G.; Carlsson, B.; Grandien, K.; Enmark, E.; Häggblad, J.; Nilsson, S.; Gustafsson, J.A. Comparison of the Ligand Binding Specificity and Transcript Tissue Distribution of Estrogen Receptors α and β . *Endocrinology* **1997**, *138*, 863–870. [[CrossRef](#)]
35. Russo, J.; Russo, I.H. The role of estrogen in the initiation of breast cancer. *J. Steroid Biochem. Mol. Biol.* **2006**, *102*, 89–96. [[CrossRef](#)]
36. Cuna, S.; Hoffmann, P.; Pujol, P. Estrogens and epithelial ovarian cancer. *Gynecol. Oncol.* **2004**, *94*, 25–32. [[CrossRef](#)]
37. Kumar, M.M.; Davuluri, S.; Poojar, S.; Mukherjee, G.; Bajpai, A.K.; Bafna, U.D.; Devi, U.K.; Kallur, P.P.R.; Kshitish, A.K.; Jayshree, R.S. Role of estrogen receptor alpha in human cervical cancer-associated fibroblasts: A transcriptomic study. *Tumor Biol.* **2016**, *37*, 4409–4420. [[CrossRef](#)]
38. Di Zazzo, E.; Galasso, G.; Giovannelli, P.; Di-Donato, M.; Castoria, G. Estrogens and Their Receptors in Prostate Cancer: Therapeutic Implications. *Front. Oncol.* **2018**, *8*, 1–7. [[CrossRef](#)]
39. Pearce, S.T.; Jordan, V.C. The biological role of estrogen receptors α and β in cancer. *Crit. Rev. Oncol. Hematol.* **2004**, *50*, 3–22. [[CrossRef](#)]
40. Vaquero, J.; Marcos, M.L.; Martínez, R.; Bravo, G. Estrogen- and progesterone-receptor proteins in intracranial tumors. *Surg. Neurol.* **1983**, *19*, 11–13. [[CrossRef](#)]
41. Carroll, R.S.; Zhang, J.; Dashner, K.; Sar, M.; Black, P.M. Steroid Hormone Receptors in Astrocytic Neoplasms. *Neurosurgery* **1995**, *37*, 496–504. [[CrossRef](#)] [[PubMed](#)]
42. Khalid, H.; Yasunaga, A.; Kishikawa, M.; Shibata, S. Immunohistochemical expression of the estrogen receptor-related antigen (ER-D5) in human intracranial tumors. *Cancer* **1995**, *75*, 2571–2578. [[CrossRef](#)]

43. Batistatou, A.; Stefanou, D.; Goussia, A.; Arkoumani, E.; Papavassiliou, A.; Agnantis, N. Estrogen receptor beta (ER β) is expressed in brain astrocytic tumors and declines with dedifferentiation of the neoplasm. *J. Cancer Res. Clin. Oncol.* **2004**, *130*, 405–410. [[CrossRef](#)] [[PubMed](#)]
44. Sareddy, G.R.; Nair, B.C.; Gonugunta, V.K.; Zhang, Q.g.; Brenner, A.; Brann, D.W.; Tekmal, R.R.; Vadlamudi, R.K. Therapeutic Significance of Estrogen Receptor Agonists in Gliomas. *Mol. Cancer* **2012**, *11*, 1174–1182. [[CrossRef](#)] [[PubMed](#)]
45. González-Arenas, A.; Hansberg-Pastor, V.; Hernández-Hernández, O.T.; González-García, T.K.; Henderson-Villalpando, J.; Lemus-Hernández, D.; Cruz-Barrios, A.; Rivas-Suárez, M.; Camacho-Arroyo, I. Estradiol increases cell growth in human astrocytoma cell lines through ER α activation and its interaction with SRC-1 and SRC-3 coactivators. *Biochim. Biophys. Acta* **2012**, *1823*, 379–386. [[CrossRef](#)] [[PubMed](#)]
46. Li, W.; Winters, A.; Poteet, E.; Ryou, M.G.; Lin, S.; Hao, S.; Wu, Z.; Yuan, F.; Hatanpaa, K.J.; Simpkins, J.W.; et al. Involvement of estrogen receptor β 5 in the progression of glioma. *Brain Res.* **2013**, *1503*, 97–107. [[CrossRef](#)]
47. Dueñas, J.M.; Candanedo, A.; Santerre, A.; Orozco, S.; Sandoval, H.; Feria, I.; López-Elizalde, R.; Venegas, M.A.; Netel, B.; de la Torre-Valdovinos, B.; et al. Aromatase and estrogen receptor alpha mRNA expression as prognostic biomarkers in patients with astrocytomas. *J. Neurooncol.* **2014**, *119*, 275–284. [[CrossRef](#)]
48. Liu, C.; Zhang, Y.; Zhang, K.; Bian, C.; Zhao, Y.; Zhang, J. Expression of estrogen receptors, androgen receptor and steroid receptor coactivator-3 is negatively correlated to the differentiation of astrocytic tumors. *Cancer Epidemiol.* **2014**, *38*, 291–297. [[CrossRef](#)]
49. Tavares, C.B.; Gomes-Braga, F.; Sousa, E.B.; Borges, U.S.; Escórcio-Dourado, C.S.; Da Silva-Sampaio, J.P.; Borges da Silva, B. Evaluation of estrogen receptor expression in low-grade and high-grade astrocytomas. *Rev. Assoc. Med. Bras.* **2018**, *64*, 1129–1133. [[CrossRef](#)]
50. Wan, S.; Jiang, J.; Zheng, C.; Wang, N.; Zhai, X.; Fei, X.; Wu, R.; Jiang, X. Estrogen nuclear receptors affect cell migration by altering sublocalization of AQP2 in glioma cell lines. *Cell Death Discov.* **2018**, *4*, 49. [[CrossRef](#)]
51. Park, S.H.; Cheung, L.W.T.; Wong, A.S.T.; Leung, P.C.K. Estrogen Regulates Snail and Slug in the Down-Regulation of E-Cadherin and Induces Metastatic Potential of Ovarian Cancer Cells through Estrogen Receptor α . *Mol. Endocrinol.* **2008**, *22*, 2085–2098. [[CrossRef](#)] [[PubMed](#)]
52. Mishra, S.; Tai, Q.; Gu, X.; Schmitz, J.; Poullard, A.; Fajardo, R.J.; Mahalingam, D.; Chen, X.; Zhu, X.; Sun, L.Z. Estrogen and Estrogen Receptor Alpha Promotes Malignancy and Osteoblastic Tumorigenesis in Prostate Cancer. *Oncotarget* **2015**, *6*, 44388–44402. [[CrossRef](#)] [[PubMed](#)]
53. Shi, X.; Peng, Y.; Du, X.; Liu, H.; Klocker, H.; Lin, Q.; Shi, J.; Zhang, J. Estradiol promotes epithelial-to-mesenchymal transition in human benign prostatic epithelial cells. *Prostate* **2017**, *77*, 1424–1437. [[CrossRef](#)] [[PubMed](#)]
54. Dhasarathy, A.; Kajita, M.; Wade, P.A. The Transcription Factor Snail Mediates Epithelial to Mesenchymal Transitions by Repression of Estrogen Receptor- α . *Mol. Endocrinol.* **2007**, *21*, 2907–2918. [[CrossRef](#)]
55. Al Saleh, S.; Al Mulla, F.; Luqmani, Y.A. Estrogen receptor silencing induces epithelial to mesenchymal transition in human breast cancer cells. *PLoS ONE* **2011**, *6*, e20610. [[CrossRef](#)]
56. Bouris, P.; Skandalis, S.S.; Piperigkou, Z.; Afratis, N.; Karamanou, K.; Aletras, A.J.; Moustakas, A.; Theocharis, A.D.; Karamanos, N.K. Estrogen receptor alpha mediates epithelial to mesenchymal transition, expression of specific matrix effectors and functional properties of breast cancer cells. *Matrix Biol.* **2015**, *43*, 42–60. [[CrossRef](#)]
57. Scherbakov, A.M.; Andreeva, O.E.; Shatskaya, V.A.; Krasil’nikov, M.A. The relationships between snail1 and estrogen receptor signaling in breast cancer cells. *J. Cell Biochem.* **2012**, *113*, 2147–2155. [[CrossRef](#)]
58. Wik, E.; Ræder, M.B.; Krakstad, C.; Trovik, J.; Birkeland, E.; Hoivik, E.A.; Mjos, S.; Werner, H.M.J.; Mannelqvist, M.; Stefansson, I.M.; et al. Lack of estrogen receptor- α is associated with epithelial-mesenchymal transition and PI3K alterations in endometrial carcinoma. *Clin. Cancer Res.* **2013**, *19*, 1094–1105. [[CrossRef](#)]
59. Colaprico, A.; Silva, T.C.; Olsen, C.; Garofano, L.; Cava, C.; Garolini, D.; Sabedot, T.S.; Malta, T.M.; Pagnotta, S.M.; Castiglioni, I.; et al. TCGAAbiolinks: An R/Bioconductor package for integrative analysis of TCGA data. *Nucleic Acids Res.* **2016**, *44*, e71. [[CrossRef](#)]
60. Costa-Silva, J.; Domingues, D.; Lopes, F.M. RNA-Seq differential expression analysis: An extended review and a software tool. *PLoS ONE* **2017**, *12*, e0190152. [[CrossRef](#)]
61. Bakal, C.; Church, G.; Perrimon, N. Quantitative Morphological Signatures Define Local Signaling Networks Regulating Cell Morphology. *Science* **2007**, *316*, 1753–1756. [[CrossRef](#)] [[PubMed](#)]

62. Carpenter, A.E.; Jones, T.R.; Lamprecht, M.R.; Clarke, C.; Kang, I.; Friman, O.; Guertin, D.A.; Chang, J.H.; Lindquist, R.A.; Moffat, J.; et al. CellProfiler: Image analysis software for identifying and quantifying cell phenotypes. *Genome Biol.* **2006**, *7*, R100. [[CrossRef](#)] [[PubMed](#)]
63. Chen, S.; Zhao, M.; Wu, G.; Yao, C.; Zhang, J. Recent Advances in Morphological Cell Image Analysis. *Comput. Math. Methods Med.* **2012**, *2012*, 101536. [[CrossRef](#)] [[PubMed](#)]
64. Ren, Z.X.; Yu, H.B.; Li, J.S.; Shen, J.L.; Du, W.S. Suitable parameter choice on quantitative morphology of A549 cell in epithelial—mesenchymal transition. *Biosci. Rep.* **2015**, *35*, e00202. [[CrossRef](#)]
65. Schmittgen, T.D.; Livak, K.J. Analyzing real-time PCR data by the comparative CT method. *Nat. Protoc.* **2008**, *3*, 1101–1108. [[CrossRef](#)]
66. Pfaffl, M.W. A new mathematical model for relative quantification in real-time RT-PCR. *Nucleic Acids Res.* **2001**, *29*, e45. [[CrossRef](#)]
67. Sottoriva, A.; Spiteri, I.; Piccirillo, S.G.M.; Touloumis, A.; Collins, V.P.; Marioni, J.C.; Curtis, C.; Watts, C.; Tavaré, S. Intratumor heterogeneity in human glioblastoma reflects cancer evolutionary dynamics. *Proc. Natl. Acad. Sci. USA* **2013**, *110*, 4009–4014. [[CrossRef](#)]
68. Patel, A.P.; Tirosh, I.; Trombetta, J.J.; Shalek, A.K.; Gillespie, S.M.; Wakimoto, H.; Cahill, D.P.; Nahed, B.V.; Curry, W.T.; Martuza, R.L.; et al. Single-cell RNA-seq highlights intratumoral heterogeneity in primary glioblastoma. *Science* **2014**, *344*, 1396–1401. [[CrossRef](#)]
69. Lin, N.; Yan, W.; Gao, K.; Wang, Y.; Zhang, J.; You, Y. Prevalence and clinicopathologic characteristics of the molecular subtypes in malignant glioma: A multi-institutional analysis of 941 cases. *PLoS ONE* **2014**, *9*, e94871. [[CrossRef](#)]
70. Olar, A.; Aldape, K.D. Using the molecular classification of glioblastoma to inform personalized treatment. *J. Pathol.* **2014**, *232*, 165–177. [[CrossRef](#)]
71. Ozawa, T.; Riester, M.; Cheng, Y.; Huse, J.T.; Squatrito, M.; Helmy, K.; Charles, N.; Michor, F.; Holland, E.C. Most Human Non-GCIMP Glioblastoma Subtypes Evolve from a Common Proneural-like Precursor Glioma. *Cancer Cell* **2014**, *26*, 288–300. [[CrossRef](#)] [[PubMed](#)]
72. Segerman, A.; Niklasson, M.; Haglund, C.; Bergström, T.; Jarvius, M.; Xie, Y.; Westermark, A.; Sönmez, D.; Hermansson, A.; Kastemar, M.; et al. Clonal Variation in Drug and Radiation Response among Glioma-Initiating Cells Is Linked to Proneural-Mesenchymal Transition. *Cell Rep.* **2016**, *17*, 2994–3009. [[CrossRef](#)] [[PubMed](#)]
73. Fedele, M.; Cerchia, L.; Pegoraro, S.; Sgarra, R.; Manfioletti, G. Proneural-mesenchymal transition: Phenotypic plasticity to acquire multitherapy resistance in glioblastoma. *Int. J. Mol. Sci.* **2019**, *20*, 2746. [[CrossRef](#)] [[PubMed](#)]
74. Wang, Q.; Hu, B.; Hu, X.; Kim, H.; Squatrito, M.; Scarpace, L.; deCarvalho, A.C.; Lyu, S.; Li, P.; Li, Y.; et al. Tumor Evolution of Glioma-Intrinsic Gene Expression Subtypes Associates with Immunological Changes in the Microenvironment. *Cancer Cell* **2017**, *32*, 42–56. [[CrossRef](#)]
75. Stanzani, E.; Martínez-Soler, F.; Mateos, T.M.; Vidal, N.; Villanueva, A.; Pujana, M.A.; Serra-Musach, J.; Iglesia, N.; Giménez-Bonafé, P.; Tortosa, A. Radioresistance of mesenchymal glioblastoma initiating cells correlates with patient outcome and is associated with activation of inflammatory program. *Oncotarget* **2017**, *8*, 73640–73653. [[CrossRef](#)]
76. Kaffes, I.; Szulzewsky, F.; Chen, Z.; Herting, C.J.; Gabanic, B.; Velazquez, J.E.; Shelton, J.; Switchenko, J.M.; Ross, J.L.; McSwain, L.F.; et al. Human Mesenchymal glioblastomas are characterized by an increased immune cell presence compared to Proneural and Classical tumors presence compared to Proneural and Classical tumors. *Oncoimmunology* **2019**, *8*, e1655360. [[CrossRef](#)]
77. Quail, D.F.; Joyce, J.A. The Microenvironmental Landscape of Brain Tumors. *Cancer Cell* **2017**, *31*, 326–341. [[CrossRef](#)]
78. Bruce-Keller, A.J.; Keeling, J.L.; Keller, J.N.; Huang, F.F.; Camondola, S.; Mattson, M.P. Antiinflammatory effects of estrogen on microglial activation. *Endocrinology* **2000**, *141*, 3646–3656. [[CrossRef](#)]
79. Baker, A.E.; Brautigam, V.M.; Watters, J.J. Estrogen modulates microglial inflammatory mediator production via interactions with estrogen receptor β . *Endocrinology* **2004**, *145*, 5021–5032. [[CrossRef](#)]
80. Acáz-Fonseca, E.; Sanchez-Gonzalez, R.; Azcoitia, I.; Arevalo, M.A.; Garcia-Segura, L.M. Role of Astrocytes in the Neuroprotective Actions of 17β -estradiol and Selective Estrogen Receptor Modulators. *Mol. Cell Endocrinol.* **2014**, *389*, 48–57. [[CrossRef](#)]

81. Pinacho-Garcia, L.M.; Valdez, R.A.; Navarrete, A.; Cabeza, M.; Segovia, J.; Romano, M.C. The Effect of Finasteride and Dutasteride on the Synthesis of Neurosteroids by Glioblastoma Cells. *Steroids* **2020**, *155*, 108556. [[CrossRef](#)] [[PubMed](#)]
82. Reijm, E.; Jansen, M.; Ruigrok-Ritstier, K.; van Staveren, I.L.; Look, M.; van Gelder, M.E.M.; Sieuwerts, A.M.; Sleijfer, S.; Foekens, J.A.; Berns, E.M.J.J. Decreased expression of EZH2 is associated with upregulation of ER and favorable outcome to tamoxifen in advanced breast cancer. *Breast Cancer Res Treat* **2011**, *125*, 387–394. [[CrossRef](#)] [[PubMed](#)]
83. Frasor, J.; Weaver, A.; Pradhan, M.; Dai, Y.; Miller, L.D.; Lin, C.Y.; Stanculescu, A. Positive cross-talk between estrogen receptor and NF- κ B in breast cancer. *Cancer Res.* **2009**, *14*, 8918–8925. [[CrossRef](#)] [[PubMed](#)]
84. Frasor, J.; El-Shennawy, L.; Stender, J.; Kastrati, I. NF κ B affects estrogen receptor expression and activity in breast cancer through multiple mechanisms. *Mol. Cell Endocrinol.* **2015**, *418*, 235–239. [[CrossRef](#)] [[PubMed](#)]
85. Hui, H.; Hongying, Z.; Qingbin, K.; Yangfu, J. Mechanisms for estrogen receptor expression in human cancer. *Exp. Hematol. Oncol.* **2018**, *7*, 24. [[CrossRef](#)]
86. Katzenellenbogen, J.; Mayne, C.; Katzenellenbogen, B.; Greene, G.; Chandralapaty, S. Structural Underpinnings of Estrogen Receptor Mutations in Endocrine Therapy Resistance. *Nat. Rev. Cancer* **2018**, *18*, 377–388. [[CrossRef](#)]
87. Christoforos, T.; Gustafsson, J. Estrogen receptor mutations and functional consequences for breast cancer. *Trends Endocrinol Metab* **2015**, *26*, 467–476. [[CrossRef](#)]
88. Thompson, S.; Petti, F.; Sujka-Kwok, I.; Mercado, P.; Bean, J.; Monaghan, M.; Seymour, S.L.; Argast, G.M.; Epstein, D.M.; Haley, J.D. A systems view of epithelial-mesenchymal transition signaling states. *Clin Exp Metastasis* **2011**, *28*, 137–155. [[CrossRef](#)]
89. D'Souza, R.; Knitte, A.; Nagaraj, N.; van Dinther, M.; Choudhary, C.; Dijke, P.; Mann, M.; Sharma, K. Time-resolved dissection of early phosphoproteome and ensuing proteome changes in response to TGF- β . *Sci Signal* **2014**, *7*, 5. [[CrossRef](#)]
90. Rojas-Puente, L.; Cardona, A.; Carranza, H.; Vargas, C.; Jaramillo, L.; Zea, D.; Cetina, L.; Wills, B.; Ruiz-Garcia, E.; Arrieta, O. Epithelial-mesenchymal transition, proliferation, and angiogenesis in locally advanced cervical cancer treated with chemoradiotherapy. *Cancer Med.* **2016**, *5*, 1989–1999. [[CrossRef](#)]
91. Qun-Ying, L.; Zhang, H.; Zhao, B.; Zheng-Yu, Z.; Bai, F.; Xin-Hai, P.; Zhao, S.; Xiong, Y.; Kun-Liang, G. TAZ promotes cell proliferation and epithelial-mesenchymal transition and is inhibited by the hippo pathway. *Mol. Cell Biol.* **2008**, *28*, 2426–2436. [[CrossRef](#)]
92. Castruccio, C.; Longhitano, L.; Distefano, A.; Anfusio, D.; Kalampoka, S.; Spina, E.L.; Astuto, M.; Avola, R.; Caruso, M.; Nicolosi, D.; et al. Role of 17 β -Estradiol on Cell Proliferation and Mitochondrial Fitness in Glioblastoma Cells. *J. Oncol.* **2020**, *2020*, 2314693. [[CrossRef](#)]
93. DePasquale, J.A. Rearrangement of the F-actin cytoskeleton in estradiol-treated MCF-7 breast carcinoma cells. *Histochem. Cell Biol.* **1999**, *112*, 341–350. [[CrossRef](#)] [[PubMed](#)]
94. Briz, V.; Baudry, M. Estrogen regulates protein synthesis and actin polymerization in hippocampal neurons through different molecular mechanisms. *Front. Endocrinol* **2014**, *5*, 22. [[CrossRef](#)] [[PubMed](#)]
95. Carnesecchi, J.; Malbouyres, M.; De Mets, R.; Bolland, M.; Beauchef, G.; Vié, K.; Chamot, C.; Lionnet, C.; Ruggiero, F.; Vanacker, J.M. Estrogens Induce Rapid Cytoskeleton Re-Organization in Human Dermal Fibroblasts via the Non-Classical Receptor GPR30. *PLoS ONE* **2015**, *10*, e0120672. [[CrossRef](#)]
96. Flamini, M.I.; Sanchez, A.M.; Goglia, L.; Tosi, V.; Genazzani, A.R.; Simoncini, T. Differential actions of estrogen and SERMs in regulation of the actin cytoskeleton of endometrial cells. *Mol. Hum. Reprod.* **2009**, *15*, 675–685. [[CrossRef](#)]
97. O'Neill, G.M. The coordination between actin filaments and adhesion in mesenchymal migration. *Cell Adhes. Migr.* **2009**, *3*, 355–357. [[CrossRef](#)]
98. Hotulainen, P.; Lappalainen, P. Stress fibers are generated by two distinct actin assembly mechanisms in motile cells. *J. Cell Biol.* **2006**, *173*, 383–394. [[CrossRef](#)]
99. Zaidel-Bar, R.; Ballestrem, C.; Kam, Z.; Geiger, B. Early molecular events in the assembly of matrix adhesions at the leading edge of migrating cells. *J. Cell Sci.* **2003**, *116*, 4605–4613. [[CrossRef](#)]
100. Saitoh, M. Involvement of partial EMT in cancer progression. *J. Biochem.* **2018**, *164*, 257–264. [[CrossRef](#)]
101. Aiello, N.M.; Maddipati, R.; Norgard, R.J.; Balli, D.; Li, J.; Yuan, S.; Yamazoe, T.; Black, T.; Sahnoud, A.; Furth, E.E.; et al. EMT Subtype Influences Epithelial Plasticity and Mode of Cell Migration. *Dev. Cell* **2018**, *45*, 681–695.e4. [[CrossRef](#)] [[PubMed](#)]

102. Yang, J.; Antin, P.; Berx, G.; Blanpain, C.; Brabletz, T.; Bronner, M.; Campbell, K.; Cano, A.; Casanova, J.; Christofori, G.; et al. Guidelines and definitions for research on epithelial–mesenchymal transition. *Nat. Rev. Mol. Cell Biol.* **2020**, *21*, 341–352. [[CrossRef](#)] [[PubMed](#)]
103. Bazzoni, G.; Martínez-Estrada, O.M.; Orsenigo, F.; Cordenonsi, M.; Citi, S.; Dejana, E. Interaction of junctional adhesion molecule with the tight junction components ZO-1, cingulin, and occludin. *J. Biol. Chem.* **2000**, *275*, 20520–20526. [[CrossRef](#)]
104. Ebnet, K.; Schulz, C.U.; Meyer Zu Brickwedde, M.K.; Pendl, G.G.; Vestweber, D. Junctional adhesion molecule interacts with the PDZ domain-containing proteins AF-6 and ZO-1. *J. Biol. Chem.* **2000**, *275*, 27979–27988. [[CrossRef](#)]
105. McNeil, E.; Capaldo, C.T.; Macara, I.G. Zonula Occludens-1 Function in the Assembly of Tight Junctions in Madin-Darby Canine Kidney Epithelial Cells. *Mol. Biol. Cell* **2006**, *17*, 1922–1932. [[CrossRef](#)] [[PubMed](#)]
106. Fanning, A.S.; Anderson, J.M. Zonula Occludens-1 and -2 Are Cytosolic Scaffolds That Regulate the Assembly of Cellular Junctions. *Ann. N. Y. Acad. Sci.* **2009**, *1165*, 113–120. [[CrossRef](#)]
107. Patil, V.; Pal, J.; Somasundaram, K. Elucidating the cancer-specific genetic alteration spectrum of glioblastoma derived cell lines from whole exome and RNA sequencing. *Oncotarget* **2015**, *6*, 43452–43471. [[CrossRef](#)]
108. Li, H.; Lei, B.; Xiang, W.; Wang, H.; Feng, W.; Liu, Y.; Qi, S. Differences in protein expression between the U251 and U87 cell lines. *Turk. Neurosurg.* **2017**, *27*, 894–903. [[CrossRef](#)]
109. Derycke, L.D.M.; Bracke, M.E. N-cadherin in the spotlight of cell-cell adhesion, differentiation, embryogenesis, invasion and signalling. *Int. J. Dev. Biol.* **2004**, *48*, 463–476. [[CrossRef](#)]
110. Shih, W.; Yamada, S. N-cadherin-mediated cell-cell adhesion promotes cell migration in a three-dimensional matrix. *J. Cell Sci.* **2012**, *125*, 3661–3670. [[CrossRef](#)]
111. Shih, W.; Yamada, S. N-cadherin as a key regulator of collective cell migration in a 3D environment. *Cell Adhes. Migr.* **2012**, *6*, 513–517. [[CrossRef](#)] [[PubMed](#)]
112. Katsumoto, T.; Mitsushima, A.; Kurimura, T. The role of the vimentin intermediate filaments in rat 3Y1 cells elucidated by immunoelectron microscopy and computer-graphic reconstruction. *Biol. Cell* **1990**, *68*, 139–146. [[CrossRef](#)]
113. Chang, L.; Goldman, R.D. Intermediate filaments mediate cytoskeletal crosstalk. *Nat. Rev. Mol. Cell Biol.* **2004**, *5*, 601–613. [[CrossRef](#)]
114. Goldman, R.D.; Khuon, S.; Chou, Y.H.; Opal, P.; Steinert, P.M. The function of intermediate filaments in cell shape and cytoskeletal integrity. *J. Cell Biol.* **1996**, *134*, 971–983. [[CrossRef](#)] [[PubMed](#)]
115. Stauffer, S.R.; Coletta, C.J.; Tedesco, R.; Nishiguchi, G.; Carlson, K.; Sun, J.; Katzenellenbogen, B.S.; Katzenellenbogen, J.A. Pyrazole ligands: Structure-Affinity/activity relationships and estrogen receptor- α -selective agonists. *J. Med. Chem.* **2000**, *43*, 4934–4947. [[CrossRef](#)] [[PubMed](#)]
116. Sun, J.; Huang, Y.R.; Harrington, W.R.; Sheng, S.; Katzenellenbogen, J.A.; Katzenellenbogen, B.S. Antagonists selective for estrogen receptor α . *Endocrinology* **2002**, *143*, 941–947. [[CrossRef](#)]
117. Meyers, M.J.; Sun, J.; Carlson, K.E.; Marriner, G.A.; Katzenellenbogen, B.S.; Katzenellenbogen, J.A. Estrogen receptor- β potency-selective ligands: Structure-activity relationship studies of diarylpropionitriles and their acetylene and polar analogues. *J. Med. Chem.* **2001**, *44*, 4230–4251. [[CrossRef](#)]



Article

LPA₁ Receptor Promotes Progesterone Receptor Phosphorylation through PKC α in Human Glioblastoma Cells

Silvia Anahi Valdés-Rives ¹, Denisse Arcos-Montoya ¹, Marisol de la Fuente-Granada ¹, Carmen J. Zamora-Sánchez ², Luis Enrique Arias-Romero ³, Olga Villamar-Cruz ³, Ignacio Camacho-Arroyo ², Sonia M. Pérez-Tapia ^{4,5} and Aliesha González-Arenas ^{1,*}

- ¹ Departamento de Medicina Genómica y Toxicología Ambiental, Instituto de Investigaciones Biomédicas, Universidad Nacional Autónoma de México (UNAM), Ciudad de México 04510, Mexico; anahivaldes@gmail.com (S.A.V.-R.); diam.denisse@gmail.com (D.A.-M.); mdelafuente@iibiomedicas.unam.mx (M.d.l.F.-G.)
 - ² Unidad de Investigación en Reproducción Humana, Instituto Nacional de Perinatología-Facultad de Química, Universidad Nacional Autónoma de México (UNAM), Ciudad de México 04510, Mexico; carmenjaninzamora@comunidad.unam.mx (C.J.Z.-S.); camachoarroyo@gmail.com (I.C.-A.)
 - ³ Unidad de Investigación en Biomedicina (UBIMED), Facultad de Estudios Superiores-Iztacala, Universidad Nacional Autónoma de México (UNAM), Tlalnepantla, Estado de México 54090, Mexico; vicovc@gmail.com (O.V.-C.); larias@unam.mx (L.E.A.-R.)
 - ⁴ Unidad de Desarrollo e Investigación en Bioprocesos (UDIBI), Escuela Nacional de Ciencias Biológicas, Instituto Politécnico Nacional, Ciudad de México 11350, Mexico; sperez@ipn.mx
 - ⁵ Departamento de Inmunología, Escuela Nacional de Ciencias Biológicas, Instituto Politécnico Nacional, Ciudad de México 11340, Mexico
- * Correspondence: alieshag@iibiomedicas.unam.mx; Tel.: +52-55-5622-9209



Citation: Valdés-Rives, S.A.; Arcos-Montoya, D.; de la Fuente-Granada, M.; Zamora-Sánchez, C.J.; Arias-Romero, L.E.; Villamar-Cruz, O.; Camacho-Arroyo, I.; Pérez-Tapia, S.M.; González-Arenas, A. LPA₁ Receptor Promotes Progesterone Receptor Phosphorylation through PKC α in Human Glioblastoma Cells. *Cells* **2021**, *10*, 807. <https://doi.org/10.3390/cells10040807>

Academic Editor: Stephen Yarwood

Received: 10 March 2021

Accepted: 31 March 2021

Published: 4 April 2021

Publisher's Note: MDPI stays neutral with regard to jurisdictional claims in published maps and institutional affiliations.



Copyright: © 2021 by the authors. Licensee MDPI, Basel, Switzerland. This article is an open access article distributed under the terms and conditions of the Creative Commons Attribution (CC BY) license (<https://creativecommons.org/licenses/by/4.0/>).

Abstract: Lysophosphatidic acid (LPA) induces a wide range of cellular processes and its signaling is increased in several cancers including glioblastoma (GBM), a high-grade astrocytoma, which is the most common malignant brain tumor. LPA₁ receptor is expressed in GBM cells and its signaling pathways activate protein kinases C (PKCs). A downstream target of PKC, involved in GBM progression, is the intracellular progesterone receptor (PR), which can be phosphorylated by this enzyme, increasing its transcriptional activity. Interestingly, in GBM cells, PKC α isotype translocates to the nucleus after LPA stimulation, resulting in an increase in PR phosphorylation. In this study, we determined that LPA₁ receptor activation induces protein-protein interaction between PKC α and PR in human GBM cells; this interaction increased PR phosphorylation in serine400. Moreover, LPA treatment augmented *VEGF* transcription, a known PR target. This effect was blocked by the PR selective modulator RU486; also, the activation of LPA₁/PR signaling promoted migration of GBM cells. Interestingly, using TCGA data base, we found that mRNA expression of *LPA1* increases according to tumor malignancy and correlates with a lower survival in grade III astrocytomas. These results suggest that LPA₁/PR pathway regulates GBM progression.

Keywords: glioblastoma; LPA₁ receptor; protein kinase C α ; progesterone receptor

1. Introduction

Glioblastoma (GBM), an astrocytoma grade IV, represents the maximal evolution grade of astrocytomas and it is among the most lethal human malignancies [1,2]. The median survival for GBM patients with the best therapy is 12–15 months and only a minor percentage of the patients (3–5%) survive for more than three years. In the Mexican population, it has been estimated that the mean age of incidence is 45 ± 15 years, compared to the global estimate of 60 ± 15 years [3,4].

The lysophosphatidic acid (LPA) is a small molecule with a phosphate head group and an acyl (or alkyl) chain at the sn-1 (or sn-2) position of the glycerol backbone [5]. It interacts with at least six GPCRs (i.e., LPA₁₋₆) coupled to the G α proteins: G α q/11,

$G\alpha i/0$, $G\alpha 12/13$, $G\alpha s$; LPA can exert an extensive range of physiological effects such as wound healing, proliferation, neurogenesis, angiogenesis and survival, depending on the cellular context [6,7]. LPA is mainly synthesized by the cleavage of membrane phospholipids into lysophospholipids by removing a fatty acid chain through phospholipase A (PLA1 or PLA2) [8]. Subsequently, autotaxin (ATX) cleaves the head group (e.g., choline, ethanolamine, or serine) on the lysophospholipids and turns them into LPA [8,9]. ATX (also known as *ENPP2*) is a 125 kDa enzyme from the family of ectonucleotide pyrophosphatases/phosphodiesterases. This enzyme is secreted to the extracellular space in a constitutively activated form and is the responsible for the main LPA production in many pathologies [8,10].

Aberrant LPA signaling has been linked to diverse conditions such as cancer [8,11]; besides, the high expression of the LPA_1 receptor has been associated with malignant progression by enhancing proliferation, migration, angiogenesis and cancer stem-cell maintenance in several tumors such as breast cancer, pancreatic cancer, ovarian cancer and GBM [12–15]. In GBM cells, the LPA_1 receptor is redistributed in the cell membrane, increasing its coupling to $G\alpha q$ and $G\alpha 12$ proteins. This activates protein kinases C (PKCs) [16,17] and turns on a signaling pathway to induce malignant progression [17–20].

The role of PKCs in cancer progression is well-known [21]. In GBM, the kinase with the highest expression is $PKC\alpha$, [16,22]. This PKC isotype induces a pro-survival and proliferative effects in GBM cells [23,24]; however, since this kinase has a wide range of actions, its contribution to GBM progression through specific signaling pathways is poorly understood [21]. We have previously demonstrated that LPA, through its LPA_1 receptor, promotes $PKC\alpha$ nuclear translocation, inducing progesterone receptor (PR) phosphorylation at S400 [25].

In previous work, we have demonstrated that activation of PKCs phosphorylates PR at S400 and that this phosphorylation induces PR transcriptional activity [24,25]. The activation of PR is known to increase proliferation, migration and invasion of GBM cells [26–28] through the transcription of essential factors for tumor growth, such as *VEGF*, *cyclin D1* and *EGFR* [29]; however, it is unknown whether PR phosphorylation by PKC is through a direct or an indirect interaction and if this posttranslational modification results in activation of PR targets transcription.

Therefore, this study aimed to evaluate if LPA induces $PKC\alpha$ /PR interaction and if this association phosphorylates and activates PR, thereby increasing GBM cell migration. Using the TCGA database, we correlated patient survival with mRNA expression of *LPAR1*, *LPAR3* and *ENPP2* genes.

2. Materials and Methods

2.1. Cell Culture and Treatments

Human glioblastoma-derived cell lines U251 and LN229 (American Type Culture Collection, Manassas, VA, USA (ATCC)) were grown in 10-cm dishes and maintained in DMEM medium (In Vitro, CDMX, Mexico), supplemented with 10% fetal bovine serum at 37 °C under a 95% air, 5% CO₂ atmosphere. 1-Oleoyl Lysophosphatidic Acid (LPA; 62215; Cayman Chemical, Ann Arbor, MI, USA) was used to activate LPA receptors and subsequently $PKC\alpha$. $LPA_{1/3}$ receptor antagonist Ki16425 (SML0971; Sigma-Aldrich, St. Louis, MO, USA) was added 30 min before the LPA treatment when used. Progesterone (P4) (SML0971; Sigma-Aldrich, St. Louis, MO, USA) was used to activate PR; selective PR modulator, RU486 (M8046; Sigma-Aldrich, St. Louis, MO, USA), was added 30 min before the P4 treatment when used.

The National Institute of Genomic Medicine in Mexico City did proof of cell validation for the U251 cell line and for LN229, we get the ATCC certificate analysis.

2.2. Proximity Ligation Assay

PLA experiments were performed using Duolink[®] kit (DUO92101, Sigma-Aldrich, St. Louis, MO, USA) according to the manufacturer's instructions. A total of 4000 cells

were plated in 16 well chambers (178599, Nunc Lab-Teck, Thermo Scientific, Waltham, MA, USA) in DMEM medium with 10% fetal bovine serum for 24 h. Eighteen hours before treatments, the medium was changed for phenol red-free DMEM without fetal bovine serum and cells were incubated at 37 °C under a 95% air and 5% CO₂ atmosphere. Afterward, cells were stimulated for 0, 5 and 15 min with LPA 100 nM, washed twice with ice-cold PBS, fixed for 15 min with PBS/Paraformaldehyde 4% and permeabilized with 0.5% Triton X-100 for 30 min. Then, cells were blocked with 40 µL of blocking solution for 1 h at 37 °C in a humidity chamber and incubated overnight at 4 °C with the primary antibodies: monoclonal mouse antibody against PKCα (2 µg/mL; sc-8393; Santa Cruz Biotechnology, Dallas, TX, USA) and polyclonal rabbit antibody against total Progesterone Receptor (2 µg/mL; sc-7208; Santa Cruz Biotechnology, Dallas, TX, USA). To detect the primary antibodies, secondary proximity probes binding rabbit and mouse immunoglobulin (PLA probe rabbit PLUS and PLA probe mouse MINUS, Olink Bioscience, Sigma-Aldrich, St. Louis, MO, USA) were diluted 1:15 and 1:5 in blocking solution, respectively. The cells were then incubated with the proximity probe solution for 1 h at 37 °C, washed three times in 50 mM Tris pH 7.6, 150 mM NaCl, 0.05% Tween-20 (TBS-T) and incubated with the hybridization solution containing connector oligonucleotides (Olink Bioscience, Sigma-Aldrich, St. Louis, MO, USA) for 45 min at 37 °C. Samples were washed with TBS-T and subsequently incubated in the ligation solution for 45 min at 37 °C. The ligation solution contained T4 DNA ligase (Fermentas, Sigma-Aldrich, St. Louis, MO, USA), allowing the ligation of secondary proximity probes and connector oligonucleotides to form a circular DNA strand. Subsequently, the samples were washed in TBS-T and incubated with the amplification solution, containing phi29 DNA polymerase (Fermentas, Sigma-Aldrich, St. Louis, MO, USA) for the roller cycle amplification for 90 min at 37 °C and washed three times with TBS-T. Finally, the samples were incubated with the detection mix solution (containing Texas Red-labeled detection probes that recognize the amplified product, Olink Bioscience, Sigma-Aldrich, St. Louis, MO, USA) for 1 h at 37 °C, washed twice in SSC-T buffer (150 mM NaCl, 15 mM sodium citrate, 0.05% Tween-20, pH 7) and were coverslipped with a fluorescence mounting medium (Biocare Medical, Pacheco, CA, USA). Fluorescent signals were detected by laser scanning microscopy (Nikon TE2000, Amsterdam, Netherlands) and PLA-positive signals were quantified using MetaMorph software. At least 50 nuclei were measured for each experimental condition.

2.3. RNA Extraction and RT-qPCR

To evaluate the effect of LPA on the gene expression induced by PR, we quantified VEGF, EGFR, TGFβ1 and cyclin D1 expression 24 h after LPA or P4 stimulation. 2×10^5 U251 cells were plated per well in six-well plates. At 24 h before treatment, the growth medium was replaced by phenol red-free DMEM supplemented with 10% charcoal-dextran filtered SFB. Then, cells were treated for 24 h with LPA (100 nM), P4 (10 nM), RU 486 (1 µM) and the conjunct treatments LPA + RU486 or P4 + RU486 (same concentrations). After treatment, cells were washed with PBS and TRIzol[®] LS Reagent (Invitrogen, Carlsbad, CA, USA) was added to detach cells from the plate. The RNA extraction was performed according to the manufacturer recommendations by the phenol-guanidine isothiocyanate-chloroform method. After extraction, RNA quantity and purity were measured with the NanoDrop 2000 Spectrophotometer (Thermo Fisher Scientific, Waltham, MA, USA). Additionally, optimal RNA integrity was assessed by the electrophoresis of 1 µg of total RNA in a 1% agarose gel in 0.5× TB buffer. cDNA was synthesized from 1 µg of total RNA with the M-MLV Reverse Transcriptase (Invitrogen, Carlsbad, CA, USA) and oligonucleotides (dT)12–18 Primer (Invitrogen, Carlsbad, CA, USA) according to the manufacturer's protocol. A total of 2 µL of such reaction was used to determine the expression of VEGF, EGFR, or the 18S ribosomal gene as expression control by qPCR with the LightCycler[®] FastStar DNA Master SYBR Green I and the LightCycler 1.5 (Roche Molecular Systems, Pleasanton, CA, USA) according to the manufacturer's protocol. Oligonucleotide sequences were: 5'-CCACACCATCACCATCGACA-3' for-

ward VEGF primer, 5'-CCAATTCCAAGAGGGACCGT-3' reverse VEGF primer (amplified fragment of 153 bp); 5'-GCCTTGACTGAGGACAGGCAT-3' forward EGFR primer, 5'-TGGTAGTGTGGGTCTCTGCT-3' reverse EGFR primer (amplified fragment of 152 bp); 5'-AGTGAAACTGCAATGGCTC-3' forward 18S primer, 5'-CTGACCGGGTTGGTTTTGAT-3' reverse 18S primer (amplified fragment of 167 bp). A reaction without RT was performed as a negative control. The relative gene expression was calculated with the $2^{-\Delta C_t}$ [30,31]. One-way ANOVA and a Tukey test were performed to determine statistical differences between treatments by using the GraphPad Prism 8.0 software (GraphPad Software, San Diego, CA, USA).

2.4. Immunofluorescence

Eight thousand cells per well were plated in Millicell EZ 4-well glass slides (Millipore, Burlington, MA, USA). Eighteen hours before treatments, the medium was changed for phenol red-free DMEM without fetal bovine serum and cells were incubated at 37 °C under a 95% air, 5% CO₂ atmosphere. After the treatments, cells were fixed for 20 min in 4% paraformaldehyde solution at 37 °C and permeabilized with 100% methanol for 6 min at −4 °C. Next, fixed cells were blocked with 1% bovine serum albumin in PBS for 1 h at room temperature and incubated at 4 °C for 24 h with 1 µg/mL of rabbit anti-pS400PR (ab60954, Abcam, Cambridge, UK) in 0.5% bovine serum albumin in PBS. The samples were rinsed thrice in PBS for 5 min each and incubated in the dark with 0.5 µg/mL anti-mouse Alexa Fluor 488-labeled secondary antibodies (A11034, Invitrogen, Carlsbad, CA, USA) for 45 min. Nuclei were stained with 1 µg/mL Hoechst 33342 solution (Thermo Scientific, Waltham, MA, USA). The cells were coverslipped with a fluorescence mounting medium (Biocare Medical, Pacheco, CA, USA). The samples were visualized in a Nikon A1R + STORM confocal microscope.

Specific characteristics of the antibodies described in Sections 2.2 and 2.4 can be consulted in Table S1.

2.5. Migration Assay

To evaluate if blocking LPA₁/PR signaling pathway affects migration, the scratch-wound assay was used. 300,000 cells were plated with DMEM medium in six-well plates until 90% confluence and the formation of a uniform monolayer were observed. With a 200 mL pipet tip, a scratch per well was made in a previously marked well to allow the identification of 4 separate segments of scratch.

The detached cells were washed by aspiration. Cells were incubated with DMEM medium with DNA synthesis inhibitor cytosine β-D-arabino-furanoside hydrochloride (10 µM, AraC; Sigma-Aldrich, St. Louis, MO, USA). One hour later, RU486 and Ki16425 were added and the scratch images were taken with an inverted microscope Olympus IX71 (Olympus Corporation, Shinjuku City, Tokyo, Japan), at 4X magnification at 0 and 24 h. The percentage of wound closure from migrating cells in the scratch area was calculated as the mean of four fields using the ImageJ software (National Institutes of Health, Bethesda, MD, USA) and the formula:

$$\text{Wound closure \%} = \left[\frac{At0h - At\Delta h}{At0h} \right] \times 100 \quad (1)$$

where: $At0h$ = total area at time 0; $At\Delta h$ = total area after “×” hours.

2.6. LPAR1/3 and ENPP2 Gene Expression Evaluation

For LPAR1, LPAR3 and ENPP2 (ATX gene) mRNA determination, we used the California University, Santa Cruz platform: UCSC Xena ([XenaBrowser.net](https://xenabrowser.net); accessed on 18 March 2021) and the database from TCGA. After applying the filters and deleting the duplicated ones, we obtained 258 samples for grade II (GII), 271 for grade III (GIII) and 166 for grade IV astrocytomas (GIV or GBM). mRNA levels were obtained and plotted on Graph Pad Prism 5.0.

2.7. Survival Curves

For the evaluation of *LPAR1*, *LPAR1* and *ENPP2* (ATX gene) mRNA relationship with patient survival, Kaplan–Meier curves were performed using the platform of the California University, Santa Cruz: UCSC Xena (XenaBrowser.net; accessed on 18 March 2021) and the database from TCGA for tumor tissue. We obtained the following data from “TCGA low-grade astrocytoma and glioblastoma” and after applying the filters and deleting the duplicated ones: for *LPAR1*: Grade II: 65 samples, Grade III: 132 samples and Grade IV: 166 samples. For *LPAR3*: Grade II: 129 samples, Grade III: 134 samples and Grade IV: 96 samples. For *ENPP2*: Grade II: 254 samples, Grade III: 265 samples and Grade IV: 153 samples. Statistical analysis between high and low expression was performed with a Log-rank (Mantel–Cox) test. A value $p < 0.05$ was considered statistically significant, as stated in figure legends. All these analyses were performed in GraphPad Prism 8.0 (Graph Pad Software, San Diego, CA, USA).

2.8. Spearman Correlations

To obtain the correlation between the degree of expression of *PGR* and *LPAR1* or *ENPP2*, the gene expression database called “TCGA Glioblastoma (GBM)” was extracted from which the samples that did not have data for both genes were eliminated; 155 samples were used for each graph and the Spearman coefficient was determined using the GraphPad Prism 8.0.2 program.

2.9. Statistical Analysis

All data were analyzed and plotted using the GraphPad Prism 5.0 software for Windows XP (GraphPad Software, San Diego, CA, USA). Statistical analysis of comparable groups was performed using a one-way ANOVA with a Bonferroni or Tukey’s post-test. A value of $p = 0.05$ or less was considered statistically significant, as stated in figure legends.

3. Results

3.1. PKC α Interacts with PR after LPA₁ Receptor Activation

Our previous work showed that PKC α immunoprecipitated with total and phosphorylated PR at residue S400 [25]; we have also demonstrated that LPA induces PKC α nuclear translocation [26]. To investigate if these proteins could interact in the same compartment after LPA₁ receptor activation, a Proximity Ligation Assay (PLA) was performed (Figure 1).

Our results show that in the U251 cell line, the stimulation with LPA at 5 and 15 min induced a protein-protein interaction between PKC α and PR with a peak at 15 min. Additionally, the puncta were located both in the cytoplasmatic and the nuclear compartments. Interestingly, a scarce basal interaction of both proteins was observed.

3.2. PR Phosphorylated in Serine 400 (PRpS400) Has a Nuclear Localization

We have previously demonstrated LPA stimulation-induced PRpS400 and PKC α nuclear translocation [25]. We were interested in knowing if PRpS400 was cytoplasmic or/and nuclear since PKC α and PR interaction occurred in both compartments.

To assess the phosphorylation of PRpS400, we used immunofluorescence after 15 min of stimulation with 100 nM of LPA and/or 2.5 μ M of Ki16425 in U251 and LN229 cell lines (Figure 2).

Interestingly, our results show nuclear puncta of PRpS400 in both cell lines at 15 min after LPA stimulation. We measured the signal at 15 min because we have previously demonstrated that PRpS400 reaches its maximum level at this timepoint [25].

In contrast, Ki16425, an inhibitor of LPA_{1/3} receptors, blocked this effect on both cell lines. We have previously demonstrated that U251 cells express the LPA₁ receptor at a protein level and LN229 cells express LPA₁/LPA₃ receptors [25]. In the LN229 cell line, PRpS400 could be promoted by both LPA receptors; meanwhile, in U251, this phosphorylation is induced through the LPA₁ receptor.

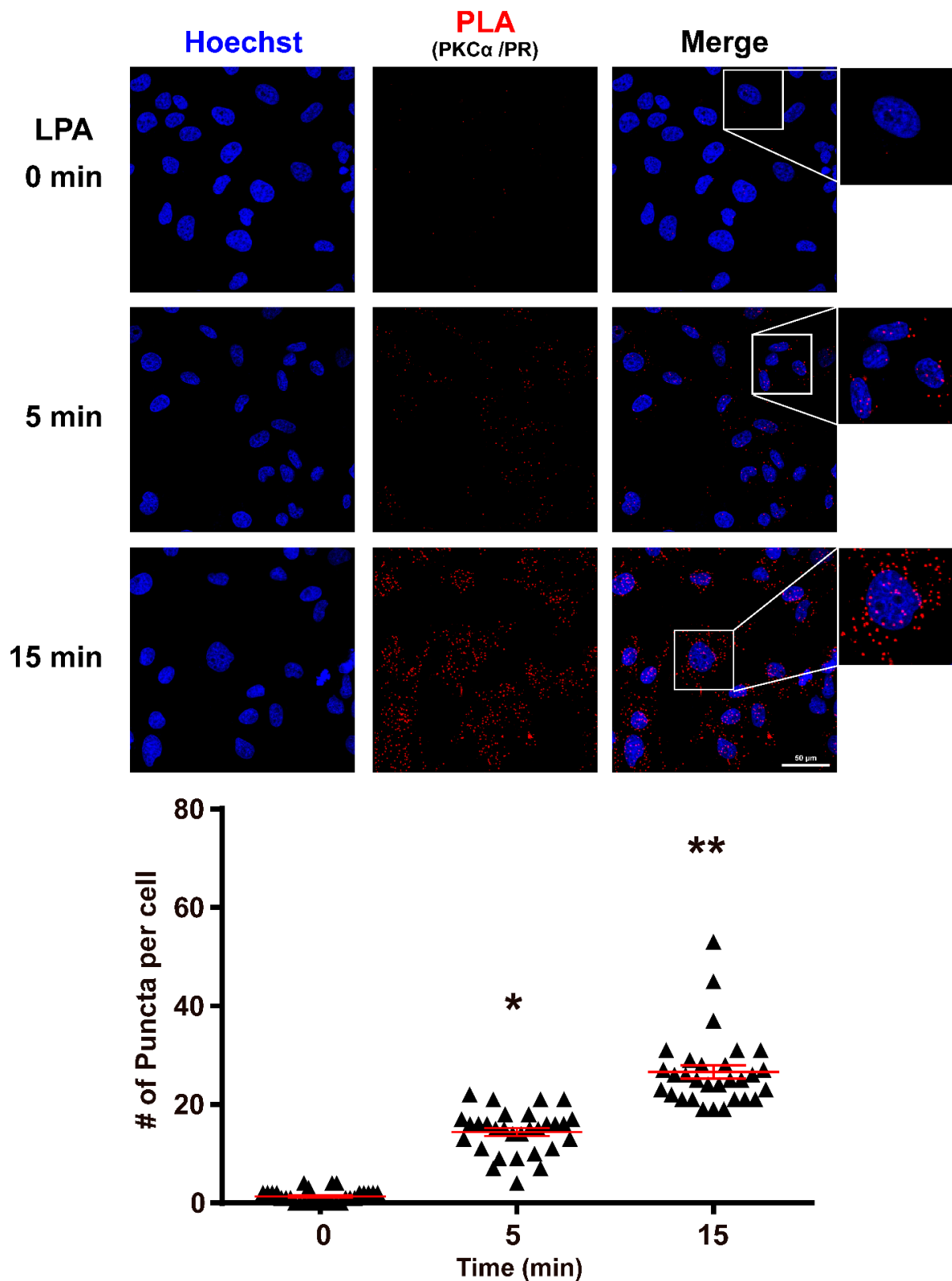


Figure 1. LPA induces the interaction of PKC α and PR. Top panel: representative images of the PLA assay. The red dots denote the proximity (distance less than 40 nm) of PKC α and PR at 0, 5 and 15 min of stimulation with 100 nM of LPA in the U251 cell line. Lower panel: graphic representation of the interactions. Results are expressed as the mean \pm S.E.M. of 30 cells nuclei per condition. A one-way ANOVA statistical test followed by a Tukey's post-test was used. * $p < 0.001$, compared to control (0) and 15 min, ** $p < 0.001$ compared to control (0).

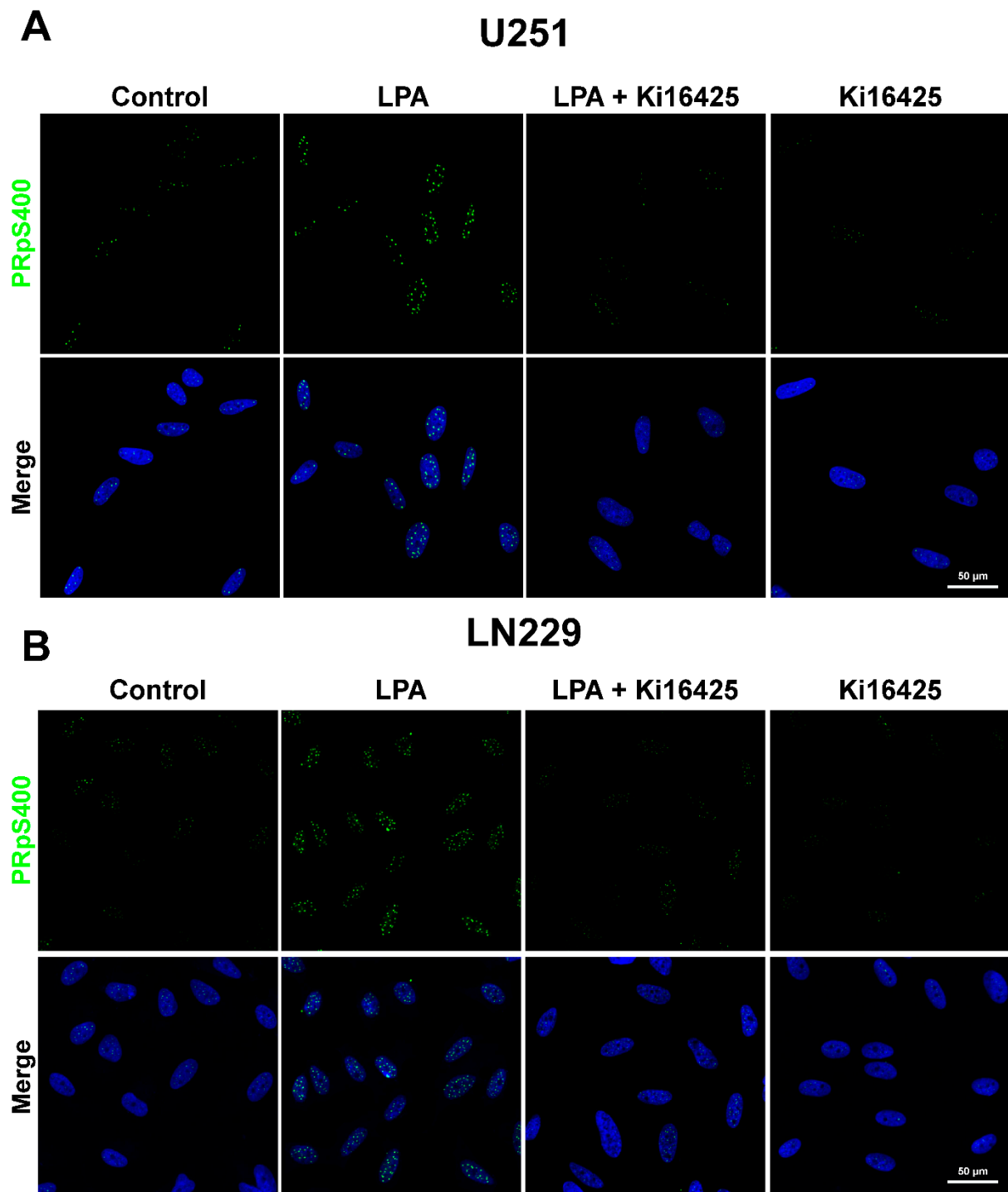


Figure 2. Localization of PRpS400 in GBM cell lines. PRpS400 localization in cell nuclei. The treatment with Ki16425 (2.5 μ M) inhibited the effect of LPA (100 nM) on the phosphorylation of PR at S400 at 15 min of stimulation in the GBM cell lines (A) U251, (B) LN229. PRpS400 (Green puncta), Hoechst (Blue). Representative images from 3 independent experiments. The photographs were taken at 60 \times magnification.

3.3. PR Induces the Expression of VEGF after Its Activation via the LPA₁ Receptor

In previous work, we showed that activating the LPA₁ receptor with its ligand induces PKC α translocation to the nucleus at 5 and 15 min [26]. Since this kinase interacts with PR and induces its phosphorylation at S400 [25], we wanted to test whether PR gene targets

could be induced by LPA treatment. We chose two important PR (*VEGF* and *EGFR*) targets known to contribute to GBM progression.

To evaluate whether LPA receptors activation modulates the expression of PR target genes, we measured their respective mRNAs with RT-qPCR after 24 h of stimulation with 10 nM of P4, 100 nM of LPA, 1 μ M of RU486 (selective modulator of PR) and the combination of RU486 with P4 or LPA in U251 cell line (Figure 3).

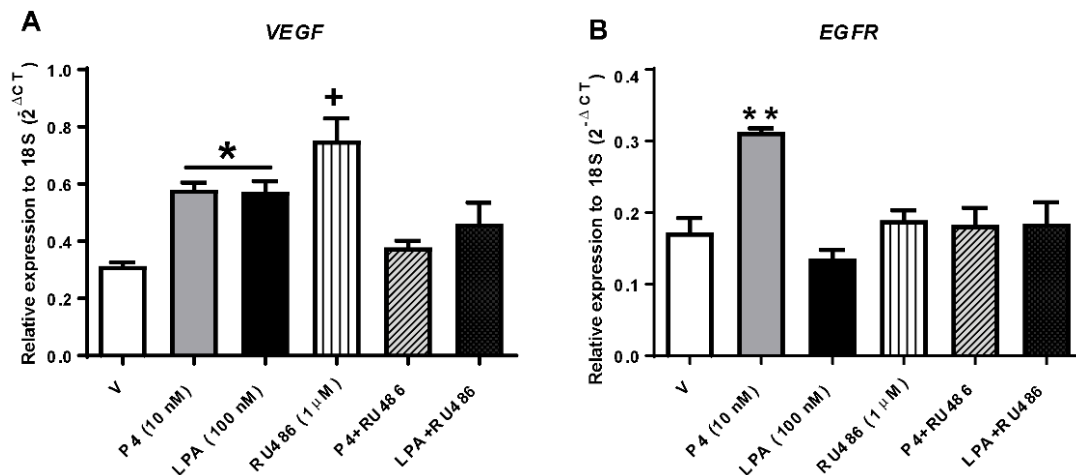


Figure 3. LPA modulates *VEGF* but not *EGFR* mRNA expression levels in GBM cells. U251 cells were treated with P4, LPA, RU486 and the combination of these treatments: P4 + RU486, LPA + RU486, or V (Vehicle; 0.1% ethanol) for 24 h, subsequently the gene expression of (A) *VEGF* and (B) *EGFR* was determined by RT-qPCR. Each column denotes the mean \pm S.E.M. of each treatment, $n = 4$. The one-way ANOVA statistical test followed by a Tukey post-test determined the statistical difference * $p < 0.02$ P4 and LPA vs. V; + $p < 0.009$ vs. V and the combined treatments; ** $p < 0.01$ P4 vs. all other treatments.

The results show that LPA modulated *VEGF* expression, similarly to P4, after 24 h of stimulation. The mRNA expression was downregulated when stimuli were combined with the selective PR modulator, RU486. However, this modulator acted as a receptor agonist when used alone. *EGFR* mRNA expression increased after P4 treatment and RU486 blocked this effect; however, no regulation by LPA was observed (Figure 3B).

3.4. LPA/PR Pathway Induces Migration

VEGF, a PR downstream target, is known to promote tumor progression. Migration of cancer cells and new vessel formation are vital factors in sustaining a growing tumor [32]. In GBM, a highly vascular tumor, VEGF is an important growth factor known to induce migration of both: GBM and endothelial cells [33].

We were interested in assessing if the LPA/PR pathway could induce migration in U251 and LN229 cell lines. We evaluated this process through a wound-healing assay with 10% FBS as LPA source combined with Ki1645 and/or RU486 at 0 h and 24 h (Figure 4).

The percentage of wound closure without or after treatment with DMSO or EtOH was 85% for U251 and 70% for LN229. In the U251 cell line, the effect of Ki16425 and RU486, in wound closure was 60 and 65%, respectively; meanwhile, in LN229 was 35% with Ki16425 and 49% with RU486. Interestingly, both compounds (RU486 and Ki16425) caused a 55% closure in U251 and a 30% in LN229, suggesting a slightly additive effect of both inhibitors.

Ki16425 is an antagonist for LPA_{1/3} receptors. We have previously demonstrated that U251 cells express the LPA₁ receptor at a protein level and LN229 cells express LPA₁/LPA₃ receptors [25]; thus, in the LN229 cell line, inhibition of migration could be promoted by both LPA receptors.

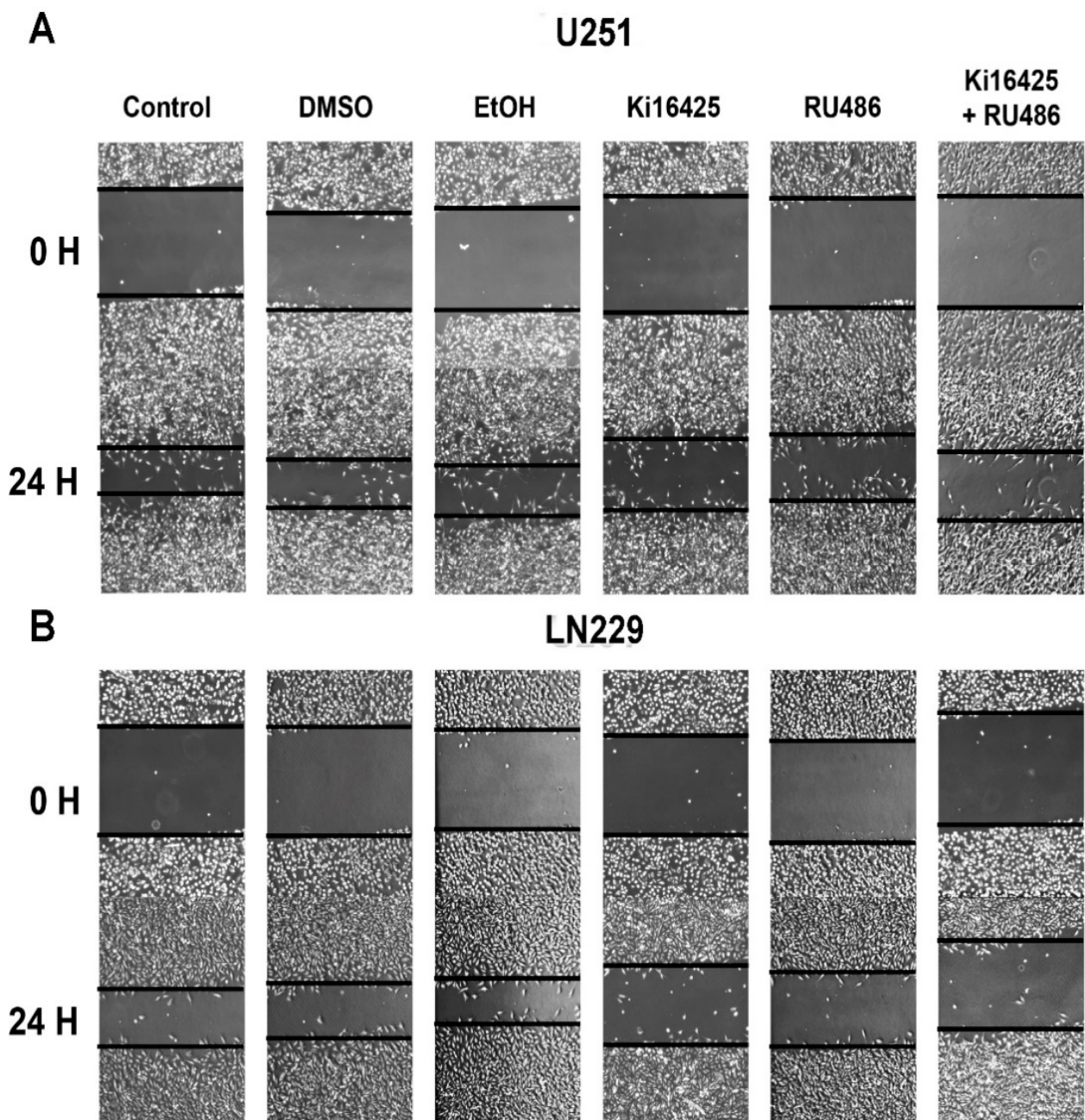


Figure 4. LPA/PR pathway signaling induces migration in GBM cells. (A) U251 and (B) LN299 cells were incubated for 24 h with complete medium (10% FBS), vehicles (DMSO and EtOH) and complete medium with Ki16425 (2.5 μ M), RU486 (1 μ M), or its combination. FBS was used as an LPA source. A total of 4 sections of the wound assay were analyzed per experiment and treatment. Representative images of two independent experiments are shown.

3.5. LPA_1 , LPA_3 and ATX Expression in the Survival of GBM Patients

Our results showed that LPA_1 /PR pathway induced PR targets transcription and migration of GBM cells; therefore, it is probable that this signaling pathway enhances tumor progression. Thus, we questioned whether LPA receptors ($LPAR1$, Figure 5A; $LPAR3$, Figure 6A) or ATX ($ENPP2$; Figure 7A) expression is modified at mRNA level in different astrocytoma grades. Additionally, we were interested in studying the correlation between these genes' expression and patient survival. Therefore, we constructed Kaplan–Meier graphs using TCGA data for astrocytoma grades II, III and IV with low and high expression of $LPAR1$ (Figure 5B–D), $LPAR3$ (Figure 6B–D) and $ENPP2$ (Figure 7B–D).

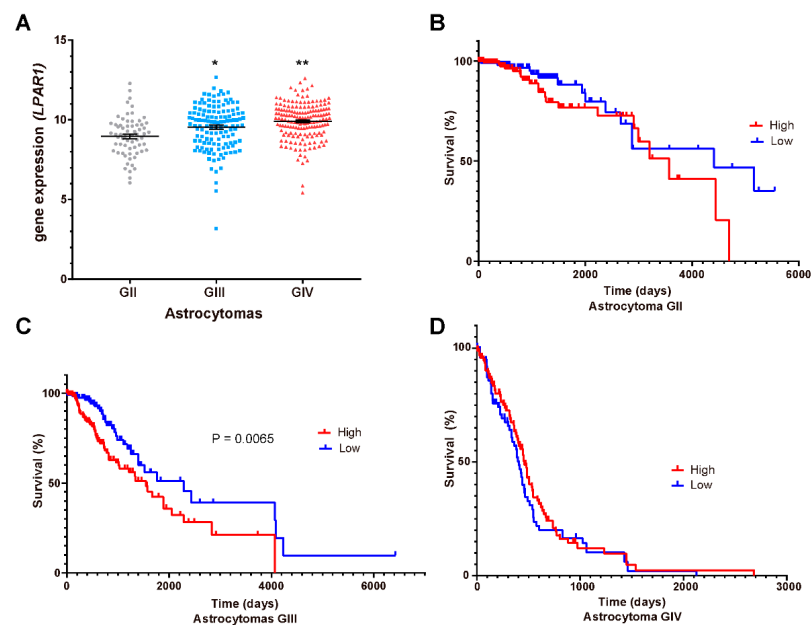


Figure 5. *LPAR1* mRNA expression and astrocytoma patient's survival. (A) *LPAR1* mRNA expression (RNA-seq Illumina HiSeq, $\log_2(\text{norm count} + 1)$) in TCGA datasets \pm SEM in different grades (G) of astrocytomas. The one-way ANOVA statistical test followed by a Tukey post-test determined the statistical difference * $p < 0.05$ GIII vs. GII and GIV, ** $p < 0.05$ GIV vs. GII and GIII. The Kaplan–Meier graphs show survival curves in patients that express low or high levels of *LPAR1* in astrocytomas (B) GII, (C) GIII and (D) GIV (GBM). Statistical analysis between high and low expression of *LPAR1* was performed with a Log-rank (Mantel–Cox) test. A value $p < 0.05$ was considered statistically significant, (B,D) were non-significant.

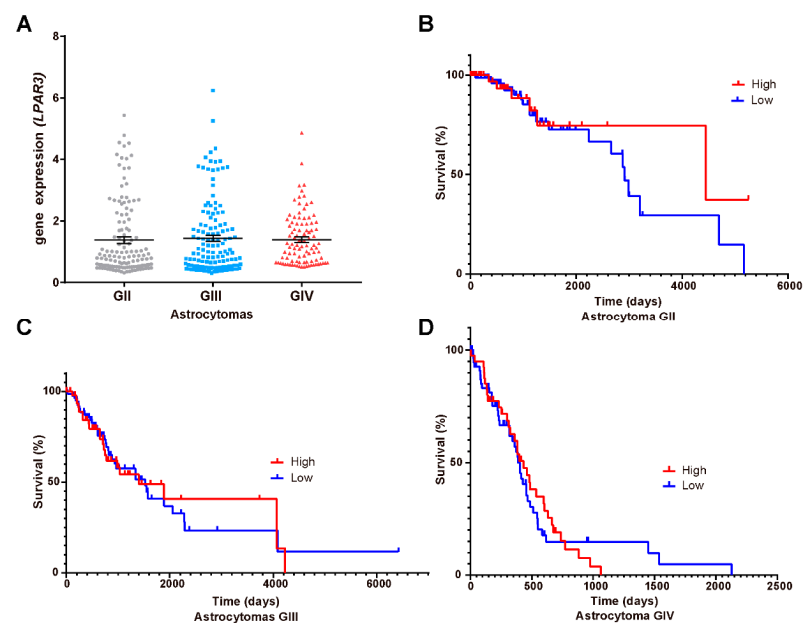


Figure 6. *LPAR3* mRNA expression and astrocytoma patient's survival. (A) *LPAR3* mRNA expression (RNA-seq Illumina HiSeq, $\log_2(\text{norm count} + 1)$) in TCGA datasets \pm SEM in different grades (G) of astrocytomas. The one-way ANOVA statistical test followed by a Tukey post-test determined the statistical difference. The Kaplan–Meier graphs show survival curves in patients that express low or high levels of *LPAR3* in astrocytomas (B) GII, (C) GIII and (D) GIV (GBM). Statistical analysis between high and low expression of *LPAR3* was performed with a Log-rank (Mantel–Cox) test. No statistical difference was observed.

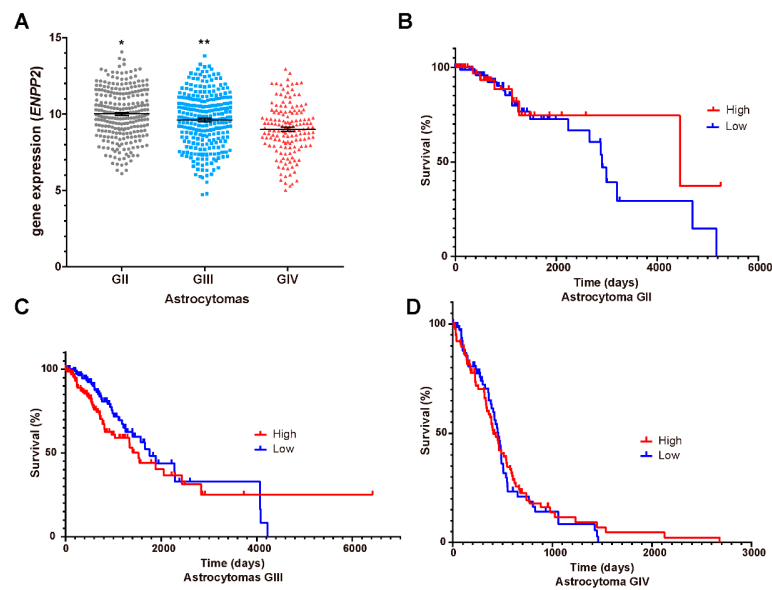


Figure 7. *ENPP2* mRNA expression and astrocytoma patient's survival. (A) *ENPP2* mRNA expression (RNA-seq Illumina HiSeq, $\log_2(\text{norm count} + 1)$) in TCGA datasets \pm SEM in different grades (G) of astrocytomas. The one-way ANOVA statistical test followed by a Tukey post-test determined the statistical difference. * $p < 0.05$ GII vs. GIII and GIV, ** $p < 0.05$ GIII vs. GII and GIV. The Kaplan–Meier graphs show survival curves in patients that express low or high levels of *ENPP2* in astrocytomas (B) GII, (C) GIII and (D) GIV (GBM). Statistical analysis between high and low expression of *ENPP2* was performed with a Log-rank (Mantel–Cox) test. No statistical difference was observed.

These results showed that the expression of *LPAR1* among the different grades of astrocytomas is increased with tumor malignancy (Figure 5A) while *LPAR3* and *ENPP2* expression does not (Figures 6A and 7A); in fact, *ENPP2* expression decreases according to tumor malignancy. For Kaplan–Meier curves, we found that *LPAR1* low expression is the only one related to overall survival in astrocytoma grade III patients (Figure 5C).

3.6. Correlation between PGR and *ENPP2* Gene Expression

Although *LPAR1* mRNA expression was associated with poor prognosis only in grade III astrocytomas, we were interested in evaluating whether there was a correlation between *PGR* and *LPAR1* expression (Figure 8A).

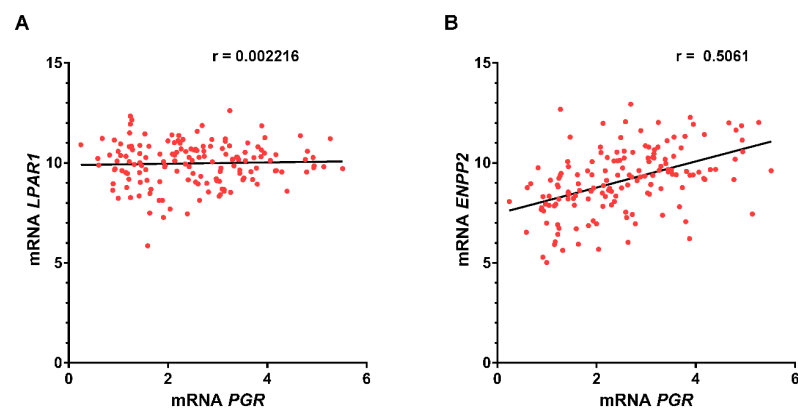


Figure 8. Correlation between *LPAR1/PGR* and *ENPP2/PGR* expression in GBM. The Spearman correlation coefficient was calculated to measure the association between (A) *LPAR1/PGR* and (B) *ENPP2/PGR* in GBM samples from the TCGA database.

Our results show that there was no correlation between the expression of *LPA1* and *PGR* genes. Since LPA production is mainly due to the enzyme ATX [8–10], it is possible that the expression of this enzyme could impact the LPA₁/PR signaling pathway. Therefore, we also analyzed if there was a correlation between *ENPP2* (ATX gene) and *PGR* mRNA expression. In this case, there was a positive correlation between these genes' expression (Figure 8B).

Additionally, by using PROMO-ALGGEN software (<http://alggen.lsi.upc.es/>; accessed on 5 March 2021), we investigated if *ENPP2* had possible progesterone response elements (PRE) in its promoter (*ENPP2* promoter sequence was obtained at the Eukaryotic Promoter Database (<https://epd.epfl.ch//index.php>; accessed on 5 March 2021) for PR binding that could, further, explain their correlation. We found seven possible binding sites in the *ENPP2* promoter with over 90% probability and one with over 95% (Figure 9) for both PR receptor isoforms (PRA and PRB).

Factors predicted within a similarity margin more or equal than 90 %

■ PR - A
 ■ PR - B

	1	10	20	30	40	50	60	70	80	90	100	110	120	130	140	150	160	170	180	190	200	210	220	230	240	250	260	270	280	290	300	310		
<i>ENPP2</i> promoter sequence																			■					■								■	■	
	320	330	340	350	360	370	380	390	400	410	420	430	440	450	460	470	480	490	500	510	520	530	540	550	560	570	580	590	600	610				
				■			■			■																								

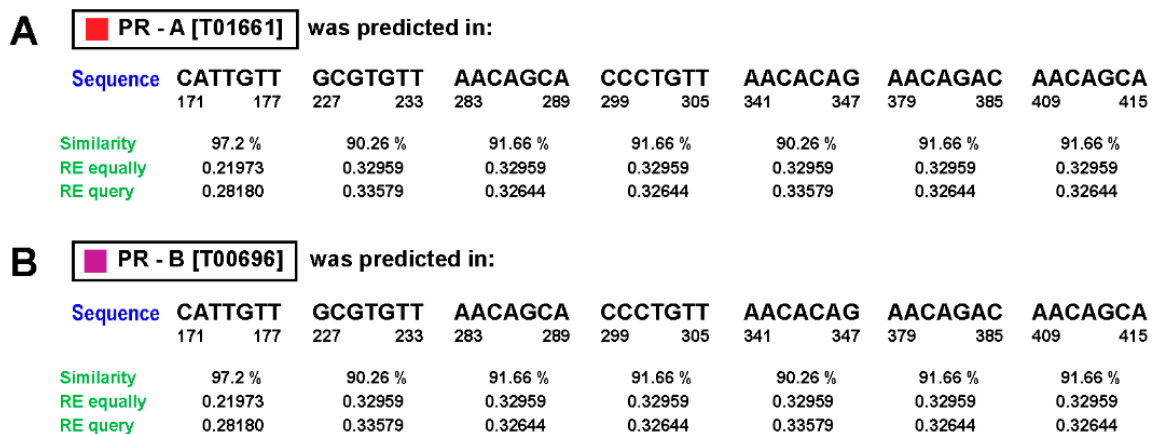


Figure 9. Possible binding sites for PR receptor in the *ENPP2* promoter sequence. Seven potential sequences were found for (A) PR isoform A and (B) PR isoform B in the *ENPP2* promoter.

4. Discussion

In this work, using the PLA assay, we evaluated whether there is a protein-protein interaction between PR and PKC α . The in situ PLA assay identifies the physical proximity of proteins; a signal will only be produced if two proteins are at a distance of less than 40 nm; this provides high selectivity for protein-protein interaction detection [34].

This assay demonstrated that after 5 and 15 min of 100 nM LPA stimulation, the proximity between PR and PKC α increased in a time-dependent manner. This result suggests a direct interaction of the kinase with the receptor that leads to the latter's phosphorylation. It is interesting to point out that U251 cells reached a high level of interaction between PR and PKC α at 15 min after LPA treatment, at the same time in which the highest accumulation of PKC α in the nucleus and the phosphorylation peak of PRpS400 were observed [25]. Furthermore, the protein-protein interaction location was cytoplasmatic and nuclear; this result proves that the PKC α /PR association could occur in both compartments, although the accumulation of PRpS400 was mainly nuclear.

Additionally, we wanted to evaluate whether the LPA₁/PKC α /PRpS400 pathway could modulate PR target genes' expression. Previous work from our laboratory reported that activation of PKC α increased PR phosphorylation that induced its transcriptional activity. In turn, PR increased the mRNA expression of the blocking factor induced by progesterone (PIBF) [27], a known PR target gene that causes cellular proliferation of GBM [24].

Other genes involved in GBM cell proliferation and migration are *EGFR* and *VEGF*, which are regulated by PR [29]. Therefore, we analyzed whether PR activation by LPA could modulate the expression of these two genes. We observed that *VEGF* expression was upregulated after LPA treatment similarly as P4 did it. In contrast, *EGFR* expression was only increased when the cells were treated with P4.

EGFR and *VEGF* are differentially regulated. *VEGF* has PRE consensus sites in addition to AP1 and SP1 sites in its promoter [35,36]. In previous work, we demonstrated that PKC activation induced a two-fold increase in PR transcriptional activity when GBM cells (U251) were transfected with the MMTV-Luc reporter plasmid carrying two PRE [24]; thus, LPA treatment induces PKC α activation (through LPA₁ receptor), that in turns phosphorylates PR, modulating *VEGF* expression by PRE.

Conversely, *EGFR* has SP1 sites but does not have canonical PREs. It is known that PR can activate MAPK or c-Src after its stimulation with P4 and that these signaling cascades promote receptor phosphorylations in different sites. Phosphorylations can promote PR binding to SP1 sites (e.g., PRpS345 by MAPK), inducing the transcription of genes without PRE in their promoters [37–39], which also explains the lack of RU486 effects on *EGFR* expression.

Although the selective modulator RU486 combined with P4 and LPA inhibits *VEGF* expression, we observed an increase in this gene transcription when used alone. This may be due to the role of RU486 as a partial agonist [40,41].

In addition, RU486 is a modulator of the glucocorticoid receptor, which could also induce *VEGF* transcription [42].

Additionally, the wound healing assay showed that inhibition of LPA₁/PR reduces cell motility. Interestingly, the inhibitors' combined effect had a slight additive impact suggesting that other pathways such as MAPK could contribute to cell migration through LPA₁ receptor signaling cascade or non-canonical PR pathways. It is worth noting that despite using a complete medium as a source of LPA, which includes growth factors, the effects of inhibiting LPA₁/PR or both were marked. Thus, due to the invasiveness nature of GBM, these results suggest that targeting both proteins is potentially beneficial at a therapeutical level. Moreover, the signaling from both proteins impacts more than just migration; although further studies are needed to corroborate our findings, they could also affect invasion, proliferation, survival and other important tumor progression features. It would be essential to point out that U251 cells express the LPA₁ receptor at a protein level and LN229 cells express LPA₁/LPA₃ receptors [25]; thus, the results found in the LN229 cell line could be promoted by both LPA receptors; meanwhile, in U251, LPA₁ receptor would be the main receptor involved in PR phosphorylation by PKC and in promoting cell migration.

We were also interested in analyzing if the mRNA of these LPA receptors and autotaxin could function as a predictor of patient survival among astrocytomas. Remarkably, *LPAR1* increases with tumor malignancy. However, it was only linked to survival in astrocytomas grade III. *LPAR3* mRNA expression did not vary among grades and *ENPP2* (ATX gene) decreased with malignancy; neither mRNAs had a link to patient prognosis. It is worth noting that the TCGA database does not harbor data of mutations of LPA receptor or ATX; therefore, we cannot account for mutants derived from *LPAR1*, *LPAR3* and *ENPP2* that could impact patient survival.

Additionally, GBM differences between the transcriptome and proteome have been found, suggesting that mRNA levels do not always reflect protein content. Leme e et al. found a poor correlation between mRNA and protein content of the neurofilament light

polypeptide and synapsin 1 in GBM patient samples [43]. Moreover, Song et al. performed a proteomic and genomic profiling of GBM and normal brain tissue and found mRNA expression rarely correlated with protein content [44]. The latter suggests that despite levels of *LPAR3* and *ENPP2* gene expression, we cannot disregard their protein role in GBM progression. In contrast, it would seem that *LPAR1* mRNA levels could be correlated with high protein levels, as demonstrated previously [25] and it has a functional role in tumor progression. However, none of the mRNA evaluated in this work could be markers for survival prognosis in GBM.

Furthermore, in a recent work from our lab, we have shown that PR protein expression increases with tumor malignancy, although mRNA levels seemed to decrease with tumor grade [45]. Moreover, PR mRNA does not correlate with survival prognosis in GBM. Several critical factors implicated in mRNA translation into its protein can be altered in GBM (e.g., regulatory proteins and siRNAs that need to be investigated [46]); therefore, the causes of mRNA/protein inconsistency in GBM remain unknown.

Despite the latter, our data suggested a possible correlation of *ENPP2* regulation by *PGR*, which could be through a positive feedback loop since we found probable PRE in the *ENPP2* promoter; thus, PRpS400 through LPA₁ receptor activation may upregulate ATX in GBM. However, the evidence so far is insufficient and requires further investigation.

5. Conclusions

LPA stimulates PKC α -PR interaction inducing receptor phosphorylation at S400, mainly in the cell nucleus. LPA₁/PR signaling cascade upregulates *VEGF* expression and induces cell migration contributing to GBM progression.

The expression of *LPAR3* and *ENPP2* mRNAs is not a biomarker for prognosis in patients' survival.

Supplementary Materials: The following are available online at <https://www.mdpi.com/article/10.3390/cells10040807/s1>, Table S1 Characteristics of the antibodies.

Author Contributions: S.A.V.-R. and A.G.-A. designed experiments and wrote the manuscript. S.A.V.-R. performed IF and confocal microscopy experiments. M.d.l.F.-G. and S.A.V.-R. performed cell culture and migration experiments. D.A.-M. performed survival curves and spearman correlations. O.V.-C. and L.E.A.-R. performed PLA assays. C.J.Z.-S. performed RNA extraction and RT-qPCR experiments. A.G.-A., I.C.-A. and S.M.P.-T. supervised the project. All authors have read and agreed to the published version of the manuscript.

Funding: This research was funded by UNAM-PAPIIT projects IA200718 and IA201120.

Institutional Review Board Statement: Not applicable.

Informed Consent Statement: Not applicable.

Data Availability Statement: The data presented in this study for survival curves are openly available in: TCGA: low-grade astrocytomas: URL: <https://portal.gdc.cancer.gov/projects/TCGA-LGG> accessed on 5 March 2021, and high-grade astrocytomas: URL: <https://portal.gdc.cancer.gov/projects/TCGA-GBM>, accessed on 18 March 2021. Promotor sequence obtained from URL: https://www.ensembl.org/Homo_sapiens/Gene/Sequence?db=core;g=ENSG00000136960;r=8:119557086-119673453, accessed on 5 March 2021.

Acknowledgments: This work was supported by UNAM-PAPIIT IA200718 and IA201120. Denisse Arcos-Montoya is a PhD student from Programa de Maestría y Doctorado en Ciencias Bioquímicas, Universidad Nacional Autónoma de México (UNAM) and received a fellowship 894557 from CONACyT. We thank Miguel Tapia-Rodriguez (Unidad de Microscopia, Instituto de Investigaciones Biomédicas, UNAM) for his technical support.

Conflicts of Interest: The authors declare no conflict of interest.

References

1. Louis, D.N.; Ohgaki, H.; Wiestler, O.D.; Cavenee, W.K.; Burger, P.C.; Jouvet, A.; Scheithauer, B.W.; Kleihues, P. The 2007 WHO Classification of Tumors of the Central Nervous System. *Acta Neuropathol.* **2007**, *114*, 97–109. [[CrossRef](#)] [[PubMed](#)]
2. Ostrom, Q.T.; Gittleman, H.; Truitt, G.; Boscia, A.; Kruchko, C.; Barnholtz-Sloan, J.S. CBTRUS Statistical Report: Primary Brain and Other Central Nervous System Tumors Diagnosed in the United States in 2011–2015. *Neuro. Oncol.* **2018**, *20*, iv1–iv86. [[CrossRef](#)]
3. Wegman-Ostrosky, T.; Reynoso-Noverón, N.; Mejía-Pérez, S.I.; Sánchez-Correa, T.E.; Alvarez-Gómez, R.M.; Vidal-Millán, S.; Cacho-Díaz, B.; Sánchez-Corona, J.; Herrera-Montalvo, L.A.; Corona-Vázquez, T. Clinical Prognostic Factors in Adults with Astrocytoma: Historic Cohort. *Clin. Neurol. Neurosurg.* **2016**, *146*, 116–122. [[CrossRef](#)] [[PubMed](#)]
4. Louis, D.N.; Perry, A.; Reifenberger, G.; von Deimling, A.; Figarella-Branger, D.; Cavenee, W.K.; Ohgaki, H.; Wiestler, O.D.; Kleihues, P.; Ellison, D.W. The 2016 World Health Organization Classification of Tumors of the Central Nervous System: A Summary. *Acta Neuropathol.* **2016**, *131*, 803–820. [[CrossRef](#)] [[PubMed](#)]
5. Moolenaar, W.H. Development of Our Current Understanding of Bioactive Lysophospholipids. *Ann. N. Y. Acad. Sci.* **2000**, *905*, 1–10. [[CrossRef](#)] [[PubMed](#)]
6. Yung, Y.C.; Stoddard, N.C.; Mirendil, H.; Chun, J. Lysophosphatidic Acid Signaling in the Nervous System. *Neuron.* **2015**, *85*, 669–682. [[CrossRef](#)]
7. Gonzalez-Gil, I.; Zian, D.; Vazquez-Villa, H.; Ortega-Gutierrez, S.; Lopez-Rodriguez, M.L. The Status of the Lysophosphatidic Acid Receptor Type 1 (LPA1R). *Medchemcomm* **2015**, *6*, 13–23. [[CrossRef](#)]
8. Valdés-Rives, S.A.; González-Arenas, A. Autotaxin-Lysophosphatidic Acid: From Inflammation to Cancer Development. *Mediat. Inflamm.* **2017**, *2017*. [[CrossRef](#)]
9. Aoki, J.; Inoue, A.; Okudaira, S. Two Pathways for Lysophosphatidic Acid Production. *Biochim. Biophys. Acta* **2008**, *1781*, 513–518. [[CrossRef](#)]
10. Perrakis, A.; Moolenaar, W.H. Autotaxin: Structure-Function and Signaling. *J. Lipid Res.* **2014**, *55*, 1010–1018. [[CrossRef](#)]
11. Yung, Y.C.; Stoddard, N.C.; Chun, J. LPA Receptor Signaling: Pharmacology, Physiology, and Pathophysiology. *J. Lipid Res.* **2014**, *55*, 1192–1214. [[CrossRef](#)] [[PubMed](#)]
12. Zhang, H.; Xu, X.; Gajewiak, J.; Tsukahara, R.; Fujiwara, Y.; Liu, J.; Fells, J.I.; Perygin, D.; Parrill, A.L.; Tigy, G.; et al. Dual Activity Lysophosphatidic Acid Receptor Pan-Antagonist/Autotaxin Inhibitor Reduces Breast Cancer Cell Migration In Vitro and Causes Tumor Regression In Vivo. *Cancer Res.* **2009**, *69*, 5441–5449. [[CrossRef](#)] [[PubMed](#)]
13. Lee, S.-C.; Fujiwara, Y.; Liu, J.; Yue, J.; Shimizu, Y.; Norman, D.D.; Wang, Y.; Tsukahara, R.; Szabo, E.; Patil, R.; et al. Autotaxin and LPA 1 and LPA 5 Receptors Exert Disparate Functions in Tumor Cells versus the Host Tissue Microenvironment in Melanoma Invasion and Metastasis. *Mol. Cancer Res.* **2015**, *13*, 174–185. [[CrossRef](#)] [[PubMed](#)]
14. Seo, E.J.; Kwon, Y.W.; Jang, I.H.; Kim, D.K.; Lee, S.I.; Choi, E.J.; Kim, K.; Suh, D.; Lee, J.H.; Choi, K.U.; et al. Autotaxin Regulates Maintenance of Ovarian Cancer Stem Cells through Lysophosphatidic Acid-Mediated Autocrine Mechanism. *Stem Cells* **2016**, *34*, 551–564. [[CrossRef](#)] [[PubMed](#)]
15. Fukushima, K.; Takahashi, K.; Yamasaki, E.; Onishi, Y.; Fukushima, N.; Honoki, K.; Tsujiuchi, T. Lysophosphatidic Acid Signaling via LPA1 and LPA3 Regulates Cellular Functions during Tumor Progression in Pancreatic Cancer Cells. *Exp. Cell Res.* **2017**, *352*, 139–145. [[CrossRef](#)]
16. Koivunen, J.; Aaltonen, V.; Peltonen, J. Protein Kinase C (PKC) Family in Cancer Progression. *Cancer Lett.* **2006**, *235*, 1–10. [[CrossRef](#)] [[PubMed](#)]
17. Steinberg, S.F. Structural Basis of Protein Kinase C Isoform Function. *Physiol. Rev.* **2008**, *88*, 1341–1378. [[CrossRef](#)] [[PubMed](#)]
18. Kishi, Y.; Okudaira, S.; Tanaka, M.; Hama, K.; Shida, D.; Kitayama, J.; Yamori, T.; Aoki, J.; Fujimaki, T.; Arai, H. Autotaxin Is Over-expressed in Glioblastoma Multiforme and Contributes to Cell Motility of Glioblastoma by Converting Lysophosphatidylcholine TO Lysophosphatidic Acid. *J. Biol. Chem.* **2006**, *281*, 17492–17500. [[CrossRef](#)] [[PubMed](#)]
19. Tabuchi, S. The Autotaxin-Lysophosphatidic Acid–Lysophosphatidic Acid Receptor Cascade: Proposal of a Novel Potential Therapeutic Target for Treating Glioblastoma Multiforme. *Lipids Health Dis.* **2015**, *14*, 56. [[CrossRef](#)]
20. Loskutov, Y.V.; Griffin, C.L.; Marinak, K.M.; Bobko, A.; Margaryan, N.V.; Geldenhuys, W.J.; Sarkaria, J.N.; Pugacheva, E.N. LPA Signaling Is Regulated through the Primary Cilium: A Novel Target in Glioblastoma. *Oncogene* **2018**, *1*. [[CrossRef](#)]
21. do Carmo, A.; Balça-Silva, J.; Matias, D.; Lopes, M. PKC Signaling in Glioblastoma. *Cancer Biol. Ther.* **2013**, *14*, 287–294. [[CrossRef](#)] [[PubMed](#)]
22. Mandil, R.; Ashkenazi, E.; Blass, M.; Kronfeld, I.; Kazimirsky, G.; Rosenthal, G.; Umansky, F.; Lorenzo, P.S.; Blumberg, P.M.; Brodie, C. Protein Kinase C α and Protein Kinase C δ Play Opposite Roles in the Proliferation and Apoptosis of Glioma Cells. *Cancer Res.* **2001**, *61*, 4612–4619.
23. Cameron, A.J.; Procyk, K.J.; Leitges, M.; Parker, P.J. PKC Alpha Protein but Not Kinase Activity Is Critical for Glioma Cell Proliferation and Survival. *Int. J. Cancer* **2008**, *123*, 769–779. [[CrossRef](#)]
24. González-Arenas, A.; Peña-Ortiz, M.Á.; Hansberg-Pastor, V.; Marquina-Sánchez, B.; Baranda-Ávila, N.; Nava-Castro, K.; Cabrera-Wrooman, A.; González-Jorge, J.; Camacho-Arroyo, I. Pkc α and Pkc δ Activation Regulates Transcriptional Activity and Degradation of Progesterone Receptor in Human Astrocytoma Cells. *Endocrinology* **2015**, *156*, 1010–1022. [[CrossRef](#)] [[PubMed](#)]

25. Valdés-Rives, S.A.; de la Fuente-Granada, M.; Velasco-Velázquez, M.A.; González-Flores, O.; González-Arenas, A. LPA1 Receptor Activation Induces PKC α Nuclear Translocation in Glioblastoma Cells. *Int. J. Biochem. Cell Biol.* **2019**, *110*, 91–102. [[CrossRef](#)] [[PubMed](#)]
26. Piña-Medina, A.G.; Hansberg-Pastor, V.; González-Arenas, A.; Cerbón, M.; Camacho-Arroyo, I. Progesterone Promotes Cell Migration, Invasion and Cofilin Activation in Human Astrocytoma Cells. *Steroids* **2016**, *105*, 19–25. [[CrossRef](#)] [[PubMed](#)]
27. Marquina-Sánchez, B.; González-Jorge, J.; Hansberg-Pastor, V.; Wegman-Ostrosky, T.; Baranda-Ávila, N.; Mejía-Pérez, S.; Camacho-Arroyo, I.; González-Arenas, A. The Interplay between Intracellular Progesterone Receptor and PKC Plays a Key Role in Migration and Invasion of Human Glioblastoma Cells. *J. Steroid Biochem. Mol. Biol.* **2016**. [[CrossRef](#)] [[PubMed](#)]
28. González-Agüero, G.; Gutiérrez, A.; González-Espinosa, D.; Solano, J.; Morales, R.; González-Arenas, A.; Cabrera-Muñoz, E.; Camacho-Arroyo, I. Progesterone Effects on Cell Growth of U373 and D54 Human Astrocytoma Cell Lines. *Endocrine* **2007**, *32*, 129–135. [[CrossRef](#)]
29. Hernández-Hernández, O.T.; González-García, T.K.; Camacho-Arroyo, I. Progesterone Receptor and SRC-1 Participate in the Regulation of VEGF, EGFR and Cyclin D1 Expression in Human Astrocytoma Cell Lines. *J. Steroid Biochem. Mol. Biol.* **2012**, *132*, 127–134. [[CrossRef](#)]
30. Schmittgen, T.D.; Livak, K.J. Analyzing Real-Time PCR Data by the Comparative CT Method. *Nat. Protoc.* **2008**, *3*, 1101–1108. [[CrossRef](#)]
31. Pfaffl, M.W. A New Mathematical Model for Relative Quantification in Real-Time RT-PCR. *Nucleic Acids Res.* **2001**, *29*, e45. [[CrossRef](#)]
32. Peña-Ortiz, M.Á.; Germán-Castelán, L.; González-Arenas, A. Growth Factors and Kinases in Glioblastoma Growth. *Adv. Mod. Oncol. Res.* **2016**, *2*, 248–260. [[CrossRef](#)]
33. Cheng, S.-Y.; Chen, N.-F.; Lin, P.-Y.; Su, J.-H.; Chen, B.-H.; Kuo, H.-M.; Sung, C.-S.; Sung, P.-J.; Wen, Z.-H.; Chen, W.-F. Anti-Invasion and Antiangiogenic Effects of Stelletin B through Inhibition of the Akt/Girdin Signaling Pathway and VEGF in Glioblastoma Cells. *Cancers* **2019**, *11*, 220. [[CrossRef](#)]
34. Fredriksson, S.; Gullberg, M.; Jarvius, J.; Olsson, C.; Pietras, K.; Gústafsdóttir, S.M.; Östman, A.; Landegren, U. Protein Detection Using Proximity-Dependent DNA Ligation Assays. *Nat. Biotechnol.* **2002**, *20*, 473–477. [[CrossRef](#)] [[PubMed](#)]
35. Mueller, M.D.; Vigne, J.-L.; Pritts, E.A.; Chao, V.; Dreher, E.; Taylor, R.N. Progestins Activate Vascular Endothelial Growth Factor Gene Transcription in Endometrial Adenocarcinoma Cells. *Fertil. Steril.* **2003**, *79*, 386–392. [[CrossRef](#)]
36. Tischer, E.; Mitchell, R.; Hartman, T.; Silva, M.; Gospodarowicz, D.; Fiddes, J.C.; Abraham, J.A. The Human Gene for Vascular Endothelial Growth Factor. Multiple Protein Forms Are Encoded through Alternative Exon Splicing. *J. Biol. Chem.* **1991**, *266*, 11947–11954. [[CrossRef](#)]
37. Hagan, C.R.; Daniel, A.R.; Dressing, G.E.; Lange, C.A. Role of Phosphorylation in Progesterone Receptor Signaling and Specificity. *Mol. Cell. Endocrinol.* **2012**, *357*, 43–49. [[CrossRef](#)] [[PubMed](#)]
38. Hudson, L.G.; Thompson, K.L.; Xu, J.; Gill, G.N. Identification and Characterization of a Regulated Promoter Element in the Epidermal Growth Factor Receptor Gene. *Proc. Natl. Acad. Sci. USA* **1990**, *87*, 7536–7540. [[CrossRef](#)] [[PubMed](#)]
39. Lange, C.A.; Shen, T.; Horwitz, K.B. Phosphorylation of Human Progesterone Receptors at Serine-294 by Mitogen-Activated Protein Kinase Signals Their Degradation by the 26S Proteasome. *Proc. Natl. Acad. Sci. USA* **2000**, *97*, 1032–1037. [[CrossRef](#)] [[PubMed](#)]
40. Chen, J.; Wang, J.; Shao, J.; Gao, Y.; Xu, J.; Yu, S.; Liu, Z.; Jia, L. The Unique Pharmacological Characteristics of Mifepristone (RU486): From Terminating Pregnancy to Preventing Cancer Metastasis. *Med. Res. Rev.* **2014**, *34*, 979–1000. [[CrossRef](#)]
41. Germán-Castelán, L.; Manjarrez-Marmolejo, J.; González-Arenas, A.; González-Morán, M.G.M.G.; Camacho-Arroyo, I. Progesterone Induces the Growth and Infiltration of Human Astrocytoma Cells Implanted in the Cerebral Cortex of the Rat. *Biomed Res. Int.* **2014**, *2014*. [[CrossRef](#)] [[PubMed](#)]
42. Pagès, G.; Pouysségur, J. Transcriptional Regulation of the Vascular Endothelial Growth Factor Gene—a Concert of Activating Factors*. *Cardiovasc. Res.* **2005**, *65*, 564–573. [[CrossRef](#)] [[PubMed](#)]
43. Lemée, J.M.; Clavreul, A.; Aubry, M.; Com, E.; De Tayrac, M.; Mosser, J.; Menei, P. Integration of Transcriptome and Proteome Profiles in Glioblastoma: Looking for the Missing Link. *BMC Mol. Biol.* **2018**, *19*, 13. [[CrossRef](#)] [[PubMed](#)]
44. Song, Y.C.; Lu, G.X.; Zhang, H.W.; Zhong, X.M.; Cong, X.L.; Xue, S.B.; Kong, R.; Li, D.; Chang, Z.Y.; Wang, X.F.; et al. Proteogenomic Characterization and Integrative Analysis of Glioblastoma Multiforme. *Oncotarget* **2017**, *8*, 97304–97312. [[CrossRef](#)]
45. Arcos-Montoya, D.; Wegman-Ostrosky, T.; Mejía-Pérez, S.; De la Fuente-Granada, M.; Camacho-Arroyo, I.; García-Carrancá, A.; Velasco-Velázquez, M.A.; Manjarrez-Marmolejo, J.; González-Arenas, A. Progesterone Receptor Together with PKC α Expression as Prognostic Factors for Astrocytomas Malignancy. *Onco. Targets. Ther.* **2021**. (In press)
46. Maier, T.; Güell, M.; Serrano, L. Correlation of mRNA and Protein in Complex Biological Samples. *FEBS Lett.* **2009**, *3966–3973*. [[CrossRef](#)]

Review

Rapid Actions of the Nuclear Progesterone Receptor through cSrc in Cancer

Claudia Bello-Alvarez, Carmen J. Zamora-Sánchez  and Ignacio Camacho-Arroyo *

Unidad de Investigación en Reproducción Humana, Instituto Nacional de Perinatología-Facultad de Química, Universidad Nacional Autónoma de México, Ciudad de México C.P. 0451, Mexico; clautus.bello@gmail.com (C.B.-A.); carmenjaninzamora@comunidad.unam.mx (C.J.Z.-S.)

* Correspondence: camachoarroyo@gmail.com; Tel.: +52-55-56223732

Abstract: The nuclear progesterone receptor (PR) is mainly known for its role as a ligand-regulated transcription factor. However, in the last ten years, this receptor's extranuclear or rapid actions have gained importance in the context of physiological and pathophysiological conditions such as cancer. The PR's polyproline (PXPP) motif allows protein–protein interaction through SH3 domains of several cytoplasmatic proteins, including the Src family kinases (SFKs). Among members of this family, cSrc is the most well-characterized protein in the scenario of rapid actions of the PR in cancer. Studies in breast cancer have provided the most detailed information on the signaling and effects triggered by the cSrc–PR interaction. Nevertheless, the study of this phenomenon and its consequences has been underestimated in other types of malignancies, especially those not associated with the reproductive system, such as glioblastomas (GBs). This review will provide a detailed analysis of the impact of the PR–cSrc interplay in the progression of some non-reproductive cancers, particularly, in GBs.

Keywords: nuclear progesterone receptor; cSrc; rapid actions; breast cancer; glioblastoma



Citation: Bello-Alvarez, C.; Zamora-Sánchez, C.J.;

Camacho-Arroyo, I. Rapid Actions of the Nuclear Progesterone Receptor through cSrc in Cancer. *Cells* **2022**, *11*, 1964. <https://doi.org/10.3390/cells11121964>

Academic Editors: James K. Pru and Wipawee Winuthayanon

Received: 6 May 2022

Accepted: 15 June 2022

Published: 18 June 2022

Publisher's Note: MDPI stays neutral with regard to jurisdictional claims in published maps and institutional affiliations.



Copyright: © 2022 by the authors. Licensee MDPI, Basel, Switzerland. This article is an open access article distributed under the terms and conditions of the Creative Commons Attribution (CC BY) license (<https://creativecommons.org/licenses/by/4.0/>).

1. Introduction

Progesterone (P4) is one of the most studied and characterized female sex hormones in the scenario of cancer [1–3]. P4 actions can be exerted by a diverse group of receptors, including nuclear progesterone receptors (PRs), membrane progesterone receptors (mPRs), and membrane-associated progesterone receptor components (PGRMCs). The mechanisms of P4 actions are classified as genomic or non-rapid effects when involving the transcription of P4-responsive genes and non-genomic or rapid effects when P4 effects are mediated by signaling through cytoplasmatic proteins [4,5].

Although the PR is primarily known for its function as a ligand-activated transcription factor, its interaction with P4 also triggers rapid or transcription-independent effects. Immediate effects mainly occur through the activation of mPRs [6] and PGRMCs [7–9], whereas nuclear actions are exerted by the PR [10], but the latter is the only one that can exert both effects. In addition to the domains involved in its function as a transcription factor, the PR possesses a polyproline-rich (PXPP) motif between aa 421 and 428 that binds to the SH3 domains of several cytoplasmic molecules, including cSrc (Figure 1), hematopoietic cell kinase (HCK), Fyn, and other kinases or adapter proteins such as the regulatory subunit of PI3K (p85), CRK proto-oncogene adaptor protein (Crk), and growth factor receptor-bound protein 2 (Grb2) [11]. cSrc is one of the most well-studied and well-characterized non-receptor tyrosine kinases in cancer progression. Unlike other proteins associated with the hallmarks of cancer, cSrc has no mutations but exhibits high enzymatic activity [12].

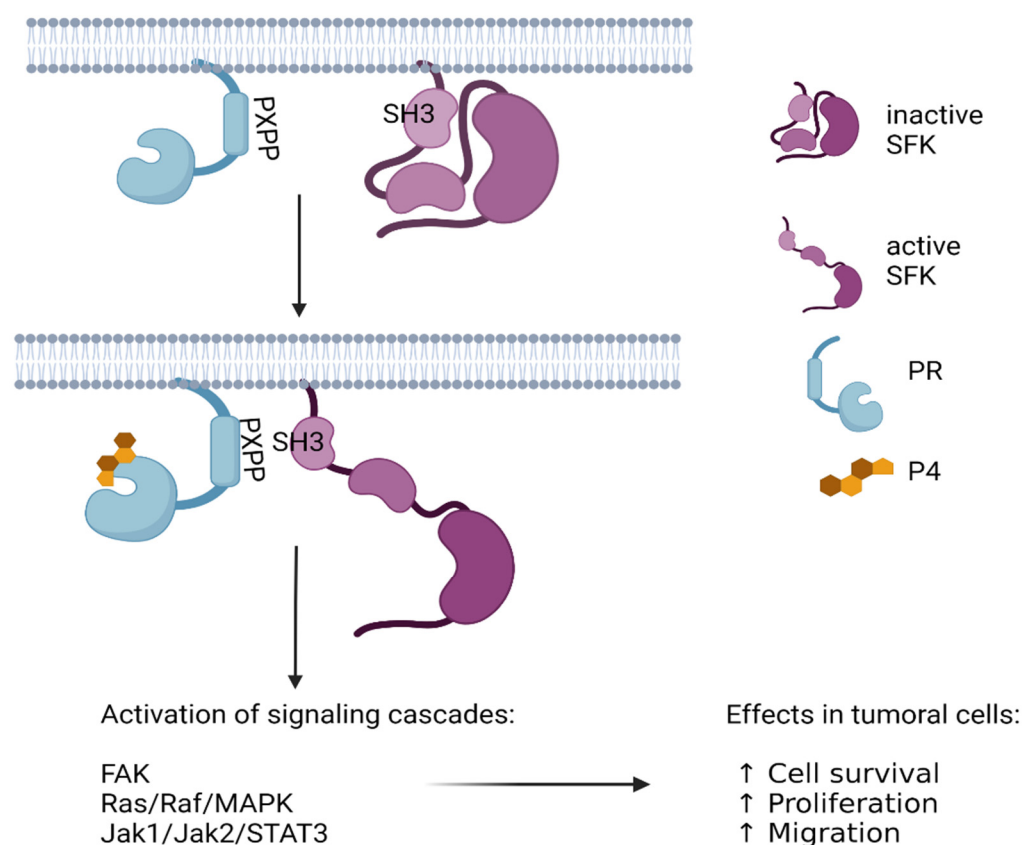


Figure 1. Activation of SFKs by SH3–PXPP interaction. In the cytoplasm or even anchored to the plasma membrane, PR interacts with other cytoplasmic molecules leading to the activation of various signaling cascades. Via PXPP, this receptor interacts with the SH3 domains of several molecules such as cSrc kinase. A direct interaction between cSrc and PR causes a conformational change in cSrc towards its active form and promotes the activation of other signaling cascades such as mitogen-activated protein kinases (MAPKs) that favor cancer progression by enhancing cell survival, proliferation, and migration.

PR–cSrc interaction has mainly been studied in breast cancer. Since the late 1990s, a large body of evidence has accumulated about the effect of P4 on breast cancer cells through rapid PR actions [13,14]. In several breast cancer-derived cell lines, it has been described that once stimulated by P4, the PXPP motif of the PR binds to the SH3 domain of cSrc, promoting a conformational change in this kinase that exposes its autocatalytic domain, followed by its activation (Figure 1) [15,16]. The interplay between the PR and cSrc in breast cancer leads to the activation of signaling pathways involved in proliferation (ERK–MAPKs) (19), migration, and invasion (focal adhesion kinase (Fak)—focal adhesion complexes) (Figure 1) [17,18]. In breast cancer, some evidence suggests that the nuclear estrogen receptor (ER) mediates the PR–cSrc interaction [13,14]. However, many elements in the mechanism of cSrc activation through the PR remain to be elucidated, for example, whether other proteins stabilize the PR–cSrc interaction. Another aspect of interest is to elucidate the PR regulation by cSrc. In this review, we aimed to discuss these aspects, the unknown processes in this mechanism, and the impact on cancer progression.

2. SH3 Domain–PXPP Motif Interaction: Structural Basis and Functions

The protein–protein interactions mediated by SH3 domain–PXPP motifs are one of the most abundant and studied processes in cells since they are necessary for activating signaling pathways and for protein subcellular localization. Although the SH3 domain was first described as an extra-catalytic domain of the Src family kinases (SFKs) in the 1980s, they are present in a wide variety of proteins: other tyrosine kinases such as the Abl family

and cytoskeletal proteins such as actin and myosin [19,20]. Around 300 SH3 domains have been identified in the human genome and in more than 200 different proteins [21].

In the case of SFKs, the protein–protein interaction mediated by the SH3 domain promotes their activation. Once activated, such kinases regulate diverse signaling pathways whose final effect is inducing cellular proliferation, cell survival, and migration, among other effects. Their broad cross-talk with many different transduction pathways makes them key regulators in pathologies such as cancer [22].

The SH3 domains consist of approximately 55–85 amino acids with a conserved structure folding [23]: five to six β -strands arranged as antiparallel β -sheets or as β -barrels connected by three loops and one helix. In addition, the SH3 domain is rich in aromatic amino acid residues that stabilize the binding site interaction with their ligand. These last elements are relevant to peptide ligand recognition [24]. The canonical ligands of SH3 domains are the PXPP left-handed helices [25].

The PXPP motifs are highly abundant in the human proteome [26]. Such protein motifs have a pseudo-symmetrical structure, which could be recognized in two different orientations by the PXXP-binding site of the SH3 domain. There are two classes of the PXPP motifs ligands which differ in the consensus sequence orientation: The class I consensus sequence is RXLPPXP, whereas class II is constituted of the consensus sequence XPPLXPR (the opposite orientation from class I) [27]. Positive amino acids such as arginine and lysine are necessary for the recognition of the polyproline motif by the SH3 domain. Such residue is recognized by the specificity pocket of the SH3 domain, formed by negative amino acid residues adjacent to the PXPP motif binding site [28,29]. In the particular case of SFKs, it was reported that they bind to the class I consensus sequence of polyproline motifs [27].

The Src kinases family is constituted by nine members whose structural organization is highly conserved in humans. Near their N-terminal domain (NTD), the SH4 domain is located, and its post-translational modifications such as myristoylation and palmitoylation are involved in attaching the kinase to the cell membrane. The SH4 domain is also one of the most variable regions among SFKs. Aside from SH4, the SH3 and SH2 domains regulate protein–protein interactions and the catalytic activity of the Src family. Interactions mediated by SH3 domain–PXPP motifs are key regulators in the function of SFKs. The SH2 is attached with a linker section to the SH1 domain, which is the enzyme's catalytic center. It is followed by the C-terminal short section containing an autoinhibitory phosphorylation residue.

When the C-terminal residue is phosphorylated, it remains bound to SH2, maintaining Src in an inactive conformation. The SFKs will change to their active form if dephosphorylation of such residue occurs or if a protein–protein interaction occurs in the SH2 or SH3 domains and induces their conformational change [30]. Many protein substrates can recruit and activate SFKs by interacting with the SH3 and/or SH2 domains. Some ligands of Src are growth factor receptors, integrins, other kinases such as Fak, and intracellular steroid receptors such as the PR (Figure 1) [31,32].

The PR belongs to the superfamily of nuclear receptors, which are best characterized by their function as transcription factors. The PR is part of the nuclear receptor subfamily 3, which comprises other steroid receptors such as ER, androgen (AR), glucocorticoid, and mineralocorticoid receptors. This family of receptors has very high variability in the NTD, favoring their interaction with specific proteins such as coactivators, other nuclear receptors, and hub proteins of different signaling pathways such as the Src family [33]. Two main PR isoforms in humans have been reported: PR-A and PR-B. Although their transcription is regulated by two distinct promoters, they are coded by the same gene (11q22–23). Structurally, the PR-B is the longer isoform and has 164 more amino acids than the PR-A in the NTD region [34].

The membrane or cytoplasmatic localization of steroid receptors is crucial to their participation in activating rapid non-transcriptional pathways. In the case of the PR, ER, and AR, their attachment to caveolae lipid rafts of the plasma membrane is mediated by their palmitoylation at the ligand-binding domain (LBD) [35,36]. This post-translational

modification is promoted by the heat shock protein 27 (Hsp27) in the ER [36]. Once attached to the plasmatic membrane, steroid receptors can interact with other proteins of the focal adhesion complexes. These stable structures at the plasma membrane interact with extracellular matrix components that mediate cellular responses to the external and inner signals regulating metabolic activity, proliferation, and motility [35].

In the PR-B, the PXPP motif is located between the 421 and 428 amino acids in the NTD region. When a direct interaction exists between cSrc and the PR, the former transits to its active form and promotes the activation of other kinases such as the mitogen-activated protein kinases (MAPKs) [16] (Figure 1). The activation of such signaling cascades has high repercussions in the cells, particularly, in different cancers, as described in the incoming sections (Figure 1). It is also important to mention that other steroid receptors also promote the activation of such signaling cascades, although their interaction with cSrc proteins could be different from the PR. The interaction between the AR and cSrc is also mediated by the interaction of SH3–PXPP, but the ER interacts with this kinase at the SH2 domain [37,38].

3. Functions of the Polyproline Motif of PR in Breast Cancer

Most research about rapid PR actions has been conducted on hormone-dependent cancers. Most PR rapid effects depend on the activation of cSrc by SH3–PXPP motif interactions or through its indirect interaction mediated by the ER [13–15].

In the first half of the 1990s, the molecular mechanisms involved in breast cancer progression by the action of sex hormones were still unknown. In 1998, Migliaccio et al. first reported progestin-dependent activation of cSrc and that this effect was dependent on the formation of the ER–cSrc–PR complex [13]. Interestingly, three years later, Boonyaratanakornkit et al. reported that activation of cSrc by the synthetic progestin R5020 was not dependent on the presence of the ER and that the PR could directly interact through the PXPP motif–SH3 domain [15]. Subsequent studies have shown that the PR and ER can directly interact with cSrc; however, the mechanisms that allow this interaction are specific for each receptor [11]. The dynamic of the interaction in cells expressing both receptors is not known. Answering in which contexts the participation of the ER is essential for activation of cSrc through the PR (Figure 2) would provide valuable information for the development of more effective therapies against breast cancer.

In vitro models of breast cancer have enlightened the relevance of PR interaction with kinases attached to the plasma membrane. The cell proliferation enhanced by progestins has been extensively reported in breast cancer [39]. In the T47D breast cancer cell line, Skildum et al. demonstrated that the mutant form of the PR-B (S294A PR-B) with low transcriptional activity and diminished proteasomal degradation [40] could activate the Ras/Raf/MAPK cascade in a ligand-dependent manner. In addition, the S294A PR-B and wt-PR induce cell cycle progression [41]. This is interesting considering that only about 5% of the PR is at the plasma membrane [15]. The direct cSrc activation by the PR is as fast as 5 to 10 min, and apart from MAPK activation, such effects activate ERK and EGFR, which in T47D also activate transcription factors such as Sp1, which promotes the expression of genes without PRE, like p21 protein [41,42].

Moreover, the positive feedback between PR rapid signaling and growth factor-activated pathways was reported in breast cancer cell lines. The co-localization of EGFR, PR, and cSrc has been reported in the focal adhesion complexes. In this context, the activation of EGFR depends on the ligand-dependent activation of the PR-B [42]. In addition, the Jak/STAT pathway is activated by PR–cSrc in T47D and the mammary-induced tumor model with C4HD cells. In such models, the progestin medroxyprogesterone induces the rapid activation of cSrc with the subsequent activation of the signal cascade Jak1/Jak2/STAT3.

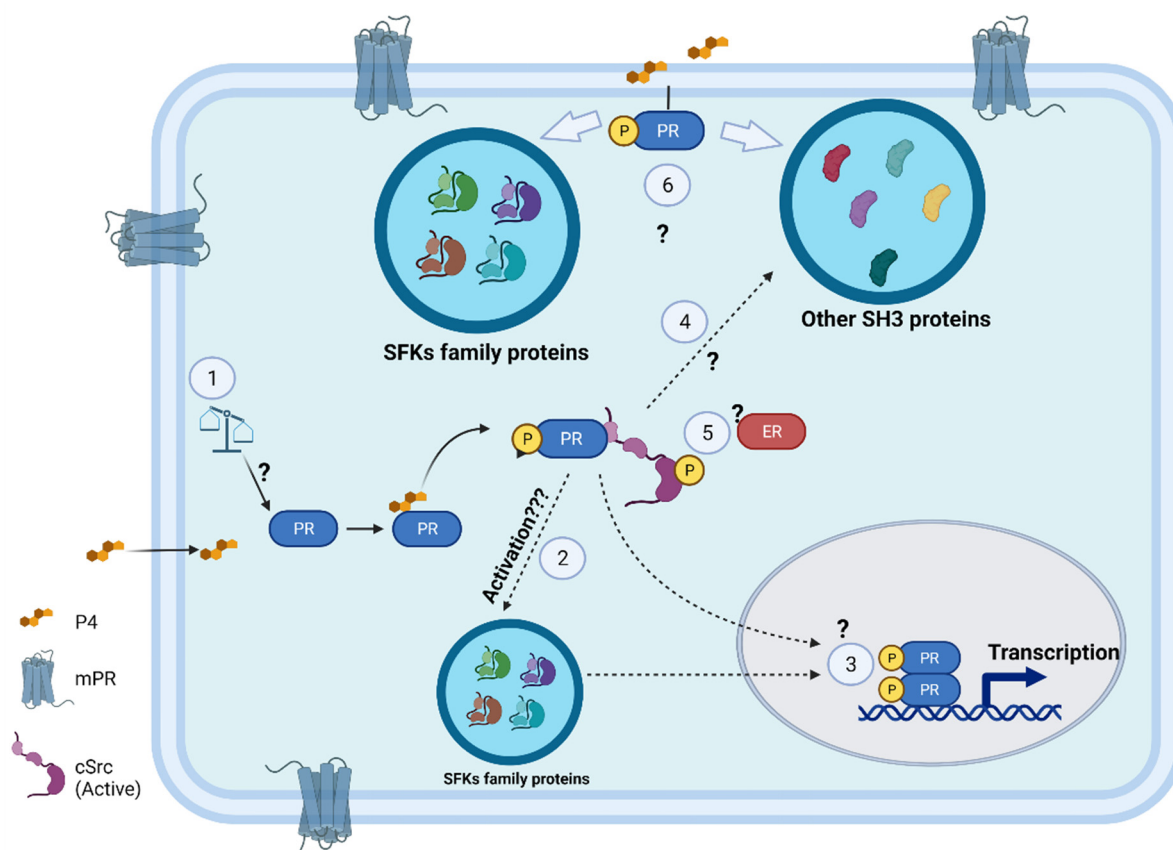


Figure 2. Potential extranuclear effects of PR. In breast cancer cells, cSrc kinase has been reported to bind PR through SH3–PXPP interaction. This interaction promotes the activation of cSrc by a conformational change that exposes the tyrosine residue 416. Other SH3-domain proteins could interact with the PR. Although its main localization is nuclear and cytoplasmic, the PR has been found to be anchored to the plasma membrane. However, there is still a lack of knowledge about many of the proteins and effects involved in the extranuclear signaling of the receptor. 1: What role does P4 concentration play in the induction of rapid PR effects? 2: What other kinases of the SFKs family can be activated by their interaction with the PR? 3: What is the role of cSrc and other SFKs in PR phosphorylation? 4: Which other proteins with SH3 domains can interact with the PR, and what effects are triggered? 5: In what context is the ER essential for the activation of cSrc through the PR? 6: What are the mechanisms allowing PR anchoring to the plasma membrane? What protein complexes would form in this area? Furthermore, is this PR localization essential for extranuclear signaling?

Additionally, in the longer term (48 h), medroxyprogesterone also promotes an augment in STAT3 levels [43]. In T47D breast cancer cells, P4 enhances breast cancer cell migration and invasion via activating Fak through extranuclear actions of the PR [17]. The Fak kinase also contains an SH3 domain that mediates the interaction with several of the components of focal adhesions, including cSrc [44]. However, it is unknown whether the SH3 domain of Fak has an affinity for the PXPP motif of the PR and its role in PR localization in the plasma membrane near the focal adhesion complexes.

4. Role of PR and cSrc in Glioblastoma Progression

4.1. Contribution of cSrc to Malignancy of Glioblastoma

Glioblastoma (GB) is the most frequent and aggressive malignant brain tumor in adults. The current standard of care for patients with GB does not offer a survival of more than 15 months [45]. cSrc is one of the oldest proto-oncogenes associated with the progression of cancer. For a long time, it was thought that the central role of this kinase (cSrc) was related to cellular proliferation and tumor growth. However, in the last two

decades, interest in this kinase has emerged in the context of cell adhesion, invasion, and motility [12]. cSrc activity has been reported to be higher in GBs than in normal brain cells [46,47]. One of the first studies on the role of cSrc in GBs was performed in transgenic mice constitutively expressing the mutated variant of cSrc lacking the negative regulatory domain at the C-terminal end (*v*-SRC). In these animals, glial tumors grew with molecular and morphological characteristics closely resembling those of a human GB [48]. The role of cSrc in regulating GB cell motility was reported by Angers-Loustau et al. in 2004. They implanted spheroids of the human GB cell line (U251) in three-dimensional type I collagen matrices. It was observed that specific pharmacological inhibitors of the Src family, PP2 and SU6656, significantly reduced cell invasion. In addition, PP2 interfered with actin filament rearrangement in lamellipodia formation [49]. In 2015, Lewis-Tuffin et al. found that the silencing of cSrc, Fyn, Yes, and Lyn decreased proliferation and migration in human GB-derived cell lines LN229, U87, U251, TP483, and SF767 [50]. In GB cells with positive expression of the stemness marker CD133, the inhibition of expression and activity of cSrc and Fyn decreased these cells' migratory and invasive capacity [51]. In 2017, it was shown that in patient-derived GB (SOX2+/Nestin+) stem cells, the addition of a penetrating peptide, whose sequence corresponded to amino acids 266–283 of the connexin 43 sequence, significantly reduced the motility and invasive capacity of these cells through the inhibition of cSrc and Fak [52]. Although the evidence suggests that cSrc is a potent drug target, clinical trials with cSrc inhibitors have not been satisfactory [53]. One of the factors analyzed is the failure of Src inhibitors to cross the blood–brain barrier. In this regard, it may be helpful to address proteins that participate in the activation of cSrc which have inhibitors or antagonists that can cross the blood–brain barrier.

4.2. PR: An Underappreciated Villain in GB Progression

Since 1997, several studies have correlated PR content with gliomas' malignancy. Khalid et al. found that the protein content of the PR was higher in GBs (grade IV gliomas) than in grade I and II gliomas from the biopsies of 86 patients [54]. Recently, Arcos-Montoya et al. reported that the PR content, determined with immunofluorescence, was higher in samples derived from patients with GBs than in samples from patients with lower-grade gliomas or normal tissue [55]. In addition to the positive correlation between protein expression and grade of malignancy in gliomas, there is functional evidence of the PR's role in the progression of GBs. Gonzalez-Aguero et al. treated human GB-derived cell lines with P4 (10 nM) and observed a significant increase in the proliferation rate compared to the vehicle. When RU486, a PR antagonist, was added to the cells, the effect of P4 was blocked, suggesting that this hormone induces GB cell proliferation through the PR [56]. The effects mediated through PRs on GB cells are not limited to modifying proliferation-associated events. Piña-Medina et al. found that P4 increased the migratory and invasive capacity of the GB-derived cell line, U251. This effect was partially blocked when RU486 or antisense oligonucleotides against the expression of PRs were added [57]. However, these effects have generally been associated with the transcriptional activity of the receptor without considering its extranuclear role in the activation of signaling pathways in the cytoplasm. In breast cancer, PR extranuclear functions have been extensively characterized; however, in other types of tumors not associated with the reproductive system, such as GBs, this aspect has been underestimated.

4.3. PR–cSrc Interaction in GBs: Experimental Evidence and Future Perspectives

In breast cancer, the interplay between PR and cSrc has been widely characterized [13–15]; however, in other non-reproductive cancer, knowledge about this phenome is scarce. In the GB context, accumulating evidence suggests that the PR participates in the progression of the tumors when stimulated with low concentrations of P4 [56–59]. However, these effects have been primarily associated with transcriptional activity [60]. Recently, Bello-Alvarez et al. identified rapid effects induced by low P4 doses (50 nM) in GB-derived cell lines. Firstly, P4 induced cSrc activation after ten minutes of stimulation. When a siRNA against PR expression

was added, this effect was abolished, suggesting the role of the PR in the kinase activation. In addition, P4 activated Fak after twenty minutes of treatment, and this effect was partially suppressed when a siRNA against cSrc expression was incorporated. These results suggest that once stimulated by P4, the PR induces rapid signaling in GB-derived cell lines through the activation of cSrc and Fak, both essential proteins that regulate the focal adhesion complex assembly and disassembly, and contribute to migration and invasion.

The authors also reported the PR–cSrc interaction by co-immunoprecipitation assay [59]. In summary, the findings of this publication propose that in GBs, the PR operates via a rapid mechanism as in the case of breast cancer [61]. Nevertheless, there are still many missing elements in this mechanism that need to be elucidated. For example, the activation of other Src family proteins by the PR (Figure 2), especially Lyn, whose activity is the highest in GBs [62]. According to Boonyaratankornkit et al., in breast cancer cells expressing PRs and ERs, the activation of cSrc by P4 involves the formation of an ER–cSrc–PR ternary complex [11]. In GBs, the expression of both receptors and their participation in the progression of these tumors has been verified [63]. Hernández-Vega et al. demonstrated that E2 stimulated epithelial–mesenchymal transition, migration, and invasion of glioblastoma cells. Interestingly, these effects were only mediated by the ER α subtype [64]. It would be of great interest to determine the specific ER subtype that participates in the activation of cSrc through the PR in GB cells (Figure 2).

In breast cancer cells, it was reported that cSrc phosphorylates the Tyr537 residue of ER α , which in vitro and in vivo enhances ER α binding to EREs [65]. In silico analysis performed by Bello-Alvarez et al. proposed the residue Tyr87 of the PR as a putative site for cSrc phosphorylation [59]. This result encourages us to extend this field of research to find out which kinases of the Src family are involved in PR phosphorylation and their effects on the transcriptional activity of this receptor (Figure 2).

Kawprasertsri et al. reported in lung cancer cells without progestin stimulation that the rapid PR signaling interferes with the activation of the EGFR–ERK1/ERK2 pathway. Through its PXPP motif, the PR can bind to the adaptor protein GrB2, which is essential for signaling through EGFR. Although not demonstrated, these authors suggested that the PR limits the availability of GrB2 to EGFR [66], which has signaling that is one of the most studied phenomena in the context of GB and is known to contribute to its progression [67]. However, there is no information about the possible cross-talk between extranuclear PR activity and EGFR-mediated effects in GBs. This result is exciting because it highlights the possibility that the PR could promote glioblastoma progression depending on the type of SH3-domain interacting protein. These findings lead us to the following question: which other proteins with SH3 domains can interact with the PR, and what effects are triggered? (Figure 2).

5. Relevance of Possible cSrc–PR Interaction in Other Cancers

Lung and colorectum carcinomas are non-reproductive cancers with the highest incidence and mortality (Global Cancer Observatory—<https://gco.iarc.fr/>, accessed on 20 April 2022). As SRC is one of the most studied and characterized proto-oncogenes, the role of cSrc in the progression of both entities has been widely reported [68–71].

Non-small cell lung cancer (NSCLC) is the most prevalent form of lung cancer and is regulated by a complex signaling network [72]. In NSCLC, the role of cSrc is closely linked to EGFR. Zhang et al. reported that in two EGFR-dependent NSCLC cell lines (HCC827 and H3255), the phosphorylation of SFKs was higher than in non-EGFR-dependent cell lines. In both cell lines, treatment with the SFK inhibitors PP1 or SKI-606 induced apoptosis [73]. Although outside the context of non-reproductive cancers, the role of the PR is less well-known, there is evidence about its function in NSCLC. In contrast to cSrc, PR expression in NSCLC has been associated with a favorable prognosis [74,75]. Kawprasertsri et al. found the presence of the PR-B, but not that of the PR-B Δ SH3 (PR variant with a mutation in the PXPP motif which inhibits the interaction with SH3 domains), and a decrease in EGF-induced A549 proliferation and ERK1/2 activation, suggesting the role of the extranuclear

function of the PR through its PXPP motif in EGFR signaling [66]. cSrc is one of the main downstream regulators of EGFR signaling [71]. The PR has been reported to participate in EGFR transcription [60,76]. It would be interesting to evaluate whether there is a cooperation among cSrc, EGFR, and PR. A possible scenario would include the activation of cSrc by its interaction with EGFR, and once activated, the phosphorylation of different tyrosine residues in the PR, which could modify its transcriptional activity.

cSrc has been extensively investigated in colon cancer. Evidence suggests that in this malignancy, instead of inducing proliferation, cSrc promotes the assembly of integrin adhesions, strengthening the ability of cells to spread on a substrate. The proposed mechanism regulates focal adhesions through its interaction with integrins and other focal proteins, including paxillin [70]. In colorectal cancer cell lines, it was found that the PR induced folic acid-mediated antiproliferative effects through cSrc activation [77]. Considering that P4 effects differ according to the concentration used, favoring (10–50 nM) [57,59] or decreasing (80–300 μ M) [78,79] GB progression, it would be of great interest to evaluate its effects at different concentrations (Figure 2) on PR extranuclear functions in non-reproductive cancers.

Sex steroid receptors, including the PR, have been located in the plasma membrane. Among the events regulating this phenomenon is palmitoylation in the ligand-binding domain. In the case of the ER, the heat shock protein Hsp27 is essential for membrane tethering [36], but in the case of the PR, the proteins involved in translocation and anchoring to the membrane have been poorly studied. Another new aspect, even in breast cancer, is whether the PR needs to be associated with the plasma membrane to initiate signal transduction and the complex of proteins associated with the PR once it is anchored to the membrane.

6. Conclusions and Perspectives

In addition to its role as a transcription factor, the PR activates signaling cascades in the cytoplasm through its PXPP motif with the SH3 domain of a diverse group of proteins. This mechanism has been widely studied in breast cancer cells [11,13–15]. However, its potential involvement in the progression or arrest of other malignancies has been underestimated. In the context of the rapid actions of the PR, there remain numerous unanswered questions. First, it is unknown which proteins with SH3 domains interact with the PR and the effect of this interaction. It is unknown how the PR's stability and transcriptional activity can be regulated through its phosphorylation at different tyrosine residues by the SFKs. Another aspect to consider is to evaluate the effect of P4 concentration in PR extranuclear actions. In *in vitro* and *in vivo* models of prostate cancer, the addition of a PXPP peptide targeting the AR–cSrc association decreased cell proliferation in the LNCaP cell line and tumor growth in mice compared to the effects of the control peptide [80]. This result suggests the potential of this type of strategy for cancer treatment and the importance of extending the study of the rapid mechanism of the PR and other members of the nuclear receptor family to non-reproductive cancers.

Author Contributions: C.B.-A. conceptualized the article and selected the topics to be covered. C.B.-A. and C.J.Z.-S. wrote and prepared the original draft. I.C.-A. provided critical commentary, corrected the text, and acquired funding. All authors have read and agreed to the published version of the manuscript.

Funding: For this work: C.J.Z.-S. and C.B.-A. were funded by the Programa de Apoyo a Proyectos de Investigación e Innovación Tecnológica (PAPIIT), project number: IN217120, DGAPA-UNAM, México.

Institutional Review Board Statement: Not applicable.

Informed Consent Statement: Not applicable.

Data Availability Statement: Not applicable.

Conflicts of Interest: The authors declare no conflict of interest.

References

1. Tania Hernandez-Hernandez, O.; Camacho-Arroyo, I. Regulation of Gene Expression by Progesterone in Cancer Cells: Effects on Cyclin D1, EGFR and VEGF. *Mini Rev. Med. Chem.* **2013**, *13*, 635–642. [[CrossRef](#)]
2. Valadez-Cosmes, P.; Vázquez-Martínez, E.R.; Cerbón, M.; Camacho-Arroyo, I. Membrane Progesterone Receptors in Reproduction and Cancer. *Mol. Cell. Endocrinol.* **2016**, *434*, 166–175. [[CrossRef](#)]
3. Brisken, C.; Scabia, V. 90 years of progesterone: Progesterone Receptor Signaling in the Normal Breast and Its Implications for Cancer. *J. Mol. Endocrinol.* **2020**, *65*, T81–T94. [[CrossRef](#)]
4. Singh, M.; Su, C.; Ng, S. Non-Genomic Mechanisms of Progesterone Action in the Brain. *Front. Neurosci.* **2013**, *7*, 159. [[CrossRef](#)]
5. Garg, D.; Ng, S.S.M.; Baig, K.M.; Driggers, P.; Segars, J. Progesterone-Mediated Non-Classical Signaling. *Trends Endocrinol. Metab.* **2017**, *28*, 656–668. [[CrossRef](#)]
6. Moussatche, P.; Lyons, T.J. Non-Genomic Progesterone Signalling and Its Non-Canonical Receptor. *Biochem. Soc. Trans.* **2012**, *40*, 200–204. [[CrossRef](#)]
7. Peluso, J.J.; Pru, J.K. Non-Canonical Progesterone Signaling in Granulosa Cell Function. *Reproduction* **2014**, *147*, R169–R178. [[CrossRef](#)]
8. Peluso, J.J.; Pru, J.K. Progesterone Receptor Membrane Component (PGRMC)1 and PGRMC2 and Their Roles in Ovarian and Endometrial Cancer. *Cancers* **2021**, *13*, 5953. [[CrossRef](#)] [[PubMed](#)]
9. Asperger, H.; Stamm, N.; Gierke, B.; Pawlak, M.; Hofmann, U.; Zanger, U.M.; Marton, A.; Katona, R.L.; Buhala, A.; Vizler, C.; et al. Progesterone Receptor Membrane Component 1 Regulates Lipid Homeostasis and Drives Oncogenic Signaling Resulting in Breast Cancer Progression. *Breast Cancer Res.* **2020**, *22*, 75. [[CrossRef](#)] [[PubMed](#)]
10. Camacho-Arroyo, I.; Hansberg-Pastor, V.; Vázquez-Martínez, E.R.; Cerbón, M. Mechanism of Progesterone Action in the Brain. In *Hormones, Brain and Behavior*; Elsevier: Oxford, UK, 2017; pp. 181–214.
11. Boonyaratanakornkit, V.; Edwards, D.P. Receptor Mechanisms Mediating Non-Genomic Actions of Sex Steroids. *Semin. Reprod. Med.* **2007**, *25*, 139–153. [[CrossRef](#)] [[PubMed](#)]
12. Yeatman, T.J. A Renaissance for SRC. *Nat. Rev. Cancer* **2004**, *4*, 470–480. [[CrossRef](#)]
13. Migliaccio, A.; Piccolo, D.; Castoria, G.; Di Domenico, M.; Bilancio, A.; Lombardi, M.; Gong, W.; Beato, M.; Auricchio, F. Activation of the Src/P21ras/Erk Pathway by Progesterone Receptor via Cross-Talk with Estrogen Receptor. *EMBO J.* **1998**, *17*, 2008. [[CrossRef](#)]
14. Ballaré, C.; Uhrig, M.; Bechtold, T.; Sancho, E.; Di Domenico, M.; Migliaccio, A.; Auricchio, F.; Beato, M. Two Domains of the Progesterone Receptor Interact with the Estrogen Receptor and Are Required for Progesterone Activation of the C-Src/Erk Pathway in Mammalian Cells. *Mol. Cell. Biol.* **2003**, *23*, 1994–2008. [[CrossRef](#)]
15. Boonyaratanakornkit, V.; Scott, M.P.; Ribon, V.; Sherman, L.; Anderson, S.M.; Maller, J.L.; Miller, W.T.; Edwards, D.P. Progesterone Receptor Contains a Proline-Rich Motif That Directly Interacts with SH3 Domains and Activates c-Src Family Tyrosine Kinases. *Mol. Cell* **2001**, *8*, 269–280. [[CrossRef](#)]
16. Boonyaratanakornkit, V.; McGowan, E.; Sherman, L.; Mancini, M.A.; Cheskis, B.J.; Edwards, D.P. The Role of Extranuclear Signaling Actions of Progesterone Receptor in Mediating Progesterone Regulation of Gene Expression and the Cell Cycle. *Mol. Endocrinol.* **2007**, *21*, 359–375. [[CrossRef](#)] [[PubMed](#)]
17. Fu, X.D.; Goglia, L.; Sanchez, A.M.; Flamini, M.; Giretti, M.S.; Tosi, V.; Genazzani, A.R.; Simoncini, T. Progesterone Receptor Enhances Breast Cancer Cell Motility and Invasion via Extranuclear Activation of Focal Adhesion Kinase. *Endocr. Relat. Cancer* **2010**, *17*, 431–443. [[CrossRef](#)]
18. Wang, H.C.; Lee, W. Sen Molecular Mechanisms Underlying Progesterone-Enhanced Breast Cancer Cell Migration. *Sci. Rep.* **2016**, *6*, 31509. [[CrossRef](#)] [[PubMed](#)]
19. Mayer, B.J.; Hamaguchi, M.; Hanafusa, H. A Novel Viral Oncogene with Structural Similarity to Phospholipase C. *Nature* **1988**, *332*, 272–275. [[CrossRef](#)]
20. Stahl, M.L.; Ferenz, C.R.; Kelleher, K.L.; Kriz, R.W.; Knopf, J.L. Sequence Similarity of Phospholipase C with the Non-Catalytic Region of Src. *Nature* **1988**, *332*, 269–272. [[CrossRef](#)]
21. Teyra, J.; Huang, H.; Jain, S.; Guan, X.; Dong, A.; Liu, Y.; Tempel, W.; Min, J.; Tong, Y.; Kim, P.M.; et al. Comprehensive Analysis of the Human SH3 Domain Family Reveals a Wide Variety of Non-Canonical Specificities. *Structure* **2017**, *25*, 1598–1610.e3. [[CrossRef](#)] [[PubMed](#)]
22. Lehmann, J.M.; Riethmüller, G.; Johnson, J.P. Nck, a Melanoma CDNA Encoding a Cytoplasmic Protein Consisting of the Src Homology Units SH2 and SH3. *Nucleic Acids Res.* **1990**, *18*, 1048. [[CrossRef](#)] [[PubMed](#)]
23. Kurochkina, N.; Guha, U. SH3 Domains: Modules of Protein-Protein Interactions. *Biophys. Rev.* **2013**, *5*, 29–39. [[CrossRef](#)]
24. Saksela, K.; Permi, P. SH3 Domain Ligand Binding: What's the Consensus and Where's the Specificity? *FEBS Lett.* **2012**, *586*, 2609–2614. [[CrossRef](#)] [[PubMed](#)]
25. Brown, A.M.; Zondlo, N.J. A Propensity Scale for Type II Polyproline Helices (PPII): Aromatic Amino Acids in Proline-Rich Sequences Strongly Disfavor PPII Due to Proline-Aromatic Interactions. *Biochemistry* **2012**, *51*, 5041–5051. [[CrossRef](#)] [[PubMed](#)]
26. Chandra, B.R.; Gowthaman, R.; Akhouri, R.R.; Gupta, D.; Sharma, A. Distribution of Proline-rich (PxxP) Motifs in Distinct Proteomes: Functional and Therapeutic Implications for Malaria and Tuberculosis. *Protein Eng. Des. Sel.* **2004**, *17*, 175–182. [[CrossRef](#)]

27. Feng, S.; Chen, J.K.; Yu, H.; Simon, J.A.; Schreiber, S.L. Two Binding Orientations for Peptides to the Src SH3 Domain: Development of a General Model for SH3-Ligand Interactions. *Science* **1994**, *266*, 1241–1247. [[CrossRef](#)]
28. Yu, H.; Chen, J.K.; Feng, S.; Dalgarno, D.C.; Brauer, A.W.; Schreiber, S.L. Structural Basis for the Binding of Proline-Rich Peptides to SH3 Domains. *Cell* **1994**, *76*, 933–945. [[CrossRef](#)]
29. Weng, Z.; Rickles, R.J.; Feng, S.; Richard, S.; Shaw, A.S.; Schreiber, S.L.; Brugge, J.S. Structure-Function Analysis of SH3 Domains: SH3 Binding Specificity Altered by Single Amino Acid Substitutions. *Mol. Cell. Biol.* **1995**, *15*, 5627–5634. [[CrossRef](#)]
30. Fajer, M.; Meng, Y.; Roux, B. The Activation of C-Src Tyrosine Kinase: Conformational Transition Pathway and Free Energy Landscape. *J. Phys. Chem. B* **2017**, *121*, 3352–3363. [[CrossRef](#)]
31. Sieg, D.J.; Hauck, C.R.; Schlaepfer, D.D. Required Role of Focal Adhesion Kinase (FAK) for Integrin-Stimulated Cell Migration. *J. Cell Sci.* **1999**, *112*, 2677–2691. [[CrossRef](#)]
32. Anand-Apte, B.; Zetter, B.R.; Viswanathan, A.; Qiu, R.G.; Chen, J.; Ruggieri, R.; Symons, M. Platelet-Derived Growth Factor and Fibronectin-Stimulated Migration Are Differentially Regulated by the Rac and Extracellular Signal-Regulated Kinase Pathways. *J. Biol. Chem.* **1997**, *272*, 30688–30692. [[CrossRef](#)] [[PubMed](#)]
33. Weikum, E.R.; Liu, X.; Ortlund, E.A. The Nuclear Receptor Superfamily: A Structural Perspective. *Protein Sci.* **2018**, *27*, 1876–1892. [[CrossRef](#)] [[PubMed](#)]
34. Kastner, P.; Krust, A.; Turcotte, B.; Stropp, U.; Tora, L.; Gronemeyer, H.; Chambon, P. Two Distinct Estrogen-Regulated Promoters Generate Transcripts Encoding the Two Functionally Different Human Progesterone Receptor Forms A and B. *EMBO J.* **1990**, *9*, 1603–1614. [[CrossRef](#)] [[PubMed](#)]
35. Pedram, A.; Razandi, M.; Sainson, R.C.A.; Kim, J.K.; Hughes, C.C.; Levin, E.R. A Conserved Mechanism for Steroid Receptor Translocation to the Plasma Membrane. *J. Biol. Chem.* **2007**, *282*, 22278–22288. [[CrossRef](#)]
36. Razandi, M.; Pedram, A.; Levin, E.R. Heat Shock Protein 27 Is Required for Sex Steroid Receptor Trafficking to and Functioning at the Plasma Membrane. *Mol. Cell. Biol.* **2010**, *30*, 3249. [[CrossRef](#)]
37. Shupnik, M.A. Crosstalk between Steroid Receptors and the C-Src-Receptor Tyrosine Kinase Pathways: Implications for Cell Proliferation. *Oncogene* **2004**, *23*, 7979–7989. [[CrossRef](#)]
38. Simoncini, T.; Genazzani, A.R. Non-Genomic Actions of Sex Steroid Hormones. *Eur. J. Endocrinol.* **2003**, *148*, 281–292. [[CrossRef](#)]
39. Moore, M.R.; Conover, J.L.; Franks, K.M. Progesterone Effects on Long-Term Growth, Death, and Bcl-XL in Breast Cancer Cells. *Biochem. Biophys. Res. Commun.* **2000**, *277*, 650–654. [[CrossRef](#)]
40. Lange, C.A.; Shen, T.; Horwitz, K.B. Phosphorylation of Human Progesterone Receptors at Serine-294 by Mitogen-Activated Protein Kinase Signals Their Degradation by the 26S Proteasome. *Proc. Natl. Acad. Sci. USA* **2000**, *97*, 1032–1037. [[CrossRef](#)]
41. Skildum, A.; Faivre, E.; Lange, C.A. Progesterone Receptors Induce Cell Cycle Progression via Activation of Mitogen-Activated Protein Kinases. *Mol. Endocrinol.* **2005**, *19*, 327–339. [[CrossRef](#)]
42. Faivre, E.J.; Daniel, A.R.; Hillard, C.J.; Lange, C.A. Progesterone Receptor Rapid Signaling Mediates Serine 345 Phosphorylation and Tethering to Specificity Protein 1 Transcription Factors. *Mol. Endocrinol.* **2008**, *22*, 823–837. [[CrossRef](#)]
43. Proietti, C.; Salatino, M.; Rosembli, C.; Carnevale, R.; Pecci, A.; Kornblihtt, A.R.; Molinolo, A.A.; Frahm, I.; Charreau, E.H.; Schillaci, R.; et al. Progesterone Induces Transcriptional Activation of Signal Transducer and Activator of Transcription 3 (Stat3) via a Jak- and Src-Dependent Mechanism in Breast Cancer Cells. *Mol. Cell. Biol.* **2005**, *25*, 4826–4840. [[CrossRef](#)] [[PubMed](#)]
44. Mitra, S.K.; Hanson, D.A.; Schlaepfer, D.D. Focal Adhesion Kinase: In Command and Control of Cell Motility. *Nat. Rev. Mol. Cell Biol.* **2005**, *6*, 56–68. [[CrossRef](#)]
45. Ostrom, Q.T.; Cioffi, G.; Waite, K.; Kruchko, C.; Barnholtz-Sloan, J.S. CBTRUS Statistical Report: Primary Brain and Other Central Nervous System Tumors Diagnosed in the United States in 2014–2018. *Neuro. Oncol.* **2021**, *23*, III1–III105. [[CrossRef](#)] [[PubMed](#)]
46. McLendon, R.; Friedman, A.; Bigner, D.; Van Meir, E.G.; Brat, D.J.; Mastrogiannis, G.M.; Olson, J.J.; Mikkelsen, T.; Lehman, N.; Aldape, K.; et al. Comprehensive Genomic Characterization Defines Human Glioblastoma Genes and Core Pathways. *Nature* **2008**, *455*, 1061–1068. [[CrossRef](#)]
47. Du, J.; Bernasconi, P.; Clauser, K.R.; Mani, D.R.; Finn, S.P.; Beroukhim, R.; Burns, M.; Julian, B.; Peng, X.P.; Hieronymus, H.; et al. Bead-Based Profiling of Tyrosine Kinase Phosphorylation Identifies SRC as a Potential Target for Glioblastoma Therapy. *Nat. Biotechnol.* **2009**, *27*, 77–83. [[CrossRef](#)]
48. Weissenberger, J.; Steinbach, J.P.; Malin, G.; Spada, S.; Rülcke, T.; Aguzzi, A. Development and Malignant Progression of Astrocytomas in GFAP-v-Src Transgenic Mice. *Oncogene* **1997**, *14*, 2005–2013. [[CrossRef](#)]
49. Angers-Loustau, A.; Hering, R.; Werbowetski, T.E.; Kaplan, D.R.; Del Maestro, R.F. Src Regulates Actin Dynamics and Invasion of Malignant Glial Cells in Three Dimensions. Alex Pavanel and Franco Di Giovanni Funds for Brain Tumor Research (R.F. Del Maestro), Canadian Cancer Society and National Cancer Institute of Canada (D.R. Kaplan). *Mol. Cancer Res.* **2004**, *2*, 595–605. [[CrossRef](#)]
50. Lewis-Tuffin, L.J.; Feathers, R.; Hari, P.; Durand, N.; Li, Z.; Rodriguez, F.J.; Bakken, K.; Carlson, B.; Schroeder, M.; Sarkaria, J.N.; et al. Src Family Kinases Differentially Influence Glioma Growth and Motility. *Mol. Oncol.* **2015**, *9*, 1783–1798. [[CrossRef](#)]
51. Han, X.; Zhang, W.; Yang, X.; Wheeler, C.G.; Langford, C.P.; Wu, L.; Filippova, N.; Friedman, G.K.; Ding, Q.; Fathallah-Shaykh, H.M.; et al. The Role of Src Family Kinases in Growth and Migration of Glioma Stem Cells. *Int. J. Oncol.* **2014**, *45*, 302–310. [[CrossRef](#)]

52. Jaraíz-Rodríguez, M.; Tabernero, M.D.; González-Tablas, M.; Otero, A.; Orfao, A.; Medina, J.M.; Tabernero, A. A Short Region of Connexin43 Reduces Human Glioma Stem Cell Migration, Invasion, and Survival through Src, PTEN, and FAK. *Stem Cell Reports* **2017**, *9*, 451–463. [[CrossRef](#)] [[PubMed](#)]
53. Galanis, E.; Anderson, S.K.; Twohy, E.L.; Carrero, X.W.; Dixon, J.G.; Tran, D.D.; Jeyapalan, S.A.; Anderson, D.M.; Kaufmann, T.J.; Feathers, R.W.; et al. A Phase I and Randomized Placebo-Controlled Phase II Trial of Bevacizumab plus Dasatinib in Patients with Recurrent Glioblastoma (GBM): Alliance/NCCTG N0872. *Cancer* **2019**, *125*, 3790. [[CrossRef](#)] [[PubMed](#)]
54. Khalid, H.; Shibata, S.; Kishikawa, M.; Yasunaga, A.; Iseki, M.; Hiura, T. Immunohistochemical Analysis of Progesterone Receptor and Ki-67 Labeling Index in Astrocytic Tumors—PubMed. *Cancer* **1997**, *80*, 2133–2140. [[CrossRef](#)]
55. Arcos-Montoya, D.; Wegman-Ostrosky, T.; Mejía-Pérez, S.; De la Fuente-Granada, M.; Camacho-Arroyo, I.; García-Carrancá, A.; Velasco-Velázquez, M.A.; Manjarrez-Marmolejo, J.; González-Arenas, A. Progesterone Receptor Together with PKC α Expression as Prognostic Factors for Astrocytomas Malignancy. *Onco Targets Ther.* **2021**, *14*, 3757. [[CrossRef](#)]
56. González-Agüero, G.; Gutiérrez, A.A.; González-Espinosa, D.; Solano, J.D.; Morales, R.; González-Arenas, A.; Cabrera-Muñoz, E.; Camacho-Arroyo, I. Progesterone Effects on Cell Growth of U373 and D54 Human Astrocytoma Cell Lines. *Endocrine* **2007**, *32*, 129–135. [[CrossRef](#)]
57. Piña-Medina, A.G.; Hansberg-Pastor, V.; González-Arenas, A.; Cerbón, M.; Camacho-Arroyo, I. Progesterone Promotes Cell Migration, Invasion and Cofilin Activation in Human Astrocytoma Cells. *Steroids* **2016**, *105*, 19–25. [[CrossRef](#)]
58. Germán-Castelán, L.; Manjarrez-Marmolejo, J.; González-Arenas, A.; Genoveva González-Morán, M.; Camacho-Arroyo, I. Progesterone Induces the Growth and Infiltration of Human Astrocytoma Cells Implanted in the Cerebral Cortex of the Rat. *BioMed Res. Int.* **2014**, *2014*, 393174. [[CrossRef](#)]
59. Bello-Alvarez, C.; Moral-Morales, A.D.; González-Arenas, A.; Camacho-Arroyo, I. Intracellular Progesterone Receptor and CSrc Protein Working Together to Regulate the Activity of Proteins Involved in Migration and Invasion of Human Glioblastoma Cells. *Front. Endocrinol.* **2021**, *12*, 640298. [[CrossRef](#)]
60. Hernández-Hernández, O.T.; González-García, T.K.; Camacho-Arroyo, I. Progesterone Receptor and SRC-1 Participate in the Regulation of VEGF, EGFR and Cyclin D1 Expression in Human Astrocytoma Cell Lines. *J. Steroid Biochem. Mol. Biol.* **2012**, *132*, 127–134. [[CrossRef](#)]
61. Trabert, B.; Sherman, M.E.; Kannan, N.; Stanczyk, F.Z. Progesterone and Breast Cancer. *Endocr. Rev.* **2020**, *41*, 320–344. [[CrossRef](#)]
62. Stettner, M.R.; Wang, W.; Nabors, L.B.; Bharara, S.; Flynn, D.C.; Grammer, J.R.; Gillespie, G.Y.; Gladson, C.L. Lyn Kinase Activity Is the Predominant Cellular Src Kinase Activity in Glioblastoma Tumor Cells. *Cancer Res.* **2005**, *65*, 5535–5543. [[CrossRef](#)]
63. Tavares, C.B.; Gomes-Braga, F.d.C.S.A.; Costa-Silva, D.R.; Escórcio-Dourado, C.S.; Borges, U.S.; Conde-Junior, A.M.; Barros-Oliveira, M.d.C.; Sousa, E.B.; Barros, L.d.R.; Martins, L.M.; et al. Expression of Estrogen and Progesterone Receptors in Astrocytomas: A Literature Review. *Clinics* **2016**, *71*, 481–486. [[CrossRef](#)]
64. Hernández-Vega, A.M.; Del Moral-Morales, A.; Zamora-Sánchez, C.J.; Piña-Medina, A.G.; González-Arenas, A.; Camacho-Arroyo, I. Estradiol Induces Epithelial to Mesenchymal Transition of Human Glioblastoma Cells. *Cells* **2020**, *9*, 1930. [[CrossRef](#)] [[PubMed](#)]
65. Castoria, G.; Giovannelli, P.; Lombardi, M.; De Rosa, C.; Giraldi, T.; De Falco, A.; Barone, M.V.; Abbondanza, C.; Migliaccio, A.; Auricchio, F. Tyrosine Phosphorylation of Estradiol Receptor by Src Regulates Its Hormone-Dependent Nuclear Export and Cell Cycle Progression in Breast Cancer Cells. *Oncogene* **2012**, *31*, 4868–4877. [[CrossRef](#)] [[PubMed](#)]
66. Kawprasertsri, S.; Pietras, R.J.; Marquez-Garban, D.C.; Boonyaratanakornkit, V. Progesterone Receptor (PR) Polyproline Domain (PPD) Mediates Inhibition of Epidermal Growth Factor Receptor (EGFR) Signaling in Non-Small Cell Lung Cancer Cells. *Cancer Lett.* **2016**, *374*, 279–291. [[CrossRef](#)]
67. Oprita, A.; Baloi, S.C.; Staicu, G.A.; Alexandru, O.; Tache, D.E.; Danoiu, S.; Micu, E.S.; Sevastre, A.S. Updated Insights on EGFR Signaling Pathways in Glioma. *Int. J. Mol. Sci.* **2021**, *22*, 587. [[CrossRef](#)]
68. Giaccone, G.; Zucali, P.A. Src as a Potential Therapeutic Target in Non-Small-Cell Lung Cancer. *Ann. Oncol.* **2008**, *19*, 1219–1223. [[CrossRef](#)]
69. Rothschild, S.; Gautschi, O.; Haura, E.; Johnson, F. Src Inhibitors in Lung Cancer: Current Status and Future Directions. *Clin. Lung Cancer* **2010**, *11*, 238–242. [[CrossRef](#)]
70. Jones, R.J.; Avizienyte, E.; Wyke, A.W.; Owens, D.W.; Brunton, V.G.; Frame, M.C. Elevated C-Src Is Linked to Altered Cell—Matrix Adhesion Rather than Proliferation in KM12C Human Colorectal Cancer Cells. *Br. J. Cancer* **2002**, *87*, 1128–1135. [[CrossRef](#)]
71. Kopetz, S.; Kopetz, S. Targeting Src and Epidermal Growth Factor Receptor in Colorectal Cancer: Rationale and Progress Into the Clinic. *Gastrointest. Cancer Res.* **2007**, *1*, S37.
72. Xu, H.; Zhang, L.; Yuan, M.; Xu, L.F.; Zhang, J.; Kong, S.; Wu, M.; Lao, Y. SRC and MEK Co-Inhibition Synergistically Enhances the Anti-Tumor Effect in Both Non-Small Cell Lung Cancer (NSCLC) and Erlotinib-Resistant NSCLC. *Front. Oncol.* **2019**, *9*, 586. [[CrossRef](#)]
73. Zhang, J.; Kalyankrishna, S.; Wislez, M.; Thilaganathan, N.; Saigal, B.; Wei, W.; Ma, L.; Wistuba, I.I.; Johnson, F.M.; Kurie, J.M. Src-Family Kinases Are Activated in Non-Small Cell Lung Cancer and Promote the Survival of Epidermal Growth Factor Receptor-Dependent Cell Lines. *Am. J. Pathol.* **2007**, *170*, 366. [[CrossRef](#)] [[PubMed](#)]
74. Ishibashi, H.; Suzuki, T.; Suzuki, S.; Niikawa, H.; Lu, L.; Miki, Y.; Moriya, T.; Hayashi, S.I.; Handa, M.; Kondo, T.; et al. Progesterone Receptor in Non-Small Cell Lung Cancer—a Potent Prognostic Factor and Possible Target for Endocrine Therapy. *Cancer Res.* **2005**, *65*, 6450–6458. [[CrossRef](#)] [[PubMed](#)]

75. Skjefstad, K.; Richardsen, E.; Donnem, T.; Andersen, S.; Kiselev, Y.; Grindstad, T.; Hald, S.M.; Al-Shibli, K.; Bremnes, R.M.; Busund, L.T.; et al. The Prognostic Role of Progesterone Receptor Expression in Non-Small Cell Lung Cancer Patients: Gender-Related Impacts and Correlation with Disease-Specific Survival. *Steroids* **2015**, *98*, 29–36. [[CrossRef](#)]
76. Faivre, E.J.; Lange, C.A. Progesterone Receptors Upregulate Wnt-1 to Induce Epidermal Growth Factor Receptor Transactivation and c-Src-Dependent Sustained Activation of Erk1/2 Mitogen-Activated Protein Kinase in Breast Cancer Cells. *Mol. Cell. Biol.* **2007**, *27*, 466–480. [[CrossRef](#)]
77. Kuo, C.T.; Lee, W. Sen Progesterone Receptor Activation Is Required for Folic Acid-Induced Anti-Proliferation in Colorectal Cancer Cell Lines. *Cancer Lett.* **2016**, *378*, 104–110. [[CrossRef](#)]
78. Atif, F.; Yousuf, S.; Stein, D.G. Anti-Tumor Effects of Progesterone in Human Glioblastoma Multiforme: Role of PI3K/Akt/MTOR Signaling. *J. Steroid Biochem. Mol. Biol.* **2015**, *146*, 62–73. [[CrossRef](#)]
79. Altinoz, M.A.; Ucal, Y.; Yilmaz, M.C.; Kiris, İ.; Ozisik, O.; Sezerman, U.; Ozpinar, A.; Elmaci, İ. Progesterone at High Doses Reduces the Growth of U87 and A172 Glioblastoma Cells: Proteomic Changes Regarding Metabolism and Immunity. *Cancer Med.* **2020**, *9*, 5767–5780. [[CrossRef](#)]
80. Migliaccio, A.; Varricchio, L.; De Falco, A.; Castoria, G.; Arra, C.; Yamaguchi, H.; Ciociola, A.; Lombardi, M.; Di Stasio, R.; Barbieri, A.; et al. Inhibition of the SH3 Domain-Mediated Binding of Src to the Androgen Receptor and Its Effect on Tumor Growth. *Oncogene* **2007**, *26*, 6619–6629. [[CrossRef](#)]